Back to the lithics: technological comparison of early Upper Palaeolithic assemblages from Al-Ansab/ Jordan, Românești-Dumbrăvița/ Romania and Fumane/ Italy

Inaugural-Dissertation

zur Erlangung des Doktorgrades der Philosophischen Fakultät der Universität zu Köln im Fach

Archäologie – **Ur- und Frühgeschichte**

vorgelegt von

Jacopo Gennai

geb. am **11.01.1992** in **Viareggio (LU), Italien**

Köln, 12.01.2021

This thesis was successfully defended on 05.05.2021 and was accepted by the Faculty of Arts and Humanities of the University of Cologne. No changes have been required by the Examination Committee; thus, it is deemed fit for publication by the first supervisor Prof. Dr. Jürgen Richter.

Erster referent: Professor Dr. Jürgen Richter

Zweiter referent: Professor Dr. Gerd-Christian Weniger

Acknowledgments

This dissertation would have not been possible without the multiple spiritual and material help I have been provided with. First of all, the work has been generously funded by the Deutsche Forschungsgemeinschaft (DFG, German Research Foundation) – Projektnummer 57444011 – SFB 806. I must thank my first supervisor Prof. Dr. Jürgen Richter for giving me the opportunity to pursue this Ph.D. research within the framework of the SFB806 "Our Way to Europe: Culture-Environment Interaction and Human Mobility in the Late Quaternary". I profited greatly from his and other members' assistance: in particular Dr. Wei Chu, Dr. Dirk Leder and Dr. Werner Schuck. A special thanks to my fellow Ph.D. colleague Christian Schepers for the fruitful conversations and making me feeling welcome in Cologne throughout my whole stay!

This dissertation research spans over two continents and in three countries. I appreciated greatly the support of Dr. Adrian Doboş and Dr. Alexandru Ciornei (Department of Palaeolithic Archaeology, Institute of Archaeology "Vasile Pârvan" in the Romanian Academy). Special thanks to Prof. Dr. Marco Peresani (Department of Humanities, Institute of Prehistoric and Anthropological Sciences of Ferrara University) for granting me access to the lithic assemblage of Grotta di Fumane and according me his trust and esteem throughout these years.

Finally, I have to thank my family, my parents Marco and Marina, which helped me being the person I am and constantly supported my dreams, whose this dissertation is the first achievement.

Index

List of Figures

List of Tables

1. Introduction

This chapter is aimed at portraying the state of the art of the research in both study areas, Europe and the Levant, and, thus, the context in which this analysis is conducted. Giving the vast literature and wealth of research carried out in these regions in more than 100 years, I will concentrate mostly on lithic industries, which are the focus of this dissertation. Furthermore, I will discuss only techno-cultural units traditionally attributed to the earliest Upper Palaeolithic (UP) occurrences, namely the Early Aurignacian and the Protoaurignacian in Europe and the Early Ahmarian in the Levant. The first section, 1.1, provides the research history of the Aurignacian, then splitting in two for giving the most accepted definitions of Early Aurignacian, 1.1.2, and of Protoaurignacian, 1.1.3. Section 1.2 deals with the Levantine UP record and the Early Ahmarian definition. Following, section 1.3 provides a review of assemblages assigned to the above-mentioned techno-cultural units, subdivided in geographical order, trying to build up an objective evaluation of the early UP technical behaviour. Section 1.4 deals with the problems of imposing the Aquitanian model of Aurignacian development to the rest of Europe. Section 1.5 presents the theoretical models of Anatomically Modern Humans (AMH) dispersal into Eurasia, especially the Danube Corridor Hypothesis. Section 1.6 addresses the problematics raised by current dating methods. Finally, 1.7 provides a summary of the chapter and a formulation of the research question leading to this dissertation.

1.1 Aurignacian

An industry containing all the future hallmark of the Aurignacian, especially the split-base osseous point, was presented by E. Lartet after his excavations in 1852 at Aurignac cave in Haute-Garonne, SW France (Breuil, 1913; Chu and Richter, 2020; Djindjian, 2007; Tafelmaier, 2017). At the beginning of the XX century, the Aurignacian acquired its definitive chrono-stratigraphical position, thanks to H. Breuil, who divided it in Lower, Middle and Upper Aurignacian. Breuil's definition of the Middle Aurignacian became the one, which today scholars refer as Aurignacian. It is based on the Aurignac inventory, an industry composed by an high frequency of carinated end-scrapers, less burins, heavily retouched blades, retouched bladelets and split-base osseous point (Breuil, 1913; Djindjian, 2007; Peyrony, 1933; Tafelmaier, 2017).

After his excavations in Dordogne and Corrèze, D. Peyrony (1933) split the Aurignacian in five subsequent phases using osseous points as markers:

Aurignacian I, split-base points (*pointes à base fendue*)
Aurignacian II, lozenge massive base points (*pointes losangiques plates*)
Aurignacian III, oval cross-section points (*pointes à section oval*)
Aurignacian IV, biconical points (*pointes biconiques*)

Aurignacian V, beveled base points (*pointes à base a biseau simple*)

In addition to the Aurignacian evolutive line, Peyrony established a second, contemporaneous one, featuring the apparent development of backed tools, the Perigordian (Peyrony, 1933):

Perigordian I, backed knives, Chatelperronian points, corresponding to Breuil's Lower Aurignacian
Perigordian II, backed knives and marginally backed blades and bladelets
Perigordian III, obliquely truncated blades and marginally backed blades and bladelets
Perigordian IV, Gravette points, corresponding to Breuil's Upper Aurignacian
Perigordian V, Noailles burins, foliates and tanged points

Regarding the Aurignacian, modern authors prefer the names of Early Aurignacian (Aurignacian I), Evolved Aurignacian (Aurignacian II), Late Aurignacian (Aurignacian III and IV) and they have abandoned the Aurignacian V (Laplace, 1966; Teyssandier and Zilhão, 2018).
Between the 1950-1960s Peyrony's model had been precised or modified, for instance the Perigordian was progressively dismantled, absorbed in the Chatelperronian and in the Gravettian. D. Sonneville-de Bordes recognised the marginally retouched bladelets, named Dufour bladelets, as true Aurignacian *fossiles directeurs* (Bon, 2006, 2002a; Delporte, 1991; Laplace, 1966). At the same time A. Cheynier introduced the term Mediterranean (*Mediterranéen*) comprising all industries of the Mediterranean rim, expanding from the Near East to other continents, slightly preceding or contemporaneous to the Aurignacian, featuring marginally backed bladelets (Laplace, 1966). Following that, G. Laplace moved the Perigordian II, renamed as Protoaurignacian (*Protoaurignacien*), into the Aurignacian evolutive line, which, in his theory of the leptolithic *synthetotype*, was a stage of the evolution of a more and more specialised laminar production ending with the fully-fledged Aurignacian (Laplace, 1966; Tafelmaier, 2017). The existence of a Aurignacian phase preceding the classic Aurignacian I was introduced by H. Delporte too, who renamed the Perigordian II in Aurignacian 0 (Delporte, 1991; Djindjian, 2007).
At this point, the actual chrono-stratigraphic-cultural framework was formed, even though definitions have been partially modified and the focus is shifted from different types or from typology to technology (Bon, 2002a).
The Aurignacian, in his broader sense, is perceived as the industry indisputably associated with AMHs dispersal in Europe, with a complex osseous technology, ornamental items and eventually figurative art (Conard and Bolus, 2003; Nigst et al., 2014; Tartar, 2015; Tejero et al., 2012; Teyssandier and Zilhão, 2018).
From the lithic point of view, it features the massive introduction of standardised laminar products, especially bladelets (Bon, 2006, 2002a; Le Brun-Ricalens, 2005a; Le Brun-Ricalens et al., 2009).

Here only the two earliest technocomplexes, the Early Aurignacian and the Protoaurignacian, will be dealt with.

1.1.2 Early Aurignacian

The Early Aurignacian (Typical or Classic Aurignacian, Aurignacian I) definition relies heavily on the archaeological record of South-western France. The Aquitanian Aurignacian bears a clear typological signature, due to the strong presence of carinated end-scrapers (end-scrapers on thick blanks whose front is at least 30 mm high (Demars and Laurent, 1992)) and robust blades, possibly bearing a scalar retouch referred as Aurignacian retouch (Bon, 2002a; Teyssandier, 2006). The negatives on the end-scrapers are consistent with frequent small and curved bladelets, rarely retouched in Dufour subtype Dufour bladelets (Le Brun-Ricalens et al., 2009). At the same time, Peyrony's partition was widely applied, meaning that most of the Early Aurignacian sites where determined on the grounds of the, sometimes sole, presence of split-base points (SBP) (Banks et al., 2013). The SBPs–Early Aurignacian equivalence has been criticised repeatedly on the grounds that SBPs are identified also in Protoaurignacian contexts, found without diagnostic cultural context or with later radiometric determinations not coherent with the Early Aurignacian chronological framework (Bodu et al., 2013; Laplace, 1966; Moreau et al., 2015; Tafelmaier, 2017).

Consistent and undisputed Early Aurignacian assemblages occur only in South-western France and in the AHIII and AHII of Geißenklösterle, Swabian Jura Germany (Bon, 2002a; Bordes and Tixier, 2002; Teyssandier et al., 2006).

Spanish and Italian sites are mostly attributed to the Early Aurignacian because of the appearance or the increased presence of carinated cores and antler technology; it must be noticed that the assemblages are mostly result of old excavations, which partially hampers the exact attribution (Arrizabalaga et al., 2009; Degano et al., 2019a; Tejero and Grimaldi, 2015). A strongly debated assemblage is AH 3 from the site of Willendorf II in Lower Austria; where repeated excavations throughout the XX century and the early XXI century have discovered a small and probably highly scattered assemblage, which has been referred to the Early Aurignacian (Nigst et al., 2014; Nigst and Haesaerts, 2012), although the Early Aurignacian attribution of the assemblage is severely criticised on stratigraphical and techno-typological grounds (Teyssandier and Zilhão, 2018).

Two Hungarian cave sites are often featured in the Early Aurignacian technocomplex, Istállóskő and Peskő in the Bükk mountains, particularly for their high content of bone and antler SBP and massive base points, which are have recently dated as early as ≈43 k cal BP (Hedges and Davies, 2008; Markó, 2017). Despite the antiquity, the combination of small lithic inventories, few, if none, diagnostic lithic tool types and of problematics associated with post-depositional reworking is severely hampering any meaningful technocomplex attribution; on the other hand, surface collections in the nearby site of Nagyréde feature lithic tools resembling the French Evolved Aurignacian (Lengyel et al., 2006; Markó, 2015).

Another famous site in Central Europe is Mladeč, Czech Republic, where, supposedly repeatedly, various individuals, males, females and one child, have precipitated or been deposited in the cave

through karst chimneys (Svoboda, 2001, 2000). The bodies were accompanied by bi-conical oval cross-section bone points, referred as Mladeč-type, and bone and ivory objects and ornaments (Svoboda, 2001, 2000). Calcareous crusts overlying the human remains provides minimum ages of 37.6–40.6 k cal BP and 38.8–41.1 k cal BP, but direct dating of teeth provided a younger interval 34.6–36.7 k cal BP (Nejman et al., 2011; Wild et al., 2005). Therefore, Mladeč, as most of the sites attributed to the Aurignacian in Central Europe, is related to an Evolved Aurignacian rather than an Early one (Svoboda, 2006).

Further East, the Kostenki-Borshchevo sites complex, Middle Don (Russia), has yielded prismatic laminar cores, carinated end-scrapers, curved and twisted bladelets, which some are retouched in Dufour subtype Roc-de-Combe bladelets, and an Aurignacian blade in two locations: Kostenki 14/LVA, a layer embedded in volcanic ash related to the Campanian Ignimbrite, and Kostenki 1/II and III (Anikovich et al., 2007; Bataille et al., 2018; Dinnis et al., 2019; Hoffecker et al., 2016; Sinitsyn, 1993, 2003).

F. Bon established the Early Aurignacian lithic technological signature at the beginning of this century through the analysis of the Aurignacian assemblages of the lower level of Tuto de Camalhot and layers 2F, 2DE and 2A of Grotte des Hyènes at Brassempouy (Bon, 2002a). He reconciled the typological observations to technological ones: the two typological markers, the carinated end-scrapers and the thick Aurignacian blades, are the expression of two dissociated production systems (Anderson et al., 2015; Bon, 2002b).

The first one is the reduction of unipolar prismatic cores for the obtention of blades. The cores are manufactured on blocs already presenting the desired morphological characteristics, hence a minimal or absent shaping. The striking platform is thoroughly facetted, the flaking surface is framed by perpendicular sides, giving a parallel edges morphology. The presence of lateral ridges allows the continued extraction of lateral asymmetrical blades re-establishing the necessary convexities; in alternative, partial unifacial crest can be shaped easily. The blades are knapped with direct soft organic hammer percussion. (Bon, 2006, 2002a; Bordes, 2006).

Bladelets are obtained through the carinated end-scrapers, small prismatic cores, and dihedral burins (Bon, 2002b).

The carinated end-scrapers are the most used configuration for bladelets production. They are an independent production carried out on blocs, split blocs, or thick flakes. The striking platform is always installed on a long plain surface, which in case of blanks is offered by the ventral face. The bladelet flaking surface is placed on a distal termination exploiting the core thickness. From the striking platform, flakes are knapped on the lateral core surfaces creating a central crest, which is in a distal position regarding the bladelet flaking surface and will be determinant in the obtention of the researched bladelets. On the flanks, the flaking surface is isolated by two flakes removal, creating the guide ridges for the first inwards convergent bladelets; these will likely present a twisted edge

profile. The bladelets knapping proceeds towards the centre obtaining slightly curved bladelet (Bon, 2002a; Bordes, 2006; Chiotti and Cretin, 2011).

The prismatic bladelets cores follows the same principles of the blade cores. They are obtained on worse quality raw material and the striking platform remains plain. Burins are an extemporaneous production (Bon, 2002a).

Early Aurignacian hard animal material industry, in addition to the SBPs, includes also *bâtons percés* and wedges in antler, awls and *lissoirs* in bone and ornamental artefacts, as the basket-shaped beads, in ivory (Higham et al., 2012; Rigaud et al., 2014; Tartar, 2015; Tartar et al., 2006; Tartar and White, 2013). Non-modified tools are bone retouchers, naturally bevelled fragments used as wedges, picks and engraving objects (Tartar, 2015; Tartar et al., 2006; Tartar and White, 2013).

The SBP manufacture process is the most complex. It involves sectioning the antler in different parts, these rods are split longitudinally in two, then after a long soaking, a crack is open longitudinally at the base with the aid of a pre-incision and then wedging, finally the point is shaped by scraping (Tartar, 2015; Tartar et al., 2006; Tartar and White, 2013; Tejero et al., 2012). Other experimentation provides contrasting results in the pre-soaking usefulness (Tejero et al., 2012).

Ivory beads have a similarly complex manufacture. The material is collected sub-fossil ivory. Following the desiccation cracks, the shafts are broken into fragments, shaped into rods by scraping, then uniformly divided in discs by cutting and separated by snapping, finally the obtained discs are shaped into beads through abrasion and perforation (Rigaud et al., 2014; Tartar, 2015).

The careful and repetitive manufacture processes is function of the need of standardised artefacts, either for hunting, either for social display (Tartar, 2015; Tartar et al., 2006).

The technical tradition is therefore showing a clear structuration in two domains: domestic and cynegetic. The first one is represented by big lithic tools knapped from unipolar blade cores and by bone tools, the second by the small, standardised bladelets knapped from carinated end-scrapers and by the antler points (Anderson et al., 2015; Bon, 2006, 2002a; Tartar et al., 2006). The nature of the lithic exploitation of carinated end-scrapers and production of osseous points, made on a material available only cyclically, points to a clear anticipation of the needs (Bon, 2005, 2002a; Tartar, 2015; Tartar et al., 2006).

The careful provisioning planning is also shown by lithic raw material procurement and sites distribution patterns (Anderson et al., 2015; Bon, 2002a).

It has been suggested that the Early Aurignacian cultural adaptation resulted from the onset of deteriorated climatic conditions caused by the Heinrich Event 4. This would fit with osseous technology increase, where wood-working technical operations would have been transferred to hard animal material at the time of the development of steppe-tundra open biomes naturally favouring the reindeer (Banks et al., 2013; Tartar, 2015). A Bayesian analysis of the available radiometric determinations led Banks and colleagues in confining the Early Aurignacian in the 39.8–37.9 k cal

BP timeframe and subsequently the Early Aurignacian sites distribution fitted best the Heinrich Event 4 climatic conditions (Banks et al., 2013).

Doubts on this model are cast by the exclusion of a site like Geißenklösterle, whose AHIII modelled start is determined at 43.0–41.5 k cal BP, the inclusion of radiometric determinations obtained before the introduction of the ultrafiltration protocols and the use of an imprecise definition of Early Aurignacian, heavily relying on the presence of SBPs (Higham et al., 2012; Tafelmaier, 2017).

1.1.3 Protoaurignacian

As early as the '60s, prehistorians started to recognise a different *facies* they could attribute to the Aurignacian but not to the Early Aurignacian, therefore they name it Protoaurignacian, Archaic or Initial Aurignacian and Aurignacian 0 (Bazile and Sicard, 1997; Bon, 2002a; Delporte, 1991; Laplace, 1966). Protoaurignacian originated from G. Laplace and had been applied to sites studied by him or in areas where his legacy is stronger, such as Italy (Bon, 2002b). Archaic/Initial Aurignacian was designated by F. Bazile and D. Sacchi for describing their sites in Mediterranean France (Bazile and Sicard, 1997; Bon, 2002b). Aurignacian 0 or Aurignacian Ia were employed by authors like H. Delporte and P. Y. Demars, in a sort of compromise with Peyrony's partition (Delporte, 1991; Djindjian, 2007).

Typologically, the Protoaurignacian has been defined as an industry massively featuring marginally backed bladelets, either the Dufour bladelets, with alternate or simply inverse retouch, or the Krems/Font Yves bladelets/points, with bilateral direct retouch (Broglio and Laplace, 1966; Laplace, 1966). The blanks are straight-profile, elongated and fairly big bladelets (Bon, 2002a; Demars and Laurent, 1992; Falcucci et al., 2018; Le Brun-Ricalens et al., 2009). Laplace identified two Protoaurignacian variants, the classic with marginally backed artefacts (*à pièces à dos marginal*) and the rarer, and stratigraphically later, with carinated end-scrapers (*à grattoirs carénés*) (Laplace, 1966). The latter is reminiscent of Aurignacian 0's definition given by Delporte, who noticed the absence of Aurignacian blades in some Aurignacian assemblages (Delporte, 1991; Djindjian, 2007).

The core of the Protoaurignacian sites distribution is the (wider) Mediterranean rim: therefore Cantabria (Arrizabalaga et al., 2009; Tafelmaier, 2017) and Catalunya in Spain (Ortega Cobos et al., 2005; Soler Subils et al., 2008), the French Pyrenees (Barshay-Szmidt et al., 2018; Laplace, 1966; Normand and Turq, 2005), the French Midi (Bazile and Sicard, 1997; Onoratini, 2008; Porraz et al., 2010; Slimak et al., 2006), in Italy on the Tyrrenean side, the Balzi Rossi sites in Liguria (Bazile, 2002; Kuhn and Stiner, 1998; Riel-Salvatore and Negrino, 2018), La Fabbrica in Tuscany (Dini et al., 2012), La Cala, Serino and Castelcivita in Campania (Gambassini, 1997; Wood et al., 2012) and on the Adriatic side, Paglicci in Apulia and Grotta di Fumane in Veneto (Broglio et al., 2005; Palma di Cesnola, 2006). Lately, new sites have been added for the French continental context, like Le Piage in Northern Aquitaine (Bordes, 2005), Les Cottès in the western Parisian Basin (Roussel and

Soressi, 2013), Grotte du Renne at Arcy sur Cure, Burgundy (Bon and Bodu, 2002) and Trou de la Mère Clochette in the French Jura (Bodu et al., 2013; Szmidt et al., 2010).

Sites that have been attributed or linked with the Protoaurignacian are Krems-Hundssteig in Lower Austria (Broglio and Laplace, 1966; Nigst and Haesaerts, 2012; Teyssandier, 2007), Tincova in Romania (Banks et al., 2013; Teyssandier, 2007), Kozarnika in Bulgaria (Sirakov et al., 2007; Tsanova, 2008; Tsanova et al., 2012), in Crimea Siuren I layers H and G (Bataille, 2016; Demidenko and Noiret, 2012). Recently, Dinnis and colleagues claim Protoaurignacian characters for the Kostenki 17/II assemblage of the Russian Kostenki-Borshchevo sites complex (Dinnis et al., 2019) but Bataille and colleagues have severely criticised such attribution (Bataille et al., 2019).

The lithic technological signature was illustrated again by F. Bon in collaboration with P. Bodu, when they reassessed the Aurignacian assemblage of layer VII of Grotte du Renne (Bon, 2002a; Bon and Bodu, 2002).

The main *chaîne opératoire* consists of a continuous reduction of blocs for an intercalated or subsequent knapping of slender blades and bladelets. Differently than the Early Aurignacian prismatic cores, the striking platform is kept plain, and the flaking surface has a convergent shape. This is in function of the lateral elements used for the *cintrage* and *carenage* operations that are plunging and inwards skewed blades: in this way, the proximo-mesial part of the flaking surface is maintained straight, while it rapidly curves in the distal part. The skewed lateral blades are progressively knapped more and more laterally, thus proximally expanding the striking platform and the flaking surface on the adjacent core faces, while it centres in distal part: hence, the core acquires a sub-pyramidal shape. The knapping fashion is maintained until the exhaustion of the core, therefore shifting from blades to bladelets production throughout the volume reduction.

Independent bladelets cores are recorded too, depending on the exploitation of originally small core volume, blanks edges, especially the so called carinated burins, and rare carinated end-scrapers (Bon, 2002a; Bordes, 2006). More than the question of an independent bladelet production, the important point to record is the feeble existence of independent blade knapping (Teyssandier and Liolios, 2008).

Rare osseous points, in ivory or cervid antler, sometimes SBPs, are found in El Castillo, Les Abeilles, Grotte du Renne, Le Piage, Trou de la Mère Clochette, Gatzarria and Isturitz (Anderson et al., 2015; Bodu et al., 2013; Szmidt et al., 2010; Tartar, 2015; Tejero et al., 2012). In l'Arbreda a SBP is found in a level featuring the same Protoaurignacian lithics as the inferior layer, similar situation in Fumane (Bon, 2002a; Falcucci, 2018; Tartar, 2015). By-products are identified in Trou de la Mère Clochette and Isturitz (Tartar, 2015). At Mochi a SBP is recorded just between the Early Aurignacian (F) and the Protoaurignacian (G) layers (Tafelmaier, 2017). Doubts have been cast for the Grotte du Renne, Trou de la Mère Clochette and Fumane SBPs (Teyssandier and Zilhão, 2018).

In any case, antler and bone implements are similar to the Early Aurignacian ones, and there are no significant differences in the manufacture processes (Tartar, 2015). Nevertheless, it has been argued

that no antler working can be safely attributed to the Protoaurignacian and that the manufacture of antler points is an Early Aurignacian introduction (Tejero and Grimaldi, 2015).

Ivory is used for a wider range of tools, such as non-split projectile points, domestic activities piercers and symbolic artefacts such as beads, rings and engraved rods, but most of the pendants are in shell (Tartar, 2015; Teyssandier, 2006; Teyssandier and Liolios, 2008).

Overall, some authors suggest that Protoaurignacian technical behaviour shows lesser structuration, which can be traced also in the available sites distribution, often located on big network axes and witnessing small mobile groups (Anderson et al., 2015; Porraz et al., 2010). Such conclusions are rejected for the Bombrini site, where the earliest layer suggest a more structured logistical land-use, while residential mobility is recorded in the youngest layer (Riel-Salvatore and Negrino, 2018).

There is an ongoing debate over whether the Protoaurignacian represents an early phase of the Aurignacian technocomplex, Laplace *sensu*, a contemporaneous technocomplex geographically detached from the Early Aurignacian, as hypothesised by F. Bon, or a technological adaptation to time-constraint climatic conditions (Banks et al., 2013; Bon, 2002a; Laplace, 1966).

In the few sequences where both *facies* are found, stratigraphical data is pointing towards a precedence of the Protoaurignacian (Barshay-Szmidt et al., 2012; Bordes, 2006; Laplace, 1966; Normand and Turq, 2005; Roussel and Soressi, 2013). The same was suggested for radiometric determinations, but the new dates of Geißenklösterle, where only Early Aurignacian is found, point to a contemporaneous appearance around 43-42 ka cal BP (Anderson et al., 2015; Benazzi et al., 2015; Douka et al., 2012; Higham et al., 2012). Two other sites from Southern Iberia, Bajondillo cave (Malaga bay, Spain) and Lapa do Picareiro (west-central Portugal), have been recently presented as the westernmost occurrence of the early Upper Palaeolithic (eUP) in Europe (Cortés-Sánchez et al., 2019a; Haws et al., 2020). Due to their rather small lithic assemblages it is impossible to assign them to any of the two technocomplexes at stake and, in the case of Bajondillo, some authors even question if it is a case of stratigraphical mixing (Anderson et al., 2019; Cortés-Sánchez et al., 2019b, 2019a; de la Peña, 2019; Haws et al., 2020). Traditionally, the end boundary of the Protoaurignacian was put at the Campanian Ignimbrite stratigraphical occurrence/Heinrich Event 4 onset, the technological reassessment of assemblages and new radiometric dates are suggesting a prolonged survival of the technocomplex (Banks et al., 2013; Falcucci, 2018; Giaccio et al., 2017; Palma di Cesnola, 2006; Riel-Salvatore and Negrino, 2018; Wood et al., 2012).

1.2 The Levantine UP record and the Early Ahmarian

At the time of the European Palaeolithic record systematisation, at the start of XX century, Levantine Palaeolithic research did not experience such turmoil, on the opposite, most of the European researchers in the Levant unabashedly cast the European cultural entities on the Levantine archaeological record (Monigal, 2002). De Morgan, in 1927, was among the first researchers to point out that Levantine record may had had a different development than the European one, if only for its

different geographical setting (Monigal, 2002). A general framework of Levantine cultural development was introduced only in 1934, much later than the European de Mortillet's one (Monigal, 2002).

In 1925 F. Turville-Petre began excavations in Wadi Amud in the locations of Mugharet el-Emireh and Zuttiyeh cave, where he noticed that Emireh yielded Aurignacian-like artefacts, such as end-scrapers, carinated end-scrapers and nosed end-scrapers, associated with Mousterian points and sidescrapers. D. Bate supported this association defining it a possible MP–UP Transition (Gilead, 1991; Monigal, 2002).

The most iconic Levantine sites were firstly excavated in this period:

Ksar Akil was among the first sites explored in a scientific way, findings from treasure hunters prompted E. Day to lead an excavation of 5 m deep reconstructing three arbitrary layers in 1922. Then Mme. Delcourt recognised more undetected stratification and the change of artifacts through depth, leading to the first real scientific excavation of the site in 1937-1938 by J. Doherty, who had to stop due to World War II and whose results were published only in 1947 (Bergman, 1988; Monigal, 2002).

In 1930–1933 A. Rust excavated the Yabrud rock-shelters I and II, in the Syrian Anti-Lebanon, providing a long stratigraphic sequence going from the Lower Palaeolithic to the Mesolithic. Later he was able to connect his findings with those in Palestine (Monigal, 2002).

D. Garrod was the first formal prehistorian archaeologists to work in the Levant, between 1929–1934 she supervised and excavated sites as el–Wad, Tabun, Kebara, Skhul and Wadi el–Mughara. Being also extensively trained on the European record she was able to discern different developments or to support similarities in types (Monigal, 2002).

The other founder father of Levantine Palaeolithic research is R. Neuville, roughly in the same timeframe of Garrod, he excavated and surveyed the Judean desert, discovering sites as Erq el Ahmar, Oumm Qatafa, Abou Sif, Sahba, and Qafzeh (Monigal, 2002). The works of Garrod and Neuville provided the nowadays cultural development framework (Monigal, 2002). They still show an Eurocentric perspective (Belfer-Cohen and Goring-Morris, 2014; Monigal, 2002). The main technological typological shift between the Middle Palaeolithic (MP) and UP is the adoption of serial blades–bladelets production (Belfer-Cohen and Goring-Morris, 2014; Garrod, 1957).

R. Neuville divided the Palestinian UP in six phases, the first four have noticeably European ascendants the last two are characterised by original characters (Neuville, 1934):

Phase I: characterised by a less elongated, thin, convergent blank with a basal thinning (later Emireh point), more elongated backed points, similar to Gravette points, and thin end-scrapers with short retouch on blades or oval flakes.

Phase II: the elongated backed points increase in numbers and the back is more rectilinear. Carinated end-scrapers and busked burins

Phase III: smaller and more rectilinear backed points. End-scrapers on flakes.
Phase IV: characterised by the appearance of nosed end-scrapers and end-scrapers on thick blades.
Phase V and IV: microliths, burins on concave truncations and carinated end-scrapers.

The Roman numeral identifies a unilineal evolution through time, the first four phases where broadly compared to European UP. He believed that the MP–UP passage is a change in typo/technology, hominid and environment (Monigal, 2002).

Slightly contemporaneously D. Garrod suggested a different division in (Monigal, 2002):

Lower Aurignacian: characterised by the Emireh point
Middle Aurignacian: characterised by Krems/Font-Yves points on smaller blanks. Later by the introduction of carinated and nosed end-scrapers.
Atitlian or Upper Aurignacian: polyhedric and carinated burins, with some backed points.

Later, she accepted the Neuville succession, introducing some technological characters as well (Garrod, 1957):

Phase I: blades are associated with Levallois blades and scrapers, which are resembling those of the Late Mousterian. Typical tool type is the Emireh point, triangular blank with basal thinning. Other tool types are backed knives, thin, simple end-scrapers, and some undiagnostic burins.
Phase II: represented in few sites. Backed points that are in-between those of Phase I and Phase III.
Phase III: named Lower Antelian. Characterised by backed points resembling the Font-Yves points and pointed bladelets. Carinated end-scrapers are found in the Mount Carmelo sites, but less in open-air contexts.
Phase IV: named Upper Antelian. Carinated burins and nosed end-scrapers plus rare osseous biconical points.
Phase V: named Atlitian. The carinated burins and narrow carinated end-scrapers form the big majority of the tool types.
Phase VI: named Kebaran. Characterised by small backed bladelets, pointed at the two extremities.

Later the Font-Yves points have been named el-Wad points (Belfer-Cohen and Goring-Morris, 2014; Gilead, 1991).
It is noticeable that in this late version Garrod begins the practice of distancing the Levantine industries from the European ones renaming them after local sites, implying the recognition of different and somewhat parallel evolution of the two records (Monigal, 2002).
Classification based on the UP Levantine reference stratigraphical sequence, Ksar Akil, was suggested by L. Copeland in 1975 (Belfer-Cohen and Goring-Morris, 2017; Gilead, 1991):

Ksar Akil Phase A: characterised by chamfered pieces, *chanfreins*, tools on flakes where a distal tranchet blow is struck from a prepared edge, and generic UP tools on Levallois blanks.

Ksar Akil Phase B: increase of end-scrapers and retouched blades, reduction of Levallois blanks and chamfered pieces.

Levantine Aurignacian Phase A: not found outside Ksar Akil. Dominated by el-Wad points and flat faced burins.

Levantine Aurignacian Phase B: dominated by carinated and nosed end-scrapers. Cfr. Antelian.

Levantine Aurignacian Phase C: increase in burins and bladelets. Cfr. Atlitian.

Kebaran

Ksar Akil has a complex excavation history, after World War II the excavation resumed in 1947–48, under the direction of J. Ewing and arriving 19 m deep. The excavation was restarted under Tixier in 1969–1975, thanks to the improvements in excavation techniques he managed to recognise more levels of occupation, but he had to stop at level X, upper UP section, because of the Lebanese Civil War. In total the site has a 23 m thick deposit, divided in thirty-six levels, spanning from Mousterian to the late UP, including the MP to UP transition; the stratigraphical sequence is divided in three big blocks by cave vault partial collapses associated with climatic weathering: the MP, the earliest UP (IUP and Ahmarian) and the later UP and Epi-Paleolithic (Bergman, 1988; Bergman et al., 2017; Douka et al., 2013).

A modern interpretation of Ksar Akil stratigraphical sequence and industries is developed by C. Bergman, whose the UP phases are here reported (Bergman et al., 2017; Douka et al., 2013):

Stone Complex 1, stratigraphical hiatus between the MP and the UP.

Phase X, former Ksar Akil Phase A, related to the Initial Upper Palaeolithic

Xa: levels XXV–XXIV. Opposed platforms parallel edges cores, producing elongated flakes, blades and elongated Levallois points. Chamfered pieces, end-scrapers, and burins on truncation.

Xb: levels XXIII–XXI. Single faceted platform convergent edges prismatic cores, producing elongated flakes and convergent blades similar to elongated Levallois points. Chamfered pieces, end-scrapers, and burins on truncation.

Phase IX, former Ksar Akil Phase B, related to the Northern Ahmarian *facies*. Levels XX/XIX–XVI. Opposed plain platforms parallel edges cores, producing thin blades. End-scrapers, backed blades, robust el-Wad points, and *pointes à face plan*, which are leaf-shaped points with invasive retouch and occasional basal thinning.

Stone Complex 2, Levels XV–XIV. Correlated with HE 4.

Phase VIII, former Levantine Aurignacian A, unassigned. Level XII. Production of twisted and curved bladelets and blades. Multifaceted and carinated burins, carinated and nosed end-scrapers.

Phase VII, former Levantine Aurignacian B, affinities with southern Early Ahmarian. Levels XI. Production of straight or curved blades and bladelets from single platform narrow fronted cores.

Phase VI, former Levantine Aurignacian B in VIII and C in VII, related to Levantine Aurignacian. Level X. Production of twisted and curved bladelets and blades. Multifaceted and carinated burins, carinated and nosed end-scrapers.
Phase V, tentatively identified, unassigned. Level IX. Production of twisted and curved bladelets and blades. Multifaceted and carinated burins, carinated and nosed end-scrapers.
Phase IV, former Levantine Aurignacian C, related to the Atlitian. Level VIII. Production of twisted and curved bladelets and blades. Multifaceted and carinated burins, carinated and nosed end-scrapers.
Phase III, former Levantine Aurignacian C, unassigned. Level VII. Production of twisted bladelets. End-scrapers, burins and carinated burins.
Phase II, unassigned, southern Early Ahmarian affinities. Level V. Production of curved bladelets. Retouched bladelets, burins and end-scrapers, especially microdenticulated Ksar Akil scraper.
Phase I, former Kebaran, related to the Masraqan. Level IV. Production of straight and curved bladelets. Backed bladelets, microgravettes, geometric microliths, burins, end-scrapers

During the 50s'–early 90s' period the surveys and the excavations multiplied throughout the Levant, feeding into the already established cultural development model, opening new geographical areas for research, and restructuring the Upper Palaeolithic framework. Especially after the works of Marks in the Negev and Gilead in the Sinai published in 1981 (Belfer-Cohen and Goring-Morris, 2014; Gilead, 1991; Monigal, 2002).
Nowadays the early Levantine UP is divided in (Belfer-Cohen and Goring-Morris, 2017, 2014; Bergman, 1988; Bergman et al., 2017; Gilead, 1991):

Initial UP/Emiran: a northern version found in Ksar Akil layers XXV–XXIV characterised by chamfered pieces on Levallois blades and flakes, tools which present a tranchet-blow giving a bevelled shape. In the South, namely at Boker Tachtit 1 and 2 it is characterised by the Emireh point, inversely retouched. Later North and South are joined in the production of morphologically Levallois blades and elongated points with facetted butts from single platform, unidirectional, pyramidal cores (Ksar Akil layers XXIII–XXI/XX, Tor Sadaf, Umm el Tlell layers II and III 2A).
Ahmarian: based on the work of Marks and Gilead in the Negev and Sinai, it was introduced as a new UP technical tradition else than the Aurignacian. It was found earlier in Qafzeh and in Erq el-Ahmar but failed to be recognised. Following radiometric datings, it has a prolonged chronological persistence. It is subdivided in
Early Ahmarian, characterised by single platform, unidirectional, flaking surface on narrow face cores producing series of blades and bladelets. The most typical tool type is the el-Wad point, a variedly retouched convergent blade/bladelet. Burins and end-scrapers are manufactured from flake by-products.

Late Ahmarian (Masraqan), despite showing a technological degree of continuity with the Early Ahmarian, it is chronologically assigned to the Epi-Palaeolithic.

Levantine Aurignacian: it is a discussed entity, perceived as a short intrusion from Europe. It is found only in coastal cave settings, broadly contemporaneous with the Early Ahmarian found in desertic/steppe areas. It is characterised by carinated forms on blades, Aurignacian scalar retouch, Dufour bladelets and osseous points.

Atitlian: it is an industry found in the Mediterranean cave settings, based on flake production and the manufacture of burins on truncation.

It is evident then that the earliest true volumetric UP industry in the Levant is the Early Ahmarian (Belfer-Cohen and Goring-Morris, 2009; Gilead, 1991). The Early Ahmarian features a production of microlithic, straight, convergent bladelets; they come from independent knapping or integrated continuous blades to bladelets cores; they are mostly modified in el-Wad points, which design a huge spectrum of lightly retouched, pointed through retouch or already convergent in shape blades or bladelets (Belfer-Cohen and Goring-Morris, 2008; Gilead, 1983; Gilead and Bar-Yosef, 1993; Goring-Morris and Davidzon, 2006).

The Early Ahmarian is well distributed all across the Levant mostly in open-air sites in the Southern desert–steppe regions, and in caves in the Mediterranean area (Belfer-Cohen and Goring-Morris, 2014; Bergman et al., 2017; Goring-Morris and Belfer-Cohen, 2018). Ahmarian ascendants have been proposed for the Early Baradostian in the Iranian Zagros mountains, an industry characterised by single platform prismatic cores producing straight blades and bladelets, occasionally retouched in the Arjaneh point (Belfer-Cohen and Goring-Morris, 2012; Tsanova et al., 2012). Also, Ahmarian features have been found in the Caucasus EUP (Golovanova and Doronichev, 2012).

The Early Ahmarian is divided in two cultural *facies*, the Northern one, found principally in cave sites like Ksar Akil and Üçağızlı, and the Southern one, the typical Early Ahmarian from open-air sites. The main difference is the use bidirectional plain platforms blades cores, which results in straighter blanks and the *pointe à face plan* in the Northern *facies* (Bergman, 1988; Bergman et al., 2017; Goring-Morris and Davidzon, 2006; Kadowaki, 2018; Kadowaki et al., 2015). An explanation for such dichotomy would be that the Northern Early Ahmarian represents an adaptation to a mixed forest–steppe biome, while the Southern Early Ahmarian a later adaptation to the steppe–desert conditions (Richter et al., 2020).

The Southern Early Ahmarian technological signature was established by A. Davidzon and N. Goring-Morris, through the extensive refits found at Nahal Nizzana XIII (Davidzon and Goring-Morris, 2003; Goring-Morris and Davidzon, 2006):

Raw material selection prefers lenticular siliceous large cobbles. There are several variants, all underlining a single concept: the narrow-fronted core for integrated blades–bladelets production. The flaking surface is constantly placed on the shorter, narrow face and it is exploited unidirectionally.

The striking platform and a distal crest are placed on the parallel longitudinal faces. The striking platform is prepared through a single cortical flake removing the whole longitudinal pebble edge, while the distal crest, forming the distal convexity, can be shaped through the bifacial knapping. The core flanks can be shaped, decorticated, and narrowed, by flakes struck from the striking platform. The back of the core is left untouched or flat. The striking platform is plain and steep angled, frequently renewed through total tablets struck from the flaking surface and the overhang is abraded. The frontal knapping rhythm is maintained throughout the production, blades and bladelets are knapped from one edge to another. Lateral core-edge, wider and slightly twisted blades sometime distally shaped in a unifacial crest, or lateral flakes, maintain the lateral convexities. The production is geared on straight or slightly curved blades and bladelets that are retouched in el-Wad points. The flake by-products are used for producing thick burins or end-scrapers. The envisioned techniques are direct hard hammer percussion for flakes and direct marginal soft stone hammer percussion for the laminar blanks. In cases of breaks on hinging accidents, the distal portion could be removed with a punch to restore the flaking surface.

The Early Ahmarian, especially in the Southern open-air sites, seems to show comparatively small sites with lithic production on site. This would point to small human groups moving frequently in the landscape (Belfer-Cohen and Goring-Morris, 2017; Gilead, 1991; Richter et al., 2020).

Bone technology is not well attested in the Early Ahmarian, a bone point is known from Abu Noshra II and a split base point from El Quseir D, but in generally bone tools production seems more sustained in the Levantine Aurignacian (Gilead, 1991). Most of the ornaments are fabricated on marine shells (Abulafia et al., 2019; Gilead, 1991; Kuhn et al., 2009; Richter et al., 2020).

The dating of the Early Ahmarian is quite complex, sites in desertic southern areas are dated between 38–30 k uncal BP, mostly concentrated in the younger half of the interval (Gilead, 1991). Caves in the north areas, such as Kebara and Manot, features much earlier dates around 47–46 cal BP, but both contexts have issues of re-depositions, Manot, and possible mixing, Kebara (Abulafia et al., 2019; Bar-Yosef et al., 1996; Rebollo et al., 2011; Zilhão, 2013). Ksar Akil has been recently independently dated, in one case the Ahmarian is indicated to last in the approximate 42–40 k cal BP interval, interrupted at the onset of the Heinrich Event 4, in another case it is retro-dated to at least a millennium earlier (Bosch et al., 2015; Douka et al., 2013). Üçağızlı is dated to 34–29 k uncal BP, approximately 40–33 k cal BP, or 38.5-36 k cal BP (Douka, 2013; Kuhn et al., 2009). Therefore, a similar contemporaneous age as the European Protoaurignacian and Early Aurignacian seems the best estimate.

1.3 eUP detailed technical behaviour review

In this section a review of the most significative eUP assemblages in the literature is given. Sites are divided by broad regional setting. Notions about the stratigraphical setting and integrity, the main technological information and typological characteristics, the application of a typometrical definition of blades and bladelets and the authors' cultural attribution are presented. Not all assemblages have been object of the same degree of technological analysis; most of them come from old excavations, with different methodological standards, for instance, the lack of systematic application of a sieving, in particular wet-sieving, procedure for the retrieval of smaller artefacts.

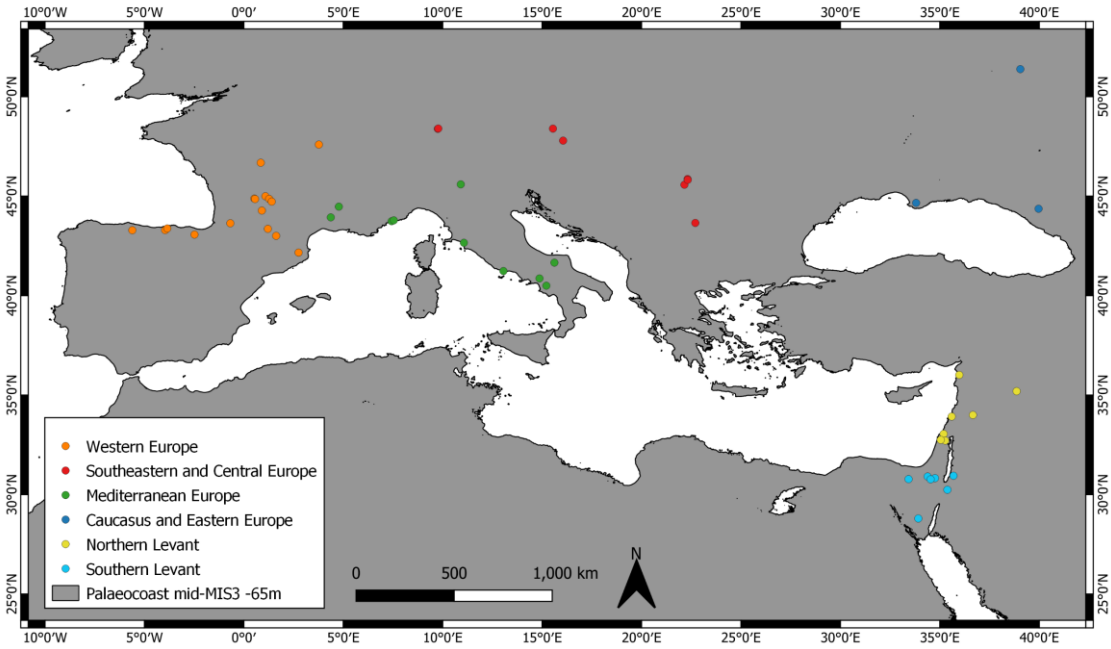

Figure 1 eUP sites mentioned in the technological review. palaeocoastlines with -65 m sea levels modified from (Zickel et al., 2016).

1.3.1 Southern Levant

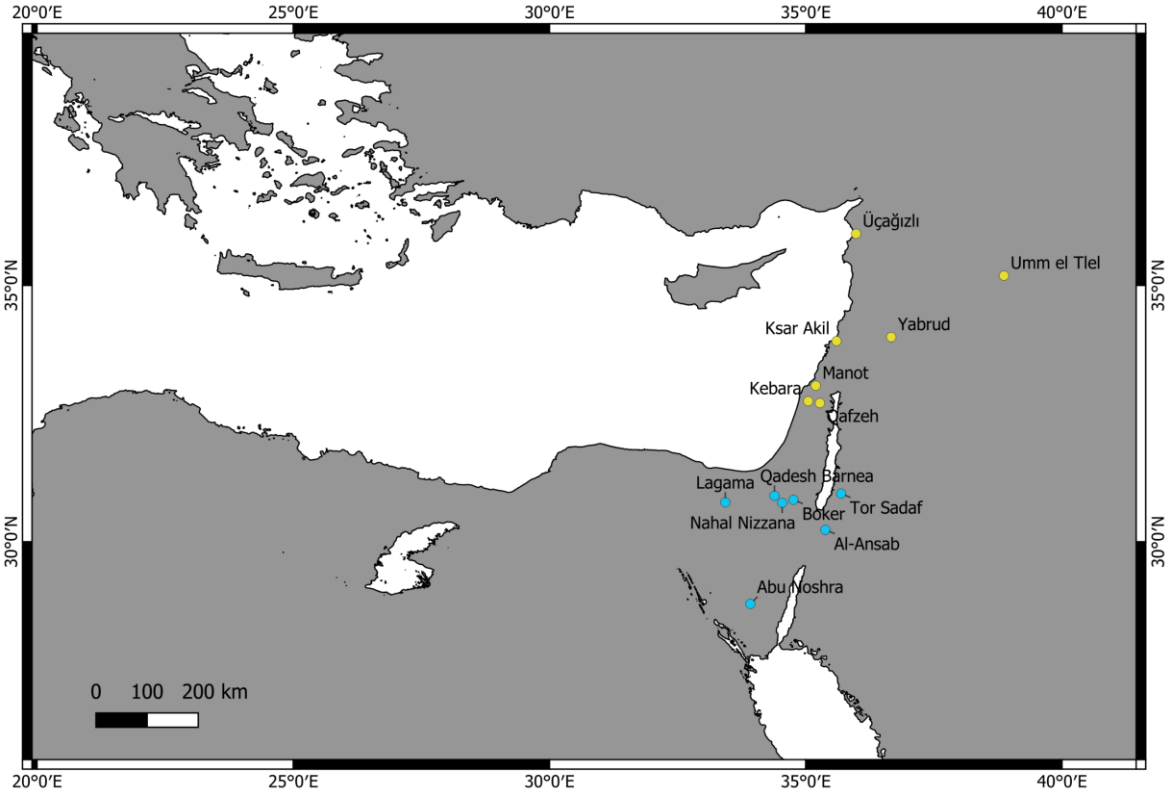

Figure 2 Detailed map of the reviewed eUP Levantine sites.

Abu Noshra I and II (Phillips, 2003, 1988).

Setting

They are open-air sites. Abu Noshra I features a main lower archaeological horizon. Abu Noshra II is 50 m apart from I, it shows a higher extension.

Technology

Raw material is mostly semi-local flint collected in a 15 km distance; some imports come from 60 km distance.

Two *chaînes opératoires* are recognised. Production of intercalated blades–bladelets and independent bladelet production.

Prismatic cores: the flaking surface is placed on the longitudinal face, it is exploited unidirectionally. The striking platform is plain and steep-angled. They are manufactured out of ovoid and cylindrical flint pieces. In some cases, blocks are imported already roughed out. They produce laminar blanks.

Longitudinal carinated cores: the flaking surface is placed on the blank longitudinal edge, it is exploited unidirectionally. It produces bladelets.

The envisioned knapping technique is direct soft hammer percussion for laminar blanks and direct hard hammer percussion for flakes blanks.

Typometry

No blades–bladelets dimensional threshold is given.

Main typological characters

The tool assemblage consists of backed and laterally retouched blades and bladelets, burins, especially dihedral, and end-scrapers on blades.

Cultural attribution

Attributed to the Lagaman, equivalent to the southern Early Ahmarian.

Gebel Maghara (Lagama) (Bar-Yosef and Belfer-Cohen, 1977; Gilead, 1983).

Setting

It is an open-air sites' complex. The sites are witnessing single occupations buried in sediments of sand and scree of wadi el-Masagid terraces, at the foot of Gebel Lagama. Some of the sites are found on the surface due to the deflation of the sedimentary context, nevertheless erosion was not powerful enough to disperse ashes from hearths.

Technology

The raw material is non-local flint imported from the central Gebel Maghara and the southern wadi el-Masagid areas.
Three *chaînes opératoires* are recognised. Continuous production of blades–bladelets.
Prismatic cores: cores are exploited unidirectionally, the striking platform is plain, and the overhang is micro-chipped. The core can be decorticated, especially creating a flat posterior face, or left untouched except for the flaking surface and striking platform. They produce blades and mostly bladelets: result of a continuous knapping and scarcity of flint in the vicinities, therefore high core reduction. While blades have curved profiles, bladelets are straight.
Longitudinal carinated cores: the flaking surface is placed on a blank longitudinal edge, it is exploited unidirectionally.
Multiplatform cores: they are a minority, mostly for exploiting more efficiently good quality raw material. Platforms can be opposed or independent.

Typometry

No blades–bladelets dimensional threshold is given. The mean width rarely exceeds 12 mm. retouched bladelets are defined as those <9 mm wide.

Main typological characters

Blades and bladelets display marginal, semi-abrupt retouch. Many are retouched in el-Wad points. Burins are low in number, mostly dihedral and on thick flakes.

Cultural attribution

Attributed to the Lagaman, equivalent to the southern Early Ahmarian.

Qadesh Barnea 601 (Gilead and Bar-Yosef, 1993).

Setting

It is an open-air site on an upper wadi terrace. The site has two occupation horizons, B, the lower and richest, and A, divided by a sterile thin layer.

Technology

The raw material is local flint.
One *chaîne opératoire* is recognised. Production of blades.
Nodules are split on anvil or by direct percussion. The core is reduced and decorticated by flakes. Then they are knapped for thin blades obtention. The striking platform is maintained through core tablets.

Typometry

The average blade is 13.6–14.3 mm wide.

Main typological characters

Few burins and end-scrapers, some end-scrapers on thick flakes. El-Wad points, with marginal, fine lateral or bi-lateral retouch are featured alongside marginally backed blades and bladelets.

Cultural attribution

Attributed to the Lagaman, equivalent to the southern Early Ahmarian.

Boker A (Monigal, 2003, 2002).

Setting

It is an open-air site. It features a single occupation.

Technology

Raw material is local flint readily available in close proximity with primary and secondary outcrops as laminated nodules and cobbles.
A single *chaîne opératoire* is recognised. Continuous production of blades and bladelets.

Prismatic on narrow face cores: the flaking surface is placed on a core narrow face, it is exploited unidirectionally. The narrow face is naturally obtained from the disc shape of the original nodule. The striking platform is plain and steep-angled, the overhang is abraded. The knapping begins preferentially on a natural ridge, occasionally it can be shaped in a crest. The knapping of thin, parallel edges blades and bladelets continues frontally until exhaustion. Management of the lateral convexities is assured by the flaking surface morphology and the knapping seriality; occasionally lateral flakes are struck and periodically central large blades are clearing the flaking surface from the numerous blade negatives.
The envisioned knapping technique is direct soft hammer percussion for the laminar blanks, direct hard hammer percussion for the shaping flakes.

Typometry

blades–bladelets dimensional threshold is put at 12 mm wide.

Main typological characters

Most of the retouched blanks are el-Wad points and inversely or backed blades and bladelets. End-scrapers are rare, burins are mostly manufactured on thick blades.

Cultural attribution

Attributed to the southern Early Ahmarian.

Ansab 1 2009-2011 campaigns (Hussain, 2015; Schyle, 2015).

Setting

It is an open-air wadi terrace site. It consists of a main find layer.

Technology

The raw material is various local flint collected in various outcrops.
Two *chaînes opératoires* are recognised. One for integrated continuous blades–bladelets production, and another for independent bladelets production. Hussain (2015) does not support a technological distinction between blades and bladelets issued from prismatic cores.
Prismatic cores on narrow face: the flaking surface is placed on a core narrow convergent face, it is exploited unidirectionally. The striking platform is plain and steep-angled, the overhang is abraded or micro-chipped. The knapping begins with distally unifacial crests or with blades on natural ridges. The convexities are maintained by embedded lateral, wider, twisted blades, and occasional lateral flank flakes. The production is oriented towards the central straight or curved regular convergent blades and bladelets.

Longitudinal carinated cores: the flaking surface is placed on a blank edge, it is exploited unidirectionally. The production is oriented towards bladelets.
The envisioned knapping technique is direct soft hammer percussion for laminar blanks and direct hard hammer percussion for flakes.

Typometry

Blades–bladelets threshold is put at 12 mm wide.

Main typological characters

El-Wad points on straight blades and bladelets, with marginal semi-abrupt or backed retouch, are prevalent. Dihedral burins and end-scrapers are made on flakes by-products.

Cultural attribution

Attributed to the southern Early Ahmarian.

Tor Sadaf (Fox, 2003).

Setting

It is a rock-shelter site. Sediments deposition appears to be continuous without any possibility of discerning sedimentological layers, except for the modern age humic soil and cobble layer, probably corresponding to a partial vault rockfall. Also, artefacts show a gradual change, with a progressive increase of laminar blanks and decrease of flakes. Overall, the artefacts have been divided in three technological analytical units, with the Early Upper Palaeolithic standing on top of a Tor Sadaf B assemblage, with IUP characteristics.

Technology

A single *chaine opératoire* is recognised. Continuous production of blades and mostly bladelets.
Prismatic cores on narrow face: the flaking surface is placed on a narrow convergent face exploited unidirectionally. The striking platform is plain. Bifacial crests and tablets are the only maintenance blanks.
The envisioned knapping technique is direct or indirect soft hammer percussion.

Typometry

No blades–bladelets dimensional threshold is given. The average width is 12.2 mm.

Main typological characters

Retouched blanks are large bladelets and small blades with lateral or bilateral inverse or direct retouch; they are affiliated to the el-Wad points.

Cultural attribution

Attributed to the southern Early Ahmarian.

1.3.2 Northern Levant

Ksar Akil levels XX–XVI (Bergman, 1988; Bergman et al., 2017; Bergman and Stringer, 1989; Williams and Bergman, 2010).

Setting

It is a rock-shelter site. Layer XX is in direct stratigraphical connection with XXI, attributed to the IUP, while level XVI is sealed by the Stone Complex 2, signalling the partial weathering of the cave vault.

Technology

A single *chaîne opératoire* is recognised. Production of blades–bladelets.
Prismatic bidirectional cores: the flaking surface has parallel edges, it is exploited bidirectionally. The striking platforms are plain and opposite, the overhang is abraded. Shaping crests seems the only convexities' preparation and maintaining operation. Production of thin blades and bladelets.
The envisioned knapping technique is direct marginal soft hammer percussion.

Typometry

No blades–bladelets threshold is given.

Main typological characters

Backed blades and bladelets, el-Wad points, pointes à face plan and simple end-scrapers.

Cultural attribution

Northern Early Ahmarian.

Üçağızlı layers B1-B4 (Kuhn, 2004; Kuhn et al., 2009).

Setting

It is a cave site. The layers are not recognised through sedimentological difference but through the density of anthropogenic material like ashes and artefacts. Layers B1-B4 feature the most sustained Ahmarian occupation(s), they are separated from the below IUP, by a less dense Ahmarian layer C, and from the above layers by a similarly less archaeologically dense layer B. the stratigraphical transition between C and B1-B4 points to an erosional event.

Technology

The raw material is large flint nodules collected in primary outcrops, imported from 15–30 km inland. A single *chaîne opératoire* is recognised. Production of blades.
Prismatic cores: the flaking surface has parallel edges; it is exploited mostly bidirectionally. The striking platforms are plain and opposite, the overhang is abraded. Production of thin blades.
The envisioned knapping technique is direct soft hammer percussion or indirect percussion.

Typometry

No blades–bladelets dimensional threshold is given.

Main typological characters

End-scrapers on blades, *pointes à face plan* and el-Wad points are the most characteristic retouched blanks.

Cultural attribution

Attributed to the northern Early Ahmarian.

Yabrud II layer 6 and 5 (Demidenko and Hauck, 2017; Pastoors et al., 2008).

Setting

It is a rock-shelter site. The site was excavated in the 1930s by A. Rust, he documented horizontal layers whose cultural content spans from the MP to the UP. Layer 6 and 5 are the first UP layers documented and they are in supposed direct stratigraphic connection with the layers above and beneath. The assemblages are severely skewed by Rust's sampling strategy.

Technology

The flint provisioning is local mostly, as witnessed by cortex surfaces, in secondary deposits and less, in primary outcrops.

6

Two *chaînes opératoires*. Independent production of bladelets and blades.
Prismatic flat cores: the flaking surface has parallel edges, and it is placed on the longitudinal face; it is exploited uni/bidirectionally. The striking platforms are plain or facetted. The convexities are maintained by lateral oblique blanks and by opposite series of negatives.
Prismatic cores: the flaking surface is placed on the longitudinal face, it is exploited unidirectionally. The striking platform is plain. Convexities are maintained by lateral oblique blanks and distally overshot ones. Also, crests are witnessed. Independent production of bladelets.

5

Three *chaînes opératoires* are recognised. Integrated production of blades–bladelets from prismatic cores and independent flakes production from a discoid core.
Prismatic cores: the flaking surface is placed on the longitudinal face, it is exploited unidirectionally. A second opposite striking platform can be used for distal convexity preparation. The knapping begins with a natural ridge or a shaped crest. Lateral convexities are maintained through oblique, convergent blanks, while the distal convexity is usually maintained through overshot blanks. The back of the remains unprepared, the core flanks join in a posterior ridge. A final stage exploitation show that cores become wider than longer. Integrated production of blades and bladelets.
Prismatic twisted cores: the flaking surface is placed obliquely regarding the striking platform, it is exploited unidirectionally. The production is independent twisted bladelets.

Typometry

No blades–bladelets threshold is given.

Main typological characters

6

no UP tool is signalled.

5

Two el-Wad points, end-scrapers and burins. Demidenko and Hauck signal carinated burins.

Cultural attribution

6

Pastoors and colleagues (2008) attribute it to the IUP, while Demidenko and Hauck (2017) to the Northern Early Ahmarian.

5

Pastoors and colleagues (2008) attribute it to the Early Ahmarian, while Demidenko and Hauck (2017) to the Levantine Aurignacian.

Manot Cave area C layers 7 and 8 (Abulafia et al., 2019; Barzilai et al., 2016; Marder et al., 2017).

Setting

It is a cave site. Area C lays at base of the Western talus, displaying 8 layers. There is a certain degree of mixing, unit 5 and 6 yields artefacts of Aurignacian and Ahmarian ascendants, while the basal

units 7 and 8 are dominated by Ahmarian finds, though some Mousterian and IUP artefacts are found as well. The reason for the mixing is probably a physical barrier at the top of the talus near the cave entrance, area E, where only Levantine Aurignacian and younger artefacts are found; periodically the sediment was moved towards the inner cave spilling over the barrier and accumulating at the base of the talus, area C: overall, excavators are confident in the regular accumulation of the units. Units 7 and 8 are, in a whole, around 1 m thick, they are divided by an erosional unconformity.

Technology

Raw material is mostly flint collected in primary and secondary deposits in a semi-local radius from the cave (10 km).

Two *chaînes opératoires* are recognised. Integrated blades–bladelets and independent blades and bladelets production.

Prismatic opposed platforms cores: the flaking surface has parallel edges morphology and is placed on the narrow longitudinal face, it is exploited bidirectionally. The striking platforms are plain, and the overhang is abraded. Morphological difference and the number and type of blanks struck between the two platforms in some cases might indicate the role of auxiliary opposite platform, more than a true bidirectional knapping. The knapping begins with a bifacially shaped crest, the convexities are maintained through neo-crests, lateral flat blades, and overshot blades. Production is focused more on straight or slightly curved blades.

Prismatic single platforms cores: the flaking surface has parallel edges or convergent morphology and is placed on the narrow longitudinal axis, it is exploited unidirectionally. The striking platform is plain, and the overhang is abraded. The knapping begins with a bifacially shaped crest, the convexities are maintained through neo-crests, lateral flat blades, and overshot blades. Production is focused more on straight or slightly curved bladelets, occasionally twisted blanks are struck.

The envisioned knapping technique is the direct soft hammer percussion.

Typometry

Blades–bladelets threshold is put at 12 mm wide.

Main typological characters

Most of the tools are retouched blades and bladelets. El-Wad points are mostly display backed or abrupt retouch, forming an awl termination or a point. End-scrapers are on blades. Burins are multiple or dihedral.

Cultural attribution

Northern Early Ahmarian

Qafzeh level E and D (Bar-Yosef and Belfer-Cohen, 2004).

Setting

It is a cave site. level E, the base of the UP stratigraphical sequence, is in direct stratigraphical connection with the Middle Palaeolithic beneath and level D above; on top of level D there is another UP layer.

Technology

E

Three *chaînes opératoires* are recognised. Two for the mostly independent blades production, one for independent bladelets production.
Prismatic bidirectional cores: the flaking surface is placed on the longitudinal face, it is exploited bidirectionally. The striking platforms are plain. Convexities are maintained through crests, laterally struck blanks, and overshot blanks. The production is mostly oriented towards straight blades.
Prismatic unidirectional cores: the flaking surface is placed on the longitudinal face, it is exploited unidirectionally. The striking platform is plain. Convexities are maintained through crests, laterally struck blanks, and overshot blanks. The production is mostly oriented towards straight blades.
Longitudinal carinated cores: the flaking surface is placed on the blank longitudinal edge, it is exploited bidirectionally. The production is oriented towards straight bladelets.

D

Mostly carinated cores correlated with the increase of twisted bladelets.

Typometry

Blades–bladelets threshold is put at 10 mm wide.

Main typological characters

E

Most of the tools are represented by el-Wad points with bilateral or unilateral abrupt direct retouch. End-scrapers on thin blades are well represented too.

D

The tool types are dominated by end-scrapers and burins, also carinated on flakes. Almost absence of el-Wad points.

Cultural attribution

E

Early Northern Ahmarian.

D

Later Ahmarian.

Umm el Tlel (Kadowaki, 2018; Ploux and Soriano, 2003).

Setting

It is an open-air site. The UP stratigraphical sequence is found mostly in sector 2, divided in various *loci* which have been partially stratigraphically correlated: North, West and South–West. Interstratified units yielding either Aurignacian or Ahmarian lithics are found between an "Intermediate Palaeolithic" with Levallois and volumetric blade–bladelet production and the Kebaran several UP levels. The Ahmarian tradition is found in levels 14'c1, FI, lp of the South–Western locus and in levels Illb, Illbl, IIlc, U2d *pro parte* of the Northern locus.

Technology

Two *chaînes opératoires* are recognised. One for the independent production of bladelets, one for intercalated blades–bladelets production.
Prismatic core on narrow surface: the flaking surface is placed on the longitudinal narrow face, it is exploited unidirectionally. The striking platform is plain and steep-angled, the overhang regulated by micro-chipping. The knapping starts with a central bifacial crest, the bladelets then are knapped from one flaking surface side to another in a convergent fashion, using a central distal nervure. Convexities and the distal central nervure are managed by lateral small-sized blades knapped from the sides, which are oblique and twisted. The bladelets, instead, are straight.
Prismatic parallel edge core: it is recognised from some bigger and regular blades, which witness the knapping of parallel edges bladelets on the guide ridges.

Typometry

Bladelets are on average 5–8 mm wide.

Main typological characters

Most of the tool types are represented by various bladelets with marginal direct, inverse or alternated semi-abrupt retouch, which are relatable with Dufour bladelets, but no el-Wad points. Some burins and simple end-scrapers on blades.

Cultural attribution

Ploux and Soriano (2003) relate these levels to the Southern Early Ahmarian tradition, nevertheless signalling the peculiarity of the el-Wad points' absence. Kadowaki (2018) instead points to a later attribution to the industries of Ksar Akil's Phase V.

Kebara layers III and IV (Bar-Yosef et al., 1996; Tostevin, 2013).

Setting

It is a cave site. The stratigraphy is divided sedimentologically in an earlier unit B containing Middle Palaeolithic industries and unit A, finely laminated in its lower part, with UP industries. Layers IV and III are the earliest UP levels, layer IV is directly superimposed to the Mousterian layer V, with whom the sedimentological difference is difficult to appreciate, a channel and some animal burrows have penetrated in both. The break in lithic industries with the upper layers II and I, Levantine Aurignacian, is evident.

Technology

Raw material is local.
Two *chaînes opératoires* are recognised, both for laminar production.
Prismatic on narrow face cores: the flaking surface is placed on the longitudinal narrow face and it has parallel edges morphology, it is exploited bidirectionally or unidirectionally. The striking platforms are plain, the overhang is abraded. The knapping begins with a shaped crest, convexities are maintained through lateral blades or neo-crests.

Typometry

No blades–bladelets dimensional threshold is given.

Main typological characters

Most of the tools are manufactured on blades. The most diagnostic types are carinated end-scrapers and el-Wad points.

Cultural attribution

Attributed to the Early Northern Ahmarian.

1.3.3 Caucasus

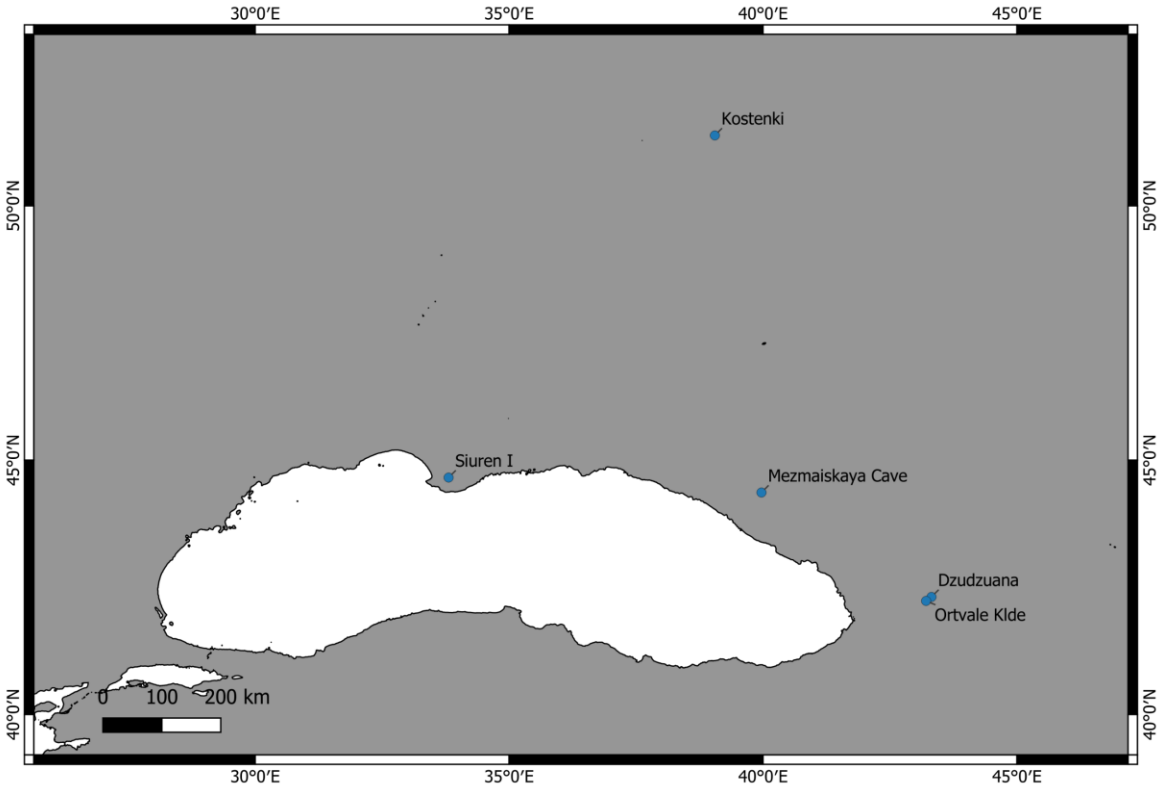

Figure 3. Detailed map of the reviewed Caucasus and Eastern Europe eUP sites.

Ortvale Klde layer 4 (Bar-Yosef et al., 2006; Golovanova and Doronichev, 2012).

Setting

It is a rock-shelter site. Layer 4 is in stratigraphical direct connection with the below Mousterian in layer 5, but the few Mousterian displaced artefacts are well recognised due to different patination.

Technology

The raw material is mostly high-quality local flint, but significant whole obsidian nodules have been imported from 100 km distance.

Two *chaîne opératoire* is recognised. Continuous production of blades and bladelets.

Prismatic cores: the flaking surface is placed on the longitudinal face and has a parallel edges morphology, it is exploited unidirectionally.

Longitudinal carinated core: the flaking surface is placed on a core longitudinal edge, it is exploited unidirectionally.

Typometry

Blades–bladelets dimensional threshold is put at 12 mm wide. Bladelets <7 mm are considered micro-bladelets.

Main typological characters

Retouched blanks are mostly laterally retouched and backed bladelets. Burins and end-scrapers on blades.

Cultural attribution

Similar to the Early Ahmarian.

Dzudzuana unit D (Bar-Yosef et al., 2011, 2006; Golovanova and Doronichev, 2012).

Setting

It is a cave site. Unit D is the earliest UP occupation of the site.

Technology

The raw material is mostly local radiolarite, rare imports of obsidian from 80–100 km distance.
A single *chaîne opératoire* is recognised. Continuous blades–bladelets production.
Prismatic cores: the flaking surface is placed on the longitudinal core face and it has convergent or parallel edges morphology, it is exploited unidirectionally.

Typometry

Blades–bladelets dimensional threshold is put at 12 mm wide. Bladelets <7 mm are considered micro-bladelets.

Main typological characters

Blades and bladelets with fine and backed retouch are prevalent. Simple end-scrapers on flakes and blades, burins, mostly dihedral ones, are rare.

Cultural attribution

Similar to the Early Ahmarian.

Mezmaiskaya layer 1C (Golovanova and Doronichev, 2012).

Setting

It is a cave site. 1C is the earliest UP layer in the cave.

Technology

The raw material is mostly local flint, also imports of flint from 60 km distance and obsidian possibly from the South-Western Caucasus.
Two *chaînes opératoires* are recognised.

Prismatic cores: the flaking surface is placed on the longitudinal core face and it has convergent or parallel edges morphology, it is exploited unidirectionally.
Transversal carinated cores: the flaking surface has convergent morphology, it is exploited unidirectionally.

Typometry

Blades–bladelets dimensional threshold is put at 12 mm wide. Bladelets <7 mm are considered micro-bladelets.

Main typological characters

Most of the retouched blanks are laterally backed bladelets and marginally directly retouched blades and bladelets. Burins, mostly dihedral, and end-scrapers are preferentially made on thick by-products flakes.

Cultural attribution

Similar to the Early Ahmarian.

1.3.4 Eastern Europe

Kostenki 17/II, 14/LVA and IVa and IVw and 1/III (Bataille et al., 2019, 2018; Dinnis et al., 2019; Hoffecker et al., 2016; Sinitsyn, 1993, 2003).

Setting

The Kostenki-Borshchevo sites complex yielded a cluster of localities featuring repeated through time open-air occupations during the MIS3 and MIS2, in a probable context of natural springs in the vicinity of the middle Don floodplain. The eUP industries are found in two palaeosols denominated Lower Humic Bed (LHB) and Upper Humic Bed (UHB) which are stratigraphically divided by the deposition of a tephra related to the Y–5 Campanian Ignimbrite one. Assemblages that have been approached to the Protoaurignacian and to the Early Aurignacian are the ones from Kostenki 17 layer II, located at the top of LHB, Kostenki 14 layer IVa and IVw, in the LHB just below the Y–5 tephra, layer LVA, directly associated with the Y–5 tephra, of Kostenki I layer III, corresponding with UHB. Dinnis and colleagues (2019) consider Kostenki I layer III affected by redeposition and mixing problems, but Hoffecker and colleagues (2016) point to the integrity of the context.

Technology

Kostenki 17 layer II

Raw material is good quality chert collected in primary outcrops in a semi-local radius, 25 km or possibly further.

Two *chaînes opératoires* are recognised.
Prismatic cores: The flaking surface has parallel edges, and it is exploited unidirectionally. The striking platform is seemingly facetted, according to the butts. The cores are used for the obtention of blades, in one case intercalated production of blades and bladelets.
Cores on longitudinal blank edge cores: the main reduction configuration. The flaking surface is installed on a longitudinal blank edge, exploited unidirectionally. The striking platform is installed on shaped truncation. It is an independent production of bladelets.
The envisioned technique is marginal direct soft hammer percussion.

Kostenki 14 layer IVw

Raw material procurement is similar to 17/II.
Only a *chaîne opératoire* is recognised. Cores are on longitudinal blank edges, with striking platform prepared on truncations, the knapping is finalised to the obtention of bladelets.

Kostenki 14 layer IVa

Two *chaînes opératoires* are recognised. The goal is the independent obtention of blades and bladelets.
Prismatic cores: the flaking surface has parallel edges, exploited unidirectionally. Production of straight and curved blades and bladelets.
Longitudinal carinated on blank edge cores: one dihedral burin, possibly used as bladelet core. Bladelets have mostly straight profiles.

Kostenki 14 layer LVA

Three *chaînes opératoires* are recognised. The goal is the independent obtention of blades and bladelets.
Prismatic cores: the flaking surface has parallel edges, exploited unidirectionally. Independent productions of straight and curved blades and bladelets.
Transversal carinated cores: flaking surface on wide distal fronts, end-scraper type. Production of mostly straight bladelets.
Longitudinal transversal on blank edge cores: flaking surface on narrow longitudinal blank edges, burin-core like. Production of mostly straight bladelets.

Kostenki 1 layer III

One main *chaîne opératoire*. Production of big blades, smaller blades and bladelets.
Prismatic cores: the flaking surface is flat or convex, exploited uni-and bidirectionally. The striking platform is plain and, in certain cases, steep angled. The convexities can be maintained through shaping or simply with the knapping of blanks on the intersection between core faces.

Transversal carinated cores: the flaking surface is convergent and can be narrow or wide, exploited unidirectionally.
Envisioned technique is the direct soft hammer percussion.

Typometry

Kostenki 17 layer II

No clear dimensional threshold blades–bladelets is put by Dinnis and colleagues (2019), retouched bladelets are less than 8 mm wide, blades are reported to be up to 38 mm wide, negatives on unipolar blades cores range from 9–20 mm wide.

Kostenki 14 layer IVa and Kostenki 14 layer LVA

Bataille and colleagues (2018) put a blades–bladelets threshold at 12 mm, bladelets less <7 mm are considered micro-bladelets.

Kostenki 1 layer III

No blades–bladelets dimensional threshold is given.

Main typological characters

Kostenki 17 layer II

6 bladelets and burin spalls, unidirectional and with straight profile, have semi-abrupt marginal direct or alternate retouch, thus fitting the Dufour bladelets subtype Dufour type.

Kostenki 14 layer IVw

9 fragmentary bladelets and burin spalls have semi-abrupt, marginal direct retouch.

Kostenki 14 layer LVA

Retouched bladelets, off-axis and twisted, have marginal and, in few cases, alternate retouch. They have been recognised as Dufour bladelets subtype Roc de Combe.

Kostenki 1 layer III

End-scrapers, also carinated, are numerous. Burins are mostly on truncation. Retouched bladelets are the most numerous tools, they are manufacture on off-axis bladelets, the retouch is marginal, direct, inverse, or alternate.

Cultural attribution

Kostenki 17 layer II, was attributed originally attributed to a local technocomplex, recognised only in Kostenki, called Spitsynian. On the grounds of the unipolar blade–bladelet reduction and the

retouched bladelets, Dinnis and colleagues (2019) approach it to the Protoaurignacian. Bataille and colleagues (2019) have instead argued against this scenario, pointing that no sub-pyramidal cores, blades–bladelets intercalated production is found in the assemblage, on the other hand the main core configuration, the burin on truncations, is not typical of the Protoaurignacian. Kostenki 14 IVa, IVw and LVA are attributed more closely to the Early Aurignacian, especially LVA given the presence of carinated end-scrapers cores. The same attribution applies to Kostenki 1 layer III.

Siuren I layer H and G (Bataille, 2016; Bataille et al., 2018; Demidenko, 2000, 2014; Demidenko and Noiret, 2012; Zwyns, 2012).

Setting

Cave site. Units H, situated just above the bedrock, and G are grouping several almost undisturbed horizontally deposited levels divided by thin sterile sediment levels; they are separated by a rock-fall from above unit F.

Technology

Two *chaînes opératoires* are recognised. The goal is the obtention of intercalated blades and, mostly, bladelets. Bladelets are mostly on-axis and with straight or slightly curved profiles. Twisted profiles blanks come from the lateral edges of the flaking surface.
Prismatic cores: it is the main core configuration. The flaking surface is exploited unidirectionally and has a wide array of morphologies, sub-pyramidal, sub-cylindrical or with parallel edges. The striking platform is plain. Convexities are shaped through lateral convergent blades and flakes and opposite flakes. Blades have wider patches of cortical surfaces.
Transversal carinated cores: the flaking surface is convergent shaped, exploited unidirectionally. The striking platform is plain, placed on the ventral blank face. The production is similar to the prismatic cores.

Typometry

Blades–bladelets dimensional threshold is put a 12 mm, bladelets <7 mm are considered micro-bladelets.

Main typological characters

Bladelets represent the most of retouched tools, they display marginal, lateral direct or inverse retouch, like Dufour, *sensu lato*, bladelets subtype Dufour.

Cultural attribution

Firstly, attributed to the Krems–Dufour Aurignacian. Another comparison is generally with the western Protoaurignacian, despite the young dates 36-34 ka calBP, which could be the result of some contamination event or bad collagen preservation.

1.3.5 South-eastern/Balkans Europe

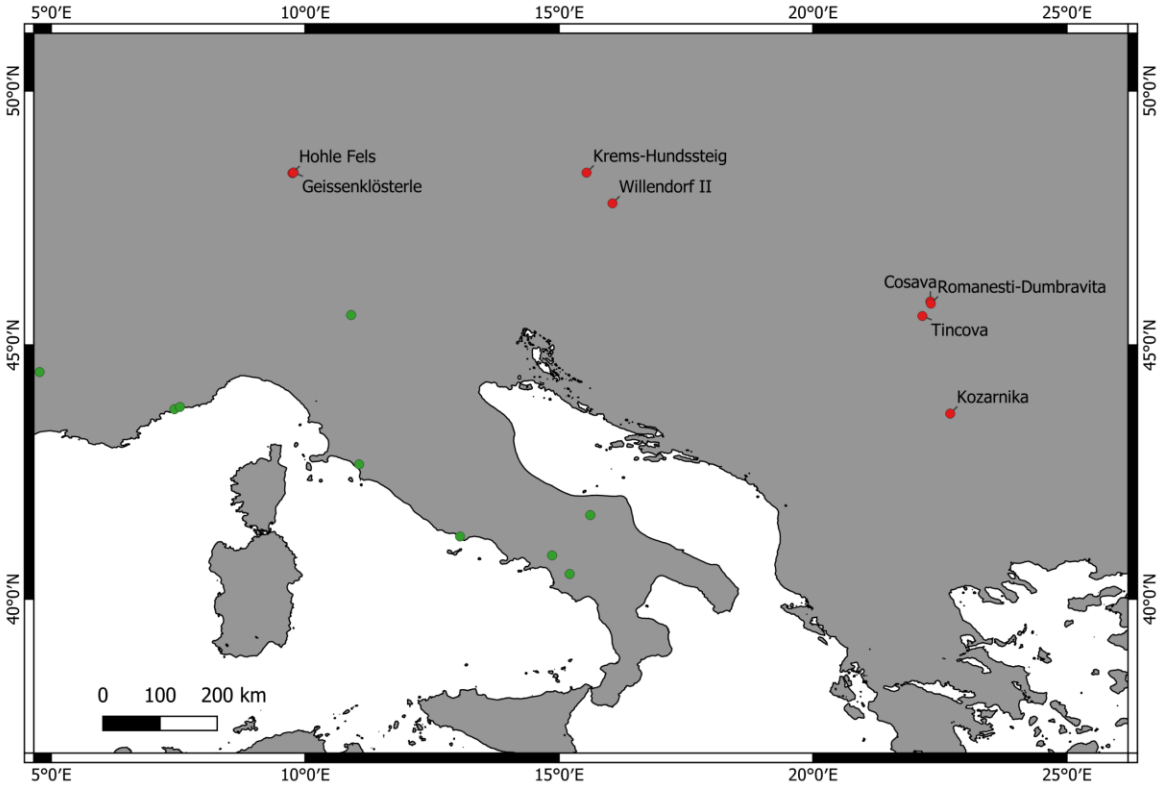

Figure 4 Detailed map of the reviewed eUP Central and South-eastern Europe sites.

Kozarnika layer VII (Sirakov et al., 2007; Tsanova, 2008).

Setting

Cave site, no sterile sedimentation in-between or erosion unconformity with the above layer VI. The layer was affected by cryoturbation, the studied assemblage comes from the less affected portion of the cave in 6 m^2 surface and 5-20 cm thickness.

Technology

Raw material of good quality is available in secondary deposition in blocks compatible with cores and blanks dimensions, a minor fraction of it witnesses a collection 80-100 km to the South.
Cores show two *chaînes opératoires*, the knapping goal is obtention of small-sized blades and large bladelets.

Prismatic sub-pyramidal cores: the flaking surface is placed on the longitudinal axis, exploited unidirectionally, broader in proximal part, distally convergent and curved. The striking platform is steep angled and plain, the overhang is abraded. Knapping rhythm is semi-circumferential, expanding on adjacent core faces in proximal part. The knapping begins directly with a cortically or partially cortical series of bladelets. Convexities are maintained through lateral laminar convergent blanks, while on the centre parallel edges bladelets are knapped. Posterior and antero-lateral crests can be shaped to help the convexities' maintaining.
Prismatic on longitudinal narrow face/blank edge cores: the flaking surface is placed on the longitudinal axis, exploited unidirectionally, using the narrow face offered by slabs or blanks' edges. The striking platform is steep angled and plain, the overhang is abraded. The knapping rhythm is frontal not invading adjacent faces. Comparatively shorter knapping series.
The knapping seems continuous, from blades to bladelets, even though some intercalation is shown. Bladelets are frequently slightly curved in distal position, meaning they are exploiting the whole flaking surface. Flakes are mostly attributed to decortication and lateral convexities shaping
The envisioned knapping is the marginal direct soft mineral or organic hammer percussion.

Typometry

The bladelets–blades threshold is fluid. The cores show mostly bladelets' negatives 4-14 mm wide at the abandonment. Most of the blanks are bladelets 5-13 mm wide. Larger blades 15-20 mm wide are few and mostly used for shaping purposes, smaller blades 10-16 mm are more frequent and issued from all knapping stages.

Main typological characters

Retouched blanks are mostly laminar. Blades are either retouched laterally or in simple end-scrapers. Burins are not frequent, simple, and made on blades or flakes. Most of the retouched bladelets witness lateral marginal direct/inverse/alternate semi-abrupt/lightly backed retouch.

Cultural attribution

Firstly, related to an embryonic development of the Gravettian, due to the small-sized backed implements, it is now related either to the western Mediterranean Protoaurignacian or to the Levantine Early Ahmarian.

Coşava (Sitlivy et al., 2014a, 2014b).

Setting

Open-air site on a hilly terrain. The context was divided in three layers and geological horizons yielding a homogenous characters industry, some evidence of partial intrusion of later Epipalaeolithic material is found on the very top of the stratigraphical sequence.

Technology

Raw material of medium quality is available in the vicinities in secondary deposition, Banat flint, some import of wider range good quality chert.

Cores show three *chaînes opératoires*, the knapping goal is obtention of small-sized blades, bladelets and micro-bladelets, continuity and intercalation between the productions is attested.

Prismatic narrow-faced cores: The flaking surface is placed on the longitudinal axis, on a narrow core face, which is exploited mostly unidirectionally. The striking platform is steep-angled and plain. Convexities are maintained through the narrowing of the lateral adjacent core faces with flakes, lateral core-edge laminar blanks and antero-lateral crests. Knapping rhythm is mostly frontal, in some case can slightly expand on adjacent lateral faces in a semi-circumferential fashion.

Carinated on longitudinal blank edge cores: The flaking surface is placed on the longitudinal axis of a blank edge, exploited mostly unidirectionally. The striking platform is steep angled and plain. The knapping begins with a central shaped crest or a natural ridge. Knapping rhythm is mostly frontal.

Transversal carinated cores: The flaking surface is placed on the distal termination of the blank exploiting transversally the thickness of the blank. The striking platform is on the ventral blank face, either plain or crudely faceted. The flaking surface, isolated by means of lateral flakes, can be wide and convergent with a semi-circumferential knapping rhythm (carinated flat end-scrapers) or narrow with a frontal knapping rhythm (nosed end-scrapers). In the first case the blanks are mostly curved and on-axis, in the second on twisted and off-axis.

Blades are mostly parallel edges with straight or slightly curved profiles, bladelets are mostly convergent with straight or slightly curved profiles. Twisted profiles are represented in either size classes.

The envisioned knapping technique is direct internal hard hammer percussion for flakes, and marginal direct soft hammer percussion for laminar blanks.

Typometry

Blades–bladelets threshold is put at 12 mm wide.

Main typological characters

Retouched tools show a good frequency of carinated and nosed end-scrapers. Laterally retouched blades, also featuring Aurignacian retouch. Laterally marginally directly or inversely retouched bladelets, Dufour *sensu lato*, are rare.

Cultural attribution

Cultural attribution is uncertain, it features a mix of Early Aurignacian and Protoaurignacian characteristics. Tentatively attributed to the Krems-Aurignacian or Early Aurignacian**.**

Tincova (Sitlivy et al., 2014b).

Setting

Single layered open-air site.

Technology

Cores show three *chaînes opératoires*, the knapping goal is obtention of blades and bladelets, independently produced from prismatic, carinated longitudinal on blank edge and carinated transversal cores.

Main typological characters

Retouched tools are dominated by simple end-scrapers. Laterally retouched blades, also featuring Aurignacian retouch are frequent. Also, laterally marginally retouched, Dufour *sensu lato*, bladelets are well represented.

Cultural attribution

Either attributed to the Protoaurignacian or to the Krems-Dufour Aurignacian.

Românești-Dumbrăvița I (Sitlivy et al., 2014b, 2012) .

Setting

Open-air site on a former river terrace in low elevation. The original sedimentary context was divided in six layers, layer III being the most abundant and widely recognised in the original excavation extension, the lowermost layer I was attributed to a Middle Palaeolithic quartzite flake entity, while the topmost layer VI to a (Epi)Gravettian industry. In the new excavations, divided in four geological horizons, GH3 corresponding to most of the central layers or to the single Layer III. Despite the high sedimentary package, lithic artefacts are distributed throughout the sedimentary succession in coherent concentrations, laying sub-horizontally.

Technology

Raw material of medium quality is available in river gravels in the nearby, Banat flint, it features also regional imports.

Cores show three *chaînes opératoires*, the knapping goal is obtention of blades and (micro)bladelets, the over-representation of blades in the old assemblage is probably related to the absence of wet sieving procedures. The production of blades and bladelets can be intercalated, independent or continuous.

Prismatic cores: The flaking surface is placed on the core longitudinal narrow face; it is exploited mostly unidirectionally. The striking platform is steep-angled and plain. The knapping rhythm can

be frontal or semi-circumferential. The core undergone a decortication through flakes. Lateral convexities are maintained through lateral narrowing flank flakes, lateral core-edges laminar blanks or antero-lateral shaped crests.
Prismatic on longitudinal narrow face/blank edge cores: the flaking surface is placed on a longitudinal narrow surface, exploited mostly unidirectionally. The knapping rhythm is frontal.
Carinated transversal cores: they are mostly present in the old collection. They are divided in flat carinated end-scrapers type, or a horse-hoof type, where the flaking surface is higher than the core thickness. The knapping rhythm is semi-circumferential.
Blades and bladelets have mostly parallel edges, blades are less on-axis than bladelets. Straight, curved, and twisted profiles share the same frequencies, but new collection bladelets have a tendency toward straight profiles.

Typometry

Blades–bladelets threshold is put a 12 mm wide. Bladelets–micro-bladelets threshold is put at 7 mm wide.

Main typological characters

In the old collection, carinated and thick end-scrapers, dihedral burins or burin on truncation and Aurignacian blades dominate the retouched tools, Dufour *sensu lato* bladelets are attested. The new collection is dominated by Dufour *sensu lato* micro-bladelets and deprived of bigger tool types.

Cultural attribution

Attribution is uncertain, more closely attributed to the Protoaurignacian.

1.3.6 Central Europe

Geißenklösterle AHIII and AHII (Teyssandier et al., 2006; Teyssandier and Liolios, 2003).

Setting

Cave site. Both units group several sub-levels, the overall integrity of the major units is guaranteed by several horizontal refits.

Technology

Raw material is good quality chert collected locally.
Two *chaînes opératoires* are recognised. Independent production of blades and bladelets.
Prismatic cores: the flaking surface has parallel edges, exploited unidirectionally. Striking platform is plain, the overhang is abraded. Knapping starts with a blade blank on the lateral core faces intersection, in fewer cases a crest is shaped. Lateral convexities are maintained through lateral

blanks and neo-crests, distal convexities through plunging blades. Mostly blades are produced, two reduced cores produced also bladelets.
Transversal carinated cores: the flaking surface is convergent, it is isolated by lateral flakes or bladelets, exploited unidirectionally. The striking platform is plain, installed on the ventral blank face. They are exclusively producing bladelets.

Typometry

No blades–bladelets dimensional threshold is given.

Main typological characters

No Aurignacian blades or Dufour bladelets are recognised.

Cultural attribution

Attributed to the Early Aurignacian.

Hohle Fels AH IV (Bataille and Conard, 2018a; Schiegl et al., 2003).

Setting

Cave site. A long stratigraphy comprising Mousterian, Aurignacian and Gravettian. The youngest Mousterian geological horizon GH9 is divided by sterile sedimentation from the earliest Aurignacian in GH8. The Aurignacian layers develop from GH8 to GH6a–GH3db. AH IV is not the earliest Aurignacian phase and it is linked with the end of the cold phase marked by the Heinrich Event 4.

Technology

The raw material is local good quality chert.
Two *chaînes opératoires* are recognised. Independent production of blades and bladelets.
Longitudinal on blank edge cores: The principal core configuration recognised in the assemblage. The flaking surface is placed on the lateral longitudinal edge of a blank, in a fashion of a burin. Most of the cores can be classified as burin on truncation, which performs the role of striking platform, the angle is steeper than prismatic cores striking platform. The production is straight profile on-axis or twisted profile bladelets and burin spalls, most of them can be classified as micro-bladelets.
Prismatic cores: the flaking surface has mostly cylindrical parallel edges morphology, in lesser fashion convergent sub-pyramidal, it is placed on the longitudinal axis either on the narrow or the wide surface. The striking platform is plain and steep angled. The distal convexity is maintained through shaping. The production is short, thick and straight profile blades.
Transversal carinated cores: they are few and corresponding to nosed end-scrapers, with lateral flakes isolating a narrow flaking surface. The striking platform is place on the ventral blank face.
The envisioned technique is the direct marginal soft hammer percussion.

Typometry

Blades-bladelets dimensional threshold is put at 12 mm, bladelets <7 mm are considered micro-bladelets.

Main typological characters

Blades are laterally retouched, sometimes in Aurignacian blades, or transformed in burins and simple end-scrapers. Bladelets and burin spalls are retouched, but no Dufour *sensu lato* are recognised.

Cultural attribution

Attributed to a different early Aurignacian *facies*.

Krems-Hundssteig (Broglio and Laplace, 1966; Nigst and Haesaerts, 2012).

Setting

Open-air site located on a fluvial terrace of the Danube. Despite being described by the original excavators, J. Strobl and H. Obermaier, as an assemblage coming from a homogeneous sedimentary context, recent authors point to mixing of several underlooked contexts, therefore challenging the archaeological and cultural value.

Technology

Prismatic cores are the only ones described, sometimes the flaking surface is sub-pyramidal.

Typometry

No blades–bladelets dimensional threshold is given.

Main typological characters

The assemblage is characterised by the numerous carinated end-scrapers and bladelets with lateral marginal retouch, inverse, direct or alternate fitting the Dufour bladelets *sensu lato* and the Krems/Font Yves points.

Cultural attribution

Attribution uncertain. The assemblage counts thousands of diagnostic Aurignacian artefacts, linking it mainly to the Protoaurignacian sites of Western Europe.

Willendorf II AH3 (Nigst et al., 2014; Nigst and Haesaerts, 2012; Teyssandier and Zilhão, 2018).

Setting

Open-air site located on a fluvial terrace of the Danube. The assemblage numbers slightly more than 500 artefacts, with a complex excavation history, most likely coming from different lenses of sediment. Most of the artefacts where found again in the collection warehouse and cannot be linked to any particular sedimentary context. Nevertheless, some refits would point to some degree of coherence.

Technology

Raw material is collected locally in fluvial gravels, a small percentage comes from long distance (200 km) procurement.
Three *chaînes opératoires* are recognised. Independent production bladelets and intercalated production of blades and bladelets.
Prismatic cores: the flaking surface is exploited unidirectionally. Striking platform is plain. Blades and bladelets have been produced directly knapping at the intersection of the flaking surface with the lateral core faces and then developing until the other edge and back.
Transversal carinated cores: they have wide fronts, carinated end-scrapers, or narrow fronts, nosed end-scrapers. Independent bladelets production.
Longitudinal on blank edge cores: they produce bladelets from blanks' lateral longitudinal edges.

Typometry

No blades–bladelets dimensional threshold is given.

Main typological characters

Carinated and nosed end-scrapers are the most diagnostic tools.

Cultural attribution

Attributed to the Early Aurignacian.

1.3.7 Western and Central Mediterranean Europe

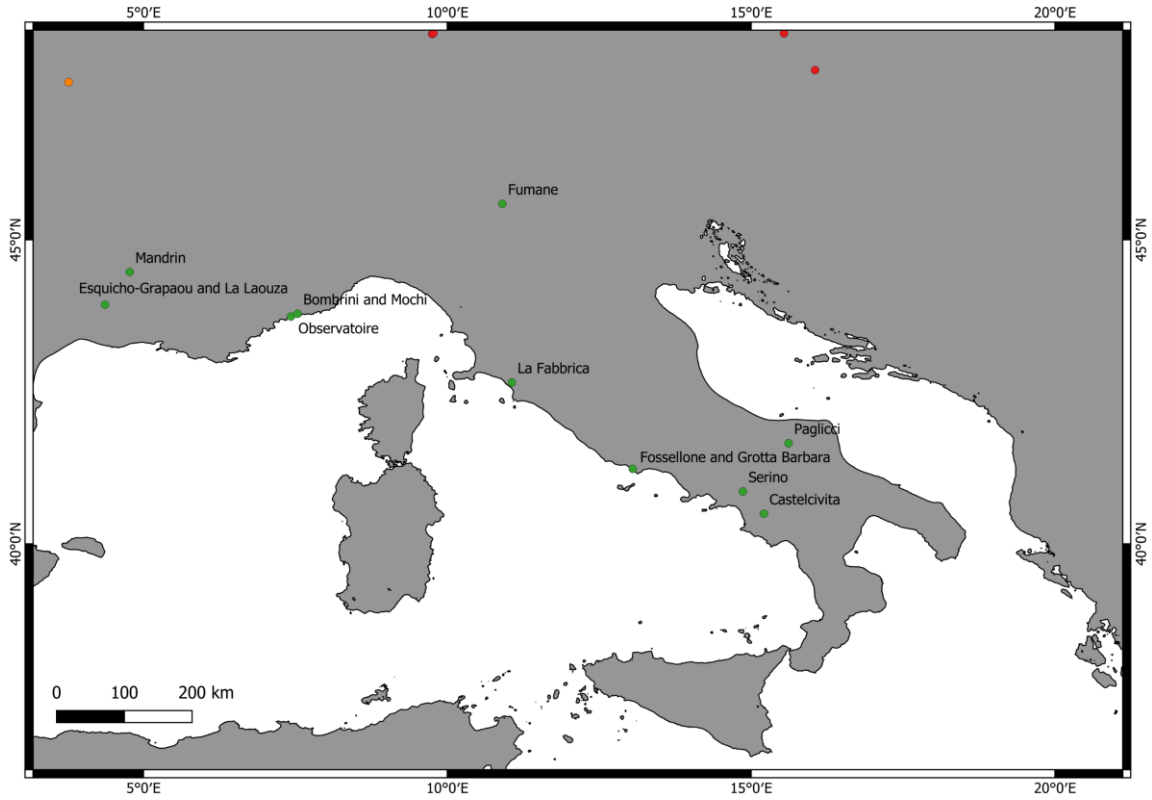

Figure 5 Detailed map of the reviewed eUP Mediterranean sites.

Esquicho-Grapaou SLC1b and SLC1a and La Laouza 2b (Bazile, 2005, 2002; Bazile and Sicard, 1997).

Setting

Esquicho–Grapaou is a cave site, while La Laouza is a rock-shelter, the two sites are 7 km far from each other. At Esquicho–Grapaou the Aurignacian layers SLC1b/a are separated from the overlying BR1, Aurignacian, and underlying BR2, Mousterian, by sterile sediments, erosion episode and concretions. At La Laouza layer 2 b is sandwiched by sterile layers.

Technology

Esquicho-Grapaou SLC1b/a

The raw material is mostly good quality local flint slabs collected in primary outcrops, complemented by riverbed flint and rare regional flint imports.

A single *chaîne opératoire* is recognised. It shows an intercalated blades–bladelets production with a focus on bladelets.

Prismatic on longitudinal narrow face cores: the flaking surface is installed on the longitudinal, narrow face of the slab, it is exploited unidirectionally. The striking platform is natural or plain, the

overhang is abraded. The knapping rhythm is frontal, convexities are maintained through lateral blanks, often shaped in antero-lateral crests, struck at the faces' intersections and, occasionally, with some opposite removals. The production is focused on straight on-axis bladelets.
The envisioned technique is the direct soft hammer percussion.

La Laouza 2b

The raw material is mostly good quality local flint, but the riverbed and regional imports flint assume more importance.
Three *chaînes opératoires* are recognised. An intercalated blades–bladelets production with a focus on bladelets and two independent bladelets production.
Prismatic on longitudinal narrow face cores: the flaking surface is installed on the longitudinal, narrow face of the slab, it is exploited unidirectionally. The striking platform is natural or plain, the overhang is abraded. The knapping rhythm is frontal, convexities are maintained through lateral blanks, often shaped in antero-lateral crests, struck at the faces' intersections and, occasionally, with some opposite removals. The production is focused on straight on-axis bladelets.
Longitudinal carinated cores: the flaking surface is placed on a narrow blank edge, it is exploited unidirectionally. The striking platform is plain and place on the longitudinal edge. The knapping rhythm is frontal, with a later expanding on the blank ventral face. Typologically can it be described as Vachons burin. The production is straight and curved bladelets.
Transversal carinated cores: the flaking surface is placed on distal end of a thick blank, it is exploited unidirectionally. The striking platform is plain and placed on the blank ventral face. The production leads to shorter and curved bladelets.
The envisioned technique is the direct soft hammer percussion.

Typometry

No blades–bladelets threshold is given. Last cores' negatives are usually ≈10 mm wide. At La Laouza blades are generally 20 mm wide, while at Esquicho–Grapaou blanks are 7–25 mm wide.

Main typological characters

Straight bladelets with lateral, marginal, inverse retouch, Dufour subtype Dufour bladelets, account for a significative number at La Laouza, while they are most of the tools in Esquicho–Grapaou. End-scrapers, also thick, are present, but not numerous. Vachons burins are well recorded in La Laouza.

Cultural attribution

Both sites are attributed to the Protoaurignacian.

Grotte Mandrin layer 1 (Slimak, 2008; Slimak et al., 2006, 2002).

Setting

It is a cave site. The Aurignacian occupation appears in the middle and upper part of layer 1 on top of the Mousterian one, the latter spanning from layer 4 until the lower layer 1.

Technology

The raw material is extremely local good quality flint collected from primary outcrops.
The assemblage is small, but coherent and witnessing all stages of knapping. Three *chaînes opératoires* are recognised. One for independent blades production from non-structured, semi-circumferential prismatic cores and two for structured bladelets production.
Prismatic on longitudinal narrow face cores: the most represented at the site. The flaking surface is placed on a longitudinal narrow face, it is exploited unidirectionally. The back of the core is shaped in a flat narrow face by flakes struck from the core sides. The lateral convexity is shaped by oblique bladelets series, struck from the core back. The distal convexity is shaped by opposite removal. The knapping rhythm is frontal. The oblique bladelets series shaping the flanks are creating bladelets bearing oblique negatives on their dorsal face, called *lamelles croisées*. The focus is the obtention of straight and highly standardised big bladelets.
Longitudinal carinated cores: the flaking surface is placed on a longitudinal blank edge, it is exploited unidirectionally. The smaller bladelets are obtained through a simple semi-circumferential knapping, maintaining the convexities through blanks issued from the adjacent wide face. Bigger, convergent bladelets, middle size class, are showing a better structuration. One core lateral face is shaped through oblique bladelet series coming from the back of the core, the other corresponds to the flake ventral face. Because of the core flank shaping, *lamelles croisées* are created as partial crests and neo-crests. Despite using a similar core blank, small bladelets and middle pointed bladelets are using two independent operative schemes.

Typometry

Bladelets are divided in three classes: the small ones, 2–3 mm wide, the middle ones, 5–6 mm wide, and the big ones, 10 mm wide.

Main typological characters

While the small bladelets have a marginal back, the big bladelets are retouched in Dufour subtype Dufour bladelets.

Cultural attribution

Attributed to the Protoaurignacian.

Grotte de l'Observatoire layers G and F (Porraz et al., 2010).

Setting

It is a cave site. The first Aurignacian layer G overlies a stalagmitic concretion which separates it from the Mousterian beneath it. F it is in direct stratigraphical connection with the overlying layer E, tentatively attributed to the Early Aurignacian because of a split-base point, but no certain stratigraphic attribution can be given to the bone point. Most of the assemblage is belonging to lower part of the layer.

Technology

The raw material is mostly high-quality flint collected 130 km east, few imports from the regional context, 40 km east, and from central Italy, 200–300 km.
Two *chaînes opératoires* are recognised. An intercalated blades–bladelets production with a focus on bladelets and one independent bladelets production.
Longitudinal carinated cores: the flaking surface is placed on the longitudinal blank edge, it is exploited unidirectionally. The striking platform is plain, and the overhang is abraded. The knapping begins with shaping a unifacial crest, creating the necessary guide ridges. The knapping rhythm is frontal, the convexities are maintained by lateral and overshot bladelets, some of them could be classified as *lamelles croisées*. The production is focused on straight or slightly curved on-axis bladelets from the central part of the flaking surface.
Prismatic cores: the flaking surface is placed on the wide face, it is exploited unidirectionally. The striking platform is plain, and the overhang is abraded. The knapping begins with a unifacial lateral crest, then it develops with a semi-circumferential rhythm. The production is oriented towards intercalated blades and bladelets

Typometry

Blades–bladelets dimensional threshold is put at 10 mm wide, which is the threshold for the Dufour subtype Dufour bladelets.

Main typological characters

A big portion of the retouched blanks consist of bladelets with lateral, marginal, and inverse semi-abrupt retouch, Dufour subtype Dufour. Burins are well represented, mostly on breakage. End-scrapers are rare.

Cultural attribution

Attributed to the Protoaurignacian.

Mochi units G and F (Douka et al., 2012; Grimaldi et al., 2014; Kuhn and Stiner, 1998; Tejero and Grimaldi, 2015).

Setting

It is a rock-shelter site. Originally the site was excavated by arbitrary 5 cm cuts and macro-units have been cast post-excavation following sedimentological and archaeological indications. Sterile units E and H separate the macro-units G and F, in direct stratigraphical connection, from the above Gravettian, D, and from the underlying Mousterian, I. H could be divided in three parts, the lower still pertaining to the Mousterian, the middle being devoid of archaeological material, and the upper part, denominated H–G, with Aurignacian archaeological material.

Technology

G

The raw material is mostly local flint, complemented by significant imports, 30% of the tools are made on imports, from Western, 200 km, and Eastern, 80–100 km, Provence as Eastern Liguria, 150 km, and Central Italy, >200 km.
Three *chaînes opératoires* are recognised. Two for an independent bladelet production, one for an independent blade production.
Prismatic cores: the flaking surface is placed on the longitudinal wide face, it has pyramidal or parallel edges morphology, and it is exploited unidirectionally. The striking platform is plain, and the overhang abraded. The only maintaining operation recognised is the shaping of crests. The focus is the production of on-axis, regular straight bladelets.
Longitudinal carinated cores: the flaking surface is placed on the blank longitudinal edge, it is exploited unidirectionally. The focus is the production of on-axis, regular bladelets.
Prismatic cores on local raw material produce blades, parallel edges and large blades are noticed among the imported flint.

Typometry

Blades–bladelets dimensional threshold is ≈10 mm wide, many are <6 mm wide.

Main typological characters

G

Most of the retouched blanks are bladelets with lateral, marginal and inverse retouch, Dufour subtype Dufour bladelets. Burins on truncations are the most present. Carinated forms and strangulated blades are rare.

F

It signals the most sustained presence of carinated end-scrapers, Aurignacian blades, and antler manufacture.

Cultural attribution

G

Attributed to the Protoaurignacian.

F

Attributed to the Early Aurignacian.

Bombrini A1 and A2 (Holt et al., 2019; Riel-Salvatore and Negrino, 2018).

Setting

It is a collapsed rock-shelter site. The site sits 50 m far from Mochi, showing many similarities. Two Aurignacian units, A1 and A2, are stratigraphically overlying the Mousterian units, MS1.

Technology

Raw material is similar to what is recorded in Mochi.
Two *chaînes opératoires* are recognised. One for an independent bladelets production from unipolar prismatic cores, one for a combined blades and flakes production.

Typometry

Bladelets are on average 7–8 mm wide.

Main typological characters

The retouched blanks are dominated by slightly curved, on-axis bladelets with marginal, bilateral, alternate, semi-abrupt retouch, the classic Dufour subtype Dufour bladelets.

Cultural attribution

Attributed to the Protoaurignacian.

La Fabbrica layers 3 and 4 (Dini et al., 2012; Dini and Tozzi, 2012).

Setting

It is a cave site. The layers 3 and 4 are directly overlying layer 2, Uluzzian, and covered by layer 5, Epigravettian. The steep slope towards the inner part of the cave is responsible of various erosional episodes.

Technology

Raw material is mostly a local wide array of siliceous rocks available in nearby river gravels, nevertheless high-quality flint collected in primary outcrops was imported for reduction on site from 160 km east.

Two *chaînes opératoires* are recognised. One for an intercalated blades–bladelets production, on the only high-quality material nodule, and one for unipolar products from globular, loosely prismatic, and non-organised cores, on local raw material.

Prismatic core on narrow face: the flaking surface is placed on the narrow and longitudinal face, it is exploited unidirectionally. The striking platform is plain, and the overhang abraded. The distal convexity is shaped through a posterodistal crest. The knapping rhythm is frontal. Production is intercalated blades–bladelets.

Typometry

No blades–bladelets dimensional threshold is given.

Main typological characters

Retouched tools feature bladelets with lateral marginal retouch and big, thick, curved blades laterally retouched.

Cultural attribution

Attributed to the Protoaurignacian.

Fossellone layer 21 (Degano et al., 2019a, 2019b).

Setting

It is a cave site. The Aurignacian layer 21 is separated from the beneath Mousterian layer 23 by a sterile clayish layer 22.

Technology

Raw material are the local ovoid Pontinian flint pebbles, which provided a challenge to the Aurignacian artisans.

A single *chaîne opératoire* is recognised. Independent production of bladelets.

Transversal carinated cores: the pebble is firstly reduced/opened through bipolar tangential technique along the longitudinal axis. In this way a ≈30 mm thick flake is obtained, the striking platform of the future carinated core is placed on the flat surface obtained from the longitudinal splitting of the cobble, while the flaking surface on a distal end of the blank. The two longitudinal edges are shaped through convergent flakes knapped from the striking platform, which put in place a central crest. The

front is shaped by lateral flakes and then by broad, off-axis bladelets. The knapping rhythm is semi-circumferential. The production focus are short, convergent bladelets issued from the centre of front.

Typometry

The desired bladelets are 3–5 mm wide.

Main typological characters

The carinated and nosed end-scrapers dominate the tool counts. Split base points are recorded too.

Cultural attribution

Attributed to the Early Aurignacian.

Grotta Barbara (D'Angelo and Mussi, 2005).

Setting

It is a cave site in the proximity of Fossellone cave. The Aurignacian layer is eroded by the nearby sea action, it survives along the cave walls and in some corridors. It overlies Mousterian layers.

Technology

The raw material is exclusively small ovoid local Pontinian flint pebbles.
Four *chaînes opératoires* are recognised. Independent production of bladelets.
Bipolar tangential technique: the flaking surface can be placed on the wider longitudinal face, the most used configuration, or the narrow longitudinal face. In this way bipolar bladelets are issued. A more complex variant uses the bipolar technique for obtaining a lateral ridge, which is afterwards used for a regular unidirectional bladelet production.
Prismatic cores: the distal part of the pebble is removed transversally to the longitudinal axis, forming a plain striking platform. The flaking surface is placed on the wider longitudinal axis and exploited unidirectionally.

Typometry

No blades–bladelets dimensional threshold is given.

Main typological characters

The retouched tools assemblage is mostly characterised by end-scrapers, also nosed and on Aurignacian blade.

Cultural attribution

Attributed to the Early Aurignacian.

Serino (Accorsi et al., 1979; Giaccio et al., 2008).

Setting

It is an open-air site. A single Aurignacian occupation overlies sterile clays, and it is sealed by a thick deposition of pumice linked with the Campanian Ignimbrite.

Technology

The raw material is exclusively flint.
Unidirectional sub-pyramidal and prismatic cores produce abundant bladelets. Striking platforms are plain.

Typometry

No blades–bladelets dimensional threshold is given. Most of the artefacts are comprised in 10 mm wide.

Main typological characters

Few bladelets with lateral, marginal retouch, approachable to Dufour bladelets. End-scrapers, also carinated are present, but in low number. Aurignacian retouch is recorded as well.

Cultural attribution

Attributed to the Protoaurignacian.

Castelcivita layers rsa, gic and ars (Gambassini, 1997; Giaccio et al., 2008).

Setting

It is a cave site. Layer rsa, short for red sandy, it is located in the II sedimentological layer and it lays on direct stratigraphical connection with the below Uluzzian layers. The above gic and ars layers constitute the I sedimentological layers and they are capped by pumice and ash layer connected with the Campanian Ignimbrite.

Technology

The raw material is mostly flint collected in the nearby river gravels.

<u>rsa</u>

Three *chaînes opératoires* are recognised. Independent bladelet production.
Prismatic cores: the flaking surface is exploited unidirectionally. The striking platform is plain. They produce straight or slightly curved on-axis bladelets.
Longitudinal carinated cores: the flaking surface is placed on the longitudinal, carinated burins, or transversal, Vachons burins, edges, it is exploited unidirectionally. They produce bladelets.

Transversal carinated cores: the flaking surface is placed on the distal end of a thick blank, it is exploited unidirectionally. The striking platform is on the blank ventral face. The flaking surface is isolated by lateral flakes, can be wide, carinated end-scrapers type, or narrow, nosed end-scrapers type. They produce bladelets.

gic and ars

The main difference is the increase of carinated forms.

Typometry

No blades–bladelets dimensional threshold is given. The majority of the artefacts is <25 mm length.

Main typological characters

rsa

Most of the retouched tools are bladelets with lateral marginal inverse or alternate semi-abrupt retouch, Dufour subtype Dufour. Carinated burins and end-scrapers are well represented, bladelets negatives are partially obliterated by subsequent retouch.

gic and ars

The retouched blanks feature the appearance of smaller, straight bladelets with marginal, convergent, direct bilateral retouch, the Castelcivita points.

Cultural attribution

rsa

Attributed to the Protoaurignacian with Dufour bladelets.

gic and ars

Attributed to the Protoaurignacian with micropoints.

Paglicci layer 24 (Giaccio et al., 2008; Palma di Cesnola, 2006).

Setting

It is a cave site. The Aurignacian layer 24 is sandwiched by a stalagmite layer, 24α, and a tephra deposition in, 23C2, linked to the Codola eruption. The layer is divided in three occupations BII–I, A4–2, A1–0. The density of artefacts grows with the stratigraphical position.

Typometry

No blades–bladelets dimensional threshold is given.

Main typological characters

The bladelets with marginal, lateral, semi-abrupt retouched, Dufour *sensu lato*, are the most represented diagnostic tool type. End-scrapers are well represented, also carinated and with bladelet retouch. The burins, also carinated and with bladelet retouch, get more important in the middle and top occupations.

Cultural attribution

Attributed to the Protoaurignacian.

Fumane (Bartolomei et al., 1992; Bertola et al., 2013; Broglio et al., 2005; Falcucci, 2018; Falcucci et al., 2017; Falcucci and Peresani, 2018).

Setting

It is a cave site. The entire stratigraphical sequence is divided in macro-units based on the sediment. The Aurignacian is found in units A, fine grain sediment, and D, mostly loose rocks from cave vault collapse. At the cave mouth, layer A2 is overlying layer A3, Uluzzian, in direct stratigraphical connection, but marked by the red sediment colour; several habitat structures are dug by the Aurignacian occupants and could displace some underlying archaeological material. The thin layer A1 is on top of A2 and ends the macro-unit A. In macro-unit D the human occupation is less dense, mostly recognised in D6, found on the eastern side of the cave, D3 (divided in D3base, D3α and D3a/b) and D1c. D1d is the last anthropised layer and attributed to the Gravettian. The inner cave is showing less stratigraphical resolution, due to compression and post-depositional processes, here the succession shows just layers A2 and the D3 complex.

Technology

Raw material is local good quality flint available in primary outcrops and river gravels.

<u>A2–A1</u>

Five *chaînes opératoires* are recognised. Independent bladelet production or intercalated blades-bladelets production. In general, the knapping focus is straight or slightly curved, on-axis bladelets. Prismatic semi-circumferential cores: the flaking surface is installed on a longitudinal axis using in continuity two adjacent core faces, the flaking surface can have parallel or convergent edges morphology; blade cores show a prevalent parallel edges morphology while bladelet ones a convergent morphology. The flaking surface is exploited unidirectionally. The striking platform is plain. The knapping procedure isolates narrow flaking surfaces through lateral or transversal-to-core-axis removals and oblique blade blanks accentuating the distal convergence, once the flaking surface is exploited knapping migrates slightly laterally reproducing the procedure, finally the core assumes

a semi-circumferential shape through the migration back and forth of the several flaking surfaces. They produce independent bladelets, blades or intercalated blades–bladelets.

Longitudinal on narrow face/blank edge cores: the flaking surface is installed on the longitudinal edge of a blank or a narrow longitudinal face of a small slab, it is exploited unidirectionally. The striking platform is plain. A posterior crest is shaped. The knapping rhythm is mostly frontal. They produce exclusively bladelets.

Transversal carinated cores: the flaking surface use the former blank thickness and it is placed on the distal end of a thick blank; it is exploited unidirectionally. The striking platform is plain and is placed on the blank ventral face. The flaking surface is isolated by lateral removals of flakes, producing a nosed morphology; they produce exclusively bladelets, shorter than the prismatic cores.

Prismatic wide faced cores: the flaking surface is installed on the wider face on the longitudinal axis, it has parallel edges morphology, and it is exploited unidirectionally. They are probably exhausted semi-circumferential cores.

Independent multiplatform cores: they have independent reduction series placed on the core volume. Knapping begins at the favourable ridges of core faces intersections creating a fully cortical laminar blank, less frequently a unilateral or bilateral crest is shaped after the first cortical blank is removed; convexities are maintained by simple naturally backed blades or neo-crested blades along the lateral edges of the core flaking surface

D3dbase–D3bα–D3ab

The lithic production remains similar to A2–A1, but an increase in the transversal carinated cores use is noticed. Also, Flakes are knapped independently.

Typometry

Blade-bladelets threshold is put at 12 mm wide, most of the inversely semi abruptly retouched blanks are inferior to that.

Main typological characters

A2–A1

A big part of the bladelets is retouched with marginal, lateral or convergent, semi-abrupt retouch. A smaller percentage of the blades is retouched laterally, some displaying scalar Aurignacian retouch. Frontally in end-scrapers or burins.

D3dbase–D3bα–D3ab

Laterally retouched bladelets are always the main type. End-scrapers, mostly carinated form, increase progressively. A split-base point is found at the interface with A1.

Cultural attribution

A2–A1

Attributed to the Protoaurignacian.

D3dbase–D3bα–D3ab

Attributed to a later phase of the Protoaurignacian.

1.3.8 Western Europe

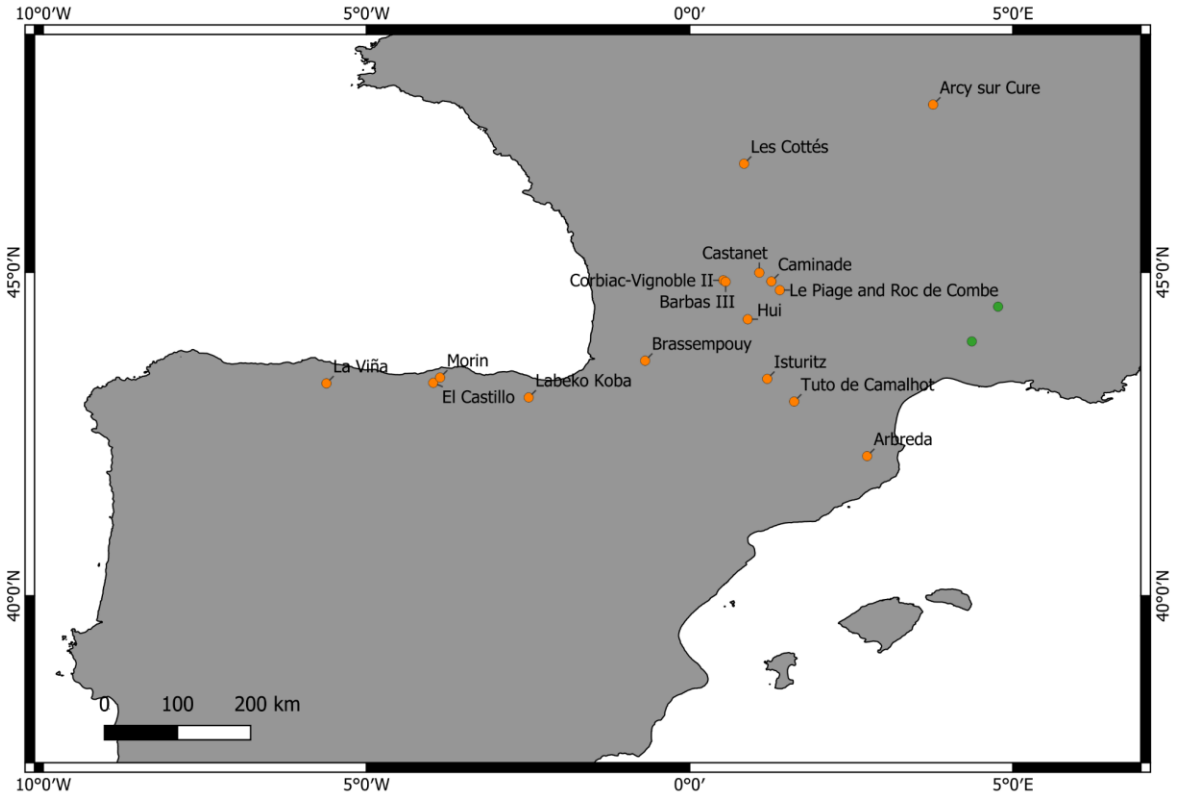

Figure 6 Detailed map of the reviewed eUP Western Europe sites.

Castanet (Chiotti et al., 2015; Chiotti and Cretin, 2011; Pelegrin and O'Farrell, 2005).

Setting

Collapsed rock-shelter site. Old excavations led by Peyrony identified two subsequent layers, recent excavation found only a single layer lying over the bedrock.

Technology

The raw material is mostly good quality chert found locally in colluvial sediments or riverbeds. Imports come primarily from primary outcrops 40–50 km far away, with a maximum distance of 140 km.

Two *chaînes opératoires* are recognised. Independent production of blades and, mostly, bladelets.

Transversal carinated cores: This is the main core configuration at the site. The flaking surface is placed at distal end of thick flakes, exploited unidirectionally. The front is 26,5 mm wide on average. The striking platform is placed on the blank ventral face. Convergent flakes are struck from the striking platform regularising the longitudinal edges and creating a central crest. The front is thus isolated and is used for a semi-circumferential knapping of bladelets taking advantage of lateral and distal convexities put in place by the flakes.

Prismatic cores: They are rare. The flaking surface has parallel edges, exploited unidirectionally. Striking platforms are facetted and the overhang frequently abraded.

Typometry

Bladelets are 3–≈20 mm wide, the most regular are comprised in the 3–10 mm wide interval.

Main typological characters

Most of the retouch tools are flat end-scrapers on blades, some showing Aurignacian lateral retouch too. Laterally retouched blades are frequent. Retouched bladelets are on irregular blanks and non-consistent retouch.

Cultural attribution

Attributed to the Early Aurignacian.

Caminade layers F and G (Bordes, 2005, 2000; Bordes and Lenoble, 2002; Bordes and Tixier, 2002).

Setting

It is a rock-shelter site. In the eastern portion of the site layers G and F correspond to a first Aurignacian phase of occupation, which is divided from the underlying Mousterian by a roof collapse and from the topmost Aurignacian units D by sterile sandy sediments.

Technology

Three *chaînes opératoires* are recognised. Independent production of blades and, mostly, bladelets.
Transversal carinated cores: the most frequent. The flaking surface is placed on the distal end of a thick laminar blank, it is exploited unidirectionally. The striking platform is plain and placed on the blanks' ventral surface. Lateral flakes are isolating the wide front. They produce straight or curved bladelets.
Prismatic on longitudinal narrow face cores: the flaking surface is placed on the longitudinal narrow face of a slab. They produce bladelets.
Prismatic cores: the flaking surface has parallel edges, exploited unidirectionally. The striking platform is facetted. The knapping starts shaping an antero-lateral crest at the flaking surface

intersection with an adjacent core face. The knapping rhythm is strictly frontal. Lateral convexities are maintained by lateral blanks or by lateral neo-crests, distal convexities are maintained by plunging blades. They produce large and thick blades.

Typometry

Bladelets negatives are 4–10 mm wide.

Main typological characters

Most of the retouched tools are carinated and nosed end-scrapers. Most of the retouched bladelets are non-twisted and display a marginal, semi-abrupt inverse retouch.

Cultural attribution

Attributed to the Early Aurignacian.

Roc de Combe layer 7 (Bordes, 2005; Bordes and Tixier, 2002).

Setting

It is a cave site. Layer 7 is formed grouping the former 7a, 7b, 7c; it is sandwiched between the Chatelperronian layer 8 and the Recent Aurignacian of layer 6 and 5.

Technology

Two *chaînes opératoires* are recognised. Independent production of blades and, mostly, bladelets. Transversal carinated cores: they are the most frequent. The flaking surface is placed on the distal end of a thick blank, it is exploited unidirectionally. The flaking surface develops in a wide front around the longitudinal volume of the blank. The striking platform is plain and placed on former blanks' ventral face. The knapping rhythm is semi-circumferential. They produce only bladelets. Prismatic cores: the flaking surface has parallel edges, exploited unidirectionally. The striking platform is facetted. The knapping starts shaping an antero-lateral crest at the flaking surface intersection with an adjacent core face. The knapping rhythm is strictly frontal. Lateral convexities are maintained by lateral blanks or by lateral neo-crests, distal convexities are maintained by plunging blades. They produce large and thick blades.

Typometry

Bladelets negatives are 4–10 mm wide.

Main typological characters

Most of the retouched bladelets are non-twisted and display a marginal, semi-abrupt inverse retouch.

Cultural attribution

Attributed to the Early Aurignacian.

Corbiac-Vignoble II (Bordes, 2005; Bordes and Tixier, 2002).

Setting

Open-air site. There a single occupation layer.

Technology

Two *chaînes opératoires* are recognised. Independent production of blades and, mostly, bladelets.
Prismatic cores: the flaking surface has parallel edges, exploited unidirectionally. The striking platform is facetted. The knapping starts shaping an antero-lateral crest at the flaking surface intersection with an adjacent core face. The knapping rhythm is strictly frontal. Lateral convexities are maintained by lateral blanks or by lateral neo-crests, distal convexities are maintained by plunging blades. They produce large and thick blades.
Transversal carinated cores: the flaking surface is placed at the distal end of a thick blade, exploited unidirectionally. The striking platform is plain and placed on the blanks' ventral surface. The knapping rhythm is semi-circumferential. They produce straight and curved profile bladelets.

Typometry

Blades are 25-50 mm wide. Bladelets are 4-11 mm wide.

Main typological characters

A single straight profile bladelet is retouched in Dufour subtype Dufour.

Cultural attribution

Attributed to the Early Aurignacian.

Le Piage (Bordes, 2006, 2005; Bordes and Tixier, 2002).

Setting

It is a rock-shelter site. Layer K is separated from the overlying layer GI by a mixed layer J.

Technology

K

Three *chaînes opératoires* are recognised. One with intercalated blades–bladelets production and the other two for independent bladelet production.

Prismatic cores: the flaking surface has sub-pyramidal morphology, it is exploited unidirectionally. Blades and bigger bladelets are knapped in continuity or intercalated.
Cores on longitudinal blanks' edge/narrow face: the flaking surface is placed on the longitudinal narrow face, it is exploited unidirectionally. They produce straight bladelets.
Transversal carinated cores: the flaking surface is placed at the distal end of a thick blade, exploited unidirectionally. The striking platform is plain and placed on the blanks' ventral surface. The knapping rhythm is semi-circumferential. They produce smaller straight and curved profile bladelets.

GI

Two *chaînes opératoires* are recognised. Independent production of blades and, mostly, bladelets.
Prismatic cores: the flaking surface has parallel edges, exploited unidirectionally. The striking platform is facetted. The knapping starts shaping an antero-lateral crest at the flaking surface intersection with an adjacent core face. The knapping rhythm is strictly frontal. Lateral convexities are maintained by lateral blanks or by lateral neo-crests, distal convexities are maintained by plunging blades. They produce large and thick blades.
Transversal carinated cores: the flaking surface is placed at the distal end of a thick blade, exploited unidirectionally. The striking platform is plain and placed on the blanks' ventral surface. The knapping rhythm is semi-circumferential. They produce straight and curved profile bladelets.

Typometry

K

No blades–bladelets dimensional threshold is given.

GI

No blades–bladelets dimensional threshold is given.

Main typological characters

K

Straight profile bladelets display marginal lateral and bilateral semi-abrupt direct, inverse, backed or alternate retouch, being compatible with Dufour bladelets subtype Dufour.

GI

Only a curved bladelet retouched in Dufour subtype Dufour.

Cultural attribution

K

Attributed to the Protoaurignacian

GI

Attributed to the Early Aurignacian.

Hui (Le Brun-Ricalens, 2005b, 1993).

Setting

Open-air site on small elevation hill. The single archaeological layer 2 is divided in arbitrary cuts 2a, 2b, 2c: most of the assemblage is found in 2b and refits prove its integrity.

Technology

The raw material is mostly local chert, with some regional radius imports.
Two *chaînes opératoires* are recognised. Independent production of blades and, mostly, bladelets.
Transversal carinated cores: the most recognised core configuration. The flaking surface is placed on the distal end of triangular and trapezoidal cross-section blocs, flakes, and thick blades. The striking platform is plain. Lateral flakes, controlling the convexities isolate a wide front, 25-30 mm. The knapping rhythm is semi-circumferential, convergent, and slightly off-axis bladelets (*lamelles de cadrage*) put in place a central guide nervure for the desired bladelets.
Prismatic cores: the flaking surface has parallel edges, it is exploited unidirectionally. The striking platform is steep angled and can be facetted, the overhang is systematically abraded. After a short decortication through flakes, the knapping start with a cortical blade on a natural lateral ridge or, less frequently, a crudely shaped crest. The knapping rhythm is frontal. The distal convexity is maintained through neo-crests, while the lateral convexity is maintained through flank narrowing flakes. Production is large and thick blades.
Envisioned knapping technique is the direct hard hammer percussion for flakes and direct soft hammer for laminar blanks.

Typometry

Blades are generally 20–30 mm wide. Desired bladelets are <15 mm long, thus at maximum ≈7 mm wide.

Main typological characters

End-scrapers are the most numerous tools. Aurignacian blades are well represented. Two bladelets have lateral marginal inverse low-angle retouch.

Cultural attribution

Attributed to the Early Aurignacian.

Barbas III C1 (Ortega Cordellat, 2005).

Setting

Open-air site on a river terrace. The layer C1 is overlying the layer C2, attributed to the Chatelperronian.

Technology

The raw material is good quality local chert, nodules up to 30 kg, with some minor regional imports. Three *chaînes opératoires* are recognised. Independent production of blades and, mostly, bladelets.
Prismatic cores: the flaking surface is placed on the longitudinal wide face; it has parallel edges, and it is exploited unidirectionally. The striking platform is plain. The knapping begins with the shaping of a bifacial crest and the rhythm is frontal. Convexities are managed by antero-lateral crests and distal shaping. The production is large and thick, straight blades.
Prismatic on longitudinal; narrow face cores: the flaking surface is placed on a longitudinal narrow face, it is exploited unidirectionally. The striking platform is plain. The knapping start with a blank removing a natural lateral ridge and the knapping rhythm is frontal. The convexities are maintained through lateral neo-crests. The production is middle sized blades.
Transversal carinated cores: the flaking surface is placed on a distal end of a thick blank, flakes or blade, exploited unidirectionally. The striking platform is plain. A single lateral flake, or two lateral flakes, isolates the flaking surface, maintaining the convexities. The production is small and curved bladelets.
Longitudinal carinated cores: the flaking surface is placed on a longitudinal blank edge, it is exploited unidirectionally. The production is long and straight bladelets.

Typometry

Big blades are 50–80 mm wide. Medium sized blades are 20–40 mm wide. Small bladelets are <10 mm wide, while big ones are on average 10 mm wide.

Main typological characters

Few bladelets are retouched.

Cultural attribution

Attributed to Early Aurignacian.

Les Cottés (Porter et al., 2019; Roussel and Soressi, 2013; Talamo et al., 2012).

Setting

It is a cave site. The stratigraphical sequence of the new excavations refers to the frontal cave talus. The layer 04 is overlying a 12 cm thick sterile layer separating it from layer 06, Chatelperronian; a sterile thin layer, 04.3bf, divides, in certain sectors, the layer 04 in two sublevels, 04inf. and 04sup.. Layer 02 is separated by a thicker low density 03 layer.

Technology

Local chert is dominant in all layers, complemented by high quality regional chert. In layer 02 the imports are dominant.

<u>04inf.</u>

Two *chaînes opératoires* finalised at the intercalated blades–bladelets knapping, but mostly at independent bladelet production. Blades are as frequent as bladelets. Bladelets are straight or slightly curved and on-axis.
Prismatic cores: the flaking surface is sub-pyramidal or sub-prismatic on the longitudinal axis, it is exploited unidirectionally. Striking platform is plain and steep-angled. Convexities are maintained by lateral blades or opposite struck flakes.
Prismatic on longitudinal narrow face/blank edge cores: the flaking surface is placed on the longitudinal narrow face of a slab or a blank, it is exploited unidirectionally.

<u>04sup.</u>

The core configurations remain similar to 04inf.. Although, blades production increase and bladelets are smaller and more curved.

<u>02.</u>

Two *chaînes opératoires* finalised at the independent production of blades and bladelets.
Prismatic cores: the flaking surface has parallel edges, and it is exploited unidirectionally. They produce large and thick blades. They are probably recycled in non-organised flake cores. Blades are straight or slightly curved.
Transversal carinated cores: the flaking surface is placed on the distal end of a blank, it is exploited unidirectionally. The striking platform is plain. The front is isolated by laterally struck flakes. Flakes are also creating a central crest shaping the distal convexity.

Typometry

Blades–bladelets dimensional threshold is put at 12 mm wide. Blades, on average, in 04inf. are 18.5 mm wide, in 04sup. 20 mm wide and in 02 22 mm wide. They record a significant difference between 04sup. and 02.

Main typological characters

04inf.

High frequency of bladelets with marginal semi-abrupt inverse continuous retouch, Dufour subtype Dufour bladelets.

04sup.

Laterally retouched thick blades, also Aurignacian blades. End-scrapers are well represented. Less and smaller retouched bladelets.

02

Aurignacian blades and nosed end-scrapers are the best represented retouched blanks.

Cultural attribution

04inf.

Attributed to the Protoaurignacian.

04sup.

Attributed to the Early Aurignacian.

02

Attributed to a later phase of the Early Aurignacian.

Isturitz (Normand et al., 2008, 2007; Normand and Turq, 2005).

Setting

It is a cave site. A big fallen rock divides in two sectors the modern excavations, the principal excavation area and the area denominated "*coupe*". The Aurignacian occupations are found in sediments characterised by the accumulation of cave vault debris, sedimentary units IV and III. Sedimentary unit V shows Mousterian occupations, the most insisted Aurignacian occupations are in sedimentary units II and III. The archaeological occupations in unit III had been affected by water run-off at the same time of deposition, which could result in material mixing. In the principal sector, layer C4c, showing mixed characters, divides layers C4b1 and C4b2 from layer C4d.

Technology

C4b1–2

The raw material is mostly regional flint collected 20 km far from the site, imports are showing a wider regional network (up to 60–80 km far) extensive long-distance network (150 km south) and one artifact coming from 200–300 km north.

Four *chaînes opératoires* are recognised. Independent blades and bladelets production.

Prismatic cores: the flaking surface has parallel edges, and it is exploited unidirectionally. The striking platform is plain, rejuvenated with total or partial tablets, the overhang is frequently abraded. The knapping starts with antero-lateral shaped crests, which maintain the convexities too. They produce blades.

Sub-pyramidal/prismatic cores: the flaking surface is placed on the longitudinal face with a convergent and distal plunging morphology, it is exploited unidirectionally. Lateral blades maintain the convexities. They produce big and straight bladelets.

Transversal carinated cores: The flaking surface is placed on the distal end of a thick blank, it is exploited unidirectionally. Convexities are maintained by lateral, off-axis, curved bladelets. They produce small curved bladelets.

Longitudinal carinated cores: the flaking surface is placed on the longitudinal edge of a blank, it is exploited unidirectionally. They produce straight bladelets.

The envisioned technique is the direct soft hammer percussion.

C4d

The raw material is mostly regional flint collected 25–30 km far from the site, some imports are coming as far as 150 km south.

Three *chaînes opératoires* are recognised. Intercalated blades–bladelets and independent bladelets production.

Sub-pyramidal/prismatic cores: similar to the same cores found in C4b1/2. The production is intercalated straight on-axis blades–bladelets.

Longitudinal carinated cores: similar to the same cores found in C4b1/2. They are more frequent. The production is independent straight on-axis bladelets.

Transversal carinated cores: similar to the same cores found in C4b1/2. They are less represented.

The envisioned technique is the direct soft hammer percussion.

Typometry

Blades–bladelets dimensional threshold is put at 12.1 mm wide, due to the presence of inverse retouch on <12 mm wide blanks.

Main typological characters

C4b1–2

Blades with lateral retouch, but very few Aurignacian blades, end-scrapers, few carinated, and Dufour subtype Dufour bladelets are the most represented.

C4d

Bladelets with lateral marginal inverse or direct retouch, Dufour subtype Dufour, are the most represented.

Cultural attribution

C4b1–2

Attributed to the Early Aurignacian.

C4d

Attributed to the Protoaurignacian.

L'Arbreda layer H (Bataille et al., 2018; Ortega Cobos et al., 2005; Soler Subils et al., 2008; Tafelmaier, 2017).

Setting

It is a cave site. The long stratigraphical sequence consists of the same lacustrine sediments, overflown from the nearby lake, and the travertine clasts of the cave. The excavation proceeds by arbitrary 5 cm thick cuts, the integrity of the archaeological occupations is given by piece-plotting and by an overall archaeological material coherence. Layer H is divided from underlying Mousterian layer I by 4 cuts of mostly archaeological sterile sedimentation, approximately the same distance separating the overlying layer G.

Technology

The raw material is exclusively good quality flint imported from 100 km north.
Three *chaînes opératoires* are recognised. Ortega Cobos and colleagues (2005) suggest the existence of independent blades and bladelets production, but Tafelmaier (2017) did not recognise any. The difference lays on the typometrical definitions of blades and bladelets.
Prismatic sub-cylindrical cores: the flaking surface is placed on the longitudinal face wide face, it is exploited unidirectionally. The striking platform is plain, and the overhang abraded. The knapping begins directly with a laminar blank knapped on a lateral natural ridge at the intersection between core's faces. The knapping rhythm is semi-circumferential. They can produce larger blades and bladelets. Bladelets are 4–7 mm wide and with straight profile.

Longitudinal carinated cores: the flaking surface is placed on the longitudinal narrow face of a blank edge, it is exploited unidirectionally. The striking platform is plain, the overhang is abraded. The back of the core ends in posterior crest used in the platform rejuvenation. The knapping begins with a central bifacial shaped crest and continues frontally, at the end the knapping can expand on a wide adjacent face. They produce smaller blades and bladelets. Bladelets are 2–4 mm wide and with straight profile.
Transversal carinated cores: for Ortega Cobos and colleagues (2005) they are the most numerous bladelets cores, Tafelmaier (2017) does not recognise the same frequency. The flaking surface is placed on a distal end of a thick blank, it is exploited unidirectionally. The striking platform is plain, the overhang is abraded. Lateral flakes isolate the front, 10–45 mm wide, and control the lateral convexities, while the distal convexity is controlled by plunging bladelets and a central shaped crest. They produce bladelets are mostly 2–7 mm wide with straight, curved, or twisted profiles.
The envisioned technique is the direct soft hammer percussion.

Typometry

Blades–bladelets dimensional threshold is based on technological and morphological assessment in Ortega Cobos and colleagues (2005), while Tafelmaier (2017) put it at 12 mm wide.

Main typological characters

Most of the retouched blanks are on-axis bladelets, Dufour subtype Dufour.

Cultural attribution

Attributed to the Protoaurignacian.

Morin (Arrizabalaga et al., 2009; Maíllo Fernández, 2006, 2005).

Setting

It is a cave site. The sub-horizontal mostly silty deposits have been affected by low energy water laminar run-off. Occupations in layers 8 and 9 are sandwiched between a Chatelperronian level 10 the Aurignacian layers 7 and 6.

Technology

8–9

The raw material is mostly local flint collected in primary deposits 5–10 km far, complemented by other varieties of siliceous material.
Three *chaînes opératoires* are recognised. One for intercalated blades–bladelets production and one for independent bladelets production. Discoid cores produce flakes.

Prismatic cores: the flaking surface is placed on the wide longitudinal face, it is slightly distally plunging and has either parallel edges or sub-pyramidal morphology, and it is exploited unidirectionally. The striking platform is plain, and the overhang is abraded. Knapping starts with cortical blade/bladelet on a natural lateral ridge, creating the convexity for the semi-circumferential knapping rhythm. Occasionally antero-lateral crests are shaped. The production is mostly geared on straight, slightly curved profiles bladelets.
Transversal carinated cores: the flaking surface has convergent morphology and is placed at the distal end of a thick blank. The striking platform is plain. The striking surface is isolated by means of lateral flakes; the guide ridges are used by twisted off-axis bladelets for maintaining the lateral convexities. They produce curved bladelets.

7

The main difference is the disassociation of blades, obtained from prismatic cores, and bladelets, obtained from transversal carinated cores, production.

Typometry

No blades–bladelets dimensional threshold is given.

Main typological characters

8–9

Laterally retouched Dufour bladelets subtype Dufour are the most indicative retouched blanks.

7

It features end-scrapers on blades, laterally retouched blades and Dufour subtype Dufour bladelets.

Cultural attribution

8–9

Attributed to the Protoaurignacian.

7

Attributed to the Early Aurignacian.

El Castillo layer 16 (Cabrera Valdés et al., 2002; Maíllo-Fernández and de Quirós, 2010; Wood et al., 2018).

Setting

It is a cave site. The front of the cave collapsed during the Pleistocene sealing layer 16, which is separated from layer 18, a contested Transitional Aurignacian layer, by the sterile layer 17. The assemblage is rather small featuring less than 300 artefacts, but indicative of the production methods.

Technology

The raw material is fine-grained quartzite.
Four *chaînes opératoires* are recognised. One for intercalated blades–bladelets production and two for independent bladelets production. Discoid cores produce flakes.
Prismatic cores: the main method used at the site. The flaking surface is installed on the longitudinal wide face, exploited unidirectionally. The striking platform is plain. The knapping begins with a cortical blank, the convexities are maintained by lateral, convergent, off-axis twisted blades/bladelets, while the centre of the flaking surface produces parallel edges, straight, on-axis bladelets. Knapping rhythm is semi-circumferential.
Transversal carinated cores: the flaking surface has convergent morphology, it is installed on a thick blank distal end, and it is exploited unidirectionally. Convergent lateral flakes maintain the convexities creating a distal central crest. Bladelets are curved or twisted.
Longitudinal carinated cores: the flaking surface is placed on the longitudinal edge, in case of carinated burin, or on the distal end of the blank, busked burin, it is exploited unidirectionally. They produce straight and distally curved bladelets.

Typometry

No blades–bladelets dimensional threshold, but most of the recognised bladelets are <12 mm wide and no blades are recognised after that size.

Main typological characters

The Dufour subtype Dufour bladelets are the most frequent retouched tools.

Cultural attribution

Attributed to the Protoaurignacian.

Labeko Koba (Arrizabalaga, 2000; Arrizabalaga et al., 2009; Bataille et al., 2018; Tafelmaier, 2017).

Setting

It is a cave site. Sterile sediments divide the Aurignacian layer VII from layer Lower IX, Chatelperronian, and the irregular layer VIII. The above Aurignacian layer VI has a sparse artefact density and separates VII from the richer layer V.

Technology

The raw material is mostly flint coming from the regional context, with long distance imports.

VII

Three *chaînes opératoires* are recognised. One for intercalated blades–bladelets production and two for independent bladelets production.
Prismatic cores: the flaking surface has parallel edges or sub-pyramidal morphology, it is exploited unidirectionally. The striking platform is plain. The knapping rhythm is semi-circumferential. Convexities are maintained by integrated laminar blanks. Blades and bladelets are intercalated, with bladelets being the focus of the production. Bladelets are big and have curved profiles.
Transversal carinated cores: the flaking surface has sub-pyramidal morphology, it is exploited unidirectionally. The striking platform is plain, placed on the blank ventral face. They produce straight and slightly curved bladelets.

Longitudinal carinated cores: the flaking surface is placed on the longitudinal edge of a blank, it is exploited unidirectionally.

V

Two *chaînes opératoires* are recognised. One for intercalated blades–bladelets production and two for independent bladelets production.
Prismatic cores: the flaking surface has parallel edges or sub-pyramidal morphology, it is exploited unidirectionally. The striking platform is plain. The knapping rhythm is semi-circumferential. Convexities are maintained by integrated laminar blanks. Blades and bladelets are intercalated, with bladelets being the focus of the production. Bladelets are big and have curved profiles.
Transversal carinated cores: this core configuration is more attested than layer VII. The flaking surface has sub-pyramidal morphology, it is exploited unidirectionally. The striking platform is plain, placed on the blank ventral face. The front is heavily isolated by two lateral flakes in most of the cases, nosed end-scrapers morphology. They produce mostly slightly curved bladelets.

Typometry

Blades–bladelets threshold is put at 12 mm wide, bladelets <7 mm are considered micro-bladelets.

Main typological characters

VII

Bladelets have a marginal semi-abrupt retouch, identified as Dufour subtype Dufour bladelets.

V

Laterally retouched blades and end-scrapers are dominant, Dufour subtype Dufour bladelets are less frequent than layer VII.

Cultural attribution

VII

Attributed to the Protoaurignacian.

V

Attributed to the Early Aurignacian.

La Viña (Santamaría Álvarez, 2012).

Setting

It is a cave site. XIIIinferior, true first Aurignacian layer is directly superimposed to XIV, Mousterian, XIIIbasal, Mousterian and Aurignacian mixing, and in some areas to the bedrock. At the base of XIIIinferior, debris is mostly vertical, contrasting the overall sub-horizontal condition of archaeological material deposition in this level. Layer XIII overlies directly and sub-horizontally layers XIIIinferior and XIIIbasal.

Technology

The raw material is mostly local quartzite, although flint imports from a wider regional context (10–50 km radius) are well attested.

XIIIinferior

Three *chaînes opératoires* are recognised. One for intercalated blades–bladelets production, one for independent bladelets production, and one for flakes issued from surface cores.
Prismatic cores: the striking platform is placed on a longitudinal wide face, it is exploited unidirectionally. The striking platform is plain, abrasion is unsystematic. The knapping begins with a laminar cortical blank on a lateral natural ridge at the cores' faces intersection. It progresses semi-

circumferentially, convexities are maintained by integrated lateral core-edge blades, neo-crests and flakes and opposite auxiliary removals. The focus of the production are bladelets, while blades are coming from the first phases of reduction.
Transversal carinated cores: the flaking surface is placed on a distal narrow edge of a thick cortical flake and it is convergent, it is exploited unidirectionally. The striking platform is plain and placed on the blank ventral surface. The flaking surface is isolated by means of lateral flakes. The production is focused on short, curved and twisted bladelets.
The envisioned technique is direct soft hammer percussion for the laminar knapping, while direct hard hammer percussion for the flakes knapping.

XIII

Three *chaînes opératoires* are recognised. One for intercalated blades–bladelets production, one for independent blades production, and two for independent bladelets production.
Prismatic cores: the flaking surface has parallel edges, and it is exploited unidirectionally. The striking platform is plain. The knapping rhythm is semi-circumferential. Most of the cores are producing blades, a minor fraction may have been recycled in bladelet cores once reduced.
Transversal carinated cores: they are the principal bladelets cores. They produce short, curved profile bladelets.
Longitudinal carinated cores: the flaking surface is placed on the longitudinal edge of a blank, it is exploited unidirectionally. They produce a minor percentage of bladelets.

Typometry

The blades–bladelets dimensional threshold is put at 12.5 mm wide.

Main typological characters

XIIIinferior

End-scrapers are well represented. Dufour subtype Dufour bladelets are less than other Protoaurignacian sites but more represented than Early Aurignacian ones.

XIII

End-scrapers, also carinated, are the most represented retouched tools. Laterally retouched blades, also featuring Aurignacian blades, are the second one. Dufour, *sensu lato*, bladelets are represented as before but manufactured on smaller blanks.

Cultural attribution

XIIIinferior

Attributed to the Protoaurignacian.

XIII

Attributed to the Early Aurignacian.

1.3.9 Synthesis

From the assemblages review no dramatic difference in raw material provisioning can be detected in the eUP: the major common point is the research of good quality material. In the Levant this is more diffused, while in Europe human groups established networks up to 300 km distance.

The Early Ahmarian is clearly divided in two different ways of exploiting the raw material, the northern *facies* preferred opposite platforms cores, while the southern one single platform cores. Also, Southern Early Ahmarian assemblages feature an independent bladelet production from longitudinal carinated cores. This difference in core configuration reflects also on the blanks obtained, opposite platform cores are more likely to be used for blades knapping, while single platform ones for bladelets knapping. This mirrors in the frequency of end-scrapers and burins on blades in the northern *facies*, while southern assemblages are more likely to use thick flakes by-products.

Surprisingly, sites in the Caucasus display a better similarity with the Southern Early Ahmarian, due to the stress on bladelets production from single platforms cores.

Single platforms cores are the rule in European eUP assemblages. The Early Aurignacian assemblages feature, generally, a bigger proportion of transversal carinated cores. Transversal carinated cores are the most represented, blanks issued from prismatic cores are often transformed in carinated cores, challenging the notion of two dissociated *chaînes opératoires*. In any case assemblages that can be confidently assigned to the Early Aurignacian tradition, eastern than the Swabian Jura, are extremely rare, in fact, only one, Kostenki 1/III. Protoaurignacian assemblages feature prismatic parallel edges and sub-pyramidal flaking surfaces, alongside to longitudinal narrow face core configurations on slabs or blanks.

The totality of the reviewed eUP assemblages reveals a non-extensive preparation of cores. The striking platform is left plain most of the times, abrasion or micro-chipping of the overhang is the only common operation. The cores having natural convexities are preferred. Embedded convexities' maintenance through lateral, off-axis and, possibly, slightly twisted is a common feature. The *lamelles croisées* in Mandrin and l'Observatoire might be a regional variant of crest shaping. Bladelets are the sought blanks size.

1.4 Critiques to the Aquitanian model and the record of Central–Eastern Europe

Many authors in the last years have criticised the imposition of the so-called Aquitanian model as an overall explanation of the Aurignacian development in Europe. H. Delporte noticed:

La séquence archéologique, qui y a été établie par Denis Peyrony (Peyrony, 1933), a en effet été abusivement imposée à d'autres régions, plus ou moins lointaines, voire à l'ensemble du continent eurasiatique (Peyrony, 1948). En fait, la recherche récente montre que cette séquence est spécifique du Périgord et qu'elle ne se retrouve pas identique dans d'autres régions, même voisines [the archaeological sequence established by Denis Peyrony, has been abusevely imposed to other near or far regions, indeed to the whole Eurasia. In fact, recent investigations show that the Peyrony sequence is specific to the Perigordian region and that it is not found identical in other regions, even if nearby.] (Delporte, 1991, p. 243)

Effectively the record of Central and Eastern Europe fails to be completely restricted in the dichotomy Early Aurignacian–Protoaurignacian:

The Banat sites are showing mixed characters, leading the authors to coin the Aurignacian 0.5 (Sitlivy et al., 2014b).

The Kostenki–Borschevo complex shows some local technocomplexes like the Streletskian and the Spitsynian which are not conforming to any Western assemblages (Bataille et al., 2018; Monigal et al., 2006). The same applies for other Eastern European assemblages (Monigal et al., 2006).

In the Swabian Jura, Hohle Fels AHIV assemblage, chronologically comparable with AHII in Geißenklösterle, is more aligned with an Evolved Aurignacian, due to the massive presence of longitudinal carinated cores and it "*highlights technological and typological variability that deviates from the western European chronological model"* (Bataille and Conard, 2018a, p. 38).

The record of Western Europe has been revised:

In Italy the Protoaurignacian seems to extend chronologically without dramatic changes in techno-typology (Falcucci, 2018; Gambassini, 1997; Palma di Cesnola, 2006; Riel-Salvatore and Negrino, 2018). No sites feature the stratigraphical succession between Protoaurignacian and Early Aurignacian, except from Mochi, where it is mostly signalled by the increased occurrence of antler working (Tejero and Grimaldi, 2015).

In South-eastern France the Early Aurignacian is virtually absent too (Onoratini, 2008).

Tafelmaier (2017) notices in her reassessment of Iberian Early Aurignacian and Protoaurignacian assemblages that:

Firstly, a highly variable independent bladelet and microblade production could be identified within the Protoaurignacian assemblages (Tafelmaier, 2017, p. 162)

Contrasting with the view of a Protoaurignacian entirely centred on a continuous reduction from blades to bladelets, reducing the role of the bladelets to undifferentiated technological role. On the contrary her and Falcucci's analyses show how blades in Protoaurignacian knapping are mostly performing shaping and supporting roles, while bladelets are the focus (Falcucci et al., 2017; Tafelmaier, 2017).

Also, she points to the presence of the purportedly typical Aurignacian typological markers as carinated end-scrapers in Protoaurignacian assemblages and she does not consider the slight increase of these in Early Aurignacian assemblages to be determinant for conclusively attributing to the Early Aurignacian the Spanish assemblages she analysed (Tafelmaier, 2017).

To be fair, the initial introducer of the Early Aurignacian techno-typological definition, F. Bon, always acknowledged the presence of an independent bladelet knapping and Aurignacian tool types in Protoaurignacian assemblages, but he pointed to the dramatic difference in shares of carinated end-scrapers between the Protoaurignacian and the Early Aurignacian (Bon, 2002a, 2002b).

One of the flagbearers of the Early Aurignacian entity clearly wrote that the technocomplex is not supposed to be found necessarily on a pan-European scale:

Here we define the Early Aurignacian not only as a typo-chronological event (e.g. Peyrony's Aurignacian I), but more generally as a specific typo-techno-economic package, which cannot be defined as a pan-European event (Teyssandier, 2003). (Teyssandier et al., 2006, p. 249)

Also Teyssandier pointed out that the dating of Willendorf II AH 3 makes it completely isolated from the Aquitanian Early Aurignacian technocomplex it has been attributed to, implying that the Early Aurignacian is probably a phenomenon restricted to South-western France (Teyssandier and Zilhão, 2018).

The introduction of the SBP, might be an adaptation to colder and more arid climatic conditions around 40 k cal BP, regardless the assemblages they are associated with (Bodu et al., 2013; Doyon, 2017; Laplace, 1966; Moreau et al., 2015; Tartar, 2015; Tejero and Grimaldi, 2015). Hence, linking the SBP with solely the Early Aurignacian is no more entirely legitimate.

Finally, there is a tendency in modern literature to reject the notion of Protoaurignacian and Early Aurignacian as chronologically bound phases or distinct traditions, but instead conceiving them as adaptive behaviours with strong regional signature (Bataille et al., 2018; Riel-Salvatore and Negrino, 2018; Tafelmaier, 2017). All these considerations invite for general revision of the eUP techno-cultural model.

1.5 Theories of AMH dispersal into Eurasia and the Danube Corridor Hypothesis

The dispersal of AMHs from Africa is a complex and heated debate. The fossil evidence is scarce and controversial, most of the times they are not associated with archaeological material and this alone cannot provide a safe species attribution at least for continental Asia and the Sunda islands, given the plethora of human forms populating these lands. Here only AMH fossil data will be discussed.

Recent data show that the early XX-discovered *Homo sapiens* fossils of Qafzeh and Skuhl, both located in Israel and dated between ≈130-90 k BP, are not the oldest and the only evidences of *Homo sapiens* pulsations from Africa to SW Asia (Groucutt et al., 2018, 2015; Hershkovitz et al., 2018). It has been suggested that groups of AMHs reached SE Asia as early as 120-80 ka BP or 63-73 ka BP on the grounds of dental remains (Groucutt et al., 2018; Liu et al., 2015; O'Connell et al., 2018). This latter evidence has been contested due to U/Th dating method controversies, effective stratigraphical association of dated material with human fossils or just because of the impossibility to ascertain safely the real stratigraphical position of the fossils (Michel et al., 2016; O'Connell et al., 2018). AMH cranial and maxillary fragments attributed to a single female individual have been found in Tam Pa Ling cave, Laos, in sediments dated through radiocarbon and OSL at 46–51 ka BP and directly dated with U/Th at 63.3 ± 6 ka BP (Demeter et al., 2012). The best preserved AMH burials in Asia/Oceania are those of Lake Mungo, New South Wales (Australia); sediments associated with Mungo I, probably cremated human rests, and Mungo III, articulated skeleton, are dated by OSL at 40 ± 2 kyr, while a lower layer containing artefacts is dated between of 50.1 ± 2.4 and 45.7 ± 2.3 kyr (Bowler et al., 2003; O'Connell et al., 2018). An AMH femur was found in Ust'-Ishim, Western Siberia, and directly radiocarbon dated at 45,9–42,9 k cal BP at 95.4% probability (Fu et al., 2014; van der Plicht et al., 2020). The retrieved genome shows more similarities with those of modern East-Asians and pre-Neolithic Eurasian individuals, showing as well a degree of Neanderthal admixture of 2.3 ± 0.3% and allowing an estimation of admixture occurrence between 50–60 k cal BP (Fu et al., 2014). AMH remains from two different layers of Ksar Akil, Lebanon, are dated to 41.5–38.3 k cal BP (modelled at 95.4% probability), associated with an Early Ahmarian context, and to 42.8–41.5 k cal BP (modelled at 95.4% probability), associated with Initial Upper Palaeolithic context (Bergman and Stringer, 1989; Douka et al., 2013). An older determination is available: 43.2–42.9 k cal BP for the Ahmarian fossil and a minimum age of 45.9 k cal BP for the IUP fossil (Bosch et al., 2015). Üçağızlı cave, Hatay in S. Turkey, has yielded AMH teeth in Early Ahmarian and IUP contexts dated respectively to 42.8–32.2 k cal BP and 45.9–37.1 k cal BP (Bosch et al., 2015; Kuhn et al., 2009). Additionally, a AMH calvaria found without context in the sealed site of Manot cave in Israel provides a minimum age of 54.7 ± 5.5 kyr ago (arithmetic mean 2σ) or 51.8 ± 4.5 kyr ago

(weighted mean 2σ), estimated through the U/Th determinations of the calcite crust adherent to the fossil (Hershkovitz et al., 2015).

Therefore the most accepted fossil and genomic data in Asia are compatible with an AMH dispersal out of Africa between 50 and 60 ka cal BP (O'Connell et al., 2018).

The oldest AMH remains in Europe are associated with two non-Aurignacian industries: the Uluzzian in Italy and the Initial Upper Palaeolithic (Bachokirian) in Bulgaria. Two deciduous molars, found in association with the transitional Uluzzian technocomplex, at Grotta del Cavallo, Apulia Italy, are attributed to AMH on morphological and enamel thickness grounds; they were found in layers EIII and EII-I, respectively dated to 45.0–43.4 k cal BP (modelled at 68.2% probability) and 44.0-43.0 k cal BP (modelled at 68.2% probability) (Benazzi et al., 2011). Though, the stratigraphical and morphological attribution is contested (Banks et al., 2013; Zilhão, 2013) (for a reply over the stratigraphical integrity (Ronchitelli et al., 2014)). The tooth and various indeterminable remains of Bacho Kiro layers I and J (former layer 11 and sublevels) are directly dated to 46.8–42.8 k cal BP (modelled at 95.4% probability) (Hublin et al., 2020).

European UP human finds are rare too. The Romanian site of Peştera cu Oase yielded exceptional remains, unfortunately without archaeological context, of an AMH mandible and a cranium, attributed to two different individuals, dated to 41.9–37.7 k cal BP at 95.4% probability (Rougier et al., 2007; Trinkaus et al., 2012, 2003; van der Plicht et al., 2020). The mandible Oase 1 yielded 7.3% of Neanderthal genome, much higher than later prehistoric individuals and modern non-Africans, estimating a close Neanderthal ancestry (fourth-, fifth- or sixth-degree relative) (Fu et al., 2015). The AMH mandible, allegedly associated with two Aurignacian blades, from Kent's Cavern, Cornwall UK, is dated to 43.1–41.9 k cal BP (modelled to 68.2% probability) (Higham et al., 2011). The stratigraphical reliability was disputed, but new analyses and dates of the sequence show an overall coherence and the few outliers are attributed to post-depositional limited-extent intrusion of younger material (Proctor et al., 2017; Zilhão, 2013). The deciduous incisors found in Protoaurignacian layers of Fumane cave and Bombrini shelter are attributed morphologically and genetically to AMHs and they are dated respectively to 41.1–38.5 k cal BP and 40.7–35.6 k cal BP (modelled to 68.2% probability) (Benazzi et al., 2015). Teeth clearly associated in Early Aurignacian context dated to 30–34 k uncal BP at Brassempouy, Landes (France), are attributed morphologically to AMHs (Bailey and Hublin, 2005). In addition human remains from eUP contexts from the Kostenki sites complex, Russia, are dated to 38.8–35.7 k cal BP, Kostenki 1 Layer III, and 38.7–36.2 k cal BP, Kostenki 14 (Benazzi et al., 2015; Hublin, 2015; Seguin-Orlando et al., 2014). Thus, AMHs are associated with eUP industries in Europe at least from ≈41 k cal BP.

Later human remains, representing several males, females and one child, are those of Mladeč, Czech Republic, dated to 31 k uncal BP (36.7–34.6 k cal BP) and associated with bone points, the Mladeč flat polished bone points (Nejman et al., 2011; Svoboda, 2001; Wild et al., 2005). Broadly

contemporaneous human remains are those of Peştera Muieri and Peştera Cioclovina, Romania, found without or with undiagnostic archaeological context (Alexandrescu et al., 2010).

If human remains are suggestive of at least two waves of dispersal into northern Eurasia, one between 50–45 k cal BP and a later one between 43–41 k cal BP, scholars have tried to resort to the notably more abundant lithic evidence.

As per the first wave, authors are suggesting that the Bohunician and the Bachokirian technical behaviour of central and Balkan Europe, must be related to the IUP of the Levant (Škrdla, 2003; Tostevin, 2000). Even sites in the Altai and Mongolia have been ascribed to the IUP, therefore explaining Ust'-Ishim fossil (Zwyns et al., 2019, 2012).

Many others have repeatedly suggested the similarities between the Protoaurignacian and the (Southern) Early Ahmarian (Anderson et al., 2015; Barzilai et al., 2016; Bon, 2002b; Bordes, 2006; Hoffecker and Holliday, 2014; Onoratini, 2008; Teyssandier, 2007, 2006; Tsanova et al., 2012). Recently, instead of the classic South-to-North Ahmarian dispersal, the opposite has been suggested, therefore further complicating the role of the Southern Early Ahmarian as the European UP direct precursor (Richter et al., 2020).

The claim of the Protoaurignacian roots in the Early Ahmarian is highly dependent on the dating of the technocomplex, hence, it is suggested or dismissed by the different dating determinations (Barzilai et al., 2016; Bosch et al., 2015; Douka et al., 2013; Kadowaki et al., 2015).

P. Mellars gave strength to this idea, compiling data and dates supporting an origin of the European Upper Palaeolithic in the Levant. In his opinion, all the characters of the Aurignacian and the Protoaurignacian, which he removed from the Aurignacian family calling it Fumanian, are present in the Levantine UP.

He figuratively envisioned a northern dispersal route, via the Danube valley, giving birth to the Early Aurignacian and a southern coastal route originating the Fumanian, interestingly sites represented on the map are identified on the grounds of SBPs recovering (Mellars, 2011, 2006a, 2006b, 1992). The absence of a UP record in Turkey, which practically hampers the continuous East-to-West dispersal, is almost ignored because of "*our virtual ignorance of early Upper Paleolithic technologies in most parts of Turkey"* (Mellars, 2006b, p. 176).

This dispersal model, in particular the role of the Danube as a movement axis, was evaluated through the density of Aurignacian, broad sense, sites in Central and South-eastern Europe. The authors of the study define a Transalpine and a Cisalpine route, divided by the gap represented by the Pannonian (Carpathian) basin; the Danube becomes an important movement axis only in its upper course, at the same time, the Protoaurignacian route is not passing along the Adriatic coast, but using the river Save and Drau (Floss et al., 2016). It must be noticed that to achieve these results, the authors used the whole Aurignacian timespan, did not make difference between sites' size and included debated sites too.

N. Conard and M. Bolus elaborated the most famous models of appearance of UP in Europe and the dispersal of AMHs:

Two models developed in Tübingen in connection with the sites of the Swabian Jura are the Danube Corridor and Kulturpumpe models (Conard, 2002a,b; Conard and Floss, 2000; Conard et al., 1999). The former postulates that modern humans rapidly entered the interior of Europe via the Danube Valley. The latter model presents competing working hypotheses to explain the early advent of fully modern behavior and the cultural innovations of the Aurignacian and Gravettian in the Swabian Jura. (Conard and Bolus, 2003, p. 333)

Both models rely on the early dates of the Swabian Jura Aurignacian (Conard and Bolus, 2003; Higham et al., 2012).

How to interpret Geißenklösterle early Early Aurignacian? at the moment, it stands out from other Early Aurignacian assemblages: the only assemblages dated as early are those of Labeko Koba VII, La Viña XIIIinferior and Isturitz C4d1, all attributed to the Protoaurignacian (Barshay-Szmidt et al., 2018; Wood et al., 2014). Willendorf II AH 3 dates are not considered here due to the reasonable doubts about the Early Aurignacian attribution on technological grounds. Repeating the concerns expressed for Willendorf II AH 3 (Teyssandier and Zilhão, 2018), it is difficult to conceive the viability of the *Kulturpumpe* model if the Early Aurignacian technical tradition is considered disjointed from the Protoaurignacian one, as in the Aquitanian model.

As for the Danube Valley, the archaeological record, though not contradicting the model, is not either suggestive of any coherent and quick advance of AMH carrying with them the Aurignacian technical package. There is a general scarcity of early sites safely attributable to the Aurignacian and the Bachokirian and the Bohunician sites in Bulgaria and Central Europe, frequently used in the Danube narrative, seem to be part of a rapid pulse unrelated with subsequent Aurignacian–Protoaurignacian population (Chu, 2018; Chu et al., 2018; Hublin et al., 2020).

An alternative dispersal hypothesis is through the Caucasus and the Eastern plains (Chu, 2018; Hoffecker and Holliday, 2014), despite being suggestive and having the credit of resolving the Anatolian gap, at the moment it does not seem more viable than the Danube way. In fact, the EUP from Caucasus has no earlier dating than the European eUP record, it has affinities with the Early Ahmarian, while the earliest occurrences of eUP in Eastern Europe, mostly Kostenki-Borschevo, cannot be ascribed to the Early Ahmarian–Protoaurignacian technical behaviour (Bataille et al., 2019; Hoffecker and Holliday, 2014; Monigal et al., 2006; Pleurdeau et al., 2016).

Hence, no relatively simple diffusion and development of the eUP (Anderson et al., 2015; Conard and Bolus, 2003) is supported so far.

1.6 Dating the eUP

One of the issues of Archaeology is the correct chronological order of the findings. The issue involves relative chronology, linked to the correct recognition of depositional processes forming the stratigraphical sequences containing the archaeological occupations, and absolute chronology, linked to the assignation of a numerical date to archaeological occurrence.

For the Palaeolithic, in general, and, in particular, the Transition from Middle-to-Upper Palaeolithic, which comprises the eUP as its termination, the right stratigraphical collocation and identification of the archaeological findings, has always played an important role. The debate over the right chrono-stratigraphical position of the Aurignacian, which has been sketched above, is a clear example.

On the other hand, with the progress of the research new questions arise and a more precise chrono-stratigraphical framework is required. eUP chronology has been refined through the years due to the advancements in absolute dating methods using the decay of radioactive isotopes (mainly ^{14}C and Uranium/Thorium) (Douka and Higham, 2017; Higham et al., 2009; Hoffmann et al., 2018a; Mellars, 2006a; Reimer et al., 2013), the luminescence expressed by trapped electrons (Thermoluminescence and Optical Stimulated Luminescence) (Jacobs et al., 2015; Klasen et al., 2013; Richter et al., 2009), the refinement of stratigraphical sequences and understanding of post-depositional and accumulation processes (mainly through the new discipline of Geo-archaeology) (Goldberg et al., 2009; Karkanas and Goldberg, 2018), and the recognition of pan-Continental or regional stratigraphical well-dated markers (tephras, especially the Campanian Ignimbrite, and the Heinrich Event 4)(Banks et al., 2013; Fedele et al., 2003; Giaccio et al., 2017, 2008; Heinrich, 1988; Hemming, 2004). All these methods, in particular the ^{14}C, are bringing solutions and problems, here I will briefly show what is their contribute to the eUP understanding.

^{14}C: discovered in the late 1940s, it measures the ratio, in organic matter, between the carbon radioisotope ^{14}C and the stable isotope ^{12}C: the theory is that while the living being is alive it acquires a constant quantity of both, upon death, ^{14}C is constantly decreasing, halving every 5730±30 years (Bradley, 2015a; Mellars, 2006a; Reimer et al., 2013). It has an effective limit of ≈50 k years, reached in the mid-2000s (Douka and Higham, 2017). All dates are followed by BP, before present, conventionally taken as AD 1950, when they are calibrated are cal BP(Reimer et al., 2013; Wood et al., 2012).

Dating with an accelerator coupled with a mass spectrometer, AMS, allows for small samples 0.5–2 mg of carbon to be measured, this has advantages such the possibility of a more aggressive pre-treatment, sub-division of the sample and multiple testing, sampling a less contaminated area, but also disadvantages like less isotope ratio stability, contamination plays a bigger role, sampling a non-representative part of an heterogeneous material (Bradley, 2015a; Bronk Ramsey et al., 2004b; Douka and Higham, 2017). Pre-treatment is a key stage of the measurement, since it is the least reproducible and more difficult to check for accuracy (Bronk Ramsey et al., 2004b). Contamination

is a serious issue, a 2% of modern carbon on a sample that real age is 40 k BP will result in an AMS measurement of 29 k BP (Douka and Higham, 2017).

Bone is a complex material to date, common pre-treatments such as demineralization and acid-base-acid remove the most ubiquitous contaminants and the humic elements contained in soils, but they leave organic molecules and degraded proteins fragments. Therefore a second treatment is applied, the ultrafiltration, which, through a molecular sieve, selects high-molecular-weight protein molecules more likely being part of the original bone collagen, it is more important in older samples and it gives older dates (Bronk Ramsey et al., 2004a; Douka and Higham, 2017; Jacobi et al., 2006). Charcoal is pre-treated with the acid-base oxidation followed by the stepped combustion method (ABOx-SC). The method consists of concentrated Acid-Base washes, followed by an oxidation of the charcoal and finally removing any labile components through low temperature combustion: this way, Oxidation Resistant Elemental Carbon is obtained and it gives older and more reliable dates. The sample needs to retain at least 50% of carbon, otherwise the concentration of contaminants leads to erroneous dates (Higham et al., 2009; Wood et al., 2012).

Another dating material are shells found in Palaeolithic contexts and believed to be collected as fresh specimen to be used in ornaments' manufacture (Douka et al., 2013). Shell carbonate can be more unstable than wood, charcoal, or bone carbon, because during diagenesis it can dissolute, recrystallize or be replaced. Pre-treatment for shells is carbonate density separation, CarDS; density separation ensures that material is separated, within an intermediate density fluid, in lower density particles floating on top and bigger density particles sinking, therefore separating the original aragonite from the lighter diagenetic calcite (Douka et al., 2010).

Since the atmospheric carbon isotopes' concentrations are changing through time due to variations in production rate and carbon cycle, a ^{14}C measurement do not equate to calendar years, hence, they need calibration against known absolute-dated record incorporating carbon at the time of formation: tree rings, plant macrofossils from varved sediments, speleothems, non-varved marine sediments and corals (Reimer et al., 2013; van der Plicht et al., 2020) The independent calibration curve, obtained firstly in 2009, allows for the comparison between dates obtained with different methods and the creation of Bayesian models and comparisons with data from climate records such as the Greenland ice core (Douka and Higham, 2017).

Any ^{14}C date has a range which includes the shortest interval in which the event falls at 95% probability or 68% (Bronk Ramsey, 2009a). A date can be wrong, i.e. non-fitting the context that is supposed to date, in this case it is called an outlier. Outliers can be removed manually; in this case the date is rejected on the grounds of arbitrary considerations with the possible help of statistical analysis defining how much agreement there is between the various dates and excluding the ones falling behind 60% agreement. Outliers can also be removed setting up statistical models which identify the probability of a date of not being in agreement with the others and down-weight it in the final PDF (Bronk Ramsey, 2009b; Higham et al., 2010). Bayesian modelling helps in determining

the reliable dates inserting prior assumptions as stratigraphical and archaeological information, the position of the sample in the stratigraphy and the confidence about the sample itself (Douka and Higham, 2017).

Uranium/Thorium: this dating method exploits the decay of the radioisotopes of uranium into thorium. It is applied to speleothems, where the uranium accumulates in solution with carbonate. With the passing of time, the decay transforms the uranium in the insoluble thorium, therefore, more thorium is present more ancient is the carbonate crust. Obtained ages are highly precise, but the method is applicable only in karst setting where a continuous carbonate deposition and a closed system, i.e. no deposition of new thorium, is assumed (Bradley, 2015a; Hoffmann et al., 2018b).

Tephra: all the pyroclastic material ejected during a volcanic eruption is referred as tephra. In explosive eruptions, this material covers large parts of the landscape, thus forming an isochronous stratigraphical marker; when it is invisible at naked eye it is called cryptotephra and it is generally distributed in a bigger area than the tephra itself. It can be dated through potassium-argon and fission-track methods on the same pyroclastic material or through other methods on included, for instance organic, material (Bradley, 2015b). The most significant tephras for the European eUP are the Campanian Ignimbrite (CI) and the Codola, both originated from the volcanic area around Naples. The CI deposits originated from the explosion of the Phlegrean Fields, north of Naples, which led to the largest volcanic eruption occurred in the Mediterranean in the past 200 k years. Its marine deposits in the Eastern Mediterranean are named Y5 or C–13 (Fedele et al., 2003; Giaccio et al., 2008). The CI is dated at 39.85 ± 0.14 k cal BP through $^{40}Ar/^{39}Ar$ dates on sanidine crystals and ^{14}C dates on a charred tree branch found in the deposits (Giaccio et al., 2017). CI deposits is accumulated over a large area comprising the whole Eastern Mediterranean, the southern Balkans and the southern Russian plains. (Fedele et al., 2003; Giaccio et al., 2008). The CI produced deposits of pumices, relative to the Plinian fallout, followed by grey and yellow tuffs, originated by the pyroclastic products, up to 80 km far from the origins. Two different chemical types of magma, coming from a more evolved upper layer and a less evolved lower layer, fed the CI eruption: the double composition is a chemical marker for recognising deposits in far settings. The CI occurs in UP sites at Serino, Castelcivita, Temnata and Kostenki-Borshchevo: at Serino, the closer site to the eruption origin, the pumices and tuffs deposits cover the human occupation, in Castelcivita the deposit consists of mm-to-cm thick basal pumice layers followed by grey ash, in Kostenki-Borshchevo the deposits are Y-shaped glass shards associated with K-feldspar and rounded quartz, it is mostly recognised chemically (Giaccio et al., 2008).

The Codola deposits are originated from an eruption of the Somma–Vesuvius volcano, they are characterised by basal fine and grey ashes, pumice lapilli fallout, followed by layers of grey coarse ashes and thin lapilli with brown and black scoria. The Codola terrestrial deposits correspond to the C–10 in the Thyrrenian marine setting, dated to 34 k cal BP. It is found as grey micro–scoria

fragments and dark–coloured glass shards with crystals of clinopyroxene and feldspar on top of the Protoaurignacian in Paglicci (Giaccio et al., 2008).

Ice-core chronology: powerful and well stratified continental climatic records are found in the long ice-cores, the reference for the Northern Hemisphere is the northern Greenland ice-core (NGRIP), which provides an ice accumulation until 123 k cal BP (North Greenland Ice Core Project members, 2004). Within the core, measurement of the oxygen isotopes $^{16}O/^{18}O$ ($\delta^{18}O$) are representative of temperatures, a more positive $\delta^{18}O$ is correlated with warmer temperatures a more negative with colder ones: observing the millennial trend, marine isotopic stages (MIS), phases of ice expansions and retreats, are defined (Sanchez Goñi and Harrison, 2010; Wolff et al., 2010). The annual ice deposition is recognised through the correlation of visual stratigraphy and peaks of concentrations of water-soluble ions, especially sodium (Na^+) and calcium (Ca^{2+}), electrical conductivity measurements and electrolytic melt water conductivity (Andersen et al., 2006; Svensson et al., 2008). Combining the $\delta^{18}O$ record with the values of Na^+ and Ca^{2+}, a good correlation is noticed: warmer temperatures mean less Ca^{2+}, representative of terrestrial dust, and less Na^+, less water salinity, and vice versa (Ram and Koenig, 1997; Wolff et al., 2010). Within the isotopic stages, there are temperature oscillations showing a consistent pattern of rapid temperature spiking, a middle part with gradual moderate cooling and a final part with a drastic cooling low-peak: these oscillations are the Dansgaard–Oeschger (D–O) events, 25 in the last glacial period (Rasmussen et al., 2014; Wolff et al., 2010). The D–O warm spikes are named Greenland Interstadials (GI) while the cold lows are named Greenland Stadials (GS); the GIs are traditionally the most visible and gets a progressive numeration through depth, the coupled GSs are getting the same numeration (Rasmussen et al., 2014; Svensson et al., 2008; Wolff et al., 2010). Once obtained the high-definition annual accumulation, the depth can be correlated to calendar years due to the comparison with known chronologies from speleothems, tephras and elements linked to particular events (Svensson et al., 2008). The eUP is all comprised in the MIS 3, 59.4–27.8 k cal BP, and specifically in the GI-11 to 8, with particular reference to GS-9, 39.9 k cal BP (Rasmussen et al., 2014; Sanchez Goñi and Harrison, 2010).

Ocean sediment cores show a cyclical increase of ice-rafted detritus, sediment released by melted floating ice, these are named Heinrich layers or Heinrich events (HE). While in the North Atlantic the detritus deposition is contemporaneous to the cooling event, in the South Atlantic it marks only the last plunge of it, therefore GS characterised by HE can be named Heinrich Stadials (HS) (Sanchez Goñi and Harrison, 2010). HE duration and age are determined through ^{14}C dates and $\delta^{18}O$ of the sediments. HS 4 is the biggest and most recognizable it is dated to 40.2–38.9 k cal BP, corresponding to GS 9 and GS 8 (Heinrich, 1988; Hemming, 2004; Sanchez Goñi and Harrison, 2010).

Luminescence: both Thermoluminscence (TL) and Optical Stimulated Luminescence (OSL) work on the principle that materials accumulate free electrons due the environmental radiation. When they are exposed to heating over 400°C, in the case of TL, or to solar power for enough time, OSL, electrons are freed, the material is said to be bleached, and the accumulation of electrons can start

again. The luminescence is function of the liberation of electrons trapped over time, therefore showing the time passed from the last bleaching event (Bradley, 2015a; Douka and Higham, 2017; Jacobs et al., 2015; Richter et al., 2009). For dating, an equivalent dose, the amount of radiation needed for producing the luminescence, and the dose rate, the rate of exposure of grains to radiation of burial time, must be found (Bradley, 2015a; Jacobs et al., 2015). The dated material in TL is mostly heated flint artefacts, in OSL grains of quartz or feldspar (Bradley, 2015a; Jacobs et al., 2015; Richter et al., 2009). TL and OSL are mostly used when the organic preservation is low and/or ^{14}C dates cannot be retrieved/relied on. The TL is preferable because the dated event is more safely linked to the human occupation (discard of a flint artefact and heating in a human-made fire), while the OSL needs the assumptions of being non-disturbed soil buried right after or contemporaneously with the human occupation (Jacobs et al., 2015; Richter et al., 2009). When compared to ^{14}C dates the standard deviation is sensibly bigger (Jacobs et al., 2015).

For a good chronometric understanding more methods should concur to the determination (Douka and Higham, 2017).
After the review of the main dating methods, it is now time to discuss if they can resolve the main eUP the chronological issues:

Is the Protoaurignacian older than the Early Aurignacian?
Is the Early Ahmarian older than the Protoaurignacian, and a possible source for the (Proto)Aurignacian development?

Despite a good number of sites had been re-dated with modern procedures, it has been shown that no coherent chronological development is available for the eUP record at continental scale. In fact, the oldest European assemblages are showing largely overlapping intervals with no structure, i.e. Protoaurignacian older than the Early Aurignacian or eastern sites older than western sites (Barshay-Szmidt et al., 2018; Bataille et al., 2018; Nigst et al., 2014; Tafelmaier, 2017). The role of continental scale climatic markers like the HE 4 or the CI is not clear, for instance the Italian Protoaurignacian continued well after (Falcucci, 2018; Giaccio et al., 2008; Riel-Salvatore and Negrino, 2018).
As for the Early Ahmarian, the only modern dated sites are northern Levant cave sites. They do show two patterns, an early chronology, starting around 46 k cal BP (Alex et al., 2017; Rebollo et al., 2011), or a chronology mostly contemporaneous with the European eUP (Bosch et al., 2015; Douka, 2013; Douka et al., 2013; Kuhn et al., 2009). The disagreeing radiocarbon determinations obtained by Bosch and colleagues (2015) and Douka and colleagues (2013) on the same material of Ksar Akil show how difficult is to have a precise age determination of a human occupation.
Waiting for the always-coming technical improvements, it seems that nowadays dating is not able to help in discerning the fine behavioural development in the eUP.

1.7 Chapter synopsis and research question formulation

The Aurignacian is the principal European cultural unit associated with the spread of the Upper Palaeolithic and of Anatomically Modern Humans. Its characteristics are laminar volumetric lithic production, geared on the massive bladelet production, bone and antler technology, widespread production of ornaments and symbolic objects and use of ochre. It has been divided in two technical traditions: the Early Aurignacian and the Protoaurignacian. The Early Aurignacian shows a production of thick blades from unipolar parallel edges prismatic cores, and, mostly, production of short slightly curved bladelets from transversal carinated cores on thick flakes and blades coming from the prismatic cores. The Protoaurignacian is more versatile; it shows a production of straight parallel edges or convergent bladelets mostly from unipolar parallel edges prismatic or convergent sub-pyramidal cores, but also from longitudinally and transversally carinated cores. The purported technological difference between the Early Aurignacian, featuring strictly disassociated blade and bladelet productions, and the Protoaurignacian, having a continuous blades-to-bladelets reduction, is questioned by several scholars. Early Aurignacian bladelets are rarely retouched, while Protoaurignacian ones are frequently transformed by lateral or bilateral marginal inverse, direct or alternated semi-abrupt retouch, identifying them as Dufour bladelets. Protoaurignacian assemblages always precedes Early Aurignacian ones in stratigraphical sequences, but they are mostly chronologically undistinguishable at the Continental scale starting both around 43–42 k cal BP. Early Aurignacian assemblages in Spain and Italy have been lately revised and not being found dramatically different from Protoaurignacian ones, the only clear occurrences of Early Aurignacian are those in South-western France and Geißenklösterle AHIII/AHII, Swabian Jura. Split-base antler points, once believed as Early Aurignacian chrono-typological hallmark, have partially lost their role and now they are ascribed to a general early Upper Palaeolithic technical behaviour. The Early Ahmarian is the earliest true Upper Palaeolithic technocomplex of the Levant. Its characteristics are laminar volumetric lithic production, the production of ornaments mostly from shells and the use of ochre. The Early Ahmarian is divided in two *facies*, the northern and the southern. The main difference is the adoption of bipolar cores in the Northern Early Ahmarian. The Southern Early Ahmarian shows a production of slender blades and bladelets from unipolar narrow-fronted cores and minor production of bladelets from longitudinal carinated cores. Blades and bladelets are transformed by lateral or bilateral marginal direct semi-abrupt and backed retouch, identifying them as el-Wad points. The Early Ahmarian is probably contemporaneous to the Early Aurignacian/Protoaurignacian. Anatomically Modern Humans started dispersing in Eurasia from Africa and SW Asia around 60–50 k cal BP, seemingly they dispersed in Europe around 43–42 k cal BP, no consensus has been reached so far on the route and the modality they followed. Dating methods advancement in the last 20 years have mostly retro-dated the eUP, but limits, as the

uncertainty given by standard deviations, are not helpful in tracing the, probably, rather quick dispersal.

As shown by the chapter, technological analysis has been applied to the early Upper Palaeolithic only recently, i.e. in the last 20 years. There is a lack of consensus in the technological description of the technocomplexes and the debate shifted mostly on radiocarbon dating, whose contribution to the understanding of cultural human behaviour development is rather limited. Repeated claims of a similarity between the Early (Southern) Ahmarian and the Protoaurignacian have been advanced, but, so far, no comprehensive technological comparison has been published or carried on (Kadowaki et al., 2015; Teyssandier et al., 2010; Tsanova et al., 2012). Therefore, this Ph.D. thesis will devote to present a technological first-hand analysis of three assemblages coming from stratified contexts, dated to the eUP timeframe, and previously attributed to the above-mentioned technocomplexes. The aim is to assess whether a common technological signature is present and to give a meaningful contribution to the eUP cultural behaviour development.

2. Material & Methods

The chapter illustrates the site context of the studied assemblages 2.1. Follows up with the sampling protocol 2.2, describing how the study samples were obtained. The analysis protocol is described in 2.3, firstly illustrating the *chaîne opératoire* (CO) approach and, secondly, the actual steps of data recording. Finally, morpho-technological and typometrical attributes are described in length in 2.4.

2.1 Sites

2.1.1 Al-Ansab

The site of Al-Ansab 1 is situated in the context of the uplifted rift connected to the Dead Sea characterising western Jordan (Bertrams et al., 2012; Klasen et al., 2013). In particular, the site was found on a slope of the northern side of the smaller Wadi Al-Ansab, at the confluence with the main Wadi Sabra (E 35.383, N 30.234) (Richter et al., 2020; Schyle, 2015).

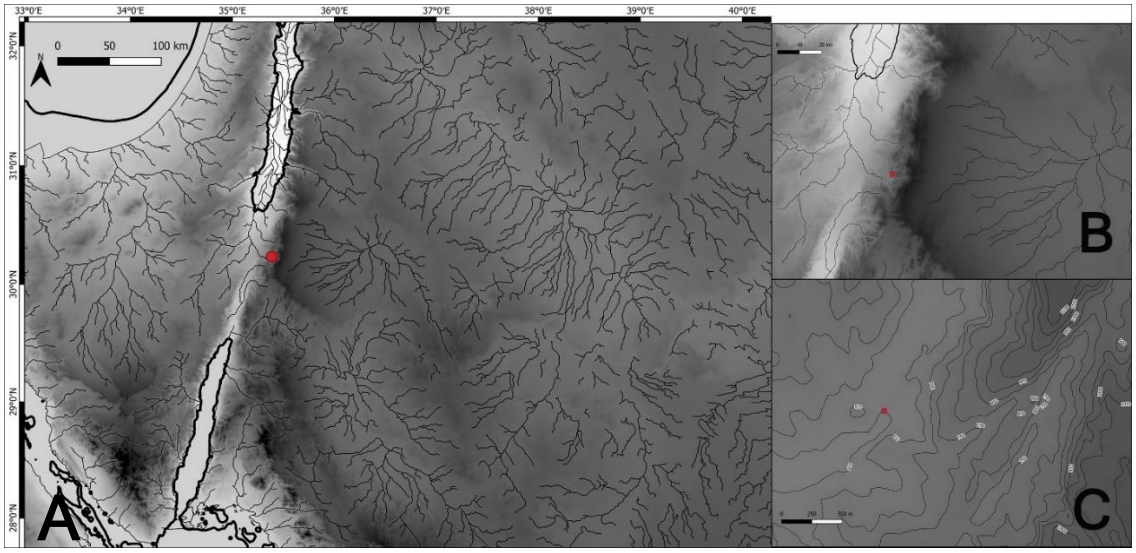

Figure 7 Topographical setting of Al-Ansab. A) Wider regional setting B) semi-local setting C) local setting. The DEM has been elaborated through SRTM (https://earthdata.nasa.gov), palaeocoastline (Zickel et al., 2016), modern coastline (https://www.marineregions.org), rivers in A and B (http://www.fao.org/geonetwork).

It sits in the Lower Wadi Sabra, characterised by a highly dynamic Upper Pleistocene wadi (fluvial) coarse sandy deposits; the wadi cuts the bedrock exposing various limestone formations bearing various quality flint seams, which were extensively employed by prehistoric occupants (Bertrams et al., 2012; Schyle, 2015). The sedimentation between 45–20 k cal BP shows a low energy environment in which the wadi bed was less incised and the alluvial plain more extended (Richter et al., 2020). Sedimentary unit I, 0.5 m thick, consists of a highly consolidated reddish-brown sand and comprises the archaeological layer (Bertrams et al., 2012). The find-layer is occurring 2 m below the modern surface, well defined by a darker colour due the diffusion of charcoal, it spans for 0.1 m, with undulated but clear upper and lower borders, it is the only one containing flint chips, the artefacts

are largely lying sub-horizontally: all indications of an *in situ* condition (Richter et al., 2020; Schoenenberg, 2018; Schyle, 2015).

The site itself was identified in 1983 due to a large scatter of artefacts on the slope, two natural calcified steps are running in W to E direction, the lower step corresponding to gridsquares 104–108 and the higher step corresponding to gridsquares 154–158 (Hussain, 2015; Richter et al., 2020; Schyle, 2015). Since 2009, the SFB806–University of Cologne has promoted extensive excavations.

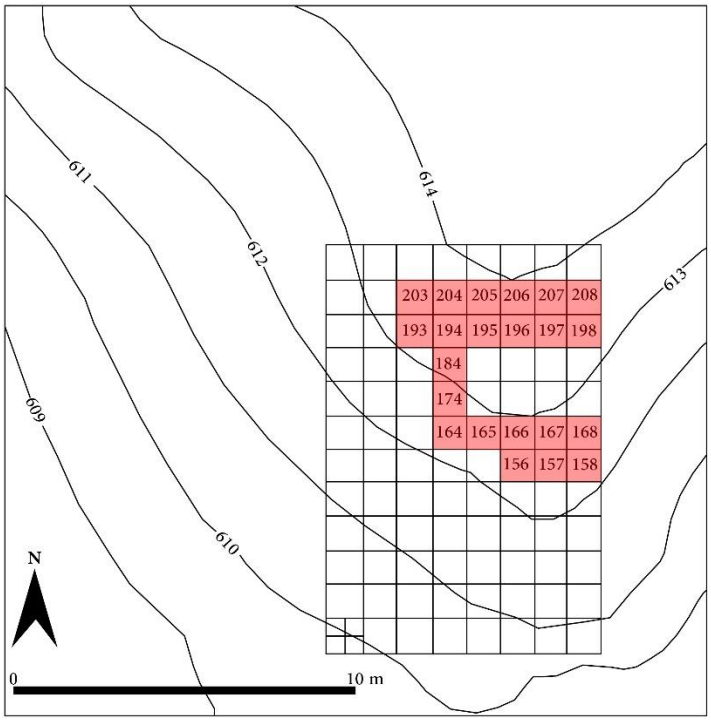

Figure 8 Al-Ansab 1 excavation grid. in red the squares that have been sampled for this dissertation. (modified from Schyle, 2015)

Excavations in years 2009, 2011 and 2013 focused on the natural steps and surroundings, retrieving the profile; during this period excavation was carried out in areas of 0.25 m^2 recovering high artefacts' concentrations, but no individual topographic measurements were taken, in addition dry sieving, 2 mm mesh, was applied on-site to the sediment (Richter et al., 2020, 2015; Schoenenberg, 2018; Schyle, 2015). The lower step was considered a secondary accumulation (Hussain, 2015; Richter et al., 2015; Schyle, 2015). From 2015 onwards the excavated area was expanded in northern direction until gridsquares 203-208, in total reaching an excavated area of approx. 25,25 m^2 (Richter et al., 2020; Schoenenberg, 2018). After 2015 individual topographic measurements are taken for artefacts >10 mm, both extremities are recorded for artefacts >20 mm, while finds <10 mm are still collected and documented on the base of the quarter square and spit (Richter et al., 2020). The measurements allowed the reconstruction of vertical and horizontal dispersal in this upper zone, the artefacts are deposited in sub-horizontal position following the natural N–S sloping and maintaining the same level in E–W direction, no particular orientation is evidenced and no significant vertical

displacement out of the find-layer is detected, confirming an *in situ* condition of the archaeological material (Richter et al., 2020).

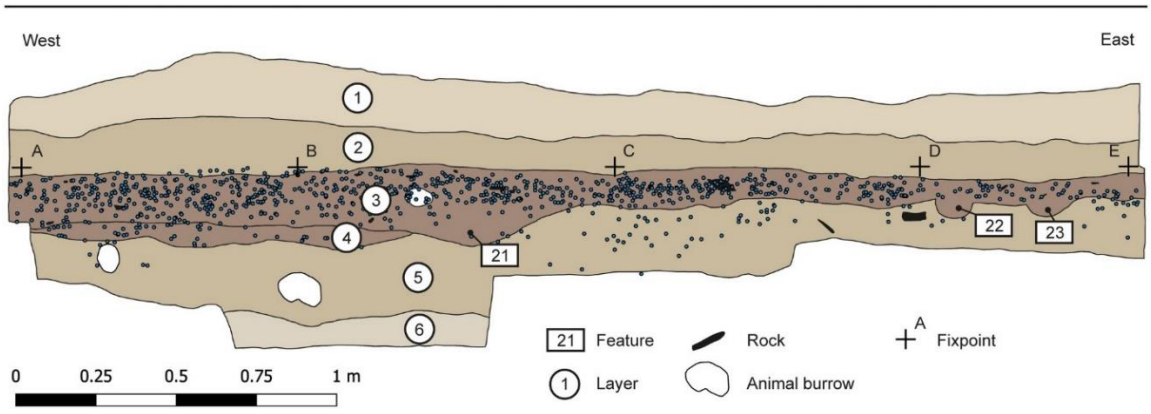

Figure 9 Al-Ansab 1 West to East profile (squares 195–198) and finds distribution from the upper excavation area. (Modified from Richter et al. 2020).

Dating was performed both with ^{14}C (AAA pre-treatment) and OSL, the wadi deposits accumulation occurred between 40-30 ka cal BP, the ^{14}C and OSL samples directly recovered in the archaeological layers points to a rapid deposition in the lower half of the period, about 38 k cal BP (Klasen et al., 2013; Richter et al., 2020).

2.1.2 Românești-Dumbrăviţa I

Românești-Dumbrăviţa I is located in South-western Romania, in the eastern part of the Banat historical region, in Timiş county (E 22.32, N 45.81). The site itself is found on a mostly flat-top river terrace at the confluence of the two branches of the river Bega (Bega Mare and Bega Mică) that originates 15 km in south-eastern direction in the Poiana Ruscă Mountains (Kels et al., 2014; Sitlivy et al., 2012).

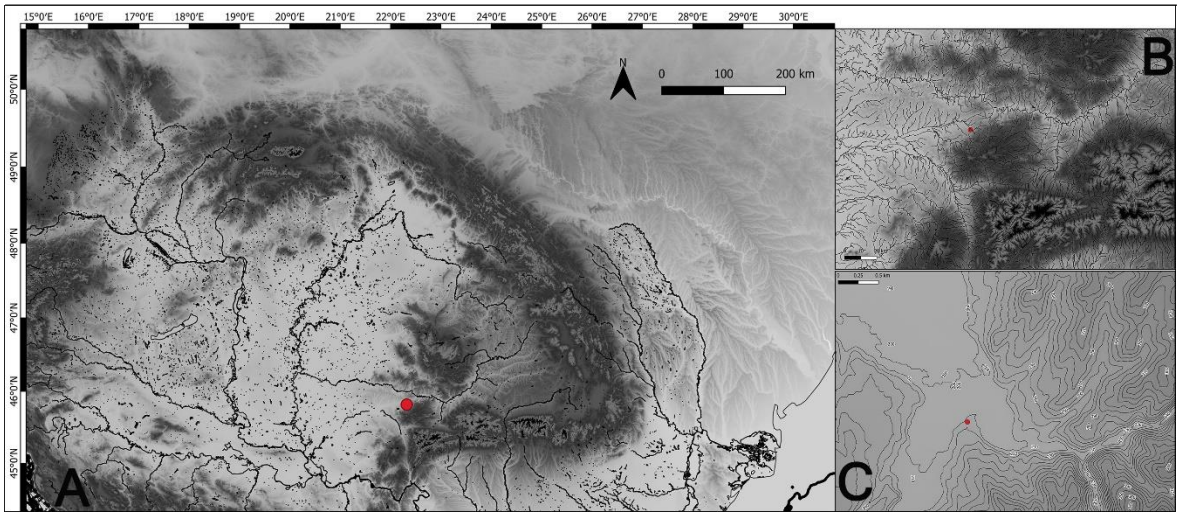

Figure 10 Topographical setting of Românești-Dumbrăviţa I. A) Wider regional setting B) semi-local setting C) local setting. The DEM has been elaborated through SRTM (https://earthdata.nasa.gov), palaeocoastline (Zickel et al., 2016), modern coastline (https://www.marineregions.org), rivers in A and B (https://land.copernicus.eu).

The site was excavated for a wide extension (450 m^2) by F. Mogoşanu during two campaigns (1960–'64, 1967–'72) (Sitlivy et al., 2012). He found several concentrations of lithic artefacts at different depths that he synthesised in an archaeological stratigraphy featuring from bottom to top (Sitlivy et al., 2012):

- Layer I, 115-105 cm deep at the upper limit of reddish clay. Containing quartzite/quartz artefacts
- Layer II, 95-90 cm deep at the base of the brown-reddish clay. Few lithic artefacts containing tools like end-scrapers, burins, blades with fine retouch, sidescrapers and flakes
- Layer III, 86-70 cm deep in brown-reddish clay sediment. Yielding the bulk of the industry attributed to the Aurignacian, including typical tools such end-scrapers, carinated ones too, fewer burins, Dufour bladelets and some retouched blades
- Layer IV, 67-60 cm deep, in the upper part of brown-reddish clay. Attributed to the Aurignacian most of tools are truncated pieces on blades and flakes, with fewer end-scrapers and Aurignacian blades and more burins, including burins on truncation
- Layer V, 50-40 cm deep, in a transitional zone between the brown-reddish clay and the above loess, an industry dominated by burins and with less common Aurignacian pieces

- Layer VI, 30-20 cm from the modern soil in loess-like sediment, attributed to the Epigravettian

Mogoşanu linked Layer III industry (and industries from neighbouring sites Coşava-Layer I and Tincova) to the one found in the Austrian site of Krems-Hundssteig, but Românești still remained undated and lacking organic material; therefore, in 2009–2010 T. Uthmaier and V. Sitlivy (SFB806–University of Cologne) carried out new small-sized excavations, implementing the missing chronological and the previous sedimentological-archaeological information (Sitlivy et al., 2012).
They retrieved a simpler, but highly comparable to the Mogoşanu's one, stratigraphical succession comprising four geological horizons (GH) (Sitlivy et al., 2012):

- GH 1, plough horizon
- GH 2, humic horizon
- GH 3, a bleached light-brown to grey horizon
- GH 4, brownish to reddish weakly clay illuviated horizon

These are the main features of Albeluvisols, especially fitting is the interfingering of tongues of bleached, lighter-coloured sediment in the lowermost clay horizon, due to possible root channels, ice-wedges and cracks (Kels et al., 2014).
Sedimentologically the succession can be divided into three units (Kels et al., 2014):

- I, below GH 4, the silt fraction is dominating, clay at its highest concentration (30%).
- II, comprising GH 4 and GH 3, silty fraction increasing with a lower concentration of clay (≈20%).
- III, comprising GH 2 and GH 1, the silty fraction reaches its maximum and clay its lowest concentration (18%). in the basal part, in the range of bleached sediment, the sand fraction has higher values.

OSL dating was performed on the sequence giving the following results (Kels et al., 2014):

- Unit I is dated to >57.9 ± 5.4 ka BP (ROM 1-3).
- Unit II provided two dates from the basal part of GH 3, 45.1 ± 4.9 ka BP (ROM 1-4a) and 35.5 ± 3.9 ka BP (ROM 1-4b).
- Unit III provided one date from GH 2, 19.2 ± 2.3 ka BP (ROM 1-5).

Archaeologically, three main and discrete artefacts levels can be distinguished in good accordance with the dating (Schmidt et al., 2013; Sitlivy et al., 2012):

- GH2 with isolated concentrations of artefacts attributed to the (Epi)Gravettian (Mogoşanu's Layer VI)

- GH3, comprises the bulk of the excavated material and attributed to the Aurignacian (Mogoşanu's Layers V, IV, because of the depth especially III and II)
- GH 4, gave isolated artefacts that could be linked to Mogoşanu's Layer I

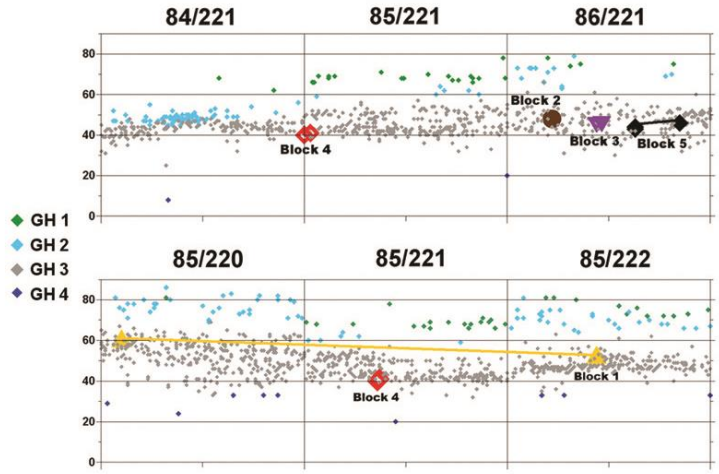

Figure 11 Românești-Dumbrăvița I E–W profile. showing 2009–2010 finds distribution and refittings (i.e. Blocks), grey dots are corresponding to GH 3 (Sitlivy et al. 2012).

Despite the general chrono-cultural accordance with Mogoşanu observations, the modern assemblage features many more small-sized findings, especially bladelets, due to the use of wet sieving (Schmidt et al., 2013; Sitlivy et al., 2012). Most of the artefacts are produced on a meso-local variety of chert called "Banat flint", which occurs in a wide variety of brownish-reddish colouration and waxy, slightly translucent appearance (Chu, 2018; Schmidt et al., 2013). The raw material is widely available in gravels and secondary deposits in a 15 km radius from the site, under the microscope it appears as a varied mixture of amorphous opal and chalcedony (Schmidt et al., 2013), but more detailed petrographic analyses combined with a detailed landscape survey are pointing towards the definition as a silicified breccia occurring in tectonic faults, causing the fracturation and the infilling of impurities like veins of quartz, in this regard the "primary" outcrops are located in a distance of 8–20 km from the site (Ciornei, personal communication; (Chu et al., 2019)).

New dating was performed with the method of TL on burnt lithic artefacts, which were recognised due to the darker brown to reddish colour (observed experimentally when heated to 400°–450° C) and common features associated with burning, such as pot-lids and craquelation (Schmidt et al. 2013). Determinations corroborate the OSL ones: GH 3 has a weighted mean date of 40.6 ± 1.5 ka BP, the only measured artefact from GH 2 dates to 15.6 ± 1.4 (Schmidt et al., 2013). The new dating and techno-typological characteristics led the authors confirming the attribution of GH 3 lithic assemblage to an early phase of the Aurignacian (for more information about the 2009-2010 assemblage analysis and Mogoşanu Layer III reevaluation (Sitlivy et al., 2014a, 2014b, 2012)). The important results obtained in 2009–2010, led to new excavation campaigns in 2016, under the direction of W. Chu and A. Szentmiklosi (SFB806- University of Cologne/Banat National Museum

of Timişoara), 2018 and 2019, under the direction of W. Chu and A. Doboş (SFB806–University of Cologne/Romanian Academy–Department of Paleolithic Archaeology), with the goal of expanding the extension of the modernly excavated area. They added 28 m^2 to the original "Swiss cross"-shaped 2009–2010 trench, yielding additional thousands of lithic artefacts.

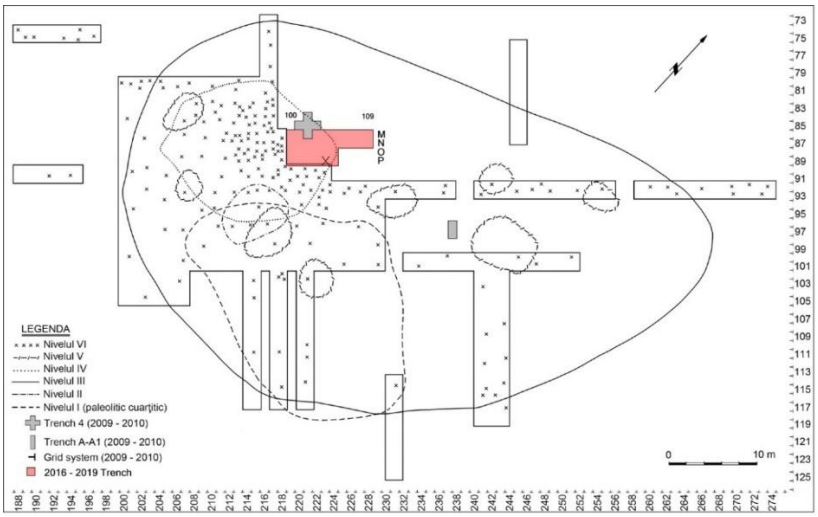

Figure 12 Românești-Dumbrăvița I grid showing the old, 2009–2010 and 2016–2019 excavations. X corresponds to square P104, which was not included in this analysis (modified from Sitlivy et al. 2012).

2016–2019 campaigns refined the stratigraphical succession introducing a new GH:

- GH 1, plough and humic horizon
- GH 2, a silty-loess light coloured horizon with laminar artefacts
- GH 2–3, a mixture of light coloured silty-loess and clay with manganese dioxide sediment corresponding to the interfingering and to the upper part of 2009–2010 GH 3, yielding a mixture of GH 2 and GH 3 artefacts
- GH 3, clay orange sediment in which a discrete Aurignacian find-level is recognised, the middle-bottom of former 2009–2010 GH 3
- GH 3–4, clay orange with manganese dioxide concentrations sediment devoid of artefacts
- GH 4, clay compact brownish sediment yielding sparse quartzite flakes

The excavation proceeds in quadrants, 0.25 m^2. Because of the absence of well-defined structures and distinguishable change of sedimentation within a single GHs, 2 cm spits are dug until the change of sediment witnessing the change of GH. Every object <5 mm is receiving an individual topographical measurement, two points for the elongated ones, the outline for bigger objects, like rocks. Thanks to the measurements, a compact vertical dispersion of artefacts is visualised. The sediment of each quadrant is collected and wet-sieved separately.

2.1.3 Fumane

Grotta di Fumane is located in the Western Lessini Mountains, eastern of Lake Garda, which are a limestone formation, part of the Venetian Pre-Alps chain, gradually rising up from the floodplain (60 a.s.l.) until ca. 1800 a.s.l.: the mid-altitude part, 800-1200 a.s.l., consisting of a high plateau. They are cut north-to-south by narrow and deeply incised valleys (*Vaj(o)*), the cave opens on the secondary Manune Vajo nearby its confluence with the main Breonio-Fumane Vajo (E 10.90, N 45.59) (Broglio et al., 2005).

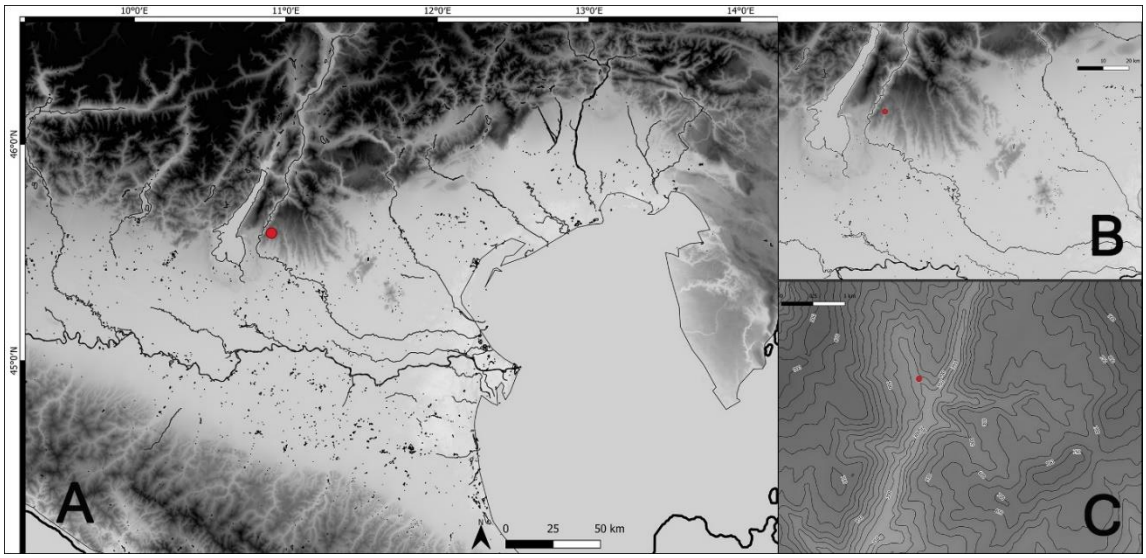

Figure 13 Topographical setting of Grotta di Fumane. A) Wider regional setting B) semi-local setting C) local setting. The DEM has been elaborated through SRTM (https://earthdata.nasa.gov), palaeocoastline (Zickel et al., 2016), modern coastline (https://www.marineregions.org), rivers in A and B (https://land.copernicus.eu).

Prehistoric inhabitants made largely use of the abundant chert material available in the different limestone formations of the Lessini Mountains that can be found in primary and secondary positions in a 5-15 kms radius from the cave (Bertola et al., 2013; Broglio et al., 2005; Falcucci et al., 2017). The most used material is the flint found in Biancone (Maiolica) formations (135-90 ma BP) in its grey and yellow-pinkish varieties. Following, flint of the Scaglia Variegata, yellow, and Scaglia Rossa, brick reddish, formations (90-70 ma BP). Less frequent are the Eocene and Oolitic flint varieties (Broglio et al., 2005; Falcucci et al., 2017).

The deposit was known since the late XIX century, but systematic excavations were started only in 1988 by a joint team of the University of Ferrara and Milan under the direction of A. Broglio and M. Cremaschi, they are carried out yearly, nowadays under the direction of M. Peresani, University of Ferrara (Broglio et al., 2005; Falcucci, 2018). Excavations led to the discovery of a 12 m thick deposit that covered entirely a closed karst opening formed by three tunnels (A left side, B the main central cave mouth and C right side), the deposit has been divided in macro-units, which features several sub-units bearing human occupations (Bartolomei et al., 1992; Broglio et al., 2005; Falcucci, 2018):

- S, the lowermost macro-unit, sediment mostly consists of dolomitic sands and limestones ice-cracked plaquettes. Artefacts are attributed to the Mousterian.

- BR, macro-unit characterised by heavy freeze and thawing processes which led to the huge deposition of horizontal layers of limestone plaquettes. Artefacts are attributed to the Mousterian.
- A, macro-unit characterised by a more insisted human (anthropic) frequentations which led to darker, finer sediments intercalated by fine horizontal layers of limestone plaquettes (especially nearby the cave walls). Sub-units A12-A4 are attributed to the Mousterian, A3 to the Uluzzian, A2-A1 is attributed to the Upper Palaeolithic (Protoaurignacian) bearing witness to the arrival of AMHs in the region (Benazzi et al., 2015).
- D, formed by huge rockfalls, that finally obliterated the cave probably around 30 ka cal BP. Nevertheless, there are still human frequentations in D6, D3 complex and D1c, attributed to a late phase of Protoaurignacian and a final, short frequentation in D1d attributed to the Gravettian.

Figure 14 Fumane upper profile . in red stratigraphical units A2 and A1 (modified from Bartolomei et al. 1992).

Macro-unit A and D have been modernly redated using radiocarbon with an enhanced purification protocol (ABOx-SC) giving the following dates for the Upper Palaeolithic (Higham et al., 2009):

- D1d, 31.6±160 k BP
- D3bα, 33.9±220 k BP
- A2, 35.7±220 k BP, 35.8±310 k BP, 34.2±270 k BP, 34.9±280 k BP, 35.2±220 ka BP (modelled start 95% probability 41.9–40.2 k cal BP, modelled end 95% probability 40.5–38.9 ka cal BP)

The entire deposit was divided in a grid of 1 m^2 squares, excavated in sub-squares of 0.11 m^2 ca. sequentially denominated a–i, from top left to bottom right. The sediment has been sieved. No electronic individual measurements have been taken for the outer part of the cave excavated between mostly between 1988 and 1991. The material has been divided in two categories between <15 mm and >15 mm in maximal dimension.

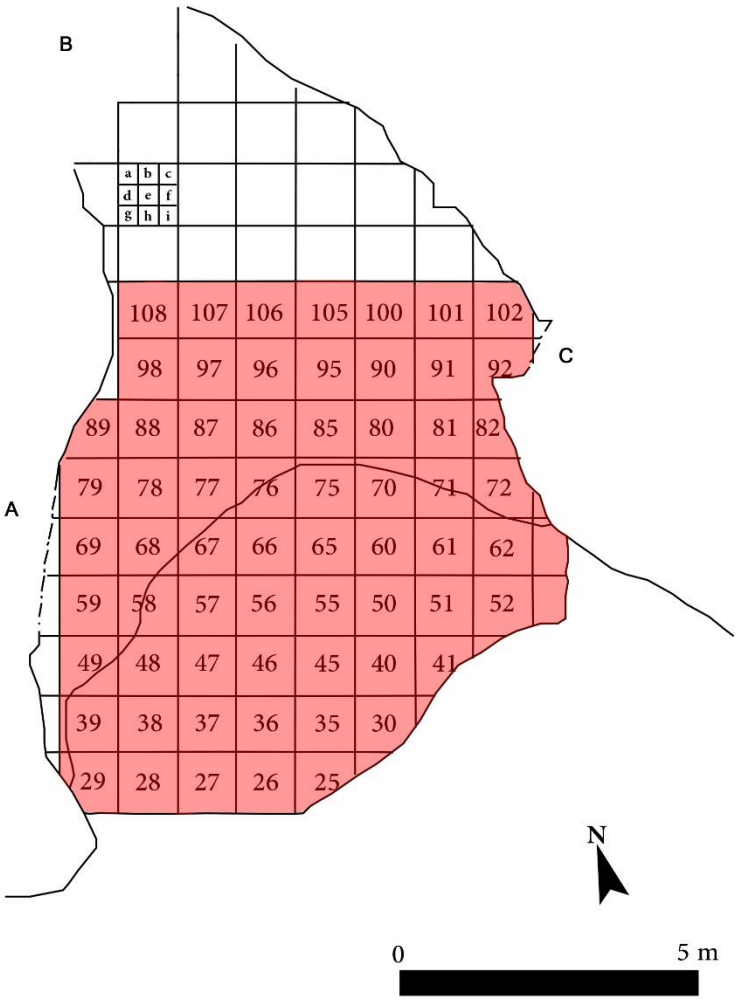

Figure 15 Fumane grid, in red the squares sampled for this analysis. Solid front line shows the modern dripline, dashed lines are the lateral tunnels still filled with archaeological deposit (modified from Falcucci et al., 2017)

A2 is well recognizable sub-horizontal dark-brownish layer, due to a high content of charcoal, ochre and anthropogenic organic material; it extends for the entire surface of the cave and outside the modern dripline, in the inner cave mouth it is covered by a sub-level, A2R (*rosso*, red), heavily coloured by ochre. In the frontal part of the cave, it is characterised by multiple features like toss

pits, structured hearths, post-holes and a cache of several tens of marine shells found in correspondence of the tunnel C. In the inner eastern part the sediment is affected by compression and tilting towards the cave wall, nevertheless, the level remains distinguishable (Bartolomei et al., 1992; Broglio et al., 2005; Falcucci, 2018; Falcucci et al., 2017). A1 covers A2 sub horizontally only out of the cave and in the frontal part of the cave mouth, therefore it is associated with A2 in the same phase of occupations (Broglio et al., 2005; Falcucci, 2018; Falcucci et al., 2017).

2.2 Sampling protocol

As shown in Chapter I, the eUP is oriented towards the production of laminar blanks, items at least twice long than wide and with subparallel lateral edges (Andrefsky, 2005; Inizan et al., 1999). In this analysis, bladelets have been recognised as laminar blanks <12 mm wide, according to several studies (Bataille et al., 2018; Bataille and Conard, 2018a; Falcucci et al., 2017; Normand and Turq, 2005; Roussel and Soressi, 2013; Tixier, 1963; Zwyns, 2012). The independent production of flakes is rarely attested. Therefore, the focus of this analysis is put on reconstructing core reductions methods and the morpho-technological attributes of blades and bladelets. Cores are recognised as a piece of raw material that shows sign of detached multiple negatives, or, in case of Pre-Cores, the shaping of a striking platform and/or flaking surface (Andrefsky, 2005; Bataille and Conard, 2018a; Conard et al., 2004; Inizan et al., 1999). The assemblages are rich, therefore sampling strategies have been singularly devised, influenced by the logistical conditions and the aim of obtaining the most technologically meaningful sample. The sampling and the results will be based on complete and semi-complete blanks, fragmented items preserving a proximal or distal part in union with a mesial portion. This approach will provide better determination of the single blanks, the maximisation of the attainable attributes and overcoming the high fragmentation pattern that small and fragile elements, as bladelets, inevitably undergo (Falcucci et al., 2018).

Al-Ansab 1

All findings from Al-Ansab are hosted on loan at the Institute of Prehistory of the University of Cologne, I analysed two assemblages coming from two detached areas excavated in different campaigns:

- The 2009-2011 campaigns material: it is retrieved from the excavation of the upper natural step, square metres 165, 166, 167, 168, 156, 157, 158, and cutting another perpendicular section along squares 164, 174, 184. The analysed sample consists of all recognised cores, blades, bladelets and flakes bearing a technological meaning.

Table 1 Al-Ansab 2009–2011 analysed sample.

Cores	Blade	Bladelet	Flake	Total
45	578	935	104	**1661**
2.70%	34.79%	56.29%	6.20%	**100.00%**

- 2018 material: it is retrieved from a higher spot of the site, stratigraphy preservation is better, allowing for the recognition of different deposition events and features, which are nevertheless grouped in the same Early Ahmarian phase of frequentation (Schoenenberg, 2018). The topographically measured artefacts from square metres 193, 194, 195, 196, 197, 198, 203, 204, 205, 206, 207, 208 has been taken in consideration. The analysed sample consists of all recognised cores, complete and semi-complete blades, bladelets and flakes.

Table 2 Al-Ansab 2018 analysed sample

Cores	Blade	Bladelet	Flake	Total
80	653	389	223	**1345**
5.94%	48.55%	28.92%	16.57%	**100.00%**

It is not possible to trace the exact stratigraphic relationship within the two areas, nevertheless the material has been confidently assigned to the same cultural phase.

Românești-Dumbrăviţa I

The object of this analysis are the artefacts retrieved during 2016, 2018 and 2019 campaigns from GH3. The material is hosted at the Institute of Archaeology "Vasile Pârvan" of the Romanian Academy, in Bucharest. Data were collected in two separate research stays, 2018 material (28.02.19-18.03.19) and 2016 & 2019 material (February 2020). 2016 artefacts were retrieved from squares N100, N101, N102, N103, N104, N105, N106, N108, N109, M101, M103, M105, M106, M107, M108, M109 directly adjacent to the small 2009–2010 excavation (sharing profile sections in squares M101, N102, M103). 2018 campaign expanded on the adjoining area formed by squares O100, O101, O102, O103, P100, P101, P102, P103. 2019 extended the excavated area to O104, O105, P104, P105. P104 artefacts have been left unwashed for further analyses and therefore have not been considered nor counted here. All topographically measured artefacts are analysed, regardless of fragmentation.

Table 3 Românești-Dumbrăviţa I determinable blanks analysed sample.

Cores	Blade	Bladelet	Flake	Total
18	616	505	710	**1849**
0.97%	33.31%	27.31%	38.39%	**100.00%**

Fumane A1–A2

All the material from Grotta di Fumane is hosted on loan at the Institute of Prehistoric and Anthropological Sciences of the Humanities Department at Ferrara University. The lithic artefacts are divided in <15 mm and >15 mm in maximal dimension, only artefacts >15 mm coming from layers A1 and A2 (and sublevels) were considered here. The sample has been recorded during a single research stay in August 2019. The sample is coming from the outer cave mouth and frontal part (outside the modern dripline), covering the square metres from the 20s line to the 100s line. A1

and A2 can be treated as a single assemblage for technological purposes, nevertheless, A1 is considerably smaller than A2 (Falcucci et al., 2017), therefore while cores, complete and semi-complete blanks are analysed for A1, only cores and complete blanks are analysed for A2.

Table 4 Fumane A1 analysed sample.

Cores	Blade	Bladelet	Flake	Total
32	271	417	95	**815**
3.92%	33.25%	51.16%	11.65%	**100.00%**

Table 5 Fumane A2 analysed sample.

Cores	Blade	Bladelet	Flake	Total
58	245	394	153	**850**
6.82%	28.82%	46.35%	18.00%	**100.00%**

2.3 Analysis protocol

2.3.1 The chaîne opératoire approach and background theory of lithic analysis

The present analysis was conducted combining *chaîne opératoire* (CO) approach with an attribute analysis. The CO is an anthropological concept introduced in Prehistoric studies by A. Leroi-Gourhan during the second half of the last century, namely as early as 1943. It stands for all the actions performed during a production, thus encompassing raw material procurement, manufacture, use and discard of the object. It takes origin from the M. Mauss conception of techniques, which included also human gestures and physical actions: the tool is not complete without the human who moves it (Cresswell, 2010; Geneste, 2010; Inizan et al., 1999; Schlanger, 2004; Sellet, 1993; Soressi and Geneste, 2011; Tostevin, 2013, 2011).

Therefore, the CO forms the base of the technological focus on prehistoric material culture, in particular lithic material, that integrated and, partially, took over the previous typological approach (Boëda et al., 1990; Inizan et al., 1999; Soressi and Geneste, 2011; Tostevin, 2013). Lithic tools, considering their diffused use and raw material procurement, are understood to be the basis of prehistoric groups' economical dynamics, influencing their movements and societal development; also, in a processual optic, the lithic sub-system interacts closely with other material culture sub-systems, for instance the hard animal raw material or the wooden ones: hence, understanding lithic production sub-systems allows for inferences about the entire societal system (Bar-Yosef and Van Peer, 2009; Geneste, 2010; Inizan et al., 1999; Sellet, 1993; Soressi and Geneste, 2011).

CO adopters and perpetrators did not often clearly state their high-range theory, which is interpreted to be the understanding of *chaîne opératoire* itself (Tostevin, 2011). On the other hand, the middle-range theory is more extensively treated, and it is resumed in achieving the overarching conceptual scheme followed by the artisan. The conceptual scheme influences the operative schemes, divided in methods and techniques, where methods are the sequence of actions and techniques are the gestures and tools used in the envisioned production (Inizan et al., 1999; Sellet, 1993; Soressi and Geneste, 2011; Tostevin, 2011). It is important to note that the operative scheme is influenced closely by the environmental factors, the physical properties and the availability of the raw material, and the human factors, such as artisan's know-how, dexterity and technical tradition (Inizan et al., 1999; Soressi and Geneste, 2011).

The technological analysis develops in three fundamental operative stages:

- Definition of the initial hypothesis achieved through a first eye assessment of the assemblage composition and characters. In this phase the analyst decides which features are important to the assemblage understanding (Inizan et al., 1999; Soressi and Geneste, 2011).
- Detailed analysis of assemblage features and reconstructions of knapping stages, based on size, cortical coverage and mostly important, the negatives' sequence. As a blank is constituted by a ventral face, obtained through the detachment of the flake from the main raw material block, and a dorsal face, characterised by the presence of the exterior surface of the block or by the traces of previous removals, it is possible to reconstruct the knapping order and direction of the removals. The latter are condensed in the diacritic scheme (Inizan et al., 1999; Sellet, 1993; Soressi and Geneste, 2011). The same, except for the ventral face recognition, is possible for cores, which are the base of the operative scheme reconstruction (Boëda, 1994, 1993; Dibble, 1995; Soressi and Geneste, 2011).
- The third phase is the final interpretation of the assemblage employed methods, techniques and knapping goals through the recognition of behavioural patterns (Inizan et al., 1999; Soressi and Geneste, 2011).

It is evident that the CO defines repetitive actions and it is less useful in defining sporadic ones, therefore the inferential power progresses with numbers of artifacts assigned to an assemblage (Soressi and Geneste, 2011). Knapping goals and operative schemes are not defined only by the presence, but also by absence: if the analyst recognises all knapping stages in an assemblage, but misses the blanks for a particular one it can be hypothesised that this stage was carried out elsewhere or the blanks were exported (Inizan et al., 1999). The CO, then, reveals complex chrono-geographical dynamics (Geneste, 2010; Inizan et al., 1999; Sellet, 1993; Soressi and Geneste, 2011).

The CO benefits from refitting and experimental knapping. Refitting is the action of recomposing the pieces of one assemblage in a more or less extensive manner. The practice is as old as Prehistoric Archaeology (Laughlin and Kelly, 2010). Site preservation greatly affects it; a rate of 20% refitted

pieces in an assemblage is considered successful, furthermore refitting is a time-consuming activity and especially difficult in case of small blank productions, such as those occurring in bifacial reduction (Bar-Yosef and Van Peer, 2009; Laughlin and Kelly, 2010). Part of the refitting methodology, is the definition of Raw Material Units, grouping artifacts by raw material colour, texture and grain size (Roebroeks et al., 1997; Sellet, 1993). Nonetheless, refittings are helpful in assessing site preservation and intra or inter sites spatial analysis (Geneste, 2010; Inizan et al., 1999; Soressi and Geneste, 2011). Technologically, they are the ultimate tool for understanding a single *chaîne opératoire* development, assessing knapping methods, blanks export and roles of a particular knapping product (Bar-Yosef and Van Peer, 2009; Davidzon and Goring-Morris, 2003; Delpiano and Peresani, 2017; Inizan et al., 1999; Soressi and Geneste, 2011). It must be remarked that, generally speaking, the negatives diacritic analysis has proven to be effective in independently reconstructing sequences refitted later on, thus, in face of the refitting above-mentioned downsides, it is a good substitute for technological analysis (Bar-Yosef and Van Peer, 2009; Falcucci et al., 2017; Inizan et al., 1999; Shott, 2003; Shott et al., 2011; Soressi and Geneste, 2011).

Experimental knapping is the practice of conducting knapping sequences to test one or more controlled parameters. It is not replication, but testing of hypotheses developed from the archaeological record investigation (Crabtree, 1966; Dibble, 1997; Soressi and Geneste, 2011). It is mostly helpful in assessing raw material behaviour, given the actualist assumption that material collected in the past had the same mechanical properties, another contribution is a better understanding of employed techniques and methods (Bar-Yosef and Van Peer, 2009; Bourguignon, 2001; Geneste, 2010; Inizan et al., 1999; Sellet, 1993; Soressi and Geneste, 2011).

The CO is not the only lithic analysis approach that makes use of a sequence concept, those generally compared with the CO are: the Lithic Reduction Sequence, the Behavioural Chain analysis and the Unified Middle-Range Theory of Artifacts Design (Bleed, 2001; Schiffer and Skibo, 1987; Shott, 2003; Tostevin, 2013, 2011).

The Lithic Reduction Sequence has long history in American Prehistoric studies, being applied for the first time at the end of the XIX century by W. H. Holmes (Shott, 2003; Tostevin, 2013). It can be matched broadly with CO for its focus on lithic knapping processes and understanding of artisan's intention and group's technical tradition, but differs in high-range theory, which is set mostly in evolutionary ecology, in the application of a continuum concept vs. a divided in stages one, probably related to the frequent bifacial reduction found in American Prehistory, and in the consequent stress on final products (Bleed, 2001; Shott, 2003; Shott et al., 2011; Tostevin, 2013, 2011). Also, it must be noticed that the CO has a much wider application, all human productions, while the Lithic Reduction Sequence is strictly devised for lithic materials (Coupaye, 2015; Cresswell, 2010; Shott, 2003; Tostevin, 2013, 2011).

The Behavioural Chain is part of the Behavioural Archaeology, it was introduced in 1976 by M. Schiffer (Schiffer and Skibo, 1987; Tostevin, 2013). Fundamentally, it uses the notion of

performance characteristics, on which the artisan's technical choices are appointed: during the manufacture and use the artisan experiments and understands which features to retain and which ones to discard (Schiffer and Skibo, 1987; Tostevin, 2013). The ultimate selection process though is socially mediated by the group adoption of the technical choices (Schiffer and Skibo, 1987). The focus of the Behavioural Chain is strictly related to the utilitarian accomplishment of a task, thus it is not entirely suitable for further social inferences (Tostevin, 2013).

The Unified Middle-Range Theory of Artifacts Design introduced by C. Carr in 1995 has its roots in the style-function approach (Tostevin, 2013). It proposes hierarchical relationships in style theory and a contextualisation of the social processes producing patterns of artefact shapes. It assigns etic meaning for establishing attributes of artifacts classes, including technological, sociocultural, behavioural, and psychological constraints and processes. The physicality of the material dictates the attributes characterizing the artifacts. Attributes can be signalling an emic group affiliation, active style or etic unconscious variations. Using ethnographical data, it ranks the attributes in three hierarchies: decision sequence (the order in which the artisan decided the attributes of the artefact), the production sequence (the relative order of attributes in which the attributes are created) and the visibility (how visible the attributes are at different scales and social contexts). The production sequence then is giving a temporal context to the visibility, which is the ultimate attribute for identification. Defining in which hierarchy the attribute is found means investigating which social process affected the variability. The more visible and later an attribute is, more is the result of a social process (Tostevin, 2013).

The main critique moved towards CO is an emic technical choices' assumption. In fact, it is criticized because while in ethnographic studies it is indeed possible to interview the makers of a certain production and understand if their technical choices are conscious, this is impossible in archaeology (Bar-Yosef and Van Peer, 2009; Monnier and Missal, 2014; Tostevin, 2013, 2011). A corollary of this criticism is the use of production stages like Initialisation, the first core shaping, or Management/Maintenance, referring to purported fixed procedures, instead of portraying a continuous reduction (Shott, 2003; Tostevin, 2011). On the other hand, following this passage, the boundary between emic and etic is unclear, and probably not useful in an archaeological context:

Wiessner (1983), however, has shown in ethnographic contexts that active, emblemic style is often unconscious, unintentional, and only etically recognized—San artisans were not conscious of making arrows whose style was diagnostic (emblemic) of their language group. Nevertheless, they could select out their own arrowheads from a pool of several groups' arrows. More importantly, they reacted with fear and suspicion to the style of an unfamiliar group's arrows, clearly evidencing the past action of emblemic style in boundary maintenance. (Tostevin, 2011, p. 356).

CO critics are also pointing to the archaeological practice of using *chaînes opératoires* as mere *"extension of typology to the reduction process*" leading to new taxonomical problems (Monnier and Missal, 2014; Shott, 2003, p. 101; Tostevin, 2011).

Another critique to the CO is that it is too descriptive and subjective, instead some scholars advocated the use of quantifiable, precisely defined attributes which in their eyes would have favoured replicable observations and overall a better understanding of the dynamics underlying the knapping practice: these observations resulted in the adoption of the Attribute Analysis (Dibble, 1995; Monnier and Missal, 2014; Scerri et al., 2016; Tryon and Potts, 2011). Emblematic the case of the early Levallois assemblage of Biache Saint-Vaast IIA: E. Boëda technological analysis determined various *chaîne opératoires* on the grounds of different cores configuration, while H. Dibble concluded, using data from the debitage, that the assemblage is better explained as different modes of exploitation on a single core and that Boëda's *chaînes opératoires* are reflecting different reduction stages (Boëda, 1994; Dibble, 1995).

Then, why using the CO approach?

Even for its critics, the CO has represented step forward in better understanding of prehistoric groups' technical traditions (Bar-Yosef and Van Peer, 2009; Monnier and Missal, 2014; Tostevin, 2013). Its holistic approach, bringing together several environmental, humans, economical and societal factors, show immense potential for expanding our knowledge of prehistoric groups' dynamics, without advocating cultural determinism (Geneste, 2010). Including in the analysis all blanks, plus failures, and a close diacritic analysis give us reasonably unbiased information about knapping processes; a technology-based taxonomy is less prone to errors occurring when using typology alone, nonetheless it must be remembered that the CO aim is not creating a taxonomy but understanding the knapping, technical and economic dynamics occurring at one or more sites (Sellet, 1993). The risks of making assumptions of emic behaviours it is relatively negligible, when compared to the illustrated benefits. It is a norm now to integrate descriptive observations with replicable and quantifiable attributes, which make conclusions much more verifiable and comparable; *chaîne opératoire* reconstructions have been discussed and evolved, now a well-established corpus of studies is present and provides a good degree of uniformity.

2.3.2 The Analysis protocol steps

Having briefly explained the theoretical background of this analysis, it is time to express the physical steps through which the analysis was performed:

1. artefacts are divided by broad categories in:

- Cores
- Debitage, artefacts where the last blow produced a ventral face, divided in

- Flakes
- Blades, items with sub-parallel edges at least 2 times longer than wide.
- Bladelets, items with sub-parallel edges at least 2 times longer than wide. Width <12 mm.

2. Debitage is ordered progressively by dimension, from longer to shorter, within the category.
3. Artefacts are ordered in classes of fragmentation: complete, Prox+Mes, proximal fragments (if analysed), mesial fragments (if analysed), Mes+Dist, distal fragments (if analysed).
4. The artefacts are divided in knapping stages, through the observation of characteristics such as cortex coverage, profile, distal termination morphology, diacritic analysis of the negatives. These stages are represented in the database as alphanumeric codes

1 Simple Flake, non-coherent or absent negatives pattern.

2 Cortical Flake, the main character is the presence of a natural unmodified surface (cortex or neo-cortex).

3 Core Tablet, an artefact which has been knapped perpendicularly to the main flaking surface, removing partially or totally the conjoining portion between the flaking surface and the platform. Usually, the point of impact (butt) is located on the flaking surface itself. The dorsal face is generally left unmodified and corresponds to the former platform.

3a Core blade tablet, an artefact removing a long and narrow portion of conjoining flaking surface-platform part. It is usually knapped from an orthogonal side, in case of complete flaking surface removal, or removing a longitudinal core edge.

4 Maintenance Flake, a flake rejuvenating the core volume.

4a Surface Cleaning Flake, it is a flaking surface rejuvenation flake, it is a category explicitly created for differentiating a rejuvenation flake coming from a main flaking surface, in opposition to Flank flakes used to narrow down core sides (Davidzon and Goring-Morris, 2003; Hussain, 2015).

5 Maintenance Blade, generic rejuvenation blade.

5a Crest, elongated artefact bearing one or bi-sided orthogonal flake removal creating a ridge used for blank removal guidance.

5b Asymmetrical Blade, a laminar blank that presents an asymmetrical cross-section, a twisted profile and an off-axis distal termination. They have been referred to also as *débordant* blades or lateral-comma blades (Falcucci et al., 2017; Hussain, 2015).

5c Overshot Blade, a laminar blank extracted from the centre of the flaking surface, generally extremely curved blunt distal ending aimed at removing a basal core portion for re-shaping the distal

convexity. Usually they bear blades and/or bladelets negatives stopping at three quarters of the length, i.e. exploiting the flaking surface for a straight profile blank.
5d Surface Cleaning Blade, a laminar blank, wide enough for removing a large portion of the flaking surface, with a blunt distal termination.

6 Simple Blade, regular elongated, ≥12 mm wide, blank consuming convexities and/or present a feathered termination.

- 6a central, the cross-section is symmetrical, termination is on-axis
- 6b lateral, the cross-section is asymmetrical, the termination can be off-axis

7 Simple Bladelet, regular elongated, <12 mm wide, blank consuming convexities and/or present a feathered termination

- 7a central, the cross-section is symmetrical, termination is on-axis
- 7b lateral, the cross-section is asymmetrical, the termination can be off-axis

7c Burin Spall, particular on-axis artefact removing a longitudinal profile of an artefact; thus, they are generally triangular in cross-section and presents two ventral faces, their own and the one of the parent artefact.

5. Retouched tools, if any, are analysed together with their category of belonging.
6. Every piece is put in relation with the others in the single category and in wider relation with other categories.
7. Singular pieces are then analysed for attributes recorded in a Microsoft Access database.
8. Cores are all platform cores (Conard et al., 2004), they have been categorised according to negative patterns and final morphology:
    - **Semi *Tournant***, blanks are knapped on the longitudinal side, negatives cover the flaking surface extending to the lateral surfaces.
    - **One face (sub) parallel edges**, they are cores with a flaking surface exploited frontally, i.e. not semi-circumferentially, framed by perpendicular parallel edges.
    - **Narrow Fronted**, blanks are knapped on the longitudinal side, the flaking surface is laterally delimited by negatives.
    - **Narrow Fronted *sur Tranche***, blanks are knapped on the longitudinal side, no formal narrowing, generally provided by cortical surfaces or ventral faces. They are produced also on-blank, in this case they are referred in publications as Lateral Carinated cores or, simply, Burin cores.
    - **Transversal Carinated**, blanks are knapped on the short side transversally the thickness of the piece. In publications they are referred as Carinated End-scrapers.

- **Pre-core**, abandoned at an early stage.

2.3.3 Recognising knapping techniques

Techniques are defined as the material actions needed for fulfilling a task. Regarding lithic artifacts, techniques are the gestures and the tools used for applying force to the raw material for knapping the blanks (Inizan et al., 1999). Upper Palaeolithic laminar assemblages are generally considered been knapped, at least the main series, using organic soft hammers with a tangential movement coming towards the core and the knapper; it is a technique opposed to the hard (stone) hammer direct percussion with internal perpendicular movement (Inizan et al., 1999; Pelegrin, 2011, 2000). To determine the technique, I used the experimental observations presented by J. Pelegrin (Pelegrin, 2011, 2000). Recent experiments, despite confirming Pelegrin's empirical observations, failed to find a statistical significance between different hammers applied to laminar volumetric knapping (Driscoll and García-Rojas, 2014), therefore techniques' determination through proxies is still a cautious operation. In particular, a blank is considered detached with hard hammer direct percussion if the ventral face bulb is prominent, if it presents small lines departing from the point of impact, if the point of impact is creating an incipient Hertzian cone, the bulb can also present a bulbar scar. A blank is considered detached with soft hammer direct percussion if the ventral face bulb is diffused, the butt protrudes in a lip, as consequence of the tangential knapping movement, on the dorsal face the overhang, connection between the flaking surface and the striking platform, is abraded for favouring the hammer impact. The prominence of the bulb as a hard hammer direct percussion proxy has been played down (Roussel et al., 2009), here I used it mainly in opposition with the diffused bulbs and in connection with the other proxies.

2.4 Attributes and measurements

2.4.1 Technological attributes

1. Entirety

- Complete, the blank is whole or presents a minimal breakage not influencing the dimensional development.
- Prox+Mes, the blank preserves the proximal and a portion of mesial parts.
- Mes+Dist, the blank preserves the distal termination and a portion of the mesial part.
- Proximal fragment, the blank just preserves the butt and the immediate neighbouring part.
- Mesial fragment, the blank does not preserve proximal and distal part.
- Distal fragment, the blank just preserves the distal termination.

2. Butt type:

- Natural, cortical.
- Plain, just one negative.

- Dihedral, two negatives forming a central ridge.
- Facetted, multiple negatives.
- Linear, a narrow strip along the proximal end.
- Punctiform, a small surface at the centre of the proximal end.

3. Bulb morphology
- Pronounced, evident Hertzian cone on the proximal ventral face.
- Diffused, perceived at touching, but well distributed flatly.
- With bulbar scar, pronounced and with the detachment of a small contextual flake.

4. Presence of a lip, a small protrusion on the very top of the ventral face.

5. Presence of Overhang Abrasion, micro-chipping on the very top of the dorsal face. Recorded for laminar items.

6. Negative types and numbers, types can be Bladelets, Blades or Flakes and combinations.

7. Negative orientation
- Unipolar, the negatives follow the blank flaking direction.
- Bipolar, negatives coming from two opposite parallel directions.
- Convergent, negatives converge obliquely from two sides.
- Crossed, negatives cut obliquely the blank flaking direction.
- Orthogonal, negatives cut perpendicularly the blank flaking direction.

2.4.2. Morpho-technological attributes

they are generally used in publications for laminar blanks

1. Outline, the blank edges in upper view
- (sub)Parallel Edges, when the edges are following two separate parallel courses.
- Convergent, edges are progressing constantly towards each other.
- Off-axis, the morphological axis does not correspond to the flaking direction (déjète).

2. Profile, the morphology of the longitudinal edge. It is assessed just for Complete and Semi-complete blanks. Profile assessment followed the methodology illustrated by F. Bon (Bon, 2002a). In case of Complete blanks, it is following the interval calculated with Curvature values (see measurements)
- Straight, the edge is sub-horizontal.
- Slightly Curved.
- Curved.
- Very Curved.
- Twisted, from perpendicular view, the artefact ventral face is partially exposed towards the viewer as schematically represented by F. Le Brun-Ricalens and colleagues (Le Brun-Ricalens et al., 2009).

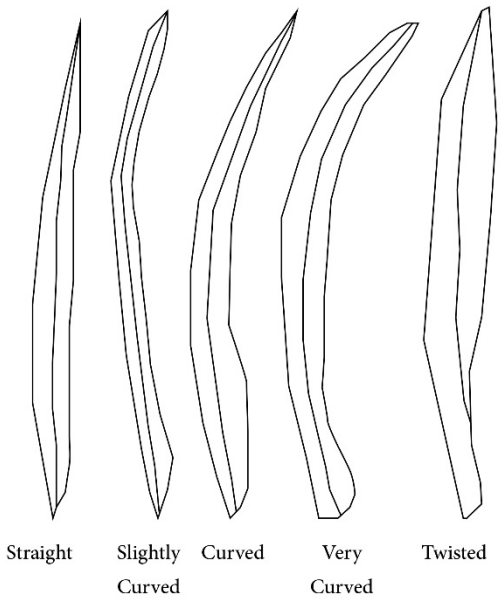

Figure 16 Longitudinal profile determination.

3. Distal end morphology, it is recorded just on Complete and Mes+Dist fragments, or distal fragments.

- Feathered, when straight and forming a sharp termination.
- Plunging, when inclined downwards with accentuated curvature.
- Hinged, when blunt, evident stopping ripples on the ventral face and curving upwards.
- Stepped, when terminating briskly with a perpendicular surface (i.e. overshot removing a plane opposite surface).

4. Crossed transversal section, it is judged as the cross-section cut transversally at artefact midpoint

- Triangular (just one ridge)
    - Symmetrical.
    - Asymmetrical.
- Trapezoidal (more ridges)
    - Symmetrical.
    - Asymmetrical.
- Flat (no ridges).

2.4.3 Measurements

They are taken as follows:

Length, it measures the maximum extent of the blank according to its debitage axis. Despite resulting in shorter measurements in case of *déjète* blanks, it is preferred to the maximum morphological axis due to its better adherence to the orientation of the blank and to the true position on the core volume

(Andrefsky, 2005; Inizan et al., 1999). In cores, it corresponds to the maximum length recorded on the flaking surface according to the main negatives' orientation.

Width, it measures the maximum extent of roughly mid-blank area perpendicularly to the Length. In cores it equates to the midpoint of the flaking surface.

Thickness, it is the maximum measure obtained transversally to the length on the artefact mid-point.

Fléche, it is the maximum distance between the blank lateral edge and a plain surface when both proximal and distal ending is touching the plain surface.

Flaking Angle, the angle formed by the ventral face and butt.

Exterior Angle (*Angle de Chasse*), the angle measured between the striking platform and the flaking surface. In blanks, calculated subtracting the Flaking Angle from a straight angle.

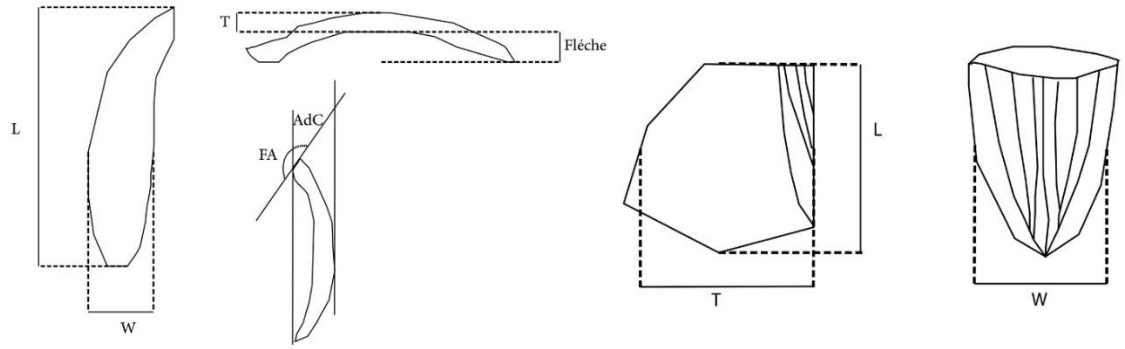

Figure 17 Modalities of measurements-taking in blanks (left) and cores (right).

Length and Width of the last preserved negative, according to the striking axis.

Derived indexes:

Elongation Index, $\frac{Length}{Width}$

Profile curvature is assessed only on Complete laminar blanks; it is calculated using this formula $\frac{Fléche*100}{Length}$, and gives values that are considered within intervals: **Straight: 0-2,9 Slightly curved 3-5,9 Curved:6-8,9 Very Curved: 9-14,9.**

2.4.4 Graphs and statistics

All graphs have been made in the open access software R (R Core Team, 2020), in particular the package ggplot2 (Wickham, 2016). Bar plots have been used to portray frequencies of single observations (i.e. profile values), while box-plots show measurements, naturally implementing a statistical summary of the measurement distribution (Slutsky, 2014). As the numerical measurements do not follow a normal distribution, they have been tested with the non-parametric Mann-Whitney-Wilcoxon U test. Categorical variables have been tested with Chi-Square Goodness of Fit test against a hypothetical distribution.

3. Results

In this chapter the data from the three sites will be illustrated. The 3.1 section presents the two assemblages from Al-Ansab 1. They are kept separated because of the two different sampling strategy and stratigraphic locations, finally an overall conclusion will establish if a difference in production processes can be noticed. The 3.2 section presents Românești-Dumbrăvița I GH3 assemblage. And finally, the 3.3 section presents the A1–A2 Fumane assemblages. As for Al-Ansab, the two assemblages are kept separated and a conclusion will be drawn later. The sites' sections are divided in Assemblage Composition, stating the structure of the assemblage, its fragmentation values and metric attributes recorded for the broad categories. Technical Observations, all the attributes defining the envisioned knapping technique as the Lipping, the Overhang Abrasion and the Bulb values. The Morpho-Technological observations, all the attributes defining knapping methods observed on Cores and Blanks. The final section gives the operative scheme reconstruction. Tables showing the exact numbers and percentages are presented in the Appendix.

3.1 Al-Ansab 1

3.1.1 Assemblage Composition

Both assemblages are laminar oriented. Bladelets are noticeably more represented in 2009–2011 than in 2018 assemblage: they are more than half of the blanks in 2009–2011 (52.64%) and slightly less than a third of 2018 ones (30.75%). Considering the laminar assemblage, bladelets account for the 57.66% in 2009–2011 of laminar blanks and the 37.33% one in 2018.

Table 6 Comparison of assemblages' compositions using complete and semi-complete blanks.

Blade		Bladelet		Flake		Total	
2009-2011	**2018**	**2009-2011**	**2018**	**2009-2011**	**2018**	**2009-2011**	**2018**
307 (38.66%)	653 (51.62%)	418 (52.64%)	389 (30.75%)	69 (8.69%)	223 (17.63%)	794 (100.00%)	1265 (100.00%)

Table 7 Laminar assemblages' compositions.

Blade		Bladelet		Total Blade and Bladelet	
2009-2011	**2018**	**2009-2011**	**2018**	**2009-2011**	**2018**
307 (42.34%)	653 (62.67%)	418 (57.66%)	389 (37.33%)	725 (100.00%)	1042 (100.00%)

3.1.1.1 Fragmentation

Only complete and semi-complete blanks are taken in account here.

Complete blanks are recording the higher values in both 2009–2011 and 2018 assemblages. Bigger blanks such as blades and flakes show the same tendency of being mostly complete, especially flakes

with percentages over 90%. Considering the bladelets, 2018 ones have a higher percentage of complete blanks, while 2009–2011 bladelets have a considerable share of proximal fragments.

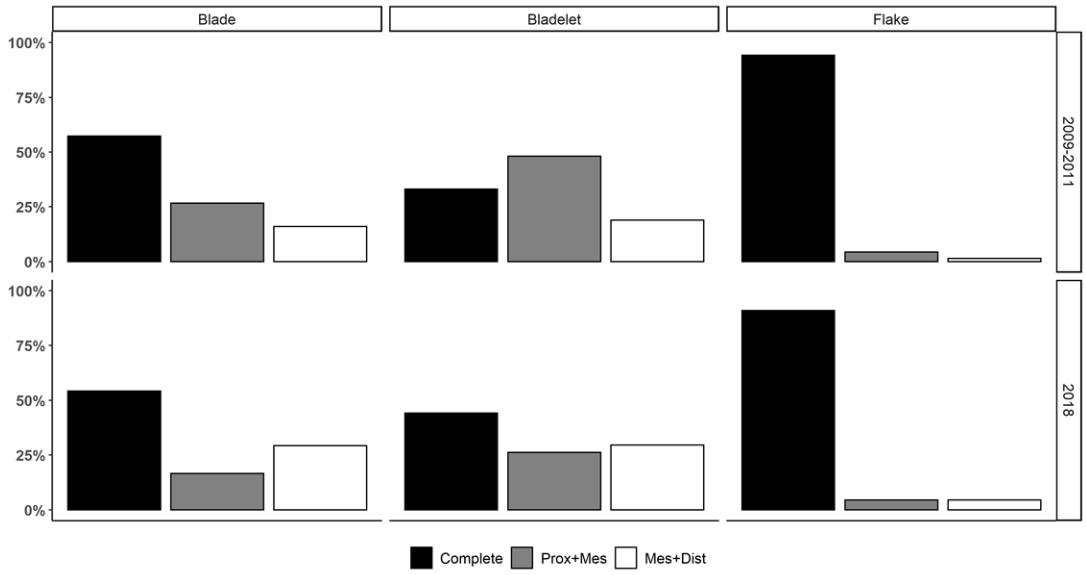

Graph 1 Fragmentation values in both assemblages.

3.1.1.2 Metric Attributes

Regarding measurements both assemblages show a similar trend, 2018 assemblage is dimensionally slightly larger. The recorded median length of blades is 48.00 mm in 2009–2011 and 48.09 mm in 2018, management blades 56.50 mm in 2009–2011 and 57.05 mm in 2018. 2009-2011 bladelets are shorter than 2018 ones (median 24.00/32.61 mm), while management bladelets have a similar median value 38.00/36.29 mm. The recorded median width of blades is 14.00 mm in 2009–2011 and 15.80 mm in 2018, management blades 18.00 mm in 2009–2011 and 19.82 mm in 2018. Bladelets recorded median width is 8.00 mm in 2009–2011 and 9.37 mm in 2018, management bladelets 9.00 mm in 2009–2011 and 10.00 mm in 2018. Last complete negatives measurements are mostly similar to bladelets: median width 5.00/6.64 mm on blanks 10.50/9.36 mm on cores. Median thickness of blades is 3.5/4.24 mm, management blades 6.00/6.70 mm, bladelets 2.00/2.43 mm, management bladelets 3.00/3.71 mm.

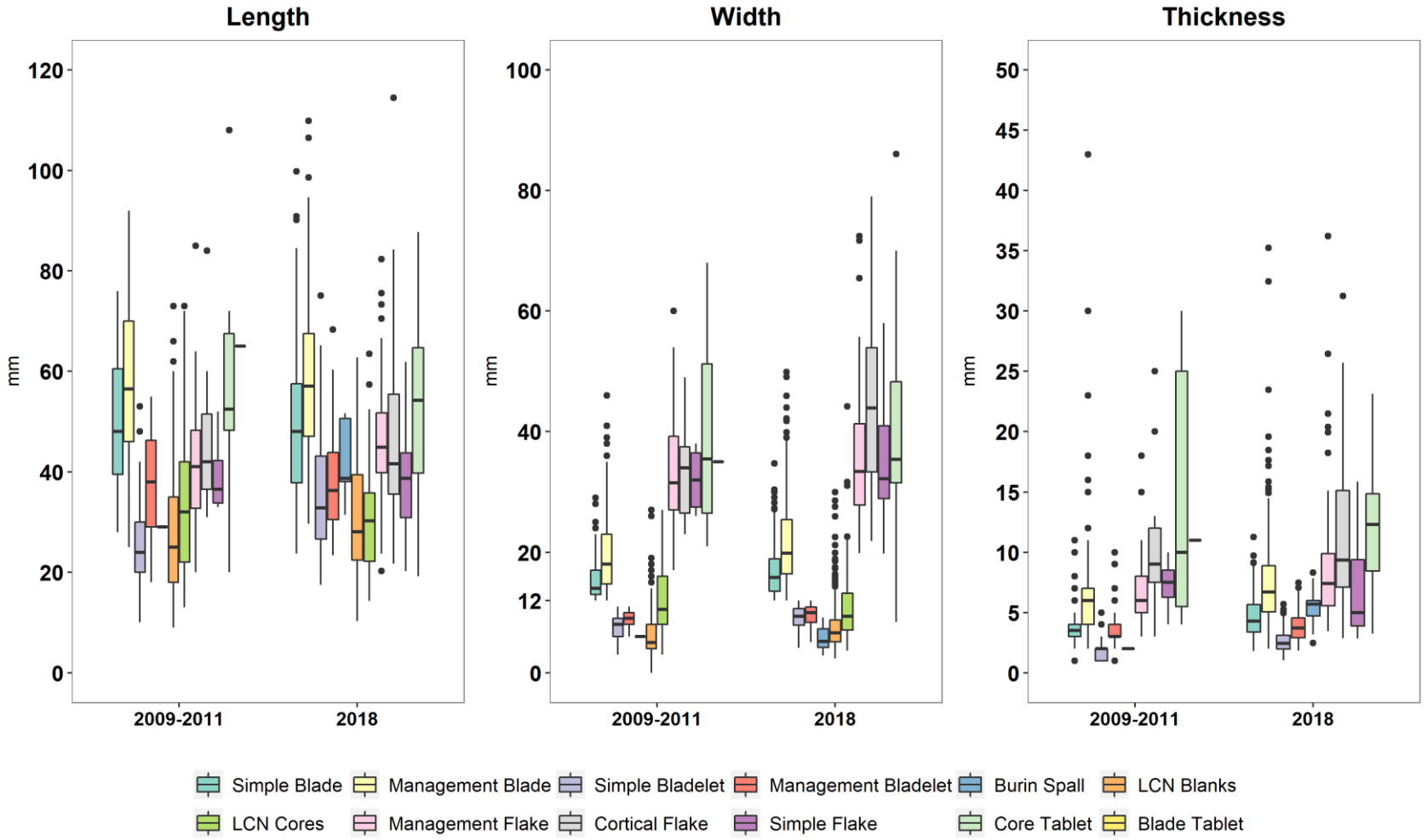

Graph 2 Length, width, and thickness values of blanks. Length and width are compared to those measured for last complete negatives (LCNs) in cores and blanks. Boxes represent the interquartile range (central 50% of the values), bold horizontal line is the median value

3.1.2 Technical Observations

3.1.2.1 Lipping

30.08% of the 2009–2011 assemblage presents a lip, while 46.36% of the 2018 one does. As a general trend in both assemblages, lipping is more marked in management blades, blades, core tablets and cortical flakes, in the 2018 assemblage also management flakes present a lip in most of the cases. Bladelets are mostly devoid of lips in both assemblages.

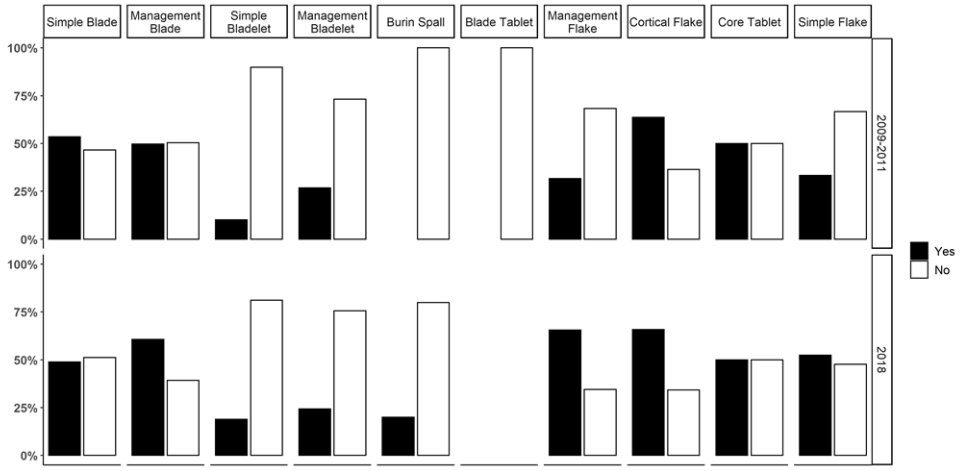

Graph 3 Lipping in both assemblages, only Complete and Prox+Mes blanks.

3.1.2.2 Overhang Abrasion

The overhang is systematically removed through abrasion or micro-chipping in cores and laminar blanks. The core category which shows less abrasion is the Narrow-Fronted *sur Tranche*.

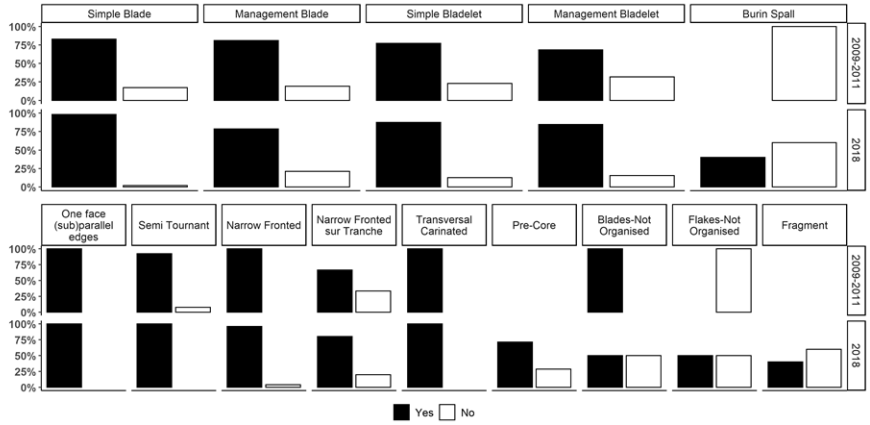

Graph 4 Overhang abrasion in laminar blanks and Cores.

3.1.2.3 Bulb

Bulbs are mostly non-marked. Diffused and not perceived bulbs account together for 72.48% in 2009–2011 and 76.5% in 2018. Most of the diffused bulbs are present in laminar blanks. Marked bulbs, pronounced ones and those with a bulbar scar, account for 25.25% in 2009–2011 and 21.18%

in 2018. Most of the marked bulbs are present in flakes, 2009–2011 simple blades are showing the highest percentage in laminar blanks, 29.31%.

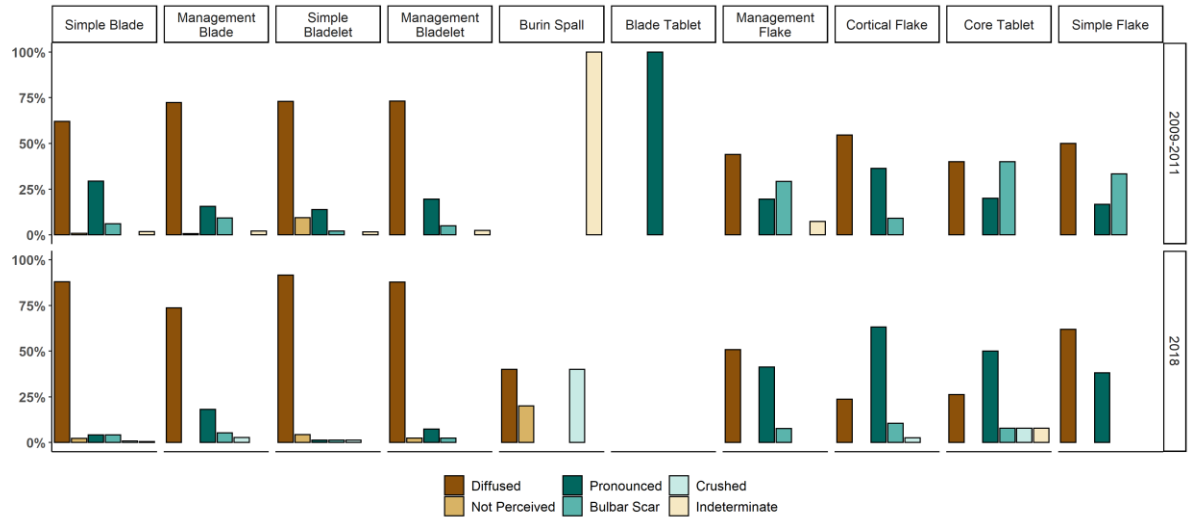

Graph 5 Bulbs in Complete and Prox+Mes blanks.

3.1.2.4 Angle

The exterior angle defined by the platform and the flaking surface is generally really acute, less than 70 degrees. This observation is broadly confirmed by the blanks, 2009–2011 ones having more acute angles while 2018 blanks are more distributed between 70 and 90 degrees.

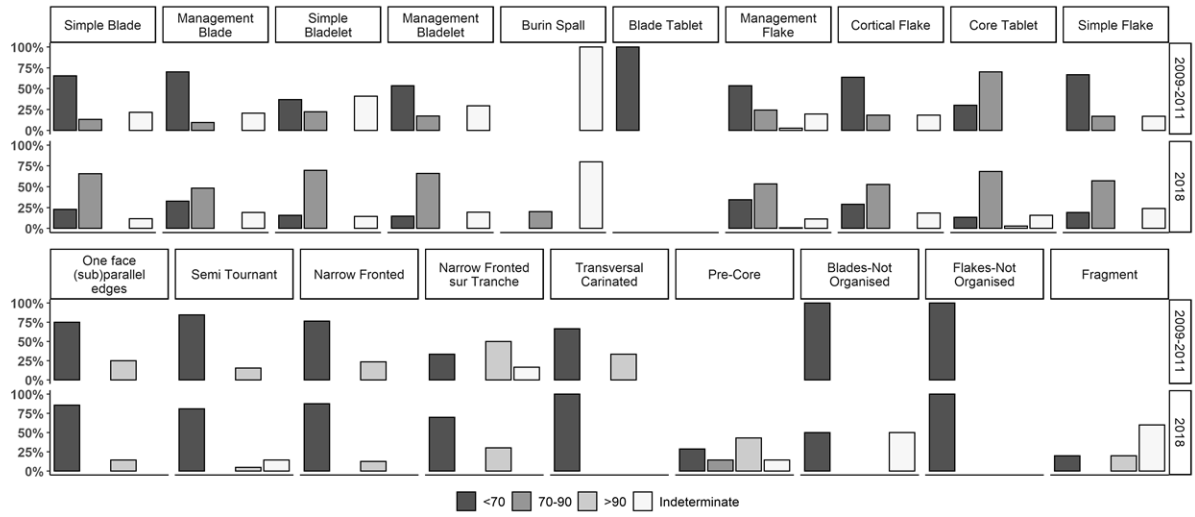

Graph 6 Knapping angle in blanks and cores.

3.1.2.5 Synthetic considerations on knapping technique

Following the considerations of J. Pelegrin (Pelegrin, 2011, 2000) both studied assemblages fit the eUP assemblages knapping techniques. In fact, the laminar blanks have usually less marked bulbs, acute knapping angle, well abraded overhang and lips due to a probable direct tangential soft hammer percussion. Flakes might be knapped through direct inner soft or hard stone hammer percussion.

3.1.3 Morpho-technological Observations

3.1.3.1 Cores

Table 8 Cores Categories in both analysed Al-Ansab 1 assemblages.

	2009-2011	2018
Pre-Core	0 (0.00%)	7 (8.75%)
One face (sub)parallel edges	4 (8.89%)	7 (8.75%)
Semi *Tournant*	13 (28.89%)	21 (26.25%)
Narrow Fronted	17 (37.78%)	24 (30.00%)
Narrow Fronted *sur Tranche*	6 (13.33%)	10 (12.50%)
Transversal Carinated	3 (6.67%)	2 (2.50%)
Blades-Not Organised	1 (2.22%)	2 (2.50%)
Flakes-Not Organised	1 (2.22%)	2 (2.50%)
Fragment	0 (0.00%)	5 (6.25%)
Total	45 (100.00%)	80 (100.00%)

Pre-Core

They are recorded just in the 2018 assemblage, accounting for the 8.75% of the 2018 cores. They are manufactured mostly using blanks or nodules. Cortex is mostly found on a lateral surface and in various combinations with the base of the core. The striking platform is plain and single originating a single surface; in one case two opposed single platforms originate two independent flaking surfaces. Negatives are mostly unipolar combinations of blades and bladelets, in the 28.57% of cases only flakes.

One face (sub) parallel edges

They account for 8.89% of the 2009–2011 cores, and for the 8.75% of 2018 cores. 2018 cores are manufactured mostly on cobbles and nodules, while 2009–2011 cores on squared chunks and nodules. The cortex is mostly found on the posterior face and laterally in both assemblages. The striking platform is mostly single and plain originating a single flaking surface, rarely the core shows an opposite platform. The negatives are mostly exclusively unipolar combinations of blades and bladelets.

Semi Tournant

They account for 28.89% of the 2009–2011 cores and for 26.25% of the 2018 cores. They are mostly manufactured on cobbles and squared chunks in 2009–2011 and cobbles and nodules in 2018. Cortex is found mostly on the posterior face. The striking platform is mostly single and plain originating a

single surface; 2018 cores show rare opposite platforms. Negatives are combinations of unipolar blades and bladelets or only bladelets.

Narrow Fronted

They account for 37.78% of 2009–2011 cores and for 30.00% of 2018 cores. In 2009–2011 assemblage they are mostly manufactured on nodules or squared chunks, while 2018 cores are mostly on cobbles. Cortex is found on posterior and lateral faces. The striking platform is plain and single originating a single flaking surface; 2018 cores show rare opposite platforms. Negatives are mostly unipolar bladelets or combinations of blades and bladelets.

Narrow Fronted sur Tranche

They account for the 13.33% of 2009–2011 cores and for the 12.50% of 2018 cores. They are manufactured mainly on blanks or natural slabs. The cortex is found on lateral faces or at the base of the core. They have strictly plain and single striking platforms originating a single flaking surface. Negatives are unipolar bladelets or combinations of unipolar blades and bladelets.

Transversal Carinated

They account for the 6.67% of 2009–2011 cores and for the 2.50% of 2018 cores. They are manufactured directly on nodules in 2009–2011 or blanks in 2018. They are mostly non cortical. The striking platform is single and plain, originating a single flaking surface; in one case of 2018 cores, two independent surfaces are recorded. The negatives are heterogeneously unipolar blades, bladelets and flakes.

Other Cores

They are represented by not organised blades and flakes productions and cores fragments, in total they account for 4.44% of 2009–2011 cores and 11.25% of 2018 ones. They are manufactured on nodules, cobbles and blanks. The cortex is found on the posterior face or on the core base, but they are largely non cortical. The striking platform is plain and mostly single, originating a single flaking surface. Negatives, regardless of their type, are unipolar.

Synthesis cores

Overall a pattern can be drawn from the two assemblages' cores. Semi *Tournant* and Narrow Fronted are the most frequent configurations. Parallel Edges and *sur Tranche* cores are branching out concepts deriving respectively from the Semi *Tournant* and the Narrow Fronted cores. Transversal Carinated cores are episodic. The four most used configurations have a flaking surface oriented along one of the biggest core axes, with Semi *Tournant* and Parallel Edges cores exploiting larger surfaces than Narrow Fronted cores. Transversal Carinated cores are using wide fronts. Knapping angles are extremely acute, and the overhang is systematically abraded regardless the core configuration. There is no selection of raw material blanks for a particular core configuration, but *sur Tranche* cores show

a preference for naturally narrow surfaces of slabs and blanks' edges. The cortex is found generally on non-extensively managed faces, therefore the posterior face and the base, and in Narrow Fronted cores whose knapping rhythm is frontal, one of the lateral faces is often left untouched in addition to the posterior ones. Most of the cores have a single plain platform and a single surface; rare cases display an opposite, often auxiliary, platform or independent flaking surfaces exploited in a different moment. All cores are showing unipolar negatives, either a combination of blades and bladelets or exclusively bladelets.

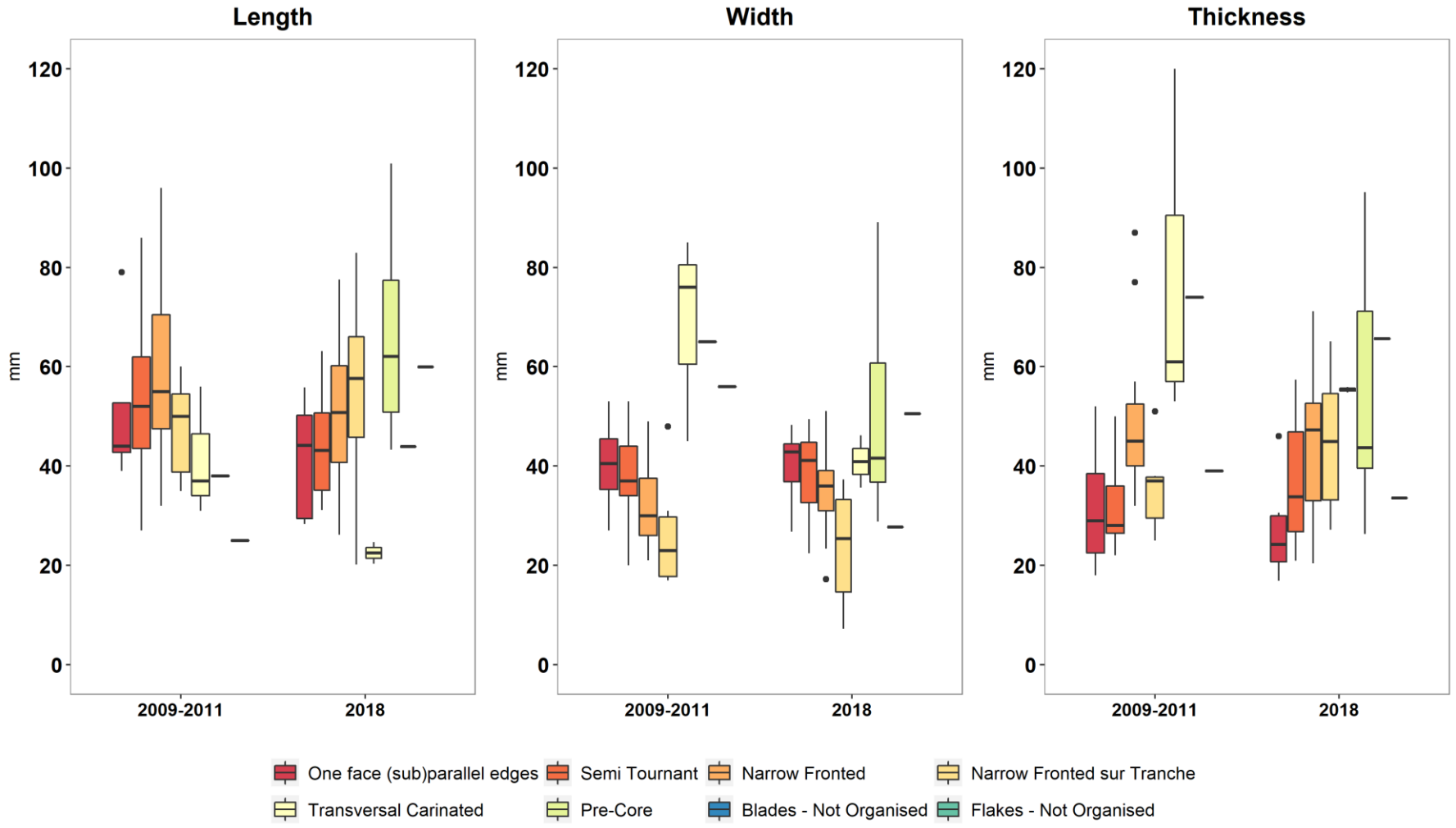

Graph 7 Cores dimensions. Boxes represent the interquartile range; the median is highlighted with a bold black line

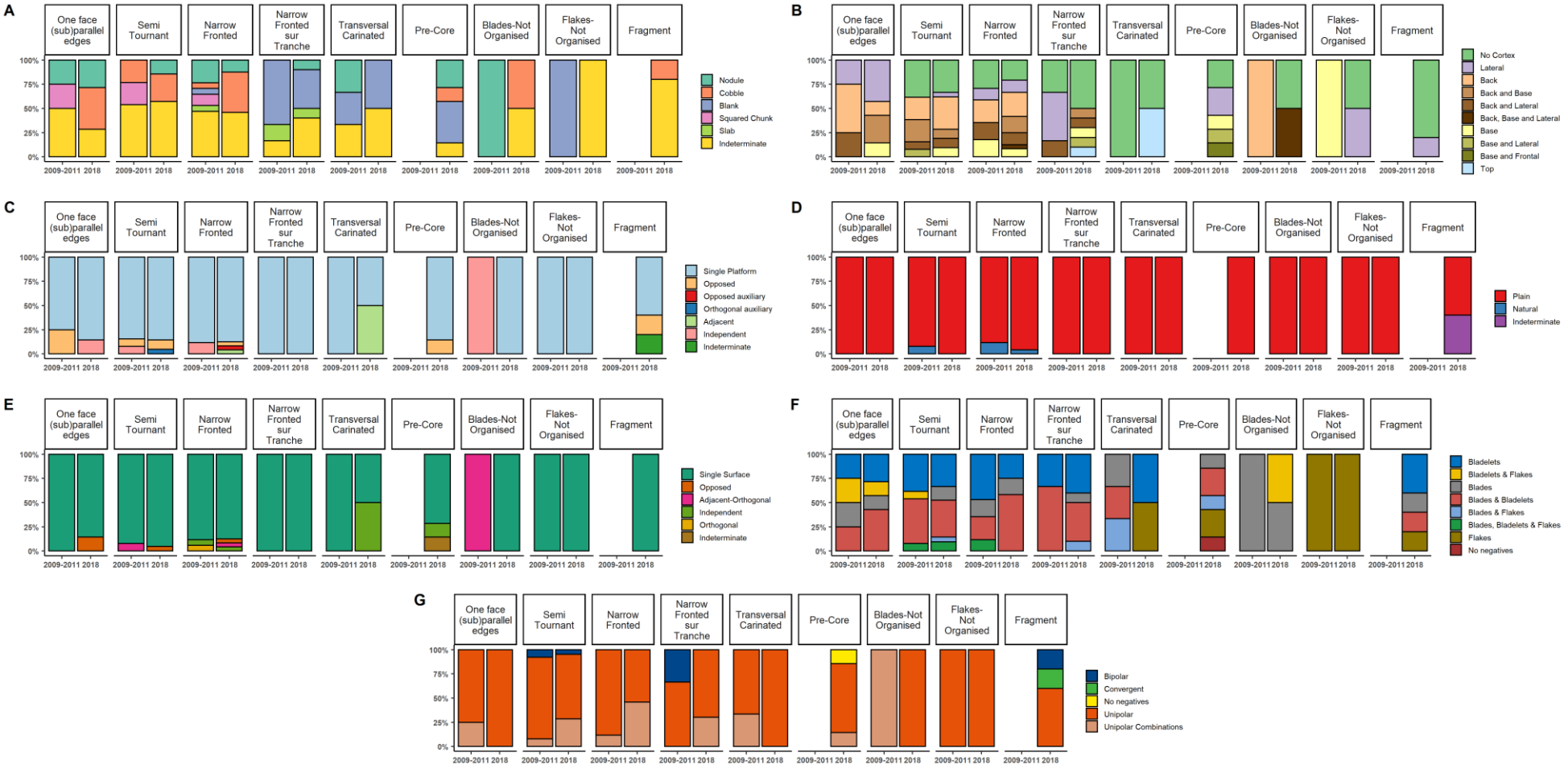

Graph 8 Cores attributes. A) Core blank. B) Cortex position. C) Striking Platform relation. D) Striking Platform type. E) Flaking Surface relation. F) Negatives' type. G) Negatives' orientation

3.1.3.2 Blanks

Table 9 Blanks categories.

	2009-2011	2018
BLADE	**307 (38.66%)**	**653 (51.62%)**
Simple Blade	138 (17.38%)	318 (25.14%)
Blade Tablet	1 (0.13%)	0 (0.00%)
Management Blanks	***168 (21.16%)***	***335 (26.48%)***
Crest	11 (1.39%)	61 (4.82%)
Asymmetrical Blade	91 (11.46%)	146 (11.54%)
Overshot Blade	53 (6.68%)	88 (6.96%)
Surface Cleaning Blade	10 (1.26%)	25 (1.98%)
Maintenance Blade	3 (0.38%)	15 (1.19%)
BLADELET	**418 (52.64%)**	**389 (30.75%)**
Simple Bladelet	360 (45.34%)	327 (25.85%)
Burin Spall	1 (0.13%)	9 (0.71%)
Management Blanks	***57 (7.18%)***	***53 (4.19%)***
Crest	2 (0.25%)	5 (0.40%)
Asymmetrical Blade	43 (5.42%)	34 (2.69%)
Overshot Blade	10 (1.26%)	9 (0.71%)
Maintenance Blade	2 (0.25%)	5 (0.40%)
FLAKE	**69 (8.69%)**	**223 (17.63%)**
Management Blanks	***41 (5.16%)***	***121 (9.57%)***
Surface Cleaning Flake	26 (3.27%)	116 (9.17%)
Maintenance Flake	15 (1.89%)	5 (0.40%)
Core Tablet	10 (1.26%)	38 (3.00%)
Cortical Flake	12 (1.51%)	41 (3.24%)
Simple Flake	6 (0.76%)	23 (1.82%)
TOTAL	**794 (100.00%)**	**1265 (100.00%)**

3.1.3.2.1 Flakes

Flakes are accounting for 8.69% of the 2009–2011 blanks and 17.63% of the 2018 ones.

Management Flakes

The **surface cleaning flakes** are the most abundant in both assemblages, accounting for 3.27% in 2009–2011 and 9.17% of blanks in 2018. Butts are mostly plain, followed by linear. Blanks are similarly non-cortical in both assemblages, followed by semi-cortical blanks mostly located in lateral position. Flakes are individually the most recorded negatives' type, but the joint laminar negatives' types are the most represented. Unipolar represents the most recorded orientation in both assemblages. Crossed is representing the second most recorded value.

Generic **maintenance flakes** account for 1.89% in 2009–2011 and 0.40% in 2018. Butts are mostly plain in both assemblages. Blanks are non-cortical in 2018 assemblage, while 2009–2011 ones are more diversified with some semi-cortical and extensively cortical blanks too. The cortex is variably located in lateral, distal or dorsal position. Negatives types have been determined only in 2009–2011, they are mostly exclusively flakes or blades. The orientation of negatives is prevalently unipolar in both assemblages, crossed negatives are again the second most recorded value in 2009–2011.

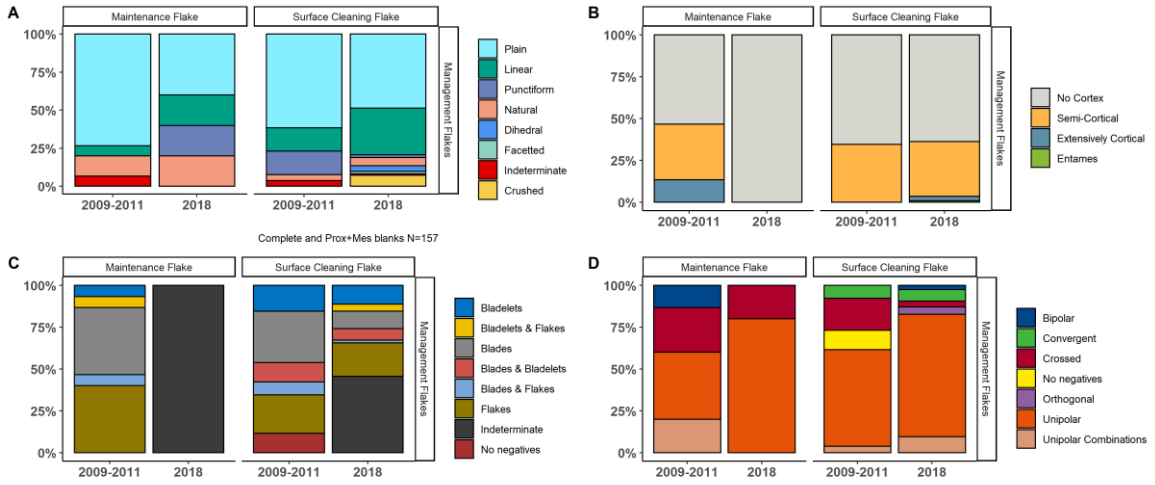

Graph 9 Management Flakes technological attributes. A) Butt values. B) Cortex coverage. C) Negatives' types. D) Negatives' orientation.

Core Tablet

Core tablets account for the 1.26% of 2009–2011 blanks and for the 3% of 2018 ones. Butts are mostly plain or facetted. While 2018 tablets are mostly non-cortical. 2009–2011 are mostly semi-cortical. But 2018 tablets feature also, primary ones completely cortical. Bladelets and combinations of blades and bladelets are the most abundant negatives' types in 2018 assemblage, while in 2009–2011 assemblage flakes are more represented. Negatives are mostly orthogonal in 2018 blanks, while unipolar and orthogonal orientations are mostly recorded in 2009–2011 blanks.

Cortical Flake

Cortical flakes account for the 1.51% of 2009–2011 blanks and 3.24% of 2018 ones. Butts are mostly plain and followed by linear in 2018 assemblage. Blanks are mostly entames, followed by extensively cortical ones, covering the dorsal blank's face. Negatives are rare, they are mostly unipolar flakes.

Simple Flake

Simple flakes account for the 0.76% 2009–2011 blanks and for the 1.82% of 2018 blanks. Butts are mostly plain. Blanks are mostly non-cortical, cortex covers only until the half of the blanks surface, mostly laterally. Determined negatives types are mostly flakes. 2018 negatives are largely unipolar, while 2009–2011 are mostly crossed.

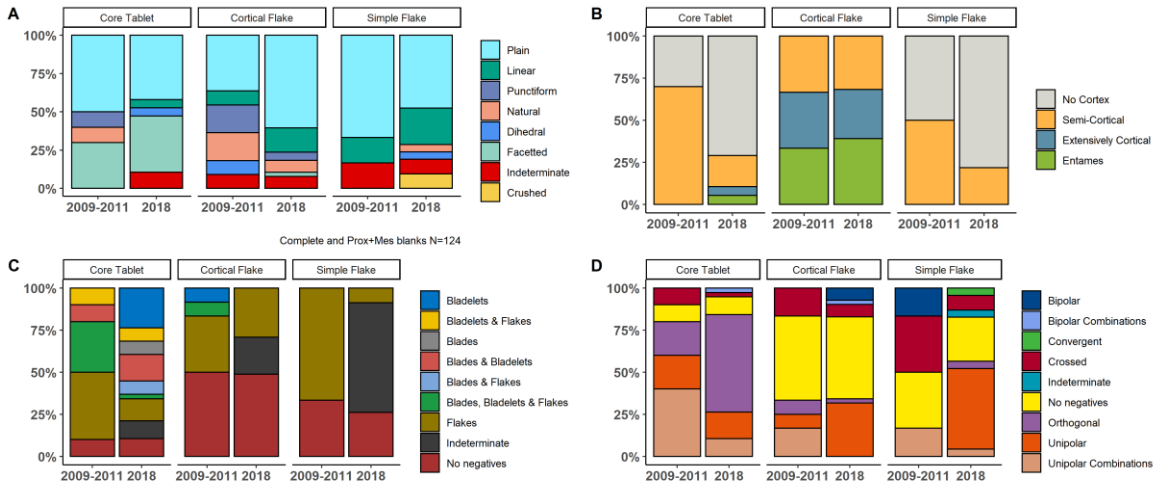

Graph 10 Core Tablet, Cortical and Simple Flakes technological attributes. A) Butt values. B) Cortex coverage. C) Negatives' types. D) Negatives' orientation.

3.1.3.2.2 Laminar

Laminar blanks are represented by blades and bladelets, blades account for 38.66% of 2009–2011 blanks and 51.62% of 2018 ones, while bladelets are 52.64% of 2009–2011 blanks and 30.75% of 2018 blanks.

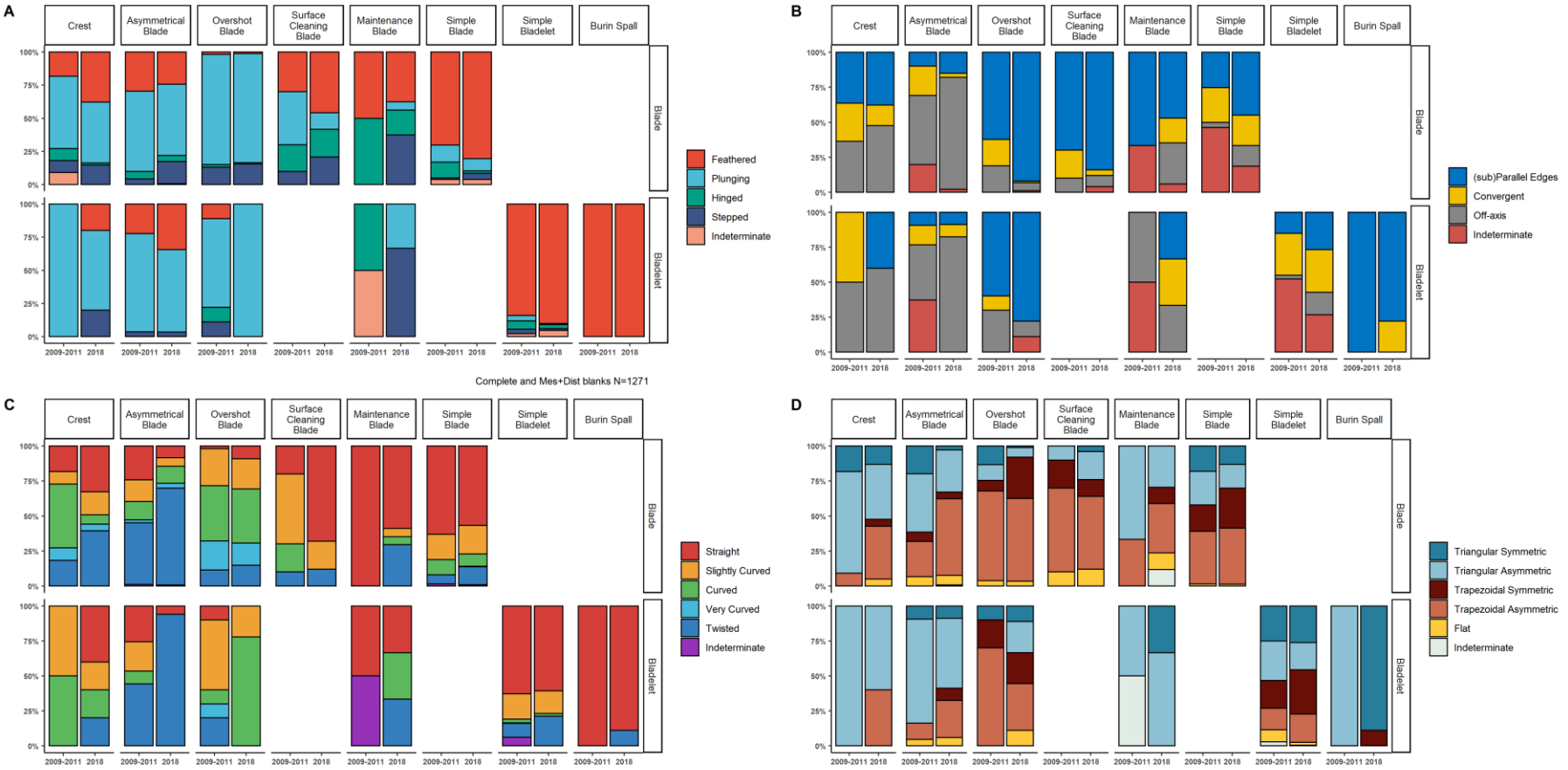

Graph 11 Laminar morphological attributes.A) Distal termination. B) Outline. C) Profile. D) Cross-section.

Management blanks

Management blanks of blade size are 21.16% of 2009–2011 blanks and 26.48% of 2018 blanks, while bladelet-size blanks are 7.18% of 2009–2011 blanks and 4.19% of 2018 blanks.

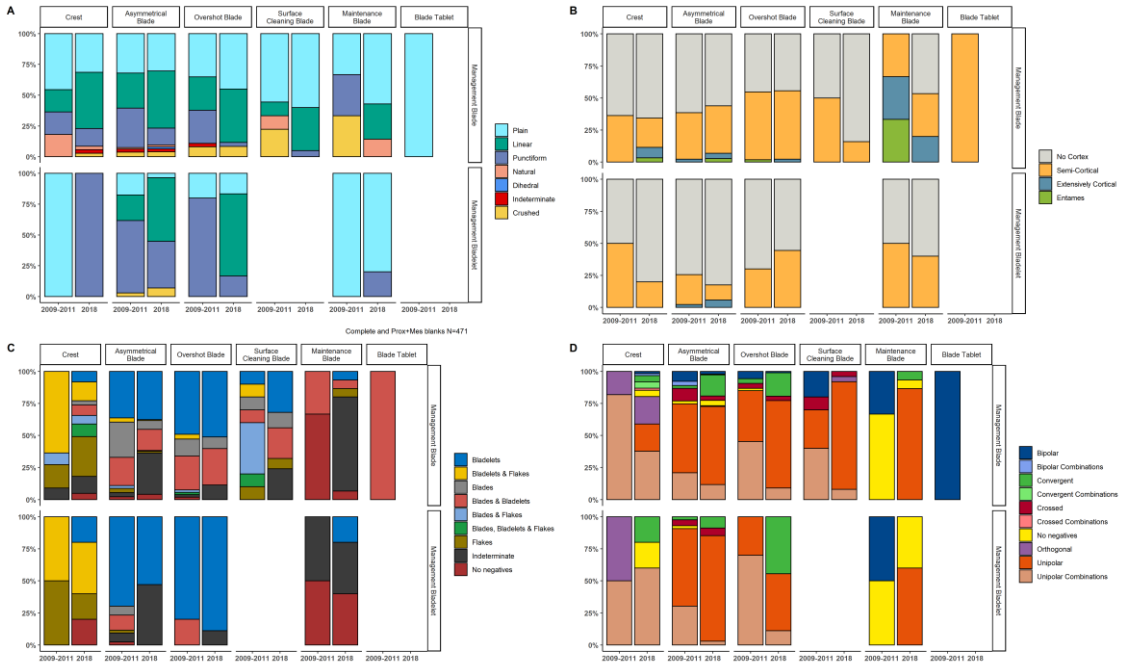

Graph 12 Management Blades technological attributes. A) Butt values. B) Cortex coverage. C) Negatives' types. D) Negatives' orientation.

Crest

Crested blades account for the 11.39% of 2009–2011 blanks and for the 4.82% of 2018 ones. Crested bladelets account for the 0.25% of 2009–2011 blanks and for the 0.40% of 2018 ones. The 2009–2011 butts are mostly plain, 2018 ones are mostly linear and plain. Blanks are mostly non-cortical, blades have a higher share of semi-cortical blanks, prevalently in lateral position. Most of the blanks display a combination of bladelets and flakes negatives or exclusively flakes ones. Orthogonal and a combination of unipolar and orthogonal are the most frequent negatives' orientations. The terminations are usually plunging, feathered terminations are more frequent in 2018 blanks. Outline is mostly distributed among sub-parallel and off-axis values. 2009–2011 profiles are mostly curved, while 2018 profiles are mostly straight and twisted. 2009–2011 cross-section is prevalently triangular, 2018 blanks' cross-section is mostly asymmetrical, either trapezoidal or triangular.

Asymmetrical blade

Blade-sized asymmetrical blades account for the 11.46% of 2009–2011 assemblage and for the 11.54% of 2018 assemblage, while bladelet-sized for the 5.42% of 2009–2011 blanks and for the 2.69% of 2018 blank. Butts are mostly linear, plain and punctiform in blades, while are mostly linear and punctiform in bladelets. Blanks are mostly non-cortical in blades and bladelets, but blades show

a higher incidence of cortex, covering mostly up to the half of the blank surface and located in lateral or distal position. Bladelets negatives, and combinations with blades, are the most frequent in blade-sized blanks; in 2009–2011 exclusive blades negatives have a higher share than 2018 ones. In bladelets-sized blanks, bladelets are almost the only determinate negatives. In both assemblages, negatives are largely unipolar, followed by convergent or unipolar and convergent. Terminations in both blades and bladelets are mostly plunging, followed by feathered terminations. The outline is generally off-axis, but 2009–2011 blanks are followed by higher representation of convergent outlines. 2009–2011 blades' profiles, apart from the dominant twisted ones, blades show higher percentages straight, slightly curved, and curved profiles, while they are mostly twisted and curved in 2018 blades. The same trend is shown by the bladelets. While 2018 blades have a mostly asymmetrical cross-section, triangular and trapezoidal, 2009–2011 blades also show a good share of symmetrical triangular cross-section. Bladelets of both assemblages have a mostly triangular asymmetrical cross-section.

Overshot blade

Blade-sized blanks account for the 6.68% of 2009–2011 ones and for 6.96% of 2018 blanks, bladelet-sized blanks account for the 1.26% of 2009–2011 blanks and for the 0.71% of 2018 ones. 2018 blades' butts are mostly plain and linear, while 2009–2011 ones are plain, linear and punctiform. 2018 bladelets have mostly linear butts, 2009–2011 ones are mostly punctiform. Both 2018 and 2009–2011 blades are frequently semi-cortical on the distal part, while bladelets shows a higher incidence of non-cortical blanks. Bladelets negatives are found on half of both assemblages' blades, followed by a combination of blades and bladelets. Bladelets negatives are typically found on bladelet-sized blanks. Negatives are prevalently unipolar, in 2009–2011 blanks the combined unipolar and convergent orientation is more represented than in 2018 blanks, while pure convergent negatives are more attested in the latter ones. Blades and bladelets terminations are prevalently plunging, followed by stepped ones. Outlines are generally sub-parallel, off-axis blanks increase in bladelets. Profiles are mostly curved; blades show an emphasis on curvature and twisting. Blades' cross-section is mostly trapezoidal asymmetrical, 2009–2011 blanks show a higher incidence of triangular cross-section while 2018 ones more trapezoidal symmetrical cross-sections

Surface Cleaning blade

They are recorded only in blade-sized blanks. They account for the 1.26% of 2009–2011 blanks and for the 1.98% of 2018 ones. Their butts are mostly plain, 2018 ones are followed by linear. Blanks are mostly non-cortical, the share of cortical blanks, only semi-cortical, is higher in 2009–2011 blanks, nonetheless cortex is located laterally or distally. 2018 blanks show mostly bladelets negatives and combination of blades and bladelets, while 2009–2011 mostly a combination of blades and flakes. Negatives are typically unipolar. Terminations are either feathered or plunging. The

outlines are prevalently sub-parallel. 2018 blanks have mostly straight profiles, while 2009–2011 slightly curved ones. The cross-section is usually trapezoidal asymmetrical.

Maintenance blade

Blade-sized blanks account for the 0.38% of 2009–2011 blanks and for the 1.19% of 2018 ones, bladelets account for the 0.25% of 2009–2011 blanks and for the 0.40% of 2018 ones. Butts are mostly plain. Non-cortical blanks are the most frequent, cortical blanks are more common in blades with some extensively cortical blanks; cortex is mostly located laterally. Negatives are mostly indeterminate. Negatives' orientation is mostly unipolar. Terminations are mostly feathered, in 2018 blanks also stepped. Outlines are mostly sub-parallel. Profiles are mostly straight; 2018 ones are followed by twisted profiles. Cross-sections are mostly asymmetrical either triangular or trapezoidal.

Simple blade and simple bladelet

Simple blades account for the 17.38% of 2009–2011 assemblage and for the 25.14% of 2018 assemblage. Simple bladelets account for the 45.34% of 2009–2011 assemblage and for the 25.85% of the 2018 assemblage. Butts are mostly linear in blades and bladelets, followed by punctiform ones in 2009–2011 blades and bladelets, by plain butts in 2018 blades and bladelets. Bladelets are almost completely non-cortical, while blades of both assemblages show a higher percentage of semi-cortical blanks, more marked in 2018 assemblage, mostly in lateral position. Bladelets are the most frequent negative type in blades and bladelets of both assemblages, in blades it is followed by a combination of blades and bladelets negatives. Negatives are mostly unipolar in blades and bladelets of both assemblages, bladelets show a higher percentage of convergent negatives than blades. Terminations are largely feathered for blades and bladelets of both assemblages, blades show a higher percentage of plunging terminations. Outlines are equally distributed in sub-parallel and convergent in blades, while bladelets have a tendency towards being more convergent. Profiles are mostly straight and slightly curved for blades and bladelets of both assemblages, blades have a higher percentage of curved blanks, mostly 2009–2011, while bladelets have more twisted ones, mostly 2018. Blades have mostly a trapezoidal cross-section, asymmetrical being more marked in both assemblages, bladelets are more equally distributed among trapezoidal and triangular cross-sections, mostly symmetrical.

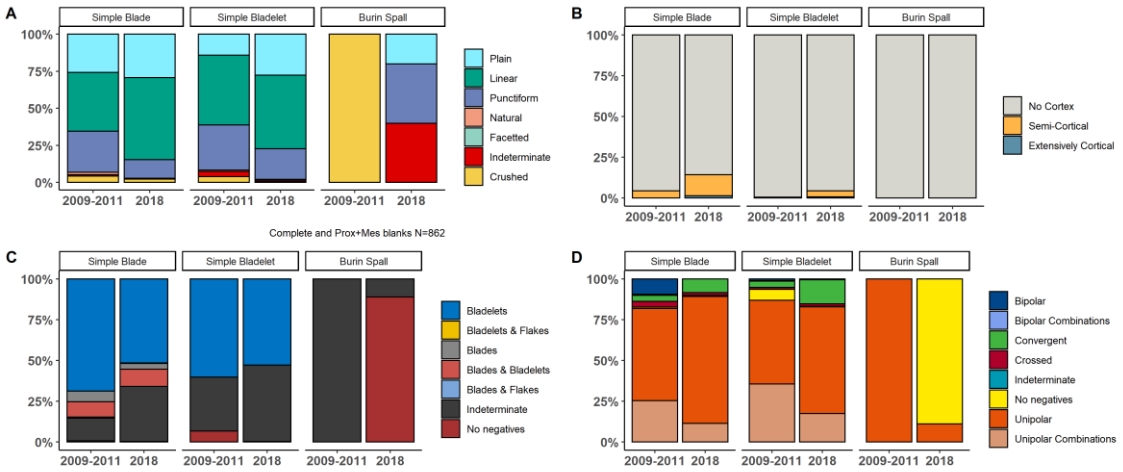

Graph 13 Simple blades, simple bladelets and burin spalls technological attributes. A) Butt values. B) Cortex coverage. C) Negatives' types. D) Negatives' orientation

Burin Spall

Burin spalls are the 0.13% of 2009–2011 assemblage and the 0.71% of 2018 one. Butts are mostly punctiform. The blanks are non-cortical. Mostly they do not have negatives. Cross-sections are triangular symmetrical. Terminations are feathered. They have mostly sub-parallel outlines. The profile is straight.

Retouched Blanks

Retouched blanks are mostly manufactured on laminar blanks in both assemblages.

Burins are the most frequent tool type in both assemblages and are largely fabricated on simple blade blanks and a core tablet. The combination of **laterally retouched bladelets and backed bladelets,** is the second biggest type group, mostly fabricated on simple bladelets. **Endscrapers** are the third most frequent types, mostly produced on management flakes and surface cleaning flakes. **El Wad points** are the fourth most frequent type, mostly fabricated on simple bladelets and blades.

3.1.4 Conclusions

The above section had the goal to present the technological analysis of Al-Ansab 1 lithic assemblages.

The two assemblages show different representation of blades and bladelets, therefore, in absence of single artefacts coordinate plotting for 2009–2011 sample, it is difficult to estimate which is the real ratio between the two products. While the 2009–2011 assemblage shows a higher frequency of bladelets, the 2018 numbers are substantially even. If only, such a high presence of fine lithic fraction would confirm again the *in-situ* nature of 2009–2011 context. On the other hand, if we assume that the archaeological material was deposited in single short-stay events and then mildly affected by water flooding from the nearby wadi (Richter et al., 2020; Schoenenberg, 2018), the original blades–bladelets numbers might be biased by grouping several single events in a palimpsest assemblage.

Nevertheless, technologically the two assemblages show the same trends.

Cores are mostly single platform ones. The striking platform is kept plain and renewed often through the knapping of core tablets, operation repeated until the core abandonment, as the wide dimensional range of tablets is showing. The two main core configurations, slightly fluid in their application, are the semi *Tournant* and the Narrow Fronted ones, which are related mostly to the choice of a narrower or a wider core faces as flaking surfaces; this could be related to a mere pragmatic exploitation of differently shaped raw material pieces. An accentuation of the morphological characteristics is evident in the Parallel Edges cores, on one hand, and in the Narrow Fronted sur Tranche, on the other hand. If Narrow Fronted cores usually reduce the core volume frontally, semi *Tournant* ones show a tendency towards the expansion over the adjacent lateral faces, mostly involved into the convexities shaping; convexities that are naturally provided if adopting a narrow flaking surface. Setting apart the, mostly, morphological differences the cores show similar tendencies. The cortical surfaces are maintained mostly in every core portion which is not involved in the knapping, as noted in Boker A (Monigal, 2003), and not extensively decorticated as in Nahal Nizzana XIII (Goring-Morris and Davidzon, 2006). The flaking angle is acute, and the overhang is systematically abraded/micro-chipped as expected in volumetric laminar knapping, the angles are less acute in blanks probably hinting towards a progression towards a higher acuteness at the end of the knapping. Negatives are unipolar, rare second platforms are opened, but mostly related to a subsequent and independent exploitation of the convexities.

Integrating with the observations made on blanks, the production is oriented towards the obtention of laminar blanks; flakes are a minority and relegated to shaping roles. The overall technical data from bulbs and lips is rather homogenous, the major technical break, if there is one, is probably more related to the size of the blanks, rather than the technological role as suggested in a previous analysis (Hussain, 2015). A tangential direct soft hammer percussion can be envisioned for products coming from the fully developed reduction, the inner direct hammer percussion may have been used for some of the initial blanks, mostly flakes.

Once the main platform is set, the core reduction starts directly with removing a natural lateral ridge, which can be distally shaped in a unilateral crest. Then, the guiding ridge produced is used for the knapping of simple blades and bladelets, arresting at around three quarters of the flaking surface extensions, i.e., not removing the distally curved part of the surface, and, thus, erasing the convexities created. Comparing the median thickness of Core Tablets (10–12 mm) with the longest blanks (slightly more than 90 mm) and median abandoned cores' length (50–60 mm), I may infer that the striking platform was renewed 3–4 times, on average. This operation was carried out "slicing" horizontally the core with a perpendicular gesture hitting either on the main core flaking surface or slightly on the side, thus resulting in "facetted" butts, due to the previous unipolar bladelets–blades negatives. Operations of convexities' management are carried out mostly by laminar blanks identified as asymmetrical blades, overshot blades or, rare, surface cleaning blades. Asymmetrical

blades, being the most frequent, are the most interesting to discuss. They generally display an off-axis outline, a plunging termination, and a twisted profile: these are proxies of a knapping at the core faces' intersection "wrapping" the lateral-framing flaking surface's ridges. Often simple bladelets and blades negatives are found on the ridge asymmetrical blades are removing/reshaping.

It is reconciling with the other main observation of this analysis: simple bladelets are, if not the majority, a consistent part of the blanks that could not be related to managing roles. They are mostly regular in shape and with straight profiles, hence matching negatives erasing convexities on blanks and cores. Bladelet-sized negatives are represented at all knapping stages. Convexities management blanks are mostly recognised in blade blanks; therefore, management choices are not influenced by the core volume reduction. Thus, it seems more conservative to interpret the knapping as a series of independent productions of combined blades and bladelets or only bladelets and not a continuous reduction in which bladelets are the result of volume loss as previously suggested for Al-Ansab 1 (Hussain, 2015), Nahal Nizzana XIII and the early Ahmarian in general (Goring-Morris and Davidzon, 2006).

As a conclusive remark, Al-Ansab 1 is undeniably showing techno-typological Early Ahmarian features, as previously noticed by other authors (Hussain, 2015; Richter et al., 2020; Schyle, 2015), the role of blades and bladelets in the production is reassessed in this analysis, the sample shows a coherent goal towards the obtention of small-sized blanks, bladelets, with largely overlapping characteristics in both assemblages.

3.2 Românești-Dumbrăviţa I

3.2.1 Assemblage Composition

The assemblage is almost equally divided amongst laminar and flake blanks. Bladelets are slightly more frequent than blades.

Table 10 Assemblage composition using complete and semi-complete blanks

Blade	Bladelet	Flake	Total
263 (24.04%)	287 (26.23%)	544 (49.73%)	1094 (100.00%)

3.2.1.1 Fragmentation

Complete blanks are representing the highest frequency in all blanks' categories, especially flakes (≈88%). While blades are mostly complete and proximal fragments, bladelets show a higher frequency of distal fragments.

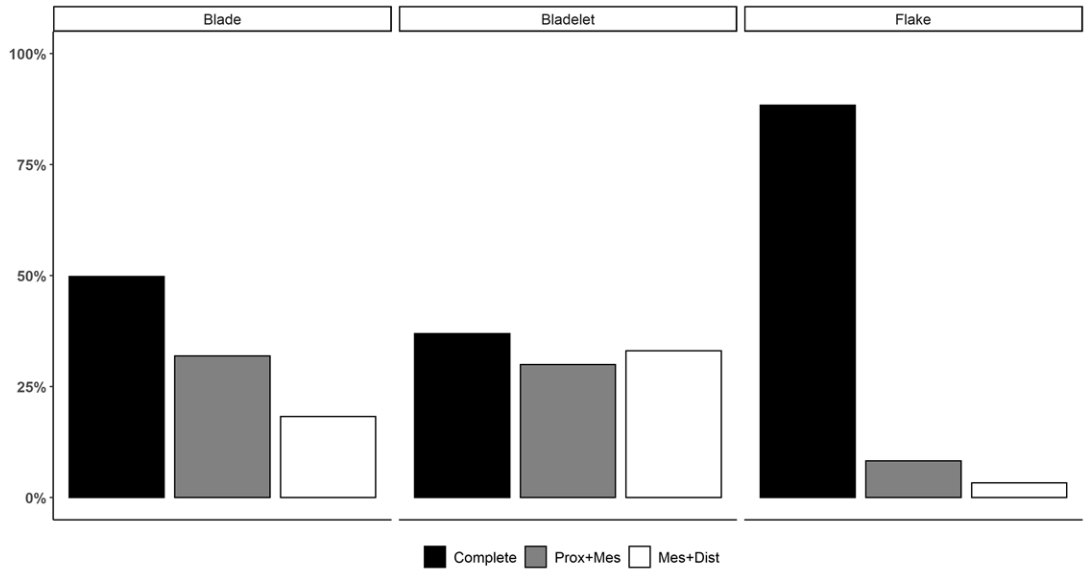

Graph 14 Fragmentation in blanks.

3.2.1.2 Metric Attributes

Blades and bladelets are showing the same trend: management blanks are usually larger and thicker. Dimensions of last complete negatives, especially regarding the width, are mostly compatible with those of the bladelets. Blades have a median length of 39.19 mm, while management blades of 42.99 mm. Bladelets have a median length of 19.99 mm, while management bladelets of 27.54 mm. Last complete negatives have a median length of 21.98 mm in blanks and 27.35 mm in cores. Blades have a median width of 15.57 mm, while management blades of 18.53 mm. Bladelets have a median width of 8.58 mm, while management bladelets of 9.66 mm. Last complete negatives have a median width of 6.94 mm in blanks and of 7.69 in cores. Blades have a median thickness of 3.70 mm, while management blades of 6.73 mm. Bladelets have a median thickness of 1.93 mm, while management bladelets of 3.05 mm.

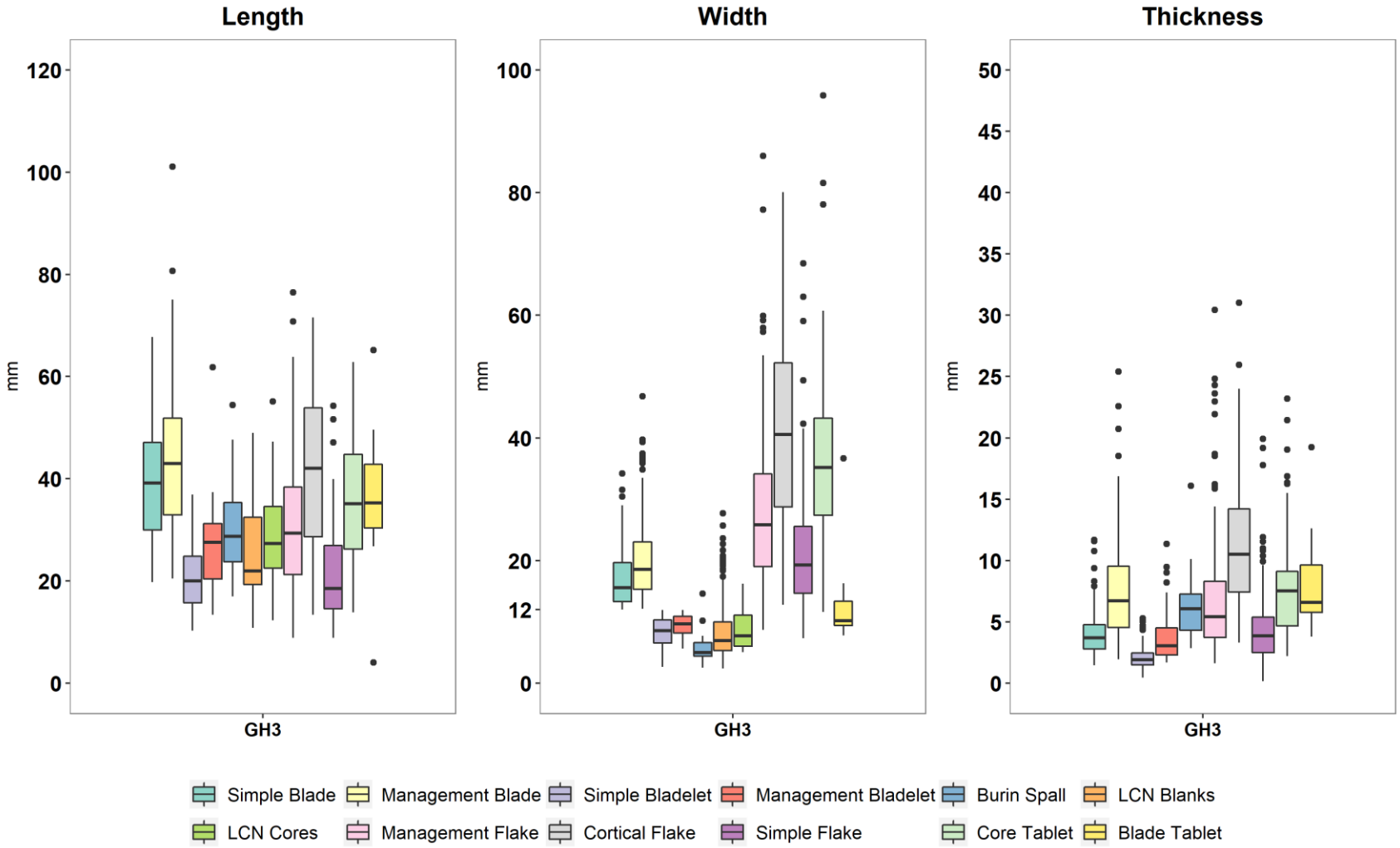

Graph 15 Length, width and thickness values of blanks. Length and width are compared to those measured for last complete negatives (LCNs) in cores and blanks. Boxes represent the interquartile range (central 50% of the values), bold horizontal line is the median value

3.2.2 Technical Observations

3.3.2.1 Lipping

Most of the blanks are non-lipped, 63.21%. Blanks showing the higher percentages of lips are, in order, blades and management flakes.

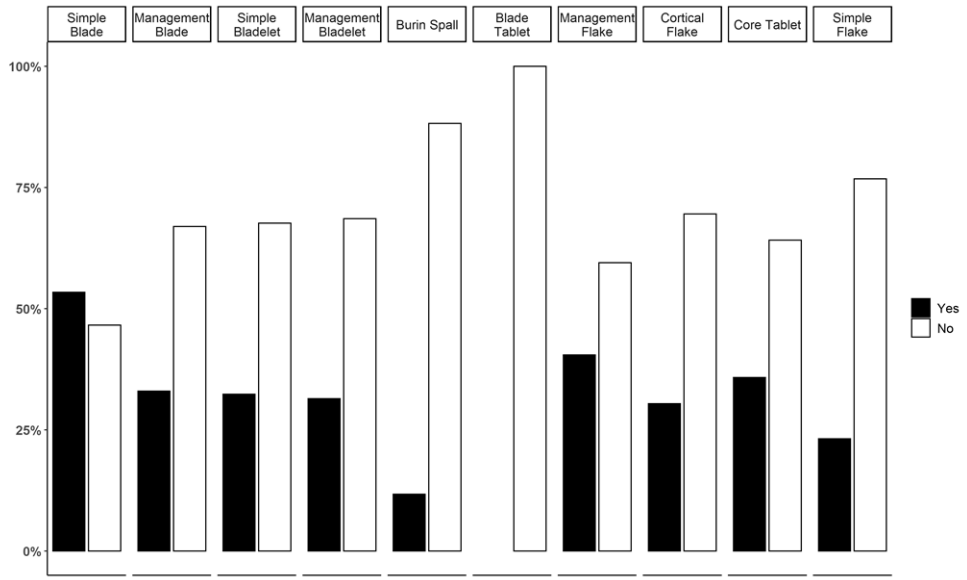

Graph 16 Lipping values

3.2.2.2 Overhang Abrasion

Overhang abrasion is detected in most of the laminar blanks (69.61%), in particular in blades, bladelets and management blades. Half of the cores shows overhang abrasion, mostly semi *Tournant* and Narrow Fronted *sur Tranche* cores.

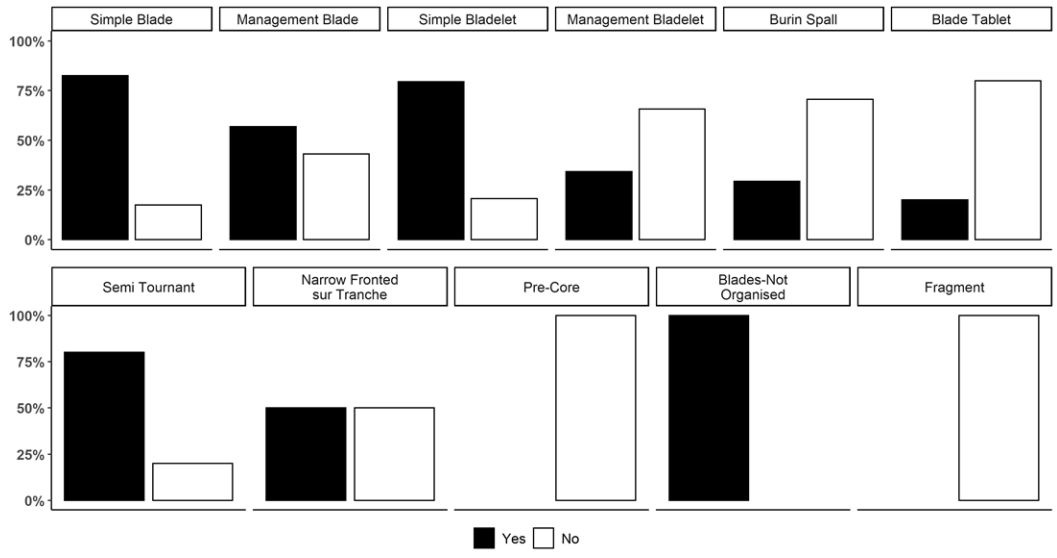

Graph 17 Overhang abrasion in blanks and cores.

3.2.2.3 Bulb

Non-marked bulbs are the majority (60.03%). Higher frequencies are recorded in laminar blanks, while flakes are almost equally divided between non-marked and marked bulbs. Pronounced bulbs are recorded, in particular, in cortical flakes and core tablets.

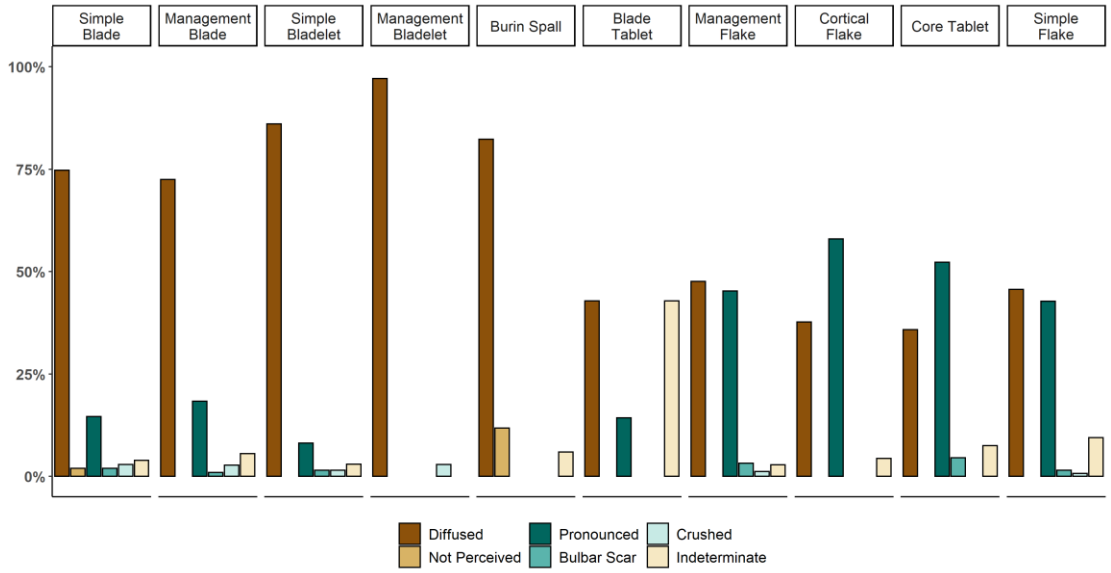

Graph 18 Bulb values in Complete and Prox+Mes blanks.

3.2.2.4 Angle

The external angle is acute, mostly comprised between 70 and 90 degrees. Roughly a quarter of the assemblages shows extremely acute angles, especially management blades, blades and management flakes. Cores follows the same trend, semi *Tournant* cores show the most acute angles.

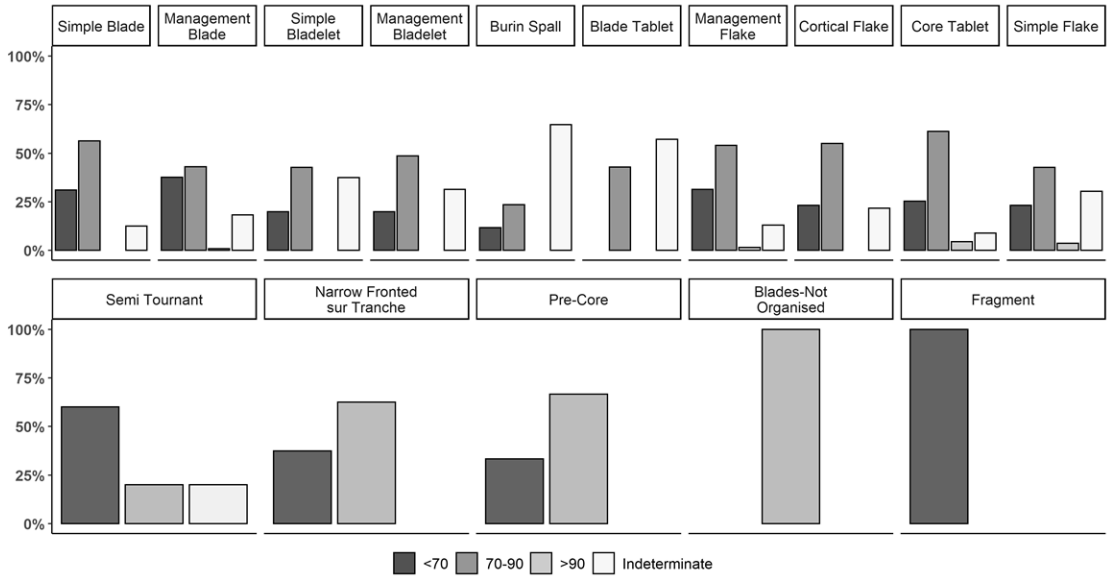

Graph 19 Knapping angles in blanks and cores.

3.2.2.5 Synthetic considerations on knapping technique

The above-mentioned observations are fitting the definition of laminar volumetric knapping through direct soft hammer tangential percussion (Pelegrin, 2011, 2000). In fact, in cores and blanks, overhang abrasion, acute knapping angle and diffused bulbs are customary. Lipping has a lesser incidence, with exception of blades, and it is equally distributed in other blanks. Early-stage flakes, such as cortical ones and some tablets, might have been produced with direct hard hammer inner percussion.

3.2.3 Morpho-technological Observations

3.2.3.1 Cores

Table 11 Cores categories

Semi Tournant	5 (27.78%)
Narrow Fronted *sur Tranche*	8 (44.44%)
Pre-Core	3 (16.67%)
Blades-Not Organised	1 (5.56%)
Fragment	1 (5.56%)
Total	18 (100.00%)

Pre-Core

They are 16.67% of the cores. They are shaped on small nodules and a squared chunk. Cortex is either on the back or on top. The striking platform is plain in all cases. It is mostly single, leading to a single surface; in one case, two independent platforms have been recognised. Negatives are either blades or bladelets, always unipolar. One core shows an extremely elaborated roughing out and central primary crest shaping and was abandoned at this stage for unknown reasons before being activated as a *sur Tranche* core.

Semi Tournant

Semi *Tournant* cores are 27.78% of the cores. They are knapped, in general, on nodules. Cortex is found on the posterior and lateral faces. The striking platform is plain and mostly single: opposed and independent platforms are rare. Negatives are mostly a combination of blades and bladelets, the rest are exclusively bladelets. They are mostly unipolar followed by unipolar and convergent combination, and bipolar negatives in one case.

Narrow Fronted sur Tranche

Narrow Fronted *sur Tranche* cores are the 44.44% of cores. They are shaped mostly on blanks or slabs, in one case on a squared chunk. Cortex is mostly on lateral faces. The striking platform is mostly plain, in the remaining cases it is natural. It is mostly single, with rare opposed and auxiliary

platforms. Negatives are mostly bladelets followed by a combination of blades and bladelets. The orientation is always unipolar.

Other Cores

Other cores are a non-organised blade core and an indeterminate fragment. Both are non-cortical. The striking platform is plain and single. Negatives are a combination of blades and bladelets and bladelets. They are unipolar or convergent.

Synthesis cores

Two main core configurations are recorded: the Narrow Fronted *sur Tranche* and the semi *Tournant*. While the latter are manufactured mostly on nodules, or rounder raw material pieces, the Narrow Fronted *sur Tranche* cores exploit the narrow edges of blanks. Pre-cores are showing that they could be fabricated from lenticular raw material pieces too. The cores are generally non-cortical, cortex patches are mostly found on lateral or posterior faces, not involved by exploitation or shaping. The striking platforms are usually plain and mostly single, in some rare cases opposed, auxiliary or independent ones are opened. Negatives on the main striking surface are either a combination of blades and bladelets or just bladelets. The orientation is largely unipolar or unipolar and convergent.

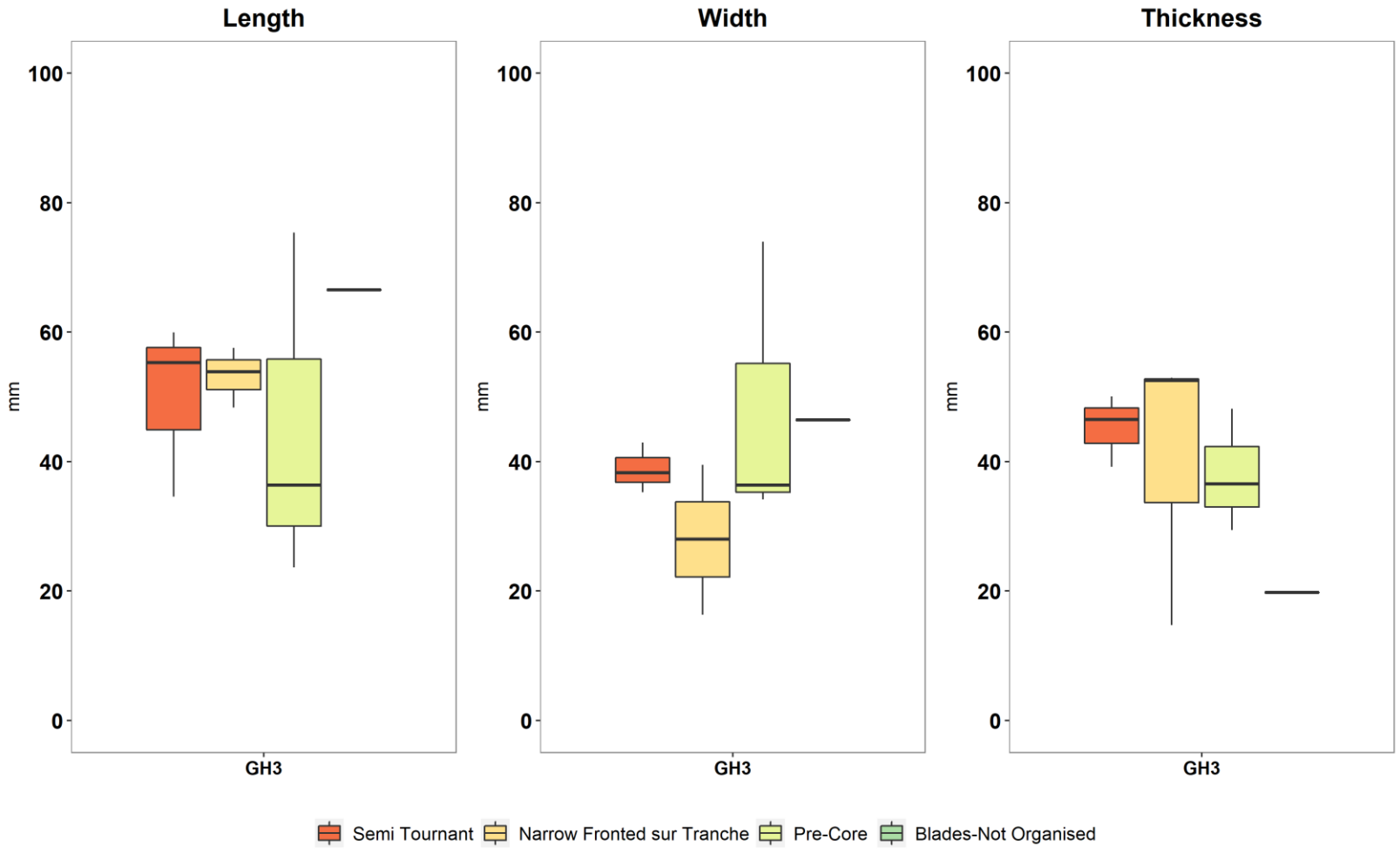

Graph 20 Cores dimensions. Box plots represent the interquartile range, the median is highlighted in a bold black line.

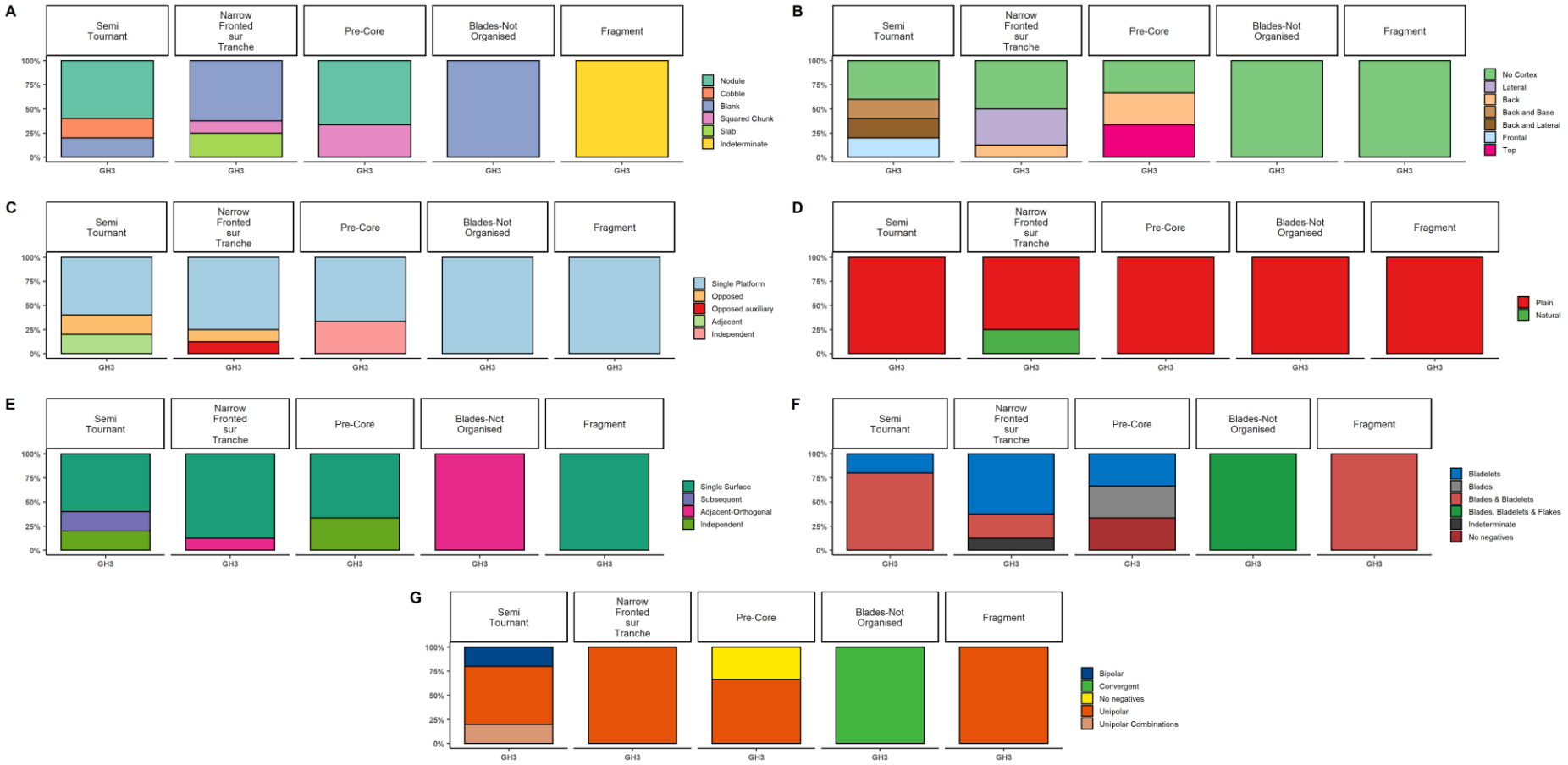

Graph 21 Cores attributes. A) Core blank. B) Cortex position. C) Striking Platform relation. D) Striking Platform type. E) Flaking Surface relation. F) Negatives' type. G) Negatives' orientation

3.2.3.2 Blanks

Table 12 Blanks categories

BLADE	**263 (24.04%)**	
Simple Blade		128 (11.70%)
Burin Spall		1 (0.09%)
Blade Tablet		2 (0.18%)
Management Blanks	***132 (12.07%)***	
Crest		9 (0.82%)
Asymmetrical Blade		73 (6.67%)
Overshot Blade		19 (1.74%)
Surface Cleaning Blade		18 (1.65%)
Maintenance Blade		13 (1.19%)
BLADELET	**287 (26.23%)**	
Simple Bladelet		196 (17.92%)
Burin Spall		29 (2.65%)
Blade Tablet		5 (0.46%)
Management Blanks	***57 (5.21%)***	
Crest		8 (0.73%)
Asymmetrical Blade		30 (2.74%)
Overshot Blade		6 (0.55%)
Surface Cleaning Blade		3 (0.27%)
Maintenance Blade		10 (0.91%)
FLAKE	**544 (49.73%)**	
Management Flakes	***266 (24.31%)***	
Surface Cleaning Flake		103 (9.41%)
Maintenance Flake		163 (14.90%)
Core Tablet		67 (6.12%)
Cortical Flake		71 (6.49%)
Simple Flake		140 (12.80%)
TOTAL	**1094 (100.00%)**	

3.2.3.2.1 Flakes

Flake blanks are the 49.73% of the assemblage, they are divided in the following categories.

Management Flakes

Management flakes account for the 24.31% of the blanks, divided in Maintenance Flake and Surface Cleaning Flake.

Surface cleaning flakes account for the 9.41% of the assemblage. Plain butts are the most common, followed by punctiform ones. Non-cortical blanks are the majority followed by semi-cortical blanks,

cortex patches are found in various locations, and the highest frequency is in distal position. As indeterminate negatives account for nearly half of the blanks, flakes are the most recorded negative type, followed by bladelets. Unipolar negatives are the most common.

Maintenance flakes account for the 14.90% of the assemblage. Plain butts are prevalent followed by Linear. Non-cortical blanks are the most common, cortical blanks are mostly semi-cortical, cortex patches are found commonly on dorsal and lateral positions. The majority of the blanks do not have determinable negatives or do not have negatives; flakes are the most recorded negative type followed by bladelets. Unipolar negatives are the most common.

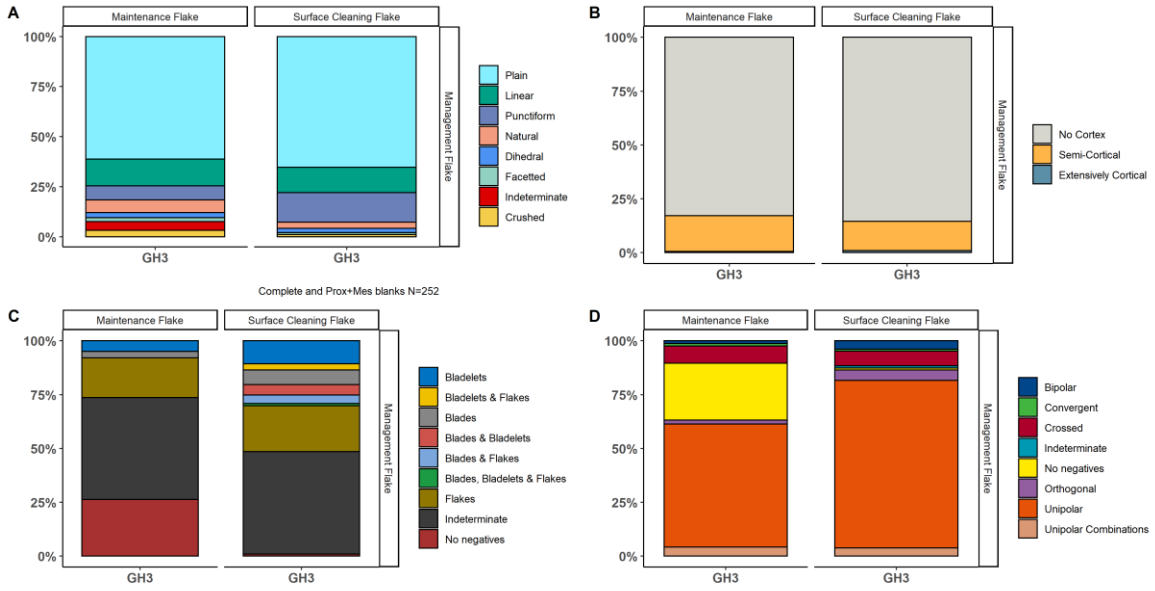

Graph 22 Management Flakes technological attributes. A) Butt values. B) Cortex coverage. C) Negatives' types. D) Negatives' orientation.

Core Tablet

Core tablets account for the 6.12% of the blanks. The butts are mostly plain followed by facetted and natural ones. Blanks are mostly non-cortical, followed by semi-cortical, mostly in proximal and distal positions. Flakes are the most recorded negative type, followed by a combination of flakes and blades and flakes and bladelets. Negatives are mostly unipolar, the combination of unipolar and orthogonal negatives being the most frequent one.

Cortical Flake

Cortical flakes account for the 6.49% of the assemblage. Butts are mostly plain followed by punctiform and natural ones. Nearly all blanks preserve a patch of cortex, extensively cortical blanks are the most frequent, followed by semi-cortical and entames, dorsal being the most common position. Blanks are mostly without negatives, flakes are the only recorded negative type. Determinate negatives are only unipolar.

Simple Flake

They account for the 12.80% of the assemblage. Butts are mostly plain, followed by punctiform and linear ones. They are mostly non-cortical, followed by semi-cortical; cortical patches are mostly in proximal position. Most of the blanks do not bear negatives, flakes are the most recorded negative type. Negatives are mostly unipolar.

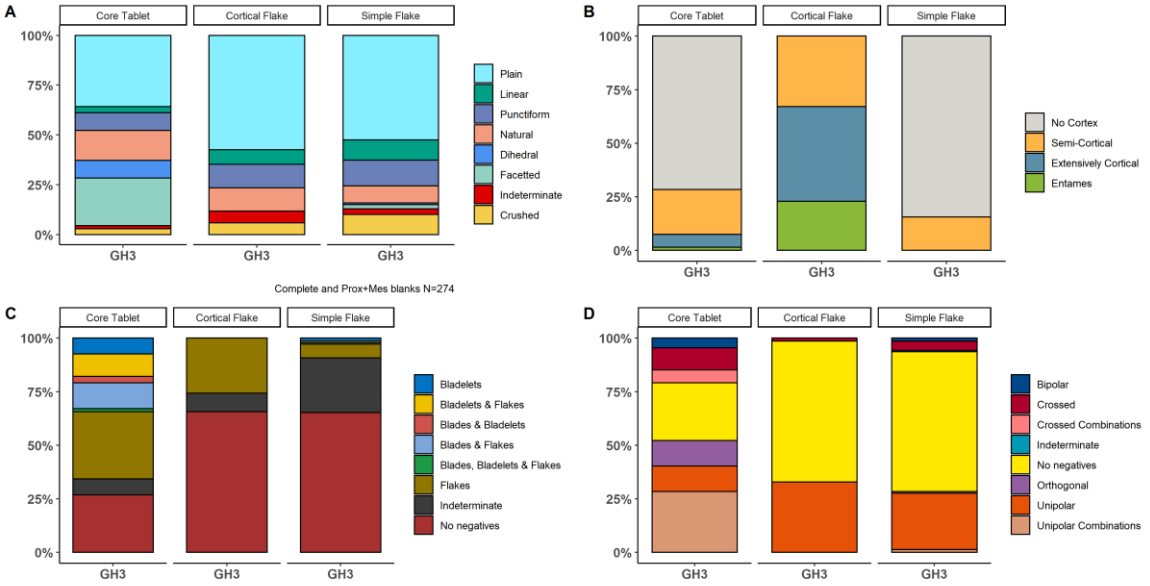

Graph 23 Core Tablets, Cortical Flakes and Simple Flakes technological attributes. A) Butt values. B) Cortex coverage. C) Negatives' types. D) Negatives' orientation.

3.2.3.2.2 Laminar

Blade blanks are the 24.04% of the assemblage, while bladelets are the 26.23%; hence, in total, laminar blanks are the 50.27% of the assemblage and they are divided in the following categories.

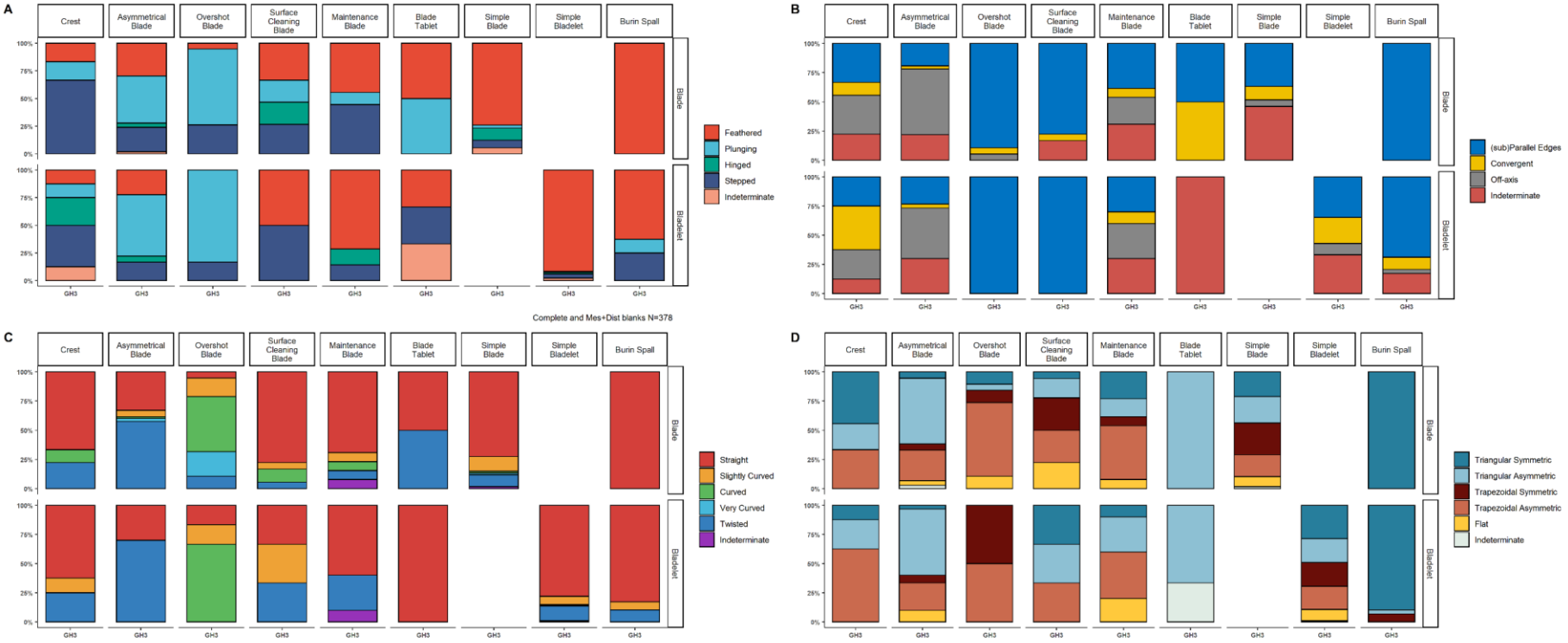

Graph 24 Laminar morphological attributes. A) Distal termination. B) Outline. C) Profile. D) Cross-section.

Management blanks

Blades are the 12.07% of the blanks, while bladelets are the 5.21%.

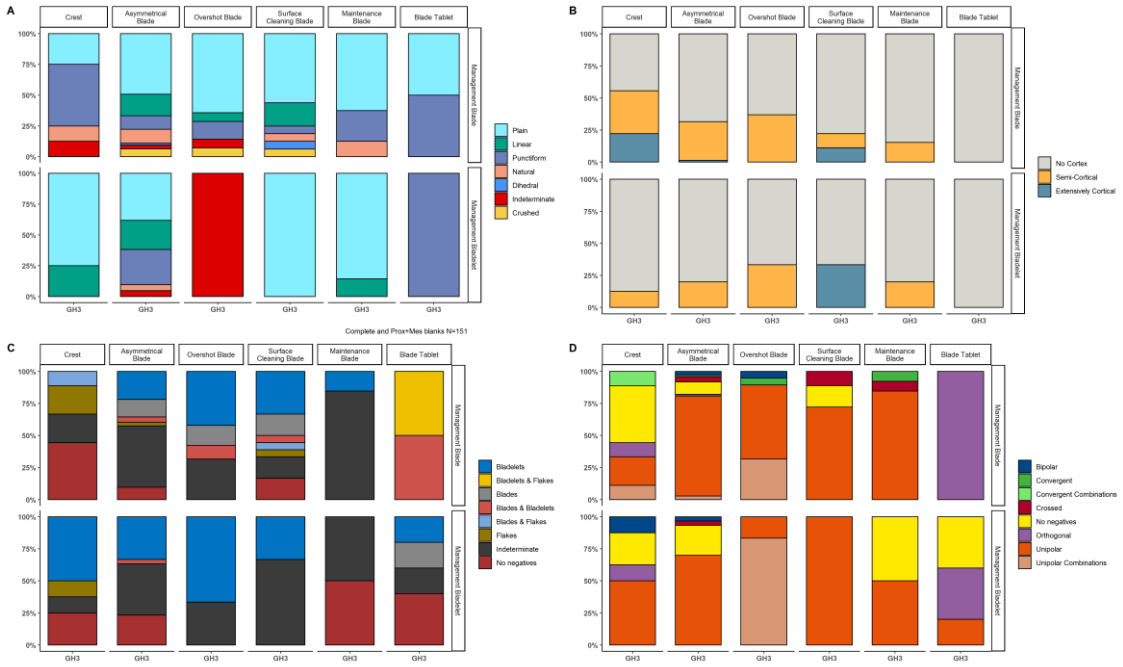

Graph 25 Management Blades technological attributes. A) Butt values. B) Cortex coverage. C) Negatives' types. D) Negatives' orientation.

Crests

Blades account for the 0.82% of the assemblage, while bladelets for the 0.73% of the assemblage. Blades butts are mostly punctiform followed by plain ones, while bladelet butts are mostly plain. Non-cortical blanks have the highest frequency, semi-cortical blanks are following; cortex patches are generally in lateral and proximal positions. Bladelets are prevalently non-cortical. Blanks with no negatives are the 44.44%, with indeterminate negatives accounting for the 22.22%, flakes is the most recorded negative type. Bladelets are the most recorded negatives on bladelets. Unipolar is the most common negatives direction. The termination is stepped. In blades, the outline is sub-parallel, while in bladelets a convergent one is the most recorded. Profiles are mostly straight. The cross-section is usually triangular and symmetrical.

Asymmetrical Blades

Asymmetrical blades account for the 6.67% of blanks, while asymmetrical bladelets for the 2.74% of blanks. Plain butts are prevalent, followed by linear ones in blades and by punctiform ones in bladelets. Most of the blanks are non-cortical, followed by semi-cortical in lateral position. Negatives' type is indeterminate in most of the cases, bladelets are the most determinate negative type. Unipolar is the prevalent orientation. The termination is mostly plunging. The outline is generally off-axis. Profiles are mostly twisted. The cross-section is usually triangular, in blades commonly asymmetrical, while in bladelets is mostly symmetrical.

Overshot Blades

Blades account for the 1.74% of the assemblage, while bladelets for the 0.55%. Butts are mostly plain, followed by punctiform ones; the only bladelet butt is indeterminate. Blanks are mostly non-cortical followed by semi-cortical blanks commonly in distal position. Bladelets are the most recorded negatives type. The unipolar orientation is the most recorded, followed, in blades, by a combination of unipolar and convergent; the latter orientation is predominant in bladelets. The distal termination is plunging. The outline is usually sub-parallel. Profiles are mostly curved, followed by very curved. The cross-section is usually trapezoidal, asymmetrical, in blades, or symmetrical, in bladelets.

Surface Cleaning Blades

Blades account for the 1.65% of the assemblage, while bladelets for the 0.27% of the assemblage. Plain butts are common, followed by linear ones. Blanks are mostly non-cortical, followed by semi-cortical and extensively cortical, usually in dorsal position. Bladelets are the most recorded negatives type. Unipolar negatives orientation is prevalent. The distal termination is mostly feathered and stepped. The outline is prevalently sub-parallel. Profiles are mostly straight in blades, while they are either straight, slightly curved or twisted in bladelets. In blades, the cross-section is mostly trapezoidal, either asymmetrical or symmetrical, while in bladelets is either triangular asymmetrical or trapezoidal asymmetrical.

Maintenance Blades

Maintenance blades account for the 1.19% of the assemblage, while bladelets for the 0.92% of the assemblage. Butts are mostly plain followed, in blades, by punctiform ones, and in bladelets, by linear ones. Most of the blanks are non-cortical, the rest being semi-cortical, in dorsal position. The most recorded negative type are bladelets. Unipolar is the prevalent negatives orientation. In blades the distal termination is mostly feathered or stepped, while in bladelets it is mostly feathered. The outline is mostly sub-parallel and off-axis. Profiles are mostly straight. In blades the cross-section is mostly trapezoidal asymmetrical, while in bladelets it is mostly triangular symmetrical.

Blade Tablet

Blades are the 0.18% of the assemblage, bladelets are the 0.46% of the assemblage. Butts are plain and punctiform in blades, punctiform in bladelets. All blanks are non-cortical. Negatives are a varied array of flakes, blades and bladelets, mostly orthogonal. Profiles are mostly straight. The outline is sub-parallel or convergent. The distal termination is feathered or plunging. The cross-section is mostly triangular, either asymmetrical or symmetrical.

Simple blade and simple bladelet

Simple blades account for the 11.70% of the assemblage, while simple bladelets for the 17.92% of the assemblage. Butts are mostly plain, followed by linear ones. Blanks are overwhelmingly non-cortical, followed in blades by semi-cortical, mostly in proximal position. Bladelets are the most recorded negatives type, followed by, in blade blanks, blades. Negatives orientation is mostly unipolar, followed by a combination of unipolar and convergent orientation. The distal termination is generally feathered. The outline is mostly sub-parallel, followed by convergent one. Profiles are mostly straight, followed by slightly curved ones and twisted ones. The cross-section in blades is almost equally divided in triangular and trapezoidal, while in bladelets is mostly trapezoidal, either asymmetrical or symmetrical.

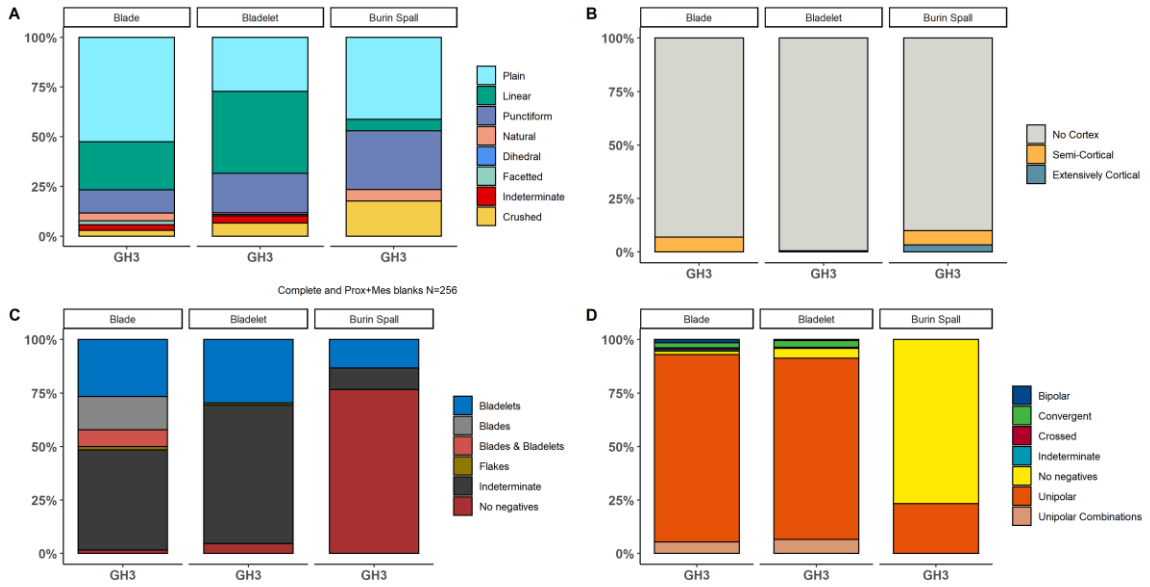

Graph 26 Simple blades, simple bladelets and burin spalls technological attributes. A) Butt values. B) Cortex coverage. C) Negatives' types. D) Negatives' orientation.

Burin Spall

Blade-sized burin spall is noticed in a single case, amounting to the 0.09% of the assemblage, bladelets burin spalls are the 2.65% of the assemblage. The butt is plain in the only blade, while it is plain and punctiform in bladelets. The blanks are mostly non-cortical. Most of the blanks do not bear negatives, bladelets are the most recorded negatives in bladelets. The distal termination is feathered. Negatives orientation is unipolar. The outline is sub-parallel. The profile is straight. The cross-section is triangular symmetrical, while in bladelets it is mostly trapezoidal asymmetrical.

Retouched Blanks

The 4.57% of the assemblage bears retouch. Most of the retouched blanks are bladelets (50.00%), followed by blades (26.00%) and flakes (24.00%).

Bladelets are mostly retouched on one edge, rarely both edges, with marginal, direct or inverse, semi-abrupt retouch. They are followed by bladelets retouched on both edges, with marginal, alternate, semi-abrupt retouch, classified as **Dufour bladelets**. The rest is represented by **laterally backed bladelets** and **dihedral burins**. Most of the bladelet retouched blanks are produced on simple bladelets.

Blades are mostly retouched in dihedral burins. Followed by **laterally retouched. And backed blades.** Most of the burins are made on management blades, while laterally retouched and backed blades on simple blades.

Flakes are bearing simple retouch, followed by burins. Most of the retouched flakes are made on management flakes.

3.2.4 Conclusions

The assemblage is focused on the production of blades and, mostly, bladelets.

All cores are platform ones. Semi *Tournant* and Narrow Fronted *sur Tranche* are the most used configurations. While the Semi *Tournant* cores are manufactured on rounder pieces of raw material, small nodules or cobbles, *sur Tranche* cores are exploiting the narrow surfaces of blanks' edges or lenticular pieces. Their frequency seems to show that *sur Tranche* cores are an established core reduction strategy in the assemblage and not simply a reuse of suitable core blanks.

If Semi *Tournant* cores evidence a mixed production of blades and bladelets, *sur Tranche* ones are mostly dedicated to bladelets. In fact, burin spalls are almost exclusively bladelet-sized.

The Semi *Tournant* reduction starts with the opening of the striking platform, which is plain, hence opened by an only flake, and mostly single. The use of a single striking platform and of a single flaking surface is shown by the strong unipolar character observed in the whole assemblage. The knapping angle, between the flaking surface and striking platform, is acute, becoming very acute in the final stages of reduction. The intersection between the striking platform and the flaking surface, the overhang, is abraded. Decortication is accomplished through the knapping of few flakes. The raw material pieces might have been decorticated prior to the import in the site or been naturally free of cortex.

The reduction follows natural convexities, which only rarely are managed through crest-shaping. Therefore, the production of mostly regular, straight, sub-parallel edges bladelets and blades can start. Convexities are managed by asymmetrical, twisted, laterally struck blades. These blades invade the lateral neighbouring faces, sometimes removing remaining lateral cortical patches, expanding laterally the flaking surface and creating the semi-circumferential morphology. The twist of the lateral profile is given by the wrapping of the two core faces' intersection. The termination is often plunging and off-axis, meaning it is invading the distal part of the other core face, also shaping the distal convexity. With fewer frequency, the distal convexity is renewed through plunging, curved, centrally struck, overshot blades. This sequence (straight bladelets struck on a ridge, renewing of the

convexity through two laterally struck twisted blades) is repeated on the opposite sides of the flaking surface until they merge into a single semi-circumferential flaking surface.

The striking platform, as witnessed also by the blanks' butts, is kept plain. It is periodically renewed by core tablets that are struck from the front or the lateral core faces, hence the orthogonal bladelets' and blades' negatives belonging to the main flaking reduction. These are accounting also for the facetted morphology of the tablets' butts. Unipolar flake negatives on the dorsal face of core tablets could be explained by temporary and localised adjustments. Some of the simple flakes morphology and dimensions are compatible with this function.

Other flakes are intervening on the flaking surface to shape convexities, localised cortex removal and cleaning the flaking surface from previous negatives.

Sur Tranche cores are relying on a more immediate, but effective, configuration. The narrow surface is already fulfilling the convexities requirements, bladelets are knapped using the central ridge, formed by the intersection of the core lateral faces, and the lateral ridges obtained by the first negative. The striking platform is plain and single. The orientation of the negatives is predominantly unipolar. The knapping angle is less acute than the Semi *Tournant* one, probably because the production stops earlier. The overhang can be abraded, but less frequently than for Semi *Tournant* cores. Since mostly blanks are used for this core configuration, one of the lateral core faces is cortical, as it was the blank's dorsal face.

Blanks' bulb, the presence, even if not marked, of lips, the abrasion of the overhang, and the acute knapping angle suggest the use of direct soft hammer tangential percussion for most of the assemblage. Some marked bulbs in flake could advocate for the minor use of direct hard hammer inner percussion.

Despite flakes constitute half of the assemblage, no core witnesses flakes production; as previously mentioned, flakes are mostly connected to decortication, core shaping and simple flakes, which cannot be related to any specific production.

Given that the production can be classified as laminar volumetric, the two products, blades and bladelets, seem to have different roles. In fact, despite being almost equally represented, blades that can be related to a convexity shaping purpose are approximately double their bladelet counterparts. On the other hand, simple laminar blanks are mostly bladelet-sized. Negatives compatible with simple bladelets are appearing on every flaking product, regardless of the size. Furthermore, simple bladelets were chosen for manufacturing most of the retouched blanks. Therefore, it suggests that bladelets were the main objective of the flaking production.

3.3 Fumane

3.3.1 Assemblage Composition

The studied assemblage comes from two different stratigraphical units, A1 and A2, superimposed to each other on the outer part of the cave. Both assemblages are dominated by laminar blanks.

Comparing the complete blanks, frequencies in the two units, are similar. For the sake of comparison between the two units, complete blanks will be used primarily throughout the chapter.

Table 13 Percentages of complete blanks' categories within the two units

Blade		Bladelet		Flake		Total	
A1	**A2**	**A1**	**A2**	**A1**	**A2**	**A1**	**A2**
113	245	160	393	86	153	359	791
(31.48%)	(30.97%)	(44.57%)	(49.68%)	(23.96%)	(19.34%)	(100.00%)	(100.00%)

3.3.1.1 Fragmentation

Fragmentation can be evaluated from the A1 assemblage. Complete blanks are representing the highest frequency in all blanks' categories, especially flakes (≈91%). Laminar blanks are similarly distributed in the complete and semi-complete classes.

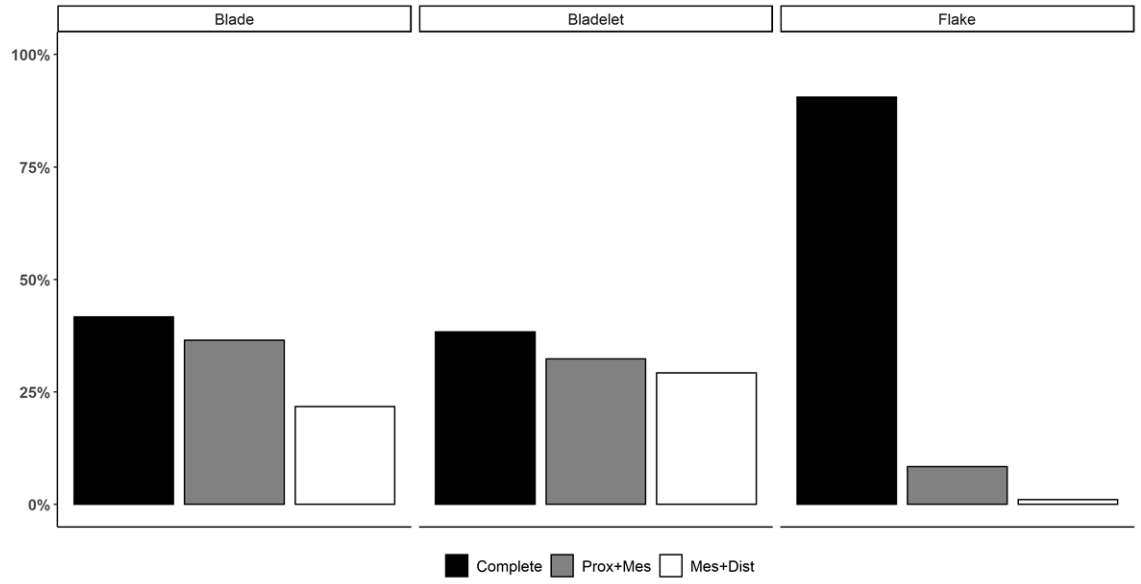

Graph 27 Fragmentation in A1.

3.3.1.2 Metric Attributes

Dimensions obtained from complete and semi-complete blanks of the two units are rather homogenous. Laminar blanks show a similar trend, management blanks are always larger and thicker than the simple ones. The last complete negatives dimensions, recorded in blanks and cores, are best fitting the ones indicated by bladelets size. In particular, blades have median length of 36.84 mm in A1 and 37.74 mm in A2, while management blades' median length is 43.85 mm in A1 and 43.07 mm in A2. Bladelets have a median length of 23.77 mm in A1 and 23.14 mm in A2, while management bladelets' median length is 30.61 mm in A1 and 28.95 mm in A2. Blades have a median width of 14.27 mm in A1 and 14.50 mm in A2, while management blades' median width is 17.05 mm in A1 and 17.21 mm in A2. Bladelets have a median width of 8.80 mm in A1 and 8.04 mm in

A2, while management bladelets' median width is 9.59 mm in A1 and 9.33 mm in A2. Blades have a median thickness of 3.59 mm in A1 and 3.39 mm in A2, management blades' median thickness is 5.83 mm in A1 and 5.49 mm in A2. Bladelets have a median thickness of 2.09 mm in A1 and 1.91 mm in A2, management bladelets' median thickness is 3.57 mm in A1 and 2.88 mm in A2. Last complete negatives are 21.06/26.14 mm long in cores and 22.55/25.68 mm long in blanks. Widths are 8.26/9.46 mm in cores and 5.59/5.38 in blanks.

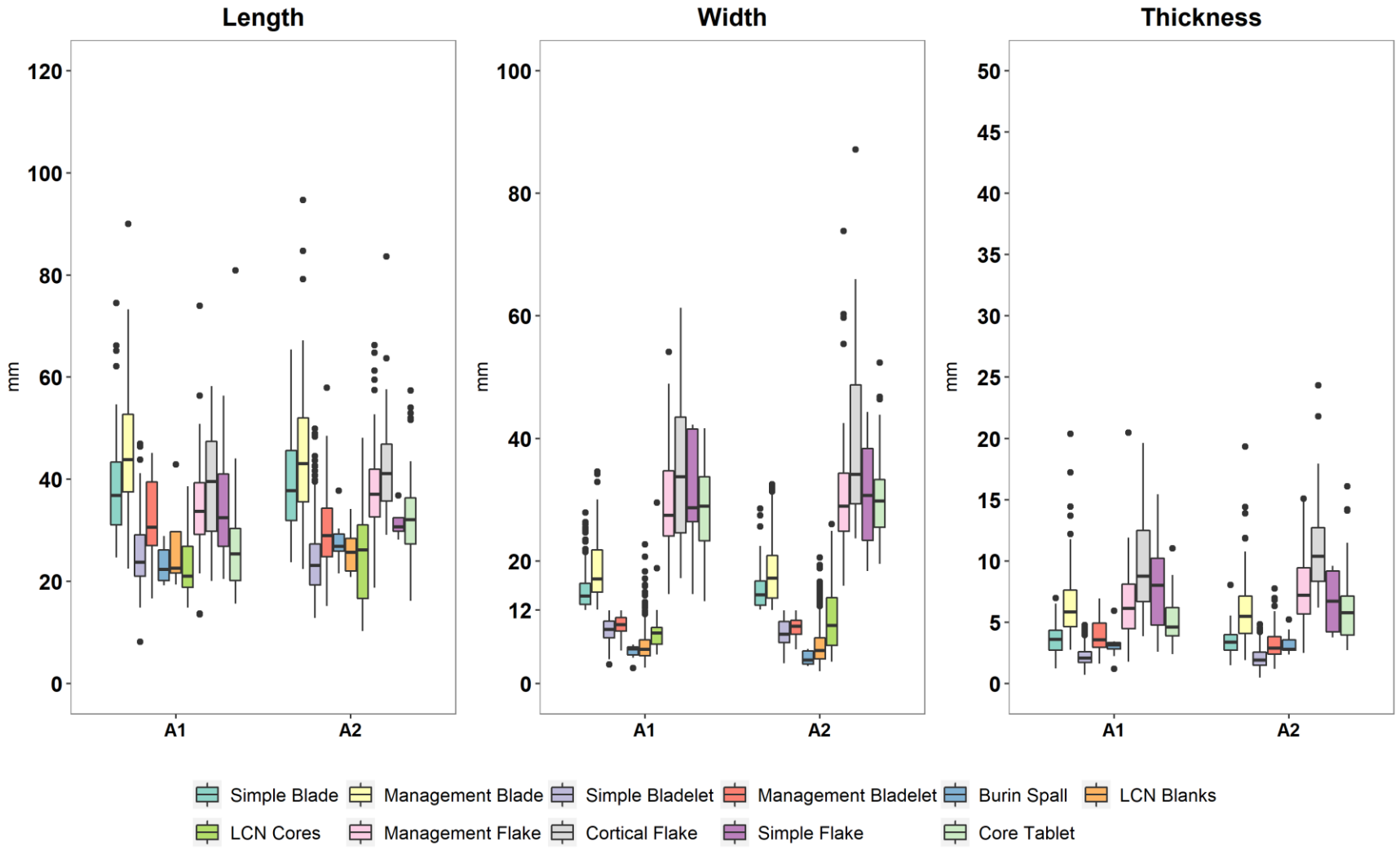

Graph 28. Length, width and thickness values of blanks. Length and width are compared to those measured for last complete negatives (LCNs) in cores and blanks. Boxes represent the interquartile range (central 50% of the values), bold horizontal line is the median value

3.3.2 Technical Observations

3.3.2.1 Lipping

Most of the blanks in both units are non-lipped, 60.45% in A1 complete blanks and 63.13% in A2. A1 blanks showing the higher percentages of lips are, in order, core tablets, management flakes, blades, management blades. In A2, while the same trend is observable, bladelets have a larger representation than in A1, despite being mostly non-lipped.

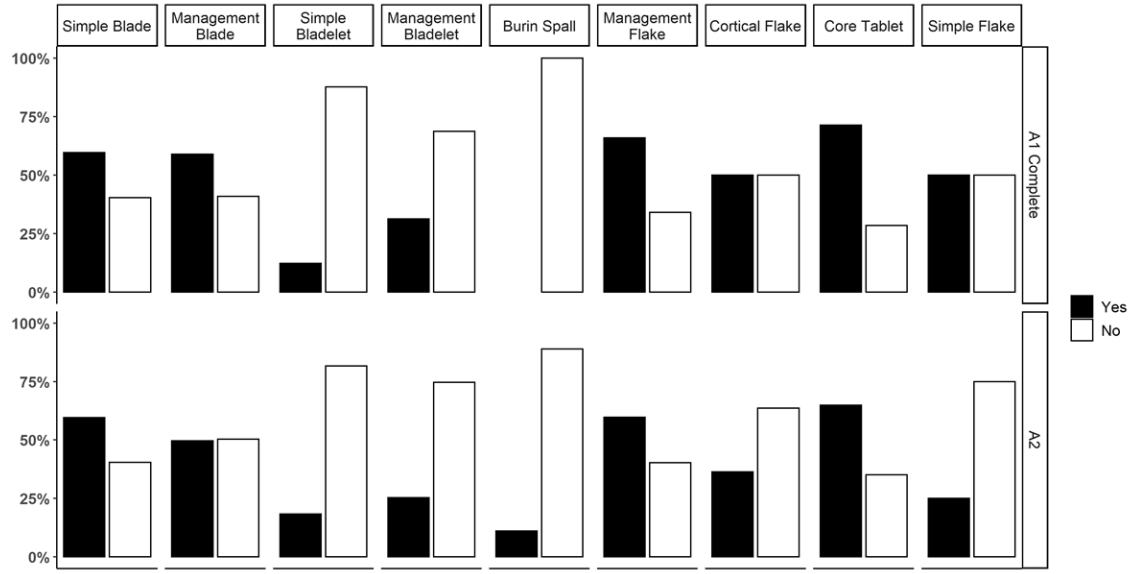

Graph 29 Lips in both assemblages' complete blanks.

3.3.2.2 Overhang Abrasion

The overhang is systematically removed through abrasion or micro-chipping in cores and laminar blanks. Higher percentages are shown in A1. The core category showing less abrasion is the Narrow-Fronted *sur Tranche.*

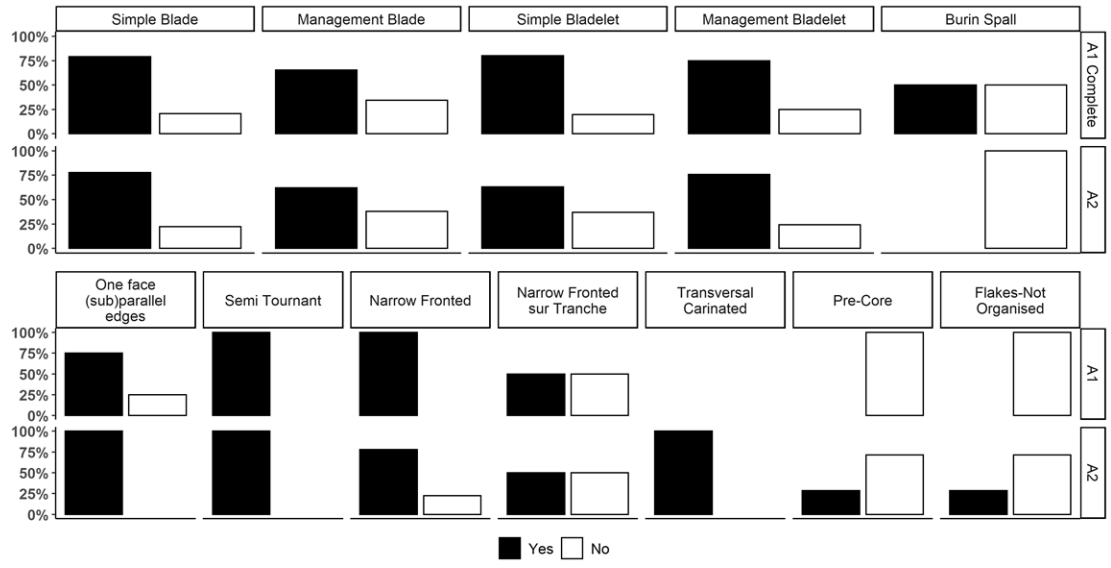

Graph 30 Overhang abrasion in cores and complete laminar blanks

3.3.2.3 Bulb

Both units have a majority of non-marked bulbs, diffused and not perceived, A1 is showing a stronger frequency, 72.14% against 66.16% of A2. Values are changing slighlty including A1 Prox+Mes blanks, 75.87%. In both units, the highest percentages of non-marked bulbs are found in bladelets, followed by blades. Flakes are generally showing a pronounced bulb, except for A1 management flakes (diffused bulbs: 61.36%).

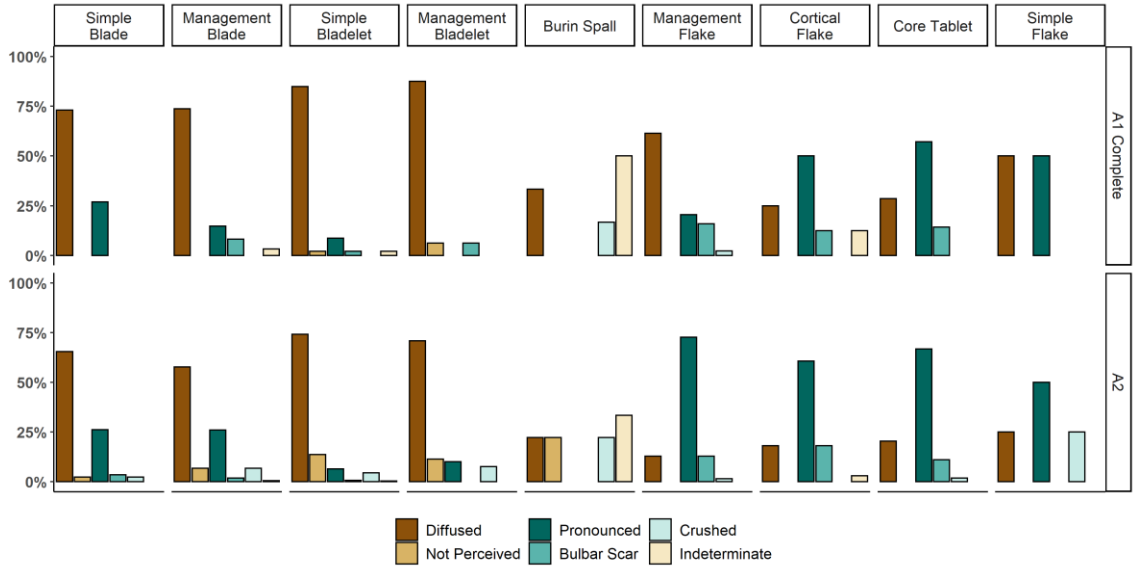

Graph 31 Bulbs in complete blanks

3.3.2.4 Angle

Exterior angles in both units are acute, comprised between 70–90° degrees, or, in lesser fashion, extremely acute, <70° degrees. Percentages are fairly stable across the main technical categories. The observation is supported by cores' striking platform–flaking surface angles. While A2 cores are mostly represented in the 70–90° degrees categories, A1 cores are equally represented in both. Cores that have a particularly acute angles are the sub-parallel edges ones in both units, and the semi *Tournant* in A1.

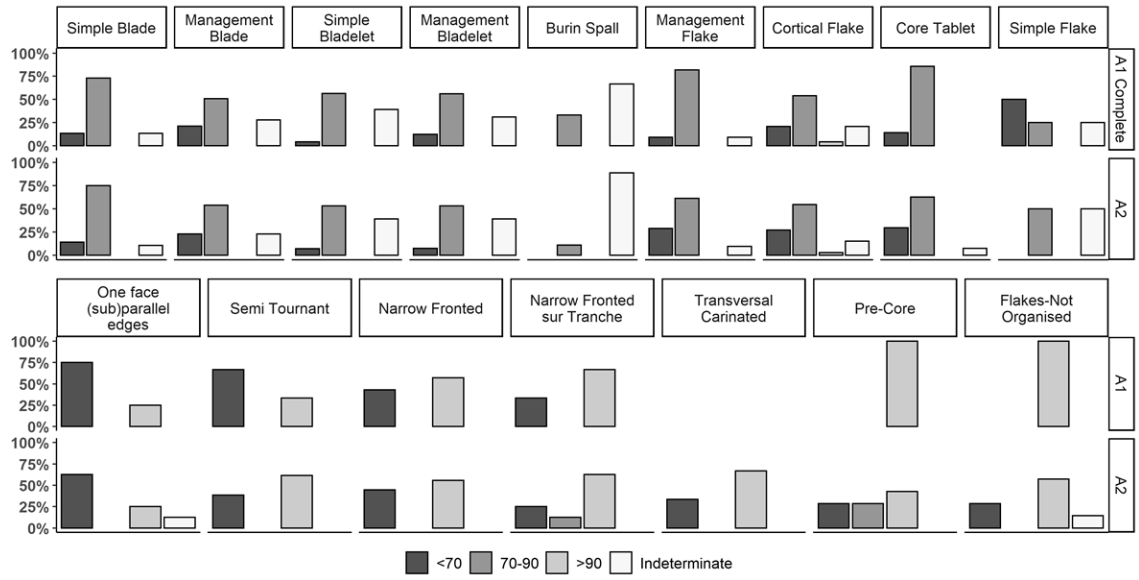

Graph 32 Knapping angles in cores and complete blanks.

3.3.2.5 Synthetic considerations on knapping technique

All above-mentioned observations are supporting the use of tangential soft hammer direct percussion. Possibly, following results in A1, also flakes from advanced management operations, such management flakes, and some core tablets, are knapped with a soft hammer direct percussion.

3.3.3 Morpho-technological Observations

3.3.3.1 Cores

Table 14 Cores categories

	A1	A2
Pre-Core	1 (3.13%)	7 (12.07%)
One face (sub)parallel edges	4 (12.50%)	8 (13.79%)
Semi *Tournant*	12 (37.50%)	13 (22.41%)
Narrow Fronted	7 (21.88%)	9 (15.52%)
Narrow Fronted *sur Tranche*	6 (18.75%)	8 (13.79%)
Transversal Carinated	0 (0.00%)	6 (10.34%)
Flakes-Not Organised	2 (6.25%)	7 (12.07%)
Total	32 (100.00%)	58 (100.00%)

Pre-Core

Pre-cores account for the 3.13% of A1 cores and the 12.07% of A2 ones. They are mostly manufactured on slabs, in A2 they are followed by cores on cobbles. The cortex is present mostly on lateral faces, in A2 followed by posterior faces. Striking platforms are mostly plain and single, originating a single flaking surface; an A2 core has an opposite auxiliary platform. Negatives in A2 cores are either flakes or a combination of blades and flakes. Negatives are mostly unipolar, followed by combinations of unipolar and other orientations.

One face (sub) parallel edges

They account for the 12.50% of A1 cores and the 13.79% of A2 cores. When the determination was possible, they have been manufactured on cobbles in A2 and a nodule in A1. Cortex is left mostly on posterior faces. Striking platforms are usually plain and single, originating a single surface; in one case, in A2, an opposed platform is related to a bipolar exploitation. Negatives are either bladelets or combinations of blades and bladelets. Negatives are unipolar or a combination of unipolar and convergent.

Semi Tournant

They account for the 37.50% of A1 cores and the 22.41% of A2 ones. They are manufactured mostly on cobbles, in one case, in A1, on a slab. Cortex is usually found on posterior faces, followed by lateral ones. Striking platforms are overwhelmingly plain and single, leading to a single striking surface; rare cases in both units are showing opposed or independent platforms leading to an opposed flaking surface or an additional one on a different core face. Negatives are either bladelets or a combination of blades and bladelets. The orientation is mostly unipolar or a combination of unipolar and convergent.

Narrow Fronted

They account for the 21.88% of A1 cores and the 15.52% of A2 cores. A1 cores are manufactured on wide array of raw material blanks, such as cobbles, nodules, squared chunks, and blanks. A2 cores are manufactured mostly on cobbles, followed by nodules and squared chunks. Cortex is found mostly on posterior faces in A2, and in lateral faces in both units. Striking platforms are mostly plain and single, leading to a single surface; in A1, rare second platforms lead to independent flaking surfaces. Negatives are mostly bladelets and combinations of blades and bladelets. The most frequent orientation is unipolar, followed by combinations of unipolar and other directions.

Narrow Fronted sur Tranche

They account for the 18.75% of A1 cores and the 13.79% of A2 cores. They are manufactured mostly on blanks, and, in lesser fashion in A2, on slabs. The only piece that shows cortex, in A2, does it on the lateral and basal face. Striking platforms are plain and single, leading to a single surface; secondary platforms can lead to independent flaking surfaces. Negatives are mostly bladelets and unipolar.

Transversal Carinated

They account for the 10.34% of A2 cores. They are manufactured mostly on blanks or squared chunks. Cortex is found either on the basal, lateral or posterior face. The striking platforms are mostly plain and single, leading to a single surface; in one case, a second platform leads to an independent flaking surface. Negatives are mostly bladelets and in one case, a combination of blades, bladelets and flakes. The orientation is unipolar or a combination of unipolar and convergent.

Other Cores

They are flake cores accounting for the 6.25% of A1 cores and the 12.07% of A2 cores. They are mostly manufactured on cobbles. The cortex is mostly found on basal face. The striking platform is either plain, in A2, or facetted. It can be single, or, in A2, adjacent leading to a single or an adjacent orthogonal flaking surface. The negatives are flakes, either centripetal or, in A2, unipolar.

Synthesis cores

A similar pattern can be drawn for the two units. Semi *Tournant* cores are the most represented, followed briefly by the Narrow Fronted and by the Narrow Fronted *sur Tranche* and Parallel Edges cores. In A2, there is a minor presence of Transversal Carinated cores. The presence of flake cores, highly resembling centripetal surface knapping can be related to postdepositional mixing with the underlying Mousterian layer in the inner cave mouth. A wide array of raw material pieces has been used for manufacturing the cores, reflecting the provisioning from nearby primary and secondary outcrops, the most frequently determined are river cobbles, followed by blanks, and in lesser fashion, nodules, slabs and squared pieces; for most of the cores, it was not possible to determine the origin given the advanced degree of reduction and the absence of cortical surfaces. If most cores are non-cortical, the cortex is left mainly on the posterior, lateral and, in A2, basal core faces. The striking platforms are generally plain, even though a minority of facetted ones is distributed evenly amongst all categories. Cores are usually displaying a single striking platform that can be accompanied in some cases, by an opposed one, in A1, or an adjacent one, in A2, leading to similarly positioned flaking surfaces. Bladelets and a combination of blades and bladelets are the most recorded negatives, whose orientation is essentially unipolar, complemented by the unipolar and convergent combination.

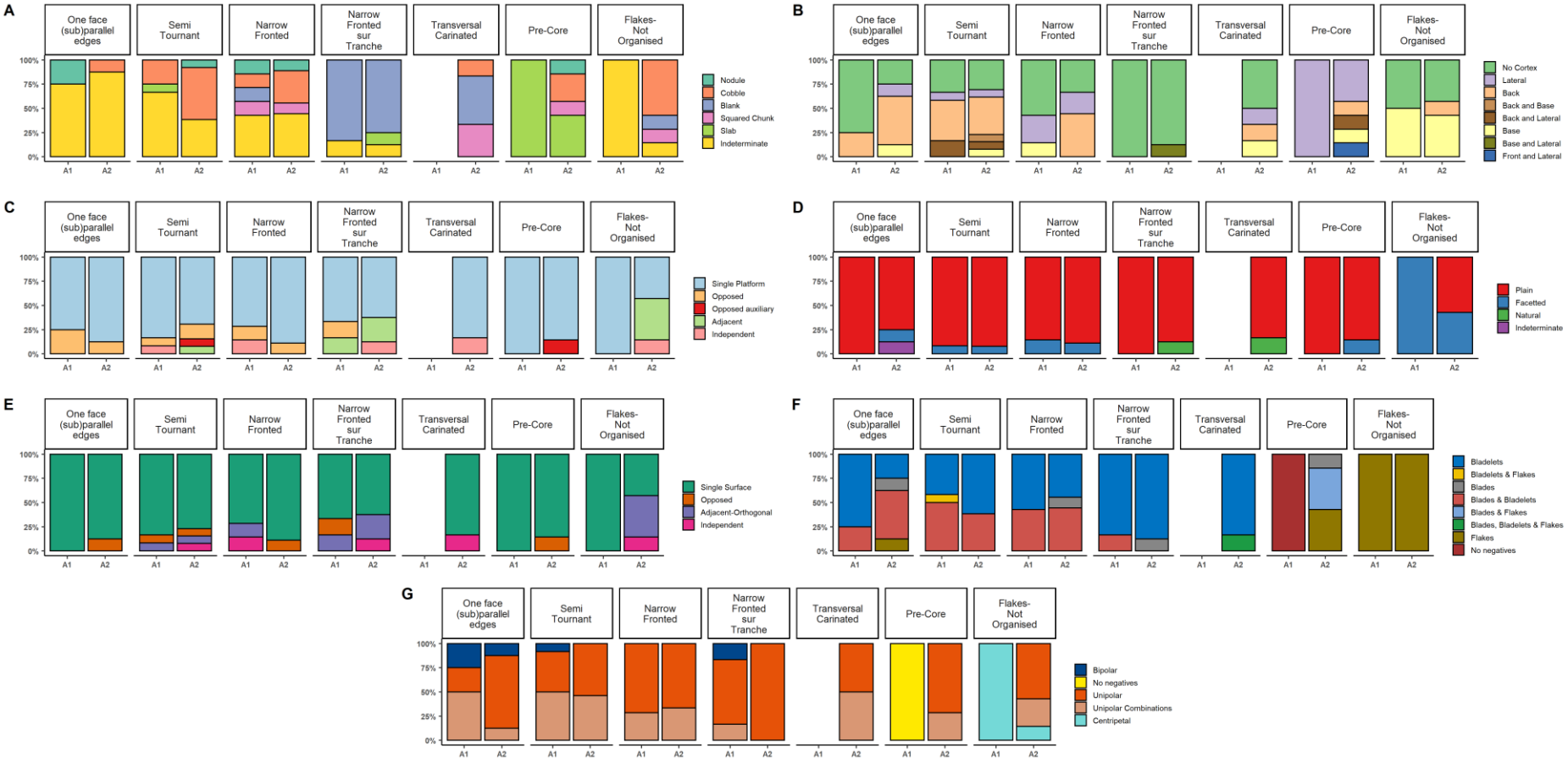

Graph 33 Cores attributes. A) Core blank. B) Cortex position. C) Striking Platform relation. D) Striking Platform type. E) Flaking Surface relation. F) Negatives' type. G) Negatives' orientation

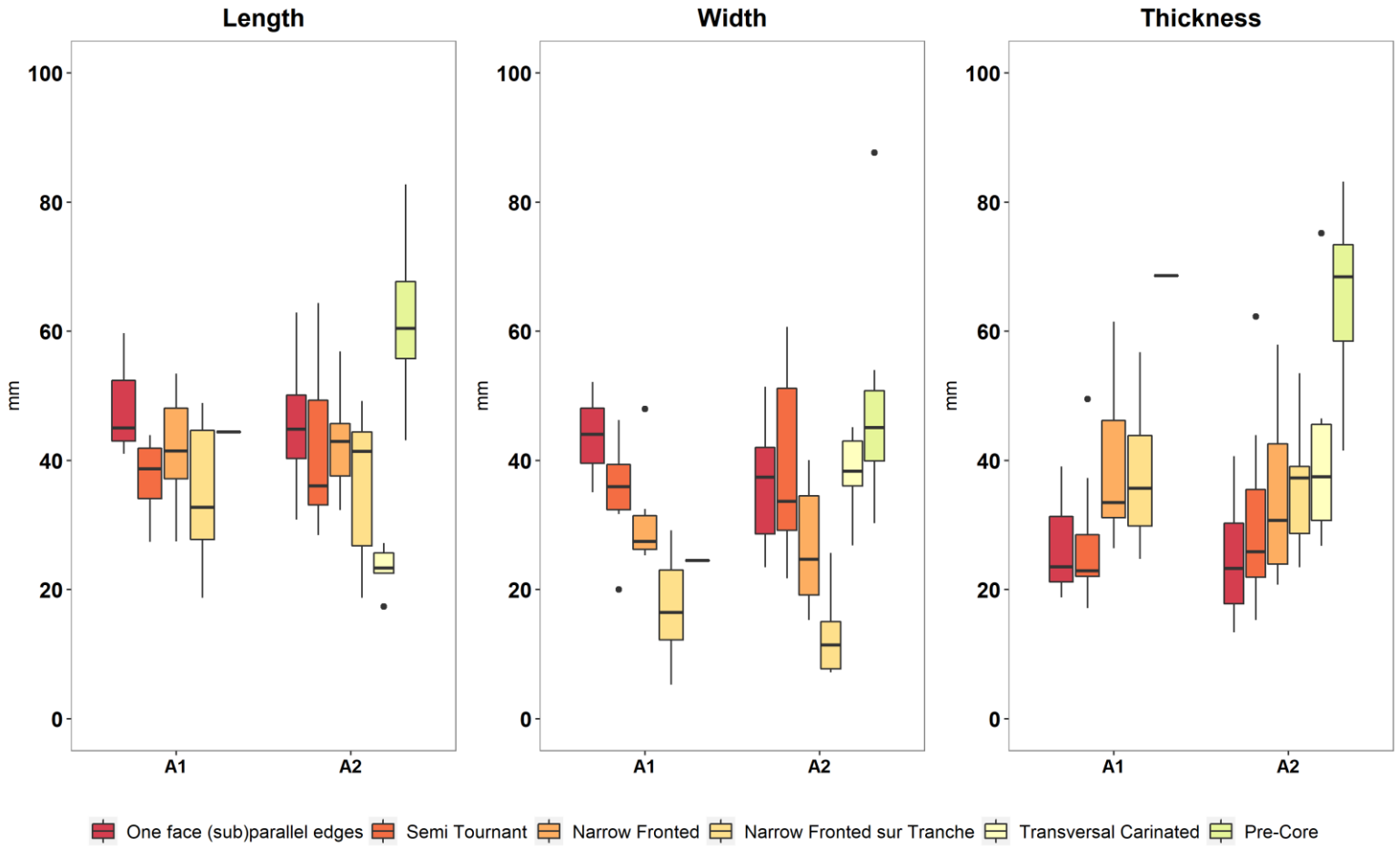

Graph 34 Cores dimensions. Box plots represent the interquartile range, the median is highlighted in a bold black line

3.3.3.2 Blanks

Table 15 Complete and semi-complete blanks divided by categories. A1Complete, just complete blanks from A1 for a better comparison with A2.

	A1 whole	A1Complete	A2
BLADE	**271 (34.61%)**	**113 (31.48%)**	**245 (30.93%)**
Simple Blade	155 (19.80%)	52 (14.48%)	84 (10.61%)
Management Blanks	***116 (14.81%)***	***61 (16.99%)***	***161 (20.33%)***
Crest	16 (2.04%)	8 (2.23%)	20 (2.53%)
Asymmetrical Blade	73 (9.32%)	36 (10.03%)	75 (9.47%)
Overshot Blade	22 (2.81%)	14 (3.90%)	36 (4.55%)
Surface Cleaning Blade	5 (0.64%)	3 (0.84%)	18 (2.27%)
Maintenance Blade	0 (0.00%)	0 (0.00%)	12 (1.52%)
BLADELET	**417 (53.26%)**	**160 (44.57%)**	**394 (49.75%)**
Simple Bladelet	359 (45.85%)	138 (38.44%)	306 (38.64%)
Burin Spall	8 (1.02%)	6 (1.67%)	9 (1.14%)
Management Blanks	***50 (6.39%)***	***16 (4.46%)***	***79 (9.97%)***
Crest	11 (1.40%)	2 (0.56%)	6 (0.76%)
Asymmetrical Blade	27 (3.45%)	10 (2.79%)	57 (7.20%)
Overshot Blade	11 (1.40%)	3 (0.84%)	8 (1.01%)
Surface Cleaning Blade	1 (0.13%)	1 (0.28%)	4 (0.51%)
Maintenance Blade	0 (0.00%)	0 (0.00%)	4 (0.51%)
FLAKE	**95 (12.13%)**	**86 (23.96%)**	**153 (19.32%)**
Management Flake	***49 (6.26%)***	***44 (12.26%)***	***62 (7.83%)***
Surface Cleaning Flake	42 (5.36%)	37 (10.31%)	44 (5.56%)
Maintenance Flake	7 (0.89%)	7 (1.95%)	18 (2.27%)
Core Tablet	15 (1.92%)	14 (3.90%)	54 (6.82%)
Cortical Flake	26 (3.32%)	24 (6.69%)	33 (4.17%)
Simple Flake	5 (0.64%)	4 (1.11%)	4 (0.51%)
TOTAL	**783 (100.00%)**	**359 (100.00%)**	**792 (100.00%)**

3.3.3.2.1 Flakes

Flakes are the 23.96% of A1 complete blanks and the 19.32% of A2 ones.

Management Flake

Management flakes are the 12.26% of A1 blanks and the 7.83% of A2 ones. They are divided in maintenance flakes and surface cleaning flakes.

Surface cleaning flakes are the 10.31% of A1 blanks and the 5.56% of A2 ones. Butts are generally plain, followed by linear and punctiform. Cortex covers typically up to half of the blanks' surface, in lateral position. Flakes are the highest recorded negatives, followed by bladelets and a combination of bladelets and flakes. Negatives are generally unipolar and a combination of unipolar and convergent.

Maintenance flakes are the 1.95% of A1 blanks and the 2.27% of A2. Butts are mostly plain, followed by linear in A2. Cortex covers mostly up to half of the blanks' surface, mostly in dorsal position. Flakes are the most recorded negatives; they are mostly unipolar or have crossed or orthogonal patterns.

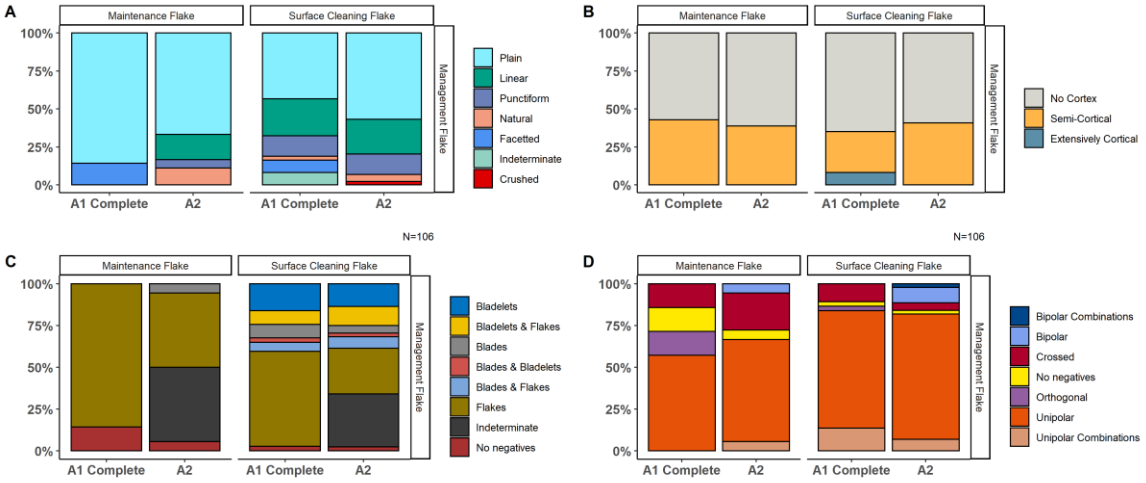

Graph 35 Management Flakes technological attributes. A) Butt values. B) Cortex coverage. C) Negatives' types. D) Negatives' orientation

Cortical Flake

They are the 6.69% of A1 blanks and the 4.17% A2 ones. Butts are usually plain, with a higher incidence of natural ones in A1. Cortex covers the entire blanks' surface in A1, while extensively cortical blanks are more frequent in A2, in both units in dorsal position. Flakes are the most recorded negatives, generally they are unipolar or, in lesser fashion, orthogonal in A2.

Core Tablet

They are 3.90% of A1 blanks and the 6.82% of A2 blanks. Butts are mostly divided between plain and facetted. Cortex covers usually up to half of the blanks' surface, in proximal position in A2 and distal position for A1. Flakes are the most recorded negatives, followed by bladelets and flakes in A2 and bladelets in A1. Negatives are generally unipolar and unipolar and orthogonal.

Simple Flake

They are 1.11% of A1 blanks and the 0.51% of A2 blanks. Butts are usually plain. Blanks are non-cortical. Flakes are the most recorded negatives, and they are largely unipolar.

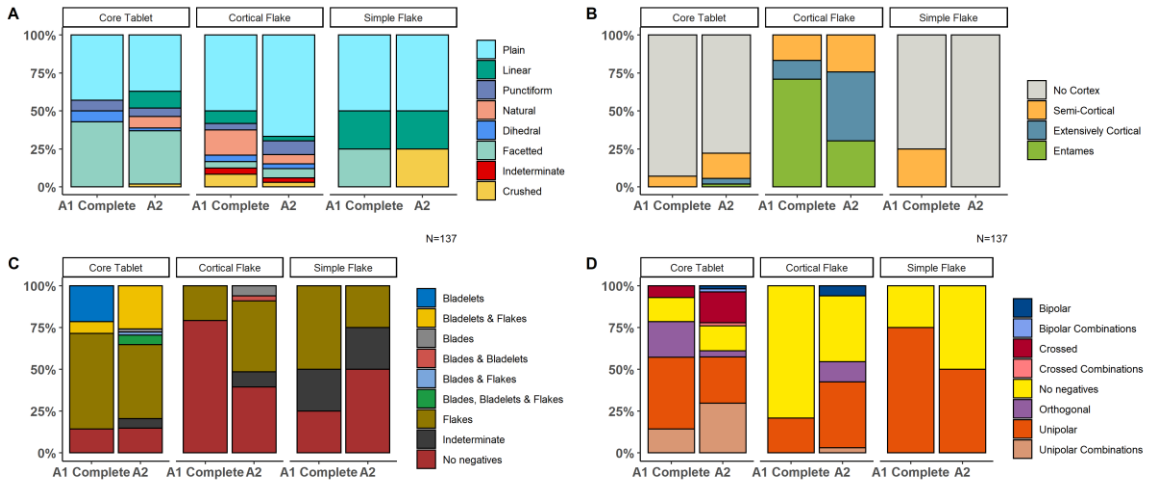

Graph 36 Core Tablets, Cortical Flakes and Simple Flakes technological attributes. A) Butt values. B) Cortex coverage. C) Negatives' types. D) Negatives' orientation.

3.3.3.2.2 Laminar

Blade blanks are the 31.48% of the A1 assemblage and the 30.93% of A2. Bladelets are the 44.57% of the A1 complete assemblage and the 49.75% of A2 one.

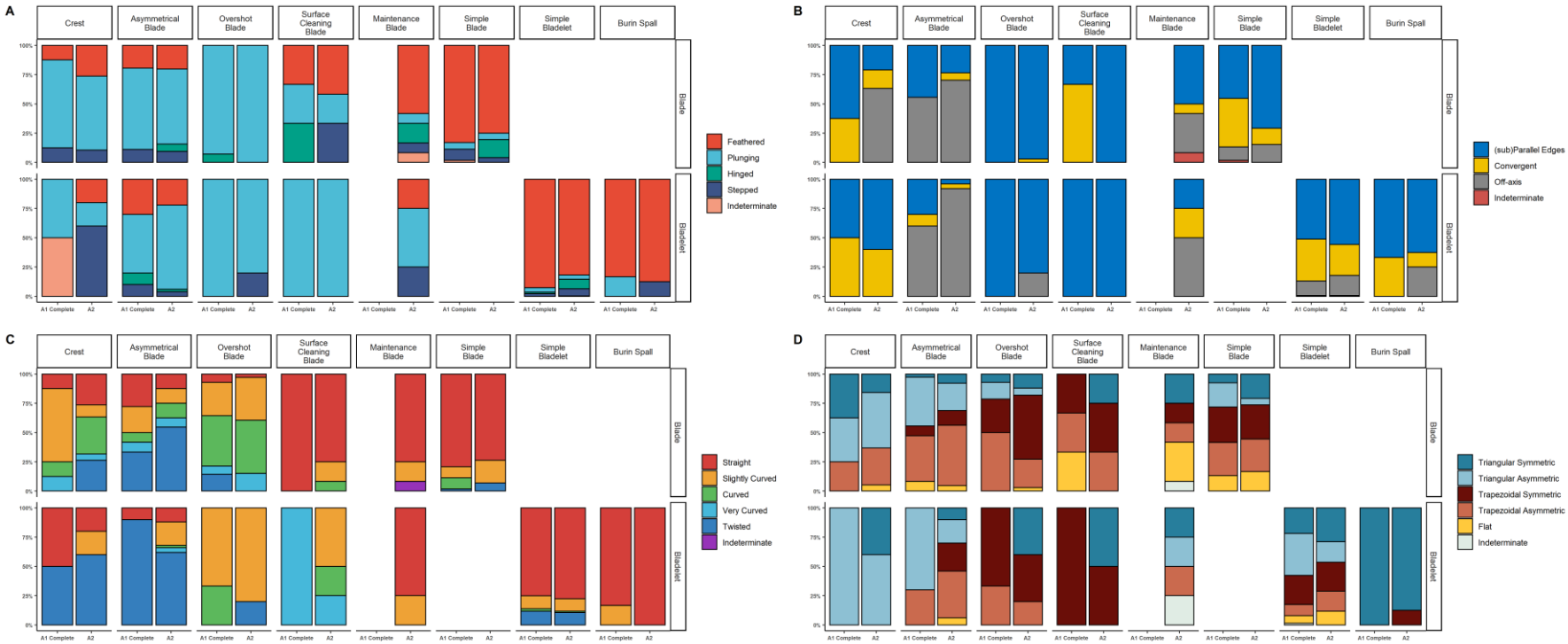

Graph 37 Laminar morphological attributes. A) Distal termination. B) Outline. C) Profile. D) Cross-section.

Management blanks

Blades are the 16.99% of A1 blanks and the 20.33% of A2 ones, bladelets are the 4.46% A1 blanks and the 9.97% of A2 ones.

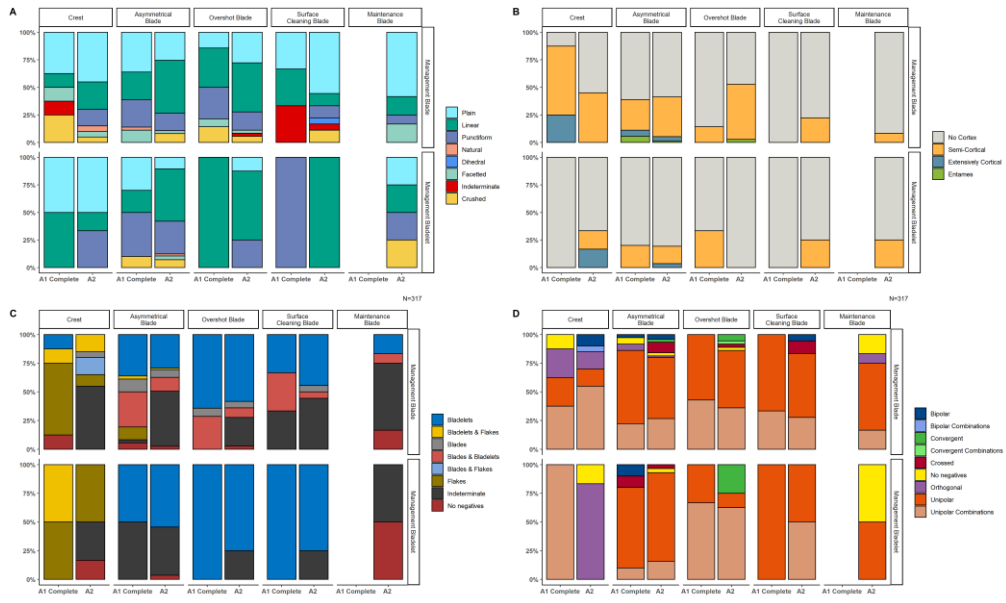

Graph 38 Management Blades technological attributes. A) Butt values. B) Cortex coverage. C) Negatives' types. D) Negatives' orientation.

Crest

Blades-sized blanks account for the 2.23% of A1 blanks and the 2.53% of A2 blanks, while bladelets-sized blanks account for the 0.56% of A1 blanks and the 0.76% of A2 blanks. Butts are mostly plain and linear. Bladelets blanks are mostly non-cortical, while blades show a higher percentage of cortical blanks; the cortex covers typically up to half of the blanks' surface, with some blades blanks being extensively cortical. A1 blades' negatives are mostly flakes, while A2 blades' negatives mostly a combination of blades or bladelets and flakes. Orientation is mostly a combination of unipolar and orthogonal and unipolar in blades, while in bladelets is mostly orthogonal. Blades' termination is mostly plunging. Blades' outline is mostly sub-parallel and convergent in A1, while off-axis in A2; bladelets are mostly sub-parallel and convergent. Profiles in blades are curved, mostly slightly curved, and twisted in A2 blades, while they are mostly twisted in bladelets. The cross-section is mostly triangular, symmetrical or asymmetrical.

Asymmetrical blade

Blades-sized blanks account for the 10.03% of A1 blanks and the 9.47% of A2 blanks, while bladelets-sized blanks account for the 2.79% of A1 blanks and the 7.20% of A2 blanks. Blades butts are mostly linear and plain, while bladelets butts are mostly linear and punctiform. Blanks' are mostly non-cortical; both blades and bladelets are mostly cortical up to a half of the blanks' surface in lateral and distal position, blades have also some extensively cortical blanks too. Bladelets and the

combination of blades and bladelets are the most recorded negatives in blades, while bladelets are the only negatives recorded in bladelets. Negatives' orientation is mostly unipolar and a combination of unipolar and convergent. The termination is mostly plunging followed by a stepped one, bladelets have more feathered terminations. The outlines are mostly off-axis. The profile is mostly twisted, followed by slightly curved ones. The cross-section is mostly asymmetrical, either triangular or trapezoidal.

Overshot blade

Blades-sized blanks account for the 3.90% of A1 blanks and the 4.55% of A2 blanks, while bladelets-sized blanks account for the 0.84% of A1 blanks and the 1.01% of the A2 blanks. Butts are mostly linear, plain and punctiform in blades and bladelets of both units. Blanks are mostly non-cortical; cortex covers up to half of the blanks' surface, mostly in distal position. Negatives are mostly bladelets in both blades and bladelets of both units. Orientation is usually unipolar and a combination of unipolar and convergent. The termination is plunging. The outline is sub-parallel. Profiles are mostly curved, bladelets are mostly slightly curved. The cross-section is mostly trapezoidal, symmetrical and asymmetrical.

Surface Cleaning blade

Blades-sized blanks account for the 0.84% of A1 blanks and the 2.27% of A2 blanks, while bladelets-sized blanks account for the 0.28% of A1 blanks and the 0.51% of A2 blanks. Butts are mostly plain and linear, bladelets' ones are either linear or punctiform. Blanks are mostly non-cortical; cortex covers up to a half of the blank surface, mostly in distal position; bladelets are less cortical. Determinate negatives are mostly bladelets and a combination of blades and bladelets. Negatives' orientation is typically unipolar and a combination of unipolar and convergent. Blades' termination is typically either feathered or plunging, while bladelets are only plunging. The outline is mostly sub-parallel in A2 and convergent in A1. Profiles are mostly straight, while bladelets are curved. The cross-section is trapezoidal, either symmetrical or asymmetrical, bladelets are more symmetrical, either trapezoidal or triangular.

Maintenance blade

Blades-sized blanks account for the 1.52% of A2 blanks, while bladelets-sized blanks account for the 0.51% of A2 blanks. Butts are mostly plain, linear, and facetted. Blanks are mostly non-cortical. Cortex covers the blanks' surface up to a half, in lateral position. Negatives are mostly bladelets and unipolar. The termination is feathered in most of the blades, while bladelets are more plunging. The outline is mostly sub-parallel, bladelets are mostly off-axis. Blades' profiles are mostly slightly curved, followed by curved, while bladelets are usually straight. Blades' cross-section is mostly symmetrical, either triangular or trapezoidal, bladelets are more asymmetrical.

Simple blade and simple bladelet

Simple blades account for the 14.48% of A1 blanks and the 10.61% of A2 ones, simple bladelets account for the 38.44% of A1 blanks and the 38.64% of A2 blanks. Butts are mostly linear, plain and punctiform in both categories, in bladelets punctiform butts are more represented than plain ones. The large part of the blanks is non-cortical, cortex covers up to half of the blanks' surface, mostly in lateral position. Bladelets are the most recorded negatives in blades, complemented by a combination of blades and bladelets, and are the only one recorded in bladelets blanks. Negatives are generally unipolar, complemented by a combination of unipolar and convergent orientation. The distal termination is mostly feathered, with some hinged and stepped ones, mostly in blades. The outline is mostly sub-parallel and convergent. The profile is mostly straight, followed by slightly curved ones, mostly in A2 blades. Bladelets follows the same trend, curved profiles are matched by twisted ones. In blades, the cross-section is almost evenly subdivided between trapezoidal symmetrical and asymmetrical one, while A1 blanks have bigger frequency of asymmetrical triangular, A2 blanks are mostly triangular symmetrical. Bladelets have mostly triangular, symmetrical and asymmetrical, and trapezoidal asymmetrical cross-sections.

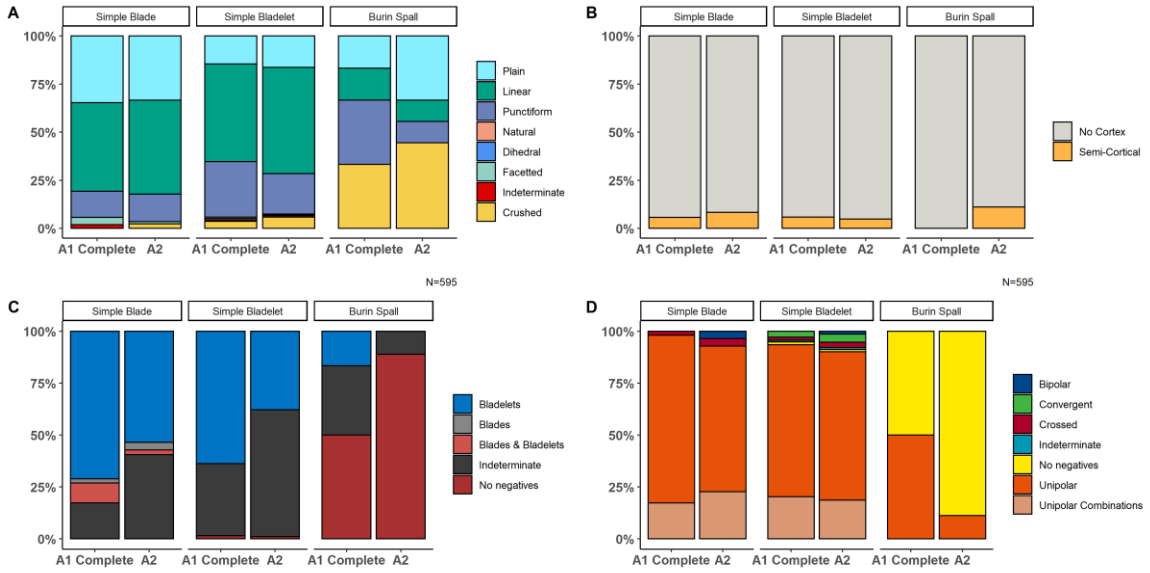

Graph 39 Simple blades, simple bladelets and burin spalls technological attributes. A) Butt values. B) Cortex coverage. C) Negatives' types. D) Negatives' orientation

Burin Spall

They are bladelet-sized blanks, and they account for the 1.67% of A1 blanks and the 1.14% of A2 ones. Butts are mostly plain in A2 and punctiform in A1. Blanks are largely non-cortical, an A2 blank is semi-cortical on dorsal position. Bladelets negatives are recorded on an A1 blank, most of the blanks are without negatives. The negatives orientation is unipolar. The distal terminations are usually feathered. Outlines are mostly sub-parallel, followed by convergent ones. Profiles are mostly straight. The cross-sections are mostly triangular symmetrical.

Retouched Blanks

Retouched blanks are 1.27% of the A1 blanks and 2.14% of A2 blanks.

Blades are the most represented, followed by bladelets and eventually by flakes. blades and flakes are mostly retouched in **burins** (simple, multiple, and busked), or displaying a direct lateral retouch, most often semi-abrupt; in one case, in A1, stepped enough for considering it an **Aurignacian blade**. Bladelets are transformed by direct lateral marginal semi-abrupt retouched in **Font-Yves points** or by alternate lateral marginal semi-abrupt retouch in **Dufour bladelets**.

3.3.4 Conclusions

Fumane units A1 and A2 assemblages show a great deal of similarity. Both technological trends and the percentages of categories in complete blanks are pointing to the same technical tradition, as evidenced by previous studies (Falcucci et al., 2017).

Cores are mostly single platform ones. The platform is usually plain, as also confirmed by the abundance of plain, linear and punctiform butts in blanks, even though rare facetted platforms are found in all core categories. The flaking surface is generally single and placed on one of the longest core axes, except for the Transversal Carinated cores. The two prevalent core categories are Semi *Tournant* and Narrow Fronted cores. They are followed by Narrow Fronted *sur Tranche* cores and Sub Parallel Edges ones. Cores are homogenous in their technical management and knapping goals. In fact, the angle between the striking platform and the flaking surface is acute to steep and the overhang is abraded thoroughly. Only Pre-Cores, Not Organised Flake cores and, partially, Narrow Fronted *sur Tranche* cores do not show the same deal of abrasion, probably in function of their less degree of technical investment due to early abandonment. All the advanced exploitation core categories are displaying bladelets or blades and bladelets negatives, only Pre-Cores and Not Organised Flake cores are displaying flake negatives on the main flaking surface. Flake cores have mostly a parallel surface exploitation pointing to an intrusion from lower Middle Palaeolithic layers (Falcucci et al., 2017).

Flakes are a minority in the assemblage, they correspond to decortication and rejuvenation activities. The decortication is represented by cortical flakes, showing extensive patches of cortex. Their small number is indicative of non-intensive decortication of cores, or it signals the import of partially decorticated piece of raw material. Management flakes, mostly represented by surface cleaning flakes, occur in a slightly more advanced knapping phase, as the cortex covering, mostly semi-cortical and lateral, is showing. Nevertheless, the knapping has not completely switched to laminar elements, including still some flakes negatives. Core tablets are used for renewing the striking platform, the ones recorded in the assemblage are mostly showing an advanced phase of exploitation, hence the low cortex presence. Also, they display previous partial management of the striking platform, unipolar flakes, and the former bladelets' negatives on the flaking surface. The tablets may be detached with perpendicular gesture, using the main flaking surface as striking platform, therefore their butts may be "facetted" due to former negatives, laying orthogonally to their knapping direction.

Laminar production starts early on, as showed by management blades dimensions. Occasionally, a crest can be shaped by the removal of one or two rows of orthogonal flakes. Blade-sized crests are more cortical, hence knapped in an earlier phase, than bladelet-sized ones. The asymmetrical cross-sections, the off-axis terminations and the twisted profiles are indicating a lateral position on the core volume, thus correcting an already existing ridge.

Nevertheless, asymmetrical blades are by far the most represented laminar management blanks, especially blade-sized ones. Blades show a higher presence of cortex, mostly on lateral and distal position, compatible with their lateral convexity maintenance. Due to their plunging, off-axis distal terminations and twisted profiles they were used for renewing the distal convexity too.

Another way of controlling the distal convexity is the knapping of plunging, curved overshot blades.

The most represented category is the simple bladelets, followed by simple blades. These blanks share the main characteristics of being typically non-cortical, having a regular sub-parallel or convergent outline, a feathered distal termination and straight or slightly curved profile. While blades have mostly trapezoidal cross-sections, bladelets have triangular ones, meaning blades are using multiple guide nervures, while bladelets typically a single central one.

Also, burin spalls are recorded, due to their morphological similarity with simple bladelets they might have been regarded as homogeneous with them.

Given that simple bladelets are the overwhelming majority of bladelet-sized blanks, while simple blades account for a minority of blade-sized blanks, negatives dimensionally compatible with a bladelet are recorded on all knapping products and cores, with the exception of decortication flakes, the most parsimonious conclusion is that the assemblage is oriented towards the production of bladelets, reserving shaping roles to blade-sized blanks.

4. Discussion

4.1 Fragmentation

It is common for eUP laminar blanks, especially bladelets, to be fragmented (Bon, 2002a; Chiotti et al., 2015; Falcucci et al., 2018; Martínez-Moreno et al., 2012; Normand et al., 2008; Paris, 2015). The analysed assemblages are no exception, in fact half of the blades are complete, but only 30–40% of the bladelets are. On the other hand, flakes are always largely represented by complete blanks. An explanation to this pattern is that, experimentally, artefacts with an area to maximum thickness ratio (A/T) inferior to 172.28 mm and with a thickness inferior to 7 mm are found most at risk to be broken by trampling (Weitzel et al., 2014). While only blades and flakes from Al-Ansab 1 exceed the critical A/T, and therefore should explain their completeness, bladelets have always the smaller value, and therefore, they are the most prone to be broken once abandoned on the ground.

Table 16 A/T values listed for the various blanks' categories in the studied assemblages

	A/T Blades	**A/T Bladelets**	**A/T Flakes**
Al-Ansab 1	179.64	117.17	192.71
Românești-Dumbrăvița I	144.74	88.40	132.72
Fumane A1–A2	148.33	97.69	154.42

For instance, in Castanet rock shelter the bladelets' fragmentation is most likely due to taphonomic reasons (Chiotti et al., 2015). Another factor to consider is that objects with similar length and width (i.e. flakes) are less likely to be fragmented accidentally (Weitzel et al., 2014). The studied assemblages confirm such empirical observation. Besides taphonomic reasons, fragmented bladelets, especially mesial fragments, are thought to be intentionally broken into smaller, regular pieces for hafting purposes (Normand et al., 2008). The widespread notion of bladelets being tips and implements for projectiles (*armatures*) is discussed below in another paragraph.

4.2 Blades–Bladelets threshold

The threshold between blades and bladelets is much debated. As shown by Section 1.3, some authors decided not to qualify precisely what a bladelet is, others preferred to give a determination using the length (Bon, 2002a), while a consistent group of authors focused themselves on the 12-mm-wide threshold. The latter did so for two reasons, the first one is that in eUP assemblages, like Isturitz or Fumane, blanks with inverse and alternate lateral retouch, characteristic of the Dufour bladelets, are mostly under the 12-mm-wide threshold (Falcucci et al., 2017; Normand et al., 2008), the second

reason is following Tixier's metrical definition of laminar blanks (Tixier, 1963). There is some concern that this would result in an arbitrary division, in fact in most of the assemblages, the distribution of the metrical values is continuous, generally skewed towards the smaller ones (Falcucci et al., 2017; Kaufman, 1986), then it is prone to be interpreted as an effect of core reduction more than a deliberate size choice. Kaufman proposed to use Discriminant analysis, in order to accentuate the differences between two *a priori* groups, defined on the assemblage tools' measurements (Kaufman, 1986). The outcome of the analysis, unfortunately, is less conclusive and objective than it could have been, in fact the statistical threshold was determined at 19 mm, but the author rejected it on the grounds of reasoned, but *ad hoc*, considerations (Kaufman, 1986). Overall, it seems that an arbitrary, but shared, threshold would be the most effective approach. Considering the analysed assemblages, width measurements are the most reliable, because they are measured also on fragmented blanks therefore resulting in larger and more representative samples. Both blade and bladelets have different width medians and the distributions are statistically significant. Despite the overlapping of the last complete negatives and bladelets, their width measurements' distributions are also statistically significant. Therefore, it can be concluded that bladelets and blades width values are statistically significant, assigning them to two different populations and, despite the overlap, last complete negatives width's measurements do not correspond to the same population of the bladelets' ones.

Table 17 results of the Wilcoxon statistical test on the distributions of blades' and bladelets' width measurements and bladelets' and last complete negatives' width measurements

Al-Ansab 1 Blade-Bladelet	**Românești-Dumbrăviţa I Blade-Bladelet**	**Fumane A1–A2 Blade-Bladelet**	**Al-Ansab 1 Bladelet-Last Complete Negatives**	**Românești-Dumbrăviţa I Bladelet-Last Complete Negatives**	**Fumane A1–A2 Bladelet-Last Complete Negatives**
W = 771188	W = 75194	W = 418476	W = 536115	W = 35753	W = 474570
p-value < 0.01	p-value < 0.01	p-value < 0.01	p-value < 0.01	p-value < 0.01	p-value < 0.01

4.3 Techniques

Defining the technique, i.e. the tool and gesture applied to a lithic reduction, without the actual finding of impactors is challenging. Historically, techniques have been hypothesised and tested through experimentation and comparison with the archaeological record; the observations that are widely accepted are those defined by J. Pelegrin through experimentation (Pelegrin, 2000). Especially for the Palaeolithic he described three types of direct percussion: with hard hammer, organic soft hammer and soft stone hammer (Pelegrin, 2000). The direct percussion with hard

hammer is characterised by an inner gesture, the impactor hits the striking platform far from the overhang, this and the mechanical properties of the impactor produce a thick butt, the small point of impact is fissured, thin lines are departing radially from the point of impact and the bulb can be pronounced or not. The direct percussion with organic soft hammer is characterised by a tangential gesture, much closer to the overhang in a sort of pulling movement: therefore, the butts are thinner, the butt extends itself forming a lip on the higher ventral face, the bulb is diffused or not perceived. The abrasion of the overhang is needed because otherwise the pulling movement would not propagate correctly, being arrested by the former removals' bulb negatives (Pelegrin, 2011, 2000). The direct percussion with soft stone hammer can be used with an inner and with a tangential gesture, in the latter case the most diagnostic features are the formations of fine and dense lines and of a bulbar scar on the ventral face. The angles formed by the striking platform and the flaking surface are acute for the tangential direct percussion, either with organic and with soft stone hammer, and more tending towards right angle for the hard hammer (Pelegrin, 2000). Roussel and colleagues confirmed Pelegrin's observation for the soft stone direct percussion, but the two other impactors, hard stone and organic hammers, left less conclusive marks (Roussel et al., 2009). In particular, they noticed that even organic soft hammers can produce pronounced bulbs (Roussel et al., 2009). Another experimentation failed to find Pelegrin's observations statistically significant or related to the type of impactor used (Driscoll and García-Rojas, 2014). This dissertation was not particularly devoted to discerning between types of impactors, therefore no experimentation has been carried out. The analysed assemblages show a high degree of overhang abrasion and acute angles, bulbs in laminar blanks are generally diffused while in flakes are more pronounced, lips are mostly present on blades while they are practically absent from bladelets. At the current state of the art these characteristics, are mostly linked to the direct organic hammer tangential percussion (Section 1.3, this dissertation). Unfortunately the hypothesised organic nature (hard wood or antler) of the impactor used in direct tangential percussion makes it difficult for such an object to preserve or to be recognised in the archaeological record (Bello et al., 2016). Therefore, caution must be used in identifying specific techniques.

4.5 Cortex

Cortex is a smooth, sometime chalky, patina covering the raw material and resulting from mechanical and chemical weathering (Andrefsky, 2005). Being the outer part of the raw material piece, cortical blanks are assumed to represent the first stages of knapping: hence, the presence of cortical blanks, alongside the other products and discarded cores, are indicative of an on-site complete reduction and it can highlight a degree of technical investment in blank production (Andrefsky, 2005). Cortical patches on cores and various cortical blanks are present in the studied assemblages, showing that raw

material was introduced on site not preformed or only slightly decorticated. In cores cortical patches are identified in posterior, lateral and basal faces, hence they witness that a complete decortication was not envisioned by the knapper, who, on the other hand, preferred to remove the cortex only in the selected areas of the core volume affected by the main reduction sequence. While nearly half of the flakes shows cortical patches, only a fifth of the blades and bladelets does, therefore the deduction that, generally, flakes are knapped for roughing out roles in early knapping stages or peripherally to the main flaking surface. Românești-Dumbrăviţa I is the least cortical assemblage, nevertheless flakes are three times more cortical than blades and bladelets. Probably due to the nature of the raw material, which is prone to internal discontinuities leading to high fragmentation; prehistoric knappers could have taken advantage of this characteristic importing on site mid-sized, already sufficiently naturally decorticated pieces of raw material. Most of the cortical blanks in the analysed assemblages, either flakes or laminar, are semi-cortical, meaning that cortex patches cover up to the half of the dorsal face, but usually smaller areas. Except for cortical flakes that are the only blanks in the assemblages featuring a dorsal face extensively, if not completely, covered with cortex. Regarding the position of the cortical patches, blanks corroborate cores' observations, in fact the most detected position is lateral, followed by the distal one. Hence, following a quick removal of cortical flakes, the main reduction sequence removed peripheral patches of cortex localised on the lateral and the basal core faces, mostly through asymmetrical and overshot blades or management flakes. Such minimal investment in cortex management is typical of other eUP assemblages. For instance, coupling the decortication with the first real laminar series is common in the Cantabrian sites (Maíllo Fernández, 2005; Maíllo-Fernández and de Quirós, 2010; Santamaría Álvarez, 2012), in Grotta Barbara (D'Angelo and Mussi, 2005), in Kozarnika VII (Tsanova, 2008), in Abu Noshra and Lagama (Bar-Yosef and Belfer-Cohen, 1977; Phillips, 1988). Blades and bladelets with lateral cortex, showing the maintaining of a lateral untouched core face, are common in l'Arbreda H, in the South-western French Early Aurignacian and in Coşava (Bon, 2002a; Bordes, 2005; Ortega Cobos et al., 2005; Sitlivy et al., 2014a). Cores showing lateral and posterior cortical areas are present in Siuren I, Isturitz, La Laouza and Esquicho Grapaou (Bataille, 2016; Bazile and Sicard, 1997; Normand and Turq, 2005). The use of cortical flakes instead of laminar blanks is also attested in Nahal Nizzana XIII and Boker A (Davidzon and Goring-Morris, 2003; Goring-Morris and Davidzon, 2006; Monigal, 2003), Qadesh Barnea 601 (Gilead and Bar-Yosef, 1993), Manot (Abulafia et al., 2019), Coşava (Sitlivy et al., 2014a). The transversal carinated cores of the Early Aurignacian contexts are showing complete roughing out through flakes (Bon, 2002a; Chiotti and Cretin, 2011; Degano et al., 2019b). Therefore, eUP decortication is quite diversified, but generally not extensive, it seems to be geared on pragmatic considerations of wasting the least possible material.

4.6 Unipolarity

The unipolar orientation is dominant in all analysed assemblages. Percentages in cores and laminar blanks are between 90–70%, combining the unipolar and unipolar and convergent orientations. On the other hand, only around half of the flakes is unipolar; although, looking closely, this is the result of the higher percentage of blanks with no negatives. Amongst the other orientations, orthogonal is important in core tablets and crests, due to their peculiar way of been struck and shaped, using the main flaking surface as striking platform. The unipolar orientation is complemented by the single striking platform and single flaking surface that cores are displaying in overwhelming majority. Opposed striking platform are episodic, and, at times, related to the distal convexity shaping. Multiple flaking surfaces on the same core are mostly independent, using another part of the core volume. The vast majority of the eUP assemblages is unipolar (Section 1.3, this dissertation). The only exception are some sites in the Northern Levant, which form the Northern Early Ahmarian technocomplex. In sites like Manot (Abulafia et al., 2019), Üçağızlı (Kuhn et al., 2009) and Ksar Akil (Bergman, 1988) the use of a single bipolar flaking surface is more common than the single platform cores. Although, in Manot the double opposite platforms are not equal in morphology and number of negatives knapped, leading the authors to define a main platform and to hypothesise that some of the opposite platforms may have shaping purposes (Abulafia et al., 2019). Also the bipolar reduction seems to be more used for blades, while bladelets are generally unipolar (Abulafia et al., 2019). Such peculiarity of the Northern Early Ahmarian has been linked to an adaptation to the Mediterranean biome (Richter et al., 2020). Also, Richter and colleagues (2020) suggest that the Early Ahmarian appeared first in such environmental context and only later the unipolar Southern Early Ahmarian appeared as a response to the colonisation of the marginal steppe and desertic Levantine areas. Such reconstruction is problematic because relies heavily on disputed chronologies, as mentioned in sections 1.2 and 1.6. In fact, so far, the only Ahmarian sites exceeding 45 ka cal BP are namely Manot and Kebara (Alex et al., 2017; Rebollo et al., 2011). Both sites are object of a heated debate concerning stratigraphy integrity, correct sampling and ^{14}C samples pre-treatment. Kebara's formation processes allows for mixing of Middle Palaeolithic charcoal in Upper Palaeolithic layers and two pre-treatment protocols (ABA and ABOx-SC) have given controversial results (Bar-Yosef et al., 1996; Goldberg et al., 2009; Rebollo et al., 2011; Zilhão, 2013), while Manot is a talus secondary accumulation which in unit 6 shows mixing between Early Ahmarian and Aurignacian artefacts and in units 7 and 8, primarily assigned to Early Ahmarian, some Mousterian and IUP artefacts are reported (Abulafia et al., 2019; Marder et al., 2017). Manot lithic industry has been reported to be studied by individual basket, because "*the correlation between sedimentological units and archaeological horizons was not straight forward*" (Abulafia et al., 2019, p. 9). In addition,

there are only two dates retrieved from unit 7 (Alex et al., 2017). The estimates for the Northern Early Ahmarian occurrence in Ksar Akil and Üçağızlı are considerably later and coming from safer contexts (Douka, 2013; Douka et al., 2013), even though a second datation of Ksar Akil Ahmarian is around 2 k years older (Bosch et al., 2015). Mughr al-Hamamah at the moment is the only site in the Levant which is dated with ABOx–SC pre-treatment and showing an early chronology (44.6–39.4 ka cal BP) from a pristine context (Stutz et al., 2015; Stutz and Stutz Nilsson, 2017). The lithic industry, despite showing no mixing and being clearly of eUP nature, is not assigned to any particular technocomplex, but from the illustrations of the cores no bipolar cores are shown, the only bipolar items reported are scaled pieces (Stutz et al., 2015; Stutz and Stutz Nilsson, 2017). All the other dates obtained from Southern Early Ahmarian sites are preceding the introduction of the ABOx–SC pre-treatment, nevertheless they are showing dates that are consistent with other conventionally (ABA) dated sites in the region and in the eUP (Higham et al., 2009; Richter et al., 2020). Therefore, it seems parsimonious not to choose an early date for the Northern Early Ahmarian development.

4.7 Cores striking platform and blanks' butts

In the analysed assemblages, cores' platforms are plain (≈90%), this is reflected in the blanks butt's composition where plain, linear and punctiform morphologies are common. According to the same concept of minimal shaping, the striking platform is opened by a single flake and it is completely renewed by a single flake, which in later stages is recognisable as a core tablet removing serial laminar negatives. Core tablets' butts are the only ones showing an important frequency of facetted morphology, result of "slicing" the core perpendicularly to the main orientation using the flaking surface as striking platform. Core tablets dorsal faces may bear one or two flake negatives, which attest the existence of partial renewals of the striking platform before the complete one. They are being removed at any stage of the reduction as their dimensional span is showing. Platform renewal through a single core tablet is typical of most of the eUP assemblages (Section 1.3, this dissertation), except for the prismatic blade cores of the Early Aurignacian which are facetted (Bon, 2002a; Bordes and Tixier, 2002).

4.8 Frontal flaking vs Semi-circumferential flaking

Two main cores knapping rhythms have been found in the eUP assemblages: frontal and semi-circumferential (Section 1.3, this dissertation). In some cases, they have been cited as identifying a particular technical tradition, for instance choosing a narrow face and exploiting it frontally is presented as a hallmark of the Early Ahmarian (Abulafia et al., 2019; Davidzon and Goring-Morris, 2003; Goring-Morris and Davidzon, 2006), while the intervention of lateral faces in core reduction

in a semi-circumferential rhythm is an essential characteristic in Protoaurignacian sub-pyramidal cores (Bon, 2002a; Bon and Bodu, 2002). Looking into details, this differentiation does not stand up in fact both knapping rhythms have been practiced in the analysed assemblages. Narrow fronted has been defined, for the purpose of this analysis, as a core which shows an active management of the narrow surface without any intervention from the main flaking surface, as described by Davidzon and Goring-Morris (Davidzon and Goring-Morris, 2003; Goring-Morris and Davidzon, 2006). Such technical investment has the task of guaranteeing the *cintrage* of the flaking surface through flakes, mostly detached on the core lateral faces.

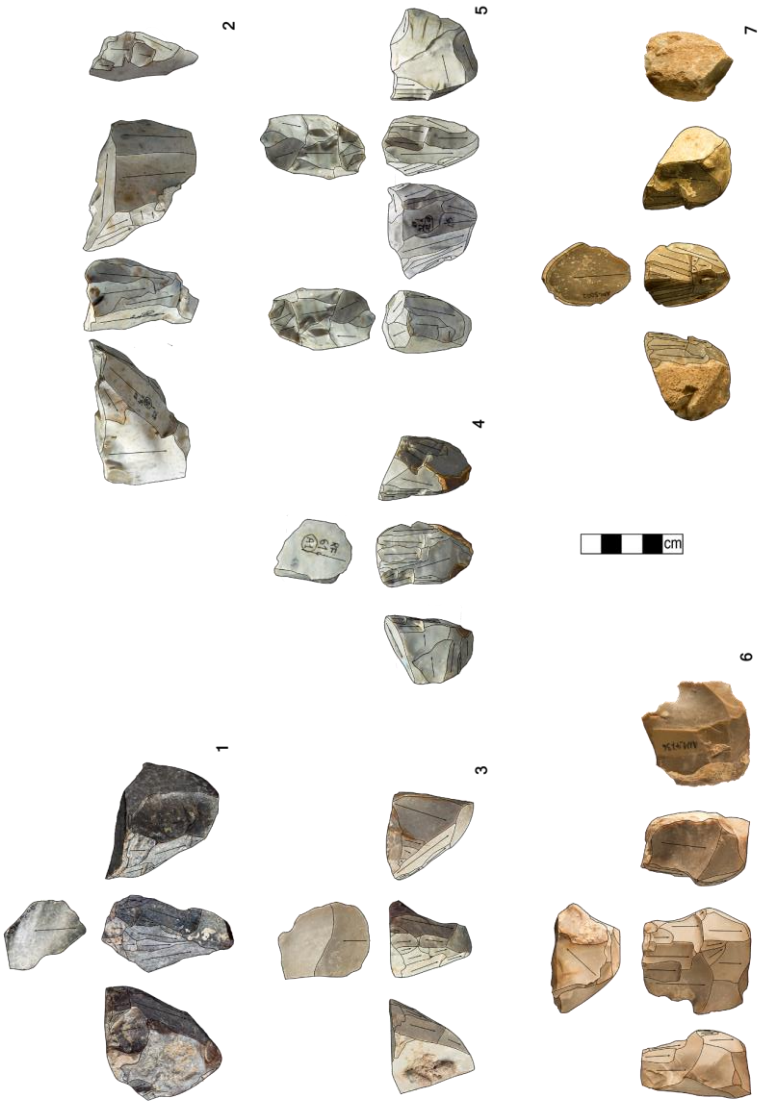

Figure 18 Narrow Fronted cores. Al-Ansab 1 (1, 3, 6, 7), Fumane A1–A2 (2, 4, 5).

Instead, semi-circumferential has been defined, for the purpose of this analysis, as the necessary involvement of core lateral faces in the main flaking surface as a way of guaranteeing the *cintrage* mostly through obliquely, inner converging blades, which gives the typical sub-pyramidal shape.

Figure 19 semi Tournant cores. Al-Ansab 1 (6, 7), Fumane A1–A2 (1, 4, 3), Românești-Dumbrăvița I (2, 3, 5).

In addition, cores showing the use of a narrow natural face, without any sign of an active narrowing, have been defined as Narrow Fronted *sur Tranche* borrowing the term from Normand and colleagues (Normand et al., 2007). In that case the name described mostly longitudinal carinated cores on blanks, in this analysis they have been merged with cores on pristine pieces of raw material that show the same course of exploitation: namely a frontal knapping rhythm aided by the natural narrowness of the chosen flaking surface.

Figure 20 Narrow Fronted sur Tranche cores. Al-Ansab 1 (1, 3), Fumane A1–A2 (2), Românești-Dumbrăvița I (4, 5).

Both Al-Ansab 1, attributed to the Southern Early Ahmarian (Richter et al., 2020), and Fumane A1–A2 assemblages, attributed to the Protoaurignacian (Falcucci et al., 2017), show the presence of Narrow Fronted and Semi *Tournant* cores. Their frequencies fail to have a significantly different distribution when tested against a theoretical even frequency: hence, at least for Al-Ansab 1 and Fumane A1–A2, Narrow Fronted and Semi *Tournant* cores are not indicative of a particular technocomplex.

Table 18 Chi-square test results of Al-Ansab 1 and Fumane A1-A2 semi Tournant and Narrow Fronted cores' frequency against a hypothetic 50-50 frequency.

	Narrow Fronted cores	**Semi Tournant cores**	**Expected frequency**	**X^2**	**p-value at 1 d.f.**
Al-Ansab 1	41	34	37.5	0.65	>0.05
Fumane A1–A2	16	25	20.5	1.98	>0.05

European eUP examples of frontal knapping on narrow faces are available in Mandrin (Slimak et al., 2002), La Laouza and Esquicho Grapaou (Bazile and Sicard, 1997), La Fabbrica (Dini et al., 2012), Coşava (Sitlivy et al., 2014a) and Kozarnika (Tsanova, 2008). At l'Observatoire both rhythms, narrow frontal and semi-circumferential, are well attested; the authors observe that narrow flaking surfaces are generally leading to bladelets, while wider ones to an intercalated production of blades and bladelets (Porraz et al., 2010). Narrow fronted cores have been described to be produced on piece of raw material naturally providing a narrow face, like slabs or flat cobbles (Bazile and Sicard, 1997; Goring-Morris and Davidzon, 2006; Porraz et al., 2010; Sitlivy et al., 2014a), therefore, a possible explanation for the application of a frontal or a semi-circumferential rhythm is an expedient decision based on the available raw material. The other cores which are forming the Narrow Fronted *sur Tranche* are represented by cores on blanks, referred into the literature as burin cores; they appear in various eUP assemblages (Section 1.3, this dissertation) but they are particularly frequent in Hohle Fels (Bataille and Conard, 2018a, 2018b) and Kostenki 17/II (Bataille et al., 2019, 2018; Dinnis et al., 2019), due to their, generally, small dimensions they are particularly suitable for bladelet production. Amongst the studied assemblage, Românești-Dumbrăvița I is showing a strong frequency of such core type. Another example of frontal knapping rhythms are prismatic parallel edges cores, mostly found in Early Aurignacian contexts (Bon, 2002a; Bordes and Tixier, 2002). Prismatic parallel edges cores are present in other eUP assemblages (Section 1.3, this dissertation), they are sometimes related to exhausted Semi *Tournant* cores (Falcucci et al., 2017; Falcucci and Peresani, 2018), in other cases they might just represent an independent configuration (Maíllo Fernández, 2006; Martínez-Moreno et al., 2012; Santamaría Álvarez, 2012). Prismatic parallel edges cores are present in small numbers in Al-Ansab 1 and Fumane A1–A2 assemblages.

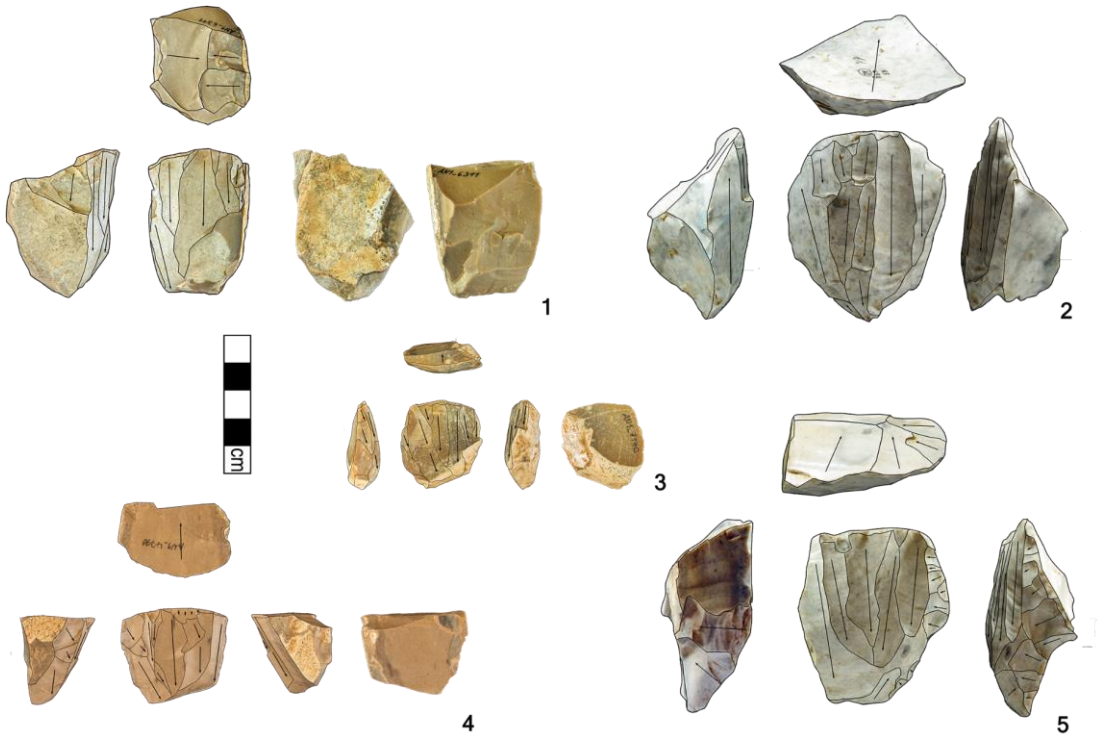

Figure 21 Parallel Edges cores. Al-Ansab 1 (1, 3, 4), Fumane A1–A2 (2, 5).

Finally, a semi circumferential knapping rhythm is recorded in transversal carinated cores (Bon, 2002a; Bordes and Tixier, 2002; Falcucci and Peresani, 2018; Le Brun-Ricalens, 2005b). They are particularly characteristic of Early Aurignacian contexts (Bon, 2002a; Bordes and Tixier, 2002; Chiotti and Cretin, 2011; Degano et al., 2019b; Le Brun-Ricalens, 2005b), but they are present in various other eUP assemblages (Section 1.3, this dissertation), including Al Ansab 1 and Fumane A1–A2. Their main characteristics is being fabricated on blanks or chunks installing the flaking surface in the thickness of the piece (Bordes and Tixier, 2002; Chiotti and Cretin, 2011).

The discussion of these two basic knapping rhythms is pivotal in understanding the different ways of guaranteeing the needed convexities to the cores. While a semi-circumferential rhythm maintains its *cintrage* slowly expanding into the adjacent lateral core faces, using lateral blades or bladelets, a frontal rhythm relies mostly on the narrowness of the flaking surface and on additional core flanks shaping. Fronted cores most common products for convexities shaping and maintaining are laterally steeply backed blades, removing the sharp angle formed by the faces intersection, they can be shaped in unifacial crests and neo-crests (Bon, 2002a; Le Brun-Ricalens, 2005b; Normand and Turq, 2005; Teyssandier et al., 2006). A peculiar type of crest is the *lamelle croisée*, in which one side remove a part of the flank shaped by oblique bladelets stricken from the back of the core (Porraz et al., 2010; Slimak et al., 2002). Instead, because the semi-circumferential rhythm expands on adjacent core faces, lateral blades have a twisted, curved profile, plunging and off-axis terminations (Bon and

Bodu, 2002; Falcucci et al., 2017; Hussain, 2015; Maíllo-Fernández and de Quirós, 2010; Zwyns, 2012).

Figure 22 Asymmetrical blades (1 – 27) and bladelets (28 – 33). Al-Ansab 1 (1, 3, 5 – 9, 12, 14, 18, 25), Fumane A1–A2 (4, 11, 13, 16, 20, 22, 24, 26 – 29, 31 – 33), Românești-Dumbrăviţa I(2, 10, 15, 17, 19, 21, 23, 30).

Such blades are the ones responsible for the maintaining of lateral and distal convexities, putting in place the guiding ridges for the central inner blades and bladelets, their mild twisting is due to the lateral position at the intersection of the flaking surface and the lateral core face. In transversal

carinated cores the same role is assumed by bladelets defined as *lamelles de cadrage* (Le Brun-Ricalens, 2005b). Asymmetrical blades are the most frequent of management blank found in the analysed assemblages, they often display a twisted profile hence witnessing the expansion of the knapping to adjacent core faces. They are followed by overshot blades, while crests are rare, leading to the interpretation that they were episodic.

Figure 23 Crests (1 – 9) and Overshot blades (10 – 20) and bladelets (21). Al-Ansab 1 (1, 5, 6, 10 –12, 16), Fumane A1–A2 (3, 4, 7, 14, 17, 19, 21), Românești-Dumbrăviţa I(2, 8, 9, 13, 15, 18, 20).

In the usual knapping reconstructions (i.e. Hussain, 2015; Richter et al., 2020), a single flaking surface is framed by two lateral asymmetrical blades, following such reconstruction a much wider

range of sizes is expected (i.e. following the progressive reduction of the core); instead, half of the blanks are concentrated in the mid-lower sizes.

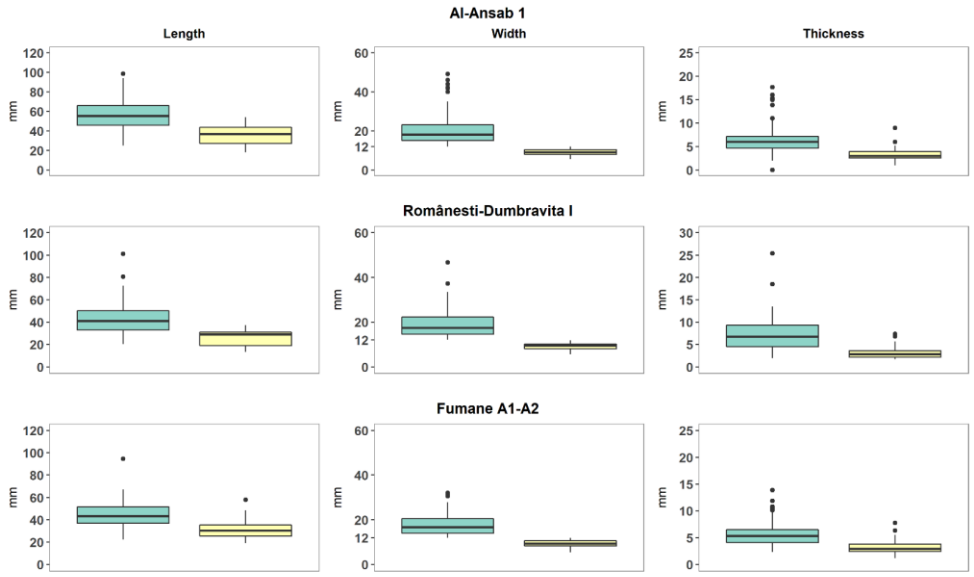

Figure 24. Dimensions of asymmetrical blades (Blue) and bladelets (Yellow). Boxes represent 50% of the pieces with the other half scattered above and beneath.

Their usage, then, could account for smaller flaking surfaces organised around local ridges (i.e. the two intersections with the core laterally adjacent faces framing the final flaking surface); such flaking surfaces would need few central overshot blades for maintaining the distal convexities, when convexities are exploited the flaking surfaces migrate laterally fusing in, after few iterations, a single flaking surface. Such hypothetical reconstruction would also reconcile with the presence of negatives of simple blades/bladelets on, seemingly, the former lateral core ridges removed by asymmetrical blades.

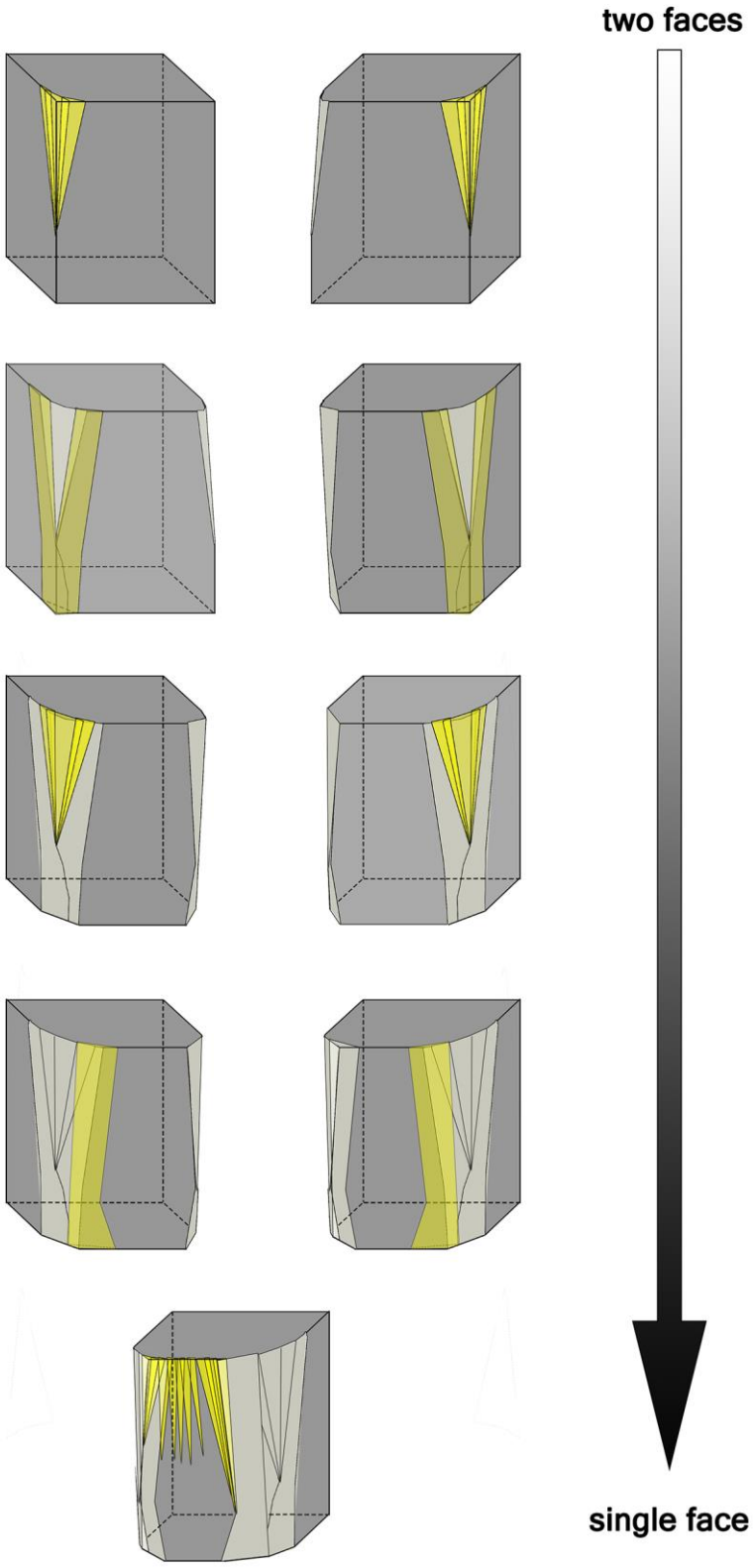

Figure 25. Hypothetical knapping progression from two flaking surfaces to a single one. Dark grey: core volume. Light grey: previous negatives. Yellow: knapped blanks.

4.9 Blade and bladelets morphology

A big part of the analysed assemblages consists of simple blades and, primarily, simple bladelets.

Figure 26. Bladelets (1 – 45) and bladelet-sized Burin Spalls (46 –50). Al-Ansab 1 (1 – 7, 15, 16, 19, 21, 23, 25, 26, 30, 31, 36, 46), Fumane A1–A2 (10 – 14, 17, 22, 24, 28, 33 – 35, 37, 47, 48, 50), Românești-Dumbrăviţa I (8, 9, 18, 20, 27, 29, 32, 38, 39, 40 – 45, 49).

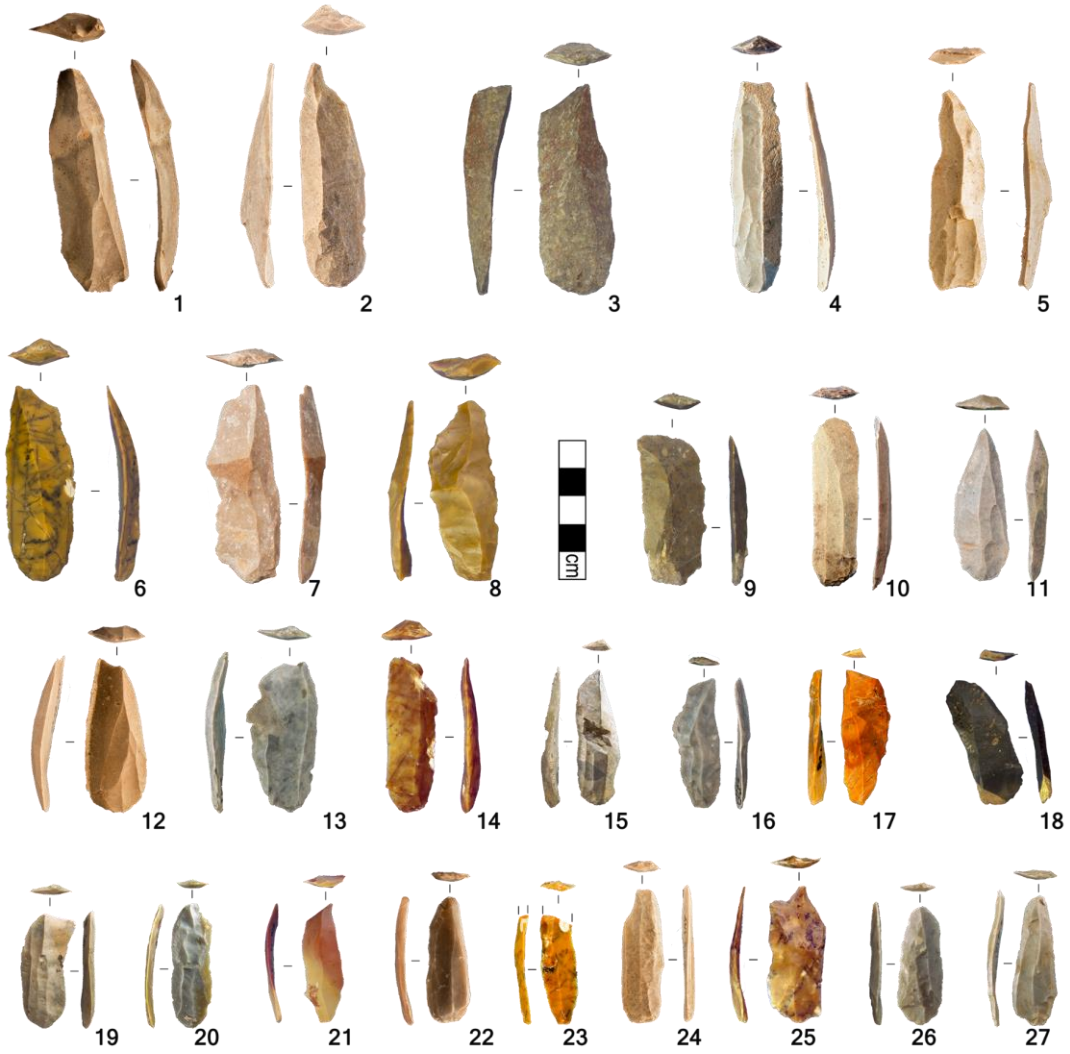

Figure 27. Blades. Al-Ansab (1, 2, 4, 5, 7, 10 – 12, 22, 24), Fumane A1–A2 (13, 15, 16, 19, 20, 26, 27), Românești-Dumbrăviţa I (3, 6, 8, 9, 14, 17, 18, 21, 23, 25).

They are largely feathered, even though blades are more likely to be plunging or occurring in a flaking accident than bladelets, probably due to their longer reaching. Both are mostly on-axis, but bladelets tend to be more convergent than sub-parallel. Both blades and bladelets have mostly straight and slightly curved profiles, while blades tend to feature more curved profiles, bladelets are more twisted. Blades have mostly trapezoidal cross-sections, meaning they used two (or more) guiding ridges, while bladelets have more triangular ones, meaning they originated from a single guiding ridge. Blades tend to be more asymmetrical, so struck from peripheral areas of the flaking surface, while bladelets are more symmetrical, then struck from a central area. Blades and bladelets are equally symmetrical in Românești-Dumbrăviţa I and in Fumane A2. Therefore, the analysed assemblages show a production tending to straight, regularly shaped, on-axis blanks: mostly expressed in bladelet sizes. Such tendency is shared with almost the entirety of the eUP assemblages

(Section 1.3, this dissertation). These blanks are reserved for lateral, direct or inverse, marginal retouch (Section 1.3, this dissertation), a similar outcome has been shown from the few retouched artefacts included in the analysis.

4.10 Flakes

Flake cores are present only in Fumane A1–A2 and Al-Ansab 1 assemblages. They do account for a small percentage of the total cores number, and, in the case of Fumane, they may well originate from a post-depositional mixing with the underlying Mousterian unit. In Al-Ansab 1, flakes cores do not differ conceptually from other cores, in fact, they have a single plain striking platform, they are unipolar, and cortex is found on the lateral or on the basal faces: overall, they do not show a particular configuration in order to obtain flakes.

Flakes are not well represented numerically in Al-Ansab 1 and Fumane, most of them can be related to decortication and core-maintenance tasks, simple flakes being rare. On the other hand, roughly a half of Românești-Dumbrăviţa I assemblage consists of flakes, with a good number of them being simple flakes, but without any core showing flake-based production.

Figure 28. Cortical flakes. Al-Ansab 1 (1, 4, 7), Fumane A1–A2 (2, 6), Românești-Dumbrăviţa I (3, 5).

Figure 29. Management Flakes (1–14) and Core Tablets (15 – 21). Al-Ansab 1 (1, 3 – 5, 7, 15, 18), Fumane A1–A2 (6, 8, 9, 11, 14, 16, 19, 21), Românești-Dumbrăviţa I (2, 10, 12, 13, 17, 20).

Flakes production in eUP contexts is generally considered subordinate to the laminar one or being expedient (Pastoors and Peresani, 2012). In level 479D of Cova Gran de Santa Linya (Pyrenees

foothills) flakes are considered to be part of the exploitation strategy alongside blades and bladelets (Martínez-Moreno et al., 2012); the authors point to the fact that no technical and technological break can be perceived between flakes and laminar blanks, although the flakes are said to cover mostly management roles, such as removing the frequent hinge accidents (Martínez-Moreno et al., 2012). Also in Siuren I flakes production is not independent from the laminar one and flake cores follow roughly the same concepts (Bataille, 2012). Cantabrian eUP contexts have been reported having an independent production of flakes from Discoid or surface cores (Maíllo Fernández, 2006; Maíllo-Fernández, 2012; Maíllo-Fernández and de Quirós, 2010; Santamaría Álvarez, 2012). In the Early Aurignacian, blades prismatic cores are said to be transformed in expedient flake cores (Bordes and Tixier, 2002; Chiotti, 2012; Roussel and Soressi, 2013). In the Early Aurignacian levels of the Pataud shelter (Dordogne, SW France), flakes are produced from prismatic unipolar cores whose flaking surface is too short for a laminar production or from S.S.D.A. cores: such production is explained with short-period occupations (Chiotti, 2012). Some flake production in Early Aurignacian contexts is also coming from the shaping of transversal carinated cores (Bon, 2002a; Chiotti, 2012; Chiotti and Cretin, 2011). Therefore, according to the literature eUP flake production is either linked to shaping and decortication, as noticed in Al-Ansab 1, Fumane A1–A2 and Românești-Dumbrăviţa I GH3 assemblages, or it stems from cores that follow the same exploitation concepts of laminar cores or are not organised. How explaining Românești-Dumbrăviţa I higher occurrence of simple flakes? These blanks are rather non-cortical, and they display either no negatives or unipolar flake negatives, they are rather small and thin, hence, it could be hypothesised that they are the results of small interventions on the core, mostly occurring on the plain striking platform.

4.11 The role of blades, bladelets and flakes: a new technical behaviour model for the eUP.

The analysed assemblages show a clear hierarchisation between the three type of blanks they consist of: flakes, blades and bladelets. Flakes have been thoroughly discussed above, it is safe to say they play a minor role in the knapping process and none regarding the main production intentions. Blades and bladelets have a more nuanced difference. Since the early 2000s', the Western European eUP record has been divided into two technical traditions, one displaying disassociated production systems for blades and bladelets and another showing a unified production of blades and bladelets from the same core: the first one was associated with the Early Aurignacian and the second one with the Protoaurignacian (Bon, 2002a; Bon and Bodu, 2002). Over the years, the focus shifted towards the smaller blanks, which have exponentially increased their presence in assemblages, thanks to improved excavation techniques, and in the academic debate (Le Brun-Ricalens, 2005a; Le Brun-Ricalens et al., 2009). In the Levant, the research tradition mostly appointed on attribute analysis or

refittings, with a higher focus on the retouched implements description, which hampers considerably the power of assemblages comparisons (Kadowaki et al., 2015). Nevertheless, the abundance of smaller blanks, i.e. bladelets, has always been a primary characteristic of Levantine eUP assemblages (Gilead, 1991; Kaufman, 1986). Production systems have been investigated in detail, paired with refittings, in the Southern Early Ahmarian Nahal Nizzana XIII and in Boker A sites (Davidzon and Goring-Morris, 2003; Goring-Morris and Davidzon, 2006; Monigal, 2003). Their conclusions show a repetitive application of the same concept in which the difference between blades and bladelets is merely due to the available core volume. Recently, various authors have challenged the proposed difference between Early Aurignacian and Protoaurignacian. Their observations, stemming from the re-analyses of different eUP assemblages, show that the difference between Early Aurignacian and Protoaurignacian production systems is more nuanced than formulated (Bataille, 2016; Falcucci, 2018; Falcucci et al., 2017; Sitlivy et al., 2014b; Tafelmaier, 2017). Mostly, they show that bladelets are not an accidental production, but sought from the start of the knapping: such intention results in independent bladelets' cores or intercalated blades–bladelets' cores, where blades are fulfilling mostly shaping roles (Bataille et al., 2018; Falcucci et al., 2017; Tafelmaier, 2017). I propose to extend such views to the Southern Early Ahmarian assemblage of Al-Ansab 1. In fact, blade-sized blanks are more likely to restore or create convexities, while bladelets-sized blanks are more likely to conform to techno-morphological attributes linked to knapping objectives in the eUP, such as: straight or slightly curved profiles, a regular morphology and a feathered ending. Bladelets-sized negatives occur all-along the reduction, leading to the rejection of a rapid core volume decrease as explanation of bladelets occurrence in the assemblages. I advocate the conscious production of bladelets as a major characteristic unifying all eUP European and Levantine assemblages under one technological behaviour. Such will be described as an extensive adoption of volumetric knapping and marginal direct soft hammer percussion. An application of such knapping technique is especially evident from the thorough overhang abrasion and the use of core tablets for renewing the striking platform. Cores can be defined as platform ones, they display frontal and semi-circumferential knapping rhythms, that is explicated in various morphological core types as sub-pyramidal convergent edges cores, sub-prismatic parallel edges cores, transversal and longitudinal carinated cores. The orientation is largely unipolar. Core shaping is kept to a minimum, resulting in a not extensive decortication, or choosing not extensively corticated raw material pieces, plain striking platforms and mostly a use of natural convexities and of embedded core convexities management. Such management is primarily achieved through the removal of asymmetrical, inwards convergent (off-axis), twisted profile and plunging distal termination blades; crests are mostly unifacial and partial, showing a slight shaping in the distal part of the guiding ridge. Overshot blades can maintain distal convexities too, but from a central area of the flaking surface. Overall, bladelets, laminar blanks <12 mm wide, are recognised as the main objective of the production; they are characterised by

straighter profiles, sub-parallel or convergent edges, regular morphology and feathered termination, therefore they mostly consume existing convexities.

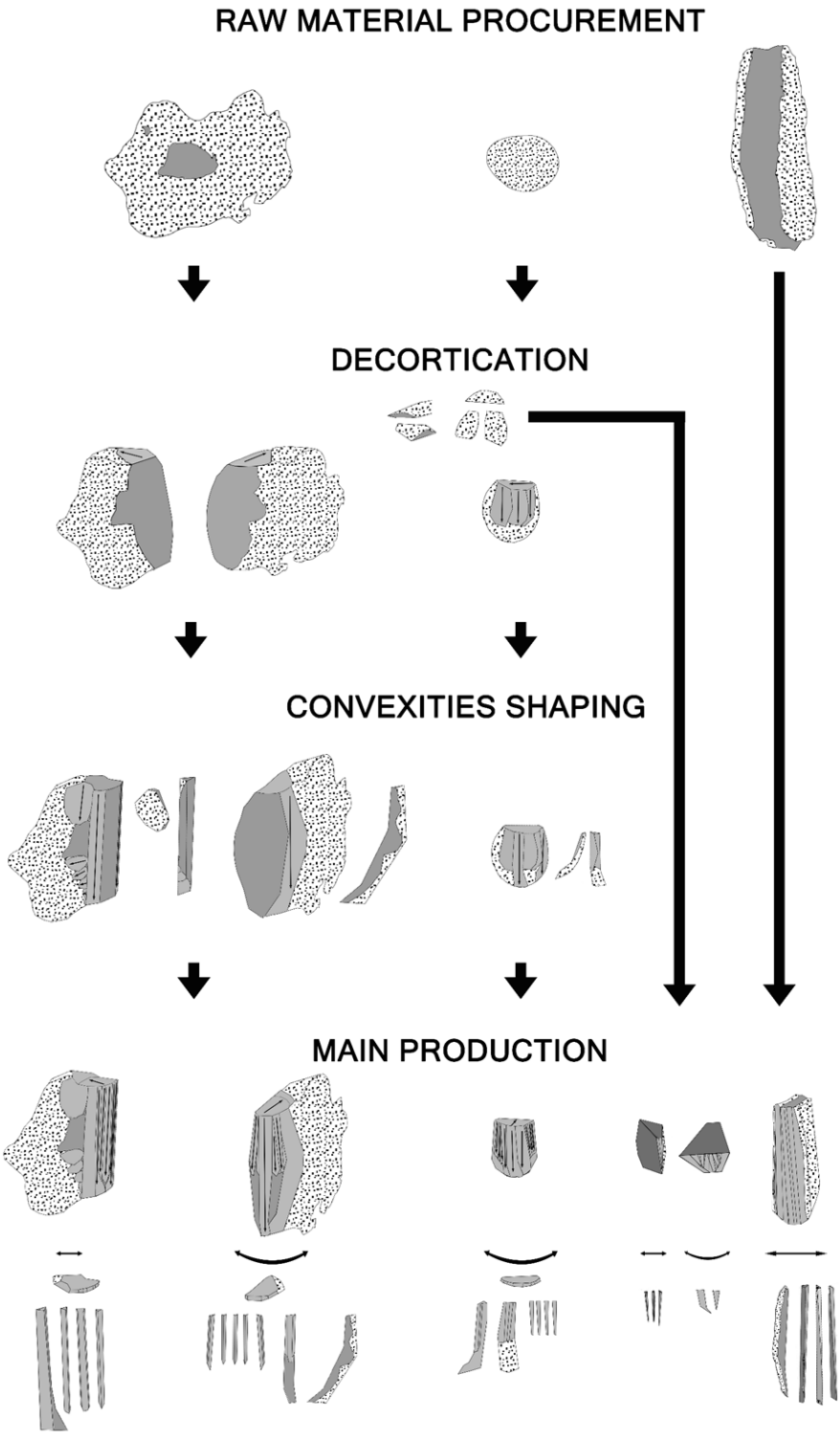

Figure 30. eUP technological behaviour concept.

4.12 The significance of lithic technology for the human dispersal

There is a long research tradition assigning the introduction of laminar technology in Eurasia to the arrival of AMH; despite laminar productions have been found also in Lower and Middle Palaeolithic contexts too, the start of the UP in Eurasia is marked by the widespread adoption of laminar technology producing bladelets (Bar-Yosef and Kuhn, 1999; De Stefani et al., 2012; Le Brun-Ricalens, 2005a). Bladelets are thought to be the durable witness of long-range projectiles, the small dimensions and regular morphologies make them perfect for the insertion in light shafts to increase the penetrative and wounding power of hunting weapons (Bon, 2005, 2002a; Teyssandier, 2007; Teyssandier et al., 2010; Tsanova et al., 2012). Another advantage of producing bladelets is a minor reliance on large nodules of good raw material: in fact, given the small dimensions of their products, bladelets can be produced from a wide range of raw material blanks, as shown by this analysis, also, a smaller piece of raw material is more likely to be homogeneous, one important qualitative characteristic of raw material against knapping accidents (Bon, 2005). In Early Aurignacian assemblages bladelets cores, especially transversal carinated forms, are representing a mobile kit, while prismatic blade cores are showing a static production linked to "household" tasks (Anderson et al., 2015; Bon, 2002a; Teyssandier, 2007; Teyssandier et al., 2010). Indeed, at least some bladelets show characteristics and traces typical of projectile use, even though others are showing a wider ranges of usage, such scraping hard materials or butchering activities (Broglio et al., 2005; Normand et al., 2008; Pelegrin and O'Farrell, 2005). In Hohle Fels bladelet-size burin spalls are related to a borer-like use (Bataille and Conard, 2018a, 2018b). More recently, the Southern Early Ahmarian bladelet based industry has been portrayed as an adaptation to more arid environments (Richter et al., 2020). According to the current chronological framework (Banks et al., 2013; Barshay-Szmidt et al., 2018; Douka et al., 2013, 2012; Higham et al., 2012; Richter et al., 2020; Schmidt et al., 2013; Stutz et al., 2015) the eUP assemblages span over the GI-11 – GI-8 (Rasmussen et al., 2014). The MIS 3 (60-30 k BP) is considered an highly instable climatic period, especially considering the abrupt and frequent oscillations between colder and milder climatic conditions corresponding to the Dansgaard-Oeschger events (Badino et al., 2020; Rasmussen et al., 2014; Sanchez Goñi and Harrison, 2010). According to the pollen data and biome modelling the Levant, during the MIS 3, was enjoying more stable climatic conditions than Europe, with enough moisture content for sustaining an Irano-Turanian steppe, mostly represented by *Artemisia* shrubs, and patches of Mediterranean woodland, mostly deciduous oak (*Quercus ithaburensis*) (Miebach et al., 2019; Richter et al., 2020). The archaeozoological record confirms such reconstruction with a better representation of gazelle and fallow deer in the northern Mediterranean area and of gazelle, wild ass

and ostrich in the southern arid environments (Rabinovich, 2017; Richter et al., 2020). In Ksar Akil, a massive accumulation of rockfall sealing the Early Ahmarian occupation, named Stone Complex 2, is associated chronologically with the HE 4 (Bergman et al., 2017; Douka et al., 2013). The HE 4 in the Levant corresponds to a peak in Amaranthaceae plants pollen signalling dryer conditions (Richter et al., 2020). Moving to the Carpathian Basin, recent studies suggest that during the MIS 3 it should have hosted mostly C_3 plants, growing in cool and humid conditions, compatible with a grasslands and steppe environments (Pötter et al., 2020). Temperatures in stadial conditions were warmer than in Western Europe and throughout the MIS 3 soil formation is detected (Hauck et al., 2018; Pötter et al., 2020). On the foothills at the margins of the basin, higher vegetations, forming a forest steppe, was present (Hauck et al., 2018). Such environment is defined as mammoth steppe, it is rich in biomass and maintained by the activity of the mammoth (*Mammuthus primigenius*) alongside ungulates as reindeers (*Rangifer tarandus*), and moose (*Alces alces*) (Hauck et al., 2018). A geographical marker is represented by the N45° latitude, northern to that a more forested environment with some deciduous trees is suggested, while southern a higher presence of *Artemisia* (Hauck et al., 2018). In loess profiles of the Lower Danube Basin, grain sizes show generally finer fraction prior to the Campanian Ignimbrite, while a bigger fraction is accumulated afterwards, showing a pattern towards stronger winds (Obreht et al., 2017). The continentalisation of climatic conditions, such as less precipitation and colder winters, is a general European feature of the late MIS 3 culminating on the substitution of boreal forest with an open steppe around 36.5 ka cal BP, on the other hand the Middle Danube Basin (Carpathian Basin) enjoyed warmer conditions due to the shift of Mediterranean air masses (Obreht et al., 2017). Such progressively cooler and drier conditions during D-O events 12 – 9 are confirmed by speleothems from the Carpathian Basin, with a low peak in GS-10 when permafrost arrived in the Northern Danube Basin and in the Eastern Carpathian mountains (Staubwasser et al., 2018). GS-9, corresponding to the HE 4, is more pronounced in Western than in Central Europe and the following interstadial oscillation, GI-8, is warmer in the Carpathian region (Staubwasser et al., 2018). In the Higher Danube Basin, interstadial conditions, corresponding to GI-11, in Willendorf II show a medium-cold steppe with boreal trees coverage in river valleys (Nigst et al., 2014). Vegetation during MIS 3 interstadials shows the presence of deciduous trees in Southern Europe, while a boreal forest was common to Western and Alpine Europe; during stadials drier conditions favoured the formation of steppe (Fletcher et al., 2010). In particular, central Italian pollen records show the presence of trees, like *Quercus*, *Abies* and *Fagus* during insterstadial conditions, while a dry steppe was forming during stadials (Fletcher et al., 2010). In Northern Italy moisture allowed continuous presence of forests dominated by conifers, with temperate trees, like *Tilia*, that persisted until 40 k cal BP with the onset of HE 4 (Pini et al., 2010). Southern and Central Italy instead show a prevalence of steppe, *Artemisia* dominated, from 45 k cal BP onwards (Badino et al., 2020). Micro and macro mammals recovered from the

Protoaurignacian layers of Grotta di Fumane broadly confirms the pollen data, in fact they outline firstly a cold and dry period, probably corresponding to the HE 4, and secondly a cold and humid period (López-García et al., 2015). Around 40 k cal BP the impact of the Campanian Ignimbrite, whose ashes' deposition interested all South Eastern Europe and partially the Russian Plain, must have been ecologically devastating (Giaccio et al., 2017; Obreht et al., 2017), leading to local abandonment of eUP sites, for instance Serino and Castelcivita in Italy (Accorsi et al., 1979; Wood et al., 2012), but seemingly spared northern areas such as Riparo Bombrini and Fumane (Falcucci, 2018; Riel-Salvatore and Negrino, 2018) or South-eastern Italy, like Grotta Paglicci (Badino et al., 2020; Palma di Cesnola, 2006). Following this, it may be concluded that bladelets eUP bearer groups thrived in relatively open environments that increased over Europe and the Levant in the mid-latter part of the MIS 3, climatic conditions were rather cool, drier during stadial conditions and more humid during interstadial ones. Moisture content affected deeply the trees coverage. Therefore, the adoption of bladelets technology could have been proved beneficial to such environments and being flexible enough for sustaining climatic overturns and major natural disasters such as the Campanian Ignimbrite. Much of the recent research on the eUP has been devoted to the AMHs dispersal in Europe, the factors that may have been favoured it and the main route(s) that AMHs could have followed (Haws et al., 2020; Mellars, 2011, 2006c; Obreht et al., 2017). Material culture, namely lithic objects, has been used to advocate one or another route of dispersal (Anderson et al., 2015; Mellars, 2011), this is why understanding eUP lithic technology is such an heated debate (Anderson et al., 2019; Bataille et al., 2019). It has been pointed out that lithic assemblages have low power in indicating an ethnic group, because they only reflect adaptive solutions: in that regard, the highest level of differentiation achievable is the recognition of regional adaptations to a particular subsistence setting (Bataille et al., 2018).Therefore, Bataille and colleagues (2018) proposed that the Protoaurignacian and the Early Aurignacian are just manifestations of a common behavioural package achieved through the network of exchanges of mobile foragers sharing the same socio-economic needs: the basal level adaptation (Aurignacian) manifests itself in local adaptations (Protoaurignacian and Early Aurignacian). According to this, a basal adaptation (eUP bladelet technology), manifests through the single adaptive *facies* (Protoaurignacian, Early Aurignacian and Early Ahmarian) due to their local settings' needs. On the contrary, this analysis shows that assemblages assigned to different *facies* are indistinguishable at a technological level. Fumane A1–A2, Românești-Dumbrăviţa I GH3, and Al-Ansab 1 assemblages failed to yield a significant difference in aims and execution of their respective lithic production, and a review of published data, as evidenced by Bataille and colleagues (2018) too, points to a very homogeneous picture. Because of that, it seems methodologically more correct to abandon named traditions. This means that, so far, a single origin and route of dispersal for such technical behaviour is not conceivable, research efforts

should be directed retrieving additional sites in gap areas such as Anatolia and further understanding the role of Central and Eastern European regions in the European dispersal of *H. sapiens*.

5. Conclusion

The thesis addressed the technical behaviour of the eUP in Europe and the Levant. The definition of eUP is the first lithic industry fully assigned to the Upper Palaeolithic, in Europe corresponding to the Protoaurignacian and the Early Aurignacian and in the Levant to the Early Ahmarian. These three lithic industries are often mentioned in the Middle – Upper Palaeolithic Transition debate because they represent the end of the transition, concluding with the final affirmation of *H. sapiens* in Eurasia at the expenses of *H. neanderthalensis*. The most evident hallmark of the eUP is the emergence of a previously episodic blank: the bladelet. Bladelets are small laminar blanks that are possibly hafted in composite tools, such as projectiles. eUP bladelets tend to be marginally modified by inverse or/and direct retouch on the longitudinal edge, sometimes the retouch creates a point sometimes it stops before the distal termination. To be consistent and to have a shared vocabulary, I decided to apply Tixier's size module definition, therefore a bladelet has a width inferior to 12 mm. Using the width allows having a larger sample, in fact also fragmented blanks, a common condition for bladelets, can be measured. Such definition is empirically proven by the concentrations of the measured values for blades' and bladelets' width, despite an apparent continuity between them, the two blanks gather around two statistically different medians above and below the arbitrary threshold. The three assemblages chosen for the analysis are coming from well-stratified, modern-fashion excavated sites with pivotal significance for the eUP. Al-Ansab 1 is one of the latest excavated, completely unexplored before, open-air sites assigned to the Southern Early Ahmarian. Românești-Dumbrăvița I provides one of the safest witness of the eUP in the Carpathian Basin and the whole South-eastern Europe. Fumane A1–A2 represent the first Protoaurignacian dispersal into the Italian Peninsula. I chose to adopt the *chaîne opératoire* approach integrated with an attribute analysis, to couple the analytical power of the diacritic analysis with the reliability of numerical and shared morpho-technological attributes, which are complementing and explaining the considerations about the core volume exploitation. The analysis evidenced similar goals and methods in the three assemblages: mostly the deliberate research of straight profile, regular bladelets. They are produced from unipolar single platform cores exploited frontally or semi-circumferentially. Blades are consistently showing characteristics associated with the maintenance of the convexities, such as a plunging or off-axis distal termination and a curved or twisted profile. Furthermore, bladelet-sized negatives are recorded through the entire reduction process and they mostly correspond to blanks located at the centre of the flaking surface, exploiting the convexities. A thorough literature review produced consistent results. Therefore, I advocate to reconsider the foundations of the Protoaurignacian, Early Aurignacian and Early Ahmarian and I propose the use of the more neutral and comprehensive term of eUP technological behaviour.

References

Abulafia, T., Goder-Goldberger, M., Berna, F., Barzilai, O., Marder, O., 2019. A technotypological analysis of the Ahmarian and Levantine Aurignacian assemblages from Manot Cave (area C) and the interrelation with site formation processes. J. Hum. Evol. 102707. https://doi.org/10.1016/j.jhevol.2019.102707

Accorsi, C.A., Aiello, E., Bartolini, C., Castelletti, L., Rodolfi, G., Ronchitelli, A., 1979. Il giacimento paleolitico di Serino (Avellino), Stratigrafia, ambienti e paletnologia. Atti Della Soc. Toscana Sci. Nat., Memorie A 86, 435–487.

Alex, B., Barzilai, O., Hershkovitz, I., Marder, O., Berna, F., Caracuta, V., Abulafia, T., Davis, L., Goder-Goldberger, M., Lavi, R., Mintz, E., Regev, L., Bar-Yosef Mayer, D., Tejero, J.-M., Yeshurun, R., Ayalon, A., Bar-Matthews, M., Yasur, G., Frumkin, A., Latimer, B., Hans, M.G., Boaretto, E., 2017. Radiocarbon chronology of Manot Cave, Israel and Upper Paleolithic dispersals. Sci. Adv. 3, e1701450. https://doi.org/10.1126/sciadv.1701450

Alexandrescu, E., Olariu, A., Skog, G., Stenström, K., Hellborg, R., 2010. Os fossiles humains des grottes Muierii et Cioclovina, Roumanie. L'Anthropologie 114, 341–353. https://doi.org/10.1016/j.anthro.2010.05.004

Andersen, K.K., Svensson, A., Johnsen, S.J., Rasmussen, S.O., Bigler, M., Röthlisberger, R., Ruth, U., Siggaard-Andersen, M.-L., Peder Steffensen, J., Dahl-Jensen, D., 2006. The Greenland Ice Core Chronology 2005, 15–42ka. Part 1: constructing the time scale. Quat. Sci. Rev. 25, 3246–3257. https://doi.org/10.1016/j.quascirev.2006.08.002

Anderson, L., Bon, F., Bordes, J.-G., Pasquini, A., Slimak, L., Teyssandier, N., 2015. Relier des espaces, construire de nouveaux réseaux: aux origines du Protoaurignacien et des débuts du Paléolithique supérieur en Europe occidentale, in: Naudinot, N., Meignen, L., Binder, D., Querré, G. (Eds.), Les Systèmes de Mobilité de La Préhistoire Au Moyen Âge XXXVe Rencontres Internationales d'archéologie et d'histoire d'Antibes. Éditions APDCA, Antibes, pp. 93–109.

Anderson, L., Reynolds, N., Teyssandier, N., 2019. No reliable evidence for a very early Aurignacian in Southern Iberia. Nat. Ecol. Evol. 3, 713–713. https://doi.org/10.1038/s41559-019-0885-3

Andrefsky, W., 2005. Lithics: macroscopic approaches to analysis, 2nd ed. ed, Cambridge manuals in archaeology. Cambridge University Press, Cambridge ; New York.

Anikovich, M.V., Sinitsyn, A.A., Hoffecker, J.F., Holliday, V.T., Popov, V.V., Lisitsyn, S.N., Forman, S.L., Levkovskaya, G.M., Pospelova, G.A., Kuz'mina, I.E., Burova, N.D., Goldberg, P., Macphail, R.I., Giaccio, B., Praslov, N.D., 2007. Early Upper Paleolithic in Eastern Europe and Implications for the Dispersal of Modern Humans. Science 315, 223–226. https://doi.org/10.1126/science.1133376

Arrizabalaga, A., 2000. The lithic technocomplexes in the archaeological site of Labeko Koba (Arrasate, Basque Country), in: Arrizabalaga, A., Altuna, J., Areso, P. (Eds.), Labeko Koba (País Vasco): hienas y humanos en los albores del paleolítico superior, Munibe. Sociedad de Ciencias Aranzadi, Zientzi Elkartea, San Sebastián-Donostia, pp. 193–343.

Arrizabalaga, A., de Quirós, F.B., Bon, F., Iriarte, M.J., Maíllo, J.M., Normand, C., 2009. Early evidence of the Aurignacian in Cantabrian Iberia and the North Pyrenees, in: Camps, M., Szmidt, C.C. (Eds.), The Mediterranean from 50 000 to 25 000 BP: Turning Points and New Directions. Oxbow Books, Oxford, pp. 255–291.

Badino, F., Pini, R., Ravazzi, C., Margaritora, D., Arrighi, S., Bortolini, E., Figus, C., Giaccio, B., Lugli, F., Marciani, G., Monegato, G., Moroni, A., Negrino, F., Oxilia, G., Peresani, M., Romandini, M., Ronchitelli, A., Spinapolice, E.E., Zerboni, A., Benazzi, S., 2020. An overview of Alpine and Mediterranean palaeogeography, terrestrial ecosystems and climate history during MIS 3 with focus on the Middle to Upper Palaeolithic transition. Quat. Int. 551, 7–28. https://doi.org/10.1016/j.quaint.2019.09.024

Bailey, S.E., Hublin, J.-J., 2005. Who made the Early Aurignacian? A Reconsideration of the Brassempouy Dental Remains. Bull. Mém. Société Anthropol. Paris 17, 115–121.

Banks, W.E., d'Errico, F., Zilhão, J., 2013. Human–climate interaction during the Early Upper Paleolithic: testing the hypothesis of an adaptive shift between the Proto-Aurignacian and the Early Aurignacian. J. Hum. Evol. 64, 39–55. https://doi.org/10.1016/j.jhevol.2012.10.001

Barshay-Szmidt, C., Normand, C., Flas, D., Soulier, M.-C., 2018. Radiocarbon dating the Aurignacian sequence at Isturitz (France): Implications for the timing and development of the Protoaurignacian and Early Aurignacian in western Europe. J. Archaeol. Sci. Rep. 17, 809–838. https://doi.org/10.1016/j.jasrep.2017.09.003

Barshay-Szmidt, C.C., Eizenberg, L., Deschamps, M., 2012. Radiocarbon (AMS) dating the Classic Aurignacian, Proto- Aurignacian and Vasconian Mousterian at Gatzarria Cave (Pyrénées-Atlantiques, France). PALEO Rev. Archéologie Préhistorique 23, 11–38.

Bartolomei, G., Broglio, A., Cassoli, P.F., Castelletti, L., Cattani, L., Cremaschi, M., Giacobini, G., Malerba, G., Maspero, A., Peresani, M., Sartorelli, A., Tagliacozzo, A., 1992. La Grotte de Fumane. Un site aurignacien au pied des Alpes. Preistoria Alp. 131–179.

Bar-Yosef, O., Arnold, M., Mercier, N., Belfer-Cohen, A., Goldberg, P., Housley, R., Laville, H., Meignen, L., Vogel, J.C., Vandermeersch, B., 1996. The Dating of the Upper Paleolithic Layers in Kebara Cave, Mt Carmel. J. Archaeol. Sci. 23, 297–306. https://doi.org/10.1006/jasc.1996.0028

Bar-Yosef, O., Belfer-Cohen, A., 2004. The Qafzeh Upper Paleolithic assemblages: 70 years later. Eurasian Prehistory 2, 145–180.

Bar-Yosef, O., Belfer-Cohen, A., 1977. The Lagaman Industry, in: Bar-Yosef, O., Phillips, J.L. (Eds.), Prehistoric Investigations in Gebel Maghara, Northern Sinai. pp. 42–85.

Bar-Yosef, O., Belfer-Cohen, A., Adler, D.S., 2006. The implications of the Middle-Upper Paleolithic chronological boundary in the Caucasus to Eurasian prehistory. Anthropologie 44, 49–60.

Bar-Yosef, O., Belfer-Cohen, A., Mesheviliani, T., Jakeli, N., Bar-Oz, G., Boaretto, E., Goldberg, P., Kvavadze, E., Matskevich, Z., 2011. Dzudzuana: an Upper Palaeolithic cave site in the Caucasus foothills (Georgia). Antiquity 85, 331–349. https://doi.org/10.1017/S0003598X0006779X

Bar-Yosef, O., Kuhn, S.L., 1999. The Big Deal about Blades: Laminar Technologies and Human Evolution. Am. Anthropol. 101, 322–338. https://doi.org/10.1525/aa.1999.101.2.322

Bar-Yosef, O., Van Peer, P., 2009. The Chaîne Opératoire Approach in Middle Paleolithic Archaeology. Curr. Anthropol. 50, 103–131. https://doi.org/10.1086/592234

Barzilai, O., Hershkovitz, I., Marder, O., 2016. The Early Upper Paleolithic Period at Manot Cave, Western Galilee, Israel. Hum. Evol. 85–100. https://doi.org/10.14673/HE2016121016

Bataille, G., 2016. Extracting the "Proto" from the Aurignacian. Distinct Production Sequences of Blades and Bladelets in the Lower Aurignacian Phase of Siuren I, Units H and G (Crimea). Mitteilungen Ges. Für Urgesch. 25, 49–85.

Bataille, G., 2012. Flakes and Blades. The role of flake production in the Aurignacian of Siuren 1 (Crimea, Ukraine), in: Pastoors, A., Peresani, M. (Eds.), Flakes Not Blades: The Role of Flake Production at the Onset of the Upper Palaeolithic in Europe, Wissenschaftliche Schriften Des Neanderthal Museums. Neanderthal Museum, Mettmann, pp. 261–293.

Bataille, G., Conard, N.J., 2018a. Blade and bladelet production at Hohle Fels Cave, AH IV in the Swabian Jura and its importance for characterizing the technological variability of the Aurignacian in Central Europe. PLOS ONE 13, e0194097. https://doi.org/10.1371/journal.pone.0194097

Bataille, G., Conard, N.J., 2018b. Burin-core technology in Aurignacian horizons IIIa and IV of Hohle Fels Cave (Southwestern Germany). Quartär 65, 7–49.

Bataille, G., Falcucci, A., Tafelmaier, Y., Conard, N.J., 2019. Technological differences between Kostenki 17/II (Spitsynskaya industry, Central Russia) and the Protoaurignacian: Reply to Dinnis et al. (2019). J. Hum. Evol. 102685. https://doi.org/10.1016/j.jhevol.2019.102685

Bataille, G., Tafelmaier, Y., Weniger, G.-C., 2018. Living on the edge – A comparative approach for studying the beginning of the Aurignacian. Quat. Int. 474, 3–29. https://doi.org/10.1016/j.quaint.2018.03.024

Bazile, F., 2005. La composante lamellaire dans l'Aurignacien Initial de la France Méditerranéene, in: Le Brun-Ricalens, F. (Ed.), Actes du XIVème congrès UISPP, Université de Liège, Belgique, 2 - 8 septembre 2001: session 6, Paléolithique supérieur ; section 6 - Upper Palaeolithic. Productions lamellaires attribuées à l'Aurignacien : Chaînes opératoires et perspectives technoculturelles, Archéologiques / Musée National d'histoire et d'art Luxembourg. Musée National d'Histoire et d'Art, Luxèmbourg, pp. 325–336.

Bazile, F., 2002. Le premier Aurignacien en France méditerranéenne : un bilan. Espac. Tiempo Forma Ser. Prehist. Arqueol. 1, 215–236. https://doi.org/10.5944/etfi.15.2002.4745

Bazile, F., Sicard, S., 1997. Le premier Aurignacien du Languedoc oriental dans son contexte méditerranéen, in: Sacchi, D. (Ed.), Congrès Préhistorique de France. XXIVe Session Carcassonne, 26-30 Septembre 1994. Colloque 1: Les Faciès Leptolithiques Du Bassin Méditerranéen Nord Occidental, Milieu Naturel et Culturel. pp. 117–125.

Belfer-Cohen, A., Goring-Morris, A.N., 2017. The Upper Palaeolithic in Cisjordan, in: Enzel, Y., Bar-Yosef, O. (Eds.), Quaternary of the Levant. Cambridge University Press, pp. 627–638. https://doi.org/10.1017/9781316106754.070

Belfer-Cohen, A., Goring-Morris, N., 2014. The Upper Palaeolithic and Earlier Epi-Palaeolithic of Western Asia, in: Renfrew, C., Bahn, P. (Eds.), The Cambridge World Prehistory 3 Volume Set. Cambridge University Press, Cambridge, pp. 1381–1407. https://doi.org/10.1017/CHO9781139017831.088

Belfer-Cohen, A., Goring-Morris, N., 2012. VI - The Earlier Upper Palaeolithic: A View from the Southern Levant, in: Otte, M., Shidrang, S., Flas, D. (Eds.), L'Aurignacien de La Grotte Yafteh et Son Contexte (Fouilles 2005-2008) /The Aurignacian of Yafteh Cave and Its Context (2005-2008 Excavations). Liège, pp. 127–136.

Belfer-Cohen, A., Goring-Morris, N., 2009. The Shift from the Middle Palaeolithic to the Upper Palaeolithic: Levantine Perspectives, in: Camps, M., Szmidt, C.C. (Eds.), The Mediterranean from 50 000 to 25 000 BP:Turning Points and New Directions. Oxbow Books, Oxford, pp. 89–100.

Belfer-Cohen, A., Goring-Morris, N., 2008. Why Microliths? Microlithization in the Levant. Archeol. Pap. Am. Anthropol. Assoc. 12, 57–68. https://doi.org/10.1525/ap3a.2002.12.1.57

Bello, S.M., Delbarre, G., De Groote, I., Parfitt, S.A., 2016. A newly discovered antler flint-knapping hammer and the question of their rarity in the Palaeolithic archaeological record: Reality or bias? Quat. Int. 403, 107–117. https://doi.org/10.1016/j.quaint.2015.11.094

Benazzi, S., Douka, K., Fornai, C., Bauer, C.C., Kullmer, O., Svoboda, J., Pap, I., Mallegni, F., Bayle, P., Coquerelle, M., Condemi, S., Ronchitelli, A., Harvati, K., Weber, G.W., 2011. Early dispersal of modern humans in Europe and implications for Neanderthal behaviour. Nature 479, 525–528. https://doi.org/10.1038/nature10617

Benazzi, S., Slon, V., Talamo, S., Negrino, F., Peresani, M., Bailey, S.E., Sawyer, S., Panetta, D., Vicino, G., Starnini, E., Mannino, M.A., Salvadori, P.A., Meyer, M., Paabo, S., Hublin, J.-J., 2015. The makers of the Protoaurignacian and implications for Neandertal extinction. Science 348, 793–796. https://doi.org/10.1126/science.aaa2773

Bergman, C., 1988. Ksar Akil and the Upper Paleolithic of the Levant. Paléorient 14, 201–210.

Bergman, C., Williams, J., Douka, K., Schyle, D., 2017. The Palaeolithic Sequence of Ksar 'Akil, Lebanon, in: Enzel, Y., Bar-Yosef, O. (Eds.), Quaternary of the Levant. Cambridge University Press, pp. 267–276. https://doi.org/10.1017/9781316106754.030

Bergman, C.A., Stringer, C.B., 1989. Fifty years after: Egbert, an early Upper Palaeolithic juvenile from Ksar Akil, Lebanon. Paléorient 15, 99–111. https://doi.org/10.3406/paleo.1989.4512

Bertola, S., Broglio, A., Cristiani, E., De Stefani, M., Gurioli, F., Negrino, F., Romandini, M., Vanhaeren, M., 2013. La diffusione del primo Aurignaziano a sud dell'arco alpino. Preistoria Alp. 47, 123–152.

Bertrams, M., Protze, J., Löhrer, R., Schyle, D., Richter, J., Hilgers, A., Klasen, N., Schmidt, C., Lehmkuhl, F., 2012. Multiple environmental change at the time of the Modern Human passage through the Middle East: First results from geoarcheological investigations on Upper Pleistocene sediments in the Wadi Sabra (Jordan). Quat. Int. 274, 55–72. https://doi.org/10.1016/j.quaint.2012.02.047

Bleed, P., 2001. Trees or Chains, Links or Branches: Conceptual Alternatives for Consideration of Stone Tool Production and Other Sequential Activities. J. Archaeol. Method Theory 8, 101–127.

Bodu, P., Bon, F., Teyssandier, N., Paris, C., 2013. L'Aurignacien et les faciès à pièces carénées entre Yonne et Yvelines, in: Bodu, P., Chehmana, L., Klaric, L., Soriano, S., Teyssandier, N. (Eds.), Le Paléolithique Supérieur Ancien de l'Europe Du Nord-Ouest Réflexions et Synthèses à Partir d'un Projet Collectif de Recherche Sur Le Centre et Le Sud Du Bassin Parisien – Actes Du Colloque de Sens (15-18 Avril 2009), Mémoire de La Société Préhistorique Français. Paris, pp. 37–61.

Boëda, É., 1994. Le concept Levallois: variabilité des méthodes, Monographie du CRA. CNRS Éd, Paris.

Boëda, E., 1993. Le débitage discoïde et le débitage Levallois récurrent centripède. Bull. Société Préhistorique Fr. 90, 392–404. https://doi.org/10.3406/bspf.1993.9669

Boëda, E., Geneste, J.-M., Meignen, L., 1990. Identification de chaînes opératoires lithiques du Paléolithique ancien et moyen. Paléo 2, 43–80. https://doi.org/10.3406/pal.1990.988

Bon, F., 2006. A brief overview of Aurignacian cultures in the context of the industries of the transition from the Middle to the Upper Paleolithic, in: Bar-Yosef, O., Zilhão, J. (Eds.), Towards a Definition of the Aurignacian: Proceedings of the Symposium Held in Lisbon, Portugal, June 25-30, 2002, Trabalhos de Arqueologia. Instituto Português de Arqueologia ; American School of Prehistoric Research, Peabody Museum, Harvard University, Lisboa : [Cambridge, Mass.], pp. 133–144.

Bon, F., 2005. Little big tool. Enquete autour du succès de la lamelle, in: Le Brun-Ricalens, F. (Ed.), Actes du XIVème congrès UISPP, Université de Liège, Belgique, 2 - 8 septembre 2001: session 6, Paléolithique supérieur ; section 6 - Upper Palaeolithic. Productions lamellaires attribuées à l'Aurignacien : Chaînes opératoires et perspectives technoculturelles, Archéologiques / Musée National d'histoire et d'art Luxembourg. Musée National d'Histoire et d'Art, Luxèmbourg, pp. 479–484.

Bon, F., 2002a. L'Aurignacien entre mer et océan: réflexion sur l'unité des phases anciennes de l'Aurignacien dans le sud le la France, Mémoire / Société Préhistorique Française. Soc. Préhistorique Française, Paris.

Bon, F., 2002b. Les termes de l´Aurignacien. Espac. Tiempo Forma Ser. Prehist. Arqueol. 1. https://doi.org/10.5944/etfi.15.2002.4737

Bon, F., Bodu, P., 2002. Analyse technologique du débitage aurignacien, in: Schmider, B. (Ed.), L'Aurignacien de La Grotte Du Renne. Les Fouilles d'André Leroi-Gourhan à Arcy-Sur-Cure (Yonne). CNRS, pp. 115–133.

Bordes, J.-G., 2006. News from the West: a reevaluation of the classical Aurignacian sequence of the Périgord, in: Bar-Yosef, O., Zilhão, J. (Eds.), Towards a Definition of the Aurignacian: Proceedings of the Symposium Held in Lisbon, Portugal, June 25-30, 2002, Trabalhos de Arqueologia. Instituto Português de Arqueologia ; American School of Prehistoric Research, Peabody Museum, Harvard University, Lisboa : [Cambridge, Mass.], pp. 147–171.

Bordes, J.-G., 2005. La séquence aurignacienne du nord de l'Aquitaine: variabilité des productions lamellaires à Caminade-Est, Roc-de-Combe, Le Piage et Corbiac-Vignoble II, in: Le Brun-Ricalens, F. (Ed.), Actes du XIVème congrès UISPP, Université de Liège, Belgique, 2 - 8 septembre 2001: session 6, Paléolithique supérieur ; section 6 - Upper Palaeolithic. Productions lamellaires attribuées à l'Aurignacien : Chaînes opératoires et perspectives technoculturelles, Archéologiques / Musée National d'histoire et d'art Luxembourg. Musée National d'Histoire et d'Art, Luxembourg, pp. 123–154.

Bordes, J.-G., 2000. La séquence aurignacienne de Caminade revisitée : l'apport des raccords d'intérêt stratigraphique. The Aurignacian sequence at Caminade Est revisited : contribution of the refittings to stratigraphie study. Paléo 12, 387–407. https://doi.org/10.3406/pal.2000.1611

Bordes, J.-G., Lenoble, A., 2002. La "lamelle Caminade" : un nouvel outil lithique aurignacien ? Bull. Société Préhistorique Fr. 99, 735–749. https://doi.org/10.3406/bspf.2002.12753

Bordes, J.-G., Tixier, J., 2002. Sur l'unité de l'Aurignacien ancien dans le Sud-Ouest de la France : la production des lames et des lamelles. Espac. Tiempo Forma Ser. Prehist. Arqueol. 1. https://doi.org/10.5944/etfi.15.2002.4743

Bosch, M.D., Mannino, M.A., Prendergast, A.L., O'Connell, T.C., Demarchi, B., Taylor, S.M., Niven, L., van der Plicht, J., Hublin, J.-J., 2015. New chronology for Ksâr 'Akil (Lebanon) supports Levantine route of modern human dispersal into Europe. Proc. Natl. Acad. Sci. 112, 7683–7688. https://doi.org/10.1073/pnas.1501529112

Bourguignon, L., 2001. Apports de l'expérimentation et de l'analyse techno-morpho-fonctionnelle à la reconnaissance du processus d'aménagement de la retouche Quina, in: Ortega, I., Frère-Sautot, M.-C. (Eds.), Préhistoire et Approche Expérimentale, Prehistoires. Monique Mergoil, Montagnac, pp. 35–66.

Bowler, J.M., Johnston, H., Olley, J.M., Prescott, J.R., Roberts, R.G., Shawcross, W., Spooner, N.A., 2003. New ages for human occupation and climatic change at Lake Mungo, Australia. Nature 421, 837–840. https://doi.org/10.1038/nature01383

Bradley, R.S., 2015a. Dating Methods I, in: Paleoclimatology. Elsevier, pp. 55–101. https://doi.org/10.1016/B978-0-12-386913-5.00003-X

Bradley, R.S., 2015b. Dating Methods II, in: Paleoclimatology. Elsevier, pp. 103–136. https://doi.org/10.1016/B978-0-12-386913-5.00004-1

Breuil, H., 1913. Les subdivisions du paléolithique supérieur et leur signification., in: Congrès International d'anthropologie et d'archéologie Préhistoriques - Compte-Rendu de La XIVème Session, Genève, 1912. Imprimerie Albert Kündig, pp. 165–238.

Broglio, A., Bertola, S., De Stefani, M., Marini, D., Lemorini, C., Rossetti, P., 2005. La production lamellaire et les armatures lamellaires de l'Aurignacien Ancien de la grotte de Fumane (Monts Lessini, Vénétie), in: Le Brun-Ricalens, F. (Ed.), Actes du XIVème congrès UISPP, Université de Liège, Belgique, 2 - 8 septembre 2001: session 6, Paléolithique supérieur ; section 6 - Upper Palaeolithic. Productions lamellaires attribuées à l'Aurignacien : Chaînes opératoires et perspectives technoculturelles, Archéologiques / Musée National d'histoire et d'art Luxembourg. Musée National d'Histoire et d'Art, Luxembourg, pp. 415–436.

Broglio, A., Laplace, G., 1966. Etudes de typologie analytique des complexes leptolithiques de l'Europe centrale. I. Les complexes aurignacoïdes de la Basse Autriche. Riv. Sci. Preistoriche XXI, 61–121.

Bronk Ramsey, C., 2009a. Bayesian Analysis of Radiocarbon Dates. Radiocarbon 51, 337–360. https://doi.org/10.1017/S0033822200033865

Bronk Ramsey, C., 2009b. Dealing with Outliers and Offsets in Radiocarbon Dating. Radiocarbon 51, 1023–1045. https://doi.org/10.1017/S0033822200034093

Bronk Ramsey, C., Higham, T., Bowles, A., Hedges, R., 2004a. Improvements to the Pretreatment of Bone at Oxford. Radiocarbon 46, 155–163. https://doi.org/10.1017/S0033822200039473

Bronk Ramsey, C., Higham, T., Leach, P., 2004b. Towards High-Precision AMS: Progress and Limitations. Radiocarbon 46, 17–24. https://doi.org/10.1017/S0033822200039308

Cabrera Valdés, V., Bernaldo de Quirós, F., Maillo Fernandez, J.M., Valladas, H., Martinez de La Riva Llorret, M., 2002. El Auriñaciense arcaico de El Castillo (Cantabria). Espac. Tiempo Forma, Prehistoria y Arqueologìa 15, 67–86.

Chiotti, L., 2012. Some evidence for flake production in the Early Aurignacian: examples from the Pataud and Castanet rock shelters (France), in: Pastoors, A., Peresani, M. (Eds.), Flakes Not Blades: The Role of Flake Production at the Onset of the Upper Palaeolithic in Europe, Wissenschaftliche Schriften Des Neanderthal Museums. Neanderthal Museum, Mettmann, pp. 105–117.

Chiotti, L., Cretin, C., 2011. Les mises en forme de grattoirs carénés \/ nucléus de l'aurignacien ancien de l'abri Castanet \(Sergeac, Dordogne\). PALEO Rev. Archéologie Préhistorique 22, 69–84.

Chiotti, L., Cretin, C., Morala, A., 2015. The Lithic Industries from Blanchard and Castanet Rock Shelters (Dordogne, France): Data from the 2005-2012 Excavations. Palethnologie 76–97. https://doi.org/10.4000/palethnologie.751

Chu, W., 2018. The Danube Corridor Hypothesis and the Carpathian Basin: Geological, Environmental and Archaeological Approaches to Characterizing Aurignacian Dynamics. J. World Prehistory 31, 117–178. https://doi.org/10.1007/s10963-018-9115-1

Chu, W., Lengyel, G., Zeeden, C., Péntek, A., Kaminská, Ľ., Mester, Z., 2018. Early Upper Paleolithic surface collections from loess-like sediments in the northern Carpathian Basin. Quat. Int. 485, 167–182. https://doi.org/10.1016/j.quaint.2017.05.017

Chu, W., Pötter, S., Doboș, A., Albert, T., Klasen, N., Ciornei, A., Bösken, J.J., Schulte, P., 2019. Geoarchaeology and geochronology of the Upper Palaeolithic site of Temerești Dealu Vinii, Banat, Romania: Site formation processes and human activity of an open-air locality. Quartär 111–134. https://doi.org/10.7485/QU66_5

Chu, W., Richter, J., 2020. Aurignacian Cultural Unit, in: Encyclopedia of Global Archaeology. Springer International Publishing, Cham, pp. 1–10. https://doi.org/10.1007/978-3-319-51726-1_3441-1

Conard, N.J., Bolus, M., 2003. Radiocarbon dating the appearance of modern humans and timing of cultural innovations in Europe: new results and new challenges. J. Hum. Evol. 44, 331–371. https://doi.org/10.1016/S0047-2484(02)00202-6

Conard, N.J., Soressi, M., Parkington, J.E., Wurz, S., Yates, R., 2004. A Unified Lithic Taxonomy Based on Patterns of Core Reduction. South Afr. Archaeol. Bull. 59, 13–17. https://doi.org/10.2307/3889318

Cortés-Sánchez, M., Jiménez-Espejo, F.J., Simón-Vallejo, M.D., Stringer, C., Lozano Francisco, M.C., García-Alix, A., Vera Peláez, J.L., Odriozola, C.P., Riquelme-Cantal, J.A., Parrilla Giráldez, R., Maestro González, A., Ohkouchi, N., Morales-Muñiz, A., 2019a. An early Aurignacian arrival in southwestern Europe. Nat. Ecol. Evol. 3, 207–212. https://doi.org/10.1038/s41559-018-0753-6

Cortés-Sánchez, M., Jiménez-Espejo, F.J., Simón-Vallejo, M.D., Stringer, C., Lozano Francisco, M.C., García-Alix, A., Vera Peláez, J.L., Odriozola, C.P., Riquelme-Cantal, J.A., Parrilla-Giráldez, R., Maestro González, A., Ohkouchi, N., Morales-Muñiz, A., 2019b. Reply to 'Dating on its own cannot resolve hominin occupation patterns' and 'No reliable evidence for a very early Aurignacian in Southern Iberia.' Nat. Ecol. Evol. 3, 714–715. https://doi.org/10.1038/s41559-019-0887-1

Coupaye, L., 2015. Chaîne opératoire, transects et théories : quelques réflexions et suggestions sur le parcours d'une méthode classique, in: Soulier, P. (Ed.), André Leroi-Gourhan, L'homme Tout Simplement: Mémoires Et Postérité D'André Leroi-Gourhan, Travaux de la MAE. Editions De Boccard, Paris, pp. 69–84.

Crabtree, D.E., 1966. A stoneworker's approach to analyzing and replicating the Lindenmeier Folsom. Tebiwa 9: 3-3. Tebiwa 9, 3–39.

Cresswell, R., 2010. Techniques et culture : les bases d'un programme de travail. Tech. Cult. 20–45. https://doi.org/10.4000/tc.4979

D'Angelo, E., Mussi, M., 2005. Galets et lamelles de l'Aurignacien du Latium (Italie Centrale): le cas de grotta Barbara, in: Le Brun-Ricalens, F. (Ed.), Actes du XIVème congrès UISPP, Université de Liège, Belgique, 2 - 8 septembre 2001: session 6, Paléolithique supérieur ; section 6 - Upper Palaeolithic. Productions lamellaires attribuées à l'Aurignacien : Chaînes opératoires et perspectives technoculturelles, Archéologiques. Musée National d'Histoire et d'Art, Luxembourg, pp. 313–322.

Davidzon, A., Goring-Morris, N., 2003. Sealed in Stone: The Upper Palaeolithic Early Ahmarian Knapping Method in the Light of Refitting Studies at Nahal Nizzana XIII, Western Negev, Israel. J. Isr. Prehist. Soc. 33, 75–205.

de la Peña, P., 2019. Dating on its own cannot resolve hominin occupation patterns. Nat. Ecol. Evol. 3, 712–712. https://doi.org/10.1038/s41559-019-0886-2

De Stefani, M., Dini, M., Klempererova, H., Peresani, M., Ranaldo, F., Ronchitelli, A., Ziggiotti, S., 2012. Continuity and replacement in flake production across the Middle-Upper Palaeolithic Transition: a view over the Italian peninsula., in: Pastoors, A., Peresani, M. (Eds.), Flakes Not Blades: The Role of Flake Production at the Onset of the Upper Palaeolithic in Europe,

Wissenschaftliche Schriften Des Neanderthal Museums. Neanderthal Museum, Mettmann, pp. 135–151.
Degano, I., Soriano, S., Villa, P., Pollarolo, L., Lucejko, J.J., Jacobs, Z., Douka, K., Vitagliano, S., Tozzi, C., 2019a. Hafting of Middle Paleolithic tools in Latium (central Italy): New data from Fossellone and Sant'Agostino caves. PLOS ONE 14, e0213473. https://doi.org/10.1371/journal.pone.0213473
Degano, I., Soriano, S., Villa, P., Pollarolo, L., Lucejko, J.J., Jacobs, Z., Douka, K., Vitagliano, S., Tozzi, C., 2019b. S1 File. Sites and assemblages: text and figures: Hafting of Middle Paleolithic tools from Latium (central Italy): New data from Fossellone and Sant'Agostino caves. PLoS ONE 14, e0213473.
Delpiano, D., Peresani, M., 2017. Exploring Neanderthal skills and lithic economy. The implication of a refitted Discoid reduction sequence reconstructed using 3D virtual analysis. Comptes Rendus Palevol 16, 865–877. https://doi.org/10.1016/j.crpv.2017.06.008
Delporte, H., 1991. La séquence aurignacienne et périgordienne sur la base des travaux récents réalisés en Périgord. Bull. Société Préhistorique Fr. 88, 243–256.
Demars, P.-Y., Laurent, P., 1992. Types d'outils lithiques du paleolithique superieur en Europe, Cahiers du quaternaire. Presses du CNRS, Paris.
Demeter, F., Shackelford, L.L., Bacon, A.-M., Duringer, P., Westaway, K., Sayavongkhamdy, T., Braga, J., Sichanthongtip, P., Khamdalavong, P., Ponche, J.-L., Wang, H., Lundstrom, C., Patole-Edoumba, E., Karpoff, A.-M., 2012. Anatomically modern human in Southeast Asia (Laos) by 46 ka. Proc. Natl. Acad. Sci. 109, 14375–14380. https://doi.org/10.1073/pnas.1208104109
Demidenko, E.Y., 2000. The European Early Aurignacian of Krems-Dufour type industries: a view from Eastern Europe. Préhistoire Eur. 16–17, 147–162.
Demidenko, E.Y., Hauck, T.C., 2017. Yabrud II rock-shelter archaeological sequence (Syria) and possible Proto- Aurignacian origin in the Levant, in: Otto, M., Le Tensorer, J.-M. (Eds.), Vocabulaire préhistoire. Hommage à Jean-Marie Le Tensorer. ERAUL, pp. 87–98.
Demidenko, E.Y., Noiret, P., 2012. The Siuren I Aurignacian of Krems-Dufour Type Industries in the Context of the European Aurignacian, in: Demidenko, E.Y., Otte, M., Noiret, P. (Eds.), From Late Middle Paleolithic and Early Upper Paleolithic to Epi-Paleolithic in Crimea. The Paleolithic of Crimea. ERAUL, Liège, pp. 343–357.
Demidenko, Y.E., 2014. Siuren I Rockshelter: From the Late Middle Paleolithic and Early Upper Paleolithic to the Epipaleolithic in Crimea, in: Smith, C. (Ed.), Encyclopedia of Global Archaeology. Springer New York, New York, NY, pp. 6711–6721. https://doi.org/10.1007/978-1-4419-0465-2_1867
Dibble, H.L., 1997. Platform Variability and Flake Morphology: A Comparison of Experimental and Archaeological Data and Implications for Interpreting Prehistoric Lithic Technological Strategies. Lithic Technol. 22, 150–170. https://doi.org/10.1080/01977261.1997.11754540
Dibble, H.L., 1995. Biache Saint-Vaast , Level IIA: A comparison of analytical approaches, in: Dibble, H.L., Bar-Yosef, O. (Eds.), The Definition and Interpretation of Levallois Technology, Monographs in World Archaeology. Madison, Winsconsin, pp. 93–116.
Dini, M., Baills, H., Conforti, J., Tozzi, C., 2012. Le Protoaurignacien de la Grotte La Fabbrica (Grosseto, Italie) dans le contexte de l'arc nord méditerranéen. L'Anthropologie 116, 550–574. https://doi.org/10.1016/j.anthro.2012.10.003
Dini, M., Tozzi, C., 2012. La Transizione Paleolitico Medio- Paleolitico Superiore nella grotta La Fabbrica (Grosseto - Toscana). Atti Della Soc. Toscana Sci. Nat. Resid. Pisa Mem. Ser. A 117–119, 17–25. https://doi.org/10.2424/ASTSN.M.2012.24
Dinnis, R., Bessudnov, A., Reynolds, N., Devièse, T., Pate, A., Sablin, M., Sinitsyn, A., Higham, T., 2019. New data for the Early Upper Paleolithic of Kostenki (Russia). J. Hum. Evol. 127, 21–40. https://doi.org/10.1016/j.jhevol.2018.11.012
Djindjian, F., 2007. Henri Delporte au Musée des antiquités nationales : les recherches sur l'Aurignacien du Périgord, in: Desbrosse, R., Thévenin, A. (Eds.), Arts et cultures de la préhistoire. Hommages à Henri Delporte, Documents préhistoriques. Éd. du CTHS, Paris, pp. 139–157.

Douka, K., 2013. Exploring “the great wilderness of prehistory”: The Chronology of the Middle to the Upper Paleolithic Transition in the Northern Levant. Mitteilungen Ges. Für Urgesch. 22, 11–40.

Douka, K., Bergman, C.A., Hedges, R.E.M., Wesselingh, F.P., Higham, T.F.G., 2013. Chronology of Ksar Akil (Lebanon) and Implications for the Colonization of Europe by Anatomically Modern Humans. PLoS ONE 8, e72931. https://doi.org/10.1371/journal.pone.0072931

Douka, K., Grimaldi, S., Boschian, G., del Lucchese, A., Higham, T.F.G., 2012. A new chronostratigraphic framework for the Upper Palaeolithic of Riparo Mochi (Italy). J. Hum. Evol. 62, 286–299. https://doi.org/10.1016/j.jhevol.2011.11.009

Douka, K., Hedges, R.E.M., Higham, T.F.G., 2010. Improved AMS ^{14}C Dating of Shell Carbonates Using High-Precision X-Ray Diffraction and a Novel Density Separation Protocol (Cards). Radiocarbon 52, 735–751. https://doi.org/10.1017/S0033822200045756

Douka, K., Higham, T., 2017. The Chronological Factor in Understanding the Middle and Upper Paleolithic of Eurasia. Curr. Anthropol. 58, S480–S490. https://doi.org/10.1086/694173

Doyon, P.L., 2017. La variabilité technologique et morphométrique des pointes de projectile aurignaciennes en matière osseuse (Doctoral thesis). Préhistoire - Université de Bordeaux et Anthropologie (archéologie préhistorique) - Université de Montréal, Bordeaux-Montreal.

Driscoll, K., García-Rojas, M., 2014. Their lips are sealed: identifying hard stone, soft stone, and antler hammer direct percussion in Palaeolithic prismatic blade production. J. Archaeol. Sci. 47, 134–141. https://doi.org/10.1016/j.jas.2014.04.008

Falcucci, A., 2018. Towards a Renewed Definition of the Protoaurignacian. Mitteilungen Ges. Für Urgesch. 27, 87–130.

Falcucci, A., Conard, N.J., Peresani, M., 2017. A critical assessment of the Protoaurignacian lithic technology at Fumane Cave and its implications for the definition of the earliest Aurignacian. PLOS ONE 12, e0189241. https://doi.org/10.1371/journal.pone.0189241

Falcucci, A., Peresani, M., 2018. Protoaurignacian Core Reduction Procedures: Blade and Bladelet Technologies at Fumane Cave. Lithic Technol. 43, 125–140. https://doi.org/10.1080/01977261.2018.1439681

Falcucci, A., Peresani, M., Roussel, M., Normand, C., Soressi, M., 2018. What’s the point? Retouched bladelet variability in the Protoaurignacian. Results from Fumane, Isturitz, and Les Cottés. Archaeol. Anthropol. Sci. 10, 539–554. https://doi.org/10.1007/s12520-016-0365-5

Fedele, F.G., Giaccio, B., Isaia, R., Orsi, G., 2003. The Campanian Ignimbrite Eruption, Heinrich Event 4, and palaeolithic change in Europe: A high-resolution investigation, in: Robock, A., Oppenheimer, C. (Eds.), Geophysical Monograph Series. American Geophysical Union, Washington, D. C., pp. 301–325. https://doi.org/10.1029/139GM20

Fletcher, W.J., Sánchez Goñi, M.F., Allen, J.R.M., Cheddadi, R., Combourieu-Nebout, N., Huntley, B., Lawson, I., Londeix, L., Magri, D., Margari, V., Müller, U.C., Naughton, F., Novenko, E., Roucoux, K., Tzedakis, P.C., 2010. Millennial-scale variability during the last glacial in vegetation records from Europe. Quat. Sci. Rev. 29, 2839–2864. https://doi.org/10.1016/j.quascirev.2009.11.015

Floss, H., Froehle, S., Wettengl, S., 2016. The Aurignacian along the Danube Its Two-Fold Role as a Transalpine and Cisalpine Passageway of Early Homo Sapiens into Europe, in: Krauss, R., Floss, H. (Eds.), Southeast Europe Before Neolithisation. Proceedings of the International Workshop within the Collaborative Research Centres SFB 1070 “RESSOURCENKULTUREN”, Schloß Hohentübingen, 9th of May 2014, RessourcenKulturen. Universität Tübingen, Tuebingen, pp. 13–39. https://doi.org/10.15496/PUBLIKATION-10762

Fox, J.R., 2003. 8. The Tor Sadaf Lithic Assemblages: A Technological Study of the Early Upper Palaeolithic in the Wadi al-Hasa, in: Goring-Morris, A.N., Belfer-Cohen, A. (Eds.), More than Meets the Eye: Studies on Upper Palaeolithic Diversity in the Near East. Oxbow ; David Brown Book Co, Oxford : Oakville, CT, pp. 80–94.

Fu, Q., Hajdinjak, M., Moldovan, O.T., Constantin, S., Mallick, S., Skoglund, P., Patterson, N., Rohland, N., Lazaridis, I., Nickel, B., Viola, B., Prüfer, K., Meyer, M., Kelso, J., Reich, D.,

Pääbo, S., 2015. An early modern human from Romania with a recent Neanderthal ancestor. Nature 524, 216–219. https://doi.org/10.1038/nature14558
Fu, Q., Li, H., Moorjani, P., Jay, F., Slepchenko, S.M., Bondarev, A.A., Johnson, P.L.F., Aximu-Petri, A., Prüfer, K., de Filippo, C., Meyer, M., Zwyns, N., Salazar-García, D.C., Kuzmin, Y.V., Keates, S.G., Kosintsev, P.A., Razhev, D.I., Richards, M.P., Peristov, N.V., Lachmann, M., Douka, K., Higham, T.F.G., Slatkin, M., Hublin, J.-J., Reich, D., Kelso, J., Viola, T.B., Pääbo, S., 2014. Genome sequence of a 45,000-year-old modern human from western Siberia. Nature 514, 445–449. https://doi.org/10.1038/nature13810
Gambassini, P., 1997. Le industrie paleolitiche di Castelcivita, in: Gambassini, P., Napoleone, G. (Eds.), Il Paleolitico di Castelcivita : culture e ambiente, Materiae. Electa Napoli, Napoli, pp. 92–145.
Garrod, D., 1957. Notes sur le Paléolithique Supérieur du Moyen Orient. Bull. Société Préhistorique Fr. 54, 439–446. https://doi.org/10.3406/bspf.1957.7854
Geneste, J.-M., 2010. Systèmes techniques de production lithique: Variations techno-économiques dans les processus de réalisation des outillages paléolithiques. Tech. Cult. 419–449. https://doi.org/10.4000/tc.5013
Giaccio, B., Hajdas, I., Isaia, R., Deino, A., Nomade, S., 2017. High-precision 14C and 40Ar/39Ar dating of the Campanian Ignimbrite (Y-5) reconciles the time-scales of climatic-cultural processes at 40 ka. Sci. Rep. 7, 45940. https://doi.org/10.1038/srep45940
Giaccio, B., Isaia, R., Fedele, F.G., Di Canzio, E., Hoffecker, J., Ronchitelli, A., Sinitsyn, A.A., Anikovich, M., Lisitsyn, S.N., Popov, V.V., 2008. The Campanian Ignimbrite and Codola tephra layers: Two temporal/stratigraphic markers for the Early Upper Palaeolithic in southern Italy and eastern Europe. J. Volcanol. Geotherm. Res. 177, 208–226. https://doi.org/10.1016/j.jvolgeores.2007.10.007
Gilead, I., 1991. The Upper Paleolithic period in the Levant. J. World Prehistory 5, 105–154. https://doi.org/10.1007/BF00974677
Gilead, I., 1983. Upper Palaeolithic Occurrences in Sinai and the transition to the Epi-palaeolithic in the Southern Levant. Paléorient 9, 39–53. https://doi.org/10.3406/paleo.1983.4330
Gilead, I., Bar-Yosef, O., 1993. Early Upper Paleolithic Sites in the Qadesh Barnea Area, NE Sinai. J. Field Archaeol. 20, 265–280.
Goldberg, P., Meignen, L., Mallol, C., 2009. Geoarcheology, Site Formation, and Transitions, in: Shea, J.J., Lieberman, D. (Eds.), Transitions in Prehistory: Essays in Honor of Ofer Bar-Yosef, American School of Prehistoric Research Monograph Series. Oxbow Books ; David Brown Book Co.], [Oxford, England] : [Oakville, Conn, pp. 431–443.
Golovanova, L.V., Doronichev, V.B., 2012. The Early Upper Paleolithic of the Caucasus in the West Eurasian Context, in: Otte, M., Shidrang, S., Flas, D. (Eds.), L'Aurignacien de La Grotte Yafteh et Son Contexte (Fouilles 2005-2008) /The Aurignacian of Yafteh Cave and Its Context (2005-2008 Excavations). Universite de Liege, Liege, pp. 137–160.
Goring-Morris, N., Belfer-Cohen, A., 2018. The Ahmarian in the Context of the Earlier Upper Palaeolithic in the Near East, in: Nishiaki, Y., Akazawa, T. (Eds.), The Middle and Upper Paleolithic Archeology of the Levant and Beyond. Springer Singapore, Singapore, pp. 87–104. https://doi.org/10.1007/978-981-10-6826-3_7
Goring-Morris, N., Davidzon, A., 2006. Straight to the point: Upper Paleolithic Ahmarian lithic technology in the Levant. Anthropologie XLIV, 93–111.
Grimaldi, S., Porraz, G., Santaniello, F., 2014. Raw material procurement and land use in the northern Mediterranean Arc: insight from the first Proto-Aurignacian of Riparo Mochi (Balzi Rossi, Italy). Quartär 61, 113–127. https://doi.org/10.7485/QU61_06
Groucutt, H.S., Grün, R., Zalmout, I.A.S., Drake, N.A., Armitage, S.J., Candy, I., Clark-Wilson, R., Louys, J., Breeze, P.S., Duval, M., Buck, L.T., Kivell, T.L., Pomeroy, E., Stephens, N.B., Stock, J.T., Stewart, M., Price, G.J., Kinsley, L., Sung, W.W., Alsharekh, A., Al-Omari, A., Zahir, M., Memesh, A.M., Abdulshakoor, A.J., Al-Masari, A.M., Bahameem, A.A., Al Murayyi, K.M.S., Zahrani, B., Scerri, E.L.M., Petraglia, M.D., 2018. Homo sapiens in Arabia by 85,000 years ago. Nat. Ecol. Evol. 2, 800–809. https://doi.org/10.1038/s41559-018-0518-2

Groucutt, H.S., Petraglia, M.D., Bailey, G., Scerri, E.M.L., Parton, A., Clark-Balzan, L., Jennings, R.P., Lewis, L., Blinkhorn, J., Drake, N.A., Breeze, P.S., Inglis, R.H., Devès, M.H., Meredith-Williams, M., Boivin, N., Thomas, M.G., Scally, A., 2015. Rethinking the dispersal of *Homo sapiens* out of Africa: Rethinking the Dispersal of *Homo sapiens* out of Africa. Evol. Anthropol. Issues News Rev. 24, 149–164. https://doi.org/10.1002/evan.21455

Hauck, T.C., Lehmkuhl, F., Zeeden, C., Bösken, J., Thiemann, A., Richter, J., 2018. The Aurignacian way of life: Contextualizing early modern human adaptation in the Carpathian Basin. Quat. Int. 485, 150–166. https://doi.org/10.1016/j.quaint.2017.10.020

Haws, J.A., Benedetti, M.M., Talamo, S., Bicho, N., Cascalheira, J., Ellis, M.G., Carvalho, M.M., Friedl, L., Pereira, T., Zinsious, B.K., 2020. The early Aurignacian dispersal of modern humans into westernmost Eurasia. Proc. Natl. Acad. Sci. 202016062. https://doi.org/10.1073/pnas.2016062117

Hedges, R., Davies, W., 2008. Dating a type-site: Fitting Szeleta Cave into its regional chronometric context. Praehistoria 9–10, 35–45.

Heinrich, H., 1988. Origin and Consequences of Cyclic Ice Rafting in the Northeast Atlantic Ocean During the Past 130,000 Years. Quat. Res. 29, 142–152. https://doi.org/10.1016/0033-5894(88)90057-9

Hemming, S.R., 2004. Heinrich events: Massive late Pleistocene detritus layers of the North Atlantic and their global climate imprint. Rev. Geophys. 42, RG1005. https://doi.org/10.1029/2003RG000128

Hershkovitz, I., Marder, O., Ayalon, A., Bar-Matthews, M., Yasur, G., Boaretto, E., Caracuta, V., Alex, B., Frumkin, A., Goder-Goldberger, M., Gunz, P., Holloway, R.L., Latimer, B., Lavi, R., Matthews, A., Slon, V., Mayer, D.B.-Y., Berna, F., Bar-Oz, G., Yeshurun, R., May, H., Hans, M.G., Weber, G.W., Barzilai, O., 2015. Levantine cranium from Manot Cave (Israel) foreshadows the first European modern humans. Nature 520, 216–219. https://doi.org/10.1038/nature14134

Hershkovitz, I., Weber, G.W., Quam, R., Duval, M., Grün, R., Kinsley, L., Ayalon, A., Bar-Matthews, M., Valladas, H., Mercier, N., Arsuaga, J.L., Martinón-Torres, M., Bermúdez de Castro, J.M., Fornai, C., Martín-Francés, L., Sarig, R., May, H., Krenn, V.A., Slon, V., Rodríguez, L., García, R., Lorenzo, C., Carretero, J.M., Frumkin, A., Shahack-Gross, R., Bar-Yosef Mayer, D.E., Cui, Y., Wu, X., Peled, N., Groman-Yaroslavski, I., Weissbrod, L., Yeshurun, R., Tsatskin, A., Zaidner, Y., Weinstein-Evron, M., 2018. The earliest modern humans outside Africa. Science 359, 456–459. https://doi.org/10.1126/science.aap8369

Higham, T., Basell, L., Jacobi, R., Wood, R., Ramsey, C.B., Conard, N.J., 2012. Testing models for the beginnings of the Aurignacian and the advent of figurative art and music: The radiocarbon chronology of Geißenklösterle. J. Hum. Evol. 62, 664–676. https://doi.org/10.1016/j.jhevol.2012.03.003

Higham, T., Brock, F., Peresani, M., Broglio, A., Wood, R., Douka, K., 2009. Problems with radiocarbon dating the Middle to Upper Palaeolithic transition in Italy. Quat. Sci. Rev. 28, 1257–1267. https://doi.org/10.1016/j.quascirev.2008.12.018

Higham, T., Compton, T., Stringer, C., Jacobi, R., Shapiro, B., Trinkaus, E., Chandler, B., Gröning, F., Collins, C., Hillson, S., O'Higgins, P., FitzGerald, C., Fagan, M., 2011. The earliest evidence for anatomically modern humans in northwestern Europe. Nature 479, 521–524. https://doi.org/10.1038/nature10484

Higham, T., Jacobi, R., Julien, M., David, F., Basell, L., Wood, R., Davies, W., Ramsey, C.B., 2010. Chronology of the Grotte du Renne (France) and implications for the context of ornaments and human remains within the Chatelperronian. Proc. Natl. Acad. Sci. 107, 20234–20239. https://doi.org/10.1073/pnas.1007963107

Hoffecker, J.F., Holliday, V.T., 2014. Landscape Archaeology and the Dispersal of Modern Humans in Eastern Europe, in: Vasil'ev, S.A., Tkach, E.S. (Eds.), Verkhnii Paleolit Severnoi Evrazii i Ameriki: Pamiatniki, Kul'tury, Traditsii. Peterburgskoe Vostokovedenie, Saint Petersburg, pp. 140–170.

Hoffecker, J.F., Holliday, V.T., Anikovich, M.V., Dudin, A.E., Platonova, N.I., Popov, V.V., Levkovskaya, G.M., Kuz'mina, I.E., Syromyatnikova, E.V., Burova, N.D., Goldberg, P.,

Macphail, R.I., Forman, S.L., Carter, B.J., Crawford, L.J., 2016. Kostenki 1 and the early Upper Paleolithic of Eastern Europe. J. Archaeol. Sci. Rep. 5, 307–326. https://doi.org/10.1016/j.jasrep.2015.11.013

Hoffmann, D.L., Standish, C.D., García-Diez, M., Pettitt, P.B., Milton, J.A., Zilhão, J., Alcolea-González, J.J., Cantalejo-Duarte, P., Collado, H., de Balbín, R., Lorblanchet, M., Ramos-Muñoz, J., Weniger, G.-Ch., Pike, A.W.G., 2018a. U-Th dating of carbonate crusts reveals Neandertal origin of Iberian cave art. Science 359, 912–915. https://doi.org/10.1126/science.aap7778

Hoffmann, D.L., Standish, C.D., García-Diez, M., Pettitt, P.B., Milton, J.A., Zilhão, J., Alcolea-González, J.J., Cantalejo-Duarte, P., Collado, H., de Balbín, R., Lorblanchet, M., Ramos-Muñoz, J., Weniger, G.-Ch., Pike, A.W.G., 2018b. Response to Comment on "U-Th dating of carbonate crusts reveals Neandertal origin of Iberian cave art." Science 362, eaau1736. https://doi.org/10.1126/science.aau1736

Holt, B., Negrino, F., Riel-Salvatore, J., Formicola, V., Arellano, A., Arobba, D., Boschian, G., Churchill, S.E., Cristiani, E., Di Canzio, E., Vicino, G., 2019. The Middle-Upper Paleolithic transition in Northwest Italy: new evidence from Riparo Bombrini (Balzi Rossi, Liguria, Italy). Quat. Int. 508, 142–152. https://doi.org/10.1016/j.quaint.2018.11.032

Hublin, J.-J., 2015. The modern human colonization of western Eurasia: when and where? Quat. Sci. Rev. 118, 194–210. https://doi.org/10.1016/j.quascirev.2014.08.011

Hublin, J.-J., Sirakov, N., Aldeias, V., Bailey, S.E., Bard, E., Delvigne, V., Endarova, E., Fagault, Y., Fewlass, H., Hajdinjak, M., Kromer, B., Krumov, I., Marreiros, J., Martisius, L.N., Paskulin, L., Sinet-Mathiot, V., Meyer, M., Pääbo, S., Popov, V., Rezek, Z., Sirakova, S., Skinner, M.M., Smith, M.G., Spasov, R., Talamo, S., Tuna, T., Wacker, L., Welker, F., Wilcke, A., Zaharlev, N., McPherron, P.S., Tsanova, T., 2020. Initial Upper Palaeolithic Homo sapiens from Bacho Kiro Cave, Bulgaria. Nature 20. https://doi.org/10.1038/s41586-020-2259-

Hussain, S.T., 2015. Betwixt seriality and sortiment: rethinking early Ahmarian blade technology in Al-Ansab 1, in: Schyle, D., Richter, J. (Eds.), Pleistocene Archaeology of the Petra Area in Jordan, Band 5. Leidorf, Rahden/Westf, pp. 131–147.

Inizan, M.-L., Reduron-Ballinger, M., Roche, H., Tixier, J., Féblot-Augustins, J. (Eds.), 1999. Technology and terminology of knapped stone: followed by a multilingual vocabulary - Arabic, English, French, German,Greek, Italian, Portuguese, Spanish, Préhistoire de la pierre taillée. CREP, Nanterre.

Jacobi, R.M., Higham, T.F.G., Ramsey, C.B., 2006. AMS radiocarbon dating of Middle and Upper Palaeolithic bone in the British Isles: improved reliability using ultrafiltration. J. Quat. Sci. 21, 557–573. https://doi.org/10.1002/jqs.1037

Jacobs, Z., Li, B., Jankowski, N., Soressi, M., 2015. Testing of a single grain OSL chronology across the Middle to Upper Palaeolithic transition at Les Cottés (France). J. Archaeol. Sci. 54, 110–122. https://doi.org/10.1016/j.jas.2014.11.020

Kadowaki, S., 2018. Ahmarian or Levantine Aurignacian? Wadi Kharar 16R and New Insights into the Upper Palaeolithic Lithic Technology in the Northeastern Levant, in: Nishiaki, Y., Akazawa, T. (Eds.), The Middle and Upper Paleolithic Archeology of the Levant and Beyond. Springer Singapore, Singapore, pp. 105–116. https://doi.org/10.1007/978-981-10-6826-3_8

Kadowaki, S., Omori, T., Nishiaki, Y., 2015. Variability in Early Ahmarian lithic technology and its implications for the model of a Levantine origin of the Protoaurignacian. J. Hum. Evol. 82, 67–87. https://doi.org/10.1016/j.jhevol.2015.02.017

Karkanas, P. (Takis), Goldberg, P., 2018. Reconstructing Archaeological Sites: Understanding the Geoarchaeological Matrix, 1st ed. Wiley. https://doi.org/10.1002/9781119016427

Kaufman, D., 1986. A Proposed Method for Distinguishing Between Blades and Bladelets. Lithic Technol. 15, 34–40. https://doi.org/10.1080/01977261.1986.11720864

Kels, H., Protze, J., Sitlivy, V., Hilgers, A., Zander, A., Anghelinu, M., Bertrams, M., Lehmkuhl, F., 2014. Genesis of loess-like sediments and soils at the foothills of the Banat Mountains,

Romania – Examples from the Paleolithic sites Românești and Coșava. Quat. Int. 351, 213–230. https://doi.org/10.1016/j.quaint.2014.04.063
Klasen, N., Hilgers, A., Schmidt, C., Bertrams, M., Schyle, D., Lehmkuhl, F., Richter, J., Radtke, U., 2013. Optical dating of sediments in Wadi Sabra (SW Jordan). Quat. Geochronol. 18, 9–16. https://doi.org/10.1016/j.quageo.2013.08.002
Kuhn, S.L., 2004. From Initial Upper Paleolithic to Ahmarian at Üçağızlı cave, Turkey. Anthropologie XLII, 249–262.
Kuhn, S.L., Stiner, M.C., 1998. The Earliest Aurignacian of Riparo Mochi (Liguria, Italy). Curr. Anthropol. 39, S175–S189. https://doi.org/10.1086/204694
Kuhn, S.L., Stiner, M.C., Güleç, E., Özer, I., Yılmaz, H., Baykara, I., Açıkkol, A., Goldberg, P., Molina, K.M., Ünay, E., Suata-Alpaslan, F., 2009. The early Upper Paleolithic occupations at Üçağızlı Cave (Hatay, Turkey). J. Hum. Evol. 56, 87–113. https://doi.org/10.1016/j.jhevol.2008.07.014
Laplace, G., 1966. Recherches sur l'origine et l'évolution des complexes leptolithiques. École Française de Rome, Rome.
Laughlin, J.P., Kelly, R.L., 2010. Experimental analysis of the practical limits of lithic refitting. J. Archaeol. Sci. 37, 427–433. https://doi.org/10.1016/j.jas.2009.10.007
Le Brun-Ricalens, F. (Ed.), 2005a. Actes du XIVème congrès UISPP, Université de Liège, Belgique, 2 - 8 septembre 2001: session 6, Paléolithique supérieur ; section 6 - Upper Palaeolithic, Archéologiques / Musée National d'histoire et d'art Luxembourg. Presented at the Congrès UISPP, Musée National d'Histoire et d'Art, Luxembourg.
Le Brun-Ricalens, F., 2005b. Reconaissance d'un "concept technoculturel" de l'Aurignacien Ancien?, in: Le Brun-Ricalens, F. (Ed.), Actes du XIVème congrès UISPP, Université de Liège, Belgique, 2 - 8 septembre 2001: session 6, Paléolithique supérieur ; section 6 - Upper Palaeolithic. Productions lamellaires attribuées à l'Aurignacien : Chaînes opératoires et perspectives technoculturelles, Archéologiques / Musée National d'histoire et d'art Luxembourg. Musée National d'Histoire et d'Art, Luxembourg, pp. 157–190.
Le Brun-Ricalens, F., 1993. Réflexions préliminaires sur le comportement litho-technologique et l'occupation du territoire du pays des Serres à l'Aurignacien: Le gisement de "Toulousète" à Beauville (Lot et Garonne). Une occupation moustérienne et aurignacienne de plein air. Paléo 5, 127–153. https://doi.org/10.3406/pal.1993.1108
Le Brun-Ricalens, F., Bordes, J.-G., Eizenberg, L., 2009. 2. A crossed-glance between southern European and Middle-Near Eastern early Upper Palaeolithic lithic technocomplexes. Existing models, new perspectives, in: Camps, M., Szmidt, C.C. (Eds.), The Mediterranean from 50 000 to 25 000 BP: Turning Points and New Directions. Oxford, pp. 11–33.
Lengyel, G., Béres, S., Fodor, L., 2006. NEW LITHIC EVIDENCE OF THE AURIGNACIAN IN HUNGARY. Eurasian Prehistory 4, 79–85.
Liu, W., Martinón-Torres, M., Cai, Y., Xing, S., Tong, H., Pei, S., Sier, M.J., Wu, Xiao-hong, Edwards, R.L., Cheng, H., Li, Y., Yang, X., de Castro, J.M.B., Wu, Xiu-jie, 2015. The earliest unequivocally modern humans in southern China. Nature 526, 696–699. https://doi.org/10.1038/nature15696
López-García, J.M., dalla Valle, C., Cremaschi, M., Peresani, M., 2015. Reconstruction of the Neanderthal and Modern Human landscape and climate from the Fumane cave sequence (Verona, Italy) using small-mammal assemblages. Quat. Sci. Rev. 128, 1–13. https://doi.org/10.1016/j.quascirev.2015.09.013
Maíllo Fernández, J.M., 2006. Archaic Aurignacian lithic technology in Cueva Morín (Cantabria, Spain), in: Bar-Yosef, O., Zilhão, J. (Eds.), Towards a Definition of the Aurignacian: Proceedings of the Symposium Held in Lisbon, Portugal, June 25-30, 2002, Trabalhos de Arqueologia. Instituto Português de Arqueologia ; American School of Prehistoric Research, Peabody Museum, Harvard University, Lisboa : [Cambridge, Mass.], pp. 111–130.
Maíllo Fernández, J.M., 2005. La production lamellaire de l'Aurignacien de la grotte Morin (Cantabrie, Espagne), in: Le Brun-Ricalens, F. (Ed.), Actes du XIVème congrès UISPP, Université de Liège, Belgique, 2 - 8 septembre 2001: session 6, Paléolithique supérieur ; section 6 - Upper Palaeolithic. Productions lamellaires attribuées à l'Aurignacien : Chaînes

opératoires et perspectives technoculturelles, Archéologiques / Musée National d'histoire et d'art Luxembourg. Musée National d'Histoire et d'Art, Luxembourg, pp. 339–357.
Maíllo-Fernández, J.M., 2012. Missing Lithics: the role of flakes in the Early Upper Palaeolithic of the Cantabrian region (Spain), in: Pastoors, A., Peresani, M. (Eds.), Flakes Not Blades: The Role of Flake Production at the Onset of the Upper Palaeolithic in Europe, Wissenschaftliche Schriften Des Neanderthal-Museums. Neanderthal Museum, Mettmann, pp. 69–84.
Maíllo-Fernández, J.M., de Quirós, F.B., 2010. L'Aurignacien archaïque de la grotte El Castillo (Espagne) : caractérisation technologique et typologique. L'Anthropologie 114, 1–25. https://doi.org/10.1016/j.anthro.2010.01.001
Marder, O., Hershkovitz, I., Barzilai, O., 2017. The Early Upper Palaeolithic of Manot Cave, Western Galilee: Chrono-Cultural, Subsistence, and Palaeo-Environmental Reconstruction, in: Enzel, Y., Bar-Yosef, O. (Eds.), Quaternary of the Levant. Cambridge University Press, pp. 277–284. https://doi.org/10.1017/9781316106754.031
Markó, A., 2017. Istállóskő revisited: the osseous artefacts from the lower layer. Acta Archaeol. Acad. Sci. Hung. 68, 193–218. https://doi.org/10.1556/072.2017.68.2.1
Markó, A., 2015. Istállóskő revisited: Lithic artefacts and assemblages, sixty years after. Acta Archaeol. Acad. Sci. Hung. 66, 5–38. https://doi.org/10.1556/072.2015.66.1.1
Martínez-Moreno, J., Mora, R., de la Torre, I., Benito-Calvo, A., 2012. The role of flakes in the early Upper Palaeolithic 497D assemblage of Cova Gan de Santa Linya (Southeastern pre-Pyrenees, Spain), in: Pastoors, A., Peresani, M. (Eds.), Flakes Not Blades: The Role of Flake Production at the Onset of the Upper Palaeolithic in Europe, Wissenschaftliche Schriften Des Neanderthal-Museums. Neanderthal Museum, Mettmann, pp. 85–104.
Mellars, P., 2011. The earliest modern humans in Europe. Nature 479, 483–485. https://doi.org/10.1038/479483a
Mellars, P., 2006a. A new radiocarbon revolution and the dispersal of modern humans in Eurasia. Nature 439, 931–935. https://doi.org/10.1038/nature04521
Mellars, P., 2006b. Archeology and the dispersal of modern humans in Europe: Deconstructing the "Aurignacian." Evol. Anthropol. Issues News Rev. 15, 167–182. https://doi.org/10.1002/evan.20103
Mellars, P., 2006c. Why did modern human populations disperse from Africa ca. 60,000 years ago? A new model. Proc. Natl. Acad. Sci. 103, 9381–9386. https://doi.org/10.1073/pnas.0510792103
Mellars, P., 1992. Archaeology and the population-dispersal hypothesis of modern human origins in Europe. Philos. Trans. R. Soc. Lond. B. Biol. Sci. 337, 225–234. https://doi.org/10.1098/rstb.1992.0100
Michel, V., Valladas, H., Shen, G., Wang, W., Zhao, J., Shen, C.-C., Valensi, P., Bae, C.J., 2016. The earliest modern Homo sapiens in China? J. Hum. Evol. 101, 101–104. https://doi.org/10.1016/j.jhevol.2016.07.008
Miebach, A., Stolzenberger, S., Wacker, L., Hense, A., Litt, T., 2019. A new Dead Sea pollen record reveals the last glacial paleoenvironment of the southern Levant. Quat. Sci. Rev. 214, 98–116. https://doi.org/10.1016/j.quascirev.2019.04.033
Monigal, K., 2003. 11. Technology, Economy, and Mobility at the Beginning of the Levantine Upper Palaeolithic, in: Goring-Morris, A.N., Belfer-Cohen, A. (Eds.), More than Meets the Eye: Studies on Upper Palaeolithic Diversity in the Near East. Oxbow ; David Brown Book Co, Oxford : Oakville, CT, pp. 118–133.
Monigal, K., 2002. The Levantine leptolithic: blade production from the Lower Paleolithic to the dawn of the Upper Paleolithic (Doctoral thesis). Dedman College-Southern Methodist University.
Monigal, K., Usik, V.I., Koulakovskaya, L., Gerasimenko, N.P., 2006. The beginning of the Upper Paleolithic in Transcarpathia, Ukraine. Anthropologie 44, 61–74.
Monnier, G.F., Missal, K., 2014. Another Mousterian Debate? Bordian facies, chaîne opératoire technocomplexes, and patterns of lithic variability in the western European Middle and Upper Pleistocene. Quat. Int. 350, 59–83. https://doi.org/10.1016/j.quaint.2014.06.053

Moreau, L., Odar, B., Higham, T., Horvat, A., Pirkmajer, D., Turk, P., 2015. Reassessing the Aurignacian of Slovenia: Techno-economic behaviour and direct dating of osseous projectile points. J. Hum. Evol. 78, 158–180. https://doi.org/10.1016/j.jhevol.2014.09.007

Nejman, L., Rhodes, E., Škrdla, P., Tostevin, G.B., Neruda, P., Nerudová, Z., Valoch, K., Oliva, M., Kaminská, L., Svoboda, J., Grün, R., 2011. New Chronological evidence for the Middle to Upper Palaeolithic Transistion in the Czech Republic and Slovakia: new optically stimulated luminescence dating results. Archaeometry 53, 1044–1066. https://doi.org/10.1111/j.1475-4754.2011.00586.x

Neuville, R., 1934. Le Préhistorique de Palestine. Rev. Biblique 43, 237–259.

Nigst, P.R., Haesaerts, P., 2012. L'Aurignacien en Basse Autriche : résultats préliminaires de l'analyse technologique de la couche culturelle 3 de Willendorf II et ses implications pour la chronologie du Paléolithique supérieur ancien en Europe centrale. L'Anthropologie 116, 575–608. https://doi.org/10.1016/j.anthro.2011.10.004

Nigst, P.R., Haesaerts, P., Damblon, F., Frank-Fellner, C., Mallol, C., Viola, B., Götzinger, M., Niven, L., Trnka, G., Hublin, J.-J., 2014. Early modern human settlement of Europe north of the Alps occurred 43,500 years ago in a cold steppe-type environment. Proc. Natl. Acad. Sci. 111, 14394–14399. https://doi.org/10.1073/pnas.1412201111

Normand, C., de Beaune, S.A., Costamagno, S., Diot, M.-F., Henry-Gambier, D., Goutas, N., Laroulandie, V., Lenoble, A., O'Farrell, M., Rendu, W., Rios Garaizar, J., Schwab, C., Tarriño Vinagre, A., Texier, J.-P., White, R., 2007. Nouvelles données sur la séquence aurignacienne de la grotte d'Isturitz (communes d'Isturitz et de Saint-Martin-d'Arberoue. Pyrénées Atlantiques), in: Jacques Evin. Un Siècle de Construction Du Discours Scientifique En Préhistoire, Vol. III " ..Aux Conceptions d'aujourd'hui ", Actes Du Congrès Préhistorique de France, XXVIe Session, Congrès Du Centenaire, 21-25 Septembre 2004, Avignon., Mémoires de La Société Préhistorique Française. pp. 277–293.

Normand, C., O'Farrell, M., Rios Garaizar, J., 2008. Quelle(s) utilisation(s) pour le productions lamellaires de l'Aurignacien Archaique? Quelques données et réflexions à partir des exemplaires de la grotte d'Isturitz (Pyrénées-Atlantiques; France), in: Lea, V. (Ed.), Recherches sur les armatures de projectiles du Paléolithique supérieur au Néolithique (actes du colloque C83, XVe congrès de l'UISPP, Lisbonne, 4-9 septembre 2006). Palaeoethnologie, pp. 7–46.

Normand, C., Turq, A., 2005. L'Aurignacien de la grotte d'Isturitz (France): la production lamellaire dans la séquence de la salle de Saint-Martin, in: Le Brun-Ricalens, F. (Ed.), Actes du XIVème congrès UISPP, Université de Liège, Belgique, 2 - 8 septembre 2001: session 6, Paléolithique supérieur ; section 6 - Upper Palaeolithic. Productions lamellaires attribuées à l'Aurignacien : Chaînes opératoires et perspectives technoculturelles, Archéologiques / Musée National d'histoire et d'art Luxembourg. Musée National d'Histoire et d'Art, Luxembourg, pp. 375–392.

North Greenland Ice Core Project members, 2004. High-resolution record of Northern Hemisphere climate extending into the last interglacial period. Nature 431, 147–151. https://doi.org/10.1038/nature02805

Obreht, I., Hambach, U., Veres, D., Zeeden, C., Bösken, J., Stevens, T., Marković, S.B., Klasen, N., Brill, D., Burow, C., Lehmkuhl, F., 2017. Shift of large-scale atmospheric systems over Europe during late MIS 3 and implications for Modern Human dispersal. Sci. Rep. 7, 1–10. https://doi.org/10.1038/s41598-017-06285-x

O'Connell, J.F., Allen, J., Williams, M.A.J., Williams, A.N., Turney, C.S.M., Spooner, N.A., Kamminga, J., Brown, G., Cooper, A., 2018. When did *Homo sapiens* first reach Southeast Asia and Sahul? Proc. Natl. Acad. Sci. 115, 8482–8490. https://doi.org/10.1073/pnas.1808385115

Onoratini, G., 2008. Le Protoaurignacien et l'Aurignacien des grottes de Grimaldi dans le contexte des cultures du Paléolithique supérieur de l'Europe méditerranéenne., in: Histoire et actualité de l'oeuvre scientifique de S.A.S. le prince Albert Ier de Monaco: 1895-2005: bilan et perspectives des connaissances sur les peuplement snéandertaliens et les premiers hommes

modernes de l'Europe méditerranéenne : actes du colloque international Paris - 2 mars 2005. Archives de l'Institut de Paléontologie Humaine, Paris, pp. 111–120.
Ortega Cobos, D., Soler Masferrer, N., Maroto Genover, J., 2005. La production des lamelles pendant l'Aurignacien Archaique dans la grotte de l'Arbreda: organisation de la production, variabilité des méthodes et des objectifs, in: Le Brun-Ricalens, F. (Ed.), Actes du XIVème congrès UISPP, Université de Liège, Belgique, 2 - 8 septembre 2001: session 6, Paléolithique supérieur ; section 6 - Upper Palaeolithic. Productions lamellaires attribuées à l'Aurignacien : Chaînes opératoires et perspectives technoculturelles, Archéologiques / Musée National d'histoire et d'art Luxembourg. Musée National d'Histoire et d'Art, Luxembourg, pp. 359–373.
Ortega Cordellat, I., 2005. La production lamellaire du niveau aurignacien de Barbas III (Creysse, Dordogne), in: Le Brun-Ricalens, F. (Ed.), Actes du XIVème congrès UISPP, Université de Liège, Belgique, 2 - 8 septembre 2001: session 6, Paléolithique supérieur ; section 6 - Upper Palaeolithic. Productions lamellaires attribuées à l'Aurignacien : Chaînes opératoires et perspectives technoculturelles, Archéologiques / Musée National d'histoire et d'art Luxembourg. Musée National d'Histoire et d'Art, Luxèmbourg, pp. 211–224.
Palma di Cesnola, A., 2006. L'Aurignacien et le Gravettien ancien de la grotte Paglicci au Mont Gargano. L'Anthropologie 110, 355–370. https://doi.org/10.1016/j.anthro.2006.06.011
Paris, C., 2015. La production de lamelles Dufour dans la couche VII d'Arcy-sur-Cure (Yonne, Aurignacien) (Master). Université de Paris I Panthéon-Sorbonne, Paris.
Pastoors, A., Peresani, M. (Eds.), 2012. Flakes not blades: the role of flake production at the onset of the Upper Palaeolithic in Europe, Wissenschaftliche Schriften des Neanderthal-Museums. Neanderthal Museum, Mettmann.
Pastoors, A., Weniger, G.-C., Kegler, J.F., 2008. The Middle – Upper Palaeolithic Transition at Yabroud II (Syria). A Re-evaluation of the Lithic Material from the Rust Excavation. Paléorient 34, 47–65. https://doi.org/10.3406/paleo.2008.5256
Pelegrin, J., 2011. Sur les débitages laminaires du Paléolithique Supérieur, in: Delpech, F., Jaubert, J. (Eds.), FRANÇOIS BORDES ET LA PRÉHISTOIRE COLLOQUE INTERNATIONAL FRANÇOIS BORDES, BORDEAUX, 22-24 AVRIL 2009, Documents préhistoriques. Ed. du CHTS, pp. 141–152.
Pelegrin, J., 2000. Les techniques de débitage laminaire au Tardiglaciaire: critères de diagnose et quelques réflexions, in: Valentin, B., Bodu, P., Christensen, M. (Eds.), L'Europe Centrale et Septentrionale Au Tardiglaciaire : Confrontation Des Modèles Régionaux de Peuplement. Actes de La Table-Ronde Internationale de Nemours, 14-16 Mai 1997. Association pour la promotion de la recherche archéologique en Ile-de-France, Nemours, pp. 73–86.
Pelegrin, J., O'Farrell, M., 2005. Les lamelles retouchées ou utilisées de Castanet, in: Le Brun-Ricalens, F. (Ed.), Actes du XIVème congrès UISPP, Université de Liège, Belgique, 2 - 8 septembre 2001: session 6, Paléolithique supérieur ; section 6 - Upper Palaeolithic. Productions lamellaires attribuées à l'Aurignacien : Chaînes opératoires et perspectives technoculturelles, Archéologiques / Musée National d'histoire et d'art Luxembourg. Musée National d'Histoire et d'Art, Luxembourg, pp. 103–121.
Peyrony, D., 1933. Les Industries « aurignaciennes » dans le bassin de la Vézère. Bull. Société Préhistorique Fr. 30, 543–559. https://doi.org/10.3406/bspf.1933.6793
Phillips, J.L., 2003. The use of chaîne opératoire approach in the Upper Palaeolithic Period in Sinai, in: Kardulias, P.N., Yerkes, R.W. (Eds.), Written in Stone: The Multiple Dimensions of Lithic Analysis. Lexington Books, Lanham, MD, pp. 7–16.
Phillips, J.L., 1988. The Upper Paleolithic of the Wadi Feiran, Southern Sinai. Paléorient 14, 183–200. https://doi.org/10.3406/paleo.1988.4467
Pini, R., Ravazzi, C., Reimer, P.J., 2010. The vegetation and climate history of the last glacial cycle in a new pollen record from Lake Fimon (southern Alpine foreland, N-Italy). Quat. Sci. Rev. 29, 3115–3137. https://doi.org/10.1016/j.quascirev.2010.06.040
Pleurdeau, D., Moncel, M.-H., Pinhasi, R., Yeshurun, R., Higham, T., Agapishvili, T., Bokeria, M., Muskhelishvili, A., Le Bourdonnec, F.-X., Nomade, S., Poupeau, G., Bocherens, H., Frouin, M., Genty, D., Pierre, M., Pons-Branchu, E., Lordkipanidze, D., Tushabramishvili, N., 2016.

Bondi Cave and the Middle-Upper Palaeolithic transition in western Georgia (south Caucasus). Quat. Sci. Rev. 146, 77–98. https://doi.org/10.1016/j.quascirev.2016.06.003
Ploux, S., Soriano, S., 2003. Umm el Tlel, une séquence du Paléolithique supérieur en Syrie centrale. Industries lithiques et chronologie culturelle. Paléorient 29, 5–34. https://doi.org/10.3406/paleo.2003.4763
Porraz, G., Simon, P., Pasquini, A., 2010. Identité technique et comportements économiques des groupes proto-aurignaciens à la grotte de l'Observatoire (principauté de Monaco). Gall. Préhistoire 52, 33–59. https://doi.org/10.3406/galip.2010.2470
Porter, S.T., Roussel, M., Soressi, M., 2019. A Comparison of Châtelperronian and Protoaurignacian Core Technology Using Data Derived from 3D Models. J. Comput. Appl. Archaeol. 2, 41–55. https://doi.org/10.5334/jcaa.17
Pötter, S., Schmitz, A., Lücke, A., Schulte, P., Obreht, I., Zech, M., Wissel, H., Marković, S.B., Lehmkuhl, F., 2020. Middle to Late Pleistocene environments based on stable organic carbon and nitrogen isotopes of loess-palaeosol sequences from the Carpathian Basin. Boreas 1–21. https://doi.org/10.1111/bor.12470
Proctor, C., Douka, K., Proctor, J.W., Higham, T., 2017. The Age and Context of the KC4 Maxilla, Kent's Cavern, UK. Eur. J. Archaeol. 20, 74–97. https://doi.org/10.1017/eaa.2016.1
R Core Team, 2020. R: A language and environment for statistical computing. R Foundation for Statistical Computing, Vienna, Austria. URL https://www.R-project.org/.
Rabinovich, R., 2017. The Archaeozoological Record in a Changing Environment of the Late Middle to the Late Pleistocene, in: Enzel, Y., Bar-Yosef, O. (Eds.), Quaternary of the Levant. Cambridge University Press, pp. 347–354. https://doi.org/10.1017/9781316106754.040
Ram, M., Koenig, G., 1997. Continuous dust concentration profile of pre-Holocene ice from the Greenland Ice Sheet Project 2 ice core: Dust stadials, interstadials, and the Eemian. J. Geophys. Res. Oceans 102, 26641–26648. https://doi.org/10.1029/96JC03548
Rasmussen, S.O., Bigler, M., Blockley, S.P., Blunier, T., Buchardt, S.L., Clausen, H.B., Cvijanovic, I., Dahl-Jensen, D., Johnsen, S.J., Fischer, H., Gkinis, V., Guillevic, M., Hoek, W.Z., Lowe, J.J., Pedro, J.B., Popp, T., Seierstad, I.K., Steffensen, J.P., Svensson, A.M., Vallelonga, P., Vinther, B.M., Walker, M.J.C., Wheatley, J.J., Winstrup, M., 2014. A stratigraphic framework for abrupt climatic changes during the Last Glacial period based on three synchronized Greenland ice-core records: refining and extending the INTIMATE event stratigraphy. Quat. Sci. Rev. 106, 14–28. https://doi.org/10.1016/j.quascirev.2014.09.007
Rebollo, N.R., Weiner, S., Brock, F., Meignen, L., Goldberg, P., Belfer-Cohen, A., Bar-Yosef, O., Boaretto, E., 2011. New radiocarbon dating of the transition from the Middle to the Upper Paleolithic in Kebara Cave, Israel. J. Archaeol. Sci. 38, 2424–2433. https://doi.org/10.1016/j.jas.2011.05.010
Reimer, P.J., Bard, E., Bayliss, A., Beck, J.W., Blackwell, P.G., Ramsey, C.B., Buck, C.E., Cheng, H., Edwards, R.L., Friedrich, M., Grootes, P.M., Guilderson, T.P., Haflidason, H., Hajdas, I., Hatté, C., Heaton, T.J., Hoffmann, D.L., Hogg, A.G., Hughen, K.A., Kaiser, K.F., Kromer, B., Manning, S.W., Niu, M., Reimer, R.W., Richards, D.A., Scott, E.M., Southon, J.R., Staff, R.A., Turney, C.S.M., van der Plicht, J., 2013. IntCal13 and Marine13 Radiocarbon Age Calibration Curves 0–50,000 Years cal BP. Radiocarbon 55, 1869–1887. https://doi.org/10.2458/azu_js_rc.55.16947
Richter, D., Tostevin, G., Škrdla, P., Davies, W., 2009. New radiometric ages for the Early Upper Palaeolithic type locality of Brno-Bohunice (Czech Republic): comparison of OSL, IRSL, TL and 14C dating results. J. Archaeol. Sci. 36, 708–720. https://doi.org/10.1016/j.jas.2008.10.017
Richter, J., Litt, T., Lehmkuhl, F., Hense, A., Hauck, T.C., Leder, D.F., Miebach, A., Parow-Souchon, H., Sauer, F., Schoenenberg, J., Al-Nahar, M., Hussain, S.T., 2020. Al-Ansab and the Dead Sea: Mid-MIS 3 archaeology and environment of the early Ahmarian population of the Levantine corridor. PLOS ONE 15, 1–36. https://doi.org/10.1371/journal.pone.0239968
Richter, J., Schyle, D., Wolter, T., 2015. The CRC 806 "Our way to Europe" - field campaigns into the archaeology of Wadi Sabra from 2008 to 2013, in: Schyle, D., Richter, J. (Eds.),

Pleistocene Archaeology of the Petra Area in Jordan, Kölner Studien Zur Prähistorischen Archäologie. Leidorf, Rahden/Westf, pp. 9–41.
Riel-Salvatore, J., Negrino, F., 2018. Proto-Aurignacian Lithic Technology, Mobility, and Human Niche Construction: A Case Study from Riparo Bombrini, Italy, in: Robinson, E., Sellet, F. (Eds.), Lithic Technological Organization and Paleoenvironmental Change, Studies in Human Ecology and Adaptation. Springer International Publishing, Cham, pp. 163–187. https://doi.org/10.1007/978-3-319-64407-3_8
Rigaud, S., Roussel, M., Rendu, W., Primault, J., Renou, S., Hublin, J.-J., Soressi, M., 2014. Les pratiques ornementales à l'Aurignacien ancien dans le Centre-Ouest de la France : l'apport des fouilles récentes aux Cottés (Vienne). Bull. Société Préhistorique Fr. 111, 19–38. https://doi.org/10.3406/bspf.2014.14362
Roebroeks, W., Kolen, J., Van Poecke, M., Van gijn, A., 1997. «Site J»: an early Weichselian (Middle Palaeolithic) flint scatter at Maastricht-Belvedere, The Netherlands. Paléo 9, 143–172. https://doi.org/10.3406/pal.1997.1231
Ronchitelli, A., Benazzi, S., Boscato, P., Douka, K., Moroni, A., 2014. Comments on "Human-climate interaction during the Early Upper Paleolithic: Testing the hypothesis of an adaptive shift between the Proto-Aurignacian and the Early Aurignacian" by William E. Banks, Francesco d'Errico, João Zilhão. J. Hum. Evol. 73, 107–111. https://doi.org/10.1016/j.jhevol.2013.12.010
Rougier, H., Milota, S., Rodrigo, R., Gherase, M., Sarcina, L., Moldovan, O., Zilhao, J., Constantin, S., Franciscus, R.G., Zollikofer, C.P.E., Ponce de Leon, M., Trinkaus, E., 2007. Pestera cu Oase 2 and the cranial morphology of early modern Europeans. Proc. Natl. Acad. Sci. 104, 1165–1170. https://doi.org/10.1073/pnas.0610538104
Roussel, M., Bourguignon, L., Soressi, M., 2009. Identification par l'expérimentation de la percussion au percuteur de calcaire au Paléolithique moyen : le cas du façonnage des racloirs bifaciaux Quina de Chez Pinaud (Jonzac, Charente-Maritime). Bull. Société Préhistorique Fr. 106, 219–238. https://doi.org/10.3406/bspf.2009.13846
Roussel, M., Soressi, M., 2013. Une nouvelle séquence du Paléolithique supérieur ancien aux marges sud-ouest du Bassin parisien : les Cottés dans la Vienne, in: Bodu, P., Chehmana, L., Klaric, L., Mevel, L., Soriano, S., Teyssandier, N. (Eds.), Le Paléolithique Supérieur Ancien de l'Europe Du Nord-Ouest. Réflexions et Synthèses à Partir d'un Projet Collectif de Recherches Sur Le Paléolithique Supérieur Ancien Du Bassin Parisien, Journées SPF, Sens, 15-18 Avril (2009). Mémoire de la Société préhistorique française, Paris, pp. 283–298.
Sanchez Goñi, M.F., Harrison, S.P., 2010. Millennial-scale climate variability and vegetation changes during the Last Glacial: Concepts and terminology. Quat. Sci. Rev. 29, 2823–2827. https://doi.org/10.1016/j.quascirev.2009.11.014
Santamaría Álvarez, D., 2012. La transición del Paleolítico medio al superior en Asturias: el abrigo de La Viña (La Manzaneda, Oviedo) y la cueva de El Sidrón (Borines, Piloña) (Doctoral thesis). Universidad de Oviedo, Oviedo.
Scerri, E.M.L., Gravina, B., Blinkhorn, J., Delagnes, A., 2016. Can Lithic Attribute Analyses Identify Discrete Reduction Trajectories? A Quantitative Study Using Refitted Lithic Sets. J. Archaeol. Method Theory 23, 669–691. https://doi.org/10.1007/s10816-015-9255-x
Schiegl, S., Goldberg, P., Pfretzschner, H.-U., Conard, N.J., 2003. Paleolithic burnt bone horizons from the Swabian Jura: Distinguishing betweenin situ fireplaces and dumping areas. Geoarchaeology 18, 541–565. https://doi.org/10.1002/gea.10080
Schiffer, M.B., Skibo, J.M., 1987. Theory and Experiment in the Study of Technological Change. Curr. Anthropol. 28, 595–622. https://doi.org/10.1086/203601
Schlanger, N., 2004. « Suivre les gestes, éclat par éclat » – la chaîne opératoire d'André Leroi-Gourhan, in: Audouze, F., Schlanger, N. (Eds.), Autour de l'homme : Contexte et Actualité d'André Leroi-Gourhan. AP-DCA, Antibes, pp. 127–147.
Schmidt, C., Sitlivy, V., Anghelinu, M., Chabai, V., Kels, H., Uthmeier, T., Hauck, T., Băltean, I., Hilgers, A., Richter, J., Radtke, U., 2013. First chronometric dates (TL and OSL) for the Aurignacian open-air site of Românești-Dumbrăviţa I, Romania. J. Archaeol. Sci. 40, 3740–3753. https://doi.org/10.1016/j.jas.2013.04.003

Schoenenberg, J., 2018. Raumstatistische Untersuchungen zum jungpaläolithischen Fundplatz Ansab 1 in Jordanien (Master). Universität zu Köln Philosophische Fakultät Institut für Ur- und Frühgeschichte, Koeln.

Schyle, D., 2015. The Ahmarian site of al-Ansab 1, in: Schyle, D., Richter, J. (Eds.), Pleistocene Archaeology of the Petra Area in Jordan, Kölner Studien Zur Prähistorischen Archäologie. Leidorf, Rahden/Westf, pp. 91–130.

Seguin-Orlando, A., Korneliussen, T.S., Sikora, M., Malaspinas, A.-S., Manica, A., Moltke, I., Albrechtsen, A., Ko, A., Margaryan, A., Moiseyev, V., Goebel, T., Westaway, M., Lambert, D., Khartanovich, V., Wall, J.D., Nigst, P.R., Foley, R.A., Lahr, M.M., Nielsen, R., Orlando, L., Willerslev, E., 2014. Genomic structure in Europeans dating back at least 36,200 years. Science 346, 1113–1118. https://doi.org/10.1126/science.aaa0114

Sellet, F., 1993. Chaine Operatoire; The Concept and Its Applications. Lithic Technol. 18, 106–112. https://doi.org/10.1080/01977261.1993.11720900

Shott, M.J., 2003. Chaîne Opératoire and Reduction Sequence. Lithic Technol. 28, 95–105. https://doi.org/10.1080/01977261.2003.11721005

Shott, M.J., Lindly, J.M., Clark, G.A., 2011. Continuous Modeling of Core Reduction: Lessons from Refitting Cores from WHS 623x, an Upper Paleolithic Site in Jordan. PaleoAnthropology 320–333.

Sinitsyn, A., 1993. Les niveaux aurignaciens de Kostienki 1, in: Kozlowski, J.K., Bánesz, L. (Eds.), Actes Du XIIe Congrés International Des Sciences Prehistoriques et Protohistoriques: Bratislava, 1-7 Septembre 1991. 4: ... Presented at the UISPP, Inst. Archéol. de l'Académie Slovaque des Sciences, Bratislava, pp. 242–259.

Sinitsyn, A.A., 2003. A Palaeolithic 'Pompeii' at Kostenki, Russia. Antiquity 77, 9–14. https://doi.org/10.1017/S0003598X00061299

Sirakov, N., Tsanova, T., Taneva, S., Krumov, I., Dimitrova, I., Kovatcheva, N., 2007. Un nouveau faciès lamellaire du début du Paléolithique Supérieur dans les Balkans. PALEO Rev. Archéologie Préhistorique 19, 131–144.

Sitlivy, V., Chabai, V., Anghelinu, M., Uthmeier, T., Kels, H., Hilgers, A., Schmidt, C., Niţă, L., Băltean, I., Veselsky, A., Hauck, T., 2012. The earliest Aurignacian in Romania: New investigations at the open air site of Românești-Dumbrăvița I (Banat). Quartär 59, 85–130.

Sitlivy, V., Chabai, V., Anghelinu, M., Uthmeier, T., Kels, H., Niţă, L., Băltean, I., Veselsky, A., Ţuţu, C., 2014a. Preliminary reassessment of the Aurignacian in Banat (South-western Romania). Quat. Int. 351, 193–212. https://doi.org/10.1016/j.quaint.2012.07.024

Sitlivy, V., Niță, L., Băltean, I., Anghelinu, M., Uthmeier, T., Hilger, A., Chabai, V.P., Hauck, T., Schmidt, C., 2014b. Placing the Aurignacian from Banat (Soutwestern Romania) into the European Early Upper Paleolithic context, in: Otte, M., Le Brun-Ricalens, F. (Eds.), Modes de Contacts et de Déplacements Au Paléolithique Eurasiatique: Actes Du Colloque International de La Commission 8 (Paléolithique Supérieur") de l'UISPP, Université de Liège, 28 - 31 Mai 2012 = Modes of Contact and Mobility during the Eurasian Palaeolithic, Archéologiques. ERAUL, Liège, pp. 243–367.

Škrdla, P., 2003. Comparison of Boker Tachtit and Stránská skála MP/UP Transitional Industries. J. Isr. Prehist. Soc. 33, 37–73.

Slimak, L., 2008. The Neronian and the historical structure of cultural shifts from Middle to Upper Palaeolithic in Mediterranean France. J. Archaeol. Sci. 35, 2204–2214. https://doi.org/10.1016/j.jas.2008.02.005

Slimak, L., Pesesse, D., Giraud, Y., 2006. Reconnaissance d'une installation du Protoaurignacien en vallée du Rhône. Implications sur nos connaissances concernant les premiers hommes modernes en France méditerranéenne. Comptes Rendus Palevol 5, 909–917. https://doi.org/10.1016/j.crpv.2006.05.002

Slimak, L., Pesesse, D., Giraud, Y., 2002. La grotte Mandrin et les premières occupations du Paléolithique supérieur en Occitanie orientale. Espac. Tiempo Forma Ser. Prehist. Arqueol. 1. https://doi.org/10.5944/etfi.15.2002.4746

Slutsky, D., 2014. The Effective Use of Graphs. J. Wrist Surg. 03, 067–068. https://doi.org/10.1055/s-0034-1375704

Soler Subils, J., Soler Masferrer, N., Maroto Genover, J., 2008. L'Arbreda's archaic Aurignacian dates clarified. Eurasian Prehistory 5, 45–55.

Soressi, M., Geneste, J.-M., 2011. The History and Efficacy of the Chaîne Opératoire Approach to Lithic Analysis: Studying Techniques to Reveal Past Societies in an Evolutionary Perspective. PaleoAnthropology 334–350.

Staubwasser, M., Drăgușin, V., Onac, B.P., Assonov, S., Ersek, V., Hoffmann, D.L., Veres, D., 2018. Impact of climate change on the transition of Neanderthals to modern humans in Europe. Proc. Natl. Acad. Sci. 115, 9116–9121. https://doi.org/10.1073/pnas.1808647115

Stutz, A.J., Shea, J.J., Rech, J.A., Pigati, J.S., Wilson, J., Belmaker, M., Albert, R.M., Arpin, T., Cabanes, D., Clark, J.L., Hartman, G., Hourani, F., White, C.E., Nilsson Stutz, L., 2015. Early Upper Paleolithic chronology in the Levant: new ABOx-SC accelerator mass spectrometry results from the Mughr el-Hamamah Site, Jordan. J. Hum. Evol. 85, 157–173. https://doi.org/10.1016/j.jhevol.2015.04.008

Stutz, A.J., Stutz Nilsson, L., 2017. Mughr el-Hamamah: An Early Upper Palaeolithic Cave Site on the Eastern Jordan Valley Flanks, in: Enzel, Y., Bar-Yosef, O. (Eds.), Quaternary of the Levant. Cambridge University Press, pp. 285–290. https://doi.org/10.1017/9781316106754.032

Svensson, A., Andersen, K.K., Bigler, M., Clausen, H.B., Dahl-Jensen, D., Davies, S.M., Johnsen, S.J., Muscheler, R., Parrenin, F., Rasmussen, S.O., Rothlisberger, R., Seierstad, I., Steffensen, J.P., Vinther, B.M., 2008. A 60 000 year Greenland stratigraphic ice core chronology. Clim Past 11.

Svoboda, J., 2006. The Aurignacian and after: chronology, geography and cultural taxonomy in the Middle Danube region, in: Bar-Yosef, O., Zilhão, J. (Eds.), Towards a Definition of the Aurignacian: Proceedings of the Symposium Held in Lisbon, Portugal, June 25-30, 2002, Trabalhos de Arqueologia. Instituto Português de Arqueologia ; American School of Prehistoric Research, Peabody Museum, Harvard University, Lisboa : [Cambridge, Mass.], pp. 259–274.

Svoboda, J., 2001. Mladeč and other caves in the Middle Danube region: early modern humans, late Neandertals, and projectiles, in: Zilhão, J., Aubry, T., de Carvalho, A.F. (Eds.), Les Premiers Hommes Modernes de La Péninsule Ibérique: Actes Du Colloque de La Commission VIII de l'UISPP: Vila Nova de Foz Côa, 22-24 Octobre 1998, Trabalhos de Arqueologia. Instituto Português de Arqueologia, Lisboa, pp. 45–60.

Svoboda, J., 2000. The depositional context of the Early Upper Paleolithic human fossils from the Koněprusy (Zlatý kůň) and Mladeč Caves, Czech Republic. J. Hum. Evol. 38, 523–536. https://doi.org/10.1006/jhev.1999.0361

Szmidt, C.C., Brou, L., Jaccottey, L., 2010. Direct radiocarbon (AMS) dating of split-based points from the (Proto)Aurignacian of Trou de la Mère Clochette, Northeastern France. Implications for the characterization of the Aurignacian and the timing of technical innovations in Europe. J. Archaeol. Sci. 37, 3320–3337. https://doi.org/10.1016/j.jas.2010.08.001

Tafelmaier, Y., 2017. Technological variability at the beginning of the Aurignacian in Northern Spain: Implications for the Proto- and Early Aurignacian distinction, Wissenschaftliche Schriften des Neanderthal Museums. Neanderthal Museum, Mettmann.

Talamo, S., Soressi, M., Roussel, M., Richards, M., Hublin, J.-J., 2012. A radiocarbon chronology for the complete Middle to Upper Palaeolithic transitional sequence of Les Cottés (France). J. Archaeol. Sci. 39, 175–183. https://doi.org/10.1016/j.jas.2011.09.019

Tartar, É., 2015. Origin and Development of Aurignacian Osseous Technology in Western Europe: a Review of Current Knowledge. Palethnologie. https://doi.org/10.4000/palethnologie.706

Tartar, E., Teyssandier, N., Bon, F., Liolios, D., 2006. Équipement de chasse, équipement domestique : une distinction efficace ? Réflexion sur la notion d'investissement technique dans les industries aurignaciennes, in: Astruc, L., Bon, F., Lea, V., Milcent, P.-Y., Philbert, S. (Eds.), Normes Techniques et Pratiques Sociales de La Simplicité Des Outillages Pré- et Protohistoriques. XXVIe Rencontres Internationales d'archéologie et d'histoire d'Antibes. Éditions APDCA, Antibes, pp. 107–117.

Tartar, É., White, R., 2013. The manufacture of Aurignacian split-based points: an experimental challenge. J. Archaeol. Sci. 40, 2723–2745. https://doi.org/10.1016/j.jas.2013.02.009
Tejero, J.-M., Christensen, M., Bodu, P., 2012. Red deer antler technology and early modern humans in Southeast Europe: an experimental study. J. Archaeol. Sci. 39, 332–346. https://doi.org/10.1016/j.jas.2011.09.018
Tejero, J.-M., Grimaldi, S., 2015. Assessing bone and antler exploitation at Riparo Mochi (Balzi Rossi, Italy): implications for the characterization of the Aurignacian in South-western Europe. J. Archaeol. Sci. 61, 59–77. https://doi.org/10.1016/j.jas.2015.05.003
Teyssandier, N., 2007. l'émergence du Paléolithique supérieur en Europe : mutations culturelles et rythmes d'évolution. PALEO Rev. Archéologie Préhistorique 19, 367–389.
Teyssandier, N., 2006. Questioning the first Aurignacian: mono or multi cultural phenomenon during the formation of the Upper Paleolithic in Central Europe and the Balkans. Anthropologie XLIV, 9–29.
Teyssandier, N., Bolus, M., Conard, N.J., 2006. The Early Aurignacian in Central Europe and its Place in a European Perspective, in: Bar-Yosef, O., Zilhão, J. (Eds.), Towards a Definition of the Aurignacian: Proceedings of the Symposium Held in Lisbon, Portugal, June 25-30, 2002, Trabalhos de Arqueologia. Instituto Português de Arqueologia ; American School of Prehistoric Research, Peabody Museum, Harvard University, Lisboa : [Cambridge, Mass.], pp. 241–256.
Teyssandier, N., Bon, F., Bordes, J.-G., 2010. Within projectile range: Some Thoughts on the Appearance of the Aurignacian in Europe. J. Anthropol. Res. 66, 209–229. https://doi.org/10.3998/jar.0521004.0066.203
Teyssandier, N., Liolios, D., 2008. Le concept d'Aurignacien : entre rupture préhistorique et obstacle épistémologique. Bull. Société Préhistorique Fr. 105, 737–747. https://doi.org/10.3406/bspf.2008.13782
Teyssandier, N., Liolios, D., 2003. Defining the earliest Aurignacian in the Swabian Alp: the relevance of the technological study of the Geissenklösterle (Baden-Württemberg, Germany) lithic and organic productions, in: Zilhão, J., d'Errico, F. (Eds.), The Chronology of the Aurignacian and of the Transitional Technocomplexes Dating, Stratigraphies, Cultural Implications.Proceedings of Symposium 6.1 of the XIVth Congress of the UISPP (University of Liège, Belgium, September 2-8, 2001), Trabalhos de Arqueologia. Presented at the UISPP, Instituto Português de Arqueologia, Lisboa, pp. 179–196.
Teyssandier, N., Zilhão, J., 2018. On the Entity and Antiquity of the Aurignacian at Willendorf (Austria): Implications for Modern Human Emergence in Europe. J. Paleolit. Archaeol. 1, 107–138. https://doi.org/10.1007/s41982-017-0004-4
Tixier, J., 1963. Typologie de l'épipaléolithique du Maghreb, Mémoires du Centre de Recherches Anthropologiques, Préhistoriques et Ethnographiques. Arts et Métiers Graphiques, Paris.
Tostevin, G.B., 2013. Seeing lithics: a middle-range theory for testing for cultural transmission in the pleistocene, American school of prehistoric research monograph series. Oakville, CT : Oxbow Books, Oxford.
Tostevin, G.B., 2011. Levels of Theory and Social Practice in the Reduction Sequence and Chaîne Opératoire Methods of Lithic Analysis. Spec. Issue Reduct. Seq. Chaîne Opératoire Methods Epistemol. Differ. Approaches Lithic Anal. 351–375.
Tostevin, G.B., 2000. The Middle to Upper Paleolithic Transition from the Levant to Central Europe: in situ development or diffusion?, in: Orschiedt, J., Weniger, G.-C. (Eds.), Neanderthals and Modern Humans-Discussing the Transition: Central and Eastern Europe from 50.000-30.000 BP. Neanderthal Museum, Mettmann, pp. 92–11.
Trinkaus, E., Constantin, S., Zilhão, J. (Eds.), 2012. Life and death at the Pestera cu Oase: a setting for modern human emergence in Europe, Human evolution series. Oxford University Press, New York.
Trinkaus, E., Moldovan, O., Milota, s., Bilgar, A., Sarcina, L., Athreya, S., Bailey, S.E., Rodrigo, R., Mircea, G., Higham, T., Ramsey, C.B., van der Plicht, J., 2003. An early modern human from the Pestera cu Oase, Romania. Proc. Natl. Acad. Sci. 100, 11231–11236. https://doi.org/10.1073/pnas.2035108100

Tryon, C.A., Potts, R., 2011. Approaches for Understanding Flake Production in the African Acheulean. PaleoAnthropology 376–389.

Tsanova, T., 2008. Les débuts du Paléolithique supérieur dans l'Est des Balkans: réflexion à partir de l'étude taphonomique et techno-économique des ensembles lithiques des sites de Bacho Kiro (couche 11), Temnata (couches VI et 4) et Kozarnika (niveau VIII), BAR international series. Archaeopress, Oxford.

Tsanova, T., Zwyns, N., Eizenberg, L., Teyssandier, N., Le Brun-Ricalens, F., Otte, M., 2012. Le plus petit dénominateur commun : réflexion sur la variabilité des ensembles lamellaires du Paléolithique supérieur ancien d'Eurasie. Un bilan autour des exemples de Kozarnika (Est des Balkans) et Yafteh (Zagros central). L'Anthropologie 116, 469–509. https://doi.org/10.1016/j.anthro.2011.10.005

van der Plicht, J., Bronk Ramsey, C., Heaton, T.J., Scott, E.M., Talamo, S., 2020. Recent developments in calibration for archaeological and environmental samples. Radiocarbon 1–23. https://doi.org/10.1017/RDC.2020.22

Weitzel, M.C., Borrazzo, K.B., Ceraso, A., Balirán, C., 2014. Trampling Fragmentation Potential of lithic artifacts: an experimental approach. Intersecc. En Antropol. 15, 97–110.

Wickham, H., 2016. ggplot2: Elegant Graphics for Data Analysis. Springer-Verlag, New York.

Wild, E.M., Teschler-Nicola, M., Kutschera, W., Steier, P., Trinkaus, E., Wanek, W., 2005. Direct dating of Early Upper Palaeolithic human remains from Mladeč. Nature 435, 332–335. https://doi.org/10.1038/nature03585

Williams, J.K., Bergman, C.A., 2010. Upper Paleolithic Levels XIII-VI (A and B) from the 1937-1938 and 1947-1948 Boston College Excavations and the Levantine Aurignacian at Ksar Akil, Lebanon. Paléorient 36, 117–161. https://doi.org/10.3406/paleo.2010.5391

Wolff, E.W., Chappellaz, J., Blunier, T., Rasmussen, S.O., Svensson, A., 2010. Millennial-scale variability during the last glacial: The ice core record. Quat. Sci. Rev. 29, 2828–2838. https://doi.org/10.1016/j.quascirev.2009.10.013

Wood, R., Bernaldo de Quirós, F., Maíllo-Fernández, J.-M., Tejero, J.-M., Neira, A., Higham, T., 2018. El Castillo (Cantabria, northern Iberia) and the Transitional Aurignacian: Using radiocarbon dating to assess site taphonomy. Quat. Int. 474, 56–70. https://doi.org/10.1016/j.quaint.2016.03.005

Wood, R., Douka, K., Boscato, P., Haesaerts, P., Sinitsyn, A.A., Higham, T.F.G., 2012. Testing the ABOx-SC method: Dating known-age charcoals associated with the Campanian Ignimbrite. Quat. Geochronol. 9, 16–26. https://doi.org/10.1016/j.quageo.2012.02.003

Wood, R.E., Arrizabalaga, A., Camps, M., Fallon, S., Iriarte-Chiapusso, M.-J., Jones, R., Maroto, J., de la Rasilla, M., Santamaría, D., Soler, J., Soler, N., Villaluenga, A., Higham, T.F.G., 2014. The chronology of the earliest Upper Palaeolithic in northern Iberia: New insights from L'Arbreda, Labeko Koba and La Viña. J. Hum. Evol. 69, 91–109. https://doi.org/10.1016/j.jhevol.2013.12.017

Zickel, M., Becker, D., Verheul, J., Yasa Yener, Willmes, C., 2016. Paleocoastlines GIS dataset. CRC806-Database. https://doi.org/10.5880/SFB806.20

Zilhão, J., 2013. Neandertal-Modern Human Contact in Western Eurasia: Issues of Dating, Taxonomy, and Cultural Associations, in: Akazawa, T., Nishiaki, Y., Aoki, K. (Eds.), Dynamics of Learning in Neanderthals and Modern Humans Volume 1. Springer Japan, Tokyo, pp. 21–57. https://doi.org/10.1007/978-4-431-54511-8_3

Zwyns, N., 2012. 19 - Small laminar blanks at Siuren I rockshelter: technological & comparative approach, in: Demidenko, E.Y., Otte, M., Noiret, P. (Eds.), From Late Middle Paleolithic and Early Upper Paleolithic to Epi-Paleolithic in Crimea. The Paleolithic of Crimea. ERAUL, Liège, pp. 359–373.

Zwyns, N., Paine, C.H., Tsedendorj, B., Talamo, S., Fitzsimmons, K.E., Gantumur, A., Guunii, L., Davakhuu, O., Flas, D., Dogandžić, T., Doerschner, N., Welker, F., Gillam, J.C., Noyer, J.B., Bakhtiary, R.S., Allshouse, A.F., Smith, K.N., Khatsenovich, A.M., Rybin, E.P., Byambaa, G., Hublin, J.-J., 2019. The Northern Route for Human dispersal in Central and Northeast Asia: New evidence from the site of Tolbor-16, Mongolia. Sci. Rep. 9, 11759. https://doi.org/10.1038/s41598-019-47972-1

Zwyns, N., Rybin, E.P., Hublin, J.-J., Derevianko, A.P., 2012. Burin-core technology and laminar reduction sequences in the initial Upper Paleolithic from Kara-Bom (Gorny-Altai, Siberia). Quat. Int. 259, 33–47. https://doi.org/10.1016/j.quaint.2011.03.036

Appendix

Table 19 Fragmentation in Al-Ansab 1

	Blade		Bladelet		Flake		Total	
	2009-2011	2018	2009-2011	2018	2009-2011	2018	2009-2011	2018
Complete	176 (57.33%)	354 (54.21%)	138 (33.01%)	172 (44.22%)	65 (94.20%)	203 (91.03%)	379 (47.73%)	729 (57.63%)
Prox+ Mes	82 (26.71%)	108 (16.54%)	201 (48.09%)	102 (26.22%)	3 (4.35%)	10 (4.48%)	286 (36.02%)	220 (17.39%)
Mes+ Dist	49 (15.96%)	191 (29.25%)	79 (18.90%)	115 (29.56%)	1 (1.45%)	10 (4.48%)	129 (16.25%)	316 (24.98%)
TOTAL	307 (100.00%)	653 (100.00%)	418 (100.00%)	389 (100.00%)	69 (100.00%	223 (100.00%)	794 (100.00%)	1265 (100.00%)

Table 20 Lipping in Al-Ansab 1.

	2009-2011			2018		
	Yes	No	Total	Yes	No	Total
Simple Blade	62 (53.45%)	54 (46.55%)	116 (100.00%)	105 (48.84%)	110 (51.16%)	215 (100.00%)
Management Blade	70 (49.65%)	71 (50.35%)	141 (100.00%)	150 (60.73%)	97 (39.27%)	247 (100.00%)
Simple Bladelet	30 (10.10%)	267 (89.90%)	297 (100.00%)	43 (18.86%)	185 (81.14%)	228 (100.00%)
Management Bladelet	11 (26.83%)	30 (73.17%)	41 (100.00%)	10 (24.39%)	31 (75.61%)	41 (100.00%)
Burin Spall	0 (0.00%)	1 (100.00%)	1 (100.00%)	1 (20.00%)	4 (80.00%)	5 (100.00%)
Blade Tablet	0 (0.00%)	1 (100.00%)	1 (100.00%)	0 (0.00%)	0 (0.00%)	0 (0.00%)
Management Flake	13 (31.71%)	28 (68.29%)	41 (100.00%)	76 (65.52%)	40 (34.48%)	116 (100.00%)
Core Tablet	5 (50.00%)	5 (50.00%)	10 (100.00%)	19 (50.00%)	19 (50.00%)	38 (100.00%)
Cortical Flake	7 (63.64%)	4 (36.36%)	11 (100.00%)	25 (65.79%)	13 (34.21%)	38 (100.00%)
Simple Flake	2 (33.33%)	4 (66.67%)	6 (100.00%)	11 (52.38%)	10 (47.62%)	21 (100.00%)
Total	200 (30.08%)	465 (69.92%)	665 (100.00%)	440 (46.36%)	509 (53.64%)	949 (100.00%)

Table 21 Overhang Abrasion in blanks and cores Al-Ansab 1.

	2009-2011			2018		
	Yes	No	Total	Yes	No	Total
Simple Blade	96 (82.76%)	20 (17.24%)	116 (100.00%)	200 (98.04%)	4 (1.96%)	204 (100.00%)
Management Blade	114 (80.85%)	27 (19.15%)	141 (100.00%)	196 (78.71%)	53 (21.29%)	249 (100.00%)
Simple Bladelet	229 (77.10%)	68 (22.90%)	297 (100.00%)	199 (87.28%)	29 (12.72%)	228 (100.00%)
Management Bladelet	28 (68.29%)	13 (31.71%)	41 (100.00%)	33 (84.62%)	6 (15.38%)	39 (100.00%)
Burin Spall	0 (0.00%)	1 (100.00%)	1 (100.00%)	2 (40.00%)	3 (60.00%)	5 (100.00%)
Total	467 (78.36%)	129 (21.64%)	596 (100.00%)	630 (86.90%)	95 (13.10%)	725 (100.00%)

	2009-2011			2018		
	Yes	**No**	**Total**	**Yes**	**No**	**Total**
One face (sub)parallel edges	4 (100.00%)	0 (0.00%)	4 (100.00%)	7 (100.00%)	0 (0.00%)	7 (100.00%)
Semi *Tournant*	12 (92.31%)	1 (7.69%)	13 (100.00%)	21 (100.00%)	(0.00%)	21 (100.00%)
Narrow Fronted	17 (100.00%)	0 (0.00%)	17 (100.00%)	23 (95.83%)	1 (4.17%)	24 (100.00%)
Narrow Fronted *sur Tranche*	4 (66.67%)	2 (33.33%)	6 (100.00%)	8 (80.00%)	2 (20.00%)	10 (100.00%)
Transversal Carinated	3 (100.00%)	0 (0.00%)	3 (100.00%)	2 (100.00%)	(0.00%)	2 (100.00%)
Pre-Core	0 (0.00%)	0 (0.00%)	0 (0.00%)	1 (50.00%)	1 (50.00%)	2 (100.00%)
Blades-Not Organised	1 (100.00%)	0 (0.00%)	1 (100.00%)	1 (50.00%)	1 (50.00%)	2 (100.00%)
Flakes-Not Organised	0 (0.00%)	1 (100.00%)	1 (100.00%)	1 (50.00%)	1 (50.00%)	2 (100.00%)
Fragment	0 (0.00%)	0 (0.00%)	0 (0.00%)	2 (40.00%)	3 (60.00%)	5 (100.00%)
Total	41 (91.11%)	4 (8.89%)	45 (100.00%)	70 (87.50%)	10 (12.50%)	80 (100.00%)

Table 22 Bulb values in Al-Ansab 1

	2009-2011					
	Diffused	**Not Perceived**	**Pronounced**	**Bulbar Scar**	**Indeterminate**	**Total**
Blade	72 (62.07%)	1 (0.86%)	34 (29.31%)	7 (6.03%)	2 (1.72%)	116 (100.00%)
Management Blade	102 (72.34%)	1 (0.71%)	22 (15.60%)	13 (9.22%)	3 (2.13%)	141 (100.00%)
Bladelet	217 (73.06%)	28 (9.43%)	41 (13.80%)	6 (2.02%)	5 (1.68%)	297 (100.00%)
Management Bladelet	30 (73.17%)	0 (0.00%)	8 (19.51%)	2 (4.88%)	1 (2.44%)	41 (100.00%)
Burin Spall	0 (0.00%)	0 (0.00%)	0 (0.00%)	0 (0.00%)	1 (100.00%)	1 (100.00%)
Blade Tablet	0 (0.00%)	0 (0.00%)	1 (100.00%)	0 (0.00%)	0 (0.00%)	1 (100.00%)
Core Tablet	4 (40.00%)	0 (0.00%)	2 (20.00%)	4 (40.00%)	0 (0.00%)	10 (100.00%)
Management Flake	18 (43.90%)	0 (0.00%)	8 (19.51%)	12 (29.27%)	3 (7.32%)	41 (100.00%)
Cortical Flake	6 (54.55%)	0 (0.00%)	4 (36.36%)	1 (9.09%)	0 (0.00%)	11 (100.00%)
Simple Flake	3 (50.00%)	0 (0.00%)	1 (16.67%)	2 (33.33%)	0 (0.00%)	6 (100.00%)
Total	452 (67.97%)	30 (4.51%)	121 (18.20%)	47 (7.07%)	15 (2.26%)	665 (100.00%)

	2018						
	Diffused	**Not Perceived**	**Pronounced**	**Bulbar Scar**	**Crushed**	**Indeterminate**	**Total**
Simple Blade	189 (87.91%)	5 (2.33%)	9 (4.19%)	9 (4.19%)	2 (0.93%)	1 (0.47%)	215 (100.00%)
Management Blade	182 (73.68%)	0 (0.00%)	45 (18.22%)	13 (5.26%)	7 (2.83%)	0 (0.00%)	247 (100.00%)
Simple Bladelet	209 (91.67%)	10 (4.39%)	3 (1.32%)	3 (1.32%)	3 (1.32%)	0 (0.00%)	228 (100.00%)
Management Bladelet	36 (87.80%)	1 (2.44%)	3 (7.32%)	1 (2.44%)	0 (0.00%)	0 (0.00%)	41 (100.00%)
Burin Spall	2 (40.00%)	1 (20.00%)	0 (0.00%)	0 (0.00%)	2 (40.00%)	0 (0.00%)	5 (100.00%)
Blade Tablet	0 (0.00%)	0 (0.00%)	0 (0.00%)	0 (0.00%)	0 (0.00%)	0 (0.00%)	0 (0.00%)
Core Tablet	10 (26.32%)	0 (0.00%)	19 (50.00%)	3 (7.89%)	3 (7.89%)	3 (7.89%)	38 (100.00%)
Management Flake	59 (50.86%)	0 (0.00%)	48 (41.38%)	9 (7.76%)	0 (0.00%)	0 (0.00%)	116 (100.00%)
Cortical Flake	9 (23.68%)	0 (0.00%)	24 (63.16%)	4 (10.53%)	1 (2.63%)	0 (0.00%)	38 (100.00%)
Simple Flake	13 (61.90%)	0 (0.00%)	8 (38.10%)	0 (0.00%)	0 (0.00%)	0 (0.00%)	21 (100.00%)
Total	709 (74.71%)	17 (1.79%)	159 (16.75%)	42 (4.43%)	18 (1.90%)	4 (0.42%)	949 (100.00%)

Table 23 Knapping angles in cores and blanks, Al-Ansab 1

	2009-2011				
	<70	**70-90**	**>90**	**Indeterminate**	**Total**
One face (sub)parallel edges	3 (75.00%)	1 (25.00%)		0 (0.00%)	4 (100.00%)
Semi Tournant	11 (84.62%)	2 (15.38%)		0 (0.00%)	13 (100.00%)
Narrow Fronted	13 (76.47%)	4 (23.53%)		0 (0.00%)	17 (100.00%)
Narrow Fronted sur Tranche	2 (33.33%)	3 (50.00%)		1 (16.67%)	6 (100.00%)
Transversal Carinated	2 (66.67%)	1 (33.33%)		0 (0.00%)	3 (100.00%)
Blades-Not Organised	1 (100.00%)	0 (0.00%)		0 (0.00%)	1 (100.00%)
Flakes-Not Organised	1 (100.00%)	0 (0.00%)		0 (0.00%)	1 (100.00%)
Total	33 (73.33%)	11 (24.44%)		1 (2.22%)	45 (100.00%)
	2018				
	<70	**70-90**	**>90**	**Indeterminate**	**Total**
One face (sub)parallel edges	6 (85.71%)	1 (14.29%)	0 (0.00%)	0 (0.00%)	7 (100.00%)
Semi Tournant	17 (80.95%)	1 (4.76%)	0 (0.00%)	3 (14.29%)	21 (100.00%)
Narrow Fronted	21 (87.50%)	3 (12.50%)	0 (0.00%)	0 (0.00%)	24 (100.00%)
Narrow Fronted sur Tranche	7 (70.00%)	3 (30.00%)	0 (0.00%)	0 (0.00%)	10 (100.00%)
Transversal Carinated	2 (100.00%)	0 (0.00%)	0 (0.00%)	0 (0.00%)	2 (100.00%)
Pre-Core	2 (28.57%)	3 (42.86%)	1 (14.29%)	1 (14.29%)	7 (100.00%)
Blades-Not Organised	1 (50.00%)	0 (0.00%)	0 (0.00%)	1 (50.00%)	2 (100.00%)
Flakes-Not Organised	2 (100.00%)	0 (0.00%)	0 (0.00%)	0 (0.00%)	2 (100.00%)
Fragment	1 (20.00%)	1 (20.00%)	0 (0.00%)	3 (60.00%)	5 (100.00%)
Total	59 (73.75%)	12 (15.00%)	1 (1.25%)	8 (10.00%)	80 (100.00%)

	2009-2011				
	<70	**70-90**	**>90**	**Indeterminate**	**Total**
Simple Blade	76 (65.52%)	15 (12.93%)	0 (0.00%)	25 (21.55%)	116 (100.00%)
Management Blade	99 (70.21%)	13 (9.22%)	0 (0.00%)	29 (20.57%)	141 (100.00%)
Simple Bladelet	109 (36.70%)	66 (22.22%)	0 (0.00%)	122 (41.08%)	297 (100.00%)
Management Bladelet	22 (53.66%)	7 (17.07%)	0 (0.00%)	12 (29.27%)	41 (100.00%)
Burin Spall	0 (0.00%)	0 (0.00%)	0 (0.00%)	1 (100.00%)	1 (100.00%)
Blade Tablet	1 (100.00%)	0 (0.00%)	0 (0.00%)	0 (0.00%)	1 (100.00%)
Management Flakes	22 (53.66%)	10 (24.39%)	1 (2.44%)	8 (19.51%)	41 (100.00%)
Core Tablet	3 (30.00%)	7 (70.00%)	0 (0.00%)	0 (0.00%)	10 (100.00%)
Cortical Flake	7 (63.64%)	2 (18.18%)	0 (0.00%)	2 (18.18%)	11 (100.00%)
Simple Flake	4 (66.67%)	1 (16.67%)	0 (0.00%)	1 (16.67%)	6 (100.00%)
Total	343 (51.58%)	121 (18.20%)	1 (0.15%)	200 (30.08%)	665 (100.00%)
	2018				
	<70	**70-90**	**>90**	**Indeterminate**	**Total**
Simple Blade	49 (22.79%)	141 (65.58%)	0 (0.00%)	25 (11.63%)	215 (100.00%)
Management Blade	81 (32.79%)	119 (48.18%)	0 (0.00%)	47 (19.03%)	247 (100.00%)
Simple Bladelet	36 (15.79%)	159 (69.74%)	0 (0.00%)	33 (14.47%)	228 (100.00%)
Management Bladelet	6 (14.63%)	27 (65.85%)	0 (0.00%)	8 (19.51%)	41 (100.00%)
Burin Spall	0 (0.00%)	1 (20.00%)	0 (0.00%)	4 (80.00%)	5 (100.00%)
Blade Tablet	0 (0.00%)	0 (0.00%)	0 (0.00%)	0 (0.00%)	0 (0.00%)
Management Flake	40 (34.48%)	62 (53.45%)	1 (0.86%)	13 (11.21%)	116 (100.00%)
Core Tablet	5 (13.16%)	26 (68.42%)	1 (2.63%)	6 (15.79%)	38 (100.00%)
Cortical Flake	11 (28.95%)	20 (52.63%)	0 (0.00%)	7 (18.42%)	38 (100.00%)
Simple Flake	4 (19.05%)	12 (57.14%)	0 (0.00%)	5 (23.81%)	21 (100.00%)
Total	232 (24.45%)	567 (59.75%)	2 (0.21%)	148 (15.60%)	949 (100.00%)

Table 24 Core blanks, Al-Ansab 1

				2009-2011			
	Blank	**Cobble**	**Indeterminate**	**Nodule**	**Slab**	**Squared Chunk**	**Total**
One face (sub)parallel edges	0 (0.00%)	0 (0.00%)	2 (50.00%)	1 (25.00%)	0 (0.00%)	1 (25.00%)	4 (100.00%)
Semi Tournant	0 (0.00%)	3 (23.08%)	7 (53.85%)	0 (0.00%)	0 (0.00%)	3 (23.08%)	13 (100.00%)
Narrow Fronted	1 (5.88%)	1 (5.88%)	8 (47.06%)	4 (23.53%)	1 (5.88%)	2 (11.76%)	17 (100.00%)
Narrow Fronted sur Tranche	4 (66.67%)	0 (0.00%)	1 (16.67%)	0 (0.00%)	1 (16.67%)	0 (0.00%)	6 (100.00%)
Transversal Carinated	1 (33.33%)	0 (0.00%)	1 (33.33%)	1 (33.33%)	0 (0.00%)	0 (0.00%)	3 (100.00%)
Blades-Not Organised	0 (0.00%)	0 (0.00%)	0 (0.00%)	1 (100.00%)	0 (0.00%)	0 (0.00%)	1 (100.00%)
Flakes-Not Organised	1 (100.00%)	0 (0.00%)	0 (0.00%)	0 (0.00%)	0 (0.00%)	0 (0.00%)	1 (100.00%)
Total	7 (15.56%)	4 (8.89%)	19 (42.22%)	7 (15.56%)	2 (4.44%)	6 (13.33%)	45 (100.00%)
				2018			
One face (sub)parallel edges	0 (0.00%)	3 (42.86%)	2 (28.57%)	2 (28.57%)	0 (0.00%)		7 (100.00%)
Semi Tournant	0 (0.00%)	6 (28.57%)	12 (57.14%)	3 (14.29%)	0 (0.00%)		21 (100.00%)
Narrow Fronted	0 (0.00%)	10 (41.67%)	11 (45.83%)	3 (12.50%)	0 (0.00%)		24 (100.00%)
Narrow Fronted sur Tranche	4 (40.00%)	0 (0.00%)	4 (40.00%)	1 (10.00%)	1 (10.00%)		10 (100.00%)
Transversal Carinated	1 (50.00%)	0 (0.00%)	1 (50.00%)	0 (0.00%)	0 (0.00%)		2 (100.00%)
Pre-Core	3 (42.86%)	1 (14.29%)	1 (14.29%)	2 (28.57%)	0 (0.00%)		7 (100.00%)
Blades-Not Organised	0 (0.00%)	1 (50.00%)	1 (50.00%)	0 (0.00%)	0 (0.00%)		2 (100.00%)
Flakes-Not Organised	0 (0.00%)	0 (0.00%)	2 (100.00%)	0 (0.00%)	0 (0.00%)		2 (100.00%)
Fragment	0 (0.00%)	1 (20.00%)	4 (80.00%)	0 (0.00%)	0 (0.00%)		5 (100.00%)
Total	8 (10.00%)	22 (27.50%)	38 (47.50%)	11 (13.75%)	1 (1.25%)		80 (100.00%)

Table 25 Cortex coverage position on cores, Al-Ansab 1.

	No Cortex	Lateral	Back	Back and Base	Back, Base and Lateral	Back and Lateral	Base	Base and Lateral	Base and Frontal	Frontal	Total
						2009-2011					
One face (sub)parallel edges	0 (0.00%)	1 (25.00%)	2 (50.00%)	0 (0.00%)		1 (25.00%)	0 (0.00%)	0 (0.00%)			4 (100.00%)
Semi Tournant	5 (38.46%)	0 (0.00%)	3 (23.08%)	3 (23.08%)		1 (7.69%)	0 (0.00%)	1 (7.69%)			13 (100.00%)
Narrow Fronted	5 (29.41%)	2 (11.76%)	4 (23.53%)	0 (0.00%)		3 (17.65%)	3 (17.65%)	0 (0.00%)			17 (100.00%)
Narrow Fronted sur Tranche	2 (33.33%)	3 (50.00%)	0 (0.00%)	0 (0.00%)		1 (16.67%)	0 (0.00%)	0 (0.00%)			6 (100.00%)
Transversal Carinated	3 (100.00%)	0 (0.00%)	0 (0.00%)	0 (0.00%)		0 (0.00%)	0 (0.00%)	0 (0.00%)			3 (100.00%)
Blades-Not Organised	0 (0.00%)	0 (0.00%)	1 (100.00%)	0 (0.00%)		0 (0.00%)	0 (0.00%)	0 (0.00%)			1 (100.00%)
Flakes-Not Organised	0 (0.00%)	0 (0.00%)	0 (0.00%)	0 (0.00%)		0 (0.00%)	1 (100.00%)	0 (0.00%)			1 (100.00%)
Total	15 (33.33%)	6 (13.33%)	10 (22.22%)	3 (6.67%)		6 (13.33%)	4 (8.89%)	1 (2.22%)			45 (100.00%)
						2018					
One face (sub)parallel edges	0 (0.00%)	3 (42.86%)	1 (14.29%)	2 (28.57%)	0 (0.00%)	0 (0.00%)	1 (14.29%)	0 (0.00%)	0 (0.00%)	0 (0.00%)	7 (100.00%)
Semi Tournant	7 (33.33%)	1 (4.76%)	7 (33.33%)	2 (9.52%)	0 (0.00%)	2 (9.52%)	2 (9.52%)	0 (0.00%)	0 (0.00%)	0 (0.00%)	21 (100.00%)
Narrow Fronted	5 (20.83%)	3 (12.50%)	6 (25.00%)	4 (16.67%)	1 (4.17%)	3 (12.50%)	2 (8.33%)	0 (0.00%)	0 (0.00%)	0 (0.00%)	24 (100.00%)
Narrow Fronted sur Tranche	5 (50.00%)	0 (0.00%)	0 (0.00%)	1 (10.00%)	0 (0.00%)	1 (10.00%)	1 (10.00%)	1 (10.00%)	0 (0.00%)	1 (10.00%)	10 (100.00%)
Transversal Carinated	1 (50.00%)	0 (0.00%)	0 (0.00%)	0 (0.00%)	0 (0.00%)	0 (0.00%)	0 (0.00%)	0 (0.00%)	0 (0.00%)	1 (50.00%)	2 (100.00%)
Pre-Core	2 (28.57%)	2 (28.57%)	0 (0.00%)	0 (0.00%)	0 (0.00%)	0 (0.00%)	1 (14.29%)	1 (14.29%)	1 (14.29%)	0 (0.00%)	7 (100.00%)
Blades-Not Organised	1 (50.00%)	0 (0.00%)	0 (0.00%)	0 (0.00%)	1 (50.00%)	0 (0.00%)	0 (0.00%)	0 (0.00%)	0 (0.00%)	0 (0.00%)	2 (100.00%)
Flakes-Not Organised	1 (50.00%)	1 (50.00%)	0 (0.00%)	0 (0.00%)	0 (0.00%)	0 (0.00%)	0 (0.00%)	0 (0.00%)	0 (0.00%)	0 (0.00%)	2 (100.00%)
Fragment	4 (80.00%)	1 (20.00%)	0 (0.00%)	0 (0.00%)	0 (0.00%)	0 (0.00%)	0 (0.00%)	0 (0.00%)	0 (0.00%)	0 (0.00%)	5 (100.00%)
Total	26 (32.50%)	11 (13.75%)	14 (17.50%)	9 (11.25%)	2 (2.50%)	6 (7.50%)	7 (8.75%)	2 (2.50%)	1 (1.25%)	2 (2.50%)	80 (100.00%)

Table 26 Striking Platform type cores, Al-Ansab 1

	2009-2011			
	Natural	**Plain**	**Indeterminate**	**Total**
One face (sub)parallel edges	0 (0.00%)	4 (100.00%)		4 (100.00%)
Semi Tournant	1 (7.69%)	12 (92.31%)		13 (100.00%)
Narrow Fronted	2 (11.76%)	15 (88.24%)		17 (100.00%)
Narrow Fronted sur Tranche	0 (0.00%)	6 (100.00%)		6 (100.00%)
Transversal Carinated	0 (0.00%)	3 (100.00%)		3 (100.00%)
Blades-Not Organised	0 (0.00%)	1 (100.00%)		1 (100.00%)
Flakes-Not Organised	0 (0.00%)	1 (100.00%)		1 (100.00%)
Total	3 (6.67%)	42 (93.33%)		45 (100.00%)
		2018		
One face (sub)parallel edges	0 (0.00%)	7 (100.00%)	0 (0.00%)	7 (100.00%)
Semi Tournant	0 (0.00%)	21 (100.00%)	0 (0.00%)	21 (100.00%)
Narrow Fronted	1 (4.17%)	23 (95.83%)	0 (0.00%)	24 (100.00%)
Narrow Fronted sur Tranche	0 (0.00%)	10 (100.00%)	0 (0.00%)	10 (100.00%)
Transversal Carinated	0 (0.00%)	2 (100.00%)	0 (0.00%)	2 (100.00%)
Pre-Core	0 (0.00%)	7 (100.00%)	0 (0.00%)	7 (100.00%)
Blades-Not Organised	0 (0.00%)	2 (100.00%)	0 (0.00%)	2 (100.00%)
Flakes-Not Organised	0 (0.00%)	2 (100.00%)	0 (0.00%)	2 (100.00%)
Fragment	0 (0.00%)	3 (60.00%)	2 (40.00%)	5 (100.00%)
Total	1 (1.25%)	77 (96.25%)	2 (2.50%)	80 (100.00%)

.

Table 27 Striking Platform relationship cores, Al-Ansab 1.

	Single	Opposed	Opposed auxiliary	Orthogonal auxiliary	Adjacent	Independent	Indeterminate	Total
				2009-2011				
One face (sub)parallel edges	3 (100.00%)	1 (25.00%)				0 (0.00%)		4 (100.00%)
Semi Tournant	11 (84.62%)	1 (7.69%)				1 (7.69%)		13 (100.00%)
Narrow Fronted	15 (88.24%)	0 (0.00%)				2 (11.76%)		17 (100.00%)
Narrow Fronted sur Tranche	6 (100.00%)	0 (0.00%)				0 (0.00%)		6 (100.00%)
Transversal Carinated	3 (100.00%)	0 (0.00%)				0 (0.00%)		3 (100.00%)
Blades-Not Organised	0 (0.00%)	0 (0.00%)				1 (100.00%)		1 (100.00%)
Flakes-Not Organised	1 (100.00%)	0 (0.00%)				0 (0.00%)		1 (100.00%)
Total	39 (86.67%)	2 (4.44%)				4 (8.89%)		45 (100.00%)
				2018				
One face (sub)parallel edges	6 (85.71%)	0 (0.00%)	0 (0.00%)	0 (0.00%)	0 (0.00%)	1 (14.29%)	0 (0.00%)	7 (100.00%)
Semi Tournant	18 (85.71%)	2 (9.52%)	0 (0.00%)	1 (4.76%)	0 (0.00%)	0 (0.00%)	0 (0.00%)	21 (100.00%)
Narrow Fronted	21 (87.50%)	1 (4.17%)	1 (4.17%)	0 (0.00%)	1 (4.17%)	0 (0.00%)	0 (0.00%)	24 (100.00%)
Narrow Fronted sur Tranche	10 (100.00%)	0 (0.00%)	0 (0.00%)	0 (0.00%)	0 (0.00%)	0 (0.00%)	0 (0.00%)	10 (100.00%)
Transversal Carinated	1 (50.00%)	0 (0.00%)	0 (0.00%)	0 (0.00%)	1 (50.00%)	0 (0.00%)	0 (0.00%)	2 (100.00%)
Pre-Core	6 (85.71%)	1 (14.29%)	0 (0.00%)	0 (0.00%)	0 (0.00%)	0 (0.00%)	0 (0.00%)	7 (100.00%)
Blades-Not Organised	2 (100.00%)	0 (0.00%)	0 (0.00%)	0 (0.00%)	0 (0.00%)	0 (0.00%)	0 (0.00%)	2 (100.00%)
Flakes-Not Organised	2 (100.00%)	0 (0.00%)	0 (0.00%)	0 (0.00%)	0 (0.00%)	0 (0.00%)	0 (0.00%)	2 (100.00%)
Fragment	3 (60.00%)	1 (20.00%)	0 (0.00%)	0 (0.00%)	0 (0.00%)	0 (0.00%)	1 (20.00%)	5 (100.00%)
Total	69 (86.25%)	5 (6.25%)	1 (1.25%)	1 (1.25%)	2 (2.50%)	1 (1.25%)	1 (1.25%)	80 (100.00%)

Table 28 Flaking Surface relationship cores, Al-Ansab 1.

2009-2011						
	Single Surface	**Opposed**	**Adjacent-Orthogonal**	**Independent**	**Indeterminate**	**Total**
One face (sub)parallel edges	4 (100.00%)		0 (0.00%)	0 (0.00%)		4 (100.00%)
Semi Tournant	12 (92.31%)		0 (0.00%)	0 (0.00%)		13 (100.00%)
Narrow Fronted	15 (88.24%)		1 (5.88%)	1 (5.88%)		17 (100.00%)
Narrow Fronted sur Tranche	6 (100.00%)		0 (0.00%)	0 (0.00%)		6 (100.00%)
Transversal Carinated	3 (100.00%)		0 (0.00%)	0 (0.00%)		3 (100.00%)
Blades-Not Organised	0 (0.00%)		0 (0.00%)	0 (0.00%)		1 (100.00%)
Flakes-Not Organised	1 (100.00%)		0 (0.00%)	0 (0.00%)		1 (100.00%)
Total	41 (91.11%)		1 (2.22%)	1 (2.22%)		45 (100.00%)
			2018			
One face (sub)parallel edges	6 (85.71%)	1 (14.29%)	0 (0.00%)	0 (0.00%)	0 (0.00%)	7 (100.00%)
Semi Tournant	20 (95.24%)	1 (4.76%)	0 (0.00%)	0 (0.00%)	0 (0.00%)	21 (100.00%)
Narrow Fronted	21 (87.50%)	1 (4.17%)	1 (4.17%)	1 (4.17%)	0 (0.00%)	24 (100.00%)
Narrow Fronted sur Tranche	10 (100.00%)	0 (0.00%)	0 (0.00%)	0 (0.00%)	0 (0.00%)	10 (100.00%)
Transversal Carinated	1 (50.00%)	0 (0.00%)	0 (0.00%)	1 (50.00%)	0 (0.00%)	2 (100.00%)
Pre-Core	5 (71.43%)	0 (0.00%)	0 (0.00%)	1 (14.29%)	1 (14.29%)	7 (100.00%)
Blades-Not Organised	2 (100.00%)	0 (0.00%)	0 (0.00%)	0 (0.00%)	0 (0.00%)	2 (100.00%)
Flakes-Not Organised	2 (100.00%)	0 (0.00%)	0 (0.00%)	0 (0.00%)	0 (0.00%)	2 (100.00%)
Fragment	5 (100.00%)	0 (0.00%)	0 (0.00%)	0 (0.00%)	0 (0.00%)	5 (100.00%)
Total	72 (90.00%)	3 (3.75%)	1 (1.25%)	3 (3.75%)	1 (1.25%)	80 (100.00%)

Table 29 Negatives types cores, Al-Ansab 1.

	Bladelets	Bladelets & Flakes	Blades	Blades & Bladelets	Blades & Flakes	Blades, Bladelets & Flakes	Flakes	No negatives	Total
					2009-2011				
One face (sub)parallel edges	1 (25.00%)	1 (25.00%)	1 (25.00%)	1 (25.00%)	0 (0.00%)	0 (0.00%)	0 (0.00%)		4 (100.00%)
Semi Tournant	5 (38.46%)	1 (7.69%)	0 (0.00%)	6 (46.15%)	0 (0.00%)	1 (7.69%)	0 (0.00%)		13 (100.00%)
Narrow Fronted	8 (47.06%)	0 (0.00%)	3 (17.65%)	4 (23.53%)	0 (0.00%)	2 (11.76%)	0 (0.00%)		17 (100.00%)
Narrow Fronted sur Tranche	2 (33.33%)	0 (0.00%)	0 (0.00%)	4 (66.67%)	0 (0.00%)	0 (0.00%)	0 (0.00%)		6 (100.00%)
Transversal Carinated	0 (0.00%)	0 (0.00%)	1 (33.33%)	1 (33.33%)	1 (33.33%)	0 (0.00%)	0 (0.00%)		3 (100.00%)
Blades-Not Organised	0 (0.00%)	0 (0.00%)	1 (100.00%)	0 (0.00%)	0 (0.00%)	0 (0.00%)	0 (0.00%)		1 (100.00%)
Flakes-Not Organised	0 (0.00%)	0 (0.00%)	0 (0.00%)	0 (0.00%)	0 (0.00%)	0 (0.00%)	1 (100.00%)		1 (100.00%)
Total	16 (35.56%)	2 (4.44%)	6 (13.33%)	16 (35.56%)	1 (2.22%)	3 (6.67%)	1 (2.22%)		45 (100.00%)
					2018				
One face (sub)parallel edges	2 (28.57%)	1 (14.29%)	1 (14.29%)	3 (42.86%)	0 (0.00%)	0 (0.00%)	0 (0.00%)	0 (0.00%)	7 (100.00%)
Semi Tournant	7 (33.33%)	0 (0.00%)	3 (14.29%)	8 (38.10%)	1 (4.76%)	2 (9.52%)	0 (0.00%)	0 (0.00%)	21 (100.00%)
Narrow Fronted	6 (25.00%)	0 (0.00%)	4 (16.67%)	14 (58.33%)	0 (0.00%)	0 (0.00%)	0 (0.00%)	0 (0.00%)	24 (100.00%)
Narrow Fronted sur Tranche	4 (40.00%)	0 (0.00%)	1 (10.00%)	4 (40.00%)	1 (10.00%)	0 (0.00%)	0 (0.00%)	0 (0.00%)	10 (100.00%)
Transversal Carinated	1 (50.00%)	0 (0.00%)	0 (0.00%)	0 (0.00%)	0 (0.00%)	0 (0.00%)	1 (50.00%)	0 (0.00%)	2 (100.00%)
Pre-Core	0 (0.00%)	0 (0.00%)	1 (14.29%)	2 (28.57%)	1 (14.29%)	0 (0.00%)	2 (28.57%)	1 (14.29%)	7 (100.00%)
Blades-Not Organised	0 (0.00%)	1 (50.00%)	1 (50.00%)	0 (0.00%)	0 (0.00%)	0 (0.00%)	0 (0.00%)	0 (0.00%)	2 (100.00%)
Flakes-Not Organised	0 (0.00%)	0 (0.00%)	0 (0.00%)	0 (0.00%)	0 (0.00%)	0 (0.00%)	2 (100.00%)	0 (0.00%)	2 (100.00%)
Fragment	2 (40.00%)	0 (0.00%)	1 (20.00%)	1 (20.00%)	0 (0.00%)	0 (0.00%)	1 (20.00%)	0 (0.00%)	5 (100.00%)
Total	22 (27.50%)	2 (2.50%)	12 (15.00%)	32 (40.00%)	3 (3.75%)	2 (2.50%)	6 (7.50%)	1 (1.25%)	80 (100.00%)

Table 30 Negatives orientation in cores, Al-Ansab 1.

	Bipolar	Convergent	Unipolar	Unipolar+ Convergent	Unipolar+ Crossed	Unipolar+ Opposite	Unipolar+ Orthogonal	No Negatives	Total
					2009-2011				
One face (sub)parallel edges	0 (0.00%)		3 (75.00%)	0 (0.00%)		1 (25.00%)	0 (0.00%)		4 (100.00%)
Semi Tournant	1 (7.69%)		11 (84.62%)	1 (7.69%)		0 (0.00%)	0 (0.00%)		13 (100.00%)
Narrow Fronted	0 (0.00%)		15 (88.24%)	1 (5.88%)		0 (0.00%)	1 (5.88%)		17 (100.00%)
Narrow Fronted sur Tranche	2 (33.33%)		4 (66.67%)	0 (0.00%)		0 (0.00%)	0 (0.00%)		6 (100.00%)
Transversal Carinated	0 (0.00%)		2 (66.67%)	1 (33.33%)		0 (0.00%)	0 (0.00%)		3 (100.00%)
Blades-Not Organised	0 (0.00%)		0 (0.00%)	1 (100.00%)		0 (0.00%)	0 (0.00%)		1 (100.00%)
Flakes-Not Organised	0 (0.00%)		1 (100.00%)	0 (0.00%)		0 (0.00%)	0 (0.00%)		1 (100.00%)
Total	3 (6.67%)		36 (80.00%)	4 (8.89%)		1 (2.22%)	1 (2.22%)		45 (100.00%)
					2018				
One face (sub)parallel edges	0 (0.00%)	0 (0.00%)	7 (100.00%)	0 (0.00%)	0 (0.00%)			0 (0.00%)	7 (100.00%)
Semi Tournant	1 (4.76%)	0 (0.00%)	14 (66.67%)	5 (23.81%)	1 (4.76%)			0 (0.00%)	21 (100.00%)
Narrow Fronted	0 (0.00%)	0 (0.00%)	13 (54.17%)	11 (45.83%)	0 (0.00%)			0 (0.00%)	24 (100.00%)
Narrow Fronted sur Tranche	0 (0.00%)	0 (0.00%)	7 (70.00%)	3 (30.00%)	0 (0.00%)			0 (0.00%)	10 (100.00%)
Transversal Carinated	0 (0.00%)	0 (0.00%)	2 (100.00%)	0 (0.00%)	0 (0.00%)			0 (0.00%)	2 (100.00%)
Pre-Core	0 (0.00%)	0 (0.00%)	5 (71.43%)	1 (14.29%)	0 (0.00%)			1 (14.29%)	7 (100.00%)
Blades-Not Organised	0 (0.00%)	0 (0.00%)	2 (100.00%)	0 (0.00%)	0 (0.00%)			0 (0.00%)	2 (100.00%)
Flakes-Not Organised	0 (0.00%)	0 (0.00%)	2 (100.00%)	0 (0.00%)	0 (0.00%)			0 (0.00%)	2 (100.00%)
Fragment	1 (20.00%)	1 (20.00%)	3 (60.00%)	0 (0.00%)	0 (0.00%)			0 (0.00%)	5 (100.00%)
Total	2 (2.50%)	1 (1.25%)	55 (68.75%)	20 (25.00%)	1 (1.25%)			1 (1.25%)	80 (100.00%)

Table 31 Butts Flakes, Al-Ansab 1.

	Plain	Linear	Punctiform	Dihedral	Facetted	Natural	Indeterminate	Crushed	Total
					2009-2011				
Management Flake									
Maintenance Flake	11 (73.33%)	1 (6.67%)	0 (0.00%)	0 (0.00%)	0 (0.00%)	2 (13.33%)	1 (6.67%)		15 (100.00%)
Surface Cleaning Flake	16 (61.54%)	4 (15.38%)	4 (15.38%)	0 (0.00%)	0 (0.00%)	1 (3.85%)	1 (3.85%)		26 (100.00%)
Core Tablet	5 (50.00%)	0 (0.00%)	1 (10.00%)	0 (0.00%)	3 (30.00%)	1 (10.00%)	0 (0.00%)		10 (100.00%)
Cortical Flake	4 (36.36%)	1 (9.09%)	2 (18.18%)	1 (9.09%)	0 (0.00%)	2 (18.18%)	1 (9.09%)		11 (100.00%)
Simple Flake	4 (66.67%)	1 (16.67%)	0 (0.00%)	0 (0.00%)	0 (0.00%)	0 (0.00%)	1 (16.67%)		6 (100.00%)
Total	40 (58.82%)	7 (10.29%)	7 (10.29%)	1 (1.47%)	3 (4.41%)	6 (8.82%)	4 (5.88%)		68 (100.00%)
					2018				
Management Flake									
Maintenance Flake	2 (40.00%)	1 (20.00%)	1 (20.00%)	0 (0.00%)	0 (0.00%)	1 (20.00%)	0 (0.00%)	0 (0.00%)	5 (100.00%)
Surface Cleaning Flake	54 (48.65%)	34 (30.63%)	2 (1.80%)	4 (3.60%)	2 (1.80%)	6 (5.41%)	1 (0.90%)	8 (7.21%)	111 (100.00%)
Core Tablet	16 (42.11%)	2 (5.26%)	0 (0.00%)	2 (5.26%)	14 (36.84%)	0 (0.00%)	4 (10.53%)	0 (0.00%)	38 (100.00%)
Cortical Flake	23 (60.53%)	6 (15.79%)	2 (5.26%)	0 (0.00%)	1 (2.63%)	3 (7.89%)	3 (7.89%)	0 (0.00%)	38 (100.00%)
Simple Flake	10 (47.62%)	5 (23.81%)	0 (0.00%)	1 (4.76%)	0 (0.00%)	1 (4.76%)	2 (9.52%)	2 (9.52%)	21 (100.00%)
Total	105 (49.30%)	48 (22.54%)	5 (2.35%)	7 (3.29%)	17 (7.98%)	11 (5.16%)	10 (4.69%)	10 (4.69%)	213 (100.00%)

Table 32 Butts in Blades and Bladelets, Al-Ansab 1.

	Plain	Linear	Punctiform	Dihedral	Facetted	Natural	Indeterminate	Crushed	Total
						2009-2011			
Crest	5 (45.45%)	2 (18.18%)	2 (18.18%)			0 (0.00%)	0 (0.00%)	0 (0.00%)	11 (100.00%)
Asymmetrical Blade	26 (32.10%)	23 (28.40%)	26 (32.10%)			3 (3.70%)	2 (2.47%)	3 (3.70%)	81 (100.00%)
Overshot Blade	13 (35.14%)	10 (27.03%)	10 (27.03%)			3 (8.11%)	1 (2.70%)	3 (8.11%)	37 (100.00%)
Surface Cleaning Blade	5 (55.56%)	1 (11.11%)	0 (0.00%)			2 (22.22%)	0 (0.00%)	2 (22.22%)	9 (100.00%)
Maintenance Blade	1 (33.33%)	0 (0.00%)	1 (33.33%)			1 (33.33%)	0 (0.00%)	1 (33.33%)	3 (100.00%)
Crest (Bladelet)	1 (100.00%)	0 (0.00%)	0 (0.00%)			0 (0.00%)	0 (0.00%)	0 (0.00%)	1 (100.00%)
Asymmetrical Bladelet	6 (17.65%)	7 (20.59%)	20 (58.82%)			1 (2.94%)	0 (0.00%)	1 (2.94%)	34 (100.00%)
Overshot Bladelet	1 (20.00%)	0 (0.00%)	4 (80.00%)			0 (0.00%)	0 (0.00%)	0 (0.00%)	5 (100.00%)
Maintenance Bladelet	1 (100.00%)	0 (0.00%)	0 (0.00%)			0 (0.00%)	0 (0.00%)	0 (0.00%)	1 (100.00%)
Blade Tablet	1 (100.00%)	0 (0.00%)	0 (0.00%)			0 (0.00%)	0 (0.00%)	0 (0.00%)	1 (100.00%)
Simple Blade	30 (25.86%)	46 (39.66%)	32 (27.59%)			5 (4.31%)	1 (0.86%)	5 (4.31%)	116 (100.00%)
Simple Bladelet	42 (14.14%)	140 (47.14%)	90 (30.30%)			12 (4.04%)	10 (3.37%)	12 (4.04%)	297 (100.00%)
Burin Spall	0 (0.00%)	0 (0.00%)	0 (0.00%)			1 (100.00%)	0 (0.00%)	1 (100.00%)	1 (100.00%)
Total	132 (22.11%)	229 (38.36%)	185 (30.99%)			28 (4.69%)	14 (2.35%)	28 (4.69%)	597 (100.00%)

	Plain	Linear	Punctiform	Dihedral	Facetted	Natural	Indeterminate	Crushed	Total
					2018				
Crest	11 (31.43%)	16 (45.71%)	5 (14.29%)	0 (0.00%)	0 (0.00%)	1 (2.86%)	1 (2.86%)	1 (2.86%)	35 (100.00%)
Asymmetrical Blade	38 (30.40%)	58 (46.40%)	17 (13.60%)	2 (1.60%)	0 (0.00%)	2 (1.60%)	3 (2.40%)	5 (4.00%)	125 (100.00%)
Overshot Blade	27 (45.00%)	26 (43.33%)	2 (3.33%)	0 (0.00%)	0 (0.00%)	0 (0.00%)	0 (0.00%)	5 (8.33%)	60 (100.00%)
Surface Cleaning Blade	12 (60.00%)	7 (35.00%)	1 (5.00%)	0 (0.00%)	0 (0.00%)	0 (0.00%)	0 (0.00%)	0 (0.00%)	20 (100.00%)
Maintenance Blade	4 (57.14%)	2 (28.57%)	0 (0.00%)	0 (0.00%)	0 (0.00%)	1 (14.29%)	0 (0.00%)	0 (0.00%)	7 (100.00%)
Crest (Bladelet)	0 (0.00%)	0 (0.00%)	1 (100.00%)	0 (0.00%)	0 (0.00%)	0 (0.00%)	0 (0.00%)	0 (0.00%)	1 (100.00%)
Asymmetrical Bladelet	1 (3.45%)	15 (51.72%)	11 (37.93%)	0 (0.00%)	0 (0.00%)	0 (0.00%)	0 (0.00%)	2 (6.90%)	29 (100.00%)
Overshot Bladelet	1 (16.67%)	4 (66.67%)	1 (16.67%)	0 (0.00%)	0 (0.00%)	0 (0.00%)	0 (0.00%)	0 (0.00%)	6 (100.00%)
Maintenance Bladelet	4 (80.00%)	0 (0.00%)	1 (20.00%)	0 (0.00%)	0 (0.00%)	0 (0.00%)	0 (0.00%)	0 (0.00%)	5 (100.00%)
Simple Blade	63 (29.30%)	119 (55.35%)	27 (12.56%)	0 (0.00%)	1 (0.47%)	0 (0.00%)	0 (0.00%)	5 (2.33%)	215 (100.00%)
Simple Bladelet	63 (27.63%)	113 (49.56%)	47 (20.61%)	0 (0.00%)	0 (0.00%)	1 (0.44%)	2 (0.88%)	2 (0.88%)	228 (100.00%)
Burin Spall	1 (20.00%)	0 (0.00%)	2 (40.00%)	0 (0.00%)	0 (0.00%)	0 (0.00%)	2 (40.00%)	0 (0.00%)	5 (100.00%)
Total	225 (30.57%)	360 (48.91%)	115 (15.63%)	2 (0.27%)	1 (0.14%)	5 (0.68%)	8 (1.09%)	20 (2.72%)	736 (100.00%)

Table 33 Cortex coverage in Flakes, Al-Ansab 1.

	No Cortex	Semi Cortical				Extensively Cortical		Entames	Total
		Lateral	*Distal*	*Dorsal*	*Proximal*	*Distal*	*Dorsal*	*Dorsal*	
					2009-2011				
Surface Cleaning Flake	17 (65.38%)	6 (23.08%)	1 (3.85%)	1 (3.85%)	1 (3.85%)	0 (0.00%)	0 (0.00%)	0 (0.00%)	26 (100.00%)
Maintenance Flake	8 (53.33%)	2 (13.33%)	0 (0.00%)	1 (6.67%)	2 (13.33%)	1 (6.67%)	1 (6.67%)	0 (0.00%)	15 (100.00%)
Core Tablet	3 (30.00%)	3 (30.00%)	0 (0.00%)	3 (30.00%)	1 (10.00%)	0 (0.00%)	0 (0.00%)	0 (0.00%)	10 (100.00%)
Cortical Flake	0 (0.00%)	2 (16.67%)	1 (8.33%)	1 (8.33%)	0 (0.00%)	0 (0.00%)	4 (33.33%)	4 (33.33%)	12 (100.00%)
Simple Flake	3 (50.00%)	2 (33.33%)	0 (0.00%)	0 (0.00%)	1 (16.67%)	0 (0.00%)	0 (0.00%)	0 (0.00%)	6 (100.00%)
Total	31 (44.93%)	15 (21.74%)	2 (2.90%)	6 (8.70%)	5 (7.25%)	1 (1.45%)	5 (7.25%)	4 (5.80%)	69 (100.00%)
					2018				
Surface Cleaning Flake	74 (63.79%)	20 (17.24%)	10 (8.62%)	7 (6.03%)	1 (0.86%)		3 (2.59%)	1 (0.86%)	116 (100.00%)
Maintenance Flake	5 (100.00%)	0 (0.00%)	0 (0.00%)	0 (0.00%)	0 (0.00%)		0 (0.00%)	0 (0.00%)	5 (100.00%)
Core Tablet	27 (71.05%)	5 (13.16%)	1 (2.63%)	1 (2.63%)	0 (0.00%)		2 (5.26%)	2 (5.26%)	38 (100.00%)
Cortical Flake	0 (0.00%)	1 (2.44%)	4 (9.76%)	7 (17.07%)	1 (2.44%)		12 (29.27%)	16 (39.02%)	41 (100.00%)
Simple Flake	18 (78.26%)	2 (8.70%)	2 (8.70%)	0 (0.00%)	1 (4.35%)		0 (0.00%)	0 (0.00%)	23 (100.00%)
Total	124 (55.61%)	28 (12.56%)	17 (7.62%)	15 (6.73%)	3 (1.35%)		17 (7.62%)	19 (8.52%)	223 (100.00%)

Table 34 Cortex coverage in Blades and Bladelets, Al-Ansab 1.

	No Cortex	Semi Cortical					Extensively Cortical		Entames		Total
		Lateral	*Distal*	*Dorsal*	*Proximal*	*Proximal and Distal*	*Lateral*	*Dorsal*	*Distal*	*Dorsal*	
						2009-2011					
Crest	7 (63.64%)	2 (18.18%)	0 (0.00%)	1 (9.09%)	1 (9.09%)		0 (0.00%)	0 (0.00%)		0 (0.00%)	11 (100.00%)
Asymmetrical Blade	56 (61.54%)	24 (26.37%)	7 (7.69%)	2 (2.20%)	0 (0.00%)		0 (0.00%)	1 (1.10%)		0 (0.00%)	91 (100.00%)
Overshot Blade	24 (45.28%)	5 (9.43%)	22 (41.51%)	1 (1.89%)	0 (0.00%)		1 (1.89%)	0 (0.00%)		1 (1.89%)	53 (100.00%)
Surface Cleaning Blade	5 (50.00%)	2 (20.00%)	2 (20.00%)	0 (0.00%)	1 (10.00%)		0 (0.00%)	0 (0.00%)		0 (0.00%)	10 (100.00%)
Maintenance Blade	0 (0.00%)	0 (0.00%)	0 (0.00%)	1 (33.33%)	0 (0.00%)		1 (33.33%)	1 (33.33%)		1 (33.33%)	3 (100.00%)
Crest (Bladelet)	1 (50.00%)	1 (50.00%)	0 (0.00%)	0 (0.00%)	0 (0.00%)		0 (0.00%)	0 (0.00%)		0 (0.00%)	2 (100.00%)
Asymmetrical Bladelet	32 (74.42%)	8 (18.60%)	1 (2.33%)	1 (2.33%)	0 (0.00%)		0 (0.00%)	1 (2.33%)		0 (0.00%)	43 (100.00%)
Overshot Bladelet	7 (70.00%)	0 (0.00%)	3 (30.00%)	0 (0.00%)	0 (0.00%)		0 (0.00%)	0 (0.00%)		0 (0.00%)	10 (100.00%)
Maintenance Bladelet	1 (50.00%)	1 (50.00%)	0 (0.00%)	0 (0.00%)	0 (0.00%)		0 (0.00%)	0 (0.00%)		0 (0.00%)	2 (100.00%)
Simple Blade	132 (95.65%)	2 (1.45%)	3 (2.17%)	1 (0.72%)	0 (0.00%)		0 (0.00%)	0 (0.00%)		0 (0.00%)	138 (100.00%)
Simple Bladelet	358 (99.44%)	1 (0.28%)	0 (0.00%)	0 (0.00%)	1 (0.28%)		0 (0.00%)	0 (0.00%)		0 (0.00%)	360 (100.00%)
Burin Spall	1 (100.00%)	0 (0.00%)	0 (0.00%)	0 (0.00%)	0 (0.00%)		0 (0.00%)	0 (0.00%)		0 (0.00%)	1 (100.00%)
Blade Tablet	0 (0.00%)	1 (100.00%)	0 (0.00%)	0 (0.00%)	0 (0.00%)		0 (0.00%)	0 (0.00%)		0 (0.00%)	1 (100.00%)
Total	624 (86.07%)	47 (6.48%)	38 (5.24%)	7 (0.97%)	3 (0.41%)		2 (0.28%)	3 (0.41%)		2 (0.28%)	725 (100.00%)

	No Cortex	Semi Cortical					Extensively Cortical		Entames		Total
		Lateral	*Distal*	*Dorsal*	*Proximal*	*Proximal and Distal*	*Lateral*	*Dorsal*	*Distal*	*Dorsal*	
						2018					
Crest	40 (65.57%)	8 (13.11%)	2 (3.28%)	4 (6.56%)	0 (0.00%)	0 (0.00%)	2 (3.28%)	3 (4.92%)	1 (1.64%)	1 (1.64%)	61 (100.00%)
Asymmetrical Blade	82 (56.16%)	32 (21.92%)	10 (6.85%)	7 (4.79%)	5 (3.42%)	0 (0.00%)	2 (1.37%)	4 (2.74%)	0 (0.00%)	4 (2.74%)	146 (100.00%)
Overshot Blade	39 (44.32%)	13 (14.77%)	29 (32.95%)	4 (4.55%)	1 (1.14%)	0 (0.00%)	0 (0.00%)	2 (2.27%)	0 (0.00%)	0 (0.00%)	88 (100.00%)
Surface Cleaning Blade	21 (84.00%)	3 (12.00%)	1 (4.00%)	0 (0.00%)	0 (0.00%)	0 (0.00%)	0 (0.00%)	0 (0.00%)	0 (0.00%)	0 (0.00%)	25 (100.00%)
Maintenance Blade	7 (46.67%)	4 (26.67%)	1 (6.67%)	0 (0.00%)	0 (0.00%)	0 (0.00%)	1 (6.67%)	2 (13.33%)	0 (0.00%)	0 (0.00%)	15 (100.00%)
Crest (Bladelet)	4 (80.00%)	0 (0.00%)	1 (20.00%)	0 (0.00%)	0 (0.00%)	0 (0.00%)	0 (0.00%)	0 (0.00%)	0 (0.00%)	0 (0.00%)	5 (100.00%)
Asymmetrical Bladelet	28 (82.35%)	2 (5.88%)	2 (5.88%)	0 (0.00%)	0 (0.00%)	0 (0.00%)	0 (0.00%)	2 (5.88%)	0 (0.00%)	0 (0.00%)	34 (100.00%)
Overshot Bladelet	5 (55.56%)	0 (0.00%)	4 (44.44%)	0 (0.00%)	0 (0.00%)	0 (0.00%)	0 (0.00%)	0 (0.00%)	0 (0.00%)	0 (0.00%)	9 (100.00%)
Maintenance Bladelet	3 (60.00%)	1 (20.00%)	1 (20.00%)	0 (0.00%)	0 (0.00%)	0 (0.00%)	0 (0.00%)	0 (0.00%)	0 (0.00%)	0 (0.00%)	5 (100.00%)
Simple Blade	273 (85.85%)	28 (8.81%)	6 (1.89%)	7 (2.20%)	0 (0.00%)	0 (0.00%)	2 (0.63%)	2 (0.63%)	0 (0.00%)	0 (0.00%)	318 (100.00%)
Simple Bladelet	313 (95.72%)	7 (2.14%)	3 (0.92%)	1 (0.31%)	0 (0.00%)	1 (0.31%)	0 (0.00%)	2 (0.61%)	0 (0.00%)	0 (0.00%)	327 (100.00%)
Burin Spall	9 (100.00%)	0 (0.00%)	0 (0.00%)	0 (0.00%)	0 (0.00%)	0 (0.00%)	0 (0.00%)	0 (0.00%)	0 (0.00%)	0 (0.00%)	9 (100.00%)
Total	824 (79.08%)	98 (9.40%)	60 (5.76%)	23 (2.21%)	6 (0.58%)	1 (0.10%)	7 (0.67%)	17 (1.63%)	1 (0.10%)	5 (0.48%)	1042 (100.00%)

Table 35 Negatives types in Flakes, Al-Ansab 1.

	Bladelets	Bladelets & Flakes	Blades	Blades & Bladelets	Blades & Flakes	Blades, Bladelets & Flakes	Flakes	No negatives	Indeterminate	Total
						2009-2011				
Surface Cleaning Flake	4 (15.38%)	0 (0.00%)	8 (30.77%)	3 (11.54%)	2 (7.69%)	0 (0.00%)	6 (23.08%)	3 (11.54%)		26 (100.00%)
Maintenance Flake	1 (6.67%)	1 (6.67%)	6 (40.00%)	0 (0.00%)	1 (6.67%)	0 (0.00%)	6 (40.00%)	0 (0.00%)		15 (100.00%)
Core Tablet	0 (0.00%)	1 (10.00%)	0 (0.00%)	1 (10.00%)	0 (0.00%)	3 (30.00%)	4 (40.00%)	1 (10.00%)		10 (100.00%)
Cortical Flake	1 (8.33%)	0 (0.00%)	0 (0.00%)	0 (0.00%)	0 (0.00%)	1 (8.33%)	4 (33.33%)	6 (50.00%)		12 (100.00%)
Simple Flake	0 (0.00%)	0 (0.00%)	0 (0.00%)	0 (0.00%)	0 (0.00%)	0 (0.00%)	4 (66.67%)	2 (33.33%)		6 (100.00%)
Total	6 (8.70%)	2 (2.90%)	14 (20.29%)	4 (5.80%)	3 (4.35%)	4 (5.80%)	24 (34.78%)	12 (17.39%)		69 (100.00%)
						2018				
Surface Cleaning Flake	13 (11.21%)	5 (4.31%)	12 (10.34%)	8 (6.90%)	2 (1.72%)	0 (0.00%)	23 (19.83%)	0 (0.00%)	53 (45.69%)	116 (100.00%)
Maintenance Flake	0 (0.00%)	0 (0.00%)	0 (0.00%)	0 (0.00%)	0 (0.00%)	0 (0.00%)	0 (0.00%)	0 (0.00%)	5 (100.00%)	5 (100.00%)
Core Tablet	9 (23.68%)	3 (7.89%)	3 (7.89%)	6 (15.79%)	3 (7.89%)	1 (2.63%)	5 (13.16%)	4 (10.53%)	4 (10.53%)	38 (100.00%)
Cortical Flake	0 (0.00%)	0 (0.00%)	0 (0.00%)	0 (0.00%)	0 (0.00%)	0 (0.00%)	12 (29.27%)	20 (48.78%)	9 (21.95%)	41 (100.00%)
Simple Flake	0 (0.00%)	0 (0.00%)	0 (0.00%)	0 (0.00%)	0 (0.00%)	0 (0.00%)	2 (8.70%)	6 (26.09%)	15 (65.22%)	23 (100.00%)
Total	22 (9.87%)	8 (3.59%)	15 (6.73%)	14 (6.28%)	5 (2.24%)	1 (0.45%)	42 (18.83%)	30 (13.45%)	86 (38.57%)	223 (100.00%)

Table 36 Negatives types in Blades and Bladelets, Al-Ansab 1.

	Bladelets	Bladelets & Flakes	Blades	Blades & Bladelets	Blades & Flakes	Blades, Bladelets & Flakes	Flakes	No negatives	Indeterminate	Total
2009-2011										
Crest	0 (0.00%)	7 (63.64%)	0 (0.00%)	0 (0.00%)	1 (9.09%)	0 (0.00%)	2 (18.18%)	0 (0.00%)	1 (9.09%)	11 (100.00%)
Asymmetrical Blade	33 (36.26%)	3 (3.30%)	25 (27.47%)	20 (21.98%)	2 (2.20%)	0 (0.00%)	3 (3.30%)	2 (2.20%)	3 (3.30%)	91 (100.00%)
Overshot Blade	26 (49.06%)	2 (3.77%)	7 (13.21%)	14 (26.42%)	1 (1.89%)	1 (1.89%)	0 (0.00%)	1 (1.89%)	1 (1.89%)	53 (100.00%)
Surface Cleaning Blade	1 (10.00%)	1 (10.00%)	1 (10.00%)	1 (10.00%)	4 (40.00%)	1 (10.00%)	1 (10.00%)	0 (0.00%)	0 (0.00%)	10 (100.00%)
Maintenance Blade	0 (0.00%)	0 (0.00%)	0 (0.00%)	1 (33.33%)	0 (0.00%)	0 (0.00%)	0 (0.00%)	2 (66.67%)	0 (0.00%)	3 (100.00%)
Crest (Bladelet)	0 (0.00%)	1 (50.00%)	0 (0.00%)	0 (0.00%)	0 (0.00%)	0 (0.00%)	1 (50.00%)	0 (0.00%)	0 (0.00%)	2 (100.00%)
Asymmetrical Bladelet	30 (69.77%)	0 (0.00%)	3 (6.98%)	5 (11.63%)	0 (0.00%)	0 (0.00%)	1 (2.33%)	1 (2.33%)	3 (6.98%)	43 (100.00%)
Overshot Bladelet	8 (80.00%)	0 (0.00%)	0 (0.00%)	2 (20.00%)	0 (0.00%)	0 (0.00%)	0 (0.00%)	0 (0.00%)	0 (0.00%)	10 (100.00%)
Maintenance Bladelet	0 (0.00%)	0 (0.00%)	0 (0.00%)	0 (0.00%)	0 (0.00%)	0 (0.00%)	0 (0.00%)	1 (50.00%)	1 (50.00%)	2 (100.00%)
Simple Blade	95 (68.84%)	0 (0.00%)	9 (6.52%)	13 (9.42%)	1 (0.72%)	0 (0.00%)	0 (0.00%)	1 (0.72%)	19 (13.77%)	138 (100.00%)
Simple Bladelet	217 (60.28%)	0 (0.00%)	0 (0.00%)	0 (0.00%)	0 (0.00%)	0 (0.00%)	0 (0.00%)	24 (6.67%)	119 (33.06%)	360 (100.00%)
Burin Spall	0 (0.00%)	0 (0.00%)	0 (0.00%)	0 (0.00%)	0 (0.00%)	0 (0.00%)	0 (0.00%)	0 (0.00%)	1 (100.00%)	1 (100.00%)
Blade Tablet	0 (0.00%)	0 (0.00%)	0 (0.00%)	1 (100.00%)	0 (0.00%)	0 (0.00%)	0 (0.00%)	0 (0.00%)	0 (0.00%)	1 (100.00%)
Total	410 (56.55%)	14 (1.93%)	45 (6.21%)	57 (7.86%)	9 (1.24%)	2 (0.28%)	8 (1.10%)	32 (4.41%)	148 (20.41%)	725 (100.00%)

	Bladelets	Bladelets & Flakes	Blades	Blades & Bladelets	Blades & Flakes	Blades, Bladelets & Flakes	Flakes	No negatives	Indeterminate	Total
						2018				
Crest	5 (8.20%)	9 (14.75%)	2 (3.28%)	5 (8.20%)	4 (6.56%)	6 (9.84%)	19 (31.15%)	3 (4.92%)	8 (13.11%)	61 (100.00%)
Asymmetrical Blade	55 (37.67%)	1 (0.68%)	10 (6.85%)	24 (16.44%)	0 (0.00%)	1 (0.68%)	2 (1.37%)	6 (4.11%)	47 (32.19%)	146 (100.00%)
Overshot Blade	45 (51.14%)	0 (0.00%)	8 (9.09%)	25 (28.41%)	0 (0.00%)	0 (0.00%)	0 (0.00%)	0 (0.00%)	10 (11.36%)	88 (100.00%)
Surface Cleaning Blade	8 (32.00%)	0 (0.00%)	3 (12.00%)	6 (24.00%)	0 (0.00%)	0 (0.00%)	2 (8.00%)	0 (0.00%)	6 (24.00%)	25 (100.00%)
Maintenance Blade	1 (6.67%)	0 (0.00%)	0 (0.00%)	1 (6.67%)	0 (0.00%)	0 (0.00%)	1 (6.67%)	1 (6.67%)	11 (73.33%)	15 (100.00%)
Crest (Bladelet)	1 (20.00%)	2 (40.00%)	0 (0.00%)	0 (0.00%)	0 (0.00%)	0 (0.00%)	1 (20.00%)	1 (20.00%)	0 (0.00%)	5 (100.00%)
Asymmetrical Bladelet	18 (52.94%)	0 (0.00%)	0 (0.00%)	0 (0.00%)	0 (0.00%)	0 (0.00%)	0 (0.00%)	0 (0.00%)	16 (47.06%)	34 (100.00%)
Overshot Bladelet	8 (88.89%)	0 (0.00%)	0 (0.00%)	0 (0.00%)	0 (0.00%)	0 (0.00%)	0 (0.00%)	0 (0.00%)	1 (11.11%)	9 (100.00%)
Maintenance Bladelet	1 (20.00%)	0 (0.00%)	0 (0.00%)	0 (0.00%)	0 (0.00%)	0 (0.00%)	0 (0.00%)	2 (40.00%)	2 (40.00%)	5 (100.00%)
Simple Blade	164 (51.57%)	1 (0.31%)	11 (3.46%)	34 (10.69%)	0 (0.00%)	0 (0.00%)	0 (0.00%)	1 (0.31%)	107 (33.65%)	318 (100.00%)
Simple Bladelet	173 (52.91%)	0 (0.00%)	0 (0.00%)	0 (0.00%)	0 (0.00%)	0 (0.00%)	0 (0.00%)	1 (0.31%)	153 (46.79%)	327 (100.00%)
Burin Spall	0 (0.00%)	0 (0.00%)	0 (0.00%)	0 (0.00%)	0 (0.00%)	0 (0.00%)	0 (0.00%)	8 (88.89%)	1 (11.11%)	9 (100.00%)
Total	479 (45.97%)	13 (1.25%)	34 (3.26%)	95 (9.12%)	4 (0.38%)	7 (0.67%)	25 (2.40%)	23 (2.21%)	362 (34.74%)	1042 (100.00%)

Table 37 Negatives orientations in Flakes, Al-Ansab 1. Combinations having less than 1% of the total are combined.

	Bipolar	Bipolar Combinations	Convergent	Crossed	Indeterminate	No negatives	Orthogonal	Unipolar	Unipolar+ Convergent	Unipolar+ Crossed	Unipolar+ Orthogonal	Total
						2009-2011						
Surface Cleaning Flake	0 (0.00%)		2 (7.69%)	5 (19.23%)		3 (11.54%)	0 (0.00%)	15 (57.69%)	0 (0.00%)	0 (0.00%)	1 (3.85%)	26 (100.00%)
Maintenance Flake	2 (13.33%)		0 (0.00%)	4 (26.67%)		0 (0.00%)	0 (0.00%)	6 (40.00%)	1 (6.67%)	1 (6.67%)	1 (6.67%)	15 (100.00%)
Core Tablet	0 (0.00%)		0 (0.00%)	1 (10.00%)		1 (10.00%)	2 (20.00%)	2 (20.00%)	0 (0.00%)	0 (0.00%)	4 (40.00%)	10 (100.00%)
Cortical Flake	0 (0.00%)		0 (0.00%)	2 (16.67%)		6 (50.00%)	1 (8.33%)	1 (8.33%)	0 (0.00%)	0 (0.00%)	2 (16.67%)	12 (100.00%)
Simple Flake	1 (16.67%)		0 (0.00%)	2 (33.33%)		2 (33.33%)	0 (0.00%)	0 (0.00%)	0 (0.00%)	0 (0.00%)	1 (16.67%)	6 (100.00%)
Total	3 (4.35%)		2 (2.90%)	14 (20.29%)		12 (17.39%)	3 (4.35%)	24 (34.78%)	1 (1.45%)	1 (1.45%)	9 (13.04%)	69 (100.00%)
						2018						
Surface Cleaning Flake	3 (2.59%)	0 (0.00%)	8 (6.90%)	4 (3.45%)	0 (0.00%)	0 (0.00%)	5 (4.31%)	85 (73.28%)	6 (5.17%)	2 (1.72%)	3 (2.59%)	116 (100.00%)
Maintenance Flake	0 (0.00%)	0 (0.00%)	0 (0.00%)	1 (20.00%)	0 (0.00%)	0 (0.00%)	0 (0.00%)	4 (80.00%)	0 (0.00%)	0 (0.00%)	0 (0.00%)	5 (100.00%)
Core Tablet	0 (0.00%)	1 (2.63%)	0 (0.00%)	1 (2.63%)	0 (0.00%)	4 (10.53%)	22 (57.89%)	6 (15.79%)	0 (0.00%)	0 (0.00%)	4 (10.53%)	38 (100.00%)
Cortical Flake	3 (7.32%)	1 (2.44%)	0 (0.00%)	3 (7.32%)	0 (0.00%)	20 (48.78%)	1 (2.44%)	13 (31.71%)	0 (0.00%)	0 (0.00%)	0 (0.00%)	41 (100.00%)
Simple Flake	0 (0.00%)	0 (0.00%)	1 (4.35%)	2 (8.70%)	1 (4.35%)	6 (26.09%)	1 (4.35%)	11 (47.83%)	0 (0.00%)	1 (4.35%)	0 (0.00%)	23 (100.00%)
Total	6 (2.69%)	2 (0.90%)	9 (4.04%)	11 (4.93%)	1 (0.45%)	30 (13.45%)	29 (13.00%)	119 (53.36%)	6 (2.69%)	3 (1.35%)	7 (3.14%)	223 (100.00%)

Table 38 Negatives orientation in Blades and Bladelets, Al-Ansab 1. Combinations not reaching 1% of the total are combined

	Bipolar	Bipolar Combinations	Convergent	Crossed	No negatives	Orthogonal	Unipolar	Unipolar+ Convergent	Unipolar+ Crossed	Unipolar+ Orthogonal	Unipolar Combinations	Total
						2009-2011						
Crest	0 (0.00%)	0 (0.00%)	0 (0.00%)	0 (0.00%)	0 (0.00%)	2 (18.18%)	0 (0.00%)	0 (0.00%)	0 (0.00%)	8 (72.73%)	1 (9.09%)	11 (100.00%)
Asymmetrical Blade	7 (7.69%)	3 (3.30%)	2 (2.20%)	9 (9.89%)	2 (2.20%)	0 (0.00%)	49 (53.85%)	10 (10.99%)	7 (7.69%)	2 (2.20%)	0 (0.00%)	91 (100.00%)
Overshot Blade	3 (5.66%)	0 (0.00%)	2 (3.77%)	2 (3.77%)	1 (1.89%)	0 (0.00%)	21 (39.62%)	15 (28.30%)	4 (7.55%)	2 (3.77%)	3 (5.66%)	53 (100.00%)
Surface Cleaning Blade	2 (20.00%)	0 (0.00%)	0 (0.00%)	1 (10.00%)	0 (0.00%)	0 (0.00%)	3 (30.00%)	0 (0.00%)	1 (10.00%)	3 (30.00%)	0 (0.00%)	10 (100.00%)
Maintenance Blade	1 (33.33%)	0 (0.00%)	0 (0.00%)	0 (0.00%)	2 (66.67%)	0 (0.00%)	0 (0.00%)	0 (0.00%)	0 (0.00%)	0 (0.00%)	0 (0.00%)	3 (100.00%)
Crest (Bladelet)	0 (0.00%)	0 (0.00%)	0 (0.00%)	0 (0.00%)	0 (0.00%)	1 (50.00%)	0 (0.00%)	0 (0.00%)	0 (0.00%)	1 (50.00%)	0 (0.00%)	2 (100.00%)
Asymmetrical Bladelet	0 (0.00%)	0 (0.00%)	1 (2.33%)	2 (4.65%)	1 (2.33%)	0 (0.00%)	26 (60.47%)	6 (13.95%)	3 (6.98%)	4 (9.30%)	0 (0.00%)	43 (100.00%)
Overshot Bladelet	0 (0.00%)	0 (0.00%)	0 (0.00%)	0 (0.00%)	0 (0.00%)	0 (0.00%)	3 (30.00%)	5 (50.00%)	2 (20.00%)	0 (0.00%)	0 (0.00%)	10 (100.00%)
Maintenance Bladelet	1 (50.00%)	0 (0.00%)	0 (0.00%)	0 (0.00%)	1 (50.00%)	0 (0.00%)	0 (0.00%)	0 (0.00%)	0 (0.00%)	0 (0.00%)	0 (0.00%)	2 (100.00%)
Simple Blade	13 (9.42%)	1 (0.72%)	5 (3.62%)	5 (3.62%)	1 (0.72%)	0 (0.00%)	78 (56.52%)	26 (18.84%)	8 (5.80%)	1 (0.72%)	0 (0.00%)	138 (100.00%)
Simple Bladelet	4 (1.11%)	1 (0.28%)	14 (3.89%)	4 (1.11%)	24 (6.67%)	0 (0.00%)	185 (51.39%)	119 (33.06%)	6 (1.67%)	2 (0.56%)	1 (0.28%)	360 (100.00%)
Burin Spall	0 (0.00%)	0 (0.00%)	0 (0.00%)	0 (0.00%)	0 (0.00%)	0 (0.00%)	1 (100.00%)	0 (0.00%)	0 (0.00%)	0 (0.00%)	0 (0.00%)	1 (100.00%)
Blade Tablet	1 (100.00%)	0 (0.00%)	0 (0.00%)	0 (0.00%)	0 (0.00%)	0 (0.00%)	0 (0.00%)	0 (0.00%)	0 (0.00%)	0 (0.00%)	0 (0.00%)	1 (100.00%)
Total	32 (4.41%)	5 (0.69%)	24 (3.31%)	23 (3.17%)	32 (4.41%)	3 (0.41%)	366 (50.48%)	181 (24.97%)	31 (4.28%)	23 (3.17%)	5 (0.69%)	725 (100.00%)

	Bipolar	Convergent	Crossed	Indeterminate	No negatives	Orthogonal	Orthogonal Combinations	Unipolar	Unipolar+ Convergent	Unipolar+ Orthogonal	Unipolar Combinations	Total
							2018					
Crest	1 (1.64%)	3 (4.92%)	0 (0.00%)	0 (0.00%)	3 (4.92%)	13 (21.31%)	5 (8.20%)	13 (21.31%)	3 (4.92%)	19 (31.15%)	1 (1.64%)	61 (100.00%)
Asymmetrical Blade	3 (2.05%)	24 (16.44%)	5 (3.42%)	0 (0.00%)	6 (4.11%)	1 (0.68%)	1 (0.68%)	89 (60.96%)	16 (10.96%)	0 (0.00%)	1 (0.68%)	146 (100.00%)
Overshot Blade	1 (1.14%)	16 (18.18%)	3 (3.41%)	0 (0.00%)	0 (0.00%)	0 (0.00%)	0 (0.00%)	60 (68.18%)	7 (7.95%)	0 (0.00%)	1 (1.14%)	88 (100.00%)
Surface Cleaning Blade	0 (0.00%)	0 (0.00%)	1 (4.00%)	0 (0.00%)	0 (0.00%)	1 (4.00%)	0 (0.00%)	21 (84.00%)	2 (8.00%)	0 (0.00%)	0 (0.00%)	25 (100.00%)
Maintenance Blade	0 (0.00%)	1 (6.67%)	0 (0.00%)	0 (0.00%)	1 (6.67%)	0 (0.00%)	0 (0.00%)	13 (86.67%)	0 (0.00%)	0 (0.00%)	0 (0.00%)	15 (100.00%)
Crest (Bladelet)	0 (0.00%)	1 (20.00%)	0 (0.00%)	0 (0.00%)	1 (20.00%)	0 (0.00%)	0 (0.00%)	0 (0.00%)	0 (0.00%)	3 (60.00%)	0 (0.00%)	5 (100.00%)
Asymmetrical Bladelet	0 (0.00%)	3 (8.82%)	2 (5.88%)	0 (0.00%)	0 (0.00%)	0 (0.00%)	0 (0.00%)	28 (82.35%)	1 (2.94%)	0 (0.00%)	0 (0.00%)	34 (100.00%)
Overshot Bladelet	0 (0.00%)	4 (44.44%)	0 (0.00%)	0 (0.00%)	0 (0.00%)	0 (0.00%)	0 (0.00%)	4 (44.44%)	1 (11.11%)	0 (0.00%)	0 (0.00%)	9 (100.00%)
Maintenance Bladelet	0 (0.00%)	0 (0.00%)	0 (0.00%)	0 (0.00%)	2 (40.00%)	0 (0.00%)	0 (0.00%)	3 (60.00%)	0 (0.00%)	0 (0.00%)	0 (0.00%)	5 (100.00%)
Simple Blade	0 (0.00%)	27 (8.49%)	5 (1.57%)	1 (0.31%)	1 (0.31%)	0 (0.00%)	0 (0.00%)	248 (77.99%)	32 (10.06%)	2 (0.63%)	2 (0.63%)	318 (100.00%)
Simple Bladelet	2 (0.61%)	48 (14.68%)	5 (1.53%)	0 (0.00%)	1 (0.31%)	0 (0.00%)	0 (0.00%)	214 (65.44%)	54 (16.51%)	0 (0.00%)	3 (0.92%)	327 (100.00%)
Burin Spall	0 (0.00%)	0 (0.00%)	0 (0.00%)	0 (0.00%)	8 (88.89%)	0 (0.00%)	0 (0.00%)	1 (11.11%)	0 (0.00%)	0 (0.00%)	0 (0.00%)	9 (100.00%)
Total	7 (0.67%)	127 (12.19%)	21 (2.02%)	1 (0.10%)	23 (2.21%)	15 (1.44%)	6 (0.58%)	694 (66.60%)	116 (11.13%)	24 (2.30%)	8 (0.77%)	1042 (100.00%)

Table 39 Distal termination in Blades and Bladelets, Al-Ansab 1

	2009-2011					
	Feathered	**Plunging**	**Hinged**	**Stepped**	**Indeterminate**	**Total**
Crest	2 (18.18%)	6 (54.55%)	1 (9.09%)	1 (9.09%)	1 (9.09%)	11 (100.00%)
Asymmetrical Blade	21 (29.58%)	43 (60.56%)	4 (5.63%)	3 (4.23%)	0 (0.00%)	71 (100.00%)
Overshot Blade	1 (1.89%)	44 (83.02%)	1 (1.89%)	7 (13.21%)	0 (0.00%)	53 (100.00%)
Surface Cleaning Blade	3 (30.00%)	4 (40.00%)	2 (20.00%)	1 (10.00%)	0 (0.00%)	10 (100.00%)
Maintenance Blade	1 (50.00%)	0 (0.00%)	1 (50.00%)	0 (0.00%)	0 (0.00%)	2 (100.00%)
Crest (Bladelet)	0 (0.00%)	2 (100.00%)	0 (0.00%)	0 (0.00%)	0 (0.00%)	2 (100.00%)
Asymmetrical Bladelet	6 (22.22%)	20 (74.07%)	0 (0.00%)	1 (3.70%)	0 (0.00%)	27 (100.00%)
Overshot Bladelet	1 (11.11%)	6 (66.67%)	1 (11.11%)	1 (11.11%)	0 (0.00%)	9 (100.00%)
Maintenance Bladelet	0 (0.00%)	0 (0.00%)	1 (50.00%)	0 (0.00%)	1 (50.00%)	2 (100.00%)
Simple Blade	54 (70.13%)	10 (12.99%)	9 (11.69%)	1 (1.30%)	3 (3.90%)	77 (100.00%)
Simple Bladelet	148 (84.09%)	7 (3.98%)	11 (6.25%)	6 (3.41%)	4 (2.27%)	176 (100.00%)
Burin Spall	1 (100.00%)	0 (0.00%)	0 (0.00%)	0 (0.00%)	0 (0.00%)	1 (100.00%)
Total	238 (53.97%)	142 (32.20%)	31 (7.03%)	21 (4.76%)	9 (2.04%)	441 (100.00%)
	2018					
	Feathered	**Plunging**	**Hinged**	**Stepped**	**Indeterminate**	**Total**
Crest	23 (37.70%)	28 (45.90%)	1 (1.64%)	9 (14.75%)	0 (0.00%)	61 (100.00%)
Asymmetrical Blade	31 (24.41%)	68 (53.54%)	6 (4.72%)	21 (16.54%)	1 (0.79%)	127 (100.00%)
Overshot Blade	1 (1.19%)	69 (82.14%)	1 (1.19%)	13 (15.48%)	0 (0.00%)	84 (100.00%)
Surface Cleaning Blade	11 (45.83%)	3 (12.50%)	5 (20.83%)	5 (20.83%)	0 (0.00%)	24 (100.00%)
Maintenance Blade	6 (37.50%)	1 (6.25%)	3 (18.75%)	6 (37.50%)	0 (0.00%)	16 (100.00%)
Crest (Bladelet)	1 (20.00%)	3 (60.00%)	0 (0.00%)	1 (20.00%)	0 (0.00%)	5 (100.00%)
Asymmetrical Bladelet	10 (34.48%)	18 (62.07%)	0 (0.00%)	1 (3.45%)	0 (0.00%)	29 (100.00%)
Overshot Bladelet	0 (0.00%)	8 (100.00%)	0 (0.00%)	0 (0.00%)	0 (0.00%)	8 (100.00%)
Maintenance Bladelet	0 (0.00%)	1 (33.33%)	0 (0.00%)	2 (66.67%)	0 (0.00%)	3 (100.00%)
Simple Blade	188 (80.34%)	22 (9.40%)	4 (1.71%)	11 (4.70%)	9 (3.85%)	234 (100.00%)
Simple Bladelet	207 (90.00%)	2 (0.87%)	7 (3.04%)	3 (1.30%)	11 (4.78%)	230 (100.00%)
Burin Spall	9 (100.00%)	0 (0.00%)	0 (0.00%)	0 (0.00%)	0 (0.00%)	9 (100.00%)
Total	487 (58.67%)	223 (26.87%)	27 (3.25%)	72 (8.67%)	21 (2.53%)	830 (100.00%)

Table 40 Outline in Blades and Bladelets, Al-Ansab 1

	2009-2011				
	(sub)Parallel Edges	**Convergent**	**Off-axis**	**Indeterminate**	**Total**
Crest	4 (36.36%)	3 (27.27%)	4 (36.36%)	(0.00%)	11 (100.00%)
Surface Cleaning Blade	7 (70.00%)	2 (20.00%)	1 (10.00%)	(0.00%)	10 (100.00%)
Maintenance Blade	2 (100.00%)	(0.00%)	(0.00%)	(0.00%)	2 (100.00%)
Asymmetrical Blade	9 (12.68%)	19 (26.76%)	43 (60.56%)	(0.00%)	71 (100.00%)
Overshot Blade	33 (62.26%)	10 (18.87%)	10 (18.87%)	(0.00%)	53 (100.00%)
Crest (Bladelet)	(0.00%)	1 (50.00%)	1 (50.00%)	(0.00%)	2 (100.00%)
Maintenance Bladelet	(0.00%)	(0.00%)	1 (50.00%)	1 (50.00%)	2 (100.00%)
Asymmetrical Bladelet	4 (14.81%)	6 (22.22%)	17 (62.96%)	(0.00%)	27 (100.00%)
Overshot Bladelet	6 (66.67%)	(0.00%)	3 (33.33%)	(0.00%)	9 (100.00%)
Simple Blade	35 (45.45%)	34 (44.16%)	5 (6.49%)	3 (3.90%)	77 (100.00%)
Simple Bladelet	54 (30.68%)	108 (61.36%)	10 (5.68%)	4 (2.27%)	176 (100.00%)
Burin Spall	1 (100.00%)	(0.00%)	(0.00%)	(0.00%)	1 (100.00%)
Total	155 (35.15%)	183 (41.50%)	95 (21.54%)	8 (1.81%)	441 (100.00%)
	2018				
	(sub)Parallel Edges	**Convergent**	**Off-axis**	**Indeterminate**	**Total**
Crest	23 (37.70%)	9 (14.75%)	29 (47.54%)	(0.00%)	61 (100.00%)
Surface Cleaning Blade	21 (87.50%)	1 (4.17%)	2 (8.33%)	(0.00%)	24 (100.00%)
Maintenance Blade	8 (50.00%)	3 (18.75%)	4 (25.00%)	1 (6.25%)	16 (100.00%)
Asymmetrical Blade	20 (15.75%)	4 (3.15%)	102 (80.31%)	1 (0.79%)	127 (100.00%)
Overshot Blade	78 (92.86%)	1 (1.19%)	5 (5.95%)	(0.00%)	84 (100.00%)
Crest (Bladelet)	2 (40.00%)	(0.00%)	3 (60.00%)	(0.00%)	5 (100.00%)
Maintenance Bladelet	1 (33.33%)	1 (33.33%)	1 (33.33%)	(0.00%)	3 (100.00%)
Asymmetrical Bladelet	2 (6.90%)	3 (10.34%)	24 (82.76%)	(0.00%)	29 (100.00%)
Overshot Bladelet	7 (87.50%)	(0.00%)	1 (12.50%)	(0.00%)	8 (100.00%)
Simple Blade	128 (54.70%)	67 (28.63%)	39 (16.67%)	(0.00%)	234 (100.00%)
Simple Bladelet	85 (36.96%)	98 (42.61%)	47 (20.43%)	(0.00%)	230 (100.00%)
Burin Spall	7 (77.78%)	2 (22.22%)	(0.00%)	(0.00%)	9 (100.00%)
Total	382 (46.02%)	189 (22.77%)	257 (30.96%)	2 (0.24%)	830 (100.00%)

Table 41 Profile in Blades and Bladelets, Al-Ansab 1

	2009-2011						
	Straight	**Slightly Curved**	**Curved**	**Very Curved**	**Twisted**	**Indeterminate**	**Total**
Crest	2 (18.18%)	1 (9.09%)	5 (45.45%)	1 (9.09%)	2 (18.18%)	0 (0.00%)	11 (100.00%)
Asymmetrical Blade	22 (24.18%)	14 (15.38%)	12 (13.19%)	2 (2.20%)	40 (43.96%)	1 (1.10%)	91 (100.00%)
Overshot Blade	1 (1.89%)	14 (26.42%)	21 (39.62%)	11 (20.75%)	6 (11.32%)	0 (0.00%)	53 (100.00%)
Surface Cleaning Blade	2 (20.00%)	5 (50.00%)	2 (20.00%)	0 (0.00%)	1 (10.00%)	0 (0.00%)	10 (100.00%)
Maintenance Blade	3 (100.00%)	0 (0.00%)	0 (0.00%)	0 (0.00%)	0 (0.00%)	0 (0.00%)	3 (100.00%)
Crest (Bladelet)	0 (0.00%)	1 (50.00%)	1 (50.00%)	0 (0.00%)	0 (0.00%)	0 (0.00%)	2 (100.00%)
Asymmetrical Bladelet	11 (25.58%)	9 (20.93%)	4 (9.30%)	0 (0.00%)	19 (44.19%)	0 (0.00%)	43 (100.00%)
Overshot Bladelet	1 (10.00%)	5 (50.00%)	1 (10.00%)	1 (10.00%)	2 (20.00%)	0 (0.00%)	10 (100.00%)
Maintenance Bladelet	1 (50.00%)	0 (0.00%)	0 (0.00%)	0 (0.00%)	0 (0.00%)	1 (50.00%)	2 (100.00%)
Simple Blade	87 (63.04%)	25 (18.12%)	15 (10.87%)	0 (0.00%)	9 (6.52%)	2 (1.45%)	138 (100.00%)
Simple Bladelet	226 (62.78%)	65 (18.06%)	10 (2.78%)	1 (0.28%)	36 (10.00%)	22 (6.11%)	360 (100.00%)
Burin Spall	1 (100.00%)	0 (0.00%)	0 (0.00%)	0 (0.00%)	0 (0.00%)	0 (0.00%)	1 (100.00%)
Total	357 (49.31%)	139 (19.20%)	71 (9.81%)	16 (2.21%)	115 (15.88%)	26 (3.59%)	724 (100.00%)
				2018			
Crest	20 (32.79%)	10 (16.39%)	4 (6.56%)	3 (4.92%)	24 (39.34%)	0 (0.00%)	61 (100.00%)
Asymmetrical Blade	12 (8.22%)	9 (6.16%)	18 (12.33%)	5 (3.42%)	101 (69.18%)	1 (0.68%)	146 (100.00%)
Overshot Blade	8 (9.09%)	19 (21.59%)	34 (38.64%)	14 (15.91%)	13 (14.77%)	0 (0.00%)	88 (100.00%)
Surface Cleaning Blade	17 (68.00%)	5 (20.00%)	0 (0.00%)	0 (0.00%)	3 (12.00%)	0 (0.00%)	25 (100.00%)
Maintenance Blade	10 (58.82%)	1 (5.88%)	1 (5.88%)	0 (0.00%)	5 (29.41%)	0 (0.00%)	17 (100.00%)
Crest (Bladelet)	2 (40.00%)	1 (20.00%)	1 (20.00%)	0 (0.00%)	1 (20.00%)	0 (0.00%)	5 (100.00%)
Asymmetrical Bladelet	2 (5.88%)	0 (0.00%)	0 (0.00%)	0 (0.00%)	32 (94.12%)	0 (0.00%)	34 (100.00%)
Overshot Bladelet	0 (0.00%)	2 (22.22%)	7 (77.78%)	0 (0.00%)	0 (0.00%)	0 (0.00%)	9 (100.00%)
Maintenance Bladelet	1 (33.33%)	0 (0.00%)	1 (33.33%)	0 (0.00%)	1 (33.33%)	0 (0.00%)	3 (100.00%)
Simple Blade	174 (56.68%)	63 (20.52%)	27 (8.79%)	1 (0.33%)	39 (12.70%)	3 (0.98%)	307 (100.00%)
Simple Bladelet	197 (60.62%)	53 (16.31%)	6 (1.85%)	0 (0.00%)	69 (21.23%)	0 (0.00%)	325 (100.00%)
Burin Spall	8 (88.89%)	0 (0.00%)	0 (0.00%)	0 (0.00%)	1 (11.11%)	0 (0.00%)	9 (100.00%)
Total	451 (43.83%)	163 (15.84%)	99 (9.62%)	23 (2.24%)	289 (28.09%)	4 (0.39%)	1029 (100.00%)

Table 42 Cross-sections in Blades and Bladelets, Al-Ansab 1

	2009-2011						
	Flat	**Trapezoidal Asymm**	**Trapezoidal Symm**	**Triangular Asymm**	**Triangular Symm**	**Indeterminate**	**Total**
Crest	0 (0.00%)	1 (9.09%)	0 (0.00%)	8 (72.73%)	2 (18.18%)	0 (0.00%)	11 (100.00%)
Asymmetrical Blade	6 (6.59%)	23 (25.27%)	6 (6.59%)	38 (41.76%)	18 (19.78%)	0 (0.00%)	91 (100.00%)
Overshot Blade	2 (3.77%)	34 (64.15%)	4 (7.55%)	6 (11.32%)	7 (13.21%)	0 (0.00%)	53 (100.00%)
Surface Cleaning Blade	1 (10.00%)	6 (60.00%)	2 (20.00%)	1 (10.00%)	0 (0.00%)	0 (0.00%)	10 (100.00%)
Maintenance Blade	0 (0.00%)	1 (33.33%)	0 (0.00%)	2 (66.67%)	0 (0.00%)	0 (0.00%)	3 (100.00%)
Crest (Bladelet)	0 (0.00%)	0 (0.00%)	0 (0.00%)	2 (100.00%)	0 (0.00%)	0 (0.00%)	2 (100.00%)
Asymmetrical Bladelet	2 (4.65%)	5 (11.63%)	0 (0.00%)	32 (74.42%)	4 (9.30%)	0 (0.00%)	43 (100.00%)
Overshot Bladelet	0 (0.00%)	7 (70.00%)	2 (20.00%)	0 (0.00%)	1 (10.00%)	0 (0.00%)	10 (100.00%)
Maintenance Bladelet	0 (0.00%)	0 (0.00%)	0 (0.00%)	1 (50.00%)	0 (0.00%)	1 (50.00%)	2 (100.00%)
Simple Blade	2 (1.45%)	52 (37.68%)	26 (18.84%)	33 (23.91%)	25 (18.12%)	0 (0.00%)	138 (100.00%)
Simple Bladelet	31 (8.61%)	56 (15.56%)	71 (19.72%)	102 (28.33%)	90 (25.00%)	10 (2.78%)	360 (100.00%)
Burin Spall	0 (0.00%)	0 (0.00%)	0 (0.00%)	1 (100.00%)	0 (0.00%)	0 (0.00%)	1 (100.00%)
Total	44 (6.08%)	185 (25.55%)	111 (15.33%)	226 (31.22%)	147 (20.30%)	11 (1.52%)	724 (100.00%)
				2018			
Crest	3 (4.92%)	23 (37.70%)	3 (4.92%)	24 (39.34%)	8 (13.11%)	0 (0.00%)	61 (100.00%)
Asymmetrical Blade	10 (6.85%)	80 (54.79%)	7 (4.79%)	44 (30.14%)	4 (2.74%)	1 (0.68%)	146 (100.00%)
Overshot Blade	3 (3.41%)	52 (59.09%)	26 (29.55%)	6 (6.82%)	1 (1.14%)	0 (0.00%)	88 (100.00%)
Surface Cleaning Blade	3 (12.00%)	13 (52.00%)	3 (12.00%)	5 (20.00%)	1 (4.00%)	0 (0.00%)	25 (100.00%)
Maintenance Blade	2 (11.76%)	6 (35.29%)	2 (11.76%)	5 (29.41%)	0 (0.00%)	2 (11.76%)	17 (100.00%)
Crest (Bladelet)	0 (0.00%)	2 (40.00%)	0 (0.00%)	3 (60.00%)	0 (0.00%)	0 (0.00%)	5 (100.00%)
Asymmetrical Bladelet	2 (5.88%)	9 (26.47%)	3 (8.82%)	17 (50.00%)	3 (8.82%)	0 (0.00%)	34 (100.00%)
Overshot Bladelet	1 (11.11%)	3 (33.33%)	2 (22.22%)	2 (22.22%)	1 (11.11%)	0 (0.00%)	9 (100.00%)
Maintenance Bladelet	0 (0.00%)	0 (0.00%)	0 (0.00%)	2 (66.67%)	1 (33.33%)	0 (0.00%)	3 (100.00%)
Simple Blade	4 (1.30%)	123 (40.07%)	88 (28.66%)	52 (16.94%)	40 (13.03%)	0 (0.00%)	307 (100.00%)
Simple Bladelet	7 (2.15%)	66 (20.31%)	103 (31.69%)	63 (19.38%)	85 (26.15%)	1 (0.31%)	325 (100.00%)
Burin Spall	0 (0.00%)	0 (0.00%)	1 (11.11%)	0 (0.00%)	8 (88.89%)	0 (0.00%)	9 (100.00%)
Total	35 (3.40%)	377 (36.64%)	238 (23.13%)	223 (21.67%)	152 (14.77%)	4 (0.39%)	1029 (100.00%)

Table 43 Fragmentation, Românești-Dumbrăvița I GH3

	Blade	Bladelet	Flake	Total
Complete	131 (49.81%)	106 (36.93%)	481 (88.42%)	718 (65.63%)
Mes+Dist	48 (18.25%)	95 (33.10%)	18 (3.31%)	161 (14.72%)
Prox+Mes	84 (31.94%)	86 (29.97%)	45 (8.27%)	215 (19.65%)
Total	263 (100.00%)	287 (100.00%)	544 (100.00%)	1094 (100.00%)

Table 44 Lipping in blanks, Românești -Dumbrăvița I GH3

	Yes	No	Total
Simple Blade	54 (54.00%)	46 (46.00%)	100 (100.00%)
Management Blade	36 (34.95%)	67 (65.05%)	103 (100.00%)
Simple Bladelet	44 (34.65%)	83 (65.35%)	127 (100.00%)
Management Bladelet	11 (31.43%)	24 (68.57%)	35 (100.00%)
Burin Spall	2 (14.29%)	12 (85.71%)	14 (100.00%)
Blade Tablet	0 (0.00%)	7 (100.00%)	7 (100.00%)
Management Flake	102 (41.46%)	144 (58.54%)	246 (100.00%)
Core Tablet	24 (36.92%)	41 (63.08%)	65 (100.00%)
Cortical Flake	21 (32.31%)	44 (67.69%)	65 (100.00%)
Simple Flake	32 (25.81%)	92 (74.19%)	124 (100.00%)
Total	326 (36.79%)	560 (63.21%)	886 (100.00%)

Table 45 Overhang abrasion in laminar blanks, Românești -Dumbrăvița I GH3

	Yes	No	Total
Simple Blade	84 (84.00%)	16 (16.00%)	100 (100.00%)
Management Blade	61 (59.22%)	42 (40.78%)	103 (100.00%)
Simple Bladelet	106 (83.46%)	21 (16.54%)	127 (100.00%)
Management Bladelet	12 (34.29%)	23 (65.71%)	35 (100.00%)
Blade Tablet	1 (20.00%)	4 (80.00%)	5 (100.00%)
Burin Spall	4 (28.57%)	10 (71.43%)	14 (100.00%)
Total	268 (69.61%)	117 (30.39%)	385 (100.00%)

Table 46 Overhang abrasion in Cores Românești -Dumbrăvița I GH3

	Yes	No	Total
Pre-Core	0 (0.00%)	3 (100.00%)	3 (100.00%)
Semi Tournant	4 (80.00%)	1 (20.00%)	5 (100.00%)
Narrow Fronted sur Tranche	4 (50.00%)	4 (50.00%)	8 (100.00%)
Blades-Not Organised	1 (100.00%)	0 (0.00%)	1 (100.00%)
Fragment	0 (0.00%)	1 (100.00%)	1 (100.00%)
Total	9 (50.00%)	9 (50.00%)	18 (100.00%)

Table 47 Bulbs values, Românești -Dumbrăvița I GH3

	Diffused	Not Perceived	Pronounced	Bulbar Scar	Indeterminate	Crushed	Total
Simple Blade	77 (74.76%)	2 (1.94%)	15 (14.56%)	2 (1.94%)	4 (3.88%)	3 (2.91%)	103 (100.00%)
Management Blade	79 (72.48%)	0 (0.00%)	20 (18.35%)	1 (0.92%)	6 (5.50%)	3 (2.75%)	109 (100.00%)
Simple Bladelet	117 (86.03%)	0 (0.00%)	11 (8.09%)	2 (1.47%)	4 (2.94%)	2 (1.47%)	136 (100.00%)
Management Bladelet	34 (97.14%)	0 (0.00%)	0 (0.00%)	0 (0.00%)	0 (0.00%)	1 (2.86%)	35 (100.00%)
Burin Spall	14 (82.35%)	2 (11.76%)	0 (0.00%)	0 (0.00%)	1 (5.88%)	0 (0.00%)	17 (100.00%)
Blade Tablet	3 (42.86%)	0 (0.00%)	1 (14.29%)	0 (0.00%)	3 (42.86%)	0 (0.00%)	7 (100.00%)
Management Flake	120 (47.62%)	0 (0.00%)	114 (45.24%)	8 (3.17%)	7 (2.78%)	3 (1.19%)	252 (100.00%)
Core Tablet	24 (35.82%)	0 (0.00%)	35 (52.24%)	3 (4.48%)	5 (7.46%)	0 (0.00%)	67 (100.00%)
Cortical Flake	26 (37.68%)	0 (0.00%)	40 (57.97%)	0 (0.00%)	3 (4.35%)	0 (0.00%)	69 (100.00%)
Simple Flake	63 (45.65%)	0 (0.00%)	59 (42.75%)	2 (1.45%)	13 (9.42%)	1 (0.72%)	138 (100.00%)
Total	557 (59.70%)	4 (0.43%)	295 (31.62%)	18 (1.93%)	46 (4.93%)	13 (1.39%)	933 (100.00%)

Table 48 Knapping angles in blanks, Românești -Dumbrăvița I GH3

	<70	70-90	>90	Indeterminate	Total
Simple Blade	32 (31.07%)	58 (56.31%)	0 (0.00%)	13 (12.62%)	103 (100.00%)
Management Blade	41 (37.61%)	47 (43.12%)	1 (0.92%)	20 (18.35%)	109 (100.00%)
Simple Bladelet	27 (19.85%)	58 (42.65%)	0 (0.00%)	51 (37.50%)	136 (100.00%)
Management Bladelet	7 (20.00%)	17 (48.57%)	0 (0.00%)	11 (31.43%)	35 (100.00%)
Burin Spall	2 (11.76%)	4 (23.53%)	0 (0.00%)	11 (64.71%)	17 (100.00%)
Blade Tablet	0 (0.00%)	3 (42.86%)	0 (0.00%)	4 (57.14%)	7 (100.00%)
Management Flake	79 (31.35%)	136 (53.97%)	4 (1.59%)	33 (13.10%)	252 (100.00%)
Core Tablet	17 (25.37%)	41 (61.19%)	3 (4.48%)	6 (8.96%)	67 (100.00%)
Cortical Flake	16 (23.19%)	38 (55.07%)	0 (0.00%)	15 (21.74%)	69 (100.00%)
Simple Flake	32 (23.19%)	59 (42.75%)	5 (3.62%)	42 (30.43%)	138 (100.00%)
Total	253 (27.12%)	461 (49.41%)	13 (1.39%)	206 (22.08%)	933 (100.00%)

Table 49 Knapping angles in Cores, Românești -Dumbrăvița I GH3

	<70	70-90	Indeterminate	Total
Pre-Core	1 (33.33%)	2 (66.67%)	0 (0.00%)	3 (100.00%)
Semi Tournant	3 (60.00%)	1 (20.00%)	1 (20.00%)	5 (100.00%)
Narrow Fronted sur Tranche	3 (37.50%)	5 (62.50%)	0 (0.00%)	8 (100.00%)
Blades-Not Organised	0 (0.00%)	1 (100.00%)	0 (0.00%)	1 (100.00%)
Fragment	1 (100.00%)	0 (0.00%)	0 (0.00%)	1 (100.00%)
Total	8 (44.44%)	9 (50.00%)	1 (5.56%)	18 (100.00%)

Table 50 Core blanks, Românești -Dumbrăviţa I GH3

	Blank	Cobble	Indeterminate	Nodule	Slab	Squared Chunk	Total
Semi Tournant	1 (20.00%)	1 (20.00%)	0 (0.00%)	3 (60.00%)	0 (0.00%)	0 (0.00%)	5 (100.00%)
Narrow Fronted sur Tranche	5 (62.50%)	0 (0.00%)	0 (0.00%)	0 (0.00%)	2 (25.00%)	1 (12.50%)	8 (100.00%)
Blades-Not Organised	1 (100.00%)	0 (0.00%)	0 (0.00%)	0 (0.00%)	0 (0.00%)	0 (0.00%)	1 (100.00%)
Pre-Core	0 (0.00%)	0 (0.00%)	0 (0.00%)	2 (66.67%)	0 (0.00%)	1 (33.33%)	3 (100.00%)
Fragment	0 (0.00%)	0 (0.00%)	1 (100.00%)	0 (0.00%)	0 (0.00%)	0 (0.00%)	1 (100.00%)
Total	7 (38.89%)	1 (5.56%)	1 (5.56%)	5 (27.78%)	2 (11.11%)	2 (11.11%)	18 (100.00%)

Table 51 Cortex position in cores, Românești-Dumbrăviţa I GH3

	No Cortex	Lateral	Back	Back & Base	Back & Lateral	Frontal	Top	Total
Semi Tournant	2 (40.00%)	0 (0.00%)	0 (0.00%)	1 (20.00%)	1 (20.00%)	1 (20.00%)	0 (0.00%)	5 (100.00%)
Narrow Fronted sur Tranche	4 (50.00%)	3 (37.50%)	1 (12.50%)	0 (0.00%)	0 (0.00%)	0 (0.00%)	0 (0.00%)	8 (100.00%)
Pre-Core	1 (33.33%)	0 (0.00%)	1 (33.33%)	0 (0.00%)	0 (0.00%)	0 (0.00%)	1 (33.33%)	3 (100.00%)
Blades-Not Organised	1 (100.00%)	0 (0.00%)	0 (0.00%)	0 (0.00%)	0 (0.00%)	0 (0.00%)	0 (0.00%)	1 (100.00%)
Fragment	1 (100.00%)	0 (0.00%)	0 (0.00%)	0 (0.00%)	0 (0.00%)	0 (0.00%)	0 (0.00%)	1 (100.00%)
Total	9 (50.00%)	3 (16.67%)	2 (11.11%)	1 (5.56%)	1 (5.56%)	1 (5.56%)	1 (5.56%)	18 (100.00%)

Table 52 Striking platform type, Românești -Dumbrăviţa I GH3

	Natural	Plain	Total
Semi Tournant	0 (0.00%)	5 (100.00%)	5 (100.00%)
Narrow Fronted sur Tranche	2 (25.00%)	6 (75.00%)	8 (100.00%)
Pre-Core	0 (0.00%)	3 (100.00%)	3 (100.00%)
Blades-Not Organised	0 (0.00%)	1 (100.00%)	1 (100.00%)
Fragment	0 (0.00%)	1 (100.00%)	1 (100.00%)
Total	2 (11.11%)	16 (88.89%)	18 (100.00%)

Table 53 Striking platform relationship, Românești -Dumbrăviţa I GH3

	Single	Opposed	Opposed auxiliary	Adjacent	Independent	Total
Semi Tournant	3 (60.00%)	1 (20.00%)	0 (0.00%)	1 (20.00%)	0 (0.00%)	5 (100.00%)
Narrow Fronted sur Tranche	6 (75.00%)	1 (12.50%)	1 (12.50%)	0 (0.00%)	0 (0.00%)	8 (100.00%)
Pre-Core	2 (66.67%)	0 (0.00%)	0 (0.00%)	0 (0.00%)	1 (33.33%)	3 (100.00%)
Blades-Not Organised	1 (100.00%)	0 (0.00%)	0 (0.00%)	0 (0.00%)	0 (0.00%)	1 (100.00%)
Fragment	1 (100.00%)	0 (0.00%)	0 (0.00%)	0 (0.00%)	0 (0.00%)	1 (100.00%)
Total	13 (72.22%)	2 (11.11%)	1 (5.56%)	1 (5.56%)	1 (5.56%)	18 (100.00%)

Table 54 Flaking Surface relationship, Românești -Dumbrăvița I GH3

	Single Surface	Adjacent-Orthogonal	Independent	Subsequent	Total
Semi Tournant	3 (60.00%)	0 (0.00%)	1 (20.00%)	1 (20.00%)	5 (100.00%)
Narrow Fronted sur Tranche	7 (87.50%)	1 (12.50%)	0 (0.00%)	0 (0.00%)	8 (100.00%)
Pre-Core	2 (66.67%)	0 (0.00%)	1 (33.33%)	0 (0.00%)	3 (100.00%)
Blades-Not Organised	0 (0.00%)	1 (100.00%)	0 (0.00%)	0 (0.00%)	1 (100.00%)
Fragment	1 (100.00%)	0 (0.00%)	0 (0.00%)	0 (0.00%)	1 (100.00%)
Total	13 (72.22%)	2 (11.11%)	2 (11.11%)	1 (5.56%)	18 (100.00%)

Table 55 Negatives types in Cores, Românești -Dumbrăvița I GH3

	Bladelets	Blades	Blades & Bladelets	Blades, Bladelets & Flakes	Indeterminate	No negatives	Total
Semi Tournant	1 (20.00%)	0 (0.00%)	4 (80.00%)	0 (0.00%)	0 (0.00%)	0 (0.00%)	5 (100.00%)
Narrow Fronted sur Tranche	5 (62.50%)	0 (0.00%)	2 (25.00%)	0 (0.00%)	1 (12.50%)	0 (0.00%)	8 (100.00%)
Pre-Core	1 (33.33%)	1 (33.33%)	0 (0.00%)	0 (0.00%)	0 (0.00%)	1 (33.33%)	3 (100.00%)
Blades-Not Organised	0 (0.00%)	0 (0.00%)	0 (0.00%)	1 (100.00%)	0 (0.00%)	0 (0.00%)	1 (100.00%)
Fragment	0 (0.00%)	0 (0.00%)	1 (100.00%)	0 (0.00%)	0 (0.00%)	0 (0.00%)	1 (100.00%)
Total	7 (38.89%)	1 (5.56%)	7 (38.89%)	1 (5.56%)	1 (5.56%)	1 (5.56%)	18 (100.00%)

Table 56 Negatives orientation in Cores Românești -Dumbrăvița I GH3

	Bipolar	Convergent	Unipolar	Unipolar+ Convergent	No negatives	Total
Semi Tournant	1 (20.00%)	0 (0.00%)	3 (60.00%)	1 (20.00%)	0 (0.00%)	5 (100.00%)
Narrow Fronted sur Tranche	0 (0.00%)	0 (0.00%)	8 (100.00%)	0 (0.00%)	0 (0.00%)	8 (100.00%)
Pre-Core	0 (0.00%)	0 (0.00%)	2 (66.67%)	0 (0.00%)	1 (33.33%)	3 (100.00%)
Blades-Not Organised	0 (0.00%)	1 (100.00%)	0 (0.00%)	0 (0.00%)	0 (0.00%)	1 (100.00%)
Fragment	0 (0.00%)	0 (0.00%)	1 (100.00%)	0 (0.00%)	0 (0.00%)	1 (100.00%)
Total	1 (20.00%)	1 (5.56%)	14 (77.78%)	1 (5.56%)	1 (5.56%)	18 (100.00%)

Table 57 Butts in Blades and Bladelets, Românești -Dumbrăvița I GH3.

	Plain	Linear	Punctiform	Dihedral	Facetted	Natural	Crushed	Indeterminate	Total
Crest	2 (25.00%)	(0.00%)	4 (50.00%)	(0.00%)	(0.00%)	1 (12.50%)	(0.00%)	1 (12.50%)	8 (100.00%)
Asymmetrical Blade	31 (49.21%)	11 (17.46%)	7 (11.11%)	1 (1.59%)	(0.00%)	7 (11.11%)	4 (6.35%)	2 (3.17%)	63 (100.00%)
Overshot Blade	9 (64.29%)	1 (7.14%)	2 (14.29%)	(0.00%)	(0.00%)	(0.00%)	1 (7.14%)	1 (7.14%)	14 (100.00%)
Surface Cleaning Blade	9 (56.25%)	3 (18.75%)	1 (6.25%)	1 (6.25%)	(0.00%)	1 (6.25%)	1 (6.25%)	(0.00%)	16 (100.00%)
Maintenance Blade	5 (62.50%)	(0.00%)	2 (25.00%)	(0.00%)	(0.00%)	1 (12.50%)	(0.00%)	(0.00%)	8 (100.00%)
Crest (Bladelet)	3 (75.00%)	1 (25.00%)	(0.00%)	(0.00%)	(0.00%)	(0.00%)	(0.00%)	(0.00%)	4 (100.00%)
Asymmetrical Bladelet	8 (38.10%)	5 (23.81%)	6 (28.57%)	(0.00%)	(0.00%)	1 (4.76%)	(0.00%)	1 (4.76%)	21 (100.00%)
Overshot Bladelet	(0.00%)	(0.00%)	(0.00%)	(0.00%)	(0.00%)	(0.00%)	(0.00%)	1 (100.00%)	1 (100.00%)
Surface Cleaning Bladelet	2 (100.00%)	(0.00%)	(0.00%)	(0.00%)	(0.00%)	(0.00%)	(0.00%)	(0.00%)	2 (100.00%)
Maintenance Bladelet	6 (85.71%)	1 (14.29%)	(0.00%)	(0.00%)	(0.00%)	(0.00%)	(0.00%)	(0.00%)	7 (100.00%)
Simple Blade	54 (52.43%)	25 (24.27%)	12 (11.65%)	(0.00%)	2 (1.94%)	4 (3.88%)	3 (2.91%)	3 (2.91%)	103 (100.00%)
Simple Bladelet	37 (27.21%)	56 (41.18%)	27 (19.85%)	1 (0.74%)	(0.00%)	1 (0.74%)	9 (6.62%)	5 (3.68%)	136 (100.00%)
Burin Spall	7 (41.18%)	1 (5.88%)	5 (29.41%)	(0.00%)	(0.00%)	1 (5.88%)	3 (17.65%)	(0.00%)	17 (100.00%)
Blade Tablet	1 (14.29%)	(0.00%)	6 (85.71%)	(0.00%)	(0.00%)	(0.00%)	(0.00%)	(0.00%)	7 (100.00%)
Total	174 (42.75%)	104 (25.55%)	72 (17.69%)	3 (0.74%)	2 (0.49%)	17 (4.18%)	21 (5.16%)	14 (3.44%)	407 (100.00%)

Table 58 Butts in Flakes, Românești -Dumbrăvița I GH3

	Plain	Linear	Punctiform	Dihedral	Facetted	Natural	Crushed	Indeterminate	Total
Surface Cleaning Flake	62 (65.26%)	12 (12.63%)	14 (14.74%)	2 (2.11%)	1 (1.05%)	3 (3.16%)	1 (1.05%)	0 (0.00%)	95 (100.00%)
Maintenance Flake	96 (61.15%)	21 (13.38%)	11 (7.01%)	4 (2.55%)	3 (1.91%)	10 (6.37%)	5 (3.18%)	7 (4.46%)	157 (100.00%)
Core Tablet	24 (35.82%)	2 (2.99%)	6 (8.96%)	6 (8.96%)	16 (23.88%)	10 (14.93%)	2 (2.99%)	1 (1.49%)	67 (100.00%)
Cortical Flake	39 (56.52%)	5 (7.25%)	9 (13.04%)	0 (0.00%)	0 (0.00%)	8 (11.59%)	4 (5.80%)	4 (5.80%)	69 (100.00%)
Simple Flake	73 (52.90%)	14 (10.14%)	17 (12.32%)	1 (0.72%)	3 (2.17%)	12 (8.70%)	14 (10.14%)	4 (2.90%)	138 (100.00%)
Total	294 (55.89%)	54 (10.27%)	57 (10.84%)	13 (2.47%)	23 (4.37%)	43 (8.17%)	26 (4.94%)	16 (3.04%)	526 (100.00%)

Table 59 Cortex coverage in Flakes, Românești-Dumbrăvița I GH3

	No Cortex	Semi Cortical						Extensively Cortical		Entames	Total
		Lateral	*Proximal*	*Distal*	*Distal+Lateral*	*Dorsal*	*Basal*	*Dorsal*	*Dorsal + Lateral*	*Dorsal*	
Surface Cleaning Flake	88 (85.44%)	2 (1.94%)	3 (2.91%)	5 (4.85%)	1 (0.97%)	3 (2.91%)	0 (0.00%)	1 (0.97%)	0 (0.00%)	0 (0.00%)	103 (100.00%)
Maintenance Flake	135 (82.82%)	8 (4.91%)	2 (1.23%)	5 (3.07%)	0 (0.00%)	11 (6.75%)	1 (0.61%)	1 (0.61%)	0 (0.00%)	0 (0.00%)	163 (100.00%)
Core Tablet	48 (71.64%)	2 (2.99%)	6 (8.96%)	4 (5.97%)	0 (0.00%)	2 (2.99%)	0 (0.00%)	4 (5.97%)	0 (0.00%)	1 (1.49%)	67 (100.00%)
Cortical Flake	1 (1.41%)	5 (7.04%)	3 (4.23%)	6 (8.45%)	0 (0.00%)	9 (12.68%)	0 (0.00%)	30 (42.25%)	1 (1.41%)	16 (22.54%)	71 (100.00%)
Simple Flake	118 (84.29%)	6 (4.29%)	11 (7.86%)	2 (1.43%)	0 (0.00%)	3 (2.14%)	0 (0.00%)	0 (0.00%)	0 (0.00%)	0 (0.00%)	140 (100.00%)
Total	390 (71.69%)	23 (4.23%)	25 (4.60%)	22 (4.04%)	1 (0.18%)	28 (5.15%)	1 (0.18%)	36 (6.62%)	1 (0.18%)	17 (3.13%)	544 (100.00%)

Table 60 Cortex coverage in Blades and Bladelets, Românești-Dumbrăvița I GH3.

	No Cortex	Semi Cortical						Extensively Cortical		Total
		Lateral	*Proximal*	*Proximal+Lateral*	*Proximal+Distal*	*Distal*	*Dorsal*	*Lateral*	*Dorsal*	
Crest	4 (44.44%)	1 (11.11%)	0 (0.00%)	1 (11.11%)	0 (0.00%)	1 (11.11%)	0 (0.00%)	1 (11.11%)	1 (11.11%)	9 (100.00%)
Asymmetrical Blade	50 (68.49%)	15 (20.55%)	1 (1.37%)	0 (0.00%)	1 (1.37%)	3 (4.11%)	2 (2.74%)	0 (0.00%)	1 (1.37%)	73 (100.00%)
Overshot Blade	12 (63.16%)	1 (5.26%)	0 (0.00%)	0 (0.00%)	0 (0.00%)	6 (31.58%)	0 (0.00%)	0 (0.00%)	0 (0.00%)	19 (100.00%)
Surface Cleaning Blade	14 (77.78%)	0 (0.00%)	0 (0.00%)	0 (0.00%)	1 (5.56%)	0 (0.00%)	1 (5.56%)	0 (0.00%)	2 (11.11%)	18 (100.00%)
Maintenance Blade	11 (84.62%)	0 (0.00%)	1 (7.69%)	0 (0.00%)	0 (0.00%)	0 (0.00%)	1 (7.69%)	0 (0.00%)	0 (0.00%)	13 (100.00%)
Crest (Bladelet)	7 (87.50%)	0 (0.00%)	0 (0.00%)	0 (0.00%)	0 (0.00%)	0 (0.00%)	1 (12.50%)	0 (0.00%)	0 (0.00%)	8 (100.00%)
Asymmetrical Bladelet	24 (80.00%)	3 (10.00%)	0 (0.00%)	0 (0.00%)	0 (0.00%)	2 (6.67%)	1 (3.33%)	0 (0.00%)	0 (0.00%)	30 (100.00%)
Overshot Bladelet	4 (66.67%)	0 (0.00%)	0 (0.00%)	0 (0.00%)	0 (0.00%)	2 (33.33%)	0 (0.00%)	0 (0.00%)	0 (0.00%)	6 (100.00%)
Surface Cleaning Bladelet	2 (66.67%)	0 (0.00%)	0 (0.00%)	0 (0.00%)	0 (0.00%)	0 (0.00%)	0 (0.00%)	0 (0.00%)	1 (33.33%)	3 (100.00%)
Maintenance Bladelet	8 (80.00%)	0 (0.00%)	0 (0.00%)	0 (0.00%)	0 (0.00%)	1 (10.00%)	1 (10.00%)	0 (0.00%)	0 (0.00%)	10 (100.00%)
Simple Blade	119 (92.97%)	3 (2.34%)	4 (3.13%)	0 (0.00%)	0 (0.00%)	2 (1.56%)	0 (0.00%)	0 (0.00%)	0 (0.00%)	128 (100.00%)
Simple Bladelet	195 (99.49%)	0 (0.00%)	0 (0.00%)	0 (0.00%)	0 (0.00%)	0 (0.00%)	1 (0.51%)	0 (0.00%)	0 (0.00%)	196 (100.00%)
Burin Spall	27 (90.00%)	0 (0.00%)	1 (3.33%)	0 (0.00%)	0 (0.00%)	1 (3.33%)	0 (0.00%)	0 (0.00%)	1 (3.33%)	30 (100.00%)
Blade Tablet	7 (100.00%)	0 (0.00%)	0 (0.00%)	0 (0.00%)	0 (0.00%)	0 (0.00%)	0 (0.00%)	0 (0.00%)	0 (0.00%)	7 (100.00%)
Total	484 (88.00%)	23 (4.18%)	7 (1.27%)	1 (0.18%)	2 (0.36%)	18 (3.27%)	8 (1.45%)	1 (0.18%)	6 (1.09%)	550 (100.00%)

Table 61 Negatives type in Blades and Bladelets, Românești-Dumbrăvița I GH3.

	Bladelets	Bladelets & Flakes	Blades	Blades & Bladelets	Blades & Flakes	Flakes	Indeterminate	No negatives	Total
Crest	0 (0.00%)	0 (0.00%)	0 (0.00%)	0 (0.00%)	1 (11.11%)	2 (22.22%)	2 (22.22%)	4 (44.44%)	9 (100.00%)
Asymmetrical Blade	16 (21.92%)	0 (0.00%)	10 (13.70%)	3 (4.11%)	0 (0.00%)	2 (2.74%)	35 (47.95%)	7 (9.59%)	73 (100.00%)
Overshot Blade	8 (42.11%)	0 (0.00%)	3 (15.79%)	2 (10.53%)	0 (0.00%)	0 (0.00%)	6 (31.58%)	0 (0.00%)	19 (100.00%)
Surface Cleaning Blade	6 (33.33%)	0 (0.00%)	3 (16.67%)	1 (5.56%)	1 (5.56%)	1 (5.56%)	3 (16.67%)	3 (16.67%)	18 (100.00%)
Maintenance Blade	2 (15.38%)	0 (0.00%)	0 (0.00%)	0 (0.00%)	0 (0.00%)	0 (0.00%)	11 (84.62%)	0 (0.00%)	13 (100.00%)
Crest (Bladelet)	4 (50.00%)	0 (0.00%)	0 (0.00%)	0 (0.00%)	0 (0.00%)	1 (12.50%)	1 (12.50%)	2 (25.00%)	8 (100.00%)
Asymmetrical Bladelet	10 (33.33%)	0 (0.00%)	0 (0.00%)	1 (3.33%)	0 (0.00%)	0 (0.00%)	12 (40.00%)	7 (23.33%)	30 (100.00%)
Overshot Bladelet	4 (66.67%)	0 (0.00%)	0 (0.00%)	0 (0.00%)	0 (0.00%)	0 (0.00%)	2 (33.33%)	0 (0.00%)	6 (100.00%)
Surface Cleaning Bladelet	1 (33.33%)	0 (0.00%)	0 (0.00%)	0 (0.00%)	0 (0.00%)	0 (0.00%)	2 (66.67%)	0 (0.00%)	3 (100.00%)
Maintenance Bladelet	0 (0.00%)	0 (0.00%)	0 (0.00%)	0 (0.00%)	0 (0.00%)	0 (0.00%)	5 (50.00%)	5 (50.00%)	10 (100.00%)
Simple Blade	34 (26.56%)	0 (0.00%)	20 (15.63%)	10 (7.81%)	0 (0.00%)	2 (1.56%)	60 (46.88%)	2 (1.56%)	128 (100.00%)
Simple Bladelet	58 (29.59%)	0 (0.00%)	0 (0.00%)	0 (0.00%)	0 (0.00%)	2 (1.02%)	127 (64.80%)	9 (4.59%)	196 (100.00%)
Burin Spall	4 (13.33%)	0 (0.00%)	0 (0.00%)	0 (0.00%)	0 (0.00%)	0 (0.00%)	3 (10.00%)	23 (76.67%)	30 (100.00%)
Blade Tablet	1 (14.29%)	1 (14.29%)	1 (14.29%)	1 (14.29%)	0 (0.00%)	0 (0.00%)	1 (14.29%)	2 (28.57%)	7 (100.00%)
Total	148 (26.91%)	1 (0.18%)	37 (6.73%)	18 (3.27%)	2 (0.36%)	10 (1.82%)	270 (49.09%)	64 (11.64%)	550 (100.00%)

Table 62 Negatives types in Flakes, Românești-Dumbrăvița I GH3.

	Bladelets	Bladelets & Flakes	Blades	Blades & Bladelets	Blades & Flakes	Blades, Bladelets & Flakes	Flakes	Indeterminate	No negatives	Total
Surface Cleaning Flake	11 (10.68%)	3 (2.91%)	7 (6.80%)	5 (4.85%)	4 (3.88%)	1 (0.97%)	22 (21.36%)	49 (47.57%)	1 (0.97%)	103 (100.00%)
Maintenance Flake	8 (4.91%)	0 (0.00%)	5 (3.07%)	0 (0.00%)	0 (0.00%)	0 (0.00%)	30 (18.40%)	77 (47.24%)	43 (26.38%)	163 (100.00%)
Core Tablet	5 (7.46%)	7 (10.45%)	0 (0.00%)	2 (2.99%)	8 (11.94%)	1 (1.49%)	21 (31.34%)	5 (7.46%)	18 (26.87%)	67 (100.00%)
Cortical Flake	0 (0.00%)	0 (0.00%)	0 (0.00%)	0 (0.00%)	0 (0.00%)	0 (0.00%)	18 (25.35%)	6 (8.45%)	47 (66.20%)	71 (100.00%)
Simple Flake	2 (1.43%)	1 (0.71%)	0 (0.00%)	0 (0.00%)	1 (0.71%)	0 (0.00%)	9 (6.43%)	36 (25.71%)	91 (65.00%)	140 (100.00%)
Total	26 (4.78%)	11 (2.02%)	12 (2.21%)	7 (1.29%)	13 (2.39%)	2 (0.37%)	100 (18.38%)	173 (31.80%)	200 (36.76%)	544 (100.00%)

Table 63 Negatives orientation in Flakes, Românești-Dumbrăvița I GH3. Combinations not reaching 1% of the total

	Bipolar	Bipolar + Crossed	Convergent	Crossed	Crossed + Orthogonal	Orthogonal	Unipolar	Unipolar + Crossed	Unipolar + Orthogonal	Unipolar Combinations	Indeterminate	No negatives	Total
Surface Cleaning Flake	4 (3.88%)	0 (0.00%)	1 (0.97%)	7 (6.80%)	0 (0.00%)	5 (4.85%)	80 (77.67%)	2 (1.94%)	1 (0.97%)	1 (0.97%)	1 (0.97%)	1 (0.97%)	103 (100.00%)
Maintenance Flake	2 (1.23%)	0 (0.00%)	2 (1.23%)	13 (7.98%)	0 (0.00%)	3 (1.84%)	93 (57.06%)	6 (3.68%)	1 (0.61%)	0 (0.00%)	0 (0.00%)	43 (26.38%)	163 (100.00%)
Core Tablet	3 (4.48%)	1 (1.49%)	(0.00%)	7 (10.45%)	3 (4.48%)	8 (11.94%)	8 (11.94%)	1 (1.49%)	17 (25.37%)	1 (1.49%)	0 (0.00%)	18 (26.87%)	67 (100.00%)
Cortical Flake	0 (0.00%)	0 (0.00%)	0 (0.00%)	1 (1.41%)	0 (0.00%)	(0.00%)	23 (32.39%)	0 (0.00%)	(0.00%)	0 (0.00%)	0 (0.00%)	47 (66.20%)	71 (100.00%)
Simple Flake	2 (1.43%)	0 (0.00%)	0 (0.00%)	6 (4.29%)	0 (0.00%)	1 (0.71%)	37 (26.43%)	1 (0.71%)	1 (0.71%)	0 (0.00%)	1 (0.71%)	91 (65.00%)	140 (100.00%)
Total	11 (2.02%)	1 (0.18%)	3 (0.55%)	34 (6.25%)	3 (0.55%)	17 (3.13%)	241 (44.30%)	10 (1.84%)	20 (3.68%)	2 (0.37%)	2 (0.37%)	200 (36.76%)	544 (100.00%)

Table 64 Negatives orientation in Blades and Bladelets, Românești-Dumbrăvița I GH3. Combinations not reaching 1% of the total are combined.

	Bipolar	Convergent	Convergent+ Orthogonal	Crossed	Orthogonal	Unipolar	Unipolar+ Convergent	Unipolar Combinations	Indeterminate	No negatives	Total
Crest	0 (0.00%)	0 (0.00%)	1 (11.11%)	0 (0.00%)	1 (11.11%)	2 (22.22%)	0 (0.00%)	1 (11.11%)	0 (0.00%)	4 (44.44%)	9 (100.00%)
Asymmetrical Blade	2 (2.74%)	1 (1.37%)	0 (0.00%)	3 (4.11%)	1 (1.37%)	57 (78.08%)	1 (1.37%)	1 (1.37%)	0 (0.00%)	7 (9.59%)	73 (100.00%)
Overshot Blade	1 (5.26%)	1 (5.26%)	0 (0.00%)	0 (0.00%)	0 (0.00%)	11 (57.89%)	6 (31.58%)	0 (0.00%)	0 (0.00%)	0 (0.00%)	19 (100.00%)
Surface Cleaning Blade	0 (0.00%)	0 (0.00%)	0 (0.00%)	2 (11.11%)	0 (0.00%)	13 (72.22%)	0 (0.00%)	0 (0.00%)	0 (0.00%)	3 (16.67%)	18 (100.00%)
Maintenance Blade	0 (0.00%)	1 (7.69%)	0 (0.00%)	1 (7.69%)	0 (0.00%)	11 (84.62%)	0 (0.00%)	0 (0.00%)	0 (0.00%)	0 (0.00%)	13 (100.00%)
Crest (Bladelet)	1 (12.50%)	0 (0.00%)	0 (0.00%)	0 (0.00%)	1 (12.50%)	4 (50.00%)	0 (0.00%)	0 (0.00%)	0 (0.00%)	2 (25.00%)	8 (100.00%)
Asymmetrical Bladelet	1 (3.33%)	0 (0.00%)	0 (0.00%)	1 (3.33%)	0 (0.00%)	21 (70.00%)	0 (0.00%)	0 (0.00%)	0 (0.00%)	7 (23.33%)	30 (100.00%)
Overshot Bladelet	0 (0.00%)	0 (0.00%)	0 (0.00%)	0 (0.00%)	0 (0.00%)	1 (16.67%)	5 (83.33%)	0 (0.00%)	0 (0.00%)	0 (0.00%)	6 (100.00%)
Surface Cleaning Bladelet	0 (0.00%)	0 (0.00%)	0 (0.00%)	0 (0.00%)	0 (0.00%)	3 (100.00%)	0 (0.00%)	0 (0.00%)	0 (0.00%)	0 (0.00%)	3 (100.00%)
Maintenance Bladelet	0 (0.00%)	0 (0.00%)	0 (0.00%)	0 (0.00%)	0 (0.00%)	5 (50.00%)	0 (0.00%)	0 (0.00%)	0 (0.00%)	5 (50.00%)	10 (100.00%)
Simple Blade	2 (1.56%)	3 (2.34%)	0 (0.00%)	1 (0.78%)	0 (0.00%)	112 (87.50%)	5 (3.91%)	2 (1.56%)	1 (0.78%)	2 (1.56%)	128 (100.00%)
Simple Bladelet	1 (0.51%)	6 (3.06%)	0 (0.00%)	0 (0.00%)	0 (0.00%)	166 (84.69%)	13 (6.63%)	0 (0.00%)	1 (0.51%)	9 (4.59%)	196 (100.00%)
Burin Spall	0 (0.00%)	0 (0.00%)	0 (0.00%)	0 (0.00%)	0 (0.00%)	7 (23.33%)	0 (0.00%)	0 (0.00%)	0 (0.00%)	23 (76.67%)	30 (100.00%)
Blade Tablet	0 (0.00%)	0 (0.00%)	0 (0.00%)	0 (0.00%)	4 (57.14%)	1 (14.29%)	0 (0.00%)	0 (0.00%)	0 (0.00%)	2 (28.57%)	7 (100.00%)
Total	8 (1.45%)	12 (2.18%)	1 (0.18%)	8 (1.45%)	7 (1.27%)	414 (75.27%)	30 (5.45%)	4 (0.73%)	2 (0.36%)	64 (11.64%)	550 (100.00%)

Table 65 Distal Termination in Blades and Bladelets, Românești-Dumbrăviţa I GH3

	Feathered	Plunging	Hinged	Stepped	Indeterminate	Total
Crest	1 (16.67%)	1 (16.67%)	0 (0.00%)	4 (66.67%)	0 (0.00%)	6 (100.00%)
Asymmetrical Blade	16 (29.63%)	23 (42.59%)	2 (3.70%)	12 (22.22%)	1 (1.85%)	54 (100.00%)
Overshot Blade	1 (5.26%)	13 (68.42%)	0 (0.00%)	5 (26.32%)	0 (0.00%)	19 (100.00%)
Surface Cleaning Blade	5 (33.33%)	3 (20.00%)	3 (20.00%)	4 (26.67%)	0 (0.00%)	15 (100.00%)
Maintenance Blade	4 (44.44%)	1 (11.11%)	0 (0.00%)	4 (44.44%)	0 (0.00%)	9 (100.00%)
Crest (Bladelet)	1 (12.50%)	1 (12.50%)	2 (25.00%)	3 (37.50%)	1 (12.50%)	8 (100.00%)
Asymmetrical Bladelet	4 (22.22%)	10 (55.56%)	1 (5.56%)	3 (16.67%)	0 (0.00%)	18 (100.00%)
Overshot Bladelet	0 (0.00%)	5 (83.33%)	0 (0.00%)	1 (16.67%)	0 (0.00%)	6 (100.00%)
Surface Cleaning Bladelet	1 (50.00%)	0 (0.00%)	0 (0.00%)	1 (50.00%)	0 (0.00%)	2 (100.00%)
Maintenance Bladelet	5 (71.43%)	0 (0.00%)	1 (14.29%)	1 (14.29%)	0 (0.00%)	7 (100.00%)
Simple Blade	54 (73.97%)	2 (2.74%)	8 (10.96%)	5 (6.85%)	4 (5.48%)	73 (100.00%)
Simple Bladelet	120 (91.60%)	1 (0.76%)	2 (1.53%)	5 (3.82%)	3 (2.29%)	131 (100.00%)
Burin Spall	16 (64.00%)	3 (12.00%)	0 (0.00%)	6 (24.00%)	0 (0.00%)	25 (100.00%)
Total	228 (61.13%)	63 (16.89%)	19 (5.09%)	54 (14.48%)	9 (2.41%)	373 (100.00%)

Table 66 Outline in Blades and Bladelets, Românești-Dumbrăviţa I GH3

	(sub)Parallel Edges	Convergent	Off-axis	Indeterminate	Total
Crest	3 (50.00%)	1 (16.67%)	2 (33.33%)	0 (0.00%)	6 (100.00%)
Asymmetrical Blade	14 (25.93%)	2 (3.70%)	35 (64.81%)	3 (5.56%)	54 (100.00%)
Overshot Blade	17 (89.47%)	1 (5.26%)	1 (5.26%)	0 (0.00%)	19 (100.00%)
Surface Cleaning Blade	14 (93.33%)	1 (6.67%)	0 (0.00%)	0 (0.00%)	15 (100.00%)
Maintenance Blade	5 (55.56%)	1 (11.11%)	3 (33.33%)	0 (0.00%)	9 (100.00%)
Crest (Bladelet)	2 (25.00%)	3 (37.50%)	2 (25.00%)	1 (12.50%)	8 (100.00%)
Asymmetrical Bladelet	6 (33.33%)	1 (5.56%)	11 (61.11%)	0 (0.00%)	18 (100.00%)
Overshot Bladelet	6 (100.00%)	0 (0.00%)	0 (0.00%)	0 (0.00%)	6 (100.00%)
Surface Cleaning Bladelet	2 (100.00%)	0 (0.00%)	0 (0.00%)	0 (0.00%)	2 (100.00%)
Maintenance Bladelet	3 (42.86%)	1 (14.29%)	3 (42.86%)	0 (0.00%)	7 (100.00%)
Simple Blade	47 (64.38%)	15 (20.55%)	7 (9.59%)	4 (5.48%)	73 (100.00%)
Simple Bladelet	68 (51.91%)	43 (32.82%)	18 (13.74%)	2 (1.53%)	131 (100.00%)
Burin Spall	21 (84.00%)	3 (12.00%)	1 (4.00%)	0 (0.00%)	25 (100.00%)
Total	208 (55.76%)	72 (19.30%)	83 (22.25%)	10 (2.68%)	373 (100.00%)

Table 67 Profiles in Blades and Bladelets, Românești-Dumbrăvița I GH3

	Straight	Slightly Curved	Curved	Very Curved	Twisted	Indeterminate	Total
Crest	6 (66.67%)	0 (0.00%)	1 (11.11%)	0 (0.00%)	2 (22.22%)	0 (0.00%)	9 (100.00%)
Asymmetrical Blade	24 (32.88%)	4 (5.48%)	1 (1.37%)	2 (2.74%)	42 (57.53%)	0 (0.00%)	73 (100.00%)
Overshot Blade	1 (5.26%)	3 (15.79%)	9 (47.37%)	4 (21.05%)	2 (10.53%)	0 (0.00%)	19 (100.00%)
Surface Cleaning Blade	14 (77.78%)	1 (5.56%)	2 (11.11%)	0 (0.00%)	1 (5.56%)	0 (0.00%)	18 (100.00%)
Maintenance Blade	9 (69.23%)	1 (7.69%)	1 (7.69%)	0 (0.00%)	1 (7.69%)	1 (7.69%)	13 (100.00%)
Crest (Bladelet)	5 (62.50%)	1 (12.50%)	0 (0.00%)	0 (0.00%)	2 (25.00%)	0 (0.00%)	8 (100.00%)
Asymmetrical Bladelet	9 (30.00%)	0 (0.00%)	0 (0.00%)	0 (0.00%)	21 (70.00%)	0 (0.00%)	30 (100.00%)
Overshot Bladelet	1 (16.67%)	1 (16.67%)	4 (66.67%)	0 (0.00%)	0 (0.00%)	0 (0.00%)	6 (100.00%)
Surface Cleaning Bladelet	1 (33.33%)	1 (33.33%)	0 (0.00%)	0 (0.00%)	1 (33.33%)	0 (0.00%)	3 (100.00%)
Maintenance Bladelet	6 (60.00%)	0 (0.00%)	0 (0.00%)	0 (0.00%)	3 (30.00%)	1 (10.00%)	10 (100.00%)
Simple Blade	93 (72.66%)	16 (12.50%)	2 (1.56%)	2 (1.56%)	13 (10.16%)	2 (1.56%)	128 (100.00%)
Simple Bladelet	153 (78.06%)	14 (7.14%)	1 (0.51%)	1 (0.51%)	25 (12.76%)	2 (1.02%)	196 (100.00%)
Burin Spall	25 (83.33%)	2 (6.67%)	0 (0.00%)	0 (0.00%)	3 (10.00%)	0 (0.00%)	30 (100.00%)
Total	347 (63.90%)	44 (8.10%)	21 (3.87%)	9 (1.66%)	116 (21.36%)	6 (1.10%)	543 (100.00%)

Table 68 Cross-sections in Blades and Bladelets, Românești -Dumbrăvița I GH3

	Flat	Indeterminate	Trapezoidal symm	Trapezoidal asymm	Triangular symm	Triangular asymm	Total
Crest	0 (0.00%)	0 (0.00%)	0 (0.00%)	3 (33.33%)	4 (44.44%)	2 (22.22%)	9 (100.00%)
Asymmetrical Blade	3 (4.11%)	2 (2.74%)	4 (5.48%)	19 (26.03%)	4 (5.48%)	41 (56.16%)	73 (100.00%)
Overshot Blade	2 (10.53%)	0 (0.00%)	2 (10.53%)	12 (63.16%)	2 (10.53%)	1 (5.26%)	19 (100.00%)
Surface Cleaning Blade	4 (22.22%)	0 (0.00%)	5 (27.78%)	5 (27.78%)	1 (5.56%)	3 (16.67%)	18 (100.00%)
Maintenance Blade	1 (7.69%)	0 (0.00%)	1 (7.69%)	6 (46.15%)	3 (23.08%)	2 (15.38%)	13 (100.00%)
Crest (Bladelet)	0 (0.00%)	0 (0.00%)	0 (0.00%)	5 (62.50%)	1 (12.50%)	2 (25.00%)	8 (100.00%)
Asymmetrical Bladelet	3 (10.00%)	0 (0.00%)	2 (6.67%)	7 (23.33%)	1 (3.33%)	17 (56.67%)	30 (100.00%)
Overshot Bladelet	0 (0.00%)	0 (0.00%)	3 (50.00%)	3 (50.00%)	0 (0.00%)	0 (0.00%)	6 (100.00%)
Surface Cleaning Bladelet	0 (0.00%)	0 (0.00%)	0 (0.00%)	1 (33.33%)	1 (33.33%)	1 (33.33%)	3 (100.00%)
Maintenance Bladelet	2 (20.00%)	0 (0.00%)	0 (0.00%)	4 (40.00%)	1 (10.00%)	3 (30.00%)	10 (100.00%)
Simple Blade	11 (8.59%)	2 (1.56%)	35 (27.34%)	24 (18.75%)	27 (21.09%)	29 (22.66%)	128 (100.00%)
Simple Bladelet	19 (9.69%)	2 (1.02%)	40 (20.41%)	39 (19.90%)	56 (28.57%)	40 (20.41%)	196 (100.00%)
Burin Spall	0 (0.00%)	0 (0.00%)	2 (6.67%)	0 (0.00%)	27 (90.00%)	1 (3.33%)	30 (100.00%)
Total	45 (8.29%)	6 (1.10%)	94 (17.31%)	128 (23.57%)	128 (23.57%)	142 (26.15%)	543 (100.00%)

Table 69 Fragmentation in A1, Fumane

	A1			
	Blade	**Bladelet**	**Flake**	**Total**
Complete	113 (41.70%)	160 (38.37%)	86 (90.53%)	359 (45.85%)
Prox+Mes	99 (36.53%)	135 (32.37%)	8 (8.42%)	242 (30.91%)
Mes+Dist	59 (21.77%)	122 (29.26%)	1 (1.05%)	182 (23.24%)
Total	271 (100.00%)	417 (100.00%)	95 (100.00%)	783 (100.00%)

.

Table 70 Lipping in blanks, Fumane

	A1			A1 Complete			A2		
	Yes	**No**	**Total**	**Yes**	**No**	**Total**	**Yes**	**No**	**Total**
Simple Blade	70	55	125	31	21	52	39	45	84
	(56.00%)	(44.00%)	(100.00%)	(59.62%)	(40.38%)	(100.00%)	(46.43%)	(53.57%)	(100.00%)
Simple	32	236	268	17	121	138	80	226	306
Bladelet	(11.94%)	(88.06%)	(100.00%)	(12.32%)	(87.68%)	(100.00%)	(26.14%)	(73.86%)	(100.00%)
Management	49	38	87	36	25	61	65	96	161
Blade	(56.32%)	(43.68%)	(100.00%)	(59.02%)	(40.98%)	(100.00%)	(40.37%)	(59.63%)	(100.00%)
Management	7	14	21	5	11	16	28	51	79
Bladelet	(33.33%)	(66.67%)	(100.00%)	(31.25%)	(68.75%)	(100.00%)	(35.44%)	(64.56%)	(100.00%)
Burin Spall	0	6	6	0	6	6	4	5	9
	(0.00%)	(100.00%)	(100.00%)	(0.00%)	(100.00%)	(100.00%)	(44.44%)	(55.56%)	(100.00%)
Management	32	17	49	29	15	44	34	28	62
Flake	(65.31%)	(34.69%)	(100.00%)	(65.91%)	(34.09%)	(100.00%)	(54.84%)	(45.16%)	(100.00%)
Core Tablet	11	4	15	10	4	14	26	28	54
	(73.33%)	(26.67%)	(100.00%)	(71.43%)	(28.57%)	(100.00%)	(48.15%)	(51.85%)	(100.00%)
Cortical Flake	12	13	25	12	12	24	14	19	33
	(48.00%)	(52.00%)	(100.00%)	(50.00%)	(50.00%)	(100.00%)	(42.42%)	(57.58%)	(100.00%)
Simple Flake	3	2	5	2	2	4	2	2	4
	(60.00%)	(40.00%)	(100.00%)	(50.00%)	(50.00%)	(100.00%)	(50.00%)	(50.00%)	(100.00%)
Total	216	385	601	142	217	359	292	500	792
	(35.94%)	(64.06%)	(100.00%)	(39.55%)	(60.45%)	(100.00%)	(36.87%)	(63.13%)	(100.00%)

Table 71 Overhang abrasion in laminar Blanks, Fumane

	A1			A1 Complete			A2		
	Yes	**No**	**Total**	**Yes**	**No**	**Total**	**Yes**	**No**	**Total**
Simple	105	22	127	42	11	53	67	19	86
Blade	(82.68%)	(17.32%)	(100.00%)	(79.25%)	(20.75%)	(100.00%)	(77.91%)	(22.09%)	(100.00%)
Simple	216	50	266	110	27	137	192	112	304
Bladelet	(81.20%)	(18.80%)	(100.00%)	(80.29%)	(19.71%)	(100.00%)	(63.16%)	(36.84%)	(100.00%)
Burin	3	3	6	3	3	6	0	9	9
Spall	(50.00%)	(50.00%)	(100.00%)	(50.00%)	(50.00%)	(100.00%)	(0.00%)	(100.00%)	(100.00%)
Management	56	31	87	40	21	61	100	61	161
Blade	(64.37%)	(35.63%)	(100.00%)	(65.57%)	(34.43%)	(100.00%)	(62.11%)	(37.89%)	(100.00%)
Management	16	5	21	12	4	16	60	19	79
Bladelet	(76.19%)	(23.81%)	(100.00%)	(75.00%)	(25.00%)	(100.00%)	(75.95%)	(24.05%)	(100.00%)
Total	396	111	507	207	66	273	419	220	639
	(78.11%)	(21.89%)	(100.00%)	(75.82%)	(24.18%)	(100.00%)	(65.57%)	(34.43%)	(100.00%)

Table 72 Overhang abrasion in Cores, Fumane

	A1			A2		
	Yes	**No**	**Total**	**Yes**	**No**	**Total**
One face (sub)parallel edges	3 (75.00%)	1 (25.00%)	4 (100.00%)	8 (100.00%)	0 (0.00%)	8 (100.00%)
Semi *Tournant*	12 (100.00%)	0 (0.00%)	12 (100.00%)	13 (100.00%)	0 (0.00%)	13 (100.00%)
Narrow Fronted	7 (100.00%)	0 (0.00%)	7 (100.00%)	7 (77.78%)	2 (22.22%)	9 (100.00%)
Narrow Fronted *sur Tranche*	3 (50.00%)	3 (50.00%)	6 (100.00%)	4 (50.00%)	4 (50.00%)	8 (100.00%)
Transversal Carinated	0 (0.00%)	0 (0.00%)	0 (0.00%)	6 (100.00%)	0 (0.00%)	6 (100.00%)
Pre-Core	0 (0.00%)	1 (100.00%)	1 (100.00%)	2 (28.57%)	5 (71.43%)	7 (100.00%)
Flakes-Not Organised	0 (0.00%)	2 (100.00%)	2 (100.00%)	2 (28.57%)	5 (71.43%)	7 (100.00%)
Total	25 (78.13%)	7 (21.88%)	32 (100.00%)	42 (72.41%)	16 (27.59%)	58 (100.00%)

Table 73 Knapping angles in blanks, Fumane.

			A1		
	<70	**70-90**	**>90**	**Indeterminate**	**Total**
Simple Blade	19 (15.20%)	84 (67.20%)	1 (0.80%)	21 (16.80%)	125 (100.00%)
Simple Bladelet	15 (5.60%)	163 (60.82%)	1 (0.37%)	89 (33.21%)	268 (100.00%)
Management Blade	24 (27.59%)	41 (47.13%)	0 (0.00%)	22 (25.29%)	87 (100.00%)
Management Bladelet	4 (19.05%)	11 (52.38%)	0 (0.00%)	6 (28.57%)	21 (100.00%)
Burin Spall	0 (0.00%)	2 (33.33%)	0 (0.00%)	4 (66.67%)	6 (100.00%)
Management Flake	5 (10.20%)	39 (79.59%)	1 (2.04%)	4 (8.16%)	49 (100.00%)
Core Tablet	2 (13.33%)	13 (86.67%)	0 (0.00%)	0 (0.00%)	15 (100.00%)
Cortical Flake	6 (24.00%)	13 (52.00%)	1 (4.00%)	5 (20.00%)	25 (100.00%)
Simple Flake	2 (40.00%)	2 (40.00%)	0 (0.00%)	1 (20.00%)	5 (100.00%)
Total	77 (12.81%)	368 (61.23%)	4 (0.67%)	152 (25.29%)	601 (100.00%)
			A1 Complete		
Simple Blade	7 (13.46%)	38 (73.08%)	0 (0.00%)	7 (13.46%)	52 (100.00%)
Simple Bladelet	6 (4.35%)	78 (56.52%)	0 (0.00%)	54 (39.13%)	138 (100.00%)
Management Blade	13 (21.31%)	31 (50.82%)	0 (0.00%)	17 (27.87%)	61 (100.00%)
Management Bladelet	2 (12.50%)	9 (56.25%)	0 (0.00%)	5 (31.25%)	16 (100.00%)
Burin Spall	0 (0.00%)	2 (33.33%)	0 (0.00%)	4 (66.67%)	6 (100.00%)
Management Flake	4 (9.09%)	35 (79.55%)	1 (2.27%)	4 (9.09%)	44 (100.00%)
Core Tablet	2 (14.29%)	12 (85.71%)	0 (0.00%)	0 (0.00%)	14 (100.00%)
Cortical Flake	5 (20.83%)	13 (54.17%)	1 (4.17%)	5 (20.83%)	24 (100.00%)
Simple Flake	2 (50.00%)	1 (25.00%)	0 (0.00%)	1 (25.00%)	4 (100.00%)
Total	41 (11.42%)	219 (61.00%)	2 (0.56%)	97 (27.02%)	359 (100.00%)
			A2		
Simple Blade	12 (14.29%)	63 (75.00%)	0 (0.00%)	9 (10.71%)	84 (100.00%)
Simple Bladelet	22 (7.19%)	160 (52.29%)	4 (1.31%)	120 (39.22%)	306 (100.00%)
Management Blade	37 (22.98%)	87 (54.04%)	0 (0.00%)	37 (22.98%)	161 (100.00%)
Management Bladelet	6 (7.59%)	42 (53.16%)	0 (0.00%)	31 (39.24%)	79 (100.00%)
Burin Spall	0 (0.00%)	1 (11.11%)	0 (0.00%)	8 (88.89%)	9 (100.00%)
Management Flake	18 (29.03%)	37 (59.68%)	1 (1.61%)	6 (9.68%)	62 (100.00%)
Core Tablet	16 (29.63%)	34 (62.96%)	0 (0.00%)	4 (7.41%)	54 (100.00%)
Cortical Flake	9 (27.27%)	17 (51.52%)	2 (6.06%)	5 (15.15%)	33 (100.00%)
Simple Flake	0 (0.00%)	2 (50.00%)	0 (0.00%)	2 (50.00%)	4 (100.00%)
Total	120 (15.15%)	443 (55.93%)	7 (0.88%)	222 (28.03%)	792 (100.00%)

Table 74 Knapping angles in Cores, Fumane

	<70	70-90	>90	Indeterminate	Total
			A1		
One face (sub)parallel edges	3 (60.00%)	1 (20.00%)			4 (100.00%)
Semi Tournant	8 (160.00%)	4 (80.00%)			12 (100.00%)
Narrow Fronted	3 (75.00%)	4 (100.00%)			7 (100.00%)
Narrow Fronted sur Tranche	2 (100.00%)	4 (200.00%)			6 (100.00%)
Pre-Core	0 (0.00%)	0 (0.00%)			1 (100.00%)
Flakes-Not Organised	0 (0.00%)	2 (100.00%)			2 (100.00%)
Total	16 (72.73%)	16 (72.73%)			32 (100.00%)
			A2		
One face (sub)parallel edges	5 (62.50%)	2 (25.00%)	0 (0.00%)	1 (12.50%)	8 (100.00%)
Semi Tournant	5 (38.46%)	8 (61.54%)	0 (0.00%)	0 (0.00%)	13 (100.00%)
Narrow Fronted	4 (44.44%)	5 (55.56%)	0 (0.00%)	0 (0.00%)	9 (100.00%)
Narrow Fronted sur Tranche	2 (25.00%)	5 (62.50%)	1 (12.50%)	0 (0.00%)	8 (100.00%)
Transversal Carinated	2 (33.33%)	4 (66.67%)	0 (0.00%)	0 (0.00%)	6 (100.00%)
Pre-Core	2 (28.57%)	3 (42.86%)	2 (28.57%)	0 (0.00%)	7 (100.00%)
Flakes-Not Organised	2 (28.57%)	4 (57.14%)	0 (0.00%)	1 (14.29%)	7 (100.00%)
Total	22 (37.93%)	31 (53.45%)	3 (5.17%)	2 (3.45%)	58 (100.00%)

Table 75 Bulbs values, Fumane.

	Diffused	Not perceived	Pronounced	Bulbar scar	Crushed	Indeterminate	Total
				A1			
Simple Blade	96 (76.80%)	2 (1.60%)	25 (20.00%)	1 (0.80%)	0 (0.00%)	1 (0.80%)	125 (100.00%)
Simple Bladelet	226 (84.33%)	8 (2.99%)	23 (8.58%)	3 (1.12%)	3 (1.12%)	5 (1.87%)	268 (100.00%)
Management Blade	61 (70.11%)	0 (0.00%)	11 (12.64%)	11 (12.64%)	0 (0.00%)	4 (4.60%)	87 (100.00%)
Management Bladelet	18 (85.71%)	1 (4.76%)	0 (0.00%)	2 (9.52%)	0 (0.00%)	0 (0.00%)	21 (100.00%)
Burin Spall	2 (33.33%)	0 (0.00%)	0 (0.00%)	0 (0.00%)	1 (16.67%)	3 (50.00%)	6 (100.00%)
Management Flake	28 (57.14%)	0 (0.00%)	11 (22.45%)	9 (18.37%)	1 (2.04%)	0 (0.00%)	49 (100.00%)
Core Tablet	4 (26.67%)	0 (0.00%)	8 (53.33%)	3 (20.00%)	0 (0.00%)	0 (0.00%)	15 (100.00%)
Cortical Flake	7 (28.00%)	0 (0.00%)	12 (48.00%)	3 (12.00%)	0 (0.00%)	3 (12.00%)	25 (100.00%)
Simple Flake	3 (60.00%)	0 (0.00%)	2 (40.00%)	0 (0.00%)	0 (0.00%)	0 (0.00%)	5 (100.00%)
Total	445 (74.04%)	11 (1.83%)	92 (15.31%)	32 (5.32%)	5 (0.83%)	16 (2.66%)	601 (100.00%)
				A1 Complete			
Simple Blade	38 (73.08%)	0 (0.00%)	14 (26.92%)	0 (0.00%)	0 (0.00%)	0 (0.00%)	52 (100.00%)
Simple Bladelet	117 (84.78%)	3 (2.17%)	12 (8.70%)	3 (2.17%)	0 (0.00%)	3 (2.17%)	138 (100.00%)
Management Blade	45 (73.77%)	0 (0.00%)	9 (14.75%)	5 (8.20%)	0 (0.00%)	2 (3.28%)	61 (100.00%)
Management Bladelet	14 (87.50%)	1 (6.25%)	0 (0.00%)	1 (6.25%)	0 (0.00%)	0 (0.00%)	16 (100.00%)
Burin Spall	2 (33.33%)	0 (0.00%)	0 (0.00%)	0 (0.00%)	1 (16.67%)	3 (50.00%)	6 (100.00%)
Management Flake	27 (61.36%)	0 (0.00%)	9 (20.45%)	7 (15.91%)	1 (2.27%)	0 (0.00%)	44 (100.00%)
Core Tablet	4 (28.57%)	0 (0.00%)	8 (57.14%)	2 (14.29%)	0 (0.00%)	0 (0.00%)	14 (100.00%)
Cortical Flake	6 (25.00%)	0 (0.00%)	12 (50.00%)	3 (12.50%)	0 (0.00%)	3 (12.50%)	24 (100.00%)
Simple Flake	2 (50.00%)	0 (0.00%)	2 (50.00%)	0 (0.00%)	0 (0.00%)	0 (0.00%)	4 (100.00%)
Total	255 (71.03%)	4 (1.11%)	66 (18.38%)	21 (5.85%)	2 (0.56%)	11 (3.06%)	359 (100.00%)
				A2			
Simple Blade	55 (65.48%)	2 (2.38%)	22 (26.19%)	3 (3.57%)	2 (2.38%)	0 (0.00%)	84 (100.00%)
Simple Bladelet	226 (73.86%)	42 (13.73%)	21 (6.86%)	2 (0.65%)	14 (4.58%)	1 (0.33%)	306 (100.00%)
Management Blade	93 (57.76%)	11 (6.83%)	42 (26.09%)	3 (1.86%)	11 (6.83%)	1 (0.62%)	161 (100.00%)
Management Bladelet	56 (70.89%)	9 (11.39%)	8 (10.13%)	0 (0.00%)	6 (7.59%)	0 (0.00%)	79 (100.00%)
Burin Spall	2 (22.22%)	2 (22.22%)	0 (0.00%)	0 (0.00%)	2 (22.22%)	3 (33.33%)	9 (100.00%)
Management Flake	8 (12.90%)	0 (0.00%)	45 (72.58%)	8 (12.90%)	1 (1.61%)	0 (0.00%)	62 (100.00%)
Core Tablet	11 (20.37%)	0 (0.00%)	36 (66.67%)	6 (11.11%)	1 (1.85%)	0 (0.00%)	54 (100.00%)
Cortical Flake	6 (18.18%)	0 (0.00%)	20 (60.61%)	6 (18.18%)	0 (0.00%)	1 (3.03%)	33 (100.00%)
Simple Flake	1 (25.00%)	0 (0.00%)	2 (50.00%)	0 (0.00%)	1 (25.00%)	0 (0.00%)	4 (100.00%)

Table 76 Core blanks, Fumane.

	Blank	Cobble	Indeterminate	Nodule	Slab	Squared Chunk	Total
				A1			
One face (sub)parallel edges	0 (0.00%)	0 (0.00%)	3 (75.00%)	1 (25.00%)	0 (0.00%)	0 (0.00%)	4 (100.00%)
Semi Tournant	0 (0.00%)	3 (25.00%)	8 (66.67%)	0 (0.00%)	1 (8.33%)	0 (0.00%)	12 (100.00%)
Narrow Fronted	1 (14.29%)	1 (14.29%)	3 (42.86%)	1 (14.29%)	0 (0.00%)	1 (14.29%)	7 (100.00%)
Narrow Fronted sur Tranche	5 (83.33%)	0 (0.00%)	1 (16.67%)	0 (0.00%)	0 (0.00%)	0 (0.00%)	6 (100.00%)
Pre-Core	0 (0.00%)	0 (0.00%)	0 (0.00%)	0 (0.00%)	1 (100.00%)	0 (0.00%)	1 (100.00%)
Flakes-Not Organised	0 (0.00%)	0 (0.00%)	2 (100.00%)	0 (0.00%)	0 (0.00%)	0 (0.00%)	2 (100.00%)
Total	6 (18.75%)	4 (12.50%)	17 (53.13%)	2 (6.25%)	2 (6.25%)	1 (3.13%)	32 (100.00%)
				A2			
One face (sub)parallel edges	0 (0.00%)	1 (12.50%)	7 (87.50%)	0 (0.00%)	0 (0.00%)	0 (0.00%)	8 (100.00%)
Semi Tournant	0 (0.00%)	7 (53.85%)	5 (38.46%)	1 (7.69%)	0 (0.00%)	0 (0.00%)	13 (100.00%)
Narrow Fronted	0 (0.00%)	3 (33.33%)	4 (44.44%)	1 (11.11%)	0 (0.00%)	1 (11.11%)	9 (100.00%)
Narrow Fronted sur Tranche	6 (75.00%)	0 (0.00%)	1 (12.50%)	0 (0.00%)	1 (12.50%)	0 (0.00%)	8 (100.00%)
Transversal Carinated	3 (50.00%)	1 (16.67%)	0 (0.00%)	0 (0.00%)	0 (0.00%)	2 (33.33%)	6 (100.00%)
Pre-Core	0 (0.00%)	2 (28.57%)	0 (0.00%)	1 (14.29%)	3 (42.86%)	1 (14.29%)	7 (100.00%)
Flakes-Not Organised	1 (14.29%)	4 (57.14%)	1 (14.29%)	0 (0.00%)	0 (0.00%)	1 (14.29%)	7 (100.00%)
Total	10 (17.24%)	18 (31.03%)	18 (31.03%)	3 (5.17%)	4 (6.90%)	5 (8.62%)	58 (100.00%)

Table 77 Cortex coverage in Cores, Fumane.

	No Cortex	Lateral	Back	Back and Base	Back and Lateral	Base	Base and Lateral	Lateral and Frontal	Total
					A1				
One face (sub)parallel edges	3 (75.00%)	0 (0.00%)	1 (25.00%)		0 (0.00%)	0 (0.00%)			4 (100.00%)
Semi Tournant	4 (33.33%)	1 (8.33%)	5 (41.67%)		2 (16.67%)	0 (0.00%)			12 (100.00%)
Narrow Fronted	4 (57.14%)	2 (28.57%)	0 (0.00%)		0 (0.00%)	1 (14.29%)			7 (100.00%)
Narrow Fronted sur Tranche	6 (100.00%)	0 (0.00%)	0 (0.00%)		0 (0.00%)	0 (0.00%)			6 (100.00%)
Pre-Core	0 (0.00%)	1 (100.00%)	0 (0.00%)		0 (0.00%)	0 (0.00%)			1 (100.00%)
Flakes-Not Organised	1 (50.00%)	0 (0.00%)	0 (0.00%)		0 (0.00%)	1 (50.00%)			2 (100.00%)
Total	18 (56.25%)	4 (12.50%)	6 (18.75%)		2 (6.25%)	2 (6.25%)			32 (100.00%)
					A2				
One face (sub)parallel edges	2 (25.00%)	1 (12.50%)	4 (50.00%)	0 (0.00%)	0 (0.00%)	1 (12.50%)	0 (0.00%)	0 (0.00%)	8 (100.00%)
Semi Tournant	4 (30.77%)	1 (7.69%)	5 (38.46%)	1 (7.69%)	1 (7.69%)	1 (7.69%)	0 (0.00%)	0 (0.00%)	13 (100.00%)
Narrow Fronted	3 (33.33%)	2 (22.22%)	4 (44.44%)	0 (0.00%)	0 (0.00%)	0 (0.00%)	0 (0.00%)	0 (0.00%)	9 (100.00%)
Narrow Fronted sur Tranche	7 (87.50%)	0 (0.00%)	0 (0.00%)	0 (0.00%)	0 (0.00%)	0 (0.00%)	1 (12.50%)	0 (0.00%)	8 (100.00%)
Transversal Carinated	3 (50.00%)	1 (16.67%)	1 (16.67%)	0 (0.00%)	0 (0.00%)	1 (16.67%)	0 (0.00%)	0 (0.00%)	6 (100.00%)
Pre-Core	0 (0.00%)	3 (42.86%)	1 (14.29%)	0 (0.00%)	1 (14.29%)	1 (14.29%)	0 (0.00%)	1 (14.29%)	7 (100.00%)
Flakes-Not Organised	3 (42.86%)	0 (0.00%)	1 (14.29%)	0 (0.00%)	0 (0.00%)	3 (42.86%)	0 (0.00%)	0 (0.00%)	7 (100.00%)
Total	22 (37.93%)	8 (13.79%)	16 (27.59%)	1 (1.72%)	2 (3.45%)	7 (12.07%)	1 (1.72%)	1 (1.72%)	58 (100.00%)

Table 78 Striking platform type, cores Fumane.

	A1			A2				
	Plain	**Facetted**	**Total**	**Plain**	**Natural**	**Facetted**	**Indeterminate**	**Total**
One face (sub)parallel edges	4 (100.00%)	0 (0.00%)	4 (100.00%)	6 (75.00%)	0 (0.00%)	1 (12.50%)	1 (12.50%)	8 (100.00%)
Semi Tournant	11 (91.67%)	1 (8.33%)	12 (100.00%)	12 (92.31%)	0 (0.00%)	1 (7.69%)	0 (0.00%)	13 (100.00%)
Narrow Fronted	6 (85.71%)	1 (14.29%)	7 (100.00%)	8 (88.89%)	0 (0.00%)	1 (11.11%)	0 (0.00%)	9 (100.00%)
Narrow Fronted sur Tranche	6 (100.00%)	0 (0.00%)	6 (100.00%)	7 (87.50%)	1 (12.50%)	0 (0.00%)	0 (0.00%)	8 (100.00%)
Transversal Carinated	0 (0.00%)	0 (0.00%)	0 (0.00%)	5 (83.33%)	1 (16.67%)	0 (0.00%)	0 (0.00%)	6 (100.00%)
Pre-Core	1 (100.00%)	0 (0.00%)	1 (100.00%)	6 (85.71%)	0 (0.00%)	1 (14.29%)	0 (0.00%)	7 (100.00%)
Flakes-Not Organised	0 (0.00%)	2 (100.00%)	2 (100.00%)	4 (57.14%)	0 (0.00%)	3 (42.86%)	0 (0.00%)	7 (100.00%)
Total	28 (87.50%)	4 (12.50%)	32 (100.00%)	48 (82.76%)	2 (3.45%)	7 (12.07%)	1 (1.72%)	58 (100.00%)

Table 79 Striking platform relationship, cores Fumane.

	A1					A2					
	Single	**Opposed**	**Adjacent**	**Independent**	**Total**	**Single**	**Opposed**	**Opposed auxiliary**	**Adjacent**	**Independent**	**Total**
One face (sub)parallel edges	3 (75.00%)	1 (25.00%)	0 (0.00%)	0 (0.00%)	4 (100.00%)	7 (87.50%)	1 (12.50%)	0 (0.00%)	0 (0.00%)	0 (0.00%)	8 (100.00%)
Semi Tournant	10 (83.33%)	1 (8.33%)	0 (0.00%)	1 (8.33%)	12 (100.00%)	9 (69.23%)	2 (15.38%)	1 (7.69%)	1 (7.69%)	0 (0.00%)	13 (100.00%)
Narrow Fronted	5 (71.43%)	1 (14.29%)	0 (0.00%)	1 (14.29%)	7 (100.00%)	8 (88.89%)	1 (11.11%)	0 (0.00%)	0 (0.00%)	0 (0.00%)	9 (100.00%)
Narrow Fronted sur Tranche	4 (66.67%)	1 (16.67%)	1 (16.67%)	0 (0.00%)	6 (100.00%)	5 (62.50%)	0 (0.00%)	0 (0.00%)	2 (25.00%)	1 (12.50%)	8 (100.00%)
Transversal Carinated	0 (0.00%)	0 (0.00%)	0 (0.00%)	0 (0.00%)	0 (0.00%)	5 (83.33%)	0 (0.00%)	0 (0.00%)	0 (0.00%)	1 (16.67%)	6 (100.00%)
Pre-Core	1 (100.00%)	0 (0.00%)	0 (0.00%)	0 (0.00%)	1 (100.00%)	6 (85.71%)	0 (0.00%)	1 (14.29%)	0 (0.00%)	0 (0.00%)	7 (100.00%)
Flakes-Not Organised	2 (100.00%)	0 (0.00%)	0 (0.00%)	0 (0.00%)	2 (100.00%)	3 (42.86%)	0 (0.00%)	0 (0.00%)	3 (42.86%)	1 (14.29%)	7 (100.00%)
Total	25 (78.13%)	4 (12.50%)	1 (3.13%)	2 (6.25%)	32 (100.00%)	43 (74.14%)	4 (6.90%)	2 (3.45%)	6 (10.34%)	3 (5.17%)	58 (100.00%)

Table 80 Flaking surface relationship, cores Fumane.

	A1					A2				
	Single Surface	**Adjacent-Orthogonal**	**Independent**	**Opposed**	**Total**	**Single Surface**	**Adjacent-Orthogonal**	**Independent**	**Opposed**	**Total**
One face (sub)parallel edges	4 (100.00%)	0 (0.00%)	0 (0.00%)	0 (0.00%)	4 (100.00%)	7 (87.50%)	0 (0.00%)	0 (0.00%)	1 (12.50%)	8 (100.00%)
Semi Tournant	10 (83.33%)	1 (8.33%)	0 (0.00%)	1 (8.33%)	12 (100.00%)	10 (76.92%)	1 (7.69%)	1 (7.69%)	1 (7.69%)	13 (100.00%)
Narrow Fronted	5 (71.43%)	1 (14.29%)	1 (14.29%)	0 (0.00%)	7 (100.00%)	8 (88.89%)	0 (0.00%)	0 (0.00%)	1 (11.11%)	9 (100.00%)
Narrow Fronted sur Tranche	4 (66.67%)	1 (16.67%)	0 (0.00%)	1 (16.67%)	6 (100.00%)	5 (62.50%)	2 (25.00%)	1 (12.50%)	0 (0.00%)	8 (100.00%)
Transversal Carinated	0 (0.00%)	0 (0.00%)	0 (0.00%)	0 (0.00%)	0 (0.00%)	5 (83.33%)	0 (0.00%)	1 (16.67%)	0 (0.00%)	6 (100.00%)
Pre-Core	1 (100.00%)	0 (0.00%)	0 (0.00%)	0 (0.00%)	1 (100.00%)	6 (85.71%)	0 (0.00%)	0 (0.00%)	1 (14.29%)	7 (100.00%)
Flakes-Not Organised	2 (100.00%)	0 (0.00%)	0 (0.00%)	0 (0.00%)	2 (100.00%)	3 (42.86%)	3 (42.86%)	1 (14.29%)	0 (0.00%)	7 (100.00%)
Total	26 (81.25%)	3 (9.38%)	1 (3.13%)	2 (6.25%)	32 (100.00%)	44 (75.86%)	6 (10.34%)	4 (6.90%)	4 (6.90%)	58 (100.00%)

Table 81 Negatives types in Cores, Fumane.

	A1						A2						
	Bladelets	**Bladelets & Flakes**	**Blades & Bladelets**	**Flakes**	**No negatives**	**Total**	**Bladelets**	**Blades**	**Blades & Bladelets**	**Blades & Flakes**	**Blades, Bladelets & Flakes**	**Flakes**	**Total**
One face (sub)parallel edges	3 (75.00%)	0 (0.00%)	1 (25.00%)	0 (0.00%)	0 (0.00%)	4 (100.00%)	2 (25.00%)	1 (12.50%)	4 (50.00%)	0 (0.00%)	0 (0.00%)	1 (12.50%)	8 (100.00%)
Semi Tournant	5 (41.67%)	1 (8.33%)	6 (50.00%)	0 (0.00%)	0 (0.00%)	12 (100.00%)	8 (61.54%)	0 (0.00%)	5 (38.46%)	0 (0.00%)	0 (0.00%)	0 (0.00%)	13 (100.00%)
Narrow Fronted	4 (57.14%)	0 (0.00%)	3 (42.86%)	0 (0.00%)	0 (0.00%)	7 (100.00%)	4 (44.44%)	1 (11.11%)	4 (44.44%)	0 (0.00%)	0 (0.00%)	0 (0.00%)	9 (100.00%)
Narrow Fronted sur Tranche	5 (83.33%)	0 (0.00%)	1 (16.67%)	0 (0.00%)	0 (0.00%)	6 (100.00%)	7 (87.50%)	1 (12.50%)	0 (0.00%)	0 (0.00%)	0 (0.00%)	0 (0.00%)	8 (100.00%)
Transversal Carinated	0 (0.00%)	0 (0.00%)	0 (0.00%)	0 (0.00%)	0 (0.00%)	0 (0.00%)	5 (83.33%)	0 (0.00%)	0 (0.00%)	0 (0.00%)	1 (16.67%)	0 (0.00%)	6 (100.00%)
Pre-Core	0 (0.00%)	0 (0.00%)	0 (0.00%)	0 (0.00%)	1 (100.00%)	1 (100.00%)	0 (0.00%)	1 (14.29%)	0 (0.00%)	3 (42.86%)	0 (0.00%)	3 (42.86%)	7 (100.00%)
Flakes-Not Organised	0 (0.00%)	0 (0.00%)	0 (0.00%)	2 (100.00%)	0 (0.00%)	2 (100.00%)	0 (0.00%)	0 (0.00%)	0 (0.00%)	0 (0.00%)	0 (0.00%)	7 (100.00%)	7 (100.00%)
Total	17 (53.13%)	1 (3.13%)	11 (34.38%)	2 (6.25%)	1 (3.13%)	32 (100.00%)	26 (44.83%)	4 (6.90%)	13 (22.41%)	3 (5.17%)	1 (1.72%)	11 (18.97%)	58 (100.00%)

Table 82 Negatives orientation in Cores, Fumane.

	Bipolar	Centripetal	Unipolar	Unipolar+Convergent	Unipolar+Crossed	Unipolar+Orthogonal	No negatives	Total
					A1			
One face (sub)parallel edges	1 (25.00%)	0 (0.00%)	1 (25.00%)	2 (50.00%)	0 (0.00%)	0 (0.00%)	0 (0.00%)	4 (100.00%)
Semi Tournant	1 (8.33%)	0 (0.00%)	5 (41.67%)	5 (41.67%)	1 (8.33%)	0 (0.00%)	0 (0.00%)	12 (100.00%)
Narrow Fronted	1 (14.29%)	0 (0.00%)	5 (71.43%)	0 (0.00%)	0 (0.00%)	1 (14.29%)	0 (0.00%)	7 (100.00%)
Narrow Fronted sur Tranche	2 (33.33%)	0 (0.00%)	4 (66.67%)	0 (0.00%)	0 (0.00%)	0 (0.00%)	0 (0.00%)	6 (100.00%)
Transversal Carinated	0 (0.00%)	0 (0.00%)	0 (0.00%)	0 (0.00%)	0 (0.00%)	0 (0.00%)	0 (0.00%)	#DIV/0!
Pre-Core	0 (0.00%)	0 (0.00%)	0 (0.00%)	0 (0.00%)	0 (0.00%)	0 (0.00%)	1 (100.00%)	1 (100.00%)
Flakes-Not Organised	0 (0.00%)	2 (100.00%)	0 (0.00%)	0 (0.00%)	0 (0.00%)	0 (0.00%)	0 (0.00%)	2 (100.00%)
Total	5 (15.63%)	2 (6.25%)	15 (46.88%)	7 (21.88%)	1 (3.13%)	1 (3.13%)	1 (3.13%)	32 (100.00%)
					A2			
One face (sub)parallel edges	1 (12.50%)	0 (0.00%)	6 (75.00%)	1 (12.50%)		0 (0.00%)		8 (100.00%)
Semi Tournant	2 (15.38%)	0 (0.00%)	7 (53.85%)	4 (30.77%)		0 (0.00%)		13 (100.00%)
Narrow Fronted	1 (11.11%)	0 (0.00%)	6 (66.67%)	2 (22.22%)		0 (0.00%)		9 (100.00%)
Narrow Fronted sur Tranche	0 (0.00%)	0 (0.00%)	8 (100.00%)	0 (0.00%)		0 (0.00%)		8 (100.00%)
Transversal Carinated	0 (0.00%)	0 (0.00%)	3 (50.00%)	3 (50.00%)		0 (0.00%)		6 (100.00%)
Pre-Core	1 (14.29%)	0 (0.00%)	5 (71.43%)	0 (0.00%)		1 (14.29%)		7 (100.00%)
Flakes-Not Organised	0 (0.00%)	1 (14.29%)	4 (57.14%)	0 (0.00%)		2 (28.57%)		7 (100.00%)
Total	5 (8.62%)	1 (1.72%)	39 (67.24%)	10 (17.24%)		3 (5.17%)		58 (100.00%)

Table 83 Butts in Flakes, Fumane.

	Plain	Linear	Punctiform	Dihedral	Facetted	Natural	Indeterminate	Crushed	Total
					A1				
Surface Cleaning Flake	18 (42.86%)	11 (26.19%)	5 (11.90%)	0 (0.00%)	3 (7.14%)	2 (4.76%)	3 (7.14%)	0 (0.00%)	42 (100.00%)
Maintenance Flake	6 (85.71%)	0 (0.00%)	0 (0.00%)	0 (0.00%)	1 (14.29%)	0 (0.00%)	0 (0.00%)	0 (0.00%)	7 (100.00%)
Core Tablet	6 (40.00%)	0 (0.00%)	1 (6.67%)	1 (6.67%)	7 (46.67%)	0 (0.00%)	0 (0.00%)	0 (0.00%)	15 (100.00%)
Cortical Flake	12 (48.00%)	2 (8.00%)	1 (4.00%)	1 (4.00%)	1 (4.00%)	5 (20.00%)	1 (4.00%)	2 (8.00%)	25 (100.00%)
Simple Flake	3 (60.00%)	1 (20.00%)	0 (0.00%)	0 (0.00%)	1 (20.00%)	0 (0.00%)	0 (0.00%)	0 (0.00%)	5 (100.00%)
Total	45 (47.87%)	14 (14.89%)	7 (7.45%)	2 (2.13%)	13 (13.83%)	7 (7.45%)	4 (4.26%)	2 (2.13%)	94 (100.00%)
					A1 Complete				
Surface Cleaning Flake	16 (43.24%)	9 (24.32%)	5 (13.51%)	0 (0.00%)	3 (8.11%)	1 (2.70%)	3 (8.11%)	0 (0.00%)	37 (100.00%)
Maintenance Flake	6 (85.71%)	0 (0.00%)	0 (0.00%)	0 (0.00%)	1 (14.29%)	0 (0.00%)	0 (0.00%)	0 (0.00%)	7 (100.00%)
Core Tablet	6 (42.86%)	0 (0.00%)	1 (7.14%)	1 (7.14%)	6 (42.86%)	0 (0.00%)	0 (0.00%)	0 (0.00%)	14 (100.00%)
Cortical Flake	12 (50.00%)	2 (8.33%)	1 (4.17%)	1 (4.17%)	1 (4.17%)	4 (16.67%)	1 (4.17%)	2 (8.33%)	24 (100.00%)
Simple Flake	2 (50.00%)	1 (25.00%)	0 (0.00%)	0 (0.00%)	1 (25.00%)	0 (0.00%)	0 (0.00%)	0 (0.00%)	4 (100.00%)
Total	42 (48.84%)	12 (13.95%)	7 (8.14%)	2 (2.33%)	12 (13.95%)	5 (5.81%)	4 (4.65%)	2 (2.33%)	86 (100.00%)
					A2				
Surface Cleaning Flake	25 (56.82%)	10 (22.73%)	6 (13.64%)	0 (0.00%)	0 (0.00%)	2 (4.55%)	0 (0.00%)	1 (2.27%)	44 (100.00%)
Maintenance Flake	12 (66.67%)	3 (16.67%)	1 (5.56%)	0 (0.00%)	0 (0.00%)	2 (11.11%)	0 (0.00%)	0 (0.00%)	18 (100.00%)
Core Tablet	20 (37.04%)	6 (11.11%)	3 (5.56%)	1 (1.85%)	19 (35.19%)	4 (7.41%)	0 (0.00%)	1 (1.85%)	54 (100.00%)
Cortical Flake	22 (66.67%)	1 (3.03%)	3 (9.09%)	1 (3.03%)	2 (6.06%)	2 (6.06%)	1 (3.03%)	1 (3.03%)	33 (100.00%)
Simple Flake	2 (50.00%)	1 (25.00%)	0 (0.00%)	0 (0.00%)	0 (0.00%)	0 (0.00%)	0 (0.00%)	1 (25.00%)	4 (100.00%)
Total	81 (52.94%)	21 (13.73%)	13 (8.50%)	2 (1.31%)	21 (13.73%)	10 (6.54%)	1 (0.65%)	4 (2.61%)	153 (100.00%)

	Plain	Linear	Punctiform	Facetted	Natural	Indeterminate	Crushed	Total
				A1				
Crest	4 (36.36%)	2 (18.18%)	0 (0.00%)	1 (9.09%)	0 (0.00%)	1 (9.09%)	3 (27.27%)	11 (100.00%)
Asymmetrical Blade	21 (37.50%)	16 (28.57%)	10 (17.86%)	6 (10.71%)	1 (1.79%)	0 (0.00%)	2 (3.57%)	56 (100.00%)
Overshot Blade	2 (13.33%)	5 (33.33%)	4 (26.67%)	2 (13.33%)	0 (0.00%)	0 (0.00%)	2 (13.33%)	15 (100.00%)
Surface Cleaning Blade	3 (60.00%)	1 (20.00%)	0 (0.00%)	0 (0.00%)	0 (0.00%)	1 (20.00%)	0 (0.00%)	5 (100.00%)
Crest (Bladelet)	1 (50.00%)	1 (50.00%)	0 (0.00%)	0 (0.00%)	0 (0.00%)	0 (0.00%)	0 (0.00%)	2 (100.00%)
Asymmetrical Bladelet	5 (35.71%)	3 (21.43%)	5 (35.71%)	0 (0.00%)	0 (0.00%)	0 (0.00%)	1 (7.14%)	14 (100.00%)
Overshot Bladelet	0 (0.00%)	4 (100.00%)	0 (0.00%)	0 (0.00%)	0 (0.00%)	0 (0.00%)	0 (0.00%)	4 (100.00%)
Surface Cleaning Bladelet	0 (0.00%)	0 (0.00%)	1 (100.00%)	0 (0.00%)	0 (0.00%)	0 (0.00%)	0 (0.00%)	1 (100.00%)
Simple Blade	38 (30.40%)	54 (43.20%)	23 (18.40%)	3 (2.40%)	0 (0.00%)	4 (3.20%)	3 (2.40%)	125 (100.00%)
Simple Bladelet	36 (13.43%)	143 (53.36%)	76 (28.36%)	1 (0.37%)	2 (0.75%)	1 (0.37%)	9 (3.36%)	268 (100.00%)
Burin Spall	1 (16.67%)	1 (16.67%)	2 (33.33%)	0 (0.00%)	0 (0.00%)	0 (0.00%)	2 (33.33%)	6 (100.00%)
Total	111 (21.89%)	230 (45.36%)	121 (23.87%)	13 (2.56%)	3 (0.59%)	7 (1.38%)	22 (4.34%)	507 (100.00%)
				A1 Complete				
Crest	3 (37.50%)	1 (12.50%)	0 (0.00%)	1 (12.50%)	0 (0.00%)	1 (12.50%)	2 (25.00%)	8 (100.00%)
Asymmetrical Blade	13 (36.11%)	9 (25.00%)	9 (25.00%)	4 (11.11%)	1 (2.78%)	0 (0.00%)	0 (0.00%)	36 (100.00%)
Overshot Blade	2 (14.29%)	5 (35.71%)	4 (28.57%)	1 (7.14%)	0 (0.00%)	0 (0.00%)	2 (14.29%)	14 (100.00%)
Surface Cleaning Blade	1 (33.33%)	1 (33.33%)	0 (0.00%)	0 (0.00%)	0 (0.00%)	1 (33.33%)	0 (0.00%)	3 (100.00%)
Crest (Bladelet)	1 (50.00%)	1 (50.00%)	0 (0.00%)	0 (0.00%)	0 (0.00%)	0 (0.00%)	0 (0.00%)	2 (100.00%)
Asymmetrical Bladelet	3 (30.00%)	2 (20.00%)	4 (40.00%)	0 (0.00%)	0 (0.00%)	0 (0.00%)	1 (10.00%)	10 (100.00%)
Overshot Bladelet	0 (0.00%)	3 (100.00%)	0 (0.00%)	0 (0.00%)	0 (0.00%)	0 (0.00%)	0 (0.00%)	3 (100.00%)
Surface Cleaning Bladelet	0 (0.00%)	0 (0.00%)	1 (100.00%)	0 (0.00%)	0 (0.00%)	0 (0.00%)	0 (0.00%)	1 (100.00%)
Simple Blade	18 (34.62%)	24 (46.15%)	7 (13.46%)	2 (3.85%)	0 (0.00%)	1 (1.92%)	0 (0.00%)	52 (100.00%)
Simple Bladelet	20 (14.49%)	70 (50.72%)	40 (28.99%)	1 (0.72%)	1 (0.72%)	1 (0.72%)	5 (3.62%)	138 (100.00%)
Burin Spall	1 (16.67%)	1 (16.67%)	2 (33.33%)	0 (0.00%)	0 (0.00%)	0 (0.00%)	2 (33.33%)	6 (100.00%)
Total	62 (22.71%)	117 (42.86%)	67 (24.54%)	9 (3.30%)	2 (0.73%)	4 (1.47%)	12 (4.40%)	273 (100.00%)

	A2								
	Plain	**Linear**	**Punctiform**	**Dihedral**	**Facetted**	**Natural**	**Indeterminate**	**Crushed**	**Total**
Crest	9 (45.00%)	5 (25.00%)	3 (15.00%)	0 (0.00%)	1 (5.00%)	1 (5.00%)	0 (0.00%)	1 (5.00%)	20 (100.00%)
Asymmetrical Blade	19 (25.33%)	36 (48.00%)	12 (16.00%)	0 (0.00%)	2 (2.67%)	0 (0.00%)	0 (0.00%)	6 (8.00%)	75 (100.00%)
Overshot Blade	10 (27.78%)	16 (44.44%)	6 (16.67%)	0 (0.00%)	1 (2.78%)	0 (0.00%)	1 (2.78%)	2 (5.56%)	36 (100.00%)
Surface Cleaning Blade	10 (55.56%)	2 (11.11%)	2 (11.11%)	1 (5.56%)	0 (0.00%)	0 (0.00%)	1 (5.56%)	2 (11.11%)	18 (100.00%)
Maintenance Blade	7 (58.33%)	2 (16.67%)	1 (8.33%)	0 (0.00%)	2 (16.67%)	0 (0.00%)	0 (0.00%)	0 (0.00%)	12 (100.00%)
Crest (Bladelet)	3 (50.00%)	1 (16.67%)	2 (33.33%)	0 (0.00%)	0 (0.00%)	0 (0.00%)	0 (0.00%)	0 (0.00%)	6 (100.00%)
Asymmetrical Bladelet	6 (10.53%)	27 (47.37%)	17 (29.82%)	0 (0.00%)	2 (3.51%)	1 (1.75%)	0 (0.00%)	4 (7.02%)	57 (100.00%)
Overshot Bladelet	1 (12.50%)	5 (62.50%)	2 (25.00%)	0 (0.00%)	0 (0.00%)	0 (0.00%)	0 (0.00%)	0 (0.00%)	8 (100.00%)
Surface Cleaning Bladelet	0 (0.00%)	4 (100.00%)	0 (0.00%)	0 (0.00%)	0 (0.00%)	0 (0.00%)	0 (0.00%)	0 (0.00%)	4 (100.00%)
Maintenance Bladelet	1 (25.00%)	1 (25.00%)	1 (25.00%)	0 (0.00%)	0 (0.00%)	0 (0.00%)	0 (0.00%)	1 (25.00%)	4 (100.00%)
Simple Blade	28 (33.33%)	41 (48.81%)	12 (14.29%)	0 (0.00%)	1 (1.19%)	0 (0.00%)	0 (0.00%)	2 (2.38%)	84 (100.00%)
Simple Bladelet	50 (16.34%)	169 (55.23%)	64 (20.92%)	1 (0.33%)	0 (0.00%)	2 (0.65%)	2 (0.65%)	18 (5.88%)	306 (100.00%)
Burin Spall	3 (33.33%)	1 (11.11%)	1 (11.11%)	0 (0.00%)	0 (0.00%)	0 (0.00%)	0 (0.00%)	4 (44.44%)	9 (100.00%)
Total	147 (23.00%)	310 (48.51%)	123 (19.25%)	2 (0.31%)	9 (1.41%)	4 (0.63%)	4 (0.63%)	40 (6.26%)	639 (100.00%)

Table 85 Cortex Coverage Flakes, Fumane

	Non-Cortical	Semi-Cortical					Extensively Cortical			Entames		Total
		Proximal	*Lateral*	*Lateral and Distal*	*Dorsal*	*Distal*	*Lateral*	*Dorsal*	*Distal*	*Dorsal*	*Distal*	
A1												
Surface Cleaning Flake	28 (66.67%)	2 (4.76%)	6 (14.29%)	0 (0.00%)	1 (2.38%)	2 (4.76%)	0 (0.00%)	3 (7.14%)	0 (0.00%)	0 (0.00%)	0 (0.00%)	42 (100.00%)
Maintenance Flake	4 (57.14%)	0 (0.00%)	1 (14.29%)	0 (0.00%)	2 (28.57%)	0 (0.00%)	0 (0.00%)	0 (0.00%)	0 (0.00%)	0 (0.00%)	0 (0.00%)	7 (100.00%)
Core Tablet	13 (86.67%)	0 (0.00%)	0 (0.00%)	0 (0.00%)	1 (6.67%)	1 (6.67%)	0 (0.00%)	0 (0.00%)	0 (0.00%)	0 (0.00%)	0 (0.00%)	15 (100.00%)
Cortical Flake	0 (0.00%)	1 (3.85%)	2 (7.69%)	0 (0.00%)	1 (3.85%)	0 (0.00%)	0 (0.00%)	3 (11.54%)	0 (0.00%)	19 (73.08%)	0 (0.00%)	26 (100.00%)
Simple Flake	4 (80.00%)	0 (0.00%)	0 (0.00%)	0 (0.00%)	1 (20.00%)	0 (0.00%)	0 (0.00%)	0 (0.00%)	0 (0.00%)	0 (0.00%)	0 (0.00%)	5 (100.00%)
Total	49 (51.58%)	3 (3.16%)	9 (9.47%)	0 (0.00%)	6 (6.32%)	3 (3.16%)	0 (0.00%)	6 (6.32%)	0 (0.00%)	19 (20.00%)	0 (0.00%)	95 (100.00%)
A1 Complete												
Surface Cleaning Flake	24 (64.86%)	1 (2.70%)	6 (16.22%)	0 (0.00%)	1 (2.70%)	2 (5.41%)	0 (0.00%)	3 (8.11%)	0 (0.00%)	0 (0.00%)		37 (100.00%)
Maintenance Flake	4 (57.14%)	0 (0.00%)	1 (14.29%)	0 (0.00%)	2 (28.57%)	0 (0.00%)	0 (0.00%)	0 (0.00%)	0 (0.00%)	0 (0.00%)		7 (100.00%)
Core Tablet	13 (92.86%)	0 (0.00%)	0 (0.00%)	0 (0.00%)	0 (0.00%)	1 (7.14%)	0 (0.00%)	0 (0.00%)	0 (0.00%)	0 (0.00%)		14 (100.00%)
Cortical Flake	0 (0.00%)	1 (4.17%)	2 (8.33%)	0 (0.00%)	1 (4.17%)	0 (0.00%)	0 (0.00%)	3 (12.50%)	0 (0.00%)	17 (70.83%)		24 (100.00%)
Simple Flake	3 (75.00%)	0 (0.00%)	0 (0.00%)	0 (0.00%)	1 (25.00%)	0 (0.00%)	0 (0.00%)	0 (0.00%)	0 (0.00%)	0 (0.00%)		4 (100.00%)
Total	44 (51.16%)	2 (2.33%)	9 (10.47%)	0 (0.00%)	5 (5.81%)	3 (3.49%)	0 (0.00%)	6 (6.98%)	0 (0.00%)	17 (19.77%)		86 (100.00%)
A2												
Surface Cleaning Flake	26 (59.09%)	2 (4.55%)	6 (13.64%)	2 (4.55%)	4 (9.09%)	4 (9.09%)		0 (0.00%)		0 (0.00%)		44 (100.00%)
Maintenance Flake	11 (61.11%)	2 (11.11%)	1 (5.56%)	1 (5.56%)	3 (16.67%)	0 (0.00%)		0 (0.00%)		0 (0.00%)		18 (100.00%)
Core Tablet	42 (77.78%)	5 (9.26%)	0 (0.00%)	0 (0.00%)	2 (3.70%)	2 (3.70%)		2 (3.70%)		1 (1.85%)		54 (100.00%)
Cortical Flake	0 (0.00%)	0 (0.00%)	1 (3.03%)	0 (0.00%)	6 (18.18%)	1 (3.03%)		15 (45.45%)		10 (30.30%)		33 (100.00%)
Simple Flake	4 (100.00%)	0 (0.00%)	0 (0.00%)	0 (0.00%)	0 (0.00%)	0 (0.00%)		0 (0.00%)		0 (0.00%)		4 (100.00%)
Total	83 (54.25%)	9 (5.88%)	8 (5.23%)	3 (1.96%)	15 (9.80%)	7 (4.58%)		17 (11.11%)		11 (7.19%)		153 (100.00%)

Table 86 Cortex Coverage in Blades and Bladelets, Fumane

A1											
	Non-Cortical	**Semi-Cortical**					**Extensively Cortical**			**Entames**		**Total**
		Proximal	**Lateral**	**Lateral and Distal**	**Dorsal**	**Distal**	**Lateral**	**Dorsal**	**Distal**	**Dorsal**	**Distal**	
Crest	5 (31.25%)	0 (0.00%)	4 (25.00%)	0 (0.00%)	1 (6.25%)	3 (18.75%)	1 (6.25%)	0 (0.00%)	1 (6.25%)	1 (6.25%)	0 (0.00%)	16 (100.00%)
Asymmetrical Blade	35 (47.95%)	0 (0.00%)	19 (26.03%)	2 (2.74%)	3 (4.11%)	5 (6.85%)	1 (1.37%)	3 (4.11%)	1 (1.37%)	3 (4.11%)	1 (1.37%)	73 (100.00%)
Overshot Blade	14 (63.64%)	0 (0.00%)	0 (0.00%)	0 (0.00%)	1 (4.55%)	7 (31.82%)	0 (0.00%)	0 (0.00%)	0 (0.00%)	0 (0.00%)	0 (0.00%)	22 (100.00%)
Surface Cleaning Blade	3 (60.00%)	0 (0.00%)	0 (0.00%)	0 (0.00%)	0 (0.00%)	1 (20.00%)	0 (0.00%)	1 (20.00%)	0 (0.00%)	0 (0.00%)	0 (0.00%)	5 (100.00%)
Crest (Bladelet)	10 (90.91%)	0 (0.00%)	1 (9.09%)	0 (0.00%)	0 (0.00%)	0 (0.00%)	0 (0.00%)	0 (0.00%)	0 (0.00%)	0 (0.00%)	0 (0.00%)	11 (100.00%)
Asymmetrical Bladelet	17 (62.96%)	0 (0.00%)	5 (18.52%)	0 (0.00%)	1 (3.70%)	1 (3.70%)	1 (3.70%)	2 (7.41%)	0 (0.00%)	0 (0.00%)	0 (0.00%)	27 (100.00%)
Overshot Bladelet	10 (90.91%)	0 (0.00%)	0 (0.00%)	0 (0.00%)	0 (0.00%)	1 (9.09%)	0 (0.00%)	0 (0.00%)	0 (0.00%)	0 (0.00%)	0 (0.00%)	11 (100.00%)
Surface Cleaning Bladelet	1 (100.00%)	0 (0.00%)	0 (0.00%)	0 (0.00%)	0 (0.00%)	0 (0.00%)	0 (0.00%)	0 (0.00%)	0 (0.00%)	0 (0.00%)	0 (0.00%)	1 (100.00%)
Simple Blade	146 (94.19%)	0 (0.00%)	6 (3.87%)	1 (0.65%)	2 (1.29%)	0 (0.00%)	0 (0.00%)	0 (0.00%)	0 (0.00%)	0 (0.00%)	0 (0.00%)	155 (100.00%)
Simple Bladelet	344 (95.82%)	0 (0.00%)	8 (2.23%)	0 (0.00%)	0 (0.00%)	4 (1.11%)	0 (0.00%)	2 (0.56%)	1 (0.28%)	0 (0.00%)	0 (0.00%)	359 (100.00%)
Burin Spall	8 (100.00%)	0 (0.00%)	0 (0.00%)	0 (0.00%)	0 (0.00%)	0 (0.00%)	0 (0.00%)	0 (0.00%)	0 (0.00%)	0 (0.00%)	0 (0.00%)	8 (100.00%)
Total	593 (86.19%)	0 (0.00%)	43 (6.25%)	3 (0.44%)	8 (1.16%)	22 (3.20%)	3 (0.44%)	8 (1.16%)	3 (0.44%)	4 (0.58%)	1 (0.15%)	688 (100.00%)

A1 Complete											
	Non-Cortical	Semi-Cortical					Extensively Cortical			Entames	Total
		Proximal	Lateral	Lateral and Distal	Dorsal	Distal	Lateral	Dorsal	Distal	Dorsal	
Crest	1 (12.50%)	0 (0.00%)	2 (25.00%)	0 (0.00%)	1 (12.50%)	2 (25.00%)	1 (12.50%)	0 (0.00%)	1 (12.50%)	0 (0.00%)	8 (100.00%)
Asymmetrical Blade	22 (61.11%)	0 (0.00%)	6 (16.67%)	1 (2.78%)	1 (2.78%)	2 (5.56%)	0 (0.00%)	1 (2.78%)	1 (2.78%)	2 (5.56%)	36 (100.00%)
Overshot Blade	12 (85.71%)	0 (0.00%)	0 (0.00%)	0 (0.00%)	0 (0.00%)	2 (14.29%)	0 (0.00%)	0 (0.00%)	0 (0.00%)	0 (0.00%)	14 (100.00%)
Surface Cleaning Blade	3 (100.00%)	0 (0.00%)	0 (0.00%)	0 (0.00%)	0 (0.00%)	0 (0.00%)	0 (0.00%)	0 (0.00%)	0 (0.00%)	0 (0.00%)	3 (100.00%)
Crest (Bladelet)	2 (100.00%)	0 (0.00%)	0 (0.00%)	0 (0.00%)	0 (0.00%)	0 (0.00%)	0 (0.00%)	0 (0.00%)	0 (0.00%)	0 (0.00%)	2 (100.00%)
Asymmetrical Bladelet	8 (80.00%)	0 (0.00%)	1 (10.00%)	0 (0.00%)	0 (0.00%)	1 (10.00%)	0 (0.00%)	0 (0.00%)	0 (0.00%)	0 (0.00%)	10 (100.00%)
Overshot Bladelet	2 (66.67%)	0 (0.00%)	0 (0.00%)	0 (0.00%)	0 (0.00%)	1 (33.33%)	0 (0.00%)	0 (0.00%)	0 (0.00%)	0 (0.00%)	3 (100.00%)
Surface Cleaning Bladelet	1 (100.00%)	0 (0.00%)	0 (0.00%)	0 (0.00%)	0 (0.00%)	0 (0.00%)	0 (0.00%)	0 (0.00%)	0 (0.00%)	0 (0.00%)	1 (100.00%)
Simple Blade	49 (94.23%)	0 (0.00%)	3 (5.77%)	0 (0.00%)	0 (0.00%)	0 (0.00%)	0 (0.00%)	0 (0.00%)	0 (0.00%)	0 (0.00%)	52 (100.00%)
Simple Bladelet	130 (94.20%)	0 (0.00%)	6 (4.35%)	0 (0.00%)	0 (0.00%)	2 (1.45%)	0 (0.00%)	0 (0.00%)	0 (0.00%)	0 (0.00%)	138 (100.00%)
Burin Spall	6 (100.00%)	0 (0.00%)	0 (0.00%)	0 (0.00%)	0 (0.00%)	0 (0.00%)	0 (0.00%)	0 (0.00%)	0 (0.00%)	0 (0.00%)	6 (100.00%)
Total	236 (86.45%)	0 (0.00%)	18 (6.59%)	1 (0.37%)	2 (0.73%)	10 (3.66%)	1 (0.37%)	1 (0.37%)	2 (0.73%)	2 (0.73%)	273 (100.00%)

A2									
	Non-Cortical	**Semi-Cortical**					**Extensively Cortical**	**Entames**	**Total**
		Proximal	**Lateral**	**Lateral and Distal**	**Dorsal**	**Distal**	**Dorsal**	**Dorsal**	
Crest	11 (55.00%)	3 (15.00%)	2 (10.00%)	0 (0.00%)	2 (10.00%)	2 (10.00%)	0 (0.00%)	0 (0.00%)	20 (100.00%)
Asymmetrical Blade	44 (58.67%)	1 (1.33%)	15 (20.00%)	1 (1.33%)	0 (0.00%)	10 (13.33%)	3 (4.00%)	1 (1.33%)	75 (100.00%)
Overshot Blade	17 (47.22%)	0 (0.00%)	2 (5.56%)	2 (5.56%)	2 (5.56%)	12 (33.33%)	0 (0.00%)	1 (2.78%)	36 (100.00%)
Surface Cleaning Blade	14 (77.78%)	0 (0.00%)	1 (5.56%)	0 (0.00%)	1 (5.56%)	2 (11.11%)	0 (0.00%)	0 (0.00%)	18 (100.00%)
Maintenance Blade	11 (91.67%)	0 (0.00%)	0 (0.00%)	0 (0.00%)	1 (8.33%)	0 (0.00%)	0 (0.00%)	0 (0.00%)	12 (100.00%)
Crest (Bladelet)	4 (66.67%)	0 (0.00%)	0 (0.00%)	0 (0.00%)	0 (0.00%)	1 (16.67%)	1 (16.67%)	0 (0.00%)	6 (100.00%)
Asymmetrical Bladelet	46 (80.70%)	1 (1.75%)	2 (3.51%)	0 (0.00%)	2 (3.51%)	4 (7.02%)	2 (3.51%)	0 (0.00%)	57 (100.00%)
Overshot Bladelet	8 (100.00%)	0 (0.00%)	0 (0.00%)	0 (0.00%)	0 (0.00%)	0 (0.00%)	0 (0.00%)	0 (0.00%)	8 (100.00%)
Surface Cleaning Bladelet	3 (75.00%)	0 (0.00%)	0 (0.00%)	0 (0.00%)	1 (25.00%)	0 (0.00%)	0 (0.00%)	0 (0.00%)	4 (100.00%)
Maintenance Bladelet	3 (75.00%)	0 (0.00%)	1 (25.00%)	0 (0.00%)	0 (0.00%)	0 (0.00%)	0 (0.00%)	0 (0.00%)	4 (100.00%)
Simple Blade	77 (91.67%)	0 (0.00%)	5 (5.95%)	0 (0.00%)	0 (0.00%)	2 (2.38%)	0 (0.00%)	0 (0.00%)	84 (100.00%)
Simple Bladelet	291 (95.10%)	1 (0.33%)	7 (2.29%)	0 (0.00%)	1 (0.33%)	6 (1.96%)	0 (0.00%)	0 (0.00%)	306 (100.00%)
Burin Spall	8 (88.89%)	0 (0.00%)	0 (0.00%)	0 (0.00%)	1 (11.11%)	0 (0.00%)	0 (0.00%)	0 (0.00%)	9 (100.00%)
Total	537 (84.04%)	6 (0.94%)	35 (5.48%)	3 (0.47%)	11 (1.72%)	39 (6.10%)	6 (0.94%)	2 (0.31%)	639 (100.00%)

Table 87 Negatives Types in Flakes, Fumane

A1									
	Bladelets	**Bladelets & Flakes**	**Blades**	**Blades & Bladelets**	**Blades & Flakes**	**Flakes**	**Indeterminate**	**No negatives**	**Total**
Surface Cleaning Flake	6 (14.29%)	3 (7.14%)	3 (7.14%)	1 (2.38%)	2 (4.76%)	24 (57.14%)	2 (4.76%)	1 (2.38%)	42 (100.00%)
Maintenance Flake	0 (0.00%)	0 (0.00%)	0 (0.00%)	0 (0.00%)	0 (0.00%)	6 (85.71%)	0 (0.00%)	1 (14.29%)	7 (100.00%)
Core Tablet	3 (20.00%)	1 (6.67%)	0 (0.00%)	0 (0.00%)	0 (0.00%)	9 (60.00%)	0 (0.00%)	2 (13.33%)	15 (100.00%)
Cortical Flake	0 (0.00%)	0 (0.00%)	0 (0.00%)	0 (0.00%)	0 (0.00%)	5 (19.23%)	0 (0.00%)	21 (80.77%)	26 (100.00%)
Simple Flake	0 (0.00%)	0 (0.00%)	0 (0.00%)	0 (0.00%)	0 (0.00%)	2 (40.00%)	1 (20.00%)	2 (40.00%)	5 (100.00%)
Total	9 (9.47%)	4 (4.21%)	3 (3.16%)	1 (1.05%)	2 (2.11%)	46 (48.42%)	3 (3.16%)	27 (28.42%)	95 (100.00%)

A1 Complete									
	Bladelets	**Bladelets & Flakes**	**Blades**	**Blades & Bladelets**	**Blades & Flakes**	**Flakes**	**Indeterminate**	**No negatives**	**Total**
Surface Cleaning Flake	6 (16.22%)	3 (8.11%)	3 (8.11%)	1 (2.70%)	2 (5.41%)	21 (56.76%)	0 (0.00%)	1 (2.70%)	37 (100.00%)
Maintenance Flake	0 (0.00%)	0 (0.00%)	0 (0.00%)	0 (0.00%)	0 (0.00%)	6 (85.71%)	0 (0.00%)	1 (14.29%)	7 (100.00%)
Core Tablet	3 (21.43%)	1 (7.14%)	0 (0.00%)	0 (0.00%)	0 (0.00%)	8 (57.14%)	0 (0.00%)	2 (14.29%)	14 (100.00%)
Cortical Flake	0 (0.00%)	0 (0.00%)	0 (0.00%)	0 (0.00%)	0 (0.00%)	5 (20.83%)	0 (0.00%)	19 (79.17%)	24 (100.00%)
Simple Flake	0 (0.00%)	0 (0.00%)	0 (0.00%)	0 (0.00%)	0 (0.00%)	2 (50.00%)	1 (25.00%)	1 (25.00%)	4 (100.00%)
Total	9 (10.47%)	4 (4.65%)	3 (3.49%)	1 (1.16%)	2 (2.33%)	42 (48.84%)	1 (1.16%)	24 (27.91%)	86 (100.00%)

A2										
	Bladelets	**Bladelets & Flakes**	**Blades**	**Blades & Bladelets**	**Blades & Flakes**	**Blades, Bladelets & Flakes**	**Flakes**	**Indeterminate**	**No negatives**	**Total**
Surface Cleaning Flake	6 (13.64%)	5 (11.36%)	2 (4.55%)	1 (2.27%)	3 (6.82%)	0 (0.00%)	12 (27.27%)	14 (31.82%)	1 (2.27%)	44 (100.00%)
Maintenance Flake	0 (0.00%)	0 (0.00%)	1 (5.56%)	0 (0.00%)	0 (0.00%)	0 (0.00%)	8 (44.44%)	8 (44.44%)	1 (5.56%)	18 (100.00%)
Core Tablet	0 (0.00%)	14 (25.93%)	1 (1.85%)	0 (0.00%)	1 (1.85%)	3 (5.56%)	24 (44.44%)	3 (5.56%)	8 (14.81%)	54 (100.00%)
Cortical Flake	0 (0.00%)	0 (0.00%)	2 (6.06%)	1 (3.03%)	0 (0.00%)	0 (0.00%)	14 (42.42%)	3 (9.09%)	13 (39.39%)	33 (100.00%)
Simple Flake	0 (0.00%)	0 (0.00%)	0 (0.00%)	0 (0.00%)	0 (0.00%)	0 (0.00%)	1 (25.00%)	1 (25.00%)	2 (50.00%)	4 (100.00%)
Total	6 (3.92%)	19 (12.42%)	6 (3.92%)	2 (1.31%)	4 (2.61%)	3 (1.96%)	59 (38.56%)	29 (18.95%)	25 (16.34%)	153 (100.00%)

Table 88 Negatives types Blades and Bladelets, Fumane.

	A1								
	Bladelets	**Bladelets & Flakes**	**Blades**	**Blades & Bladelets**	**Blades & Flakes**	**Flakes**	**Indeterminate**	**No negatives**	**Total**
Crest	1 (6.25%)	2 (12.50%)	0 (0.00%)	1 (6.25%)	0 (0.00%)	8 (50.00%)	2 (12.50%)	2 (12.50%)	16 (100.00%)
Asymmetrical Blade	22 (30.14%)	2 (2.74%)	8 (10.96%)	17 (23.29%)	0 (0.00%)	6 (8.22%)	11 (15.07%)	7 (9.59%)	73 (100.00%)
Overshot Blade	12 (54.55%)	0 (0.00%)	3 (13.64%)	6 (27.27%)	0 (0.00%)	0 (0.00%)	1 (4.55%)	0 (0.00%)	22 (100.00%)
Surface Cleaning Blade	2 (40.00%)	0 (0.00%)	0 (0.00%)	1 (20.00%)	0 (0.00%)	0 (0.00%)	2 (40.00%)	0 (0.00%)	5 (100.00%)
Crest (Bladelet)	1 (9.09%)	6 (54.55%)	0 (0.00%)	0 (0.00%)	1 (9.09%)	3 (27.27%)	0 (0.00%)	0 (0.00%)	11 (100.00%)
Asymmetrical Bladelet	15 (55.56%)	0 (0.00%)	0 (0.00%)	1 (3.70%)	0 (0.00%)	0 (0.00%)	9 (33.33%)	2 (7.41%)	27 (100.00%)
Overshot Bladelet	9 (81.82%)	0 (0.00%)	0 (0.00%)	0 (0.00%)	0 (0.00%)	0 (0.00%)	2 (18.18%)	0 (0.00%)	11 (100.00%)
Surface Cleaning Bladelet	1 (100.00%)	0 (0.00%)	0 (0.00%)	0 (0.00%)	0 (0.00%)	0 (0.00%)	0 (0.00%)	0 (0.00%)	1 (100.00%)
Simple Blade	120 (77.42%)	0 (0.00%)	3 (1.94%)	9 (5.81%)	0 (0.00%)	0 (0.00%)	23 (14.84%)	0 (0.00%)	155 (100.00%)
Simple Bladelet	203 (56.55%)	0 (0.00%)	0 (0.00%)	1 (0.28%)	0 (0.00%)	0 (0.00%)	152 (42.34%)	3 (0.84%)	359 (100.00%)
Burin Spall	1 (12.50%)	0 (0.00%)	0 (0.00%)	0 (0.00%)	0 (0.00%)	0 (0.00%)	2 (25.00%)	5 (62.50%)	8 (100.00%)
Total	387 (56.25%)	10 (1.45%)	14 (2.03%)	36 (5.23%)	1 (0.15%)	17 (2.47%)	204 (29.65%)	19 (2.76%)	688 (100.00%)
	A1 Complete								
Crest	1 (12.50%)	1 (12.50%)	0 (0.00%)	0 (0.00%)	0 (0.00%)	5 (62.50%)	0 (0.00%)	1 (12.50%)	8 (100.00%)
Asymmetrical Blade	13 (36.11%)	1 (2.78%)	4 (11.11%)	11 (30.56%)	0 (0.00%)	4 (11.11%)	1 (2.78%)	2 (5.56%)	36 (100.00%)
Overshot Blade	9 (64.29%)	0 (0.00%)	1 (7.14%)	4 (28.57%)	0 (0.00%)	0 (0.00%)	0 (0.00%)	0 (0.00%)	14 (100.00%)
Surface Cleaning Blade	1 (33.33%)	0 (0.00%)	0 (0.00%)	1 (33.33%)	0 (0.00%)	0 (0.00%)	1 (33.33%)	0 (0.00%)	3 (100.00%)
Crest (Bladelet)	0 (0.00%)	1 (50.00%)	0 (0.00%)	0 (0.00%)	0 (0.00%)	1 (50.00%)	0 (0.00%)	0 (0.00%)	2 (100.00%)
Asymmetrical Bladelet	5 (50.00%)	0 (0.00%)	0 (0.00%)	0 (0.00%)	0 (0.00%)	0 (0.00%)	5 (50.00%)	0 (0.00%)	10 (100.00%)
Overshot Bladelet	3 (100.00%)	0 (0.00%)	0 (0.00%)	0 (0.00%)	0 (0.00%)	0 (0.00%)	0 (0.00%)	0 (0.00%)	3 (100.00%)
Surface Cleaning Bladelet	1 (100.00%)	0 (0.00%)	0 (0.00%)	0 (0.00%)	0 (0.00%)	0 (0.00%)	0 (0.00%)	0 (0.00%)	1 (100.00%)
Simple Blade	37 (71.15%)	0 (0.00%)	1 (1.92%)	5 (9.62%)	0 (0.00%)	0 (0.00%)	9 (17.31%)	0 (0.00%)	52 (100.00%)
Simple Bladelet	88 (63.77%)	0 (0.00%)	0 (0.00%)	0 (0.00%)	0 (0.00%)	0 (0.00%)	48 (34.78%)	2 (1.45%)	138 (100.00%)
Burin Spall	1 (16.67%)	0 (0.00%)	0 (0.00%)	0 (0.00%)	0 (0.00%)	0 (0.00%)	2 (33.33%)	3 (50.00%)	6 (100.00%)
Total	159 (58.24%)	3 (1.10%)	6 (2.20%)	21 (7.69%)	0 (0.00%)	10 (3.66%)	66 (24.18%)	8 (2.93%)	273 (100.00%)

	A2								
	Bladelets	**Bladelets & Flakes**	**Blades**	**Blades & Bladelets**	**Blades & Flakes**	**Flakes**	**Indeterminate**	**No negatives**	**Total**
Crest	0 (0.00%)	3 (15.00%)	1 (5.00%)	0 (0.00%)	3 (15.00%)	2 (10.00%)	11 (55.00%)	0 (0.00%)	20 (100.00%)
Asymmetrical Blade	22 (29.33%)	1 (1.33%)	5 (6.67%)	9 (12.00%)	0 (0.00%)	0 (0.00%)	36 (48.00%)	2 (2.67%)	75 (100.00%)
Overshot Blade	21 (58.33%)	0 (0.00%)	2 (5.56%)	3 (8.33%)	0 (0.00%)	0 (0.00%)	9 (25.00%)	1 (2.78%)	36 (100.00%)
Surface Cleaning Blade	8 (44.44%)	0 (0.00%)	1 (5.56%)	1 (5.56%)	0 (0.00%)	0 (0.00%)	8 (44.44%)	0 (0.00%)	18 (100.00%)
Maintenance Blade	2 (16.67%)	0 (0.00%)	0 (0.00%)	1 (8.33%)	0 (0.00%)	0 (0.00%)	7 (58.33%)	2 (16.67%)	12 (100.00%)
Crest (Bladelet)	0 (0.00%)	0 (0.00%)	0 (0.00%)	0 (0.00%)	0 (0.00%)	3 (50.00%)	2 (33.33%)	1 (16.67%)	6 (100.00%)
Asymmetrical Bladelet	31 (54.39%)	0 (0.00%)	0 (0.00%)	0 (0.00%)	0 (0.00%)	0 (0.00%)	24 (42.11%)	2 (3.51%)	57 (100.00%)
Overshot Bladelet	6 (75.00%)	0 (0.00%)	0 (0.00%)	0 (0.00%)	0 (0.00%)	0 (0.00%)	2 (25.00%)	0 (0.00%)	8 (100.00%)
Surface Cleaning Bladelet	3 (75.00%)	0 (0.00%)	0 (0.00%)	0 (0.00%)	0 (0.00%)	0 (0.00%)	1 (25.00%)	0 (0.00%)	4 (100.00%)
Maintenance Bladelet	0 (0.00%)	0 (0.00%)	0 (0.00%)	0 (0.00%)	0 (0.00%)	0 (0.00%)	2 (50.00%)	2 (50.00%)	4 (100.00%)
Simple Blade	45 (53.57%)	0 (0.00%)	3 (3.57%)	2 (2.38%)	0 (0.00%)	0 (0.00%)	34 (40.48%)	0 (0.00%)	84 (100.00%)
Simple Bladelet	116 (37.91%)	0 (0.00%)	0 (0.00%)	0 (0.00%)	0 (0.00%)	0 (0.00%)	187 (61.11%)	3 (0.98%)	306 (100.00%)
Burin Spall	0 (0.00%)	0 (0.00%)	0 (0.00%)	0 (0.00%)	0 (0.00%)	0 (0.00%)	1 (11.11%)	8 (88.89%)	9 (100.00%)
Total	254 (39.75%)	4 (0.63%)	12 (1.88%)	16 (2.50%)	3 (0.47%)	5 (0.78%)	324 (50.70%)	21 (3.29%)	639 (100.00%)

Table 89 Negatives orientation in Flakes, Fumane.

	Crossed	Orthogonal	Unipolar	Unipolar+Convergent	Unipolar+Orthogonal	No negatives	Total
				A1			
Surface Cleaning Flake	6 (14.29%)	1 (2.38%)	28 (66.67%)	3 (7.14%)	3 (7.14%)	1 (2.38%)	42 (100.00%)
Maintenance Flake	1 (14.29%)	1 (14.29%)	4 (57.14%)	0 (0.00%)	0 (0.00%)	1 (14.29%)	7 (100.00%)
Core Tablet	1 (6.67%)	3 (20.00%)	7 (46.67%)	0 (0.00%)	2 (13.33%)	2 (13.33%)	15 (100.00%)
Cortical Flake	0 (0.00%)	0 (0.00%)	5 (19.23%)	0 (0.00%)	0 (0.00%)	21 (80.77%)	26 (100.00%)
Simple Flake	0 (0.00%)	0 (0.00%)	3 (60.00%)	0 (0.00%)	0 (0.00%)	2 (40.00%)	5 (100.00%)
Total	8 (8.42%)	5 (5.26%)	47 (49.47%)	3 (3.16%)	5 (5.26%)	27 (28.42%)	95 (100.00%)
				A1 Complete			
Surface Cleaning Flake	4 (10.81%)	1 (2.70%)	26 (70.27%)	3 (8.11%)	2 (5.41%)	1 (2.70%)	37 (100.00%)
Maintenance Flake	1 (14.29%)	1 (14.29%)	4 (57.14%)	0 (0.00%)	0 (0.00%)	1 (14.29%)	7 (100.00%)
Core Tablet	1 (7.14%)	3 (21.43%)	6 (42.86%)	0 (0.00%)	2 (14.29%)	2 (14.29%)	14 (100.00%)
Cortical Flake	0 (0.00%)	0 (0.00%)	5 (20.83%)	0 (0.00%)	0 (0.00%)	19 (79.17%)	24 (100.00%)
Simple Flake	0 (0.00%)	0 (0.00%)	3 (75.00%)	0 (0.00%)	0 (0.00%)	1 (25.00%)	4 (100.00%)
Total	6 (6.98%)	5 (5.81%)	44 (51.16%)	3 (3.49%)	4 (4.65%)	24 (27.91%)	86 (100.00%)

						A2					
	Bipolar	**Bipolar Combinations**	**Crossed**	**Crossed+ Orthogonal**	**Orthogonal**	**Unipolar**	**Unipolar+ Convergent**	**Unipolar+ Crossed**	**Unipolar+ Orthogonal**	**No negatives**	**Total**
Surface Cleaning Flake	4 (9.09%)	1 (2.27%)	2 (4.55%)	0 (0.00%)	0 (0.00%)	33 (75.00%)	2 (4.55%)	1 (2.27%)	0 (0.00%)	1 (2.27%)	44 (100.00%)
Maintenance Flake	1 (5.56%)	0 (0.00%)	4 (22.22%)	0 (0.00%)	0 (0.00%)	11 (61.11%)	0 (0.00%)	0 (0.00%)	1 (5.56%)	1 (5.56%)	18 (100.00%)
Core Tablet	1 (1.85%)	1 (1.85%)	10 (18.52%)	1 (1.85%)	2 (3.70%)	15 (27.78%)	0 (0.00%)	1 (1.85%)	15 (27.78%)	8 (14.81%)	54 (100.00%)
Cortical Flake	2 (6.06%)	0 (0.00%)	0 (0.00%)	0 (0.00%)	4 (12.12%)	13 (39.39%)	0 (0.00%)	0 (0.00%)	1 (3.03%)	13 (39.39%)	33 (100.00%)
Simple Flake	0 (0.00%)	0 (0.00%)	0 (0.00%)	0 (0.00%)	0 (0.00%)	2 (50.00%)	0 (0.00%)	0 (0.00%)	0 (0.00%)	2 (50.00%)	4 (100.00%)
Total	8 (5.23%)	2 (1.31%)	16 (10.46%)	1 (0.65%)	6 (3.92%)	74 (48.37%)	2 (1.31%)	2 (1.31%)	17 (11.11%)	25 (16.34%)	153 (100.00%)

Table 90 Negatives Orientation in Blades and Bladelets, Fumane.

	Bipolar	Convergent	Crossed	Orthogonal	Unipolar	Unipolar+ Convergent	Unipolar+ Crossed	Unipolar+ Orthogonal	Indeterminate	No negatives	Total
						A1					
Crest	0 (0.00%)	0 (0.00%)	0 (0.00%)	3 (18.75%)	4 (25.00%)	0 (0.00%)	0 (0.00%)	6 (37.50%)	1 (6.25%)	2 (12.50%)	16 (100.00%)
Asymmetrical Blade	1 (1.37%)	0 (0.00%)	1 (1.37%)	3 (4.11%)	48 (65.75%)	8 (10.96%)	1 (1.37%)	3 (4.11%)	0 (0.00%)	8 (10.96%)	73 (100.00%)
Overshot Blade	0 (0.00%)	0 (0.00%)	0 (0.00%)	0 (0.00%)	16 (72.73%)	6 (27.27%)	0 (0.00%)	0 (0.00%)	0 (0.00%)	0 (0.00%)	22 (100.00%)
Surface Cleaning Blade	0 (0.00%)	0 (0.00%)	0 (0.00%)	0 (0.00%)	4 (80.00%)	1 (20.00%)	0 (0.00%)	0 (0.00%)	0 (0.00%)	0 (0.00%)	5 (100.00%)
Crest (Bladelet)	0 (0.00%)	0 (0.00%)	0 (0.00%)	2 (18.18%)	1 (9.09%)	0 (0.00%)	0 (0.00%)	8 (72.73%)	0 (0.00%)	0 (0.00%)	11 (100.00%)
Asymmetrical Bladelet	1 (3.70%)	1 (3.70%)	2 (7.41%)	0 (0.00%)	18 (66.67%)	3 (11.11%)	0 (0.00%)	0 (0.00%)	0 (0.00%)	2 (7.41%)	27 (100.00%)
Overshot Bladelet	0 (0.00%)	1 (9.09%)	0 (0.00%)	0 (0.00%)	3 (27.27%)	7 (63.64%)	0 (0.00%)	0 (0.00%)	0 (0.00%)	0 (0.00%)	11 (100.00%)
Surface Cleaning Bladelet	0 (0.00%)	0 (0.00%)	0 (0.00%)	0 (0.00%)	1 (100.00%)	0 (0.00%)	0 (0.00%)	0 (0.00%)	0 (0.00%)	0 (0.00%)	1 (100.00%)
Simple Blade	0 (0.00%)	1 (0.65%)	2 (1.29%)	0 (0.00%)	123 (79.35%)	26 (16.77%)	3 (1.94%)	0 (0.00%)	0 (0.00%)	0 (0.00%)	155 (100.00%)
Simple Bladelet	0 (0.00%)	7 (1.95%)	6 (1.67%)	0 (0.00%)	265 (73.82%)	73 (20.33%)	3 (0.84%)	0 (0.00%)	2 (0.56%)	3 (0.84%)	359 (100.00%)
Burin Spall	0 (0.00%)	0 (0.00%)	0 (0.00%)	0 (0.00%)	3 (37.50%)	0 (0.00%)	0 (0.00%)	0 (0.00%)	0 (0.00%)	5 (62.50%)	8 (100.00%)
Total	2 (0.29%)	10 (1.45%)	11 (1.60%)	8 (1.16%)	486 (70.64%)	124 (18.02%)	7 (1.02%)	17 (2.47%)	3 (0.44%)	20 (2.91%)	688 (100.00%)
						A1 Complete					
Crest	0 (0.00%)	0 (0.00%)	0 (0.00%)	2 (25.00%)	2 (25.00%)	0 (0.00%)	0 (0.00%)	3 (37.50%)	0 (0.00%)	1 (12.50%)	8 (100.00%)
Asymmetrical Blade	1 (2.78%)	0 (0.00%)	0 (0.00%)	2 (5.56%)	23 (63.89%)	6 (16.67%)	1 (2.78%)	1 (2.78%)	0 (0.00%)	2 (5.56%)	36 (100.00%)
Overshot Blade	0 (0.00%)	0 (0.00%)	0 (0.00%)	0 (0.00%)	8 (57.14%)	6 (42.86%)	0 (0.00%)	0 (0.00%)	0 (0.00%)	0 (0.00%)	14 (100.00%)
Surface Cleaning Blade	0 (0.00%)	0 (0.00%)	0 (0.00%)	0 (0.00%)	2 (66.67%)	1 (33.33%)	0 (0.00%)	0 (0.00%)	0 (0.00%)	0 (0.00%)	3 (100.00%)
Crest (Bladelet)	0 (0.00%)	0 (0.00%)	0 (0.00%)	0 (0.00%)	0 (0.00%)	0 (0.00%)	0 (0.00%)	2 (100.00%)	0 (0.00%)	0 (0.00%)	2 (100.00%)
Asymmetrical Bladelet	1 (10.00%)	0 (0.00%)	1 (10.00%)	0 (0.00%)	7 (70.00%)	1 (10.00%)	0 (0.00%)	0 (0.00%)	0 (0.00%)	0 (0.00%)	10 (100.00%)
Overshot Bladelet	0 (0.00%)	0 (0.00%)	0 (0.00%)	0 (0.00%)	1 (33.33%)	2 (66.67%)	0 (0.00%)	0 (0.00%)	0 (0.00%)	0 (0.00%)	3 (100.00%)
Surface Cleaning Bladelet	0 (0.00%)	0 (0.00%)	0 (0.00%)	0 (0.00%)	1 (100.00%)	0 (0.00%)	0 (0.00%)	0 (0.00%)	0 (0.00%)	0 (0.00%)	1 (100.00%)
Simple Blade	0 (0.00%)	0 (0.00%)	1 (1.92%)	0 (0.00%)	42 (80.77%)	7 (13.46%)	2 (3.85%)	0 (0.00%)	0 (0.00%)	0 (0.00%)	52 (100.00%)
Simple Bladelet	0 (0.00%)	4 (2.90%)	2 (1.45%)	0 (0.00%)	101 (73.19%)	27 (19.57%)	1 (0.72%)	0 (0.00%)	1 (0.72%)	2 (1.45%)	138 (100.00%)
Burin Spall	0 (0.00%)	0 (0.00%)	0 (0.00%)	0 (0.00%)	3 (50.00%)	0 (0.00%)	0 (0.00%)	0 (0.00%)	0 (0.00%)	3 (50.00%)	6 (100.00%)
Total	2 (0.73%)	4 (1.47%)	4 (1.47%)	4 (1.47%)	190 (69.60%)	50 (18.32%)	4 (1.47%)	6 (2.20%)	1 (0.37%)	8 (2.93%)	273 (100.00%)

	A2											
	Bipolar	**Convergent**	**Crossed**	**Orthogonal**	**Unipolar**	**Unipolar+ Convergent**	**Unipolar+ Crossed**	**Unipolar+ Orthogonal**	**Unipolar Combinations**	**Indeterminate**	**No negatives**	**Total**
Crest	2 (10.00%)	1 (5.00%)	0 (0.00%)	3 (15.00%)	3 (15.00%)	1 (5.00%)	0 (0.00%)	10 (50.00%)	0 (0.00%)	0 (0.00%)	0 (0.00%)	20 (100.00%)
Asymmetrical Blade	3 (4.00%)	2 (2.67%)	7 (9.33%)	1 (1.33%)	40 (53.33%)	16 (21.33%)	2 (2.67%)	2 (2.67%)	0 (0.00%)	0 (0.00%)	2 (2.67%)	75 (100.00%)
Overshot Blade	0 (0.00%)	3 (8.33%)	1 (2.78%)	0 (0.00%)	18 (50.00%)	12 (33.33%)	0 (0.00%)	1 (2.78%)	0 (0.00%)	0 (0.00%)	1 (2.78%)	36 (100.00%)
Surface Cleaning Blade	1 (5.56%)	0 (0.00%)	2 (11.11%)	0 (0.00%)	10 (55.56%)	2 (11.11%)	0 (0.00%)	1 (5.56%)	2 (11.11%)	0 (0.00%)	0 (0.00%)	18 (100.00%)
Maintenance Blade	0 (0.00%)	0 (0.00%)	0 (0.00%)	1 (8.33%)	7 (58.33%)	2 (16.67%)	0 (0.00%)	0 (0.00%)	0 (0.00%)	0 (0.00%)	2 (16.67%)	12 (100.00%)
Crest (Bladelet)	0 (0.00%)	0 (0.00%)	0 (0.00%)	5 (83.33%)	0 (0.00%)	0 (0.00%)	0 (0.00%)	0 (0.00%)	0 (0.00%)	0 (0.00%)	1 (16.67%)	6 (100.00%)
Asymmetrical Bladelet	0 (0.00%)	0 (0.00%)	2 (3.51%)	0 (0.00%)	44 (77.19%)	9 (15.79%)	0 (0.00%)	0 (0.00%)	0 (0.00%)	0 (0.00%)	2 (3.51%)	57 (100.00%)
Overshot Bladelet	0 (0.00%)	2 (25.00%)	0 (0.00%)	0 (0.00%)	1 (12.50%)	5 (62.50%)	0 (0.00%)	0 (0.00%)	0 (0.00%)	0 (0.00%)	0 (0.00%)	8 (100.00%)
Surface Cleaning Bladelet	0 (0.00%)	0 (0.00%)	0 (0.00%)	0 (0.00%)	2 (50.00%)	1 (25.00%)	1 (25.00%)	0 (0.00%)	0 (0.00%)	0 (0.00%)	0 (0.00%)	4 (100.00%)
Maintenance Bladelet	0 (0.00%)	0 (0.00%)	0 (0.00%)	0 (0.00%)	2 (50.00%)	0 (0.00%)	0 (0.00%)	0 (0.00%)	0 (0.00%)	0 (0.00%)	2 (50.00%)	4 (100.00%)
Simple Blade	3 (3.57%)	0 (0.00%)	3 (3.57%)	0 (0.00%)	59 (70.24%)	18 (21.43%)	0 (0.00%)	1 (1.19%)	0 (0.00%)	0 (0.00%)	0 (0.00%)	84 (100.00%)
Simple Bladelet	4 (1.31%)	12 (3.92%)	8 (2.61%)	0 (0.00%)	219 (71.57%)	48 (15.69%)	8 (2.61%)	1 (0.33%)	0 (0.00%)	3 (0.98%)	3 (0.98%)	306 (100.00%)
Burin Spall	0 (0.00%)	0 (0.00%)	0 (0.00%)	0 (0.00%)	1 (11.11%)	0 (0.00%)	0 (0.00%)	0 (0.00%)	0 (0.00%)	0 (0.00%)	8 (88.89%)	9 (100.00%)
Total	13 (2.03%)	20 (3.13%)	23 (3.60%)	10 (1.56%)	406 (63.54%)	114 (17.84%)	11 (1.72%)	16 (2.50%)	2 (0.31%)	3 (0.47%)	21 (3.29%)	639 (100.00%)

Table 91 Distal termination in Blades and Bladelets, Fumane.

	Feathered	Plunging	Hinged	Stepped	Indeterminate	Total
A1						
Crest	2 (15.38%)	10 (76.92%)	0 (0.00%)	1 (7.69%)	0 (0.00%)	13 (100.00%)
Asymmetrical Blade	9 (16.98%)	39 (73.58%)	0 (0.00%)	4 (7.55%)	1 (1.89%)	53 (100.00%)
Overshot Blade	0 (0.00%)	20 (95.24%)	1 (4.76%)	0 (0.00%)	0 (0.00%)	21 (100.00%)
Surface Cleaning Blade	1 (33.33%)	1 (33.33%)	1 (33.33%)	0 (0.00%)	0 (0.00%)	3 (100.00%)
Crest (Bladelet)	5 (45.45%)	4 (36.36%)	0 (0.00%)	1 (9.09%)	1 (9.09%)	11 (100.00%)
Asymmetrical Bladelet	9 (39.13%)	12 (52.17%)	1 (4.35%)	1 (4.35%)	0 (0.00%)	23 (100.00%)
Overshot Bladelet	0 (0.00%)	10 (100.00%)	0 (0.00%)	0 (0.00%)	0 (0.00%)	10 (100.00%)
Surface Cleaning Bladelet	0 (0.00%)	1 (100.00%)	0 (0.00%)	0 (0.00%)	0 (0.00%)	1 (100.00%)
Simple Blade	67 (80.72%)	5 (6.02%)	1 (1.20%)	5 (6.02%)	5 (6.02%)	83 (100.00%)
Simple Bladelet	195 (85.53%)	17 (7.46%)	9 (3.95%)	3 (1.32%)	4 (1.75%)	228 (100.00%)
Burin Spall	7 (87.50%)	1 (12.50%)	0 (0.00%)	0 (0.00%)	0 (0.00%)	8 (100.00%)
Total	295 (64.98%)	120 (26.43%)	13 (2.86%)	15 (3.30%)	11 (2.42%)	454 (100.00%)
A1 Complete						
Crest	1 (12.50%)	6 (75.00%)	0 (0.00%)	1 (12.50%)	0 (0.00%)	8 (100.00%)
Asymmetrical Blade	7 (19.44%)	25 (69.44%)	0 (0.00%)	4 (11.11%)	0 (0.00%)	36 (100.00%)
Overshot Blade	0 (0.00%)	13 (92.86%)	1 (7.14%)	0 (0.00%)	0 (0.00%)	14 (100.00%)
Surface Cleaning Blade	1 (33.33%)	1 (33.33%)	1 (33.33%)	0 (0.00%)	0 (0.00%)	3 (100.00%)
Crest (Bladelet)	0 (0.00%)	1 (50.00%)	0 (0.00%)	0 (0.00%)	1 (50.00%)	2 (100.00%)
Asymmetrical Bladelet	3 (30.00%)	5 (50.00%)	1 (10.00%)	1 (10.00%)	0 (0.00%)	10 (100.00%)
Overshot Bladelet	0 (0.00%)	3 (100.00%)	0 (0.00%)	0 (0.00%)	0 (0.00%)	3 (100.00%)
Surface Cleaning Bladelet	0 (0.00%)	1 (100.00%)	0 (0.00%)	0 (0.00%)	0 (0.00%)	1 (100.00%)
Simple Blade	44 (83.02%)	3 (5.66%)	0 (0.00%)	5 (9.43%)	1 (1.89%)	53 (100.00%)
Simple Bladelet	127 (92.70%)	5 (3.65%)	2 (1.46%)	3 (2.19%)	0 (0.00%)	137 (100.00%)
Burin Spall	5 (83.33%)	1 (16.67%)	0 (0.00%)	0 (0.00%)	0 (0.00%)	6 (100.00%)
Total	188 (68.86%)	64 (23.44%)	5 (1.83%)	14 (5.13%)	2 (0.73%)	273 (100.00%)
A2						
Crest	5 (25.00%)	13 (65.00%)	0 (0.00%)	2 (10.00%)	0 (0.00%)	20 (100.00%)
Asymmetrical Blade	15 (20.00%)	48 (64.00%)	4 (5.33%)	8 (10.67%)	0 (0.00%)	75 (100.00%)
Overshot Blade	0 (0.00%)	36 (100.00%)	0 (0.00%)	0 (0.00%)	0 (0.00%)	36 (100.00%)
Surface Cleaning Blade	6 (33.33%)	6 (33.33%)	1 (5.56%)	5 (27.78%)	0 (0.00%)	18 (100.00%)
Maintenance Blade	7 (58.33%)	1 (8.33%)	2 (16.67%)	1 (8.33%)	1 (8.33%)	12 (100.00%)
Crest (Bladelet)	1 (16.67%)	1 (16.67%)	0 (0.00%)	4 (66.67%)	0 (0.00%)	6 (100.00%)
Asymmetrical Bladelet	11 (19.30%)	43 (75.44%)	1 (1.75%)	2 (3.51%)	0 (0.00%)	57 (100.00%)
Overshot Bladelet	0 (0.00%)	6 (75.00%)	0 (0.00%)	2 (25.00%)	0 (0.00%)	8 (100.00%)
Surface Cleaning Bladelet	0 (0.00%)	4 (100.00%)	0 (0.00%)	0 (0.00%)	0 (0.00%)	4 (100.00%)
Maintenance Bladelet	1 (25.00%)	2 (50.00%)	0 (0.00%)	1 (25.00%)	0 (0.00%)	4 (100.00%)
Simple Blade	64 (74.42%)	4 (4.65%)	13 (15.12%)	5 (5.81%)	0 (0.00%)	86 (100.00%)
Simple Bladelet	243 (80.20%)	17 (5.61%)	21 (6.93%)	22 (7.26%)	0 (0.00%)	303 (100.00%)
Burin Spall	8 (88.89%)	0 (0.00%)	0 (0.00%)	1 (11.11%)	0 (0.00%)	9 (100.00%)
Total	361 (56.58%)	181 (28.37%)	42 (6.58%)	53 (8.31%)	1 (0.16%)	638 (100.00%)

Table 92 Outline in Blades and Bladelets, Fumane.

	(sub)Parallel Edges	Convergent	Off-axis	Indeterminate	Total
			A1		
Crest	7 (53.85%)	4 (30.77%)	2 (15.38%)	0 (0.00%)	13 (100.00%)
Asymmetrical Blade	21 (39.62%)	1 (1.89%)	30 (56.60%)	1 (1.89%)	53 (100.00%)
Overshot Blade	21 (100.00%)	0 (0.00%)	0 (0.00%)	0 (0.00%)	21 (100.00%)
Surface Cleaning Blade	1 (33.33%)	2 (66.67%)	0 (0.00%)	0 (0.00%)	3 (100.00%)
Crest (Bladelet)	5 (45.45%)	5 (45.45%)	1 (9.09%)	0 (0.00%)	11 (100.00%)
Asymmetrical Bladelet	7 (30.43%)	4 (17.39%)	12 (52.17%)	0 (0.00%)	23 (100.00%)
Overshot Bladelet	8 (80.00%)	2 (20.00%)	0 (0.00%)	0 (0.00%)	10 (100.00%)
Surface Cleaning Bladelet	1 (100.00%)	0 (0.00%)	0 (0.00%)	0 (0.00%)	1 (100.00%)
Simple Blade	42 (50.60%)	31 (37.35%)	6 (7.23%)	4 (4.82%)	83 (100.00%)
Simple Bladelet	116 (50.88%)	86 (37.72%)	22 (9.65%)	4 (1.75%)	228 (100.00%)
Burin Spall	4 (50.00%)	3 (37.50%)	1 (12.50%)	0 (0.00%)	8 (100.00%)
Total	233 (51.32%)	138 (30.40%)	74 (16.30%)	9 (1.98%)	454 (100.00%)
			A1 Complete		
Crest	5 (62.50%)	3 (37.50%)	0 (0.00%)	0 (0.00%)	8 (100.00%)
Asymmetrical Blade	16 (44.44%)	0 (0.00%)	20 (55.56%)	0 (0.00%)	36 (100.00%)
Overshot Blade	14 (100.00%)	0 (0.00%)	0 (0.00%)	0 (0.00%)	14 (100.00%)
Surface Cleaning Blade	1 (33.33%)	2 (66.67%)	0 (0.00%)	0 (0.00%)	3 (100.00%)
Crest (Bladelet)	1 (50.00%)	1 (50.00%)	0 (0.00%)	0 (0.00%)	2 (100.00%)
Asymmetrical Bladelet	3 (30.00%)	1 (10.00%)	6 (60.00%)	0 (0.00%)	10 (100.00%)
Overshot Bladelet	3 (100.00%)	0 (0.00%)	0 (0.00%)	0 (0.00%)	3 (100.00%)
Surface Cleaning Bladelet	1 (100.00%)	0 (0.00%)	0 (0.00%)	0 (0.00%)	1 (100.00%)
Simple Blade	24 (45.28%)	22 (41.51%)	6 (11.32%)	1 (1.89%)	53 (100.00%)
Simple Bladelet	70 (51.09%)	49 (35.77%)	17 (12.41%)	1 (0.73%)	137 (100.00%)
Burin Spall	4 (66.67%)	2 (33.33%)	0 (0.00%)	0 (0.00%)	6 (100.00%)
Total	142 (52.01%)	80 (29.30%)	49 (17.95%)	2 (0.73%)	273 (100.00%)
			A2		
Crest	5 (25.00%)	3 (15.00%)	12 (60.00%)	0 (0.00%)	20 (100.00%)
Asymmetrical Blade	16 (21.33%)	4 (5.33%)	55 (73.33%)	0 (0.00%)	75 (100.00%)
Overshot Blade	35 (97.22%)	1 (2.78%)	0 (0.00%)	0 (0.00%)	36 (100.00%)
Surface Cleaning Blade	18 (100.00%)	0 (0.00%)	0 (0.00%)	0 (0.00%)	18 (100.00%)
Maintenance Blade	6 (50.00%)	1 (8.33%)	4 (33.33%)	1 (8.33%)	12 (100.00%)
Crest (Bladelet)	4 (66.67%)	2 (33.33%)	0 (0.00%)	0 (0.00%)	6 (100.00%)
Asymmetrical Bladelet	3 (5.26%)	2 (3.51%)	52 (91.23%)	0 (0.00%)	57 (100.00%)
Overshot Bladelet	7 (87.50%)	0 (0.00%)	1 (12.50%)	0 (0.00%)	8 (100.00%)
Surface Cleaning Bladelet	4 (100.00%)	0 (0.00%)	0 (0.00%)	0 (0.00%)	4 (100.00%)
Maintenance Bladelet	1 (25.00%)	1 (25.00%)	2 (50.00%)	0 (0.00%)	4 (100.00%)
Simple Blade	61 (70.93%)	11 (12.79%)	14 (16.28%)	0 (0.00%)	86 (100.00%)
Simple Bladelet	162 (53.47%)	77 (25.41%)	63 (20.79%)	1 (0.33%)	303 (100.00%)
Burin Spall	5 (55.56%)	2 (22.22%)	2 (22.22%)	0 (0.00%)	9 (100.00%)
Total	327 (51.25%)	104 (16.30%)	205 (32.13%)	2 (0.31%)	638 (100.00%)

Table 93 Profile in Blades and Bladelets, Fumane

	Straight	Slightly Curved	Curved	Very Curved	Twisted	Indeterminate	Total
				A1			
Crest	2 (12.50%)	8 (50.00%)	3 (18.75%)	1 (6.25%)	2 (12.50%)	0 (0.00%)	16 (100.00%)
Asymmetrical Blade	26 (35.62%)	16 (21.92%)	5 (6.85%)	4 (5.48%)	21 (28.77%)	1 (1.37%)	73 (100.00%)
Overshot Blade	1 (4.55%)	5 (22.73%)	13 (59.09%)	1 (4.55%)	2 (9.09%)	0 (0.00%)	22 (100.00%)
Surface Cleaning Blade	4 (80.00%)	1 (20.00%)	0 (0.00%)	0 (0.00%)	0 (0.00%)	0 (0.00%)	5 (100.00%)
Crest (Bladelet)	7 (63.64%)	1 (9.09%)	2 (18.18%)	0 (0.00%)	1 (9.09%)	0 (0.00%)	11 (100.00%)
Asymmetrical Bladelet	4 (14.81%)	4 (14.81%)	0 (0.00%)	2 (7.41%)	17 (62.96%)	0 (0.00%)	27 (100.00%)
Overshot Bladelet	0 (0.00%)	4 (36.36%)	5 (45.45%)	2 (18.18%)	0 (0.00%)	0 (0.00%)	11 (100.00%)
Surface Cleaning Bladelet	0 (0.00%)	0 (0.00%)	0 (0.00%)	1 (100.00%)	0 (0.00%)	0 (0.00%)	1 (100.00%)
Simple Blade	123 (78.34%)	17 (10.83%)	11 (7.01%)	0 (0.00%)	6 (3.82%)	0 (0.00%)	157 (100.00%)
Simple Bladelet	274 (76.75%)	46 (12.89%)	6 (1.68%)	0 (0.00%)	31 (8.68%)	0 (0.00%)	357 (100.00%)
Burin Spall	6 (75.00%)	1 (12.50%)	1 (12.50%)	0 (0.00%)	0 (0.00%)	0 (0.00%)	8 (100.00%)
Total	447 (64.97%)	103 (14.97%)	46 (6.69%)	11 (1.60%)	80 (11.63%)	1 (0.15%)	688 (100.00%)
				A1 Complete			
Crest	1 (12.50%)	5 (62.50%)	1 (12.50%)	1 (12.50%)	0 (0.00%)		8 (100.00%)
Asymmetrical Blade	10 (27.78%)	8 (22.22%)	3 (8.33%)	3 (8.33%)	12 (33.33%)		36 (100.00%)
Overshot Blade	1 (7.14%)	4 (28.57%)	6 (42.86%)	1 (7.14%)	2 (14.29%)		14 (100.00%)
Surface Cleaning Blade	3 (100.00%)	0 (0.00%)	0 (0.00%)	0 (0.00%)	0 (0.00%)		3 (100.00%)
Crest (Bladelet)	1 (50.00%)	0 (0.00%)	0 (0.00%)	0 (0.00%)	1 (50.00%)		2 (100.00%)
Asymmetrical Bladelet	1 (10.00%)	0 (0.00%)	0 (0.00%)	0 (0.00%)	9 (90.00%)		10 (100.00%)
Overshot Bladelet	0 (0.00%)	2 (66.67%)	1 (33.33%)	0 (0.00%)	0 (0.00%)		3 (100.00%)
Surface Cleaning Bladelet	0 (0.00%)	0 (0.00%)	0 (0.00%)	1 (100.00%)	0 (0.00%)		1 (100.00%)
Simple Blade	42 (79.25%)	5 (9.43%)	5 (9.43%)	0 (0.00%)	1 (1.89%)		53 (100.00%)
Simple Bladelet	103 (75.18%)	15 (10.95%)	3 (2.19%)	0 (0.00%)	16 (11.68%)		137 (100.00%)
Burin Spall	5 (83.33%)	1 (16.67%)	0 (0.00%)	0 (0.00%)	0 (0.00%)		6 (100.00%)
Total	167 (61.17%)	40 (14.65%)	19 (6.96%)	6 (2.20%)	41 (15.02%)		273 (100.00%)

.

	A2						
	Straight	**Slightly Curved**	**Curved**	**Very Curved**	**Twisted**	**Indeterminate**	**Total**
Crest	5 (25.00%)	2 (10.00%)	7 (35.00%)	1 (5.00%)	5 (25.00%)	0 (0.00%)	20 (100.00%)
Asymmetrical Blade	9 (12.00%)	9 (12.00%)	10 (13.33%)	6 (8.00%)	41 (54.67%)	0 (0.00%)	75 (100.00%)
Overshot Blade	1 (2.78%)	13 (36.11%)	17 (47.22%)	5 (13.89%)	0 (0.00%)	0 (0.00%)	36 (100.00%)
Surface Cleaning Blade	11 (61.11%)	4 (22.22%)	2 (11.11%)	1 (5.56%)	0 (0.00%)	0 (0.00%)	18 (100.00%)
Maintenance Blade	9 (75.00%)	2 (16.67%)	0 (0.00%)	0 (0.00%)	0 (0.00%)	1 (8.33%)	12 (100.00%)
Crest (Bladelet)	2 (33.33%)	1 (16.67%)	0 (0.00%)	0 (0.00%)	3 (50.00%)	0 (0.00%)	6 (100.00%)
Asymmetrical Bladelet	7 (12.28%)	12 (21.05%)	1 (1.75%)	2 (3.51%)	35 (61.40%)	0 (0.00%)	57 (100.00%)
Overshot Bladelet	1 (12.50%)	5 (62.50%)	1 (12.50%)	0 (0.00%)	1 (12.50%)	0 (0.00%)	8 (100.00%)
Surface Cleaning Bladelet	0 (0.00%)	2 (50.00%)	1 (25.00%)	1 (25.00%)	0 (0.00%)	0 (0.00%)	4 (100.00%)
Maintenance Bladelet	3 (75.00%)	1 (25.00%)	0 (0.00%)	0 (0.00%)	0 (0.00%)	0 (0.00%)	4 (100.00%)
Simple Blade	62 (72.09%)	17 (19.77%)	1 (1.16%)	0 (0.00%)	6 (6.98%)	0 (0.00%)	86 (100.00%)
Simple Bladelet	232 (76.57%)	29 (9.57%)	5 (1.65%)	1 (0.33%)	36 (11.88%)	0 (0.00%)	303 (100.00%)
Burin Spall	9 (100.00%)	0 (0.00%)	0 (0.00%)	0 (0.00%)	0 (0.00%)	0 (0.00%)	9 (100.00%)
Total	351 (55.02%)	97 (15.20%)	45 (7.05%)	17 (2.66%)	127 (19.91%)	1 (0.16%)	638 (100.00%)

Table 94 Cross-sections in Blades and Bladelets, Fumane

	A1						
	Flat	**Trapezoidal Asymm**	**Trapezoidal Symm**	**Triangular Asymm**	**Triangular Symm**	**Indeterminate**	**Total**
Crest	0 (0.00%)	5 (31.25%)	0 (0.00%)	6 (37.50%)	5 (31.25%)	0 (0.00%)	16 (100.00%)
Asymmetrical Blade	4 (5.48%)	24 (32.88%)	6 (8.22%)	29 (39.73%)	9 (12.33%)	1 (1.37%)	73 (100.00%)
Overshot Blade	0 (0.00%)	10 (45.45%)	6 (27.27%)	3 (13.64%)	3 (13.64%)	0 (0.00%)	22 (100.00%)
Surface Cleaning Blade	1 (20.00%)	3 (60.00%)	1 (20.00%)	0 (0.00%)	0 (0.00%)	0 (0.00%)	5 (100.00%)
Crest (Bladelet)	0 (0.00%)	2 (18.18%)	2 (18.18%)	5 (45.45%)	2 (18.18%)	0 (0.00%)	11 (100.00%)
Asymmetrical Bladelet	0 (0.00%)	10 (37.04%)	1 (3.70%)	15 (55.56%)	1 (3.70%)	0 (0.00%)	27 (100.00%)
Overshot Bladelet	0 (0.00%)	4 (36.36%)	6 (54.55%)	0 (0.00%)	1 (9.09%)	0 (0.00%)	11 (100.00%)
Surface Cleaning Bladelet	0 (0.00%)	0 (0.00%)	1 (100.00%)	0 (0.00%)	0 (0.00%)	0 (0.00%)	1 (100.00%)
Simple Blade	13 (8.28%)	49 (31.21%)	50 (31.85%)	29 (18.47%)	16 (10.19%)	0 (0.00%)	157 (100.00%)
Simple Bladelet	24 (6.72%)	45 (12.61%)	109 (30.53%)	96 (26.89%)	80 (22.41%)	3 (0.84%)	357 (100.00%)
Burin Spall	0 (0.00%)	0 (0.00%)	0 (0.00%)	0 (0.00%)	8 (100.00%)	0 (0.00%)	8 (100.00%)
Total	42 (6.10%)	152 (22.09%)	182 (26.45%)	183 (26.60%)	125 (18.17%)	4 (0.58%)	688 (100.00%)
	A1 Complete						
Crest	0 (0.00%)	2 (25.00%)	0 (0.00%)	3 (37.50%)	3 (37.50%)	0 (0.00%)	8 (100.00%)
Asymmetrical Blade	3 (8.33%)	14 (38.89%)	3 (8.33%)	15 (41.67%)	1 (2.78%)	0 (0.00%)	36 (100.00%)
Overshot Blade	0 (0.00%)	7 (50.00%)	4 (28.57%)	2 (14.29%)	1 (7.14%)	0 (0.00%)	14 (100.00%)
Surface Cleaning Blade	1 (33.33%)	1 (33.33%)	1 (33.33%)	0 (0.00%)	0 (0.00%)	0 (0.00%)	3 (100.00%)
Crest (Bladelet)	0 (0.00%)	0 (0.00%)	0 (0.00%)	2 (100.00%)	0 (0.00%)	0 (0.00%)	2 (100.00%)
Asymmetrical Bladelet	0 (0.00%)	3 (30.00%)	0 (0.00%)	7 (70.00%)	0 (0.00%)	0 (0.00%)	10 (100.00%)
Overshot Bladelet	0 (0.00%)	1 (33.33%)	2 (66.67%)	0 (0.00%)	0 (0.00%)	0 (0.00%)	3 (100.00%)
Surface Cleaning Bladelet	0 (0.00%)	0 (0.00%)	1 (100.00%)	0 (0.00%)	0 (0.00%)	0 (0.00%)	1 (100.00%)
Simple Blade	7 (13.21%)	15 (28.30%)	16 (30.19%)	11 (20.75%)	4 (7.55%)	0 (0.00%)	53 (100.00%)
Simple Bladelet	9 (6.57%)	13 (9.49%)	34 (24.82%)	49 (35.77%)	30 (21.90%)	2 (1.46%)	137 (100.00%)
Burin Spall	0 (0.00%)	0 (0.00%)	0 (0.00%)	0 (0.00%)	6 (100.00%)	0 (0.00%)	6 (100.00%)
Total	20 (7.33%)	56 (20.51%)	61 (22.34%)	89 (32.60%)	45 (16.48%)	2 (0.73%)	273 (100.00%)

	A2						
	Flat	**Trapezoidal Asymm**	**Trapezoidal Symm**	**Triangular Asymm**	**Triangular Symm**	**Indeterminate**	**Total**
Crest	1 (5.00%)	6 (30.00%)	0 (0.00%)	10 (50.00%)	3 (15.00%)	0 (0.00%)	20 (100.00%)
Asymmetrical Blade	4 (5.33%)	38 (50.67%)	10 (13.33%)	18 (24.00%)	5 (6.67%)	0 (0.00%)	75 (100.00%)
Overshot Blade	1 (2.78%)	10 (27.78%)	18 (50.00%)	3 (8.33%)	4 (11.11%)	0 (0.00%)	36 (100.00%)
Surface Cleaning Blade	0 (0.00%)	6 (33.33%)	8 (44.44%)	0 (0.00%)	4 (22.22%)	0 (0.00%)	18 (100.00%)
Maintenance Blade	4 (33.33%)	2 (16.67%)	2 (16.67%)	0 (0.00%)	3 (25.00%)	1 (8.33%)	12 (100.00%)
Crest (Bladelet)	0 (0.00%)	0 (0.00%)	0 (0.00%)	3 (50.00%)	3 (50.00%)	0 (0.00%)	6 (100.00%)
Asymmetrical Bladelet	4 (7.02%)	20 (35.09%)	14 (24.56%)	12 (21.05%)	7 (12.28%)	0 (0.00%)	57 (100.00%)
Overshot Bladelet	0 (0.00%)	1 (12.50%)	4 (50.00%)	0 (0.00%)	3 (37.50%)	0 (0.00%)	8 (100.00%)
Surface Cleaning Bladelet	0 (0.00%)	0 (0.00%)	2 (50.00%)	0 (0.00%)	2 (50.00%)	0 (0.00%)	4 (100.00%)
Maintenance Bladelet	0 (0.00%)	1 (25.00%)	0 (0.00%)	1 (25.00%)	1 (25.00%)	1 (25.00%)	4 (100.00%)
Simple Blade	12 (13.95%)	23 (26.74%)	27 (31.40%)	6 (6.98%)	17 (19.77%)	1 (1.16%)	86 (100.00%)
Simple Bladelet	32 (10.53%)	47 (15.46%)	79 (25.99%)	56 (18.42%)	90 (29.61%)	0 (0.00%)	304 (100.00%)
Burin Spall	0 (0.00%)	0 (0.00%)	1 (11.11%)	1 (11.11%)	7 (77.78%)	0 (0.00%)	9 (100.00%)
Total	58 (9.08%)	154 (24.10%)	165 (25.82%)	110 (17.21%)	149 (23.32%)	3 (0.47%)	639 (100.00%)

Curriculum Vitae

PERSONAL CONTACTS
Jacopo Gennai
Date of birth: 11/01/1992 **Nationality:** Italian **Gender:** Male **Phone:** (+39) 3470427522 **E-mail**: jacopo.gennai@hotmail.it; jgennai@uni-koeln.de **Current address:** Aachener Str. 72, 50674, Köln, Germany

EDUCATION AND TRAINING

01/04/2018 – CURRENT – Köln, Germany
PH.D. CANDIDATE – Universität zu Köln - Institut für Ur- und Frühgeschichte
03/04/2017 – 25/09/2017 – Leiden, Netherlands
ERASMUS+ TRAINEESHIP – Leiden University - Faculty of Archaeology, Human Origins Department
18/12/2014 – 14/03/2017 – Ferrara, Italy
MA IN QUATERNARY, PREHISTORY AND ARCHAEOLOGY (LM 2) – Università degli Studi di Ferrara
Field(s) of study
Arts and humanities : *History and archaeology*
110/110 cum laude
The laminar Levallois of Grotta di Fumane (VR) in the framework of the Italian Final Mousterian EQF level 7
30/09/2013 – 22/06/2014 – Leicester, United Kingdom
LLP ERASMUS FOR STUDY – University of Leicester - School of Archaeology and Ancient History
15/09/2011 – 11/02/2015 – Pisa, Italy
BA IN CULTURAL HERITAGE STUDIES (L 1); ARCHAEOLOGY CURRICULUM – Università di Pisa
Field(s) of study
Arts and humanities : *Humanities (except languages) not elsewhere classified*
110/110 cum laude The Middle/Upper Palaeolithic Transition in Italy and Europe EQF level 6
2006 – 2011 – Viareggio, Italy
DILPOMA DI ISTRUZIONE DI SCUOLA SECONDARIA – Liceo Ginnasio Statale Giosuè Carducci
82/100 EQF level 4

WORKING EXPERIENCE

01/01/2018 – CURRENT – Köln, Germany
WISSENSCHAFTLICHER MITARBEITER – UNIVERSITAET ZU KOELN

LANGUAGE SKILLS

Mother tongue(s): ITALIAN
Other language(s):

	UNDERSTANDING		SPEAKING		WRITING
	Listening	Reading	Spoken production	Spoken interaction	
ENGLISH	**C2**	**C2**	**C1**	**C1**	**C1**
FRENCH	**A2**	**B1**	**A2**	**A2**	**A2**
GERMAN	**A1**	**A1**	**A2**	**A2**	**A1**

Levels: A1 and A2: Basic user; B1 and B2: Independent user; C1 and C2: Proficient user

CONFERENCES AND SEMINARS

01/12/2020 – 05/12/2020 – Universität zu Köln
Materiality & Agency: Archaeological, Philosophical, and Anthropological Perspectives
12/12/2019 – 13/12/2019 – Universität zu Köln
Geometric Morphometrics
28/11/2019 – 29/11/2019 – RWTH Aachen
Loess-Archaeology Workshop
23/04/2019 – 27/04/2019 – Neanderthal Museum, Mettmann (DE)
Hugo Obermaier Society annual Meeting
04/06/2018 – 09/06/2018 – Paris
XVIIIe world UISPP Congress
08/04/2018 – 13/04/2018 – Vienna
EGU General Assembly
21/09/2017 – 23/09/2017 – Leiden
7th ESHE Meeting
30/08/2017 – 03/09/2017 – Maastricht
23rd EAA Meeting